

ACC. No. 645

*[Faint handwritten notes]*



# MAP OF THE MOON

BY

THOMAS GWYN ELGER, F.R.A.S.

*The Map, in four Sections, accompanying this Work,  
has also been printed as a whole, and may  
be obtained separately.*

**Price on sheet, Two Shillings and Sixpence.**

**Mounted on strong millboard and varnished,  
Four Shillings.**

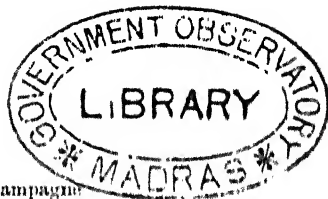
# THE MOON

## A FULL DESCRIPTION AND MAP OF ITS PRINCIPAL PHYSICAL FEATURES

BY

THOMAS GWYN ELGER, F.R.A.S.

DIRECTOR OF THE LUNAR SECTION OF THE BRITISH  
ASTRONOMICAL ASSOCIATION  
EX-PRESIDENT LIVERPOOL ASTRONOMICAL SOCIETY



"Altri fiumi, altri laghi, altre campagne  
Sono là su che non son qui tra noi,  
Altri piani, altre valli, altre montagne."  
ORLANDO FURIOSO, Canto xxxii.

LONDON  
GEORGE PHILIP & SON, 32 FLEET STREET, E.C.  
LIVERPOOL: 45 to 51 SOUTH CASTLE STREET  
1895

IIA Lib.





## PREFACE

THIS book and the accompanying map is chiefly intended for the use of lunar observers, but it is hoped it may be acceptable to many who, though they cannot strictly be thus described, take a general interest in astronomy.

The increasing number of those who possess astronomical telescopes, and devote more or less of their leisure in following some particular line of research, is shown by the great success in recent years of societies, such as the British Astronomical Association with its several branches, the Astronomical Society of the Pacific, and similar institutions in various parts of the world. These societies are not only doing much in popularising the sublimest of the sciences, but are the means of developing and organising the capabilities of their members by discouraging aimless and desultory observations, and by pointing out how individual effort may be utilised and made of permanent value in almost every department of astronomy.

The work of the astronomer, like that of the votary of almost every other science, is becoming every year more and more specialised; and among its manifold subdivisions, the study of the physical features of the moon is undoubtedly increasing in popularity and importance. To those who are pursuing such observations, it is believed that this book will be a useful companion to the telescope, and convenient for reference.

Great care has been taken in the preparation of the map, which, so far as the positions of the various objects represented are concerned, is based on the last edition of Beer and Mädler's chart, and on the more recent and much larger and elaborate map of Schmidt; while as regards the shape and details of most of the formations, the author's drawings and a large number of photographs have been utilised. Even on so small a scale as eighteen inches to the moon's diameter, more detail might have been inserted, but this, at the expense of distinctness, would have detracted from the value of the map for handy reference in the usually dim light of the observatory, without adding to its utility in other ways. Every named formation is prominently shown; and most

other features of interest, including the principal rill-systems, are represented, though, as regards these, no attempt is made to indicate all their manifold details and ramifications, which, to do effectually, would in very many instances require a map on a much larger scale than any that has yet appeared.

The insertion of meridian lines and parallels of latitude at every ten degrees, and the substitution of names for reference numbers, will add to the usefulness of the map.

With respect to the text, a large proportion of the objects in the Catalogue and in the Appendix have been observed and drawn by the author many times during the last thirty years, and described in *The Observatory* and other publications. He has had, besides, the advantage of consulting excellent sketches by Mr W. H. MAW, F.R.A.S., Dr. SHELDON, F.R.A.S., Mr. A. MEE, F.R.A.S., Mr. G. P. HALLOWES, F.R.A.S., Dr. SMART, F.R.A.S., Mr. T. GORDON, F.R.A.S., Mr. G. T. DAVIS, Herr BRENNER, Herr KRIEGER, Mr. H. CORDER, and other members of the British Astronomical Association. Through the courtesy of Professor HOLDEN, Director of the Lick Observatory, and M. PRINZ, of the Royal Observatory of Brussels, many beautiful photographs and direct photographic enlargements have been available, as have also the exquisite heliogravures received by the author from Dr. L. WEINEK, Director of the Imperial Observatory of Prague, and the admirable examples of the photographic work of MM. PAUL and PROSPER HENRY of the Paris Observatory, which are occasionally published in *Knowledge*. The numerous representations of lunar objects which have appeared from time to time in that storehouse of astronomical information, *The English Mechanic*, and the invaluable notes in "Celestial Objects for Common Telescopes," and in various periodicals, by the late REV. PREBENDARY WEBB, to whom Selenography and Astronomy generally owe so much, have also been consulted.

As a rule, all the more prominent and important features are described, though very frequently interesting details are referred to which, from their minuteness, could not be shown in the map. The measurements (given in round numbers) are derived in most instances from NEISON'S (Nevill) "Moon," though occasionally those in the introduction to Schmidt's chart are adopted.

THOMAS GYWN ELGER.

# CONTENTS

	PAGE
INTRODUCTION . . . . .	I
MARIA, OR PLAINS, TERMED "SEAS" . . . . .	4
RIDGES . . . . .	7
RING-MOUNTAINS, CRATERS, &c. . . . .	9
Walled Plains . . . . .	10
Mountain Rings . . . . .	12
Ring-Plains . . . . .	12
Craters . . . . .	14
Crater Cones . . . . .	15
Craterlets, Crater Pits . . . . .	16
MOUNTAIN RANGES, ISOLATED MOUNTAINS, &c. . . . .	17
CLEFTS, OR RILLS . . . . .	20
FAULTS . . . . .	26
VALLEYS . . . . .	26
BRIGHT RAY-SYSTEMS. . . . .	27
THE MOON'S ALBEDO, SURFACE BRIGHTNESS, &c. . . . .	30
TEMPERATURE OF THE MOON'S SURFACE . . . . .	32
LUNAR OBSERVATION . . . . .	32
PROGRESS OF SELENOGRAPHY, LUNAR PHOTOGRAPHY . . . . .	35

## CATALOGUE OF LUNAR FORMATIONS

### FIRST QUADRANT—

West Longitude $90^{\circ}$ to $60^{\circ}$ . . . . .	39
"      " $60^{\circ}$ to $40^{\circ}$ . . . . .	42
"      " $40^{\circ}$ to $20^{\circ}$ . . . . .	48
"      " $20^{\circ}$ to $0^{\circ}$ . . . . .	54

### SECOND QUADRANT—

East Longitude $0^{\circ}$ to $20^{\circ}$ . . . . .	67
"      " $20^{\circ}$ to $40^{\circ}$ . . . . .	76
"      " $40^{\circ}$ to $60^{\circ}$ . . . . .	82
"      " $60^{\circ}$ to $90^{\circ}$ . . . . .	87

## THIRD QUADRANT—

	PAGE
East Longitude $0^{\circ}$ to $20^{\circ}$ . . . . .	92
„ „ $20^{\circ}$ to $40^{\circ}$ . . . . .	105
„ „ $40^{\circ}$ to $60^{\circ}$ . . . . .	113
„ „ $60^{\circ}$ to $90^{\circ}$ . . . . .	119

## FOURTH QUADRANT—

West Longitude $90^{\circ}$ to $60^{\circ}$ . . . . .	123
„ „ $60^{\circ}$ to $40^{\circ}$ . . . . .	127
„ „ $40^{\circ}$ to $20^{\circ}$ . . . . .	133
„ „ $20^{\circ}$ to $0^{\circ}$ . . . . .	142

## MAP OF THE MOON

First Quadrant . . . . .	<i>between pages</i> 38 and 39
Second Quadrant . . . . .	„ „ 66 „ 67
Third Quadrant . . . . .	„ „ 92 „ 93
Fourth Quadrant . . . . .	„ „ 122 „ 123

## APPENDIX

Description of Map . . . . .	153
List of the Maria, or Grey Plains, termed “Seas,” &c. . . . .	155
List of some of the most Prominent Mountain Ranges, Promontories, Isolated Mountains, and Remarkable Hills . . . . .	156
List of the Principal Ray-Systems, Light-Surrounded Craters, and Light Spots . . . . .	160
Position of the Lunar Terminator . . . . .	164
Lunar Elements . . . . .	168
Alphabetical List of Formations . . . . .	170

## INTRODUCTION

WE know, both by tradition and published records, that from the earliest times the faint grey and light spots which diversify the face of our satellite excited the wonder and stimulated the curiosity of mankind, giving rise to suppositions more or less crude and erroneous as to their actual nature and significance. It is true that Anaxagoras, five centuries before our era, and probably other philosophers preceding him,—certainly Plutarch at a much later date—taught that these delicate markings and differences of tint, obvious to every one with normal vision, point to the existence of hills and valleys on her surface; the latter maintaining that the irregularities of outline presented by the “terminator,” or line of demarcation between the illumined and unillumined portion of her spherical superficies, are due to mountains and their shadows; but more than fifteen centuries elapsed before the truth of this sagacious conjecture was unquestionably demonstrated. Selenography, as a branch of observational astronomy, dates from the spring of 1609, when Galileo directed his “optic tube” to the moon, and in the following year, in the *Sidereus Nuncius*, or “the Intelligencer of the Stars,” gave to an astonished and incredulous world an account of the unsuspected marvels it revealed. In this remarkable little book we have the first attempt to represent the telescopic aspect of the moon’s visible surface in the five rude woodcuts representing the curious features he perceived thereon, whose form and arrangement, he tells us, reminded him of the “ocelli” on the feathers of a peacock’s tail,—a quaint but not altogether inappropriate simile to describe the appearance of groups of the larger ring-mountains partially illuminated by the sun, when seen in a small telescope.

The bright and dusky areas, so obvious to the unaided sight, were found by Galileo to be due to a very manifest difference in the character of the lunar surface, a large portion of the northern hemisphere, and no inconsiderable part of the south-eastern quadrant, being seen to consist of large grey monotonous tracts, often bordered by lofty mountains, while the remainder of the



superficies was much more conspicuously brilliant, and, moreover, included by far the greater number of those curious ring-mountains and other extraordinary features whose remarkable aspect and peculiar arrangement first attracted his attention. Struck by the analogy which these contrasted regions present to the land and water surfaces of our globe, he suspected that the former are represented on the moon by the brighter and more rugged, and the latter by the smoother and more level areas; a view, however, which Kepler more distinctly formulated in the dictum, "*Do maculas esse Maria, do lucidas esse terras.*" Besides making a rude lunar chart, he estimated the heights of some of the ring-mountains by measuring the distance from the terminator of their bright summit peaks, when they were either coming into or passing out of sunlight; and though his method was incapable of accuracy, and his results consequently untrustworthy, it served to demonstrate the immense altitude of these circumvallations, and to show how greatly they exceed any mountains on the earth if the relative dimensions of the two globes are taken into consideration.

Before the close of the century when selenography first became possible, Hevel of Dantzic, Scheiner, Langrenus (cosmographer to the King of Spain), Riccioli, the Jesuit astronomer of Bologna, and Dominic Cassini, the celebrated French astronomer, greatly extended the knowledge of the moon's surface, and published drawings of various phases, and charts, which, though very rude and incomplete, were a clear advance upon what Galileo, with his inferior optical means, had been able to accomplish. Langrenus, and after him Hevel, gave distinctive names to the various formations, mainly derived from terrestrial physical features, for which Riccioli subsequently substituted those of philosophers, mathematicians, and other celebrities; and Cassini determined by actual measurement the relative position of many of the principal objects on the disc, thus laying the foundation of an accurate system of lunar topography; while the labours of T. Mayer and Schröter in the last century, and of Lohrmann, Mädler, Neison (Nevill), Schmidt, and other observers in the present, have been mainly devoted to the study of the minuter detail of the moon and its physical characteristics.

As was manifest to the earliest telescopic observers, its visible surface is clearly divisible into strongly contrasted areas, differing both in colour and structural character. Somewhat less than half of what we see of it consists of comparatively level dark

tracts, some of them very many thousands of square miles in extent, the monotony of whose dusky superficies is often unrelieved for great distances by any prominent object; while the remainder, everywhere manifestly brighter, is not only more rugged and uneven, but is covered to a much greater extent with numbers of quasi-circular formations, differing widely in size, classed as walled-plains, ring-plains, craters, craterlets, crater-cones, &c. (the latter bearing a great outward resemblance to some terrestrial volcanoes), and mountain ranges of vast proportions, isolated hills, and other features.

Though nothing resembling sheets of water, either of small or large extent, have ever been detected on the surface, the superficial resemblance, in small telescopes, of the large grey tracts to the appearance which we may suppose our terrestrial lakes and oceans would present to an observer on the moon, naturally induced the early selenographers to term them *Maria*, or “seas”—a convenient name, which is still maintained, without, however, implying that these areas, as we now see them, are, or ever were, covered with water. Some, however, regard them as old sea-beds, from which every trace of fluid, owing to some unknown cause, has vanished, and that the folds and wrinkles, the ridges, swellings, and other peculiarities of structure observed upon them, represent some of the results of alluvial action. It is, of course, possible, and even probable, that at a remote epoch in the evolution of our satellite these lower regions were occupied by water, but that their surface, as it now appears, is actually this old sea-bottom, seems to be less likely than that it represents the consolidated crust of some semi-fluid or viscous material (possibly of a basaltic type) which has welled forth from orifices or rents communicating with the interior, and overspread and partially filled up these immense hollows, more or less overwhelming and destroying many formations which stood upon them before this catastrophe took place. Though this, like many other speculations of a similar character relating to lunar “geology,” must remain, at least for the present, as a mere hypothesis; indications of this partial destruction by some agency or other is almost everywhere apparent in those formations which border the so-called seas, as, for example, *Fracastorius* in the *Mare Nectaris*; *Le Monnier* in the *Mare Tranquillitatis*; *Pitatus* and *Hesiodus*, on the south side of the *Mare Nubium*; *Doppelmayer* in the *Mare Humorum*, and in many other situations; while no observer can fail to notice innumerable instances of more or less complete obliteration

tion and ruin among objects within these areas, in the form of obscure rings (mere scars on the surface), dusky craters, circular arrangements of isolated hills, reminding one of the monoliths of a Druidical temple; all of which we are justified in concluding were at one time formations of a normal type. It has been held by some selenologists—and Schmidt appears to be of the number—that, seeing the comparative scarcity of large ring-plains and other massive formations on the Maria, these grey plains represent, as it were, a picture of the primitive surface of the moon before it was disturbed by the operations of interior forces; but this view affords no explanation of the undoubted existence of the relics of an earlier lunar world beneath their smooth superficies.

MARIA.—Leaving, however, these considerations for a more particular description of the Maria, it is clearly impossible, in referring to their level relatively to the higher and brighter land surface of the moon, to appeal to any hypsometrical standard. All that is known in this respect is, that they are invariably lower than the latter, and that some sink to a greater depth than others, or, in other words, that they do not all form a part of the same sphere. Though they are more or less of a greyish-slaty hue—some of them approximating very closely to that of the pigment known as “Payne’s grey”—the tone, of course, depends upon the angle at which the solar rays impinge on that particular portion of the surface under observation. Speaking generally, they are, as would follow from optical considerations, conspicuously darker when viewed near the terminator, or when the sun is either rising or setting upon them, than under a more vertical angle of illumination. But even when it is possible to compare their colour by eye-estimation under similar solar altitudes, it is found that not only are some of the Maria, as a whole, notably darker than others, but nearly all of them exhibit *local* inequalities of hue, which, under good atmospheric and instrumental conditions, are especially remarkable. Under such circumstances I have frequently seen the surface, in many places covered with minute glittering points of light, shining with a silvery lustre, intermingled with darker spots and a network of streaks far too delicate and ethereal to represent in a drawing. In addition to these contrasts and differences in the sombre tone of these extended plains, many observers have remarked traces of a yellow or green tint on the surface of some of them. For example, the Mare Imbrium and the Mare Frigoris appear under

certain conditions to be of a dirty yellow-green hue, the central parts of the Mare Humorum dusky green, and part of the Mare Serenitatis and the Mare Crisium light green, while the Palus Somnii has been noted a golden-brown yellow. To these may be added the district round Taruntius in the Mare Fœcunditatis, and portions of other regions referred to in the catalogue, where I have remarked a very decided sepia colour under a low sun. It has been attempted to account for these phenomena by supposing the existence of some kind of vegetation; but as this involves the presence of an atmosphere, the idea hardly finds favour at the present time, though perhaps the possibility of plant growth in the low-lying districts, where a gaseous medium may prevail, is not altogether so chimerical a notion as to be unworthy of consideration. Nasmyth and others suggest that these tints may be due to broad expanses of coloured volcanic material, an hypothesis which, if we believe the Maria to be overspread with such matter, and knowing how it varies in colour in terrestrial volcanic regions, is more probable than the first. Anyway, whether we consider these appearances to be objective, or, after all, only due to purely physiological causes, they undoubtedly merit closer study and investigation than they have hitherto received.

There are twenty-three of these dusky areas which have received distinctive names; seventeen of them are wholly, or in great part, confined to the northern, and to the south-eastern quarter of the southern hemisphere—the south-western quadrant being to a great extent devoid of them. By far the largest is the vast Oceanus Procellarum, extending from a high northern latitude to beyond latitude  $10^{\circ}$  in the south-eastern quadrant, and, according to Schmidt, with its bays and inflections, occupying an area of nearly two million square miles, or more than that of all the remaining Maria put together. Next in order of size come the Mare Nubium, of about one-fifth the superficies, covering a large portion of the south-eastern quadrant, and extending considerably north of the equator, and the Mare Imbrium, wholly confined to the north-eastern quadrant, and including an area of about 340,000 square miles. These are by far the largest lunar “seas.” The Mare Fœcunditatis, in the western hemisphere, the greater part of it lying in the south-western quadrant, is scarcely half so big as the Mare Imbrium; while the Maria Serenitatis and Tranquilitatis, about equal in area (the former situated wholly north of the equator, and the latter only partially extending south of it), are still smaller. The arctic Mare Frigoris, some 100,000 square miles in

extent, is the only remaining large sea,—the rest, such as the Mare Vaporum, the Sinus Medii, the Mare Crisium, the Mare Humorum, and the Mare Humboldtianum, are of comparatively small dimensions, the Mare Crisium not greatly exceeding 70,000 square miles, the Mare Humorum (about the size of England) 50,000 square miles, while the Mare Humboldtianum, according to Schmidt, includes only about 42,000 square miles, an area which is approached by some formations not classed with the Maria. This distinction, speaking generally, prevails among the Maria,—those of larger size, such as the Oceanus Procellarum, the Mare Nubium, and the Mare Foecunditatis, are less definitely enclosed, and, like terrestrial oceans, communicate with one another; while their borders, or, if the term may be allowed, their coast-line, is often comparatively low and ill-defined, exhibiting many inlets and irregularities in outline. Others, again, of considerable area, as, for example, the Mare Serenitatis and the Mare Imbrium, are bounded more or less completely by curved borders, consisting of towering mountain ranges, descending with a very steep escarpment to their surface: thus in form and other characteristics they resemble immense wall-surrounded plains. Among the best examples of enclosed Maria is the Mare Crisium, which is considered by Neison to be the deepest of all, and the Mare Humboldtianum.

Though these great plains are described as level, this term must only be taken in a comparative sense. No one who observes them when their surface is thrown into relief by the oblique rays of the rising or setting sun can fail to remark many low bubble-shaped swellings with gently rounded outlines, shallow trough-like hollows, and, in the majority of them, long sinuous ridges, either running concentrically with their borders or traversing them from side to side. Though none of these features are of any great altitude or depth, some of the ridges are as much as 700 feet in height, and probably in many instances the other elevations often rise to 150 feet or more above the low-lying parts of the plains on which they stand. Hence we may say that the Maria are only level in the sense that many districts in the English Midland counties are level, and not that their surface is absolutely flat. The same may be said as to their apparent smoothness, which, as is evident when they are viewed close to the terminator, is an expression needing qualification, for under these conditions they often appear to be covered with wrinkles, flexures, and little asperities, which, to be visible at all, must be of considerable size. In fact,

were it possible to examine them from a distance of a few miles, instead of from a standpoint which, under the most favourable circumstances, cannot be reckoned at less than 300, and this through an interposed aerial medium always more or less perturbed, they would probably be described as rugged and uneven, as some modern lava sheets.

RIDGES.—Among the Maria which exhibit the most remarkable arrangement of ridges is the Mare Humorum, in the south-eastern quadrant. Here, if it be observed under a rising sun, a number of these objects will be seen extending from the region north of the ring-mountain Vitello in long undulating lines, roughly concentric with the western border of the “sea,” and gradually diminishing in altitude as they spread out, with many ramifications, to a distance of 200 miles or more towards the north. At this stage of illumination they are strikingly beautiful in a good telescope, reminding one of the ripple-marks left by the tide on a soft sandy beach. Like most other objects of their class, they are very evanescent, gradually disappearing as the sun rises higher in the lunar firmament, and ultimately leaving nothing to indicate their presence beyond here and there a ghostly streak or vein of a somewhat lighter hue than that of the neighbouring surface. The Mare Nectaris, again, in the south-western quadrant, presents some fine examples of concentric ridges, which are seen to the best advantage when the morning sun is rising on Rosse, a prominent crater north of Fracastorius. This “sea” is evidently concave in cross-section, the central portion being considerably lower than the margin, and these ridges appear to mark the successive stages of the change of level from the coast-line to the centre. They suggest the “caving in” of the surface, similar to that observed on a frozen pond or river, where the “cat’s ice” at the edge, through the sinking of the water beneath, is rent and tilted to a greater or less degree. The Mare Serenitatis and the Mare Imbrium, in the northern hemisphere, are also remarkable for the number of these peculiar features. They are very plentifully distributed round the margin and in other parts of the former, which includes besides one of the longest and loftiest on the moon’s visible surface—the great serpentine ridge, first drawn and described nearly a hundred years ago by the famous selenographer, Schröter of Lilienthal. Originating at a little crater under the north-east wall of great ring-plain Posidonius, it follows a winding course across the Mare toward the south, throwing out many minor branches, and ultimately dies out under a great rocky promontory

—the Promontory Acherusia, at the western termination of the Hæmus range. A comparatively low power serves to show the curious structural character of this immense ridge, which appears to consist of a number of corrugations and folds massed together, rising in places, according to Neison, to a height of 700 feet and more. The Mare Imbrium also affords an example of a ridge, which, though shorter, is nearly as prominent, in that which runs from the bright little ring-plain Piazzzi Smyth towards the west side of Plato. The region round Timocharis and other quarters of the Mare are likewise traversed by very noteworthy features of a similar class. The Oceanus Procellarum also presents good instances of ridges in the marvellous ramifications round Encke, Kepler, and Marius, and in the region north of Aristarchus and Herodotus. Perhaps the most perfect examples of surface swellings are those in the Mare Tranquilitatis, a little east of the ring-plain Arago, where there are two nearly equal circular mounds, at least ten miles in diameter, resembling tumuli seen from above. Similar, but more irregular, objects of a like kind are very plentiful in many other quarters.

It is a suggestive peculiarity of many of the lunar ridges, both on the Maria and elsewhere, that they are very generally found in association with craters of every size. Illustrations of this fact occur almost everywhere. Frequently small craters are found on the summits of these elevations, but more often on their flanks and near their base. Where a ridge suddenly changes its direction, a crater of some prominence generally marks the point, often forming a node, or crossing-place of other ridges, which thus appear to radiate from it as a centre. Sometimes they intrude within the smaller ring-mountains, passing through gaps in their walls, as, for example, in the cases of Mädler, Lassell, &c. Various hypotheses have been advanced to account for them. The late Professor Phillips, the geologist, who devoted much attention to the telescopic examination of the physical features of the moon, compared the lunar ridges to long, low, undulating mounds, of somewhat doubtful origin, called "kames" in Scotland, and "eskers" in Ireland, where on the low central plain they are commonly found in the form of extended banks (mainly of gravel), with more or less steep sides, rising to heights of from 20 to 70 feet. They are sometimes only a few yards wide at the top, while in other places they spread out into large humps, having circular or oval cavities on their summits, 50 or 60 yards across, and as much as 40 feet deep. Like the lunar ridges, they

throw out branches and exhibit many breaches of continuity. By some geologists they are supposed to represent old submarine banks formed by tidal currents, like harbour bars, and by others to be glacial deposits; in either case, to be either directly or indirectly due to alluvial action. Their outward resemblance to some of the ridges on the moon is unquestionable; and if we could believe that the Maria, as we now see them, are dried-up sea-beds, it might be concluded that these ridges had a similar origin; but their close connection with centres of volcanic disturbance, and the numbers of little craters on or near their track, point to the supposition that they consist rather of material exuded from long-extending fissures in the crust of the "seas," and in other surfaces where they are superimposed. This conjecture is rendered still more probable by the fact that we sometimes find the direction of clefts (which are undoubted surface cracks) prolonged in the form of long narrow ridges or of rows of little hillocks. We are, however, not bound to assume that all the manifold corrugations observed on the lunar plains are due to one and the same cause; indeed, it is clear that some are merely the outward indications of sudden drops in the surface, as in the case of the ridges round the western margin of the Mare Nectaris, and in other situations, where subsidence is manifested by features assuming the outward aspect of ordinary ridges, but which are in reality of a very different structural character.

The Maria, like almost every other part of the visible surface, abound in craters of a minute type, which are scattered here and there without any apparent law or ascertained principle of arrangement. Seeing how imperfect is our acquaintance with even the larger objects of this class, it is rash to insist on the antiquity or permanence of such diminutive objects, or to dogmatise about the cessation of lunar activity in connection with features where the volcanic history of our globe, if it is of any value as an analogue, teaches us it is most likely to prevail.

Most observers will agree with Schmidt, that observations and drawings of objects on the sombre depressed plains of the moon are easier and pleasanter to make than on the dazzling highlands, and that the lunar "sea" is to the working selenographer like an oasis in the desert to the traveller—a relief in this case, however, not to an exhausted body, but to a weary eye.

RING-MOUNTAINS, CRATERS, &c.—It is these objects, in their almost endless variety and bewildering number, which, more than any others, give to our satellite that marvellous appearance in the



telescope which since the days of Galileo has never failed to evoke the astonishment of the beholder. However familiar we may be with the lunar surface, we can never gaze on these extraordinary formations, whether massed together apparently in inextricable confusion, or standing in isolated grandeur, like Copernicus, on the grey surface of the plains, without experiencing, in a scarcely diminished degree, the same sensation of wonder and admiration with which they were beheld for the first time. Although the attempt to bring all these *bizarre* forms under a rigid scheme of classification has not been wholly successful, their structural peculiarities, the hypsometrical relation between their interior and the surrounding district, their size, and the character of their circumvallation, the dimensions of their cavernous opening as compared with that of the more or less truncated conical mass of matter surrounding it, all afford a basis for grouping them under distinctive titles, that are not only convenient to the selenographer, but which undoubtedly represent, as a rule, actual diversities in their origin and physical character.

These distinguishing titles, as adopted by Schröter, Lohrmann, and Mädler, and accepted by subsequent observers, are WALLED-PLAINS, MOUNTAIN RINGS, RING-PLAINS, CRATERS, CRATER-CONES, CRATERLETS, CRATER-PITS, DEPRESSIONS.

WALLED-PLAINS.—These formations, approximating more or less to the circular form, though frequently deviating considerably from it, are among the largest enclosures on the moon. They vary from upwards of 150 to 60 miles or under in diameter, and are often encircled by a complex rampart of considerable breadth, rising in some instances to a height of 12,000 feet or more above the enclosed plain. This rampart is rarely continuous, but is generally interrupted by gaps, crossed by transverse valleys and passes, and broken by more recent craters and depressions. As a rule, the area within the circumvallation (usually termed “the floor”) is only slightly, if at all, lower than the region outside: it is very generally of a dusky hue, similar to that of the grey plains or Maria, and, like them, is usually variegated by the presence of hills, ridges, and craters, and is sometimes traversed by delicate furrows, termed clefts or rills.

*Ptolemæus*, in the third quadrant, and not far removed from the centre of the disc, may be taken as a typical example of the class. Here we have a vast plain, 115 miles from side to side, encircled by a massive but much broken wall, which at one peak towers more than 9000 feet above a level floor, which includes details of

a very remarkable character. The adjoining *Alphonsus* is another, but somewhat smaller, object of the same type, as are also *Albategnius*, and *Arzachel*; and *Plato*, in a high northern latitude, with its noble many-peaked rampart and its variable steel-grey interior. *Grimaldi*, near the eastern limb (perhaps the darkest area on the moon), *Schickard*, nearly as big, on the south-eastern limb, and *Bavilly*, larger than either (still farther south in the same quadrant), although they approach some of the smaller "seas" in size, are placed in the same category. The conspicuous central mountain, so frequently associated with other types of ringed enclosures, is by no means invariably found within the walled-plains; though, as in the case of *Petavius*, *Langrenus*, *Gassendi*, and several other noteworthy examples, it is very prominently displayed. The progress of sunrise on all these objects affords a magnificent spectacle. Very often when the rays impinge on their apparently level floor at an angle of from  $1^{\circ}$  to  $2^{\circ}$ , it is seen to be coarse, rough grained, and covered with minute elevations, although an hour or so afterwards it appears as smooth as glass.

Although it is a distinguishing characteristic that there is no great difference in level between the outside and the inside of a walled-plain, there are some very interesting exceptions to this rule, which are termed by Schmidt "Transitional forms." Among these he places some of the most colossal formations, such as *Clavius*, *Maurolycus*, *Stöfler*, *Janssen*, and *Longomontanus*. The first, which may be taken as representative of the class (well known to observers as one of the grandest of lunar objects), has a deeply sunken floor, fringed with mountains rising some 12,000 feet above it, though they scarcely stand a fourth of this height above the plain on the west, which ascends with a very gentle gradient to the summit of the wall. Hence the contrast between the shadows of the peaks of the western wall on the floor at sunrise, and of the same peaks on the region west of the border at sunset is very marked. In *Gassendi*, *Phocylides*, and *Wargentin* we have similar notable departures from the normal type. The floor of the former on the north stands 2000 feet above the Mare Humorum. In *Phocylides*, probably through "faulting," one portion of the interior suddenly sinks to a considerable depth below the remainder; while the very abnormal *Wargentin* has such an elevated floor, that, when viewed under favourable conditions, it reminds one of a shallow oval tray or dish filled with fluid to the point of overflowing. These examples, very far from being exhaustive, will be sufficient to show that the walled-plains exhibit

noteworthy differences in other respects than size, height of rampart, or included detail. Still another peculiarity, confined, it is believed, to a very few, may be mentioned, viz., convexity of floor, prominently displayed in Petavius, Mersenius, and Hevel.

**MOUNTAIN RINGS.**—These objects, usually encircled by a low and broken border, seldom more than a few hundred feet in height, are closely allied to the walled-plains. They are more frequently found on the Maria than elsewhere. In some cases the ring consists of isolated dark sections, with here and there a bright mass of rock interposed; in others, of low curvilinear ridges, forming a more or less complete circumvallation. They vary in size from 60 or 70 miles to 15 miles and less. The great ring north of Flamsteed, 60 miles across, is a notable example; another lies west of it on the north of Wichmann; while a third will be found south-east of Encke;—indeed, the Mare Procellarum abounds in objects of this type. The curious formation on the Mare Imbrium immediately south of Plato (called “Newton” by Schröter), may be placed in this category, as may also many of the low dusky rings of much smaller dimensions found in many quarters of the Maria. As has been stated elsewhere, these features have the appearance of having once been formations of a much more prominent and important character, which have suffered destruction, more or less complete, through being partially overwhelmed by the material of the “seas.”

**RING-PLAINS.**—These are by far the most numerous of the ramparted enclosures of the moon, and though it is occasionally difficult to decide in which class, walled-plain or ring-plain, some objects should be placed, yet, as a rule, the difference between the structural character of the two is abundantly obvious. The ring-plains vary in diameter from sixty to less than ten miles, and are far more regular in outline than the walled-plains. Their ramparts, often very massive, are more continuous, and fall with a steep declivity to a floor almost always greatly depressed below the outside region. The inner slopes generally display subordinate heights, called terraces, arranged more or less concentrically, and often extending in successive stages nearly down to the interior foot of the wall. With the intervening valleys, these features are very striking objects when viewed under good conditions with high powers. In some cases they may possibly represent the effects of the slipping of the upper portions of the wall, from a want of cohesiveness in the material of which it is composed; but this hardly explains why the highest terrace often

stands nearly as high as the rampart. Nasmyth, in his eruption hypothesis, suggests that in such a case there may have been two eruptions from the same vent; one powerful, which formed the exterior circle, and a second, rather less powerful, which has formed the interior circle. Ultimately, however, coming to the conclusion that terraces, as a rule, are not due to any such freaks of the eruption, he ascribes them to landslips. In any case, we can hardly imagine that material standing at such a high angle of inclination as that forming the summit ridge of many of the ring-plains would not frequently slide down in great masses, and thus form irregular plateaus on the lower and flatter portions of the slope; but this fails to explain the symmetrical arrangement of the concentric terraces and intermediate valleys. The inner declivity of the north-eastern wall of Plato exhibits what to all appearance is an undoubted landslip, as does also that of Hercules on the northern side, and numerous other cases might be adduced; but in all of them the appearance is very different from that of the true terrace.

The *glacis*, or outer slope of a ring-plain, is invariably of a much gentler inclination than that which characterises the inner declivity: while the latter very frequently descends at an angle varying from  $60^{\circ}$  to  $50^{\circ}$  at the crest of the wall, to from  $10^{\circ}$  to  $2^{\circ}$  at the bottom, where it meets the floor; the former extends for a great distance at a very flat gradient before it sinks to the general level of the surrounding country. It differs likewise from the inner descent, in the fact that, though often traversed by valleys, intersected by deep gullies and irregular depressions, and covered with humpy excrescences and craters, it is only rarely that any features comparable to the terraces, usually present on the inner escarpment, can be traced upon it.

Elongated depressions of irregular outline, and very variable in size and depth, are frequently found on the outer slopes of the border. Some of them consist of great elliptical or sub-circular cavities, displaying many expansions and contractions, called "pockets," and suggesting the idea that they were originally distinct cup-shaped hollows, which from some cause or other have coalesced like rows of inosculating craters. While many of these features are so deep that they remain visible for a considerable time under a low sun, others, though perhaps of greater extent, vanish in an hour or so.

As in the case of the walled-plains, the ramparts of the ring-plains exhibit gaps and are broken by craters and depressions,

but to a much less extent. Often the lofty crest, surmounted by *aiguilles* or by blunter peaks, towering in some cases to nearly double its altitude above the interior, is perfectly continuous (like Copernicus), or only interrupted by narrow passes. It is a suggestive circumstance that gaps, other than valleys, are almost invariably found either in the north or south walls, or in both, and seldom in other positions. The buttress, or long-extending spur, is a feature frequently associated with the ring-plain rampart, as are also numbers of what, for the lack of a better name, must be termed little hillocks, which generally radiate in long rows from the outer foot of the slope. The spurs usually abut on the wall, and, either spreading out like the sticks of a fan or running roughly parallel to each other, extend for long distances, gradually diminishing in height and width till they die out on the surrounding surface. They have been compared to lava streams, which those round Aristillus, Aristoteles, and on the flank of Clavius *a*, certainly somewhat resemble, though, in the two former instances, they are rather comparable to immense ridges. In addition to the above, the spurs radiating from the south-eastern rampart of Condamine and the long undulating ridges and rows of hillocks running from Cyrillus over the eastern glaciis of Theophilus, may be named as very interesting examples.

Nelson and some other selenographers place in a distinct class certain of the smaller ring-plains which usually have a steeper outer slope, and are supposed to present clearer indications of a volcanic origin than the ring-plains, terming them "Crater-plains."

CRATERS.—Under this generic name is placed a vast number of formations exhibiting a great difference in size and outward characteristics, though generally (under moderate magnification) of a circular or sub-circular shape. Their diameter varies from 15 miles or more to 3, and even less, and their flanks rise much more steeply to the summit, which is seldom very lofty, than those of the ring-plains, and fall more gradually to the floor. There is no portion of the moon in which they do not abound, whether it be on the ramparts, floors, and outer slopes of walled and ring plains, the summits and escarpments of mountain ranges, amid the intricacies of the highlands, or on the grey surface of the Maria. In many instances they have a brighter and newer aspect than the larger formations, often being the most brilliant points on their walls, when they are found in this position. Very

frequently too they are not only very bright themselves, but stand on bright areas, whose borders are generally concentric with them, which shine with a glistening lustre, and form a kind of halo of light around them. Euclides and Bessarion A, and the craters east of Landsberg, are especially interesting examples. It seems not improbable that these areas may represent deposits formed by some kind of matter ejected from the craters, but whether of ancient or modern date, it is, of course, impossible to determine. Future observers will perhaps be in a better position to decide the question without cavil, if such eruptions should again take place. Like the larger enclosures, these smaller objects frequently encroach upon each other—crater-ring overlapping crater-ring, as in the case of Thebit, where a large crater, which has interfered with the continuity of the east wall, has, in its turn, been disturbed by a smaller crater on its own east wall. The craters in many cases, possibly in the majority if we could detect them, have central mountains, some of them being excellent tests for telescopic definition—as, for example, the central peaks of Hortensius, Bessarion, and that of the small crater just mentioned on the east wall of Thebit A. A tendency to a linear arrangement is often displayed, especially among the smaller class, as is also their occurrence in pairs.

CRATER-CONES.—These objects, plentifully distributed on the lunar surface, are especially interesting from their outward resemblance to the parasitic cones found on the flanks of terrestrial volcanoes (Etna, for instance). In the larger examples it is occasionally possible to see that the interiors are either inverted cones without a floor, or cup-shaped depressions on the summit of the object. Frequently, however, they are so small that the orifice can only be detected under oblique illumination. Under a high sun they generally appear as white spots, more or less ill-defined, as on the floors of Archimedes, Fracastorius, Plato, and many other formations, which include a great number, all of which are probably crater cones, although only a few have been seen as such. It is a significant fact that in these situations they are always found to be closely associated with the light streaks which traverse the interior of the formations, standing either on their surface or close to their edges. The instrumental and meteorological requirements necessary for a successful scrutiny of the smallest type of these features, are beyond the reach of the ordinary observer in this country, as they demand direct observation in large telescopes under the best atmospheric conditions.

Some years ago Dr. Klein of Cologne called attention to some very interesting types of crater-cones, which may be found on certain dark or smoky-grey areas on the moon. These, he considers, may probably represent active volcanic vents, and urges that they should be diligently examined and watched by observers who possess telescopes adequate to the task. The most noteworthy examples of these objects are in the following positions:—(1) West of a prominent ridge running from Beaumont to the west side of Theophilus, and about midway between these formations; (2) in the Mare Vaporum, south of Hyginus; (3) on the floor of Werner, near the foot of the north wall; (4) under the east wall of Alphonsus, on the dusky patch in the interior; (5) on the south side of the floor of Atlas. I have frequently described elsewhere with considerable detail the telescopic appearance of these features under various phases, and have pointed out that though large apertures and high powers are needed to see these cones to advantage, the dusky areas, easily traced on photograms, might be usefully studied by observers with smaller instruments, as if they represent the *ejecta* from the crater-cones which stand upon them, changes in their form and extent could very possibly be detected. In addition to those already referred to, a number of mysterious dark spots were discovered by Schmidt in the dusky region about midway between Copernicus and Gambart, which Klein describes as perforated like a sieve with minute craters. A short distance south-west of Copernicus stands a bright crater-cone surrounded by a grey nimbus, which may be classed with these objects. It is well seen under a high light, as indeed is the case with most of these features.

CRATERLETS, CRATER-PITS.—To a great extent the former term is needless and misleading, as the so-called craters merge by imperceptible gradations into very minute objects, as small as half a mile in diameter, and most probably, if we could more accurately estimate their size, still less. The crater-pit, however, has well-marked peculiarities which distinguish it from all other types, such as the absence of a distinguishable rim and extreme shallowness. They appear to be most numerous on the high-level plains and plateaus in the south-western quadrant, and may be counted by hundreds under good atmospheric conditions on the outer slopes of Walter, Clavius, and other large enclosures. In these positions they are often so closely aggregated that, as Nasmyth remarks, they remind one of an accumulation of froth. Even in an 8½-inch reflector I have frequently seen the outer

slope of the large ring-plain on the north-western side of Vendelinus, so perforated with these objects that it resembled pumice or vesicular lava, many of the little holes being evidently not circular, but square shaped and very irregular. The interior of Stadius and the region outside abounds in these minute features, but the well-known crater-row between this formation and Copernicus seems rather to consist of a number of inosculating crater-cones, as they stand very evidently on a raised bank of some altitude.

MOUNTAIN RANGES, ISOLATED MOUNTAINS, &c.—The more massive and extended mountain ranges of the moon are found in the northern hemisphere, and (what is significant) in that portion of it which exhibits few indications of other superficial disturbances. The most prominently developed systems, the *Alps*, the *Caucasus*, and the *Apennines*, forming a mighty western rampart to the Mare Imbrium and giving it all the appearance of a vast walled plain, present few points of resemblance to any terrestrial chain. The former include many hundred peaks, among which, Mont Blanc rises to a height of 12,000 feet, and a second, some distance west of Plato, to nearly as great an altitude; while others, ranging from 5000 to 8000 feet, are common. They extend in a south-west direction from Plato to the Caucasus, terminating somewhat abruptly, a little west of the central meridian, in about N. lat.  $42^{\circ}$ . One of the most interesting features associated with this range is the so-called great Alpine valley, which cuts through it west of Plato. The *Caucasus* consist of a massive wedge-shaped mountain land, projecting southwards, and partially dividing the Mare Imbrium from the Mare Serenitatis, both of which they flank. Though without peaks so lofty as those pertaining to the Alps, there is one, immediately east of the ring-plain Calippus, which, towering to 19,000 feet, surpasses any of which the latter system can boast. The *Apennines*, however, are by far the most magnificent range on the visible surface, including as they do some 3000 peaks, and extending in an almost continuous curve of more than 400 miles in length from Mount Hadley, on the north, to the fine ring-plain Eratosthenes, which forms a fitting termination, on the south. The great headland Mount Hadley rises more than 15,000 feet, while a neighbouring promontory on the south-east of it is fully 14,000 feet, and another, close by, is still higher above the Mare. Mount Huygens, again, in N. lat.  $20^{\circ}$ , and the square-shaped mass Mount Wolf, near the southern end of the chain, include peaks standing 18,000 and 12,000 feet respectively above the plain, to which their flanks descend with a steep declivity. The counterscarp of the



Apennines, in places 160 miles in width from east to west, runs down to the Mare Vaporum with a comparatively gentle inclination. It is everywhere traversed by winding valleys of a very intricate type, all trending towards the south-west, and includes some bright craters and mountain-rings. The *Carpathians*, forming in part the southern border of the Mare Imbrium, extend for a length of more than 180 miles eastward of E., long.  $16^{\circ}$ , and, embracing the ring-plain Gay-Lussac, terminate west of Mayer. They present a less definite front to the Mare than the Apennines, and are broken up and divided by irregular valleys and gaps; their loftiest peak, situated on a very projecting promontory north-west of Mayer, rising to a height of 7000 feet. Notwithstanding their comparatively low altitude, the region they occupy forms a fine telescopic picture at lunar sunrise. The *Sinus Iridum highlands*, bordering the beautiful bay on the north-east side of the Mare Imbrium, rank among the loftiest and most intricate systems on the moon, and, like the Apennines, present a steep face to the grey plain from which they rise, though differing from them in other respects. They include many high peaks, the loftiest, in the neighbourhood of the ring-plain Sharp, rising 15,000 feet. There are probably some still higher mountains in the vicinity, but the difficulties attending their measurement render it impossible to determine their altitude with any approach to accuracy.

The *Taurus Mountains* extend from the west side of the Mare Serenitatis, near Le Monnier and Littrow, in a north-westerly direction towards Geminus and Berselius, bordering the west side of the Lacus Somniorum. They are a far less remarkable system than any of the preceding, and consist rather of a wild irregular mountain region than a range. In the neighbourhood of Berselius are some peaks which, according to Neison, cannot be less than 10,000 feet in height.

On the north side of the Mare Imbrium, east of Plato, there is a beautiful narrow range of bright outlying heights, called the *Teneriffe Mountains*, which include many isolated objects of considerable altitude, one of the loftiest rising about 8000 feet. Farther towards the east lies another group of a very similar character, called the *Straight Range*, from its linear regularity. It extends from west to east for a distance of about 60 miles, being a few miles shorter than the last, and includes a peak of 6000 feet.

The *Harbinger Mountains*.—A remarkable group, north-west of Aristarchus, including some peaks as high as 7000 feet, and other details noticed in the catalogue.

The above comprise all the mountain ranges in the northern hemisphere of any prominence, or which have received distinctive names, except the *Hercynian Mountains*, on the north-east limb, east of the walled plain Otto Struve. These are too near the edge to be well observed, but, from what can be seen of them, they appear to abound in lofty peaks, and to bear more resemblance to a terrestrial chain than any which have yet been referred to.

The mountain systems of the southern hemisphere, except the ranges visible on the limb, are far less imposing and remarkable than those just described. The *Pyrenees*, on the western side of the Mare Nectaris, extend in a meridional direction for nearly 190 miles, and include a peak east of Guttemberg of nearly 12,000 feet, and are traversed in many places by fine valleys.

The *Alti Mountains* form a magnificent chain, 275 miles in length, commencing on the outer eastern slope of Piccolomini, and following a tolerably direct north-east course, with a few minor bendings, to the west side of Fermat, where they turn more towards the north, ultimately terminating about midway between Tacitus and Catherina. The region situated on the south-east is a great table-land, without any prominent features, rising gently towards the mountains, which shelve steeply down to an equally barren expanse on the north-west, to which they present a lofty face, having an average altitude of about 6000 feet. The loftiest peak, over 13,000 feet, rises west of Fermat.

The *Riphaean Mountains*, a remarkably bright group, occupying an isolated position in the Mare Procellarum south of Landsberg, and extending for more than 100 miles in a meridional direction. They are most closely aggregated at a point nearly due west of Euclides, from which they throw off long-branching arms to the north and south, those on the north bifurcating and gradually sinking to the level of the plain. The loftiest peaks are near the extremity of this section, one of them rising to 3000 feet. Two bright craters are associated with these mountains, one nearly central, and the other south of it.

The *Percy Mountains*.—This name is given to the bright highlands extending east of Gassendi towards Mersenius, forming the north-eastern border of the Mare Humorum. They abound in minute detail—bright little mountains and ridges—and include some clefts pertaining to the Mersenius rill-system; but their most noteworthy feature is the long bright mountain-arm, branching out from the eastern wall of Gassendi, and extending for more than 50 miles towards the south-east.

The principal ranges on the limb are the *Leibnitz Mountains*, extending from S. lat.  $70^\circ$  on the west to S. lat.  $80^\circ$  on the east limb. They include some giant peaks and plateaus, noteworthy objects in profile, some of which, according to Schröter and Mädler, rise to 26,000 feet. The *Dörfel Mountains*, between S. lat.  $80^\circ$  and  $57^\circ$  on the eastern limb, include, if Schröter's estimate is correct, three peaks which exceed 26,000 feet. On the eastern limb, between S. lat.  $35^\circ$  and  $18^\circ$ , extend the *Rook Mountains*, which have peaks, according to Schröter, as high as 25,000 feet. Next in order come the *Cordilleras*, which extend to S. lat.  $8^\circ$ , and the *D'Alembert Mountains*, lying east of Rocca and Grimaldi, closely associated with them, and probably part of the same system. Some of the peaks approach 20,000 feet. In addition to these mountain ranges there are others less prominent on the limb in the northern hemisphere, which have not been named.

ISOLATED MOUNTAINS are very numerous in different parts of the moon, the most remarkable are referred to in the appendix. Many remain unnamed.

CLEFTS OR RILLS.—Though Fontenelle, in his *Entretiens sur la Pluralité des Mondes*, informs his pupil, the Marchioness, that “M. Cassini discovered in the moon something which separates, then reunites, and finally loses itself in a cavity, which from its appearance seemed to be a river,” it can hardly be supposed that what the French astronomer saw, or fancied he saw, with the imperfect telescopes of that day, was one of the remarkable and enigmatical furrows termed clefts or rills, first detected by the Hanoverian selenographer Schröter; who, on October 7, 1787, discovered the very curious serpentine cleft near Herodotus, having a few nights before noted for the first time the great Alpine valley west of Plato, once classed with the clefts, though it is an object of a very different kind. Between 1787 and 1797 Schröter found ten rills; but twenty years elapsed before an addition was made to this number by the discoveries of Gruithuisen, and, a short time after, by those of Lohrmann, who in twelve months (1823–24) detected seventy. Kinau, Mädler, and finally Schmidt, followed, till, in 1866, when the latter published his work, *Ueber Rillen auf dem Monde*, the list was thus summarised:—

In the 1st or N.W. quadrant	127	rills
„ 2nd „ N.E.	75	„
„ 3rd „ S.E.	141	„
„ 4th „ S.W.	82	„

or 425 in all. Since the date of this book the number of known rills has been more than doubled; in fact, scarcely a lunation passes without new discoveries being made.

The significance of the word *rille* in German, a groove or furrow, describes with considerable accuracy the usual appearance of the objects to which it is applied, consisting as they do of long narrow channels, with sides more or less steep, and sometimes vertical. They often extend for hundreds of miles in approximately straight lines over portions of the moon's surface, frequently traversing in their course ridges, craters, and even more formidable obstacles, without any apparent check or interruption, though their ends are sometimes marked by a mound or crater. Their length ranges from ten or twelve to three hundred miles or more (as in the great Sirsalis rill), their breadth, which is very variable within certain limits, from less than half a mile to more than two, and their depth (which must necessarily remain to a great extent problematical) from 100 to 400 yards. They exhibit in the telescope a gradation from somewhat coarse grooves, easily visible at suitable times in very moderately sized instruments, to striæ so delicate as to require the largest and most perfect optical means and the best atmospheric conditions to be glimpsed at all. Viewed under moderate amplification, the majority of rills resemble deep canal-like channels with roughly parallel sides, displaying occasionally local irregularities, and fining off to invisibility at one or both ends. But, if critically scrutinised in the best observing weather with high powers, the apparent evenness of their edges entirely disappears, and we find that the latter exhibit indentations, projections, and little flexures, like the banks of an ordinary stream or rivulet, or, to use a very homely simile, the serrated edges and little jagged irregularities of a biscuit broken across. In some cases we remark crateriform hollows or sudden expansions in their course, and deep sinuous ravines, which render them still more unsymmetrical and variable in breadth. With regard to their distribution on the lunar surface; they are found in almost every region, but perhaps not so frequently on the surface of the Maria as elsewhere, though, as in the case of the Triesnecker and other systems, they often abound in the neighbourhood of disturbed regions in these plains, and in many cases along their margins, as, for example, the Gassendi-Mersenius and the Sabine-Ritter groups. The interior of walled plains are frequently intersected by them, as in Gassendi, where nearly forty, more or less delicate examples, have been seen;

in Hevel, where there is a very interesting system of crossed clefts, and within Posidonius. If we study any good modern lunar map, it is evident how constantly they appear near the borders of mountain ranges, walled-plains, and ring-plains; as, for instance, at the foot of the Apennines; near Archimedes, Aristarchus, Ramsden, and in many other similar positions. Rugged highlands also are often traversed by them, as in the case of those lying west of Le Monnier and Chacornac, and in the region west of the Mare Humorum. It may be here remarked, however, as a notable fact, that the neighbourhood of the grandest ring-mountain on the moon, Copernicus, is, strange to say, devoid of any features which can be classed as true clefts, though it abounds in crater-rows. The intricate network of rills on the west of Triesnecker, when observed with a low power, reminds one of the wrinkles on the rind of an orange or on the skin of a withered apple. Gruithuisen, describing the rill-traversed region between Agrippa and Hyginus, says that "it has quite the look of a Dutch canal map." In the subjoined catalogue many detailed examples will be given relating to the course of these mysterious furrows; how they occasionally traverse mountain arms, cut through, either completely or partially (as in Ramsden), the borders of ring-plains and other enclosures, while not unfrequently a small mound or similar feature appears to have caused them to swerve suddenly from their path, as in the case of the Ariadæus cleft, and in that of one member of the Mercator-Campanus system.

Of the actual nature of the lunar rills we are, it must be confessed, supremely ignorant. With some of the early observers it was a very favourite notion that they are artificial works, constructed presumably by Kepler's *sub-volvani*, or by other intelligences. There is perhaps some excuse to be made for the freaks of an exuberant fancy in regard to objects which, if we ignore for a moment their enormous dimensions, judged by a terrestrial standard, certainly have, in their apparent absence of any physical relation to neighbouring objects, all the appearance of being works of art rather than of nature. The keen-sighted and very imaginative Gruithuisen believed that in some instances they represent roads cut through interminable forests, and in others the dried-up beds of once-mighty rivers. His description of the Triesnecker rill-system reads like a page from a geographical primer. A portion of it is compared to the river Po, and he traces its course mile by mile up to the "delta" at its place of disembogement into the Mare Vaporum. From the position of

some rills with respect to the contour of the surrounding country, it is evident that if water were now present on the moon, they, being situated at the lowest level, would form natural channels for its reception ; but the exceptions to this arrangement are so numerous and obvious, that the idea may be at once dismissed that there is any analogy between them and our rivers. The eminent selenographer, the late W. R. Birt, compared many of them to "inverted river-beds," from the fact that, as often as not, they become broader and deeper as they attain a higher level. The branches resemble rivers more frequently than the main channels ; for they generally commence as very fine grooves, and, becoming broader and broader, join them at an acute angle. An attempt again has been made to compare the lunar clefts with those vast gorges, the marvellous results of aqueous action, called cañons, which attain their greatest dimensions in North America ; such as the Great Cañon of the Colorado, which is at least 300 miles in length, and in places 2000 yards in depth, with perpendicular or even overhanging sides ; but the analogy, at first sight specious, utterly breaks down under closer examination. Some selenographers consider them to consist of long-extending rows of confluent craters, too minute to be separately distinguished, and to be thus due to some kind of volcanic action. This is undoubtedly true in many instances, for almost every lunar region affords examples of crater-rows merging by almost imperceptible gradations into cleft-like features, and crater-rows of considerable size resemble clefts under low powers. Still it seems probable that the greater number of these features are immense furrows or cracks in the surface and nothing more ; for the higher the magnifying power employed in their examination, the less reason there is to object to this description. Dr. Klein of Cologne believes that rills of this class are due to the shrinkage of parts of the moon's crust, and that they are not as a rule the result of volcanic causes, though he admits that there may be some which have a seismic origin. No good reason has as yet been given for the fact that they so frequently cross small craters and other objects in their course, though it has been suggested that the route followed by a rill from crater to crater in these instances may be a line of least surface resistance, an explanation far from being satisfactory.

Whether variations in the visibility of lunar details, when observed under apparently similar conditions, actually occur from time to time from some unknown cause, is one of those vexed

questions which will only be determined when the moon is systematically studied by experienced observers using the finest instruments at exceptionally good stations; but no one who examines existing records of observations of rills by Gruithuisen, Lohrmann, Mädler, Schmidt, and other observers, can well avoid the conclusion that the anomalies brought to light therein point strongly to the probability of the existence of some agency which occasionally modifies their appearance or entirely conceals them from view.

The following is one illustration out of many which might be quoted. At a point in its course, nearly due north of the ring-plain Agrippa, the great Ariadæus cleft sends out a branch which runs into the well-known Hyginus cleft, reminding one, as Dr. Klein remarks, of two rivers connected in the shortest way by a canal. This uniting furrow was detected by Gruithuisen, who observed it several times. On some occasions it appeared perfectly straight, at others very irregular; but, what is very remarkable, although two such accurate observers as Lohrmann and Mädler frequently scrutinised the region, neither of them saw a trace of this object; and but for its rediscovery by Schmidt in 1862, its existence would certainly have been ignored by selenographers as a mere figment of Gruithuisen's too lively imagination. Dr. Klein has frequently seen this rill with great distinctness, and at other times sought for it in vain; though on each occasion the conditions of illumination, libration, and definition were practically similar. I have sometimes found this cleft an easy object with a 4-inch achromatic. Again, many rills described by Mädler as very delicate and difficult to trace, may now be easily followed in "common telescopes." In short, the more direct telescopic observations accumulate, and the more the study of minute detail is extended, the stronger becomes the conviction, that in spite of the absence of an appreciable atmosphere, there may be something resembling low-lying exhalations from some parts of the surface which from time to time are sufficiently dense to obscure, or even obliterate, the region beneath them.

If, as seems most probable, these gigantic cracks are due to contractions of the moon's surface, it is not impossible, in spite of the assertions of the text-books to the effect that our satellite is now "a changeless world," that emanations may proceed from these fissures, even if, under the monthly alternations of extreme temperatures, surface changes do not now occasionally take place from this cause also. Should this be so, the appearance of new rills and the extension and modification of those already

existing may reasonably be looked for. Many instances might be adduced tending to confirm this supposition, to one of which, as coming under my notice, I will briefly refer. On the evening of November 11, 1883, when examining the interior of the great ring-plain Mersenius with a power of 350 on a  $8\frac{1}{2}$  reflector; in addition to the two closely parallel clefts discovered by Schmidt, running from the inner foot of the north-eastern rampart towards the centre, I remarked another distinct cleft crossing the northern part of the floor from side to side. Shortly afterwards, M. Gaudibert, one of our most experienced selenographers, who has discovered many hitherto unrecorded clefts, having seen my drawing, searched for this object, and, though the night was far from favourable, had distinct though brief glimpses of it with the moderate magnifying power of 100. Mersenius is a formation about 40 miles in diameter, with a prominently convex interior, containing much detail which has received more than ordinary attention from observers. It has, moreover, been specially mapped by Schmidt and others, yet no trace of this rill was noted, though objects much more minute and difficult have not been overlooked. Does not an instance of this kind raise a well-grounded suspicion of recent change which it is difficult to explain away?

To see the lunar clefts to the best advantage, they must be looked for when not very far removed from the terminator, as when so situated the black shadow of one side, contrasted with the usually brightly-illuminated opposite flank, renders them more conspicuous than when they are viewed under a higher sun. Though, as a rule, invisible at full moon, some of the coarser clefts—as, for example, a portion of the Hyginus furrow, and that north of Birt—may be traced as delicate white lines under a nearly vertical light.

For properly observing these objects, a power of not less than 300 on telescopes of large aperture is needed; and in studying their minute and delicate details, we are perhaps more dependent on atmospheric conditions than in following up any other branch of observational astronomy. Few indeed are the nights, in our climate at any rate, when the rough, irregular character of the steep interior of even the coarser examples of these immense chasms can be steadily seen. We can only hope to obtain a more perfect insight into their actual structural peculiarities when they are scrutinised under more perfect climatic circumstances than they have been hitherto. When observing the Hyginus cleft,



Dr. Klein noticed that at one place the declivities of the interior displayed decided differences of tint. At many points the reflected sunlight was of a distinctly yellow hue, while in other places it was white, as if the cliffs were covered with snow. He compares this portion of the rill to the Rhine valley between Bingen and Coblentz, but adds that the latter, if viewed from the moon, would probably not present so fresh an appearance, and would, of course, be frequently obscured by clouds.

Since the erection of the great Lick telescope on Mount Hamilton, our knowledge of the details of some of the lunar clefts has been greatly increased, as in the case of the Ariadæus cleft, and many others. Professor W. H. Pickering, also, at Arequipa, has made at that ideal astronomical site many observations which, when published, will throw more light upon their peculiar characteristics.

A few years ago M. E. L. Trouvelot of Meudon drew attention to a curious appearance which he noted in connection with certain rills when near the terminator, viz., extremely attenuated threads of light on their sites and their apparent prolongations. He observed it in the ring-plain Eudoxus, crossing the southern side of the floor from wall to wall; and also in connection with the prominent cleft running from the north side of Burg to the west of Alexander, and in some other situations. He terms these phenomena *Murs enigmatiques*. Apparent prolongations of clefts in the form of rows of hillocks or small mounds are very common.

*Faults*.—These sudden drops in the surface, representing local dislocations, are far from unusual: the best examples being the straight wall, or “railroad,” west of Birt; that which strikes obliquely across Plato; another which traverses Phocylides; and a fourth that has manifestly modified the mountain arm north of Cichus. They differ from the terrestrial phenomena so designated in the fact that the surface indications of these are destroyed by denudation or masked by deposits of subsequent date. In many cases on the moon, though its course cannot be traced in its entirety by its shadow, yet the existence of a fault may be inferred by the displacement and fracture of neighbouring objects.

*VALLEYS*.—Features thus designated, differing greatly both in size and character, are met with in almost every part of the surface, except on the grey plains. While the smallest examples, from their delicacy, tenuity, and superficial resemblance to rills, are termed rill-valleys, the larger and more conspicuous assume the appearance of coarse chasms, gorges, or trough-like depres-

sions. Between these two extremes, are many objects of moderate dimensions—winding or straight ravines and defiles bounded by steep mountains, and shallow dales flanked by low rounded heights. The rill valleys are very numerous, only differing in many instances from the true rills in size, and are probably due to the same cause. Among the most noteworthy valleys of the largest class must, of course, be placed the great valley of the Alps, one of the most striking objects in the northern hemisphere, which also includes the great valley south-east of Ukert. The Rheita valley, the very similar chasm west of Reichenbach, and the gorge west of Herschel, are also notable examples in the southern hemisphere. The borders of some of the Maria (especially that of the Mare Crisium) and of many of the depressed rimless formations, furnish instances of winding valleys intersecting their borders: the hilly regions likewise often abound in long branching defiles.

BRIGHT RAY-SYSTEMS.—Reference has already been made to the faint light streaks and markings often found on the floors of the ring-mountains and in other situations, and to the brilliant *nimbi* surrounding some of the smaller craters; but, in addition to these, many objects on the moon's visible surface are associated with a much more remarkable and conspicuous phenomenon—the bright rays which, under a high sun, are seen either to radiate from them as apparent centres to great distances, or, in the form of irregular light areas, to environ them, and to throw out wide-spreading lucid beams, extending occasionally many hundreds of miles from their origin. The more striking of these systems were recognised and drawn at a very early stage of telescopic observation, as may be seen if we consult the quaint old charts of Hevel, Riccioli, Fontana, and other observers of the seventeenth century, where they are always prominently, though very inaccurately, portrayed. The principal ray-systems are those of Tycho, Copernicus, Kepler, Anaxagoras, Aristarchus, Olbers, Byrgius A, and Zuchius; while Autolycus, Aristillus, Proclus, Timocharis, Furnerius A, and Menelaus are grouped as constituting minor systems. Many additional centres exist, a list of which will be found in the appendix.

The rays emanating from Tycho surpass in extent and interest any of the others. Hundreds of distinct light streaks originate round the grey margin of this magnificent object, some of them extending over a greater part of the moon's visible superficies, and "radiating," in the words of Professor Phillips, "like false meridians, or like meridians true to an earlier pole of rotation."

No systematic attempt has yet been made to map them accurately as a whole on a large scale, for their extreme intricacy and delicacy would render the task a very difficult one, and, moreover, would demand a long course of observation with a powerful telescope in an ideal situation; but Professor W. H. Pickering, observing under these conditions at Arequipa, has recently devoted considerable attention both to the Tycho and other rays, with especially suggestive and important results, which may be briefly summarised as follows:—

(1.) That the Tycho streaks do not radiate from the apparent centre of this formation, but point towards a multitude of minute craterlets on its south-eastern or northern rims. Similar craterlets occur on the rims of other great craters, forming ray-centres.

(2.) Speaking generally, a very minute and brilliant crater is located at the end of the streak nearest the radiant point, the streak spreading out and becoming fainter towards the other end. The majority of the streaks appear to issue from one or more of these minute craters, which rarely exceed a mile in diameter.

(3.) The streaks which do not issue from minute craters, usually lie upon or across ridges, or in other similar exposed situations, sometimes apparently coming through notches in the mountain walls.

(4.) Many of the Copernicus streaks start from craterlets within the rim, flow up the inside and down the outside of the walls. Kepler includes two such craterlets, but here the flow seems to have been more uniform over the edges of the whole crater, and is not distinctly divided up into separate streams.

(5.) Though there are similar craters within Tycho, the streaks from them do not extend far beyond the walls. All the conspicuous Tycho streaks originate outside the rim.

(6.) The streaks of Copernicus, Kepler, and Aristarchus are greyish in colour, and much less white than those associated with Tycho: some white lines extending south-east from Aristarchus do not apparently belong to the system. In the case of craterlets lying between Aristarchus and Copernicus the streaks point away from the latter.

(7.) There are no very long streaks; they vary from ten to fifty miles in length, and are rarely more than a quarter of a mile broad at the crater. From this point they gradually widen out and become fainter. Their width, however, at the end farthest from the crater, seldom exceeds five miles.

These statements, especially those relating to the length of the

streaks, are utterly opposed to prevailing notions, but Professor Pickering specifies the case of the two familiar parallel rays extending from the north-east of Tycho to the region east of Bullialdus. His observations show that these streaks, originating at a number of little craters situated from thirty to sixty miles beyond the confines of Tycho, "enter a couple of broad slightly depressed valleys. In these valleys are found numerous minute craters of the kind above described, with intensely brilliant interiors. When the streaks issuing from those craters near Tycho are nearly exhausted, they are reinforced by streaks from other craters which they encounter upon the way, the streaks becoming more pronounced at these points. These streaks are again reinforced farther out. These parallel rays must therefore not be considered as two streaks, but as two series of streaks, the components of which are placed end to end."

Thus, according to Professor Pickering, we must no longer regard the rays emanating from the Tycho region and other centres as continuous, but as consisting of a succession of short lengths, diminishing in brilliancy but increasing in width, till they reach the next crater lying in their direction, when they are reinforced; and the same process of gradual diminution in brightness and reinforcement goes on from one end to the other.

The following explanation is suggested to account for the origin of the rays:—"The earth and her satellite may differ not so much as regards volcanic action as in the densities of their atmospheres. Thus if the craterlets on the rim of Tycho were constantly giving out large quantities of gas or steam, which in other regions was being constantly absorbed or condensed, we should have a wind uniformly blowing away from that summit in all directions. Should other summits in its vicinity occasionally give out gases, mixed with any fine white powder, such as pumice, this powder would be carried away from Tycho, forming streaks."

The difficulty surrounding this very ingenious hypothesis is, that though, assuming the existence of pumice-emitting craters and regions of condensation, there might be a more or less lineal and streaky deposition of this white material over large areas of the moon, why should this deposit be so definitely arranged, and why should these active little craters happen to lie on these particular lines?

The confused network of streaks round Copernicus seem to respond more happily to the requirements of Professor Pickering's hypothesis, for here there is an absence of that definiteness of

direction so manifestly displayed in the case of the Tycho rays, and we can well imagine that with an area of condensation surrounding this magnificent object beyond the limits of the streaks, and a number of active little craters on and about its rim, the white material ejected might be drawn outwards in every direction by wind currents, which possibly once existed, and, settling down, assume forms such as we see.

Nasmyth's well-known hypothesis attributes the radiating streaks to cracks in the lunar globe caused by the action of an upheaving force, and accounts for their whiteness by the outwelling of lava from them which has spread to a greater or less distance on either side. If the moon has been fractured in this way, we can easily suppose that the craters formed on these fissures, being in communication with the interior, might eject some pulverulent white matter long after the rest of the surface with its other types of craters had attained a quiescent stage.

The Tycho rays, when viewed under ordinary conditions, appear to extend in unbroken bands to immense distances. One of the most remarkable, strikes along the eastern side of Fracastorius, across the Mare Nectaris to Guttemberg, while another, more central, extends, with local variations in brightness, through Menelaus, over the Mare Serenitatis nearly to the north-west limb. This is the ray that figures so prominently in rude woodcuts of the moon, in which the Mare Serenitatis traversed by it is made to resemble the Greek letter  $\Phi$ . The Kepler, Aristarchus, and Copernicus systems, though of much smaller extent, are very noteworthy from the crossing and apparent interference of the rays;<sup>1</sup> while those near Byrgius, round Aristarchus, and the rays from Proclus, are equally remarkable.

As no branch of selenography has been more neglected than the observation of these interesting but enigmatical features, one may hope that, in spite of the exacting conditions as to situation and instrumental requirements necessary for their successful scrutiny, the fairly equipped amateur in this less favoured country will not be deterred from attempting to clear up some of the doubts and difficulties which at present exist as to their actual nature.

THE MOON'S ALBEDO, SURFACE BRIGHTNESS, &c.—Sir John

<sup>1</sup> Nichol found that the rays from Kepler cut through rays from Copernicus and Aristarchus, while rays from the latter cut through rays from the former. He therefore inferred that their relative ages stand in the order,—Copernicus, Aristarchus, Kepler.

Herschel maintained that "the actual illumination of the lunar surface is not much superior to that of weathered sandstone rock in full sunshine." "I have," he says, "frequently compared the moon setting behind the grey perpendicular façade of the Table Mountain, illuminated by the sun just risen in the opposite quarter of the horizon, when it has been scarcely distinguishable in brightness from the rock in contact with it. The sun and moon being at nearly equal altitudes, and the atmosphere perfectly free from cloud or vapour, its effect is alike on both luminaries." Zöllner's elaborate researches on this question are closely in accord with the above observational result. Though he considers that the brightest parts of the surface are as white as the whitest objects with which we are acquainted, yet, taking the reflected light as a whole, he finds that the moon is more nearly black than white. The most brilliant object on the surface is the central peak of the ring-plain Aristarchus, the darkest the floor of Grimaldi, or perhaps a portion of that of the neighbouring Riccioli. Between these extremes, there is every gradation of tone. Proctor, discussing this question on the basis of Zöllner's experiments respecting the light reflected by various substances, concludes that the dark area just mentioned must be notably darker than the dark grey syenite which figures in his tables, while the floor of Aristarchus is as white as newly fallen snow.

The estimation of lunar tints in the usual way, by eye observations at the telescope, involving as it does physiological errors which cannot be eliminated, is a method far too crude and ambiguous to form the basis of a scientific scale or for the detection of slight variations. An instrument on the principle of Dawes' solar eyepiece has been suggested; this, if used with an invariable and absolute scale of tints, would remove many difficulties attending these investigations. The scale which was adopted by Schröter, and which has been used by selenographers up to the present time, is as follows:—

0° = Black.	5° = Pure light grey.
1° = Greyish black.	6° = Light whitish grey.
2° = Dark grey.	7° = Greyish white.
3° = Medium grey.	8° = Pure white.
4° = Yellowish grey.	9° = Glittering white.
10° = Dazzling white.	

The following is a list of lunar objects published in the *Selenographical Journal*, classed in accordance with this scale:—

- 0° Black shadows.
- 1° Darkest portions of the floors of Grimaldi and Riccioli.
- 1½° Interiors of Boscovich, Billy, and Zupus.
- 2° Floors of Endymion, Le Monnier, Julius Cæsar, Crüger, and Fourier *a*.
- 2½° Interiors of Azout, Vitruvius, Pitatus, Hippalus, and Marius.
- 3° Interiors of Taruntius, Plinius, Theophilus, Parrot, Flamsteed, and Mercator.
- 3½° Interiors of Hansen, Archimedes, and Mersenius.
- 4° Interiors of Manilius, Ptolemæus, and Gueriké.
- 4½° Surface round Aristillus, Sinus Medii.
- 5° Walls of Arago, Landsberg, and Bullialdus. Surface round Kepler and Archimedes.
- 5½° Walls of Picard and Timocharis. Rays from Copernicus.
- 6° Walls of Macrobius, Kant, Bessel, Mösting, and Flamsteed.
- 6½° Walls of Langrenus, Theætetus, and Lahire.
- 7° Theon, Ariadæus, Bode B, Wichmann, and Kepler.
- 7½° Ukert, Hortensius, Euclides.
- 8° Walls of Godin, Bode, and Copernicus.
- 8½° Walls of Proclus, Bode A, and Hipparchus c.
- 9° Censorinus, Dionysius, Mösting A, and Mersenius B and c.
- 9½° Interior of Aristarchus, La Peyrouse Δ.
- 10° Central peak of Aristarchus.

TEMPERATURE OF THE MOON'S SURFACE.—Till the subject was undertaken some years ago by Lord Rosse, no approach was made to a satisfactory determination of the surface temperature of the moon. From his experiments he inferred that the maximum temperature attained, at or near the equator, about three days after full moon, does not exceed 200° C., while the minimum is not much under zero C. Subsequent experiments, however, both by himself and Professor Langley, render these results more than doubtful, without it is admitted that the moon has an atmospheric covering. Langley's results make it probable that the temperature never rises above the freezing-point of water, and that at the end of the prolonged lunar night of fourteen days it must sink to at least 200° below zero. Mr. F. W. Verrey of the Alleghany Observatory has recently conducted, by means of the bolometer, similar researches as to the distribution of the moon's heat and its variation with the phase, by which he has deduced the varying radiation from the surface in different localities of the moon under various solar altitudes.

LUNAR OBSERVATION.—In observing the moon, we enjoy an advantage of which we cannot boast when most other planetary

bodies are scrutinised ; for we see the actual surface of another world undimmed by palpable clouds or exhalations, except such as exist in the air above us ; and can gaze on the marvellous variety of objects it presents much as we contemplate a relief map of our own globe. But inasmuch as the manifold details of the relief map require to be placed in a certain light to be seen to the best advantage, so the ring-mountains, rugged highlands, and wide-extending plains of our satellite, as they pass in review under the sun, must be observed when suitable conditions of illumination prevail, if we wish to appreciate their true character and significance.

As a general rule, lunar objects are best seen when they are at no great distance from "the terminator," or the line dividing the illuminated from the unilluminated portion of the spherical surface. This line is constantly changing its position with the sun, advancing slowly onwards towards the east at a rate which, roughly speaking, amounts to about  $30'.5$  in an hour, or passing over  $10^\circ$  of lunar longitude in about 19 hrs. 40 mins. When an object is situated on this line, the sun is either rising or setting on the neighbouring region, and every inequality of the surface is rendered prominent by its shadow ; so that trifling variations in level and minor asperities assume for the time being an importance to which they have no claim. If we are observing an object at lunar sunrise, a very short time, often only a few minutes, elapses before the confusion caused by the presence of the shadows of these generally unimportant features ceases to interfere with the observation, and we can distinguish between those details which are really noteworthy and others which are trivial and evanescent. Every formation we are studying should be observed, and drawn if possible, under many different conditions of illumination. It ought, in fact, to be examined from the time when its loftiest heights are first illuminated by the rising sun till they disappear at sunset. This is, of course, practically impossible in the course of one lunation, but by utilising available opportunities, a number of observations may be obtained under various phases which will be more or less exhaustive. It cannot be said that much is known about any object until an attempt has been made to carry out this plan. Features which assume a certain appearance at one phase frequently turn out to be altogether different when viewed under another ; important details obscured by shadows, craters masked by those of neighbouring objects, or by the shadows of their own rims, are often only



revealed when the sun has attained an altitude of ten degrees or more. In short, there is scarcely a formation on the moon which does not exemplify the necessity of noting its aspect from sunrise to sunset. Regard must also be had to libration, which affects to a greater or less degree every object; carrying out of the range of observation regions near the limb at one time, and at another bringing into view others beyond the limits of the maps, which represent the moon in the mean state of libration. The area, in fact, thus brought into view, or taken out of it, is between  $\frac{1}{12}$ th and  $\frac{1}{13}$ th of the entire area of the moon, or about the  $\frac{1}{6}$ th part of the hemisphere turned away from the earth. It is convenient to bear in mind that we see an object under nearly the same conditions every  $59^{\text{d}} 1^{\text{h}} 28^{\text{m}}$ , or still more accurately, after the lapse of fifteen lunations, or  $442^{\text{d}} 23^{\text{h}}$ . Many observers avoid the observation of objects under a high light. This, however, should never be neglected when practicable, though in some cases it is not easy to carry out, owing to the difficulty in tracing details under these circumstances.

Although to observe successfully the minuter features, such as the rills and the smaller craterlets, requires instruments of large aperture located in favourable situations, yet work of permanent value may be accomplished with comparatively humble telescopic means. A 4-inch achromatic, or a silver-on-glass reflector of 6 or  $6\frac{1}{2}$  inches aperture, will reveal on a good night many details which have not yet been recorded, and the possessor of instruments of this size will not be long in discovering that the moon, despite of what is often said, has not been so exhaustively surveyed that nothing remains for him to do.

Only experience and actual trial will teach the observer to choose the particular eyepiece suitable for a given night or a given object. It will be found that it is only on very rare occasions that he can accomplish much with powers which, perhaps only on two or three nights in a year in this climate, tell to great advantage; though it sometimes happens that the employment of an eyepiece, otherwise unsuitable for the night, will, during a short spell of good definition, afford a fleeting glimpse of some difficult feature, and thus solve a doubtful point. It has often been said that the efficiency of a telescope depends to a great extent on "the man at the eye end." This is as true in the case of the moon as it is in other branches of observational astronomy.

Observers, especially beginners, frequently fall into great error

in failing to appreciate the true character of what they see. In this way a shallow surface depression, possibly only a few feet below the general level of the neighbouring country, is often described as a "vast gorge," because, under very oblique light, it is filled with black shadow; or an insignificant hillock is magnified into a mountain when similarly viewed. Hence the importance, just insisted on, of studying lunar features under as many conditions as possible before finally attempting to describe them.

However indifferent a draughtsman an observer may be, if he endeavours to portray what he sees to the best of his ability, he will ultimately attain sufficient skill to make his work useful for future reference: in any case, it will be of more value than a mere verbal description without a sketch. Doubt and uncertainty invariably attend to a greater or less extent written notes unaccompanied by drawings, as some recent controversies, respecting changes in Linné and elsewhere, testify. Now that photographs are generally available to form the basis of a more complete sketch, much of the difficulty formerly attending the correct representation of the outline and grosser features of a formation has been removed, and the observer can devote his time and attention to the insertion and description of less obvious objects.

PROGRESS OF SELENOGRAPHY.—Till within recent years, the systematic study of the lunar surface may be said to have been confined, in this country at any rate, to a very limited number of observers, and, except in rare instances, those who possessed astronomical telescopes only directed them to the moon as a show object to excite the wonder of casual visitors. The publication of Webb's "Celestial Objects" in 1859, the supposed physical change in the crater Linné, announced in 1866, and the appearance of an unrecorded black spot near Hyginus some ten years later, had the effect of awakening a more lively interest in selenography, and undoubtedly combined to bring about a change in this respect, which ultimately resulted in the number of amateurs devoting much of their time to this branch of observational astronomy being notably increased. Still, large telescopes, as a rule, held aloof for some unexplained reason, or were only employed in a desultory and spasmodic fashion, without any very definite object. When the Council of the British Association for the Advancement of Science, stimulated by the Linné controversy, deemed the moon to be worthy of passing attention, observa-

tions, directed to objects suspected of change (the phenomena on the floor of Plato) were left to three or four observers, under the able direction of Mr. Birt, the largest instruments available being an 8 $\frac{1}{4}$ -inch reflector and the Crossley refractor of 9 inches aperture ! During the last decade, however, all this has been changed, and we not only have societies, such as the British Astronomical Association, setting apart a distinct section for the systematic investigation of lunar detail, but some of the largest and most perfect instruments in the world, among them the noble refractor on Mount Hamilton, employed in photographing the moon or in scrutinising her manifold features by direct observation. Hence, it may be said that selenography has taken a new and more promising departure, which, among other results, must lead to a more accurate knowledge of lunar topography, and settle possibly, ere long, the vexed question of change, without any residuum of doubt.

Lunar photography as exemplified by the marvellous and beautiful pictures produced at the Lick Observatory under the auspices of Dr Holden, and the exquisite enlargements of them by Dr. Weinek of Prague ; at Paris by the brothers Henry, and at Brussels by M Prinz ; point to the not far distant time when we shall possess complete photographic maps on a large scale of the whole visible disc under various phases of illumination, which will be of inestimable value as topographical charts. When this is accomplished, the observer will have at his command faithful representations of any formation, or of any given region he may require, to utilise for the study of the smaller details by direct observation.

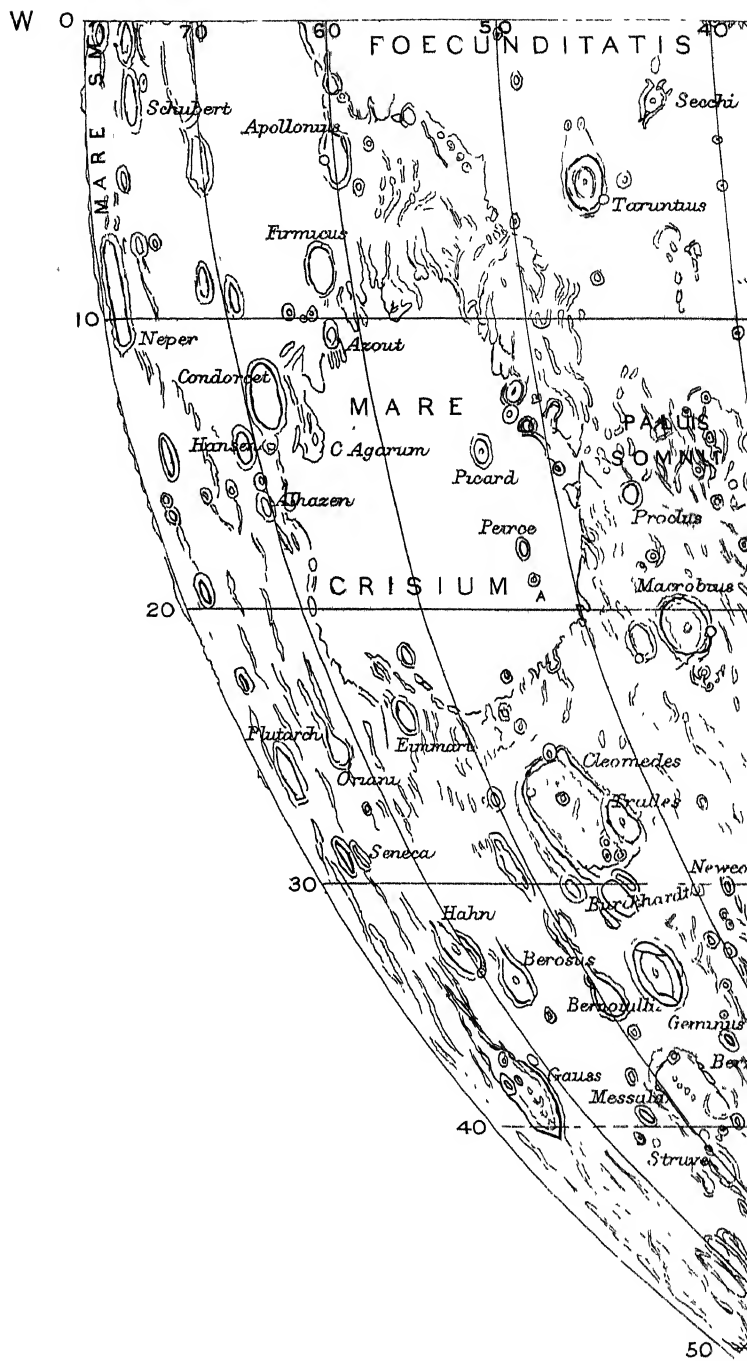
Desultory and objectless drawings and notes have hitherto been more or less characteristic of the work done, even by those who have given more than ordinary attention to the moon. Though these, if duly recorded, are valuable as illustrating the physical structure, the estimated brightness under various phases, and other peculiarities of lunar features, they do not materially forward investigations relating to the discovery of present lunar activity or to the detection of actual change. It is reiterated *ad nauseam* in many popular books that the moon is a changeless world, and it is implied that, having attained a state when no further manifestations of internal or external forces are possible, it revolves round the earth in the condition, for the most part, of a globular mass of vesicular lava or slag, possessing no interest except as a notable example of a "burnt-out planet." In answer to these dogmatic

assertions, it may be said that, notwithstanding the multiplication of monographs and photographs, the knowledge we possess, even of the larger and more prominent objects, is far too slight to justify us in maintaining that changes, which on earth we should use a strong adjective to describe, have not taken place in connection with some of them in recent years. Would the most assiduous observer assert that his knowledge of any one of the great formations, in the south-west quadrant, for example, is so complete that, if a chasm as big as the Val del Bove was blown out from its flanks, or formed by a landslide, he would detect the change in the appearance of an area (some three miles by four) thus brought about, unless he had previously made a very prolonged and exhaustive study of the object? Or, again, among formations of a different class, the craters and crater-cones; might not objects as large as Monte Nuovo or Jorullo come into existence in many regions without any one being the wiser? It would certainly have needed a persistent lunar astronomer, and one furnished with a very perfect telescope, to have noted the changes that have occurred within the old crater-ring of Somma or among the Santorin group during the past thirty years, or even to have detected the effects resulting from the great catastrophe in A.D. 79, at Vesuvius; yet these objects are no larger than many which, if they were situated on our satellite, would be termed comparatively small, if not insignificant.

One of the principal aims of lunar research is to learn as much as possible as to the present condition of the surface. Every one qualified to give an opinion will admit that this cannot be accomplished by roaming at large over the whole visible superficies, but only by confining attention to selected areas of limited extent, and recording and describing every object visible thereon, under various conditions of illumination, with the greatest accuracy attainable. This plan was suggested and inaugurated nearly thirty years ago by Mr. Birt, under the patronage of the British Association; but as he proposed to deal with the entire disc in this way, the magnitude and ambitious character of the scheme soon damped the ardour of those who at first supported it, and it was ultimately abandoned. It was, however, based on the only feasible principle which, as it seems to the writer, will not result in doubt and confusion. Now that photography has come to the assistance of the observer, Mr. Birt's proposal, if confined within narrower limits, would be far less arduous an undertaking than before, and might

be easily carried out. A complete photographic survey of a few selected regions, as a basis for an equally thorough and exhaustive scrutiny by direct observation, would, it is believed, lead to a much more satisfactory and hopeful method for ultimately furnishing irrefragable testimony as to permanency or change than any that has yet been undertaken.



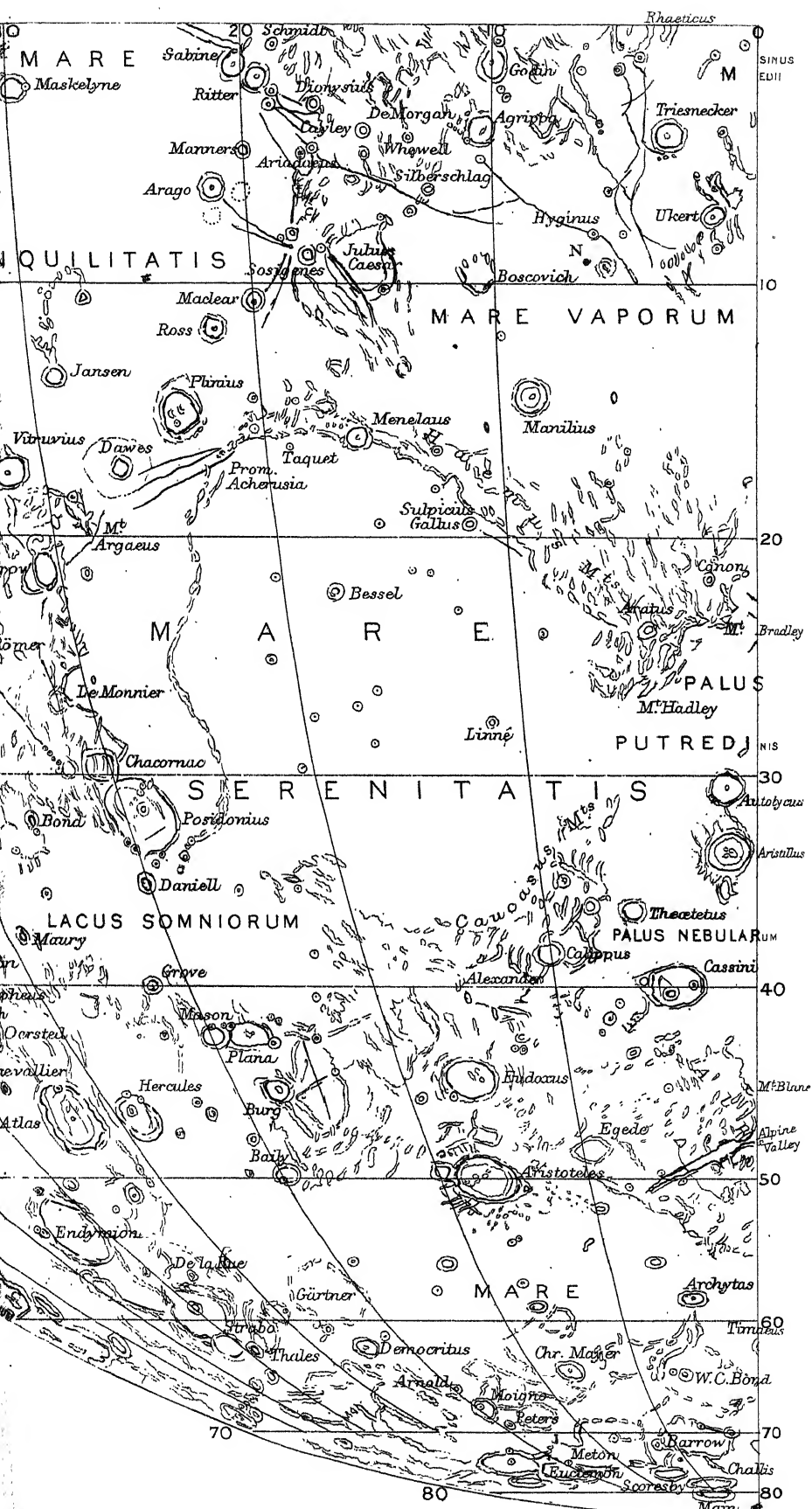


# Map of the Moon

by

T. GWYN ELGER, F.R.A.S.

FIRST QUADRANT.







# CATALOGUE OF LUNAR FORMATIONS

## FIRST QUADRANT

WEST LONGITUDE  $90^{\circ}$  TO  $60^{\circ}$

SCHUBERT.—This ring-plain, about 46 miles in diameter, situated on the N.E. side of the Mare Smythii, is too near the limb to be well observed.

NEPER.—Though still nearer the limb, this walled-plain, 74 miles in diameter, is a much more conspicuous object. It has a lofty border and a prominent central mountain, the highest portion of a range of hills which traverses the interior from N. to S.

APOLLONIUS.—A ring-plain, 30 miles in diameter, standing in the mountainous region S. of the Mare Crisium. There is a large crater on the S.W. wall, and another, somewhat smaller, adjoining it on the N. There are many brilliant craters in the vicinity.

FIRMICUS.—A somewhat larger, more regular, but, in other respects, very similar ring-plain, N.W. of the last. Some distance on the W., Mädler noted a number of dark-grey streaks which apparently undergo periodical changes, suggestive of something akin to vegetation. They are situated near a prominent mountain situated in a level region.

AZOUT.—A small ring-plain, connected with the last by a lofty ridge. It is the apparent centre of many other ridges and valleys which radiate from it towards the N.W. and the Mare Crisium. There is a central mountain, not an easy telescopic object, on its dusky floor.

CONDORCET.—A very prominent ring-plain, 45 miles in diameter, situated on the mountainous S.W. margin of the Mare Crisium. It is encircled by a lofty wall about 8000 feet in height. The dark interior of this and of the three preceding formations render them easily traceable under a high angle of illumination.

HANSEN.—A ring-plain, 32 miles in diameter, on the W. border

of the Mare Crisium N. of Condorcet. Schmidt shows a central mountain and a terraced wall.

ALHAZEN.—This ring-plain, rather smaller than the last, is the most northerly of the linear chain of formations, associated with the highlands bordering the S.W. and the W. flanks of the Mare Crisium. It has a central mountain and other minor elevations on the floor. There is a little ring between Alhazen and Hansen, never very conspicuous in the telescope, which is plainly traceable in good photographs.

EIMMART.—A conspicuous ring-plain with bright walls on the N.W. margin of the Mare Crisium. The E. border attains a height of 10,000 feet above the interior, which, according to Schmidt, has a small central mountain. There is a rill-like valley on the E. of the formation.

ORIANI.—An irregular object, 32 miles in diameter, somewhat difficult to identify, N.W. of the last. There is a conspicuous crater on the N. of it, with which it is connected by a prominent ridge.

PLUTARCH.—A fine ring-plain W. of Oriani, with regular walls, and, according to Neison, with two central mountains, only one of which I have seen. Both this formation and the last are beautifully shown in a photograph taken August 19, 1891, at the Lick Observatory, when the moon's age was 15 d. 10 hrs.

SENECA.—Rather smaller than Plutarch. Too near the limb for satisfactory observation. Schmidt shows two considerable mountains in the interior. The position of this object in Schmidt's chart is not accordant with its place in Beer and Mädler's map, nor in that of Neison.

HAHN.—A ring-plain, 46 miles in diameter, with a fine central mountain and lofty peaks on the border, which is not continuous on the S. There is a large and prominent crater on the E.

BEROSUS.—A somewhat smaller object of a similar type, N. of Hahn, but with a loftier wall. There is a want of continuity also in the border, the eastern and western sections of which, instead of joining, extend for some distance towards the S., forming a narrow gorge or valley. Outside the S.E. wall there is a small crater, and some irregular depressions on the E. The minute central mountain is only seen with difficulty under a low evening sun. The bright region between Hahn and Berosus and the western flank of Cleomedes is an extensive plain, devoid of prominent detail, and which, according to Neison, includes an area of 40,000 square miles.

GAUSS.—A large, and nearly circular walled-plain, 111 miles in diameter, situated close to the N.W. limb, and consequently always foreshortened into a more or less elongated ellipse. But for this it would be one of the grandest objects in the first quadrant. Under the designation of “Mercurius Falsus” it received great attention from Schröter, who gives several representations of it in his *Selenotopographische Fragmente*, which, though drawn in his usual conventional style, convey a juster idea of its salient features than many subsequent drawings made under far better optical conditions. The border, especially on the W., is very complex, and is discontinuous on the S., where it is intersected by more than one pass, and is prolonged far beyond the apparent limits of the formation. The most noteworthy feature is the magnificent mountain chain which traverses the floor from N. to S. It is interesting to watch the progress of sunset thereon, and see peak after peak disappear, till only the great central boss and a few minute glittering points of light, representing the loftier portions of the chain, remain to indicate its position. Mädler expatiates on the sublime view which would be obtained by any one standing on the highest peak and observing the setting sun on one side of him and the nearly “full” earth on the other; while beneath him would lie a vast plain, shrouded in darkness, surrounded by the brilliantly illuminated peaks on the lofty border, gradually passing out of sunlight. In addition to the central mountain range, there are some large rings, craters, hillocks, &c., on the floor; and on the inner slope of the W. border there is a very large circular enclosure resembling a ring-plain, not recorded in the maps. Schmidt shows a row of large craters on the outer slope of the E. border. Of these, one is very conspicuous under a low evening sun, by reason of its brilliant walls and interior. In the region between Gauss and Barosus is a number of narrow steep ridges which follow the curvature of the E. wall.

STRUVE.—A small irregularly-shaped formation, open towards the S., forming one of the curious group of unsymmetrical enclosures associated with Messala. Its dark floor and a small dusky area on the N. indicate its position under a high sun.

CARRINGTON.—A small ring-plain, belonging to the Messala group, adjoining Schumacher on the N.W.

MERCURIUS.—This formation is 25 miles in diameter. A small crater stands on the S.E. section of the wall. There is a longitudinal range in the interior, and on the W. and N.W. the remains of two large walled-plains, the more westerly of which is a note-

worthy object under suitable conditions. A short distance S. is a large, irregular, and very dark marking. On the N., lies an immense bright plain, extending nearly to the border of Endymion.

### WEST LONGITUDE $60^{\circ}$ TO $40^{\circ}$ .

TARUNTIUS.—Notwithstanding its comparatively low walls, this ring-plain, 44 miles in diameter, is a very conspicuous object under a rising sun. Like Vitello and a few other formations, it has an inner ring on the floor, concentric with the outer rampart, which I have often seen nearly complete under evening illumination. There is a small bright crater on the S.E. wall, and a larger one on the crest of the N.E. wall, with a much more minute depression on the W. of it, the intervening space exhibiting signs of disturbance. The upper portion of the wall is very steep, contrasting in this respect with the very gentle inclination of the *glacis*, which on the S. extends to a distance of at least 30 miles before it sinks to the level of the surrounding country, the gradient probably being as slight as 1 in 45. Two low dusky rings and a long narrow valley with brilliant flanks are prominent objects on the plain E. of Taruntius under a low evening sun.

SECCHI.—A partially enclosed little ring-plain S. of Taruntius, with a prominent central mountain and bright walls. There is a short cleft running in a N.E. direction from a point near the E. wall. Schmidt represents it as a row of inosculating craters.

PICARD.—The largest of the craters on the surface of the Mare Crisium, 21 miles in diameter. The floor, which includes a central mountain, is depressed about 2000 feet below the outer surface, and is surrounded by walls rising some 3000 feet above the Mare. A small but lofty ring-plain, Picard E, on the E., near the border of the Mare, is remarkable for its change of aspect under different angles of illumination. A long curved ridge running S. from this, with a lower ridge on the west, sometimes resemble a large enclosure with a central mountain. Still farther S., there is another bright deep crater, *a*, with a large low ring adjoining it on the S., abutting on the S.E. border of the Mare. Schröter bestowed much attention on these and other formations on the Mare Crisium, and attributed certain changes which he observed to a lunar atmosphere.

PEIRCE.—This formation, smaller than Picard, is also prominent, its border being very bright. There is a central peak, which, though

not an easy object, I once glimpsed with a 4-inch Cook achromatic, and have seen it two or three times since with an 8½-in. Calver reflector. A small crater, detected by Schmidt, which I once saw very distinctly under evening illumination, stands on the floor at the foot of the W. wall. Peirce A, a deeper formation, lies a little N. of Peirce, and has also, according to Neison, a very slight central hill, which is only just perceptible under the most favourable conditions. Schmidt appears to have overlooked it.

PROCLUS.—One of the most brilliant objects on the moon's visible surface, and hence extremely difficult to observe satisfactorily. It is about 18 miles in diameter, with very steep walls, and, according to Schmidt, has a small crater on its east border, where Mädler shows a break. It is questionable whether there is a central mountain. It is the centre of a number of radiating light streaks which partly traverse the Mare Crisium, and with those emanating from Picard, Peirce, and other objects thereon, form a very complicated system. ✓

MACROBIUS.—This, with a companion ring on the W., is a very beautiful object under a low sun. It is 42 miles in diameter, and is encircled by a bright, regular, but complex border, some 13,000 feet in height above the floor. Its crest is broken on the E. by a large brilliant crater, and its continuity is interrupted on the N. by a formation resembling a large double crater, which is associated with a number of low rounded banks and ridges extending some distance towards the N.W., and breaking the continuity of the *glacis*. The W. wall is much terraced, and on the N.W. includes a row of prominent depressions, well seen when the interior is about half illuminated under a rising sun. The central mountain is of the compound type, but not at all prominent. The companion ring, Macrobius c, is terraced internally on the W., and the continuity of its N. border is broken by two depressions. There is a rill-valley between its N.E. side and Macrobius. ✓

CLEOMEDES.—A large oblong enclosure, 78 miles in diameter, with massive walls, varying in altitude from 8000 to 10,000 feet above the interior. The most noteworthy features in connection with the circumvallation are the prominent depressions on the W. wall. Under a rising sun, when about one-fourth of the floor is in shadow, three of these can be easily distinguished, each resembling in form the figure  $\infty$ . There are two other curious depressions at the S.W. end of the formation. On the dark steel-grey floor are two irregular dusky areas, and a narrow ✓

but bright central mountain, on which, according to Schmidt, stand two little craters. There are two ring-plains on the S.W. quarter, and a group of three associated craters on the N. side, one of which (A) Schröter believed came into existence after he commenced to observe the formation, a supposition that has been shown by Birt and others to be very improbable.

TRALLES.—A large irregular crater, one of the deepest on the visible surface of the moon, situated on the N.E. wall of Cleomedes. There is a crater on its N. wall, and, according to Schmidt, some ridges and three closely associated craters on the floor.

BURCKHARDT.—This object, situated on an apparent extension of the W. wall of Cleomedes, is 35 miles in diameter, with a lofty border, rising on the E. to an altitude of nearly 13,000 feet. It has a prominent central mountain and some low ridges on the floor, which, together with two minute craters on the S.W. wall, I have seen under a low angle of morning illumination. It is flanked both on the E. and W. by deep irregular depressions, which present the appearance of having once been complete formations.

GEMINUS.—A fine regular ring-plain, 54 miles in diameter, nearly circular, with bright walls, rising on the E. to a height of more than 12,000 feet, and on the opposite side to nearly 16,000 feet above the floor. Their crest is everywhere very steep, and the inner slope is much terraced. There is a small but conspicuous mountain in the interior; N. of which I have seen a long ridge, where Schmidt shows some hillocks. Two fine clefts are easily visible within the ring, one running for some distance on the S.E. side of the floor, mounting the inner slope of the S.W. border to the summit ridge (where it is apparently interrupted), and then striking across the plain in a S.W. direction. Here it is accompanied for a short distance by a somewhat coarser companion, running parallel to it on the N. The other cleft occupies a very similar position on the N.W. side of the floor at the inner foot of the wall. On several occasions, when observing this formation and the vicinity, I have been struck by its peculiar colour under a low evening sun. At this time the whole region appears to be of a warm light brown or sepia tone.

BERNOUILLE.—A very deep ring-plain on the W. side of Geminus. Under evening illumination its lofty W. wall, which rises to a height of nearly 13,000 feet above the floor, is conspicuously brilliant. This formation exhibits a marked departure from the circular type, being bounded by rectilinear sides. The inner

slope of the W. wall is slightly terraced. The border on the S. is much lower than elsewhere, as is evident when the formation is on the evening terminator. On the N. is the deep crater Messala  $\alpha$ .

NEWCOMB.—The most prominent of a group of formations standing in the midst of the Hæmus Mountains. Its crest is nearly 12,000 feet above the floor, on which there are some hills.

MESSALA.—This fine walled-plain, nearly 70 miles in diameter, is, with its surroundings, an especially interesting object when observed under a low angle of illumination. Its complex border, though roughly circular, displays many irregularities in outline, due mainly to rows of depressions. The best view of it is obtained when the W. wall is on the evening terminator. At this phase, if libration is favourable, the manifold details of its very uneven and apparently convex floor are best seen. On the S.W. side is a group of large craters associated with a number of low hills, of which Schmidt shows five; but I have seen many more, together with several ridges between them and the E. wall. I noted also a cleft, or it may be a narrow valley, running from the foot of the N.W. wall towards the centre. On the floor, abutting on the N.E. border, is a semi-circular ridge of considerable height, and beyond the border on the N.E. there is another curved ridge, completing the circle, the wall forming the diameter. This formation is clearly of more ancient date than Messala, as the N.E. wall of the latter has cut through it. Where Messala joins Schumacher there is a break in the border, occupied by three deep depressions.

SCHUMACHER.—A large irregular ring-plain, 28 miles in diameter, associated with the N. wall of Messala, and having other smaller rings adjoining it on the E. and N. The interior seems to be devoid of detail.

HOOKE.—Another irregular ring-plain, 28 miles in diameter, on the N.E. of Messala. There is a bright crater of considerable size on the S.W., which is said to be more than 6000 feet in depth, and, according to Neison, is visible as a white spot at full. There is a smaller crater on the slope of the N.W. wall.

SHUCKBURGH.—A square-shaped enclosure on the N. of the last, with a comparatively low border. It has a conspicuous crater at its N.W. corner.

BERZELIUS.—A considerable ring-plain of regular form, with low walls and dark interior, on which there is a central peak, difficult to detect.



FRANKLIN.—A ring-plain, 33 miles in diameter, which displays a considerable departure from the circular type, as the border is in great part made up of rectilineal sections. Both the W. and N.E. wall is much terraced, and rises about 8000 feet above the dark floor, on the S. part of which there is a long ridge. There is a bright little isolated mountain on the plain E. of the formation, and a conspicuous craterlet on the N.W. An incomplete ring, with a very attenuated border, abuts on the S. side of Franklin.

CEPHEUS.—A peculiarly shaped ring-plain, 27 miles in diameter. The E. border is nearly rectilineal, while on the W., the wall forms a bold curve. There is a very brilliant crater on the summit of this section, and a central mountain on the floor. The W. wall is much terraced. W. of Cepheus, close to the brilliant crater, there is a cleft or narrow valley running N. towards Oersted.

OERSTED.—An oblong formation with very low walls, scarcely traceable on the S.E., except when near the terminator. There is a conspicuous crater on the N.W. side of the floor, and a curious square enclosure, with a crater on its W. border, abutting on the N.E. wall.

CHEVALLIER.—An inconspicuous object enclosed by slightly curved ridges. It includes a deep bright crater. On the N. is a low square formation and a long ridge running N. from it. Just beyond the N.E. wall is the fine large crater, Atlas A, with a much smaller but equally conspicuous crater beyond. A has a central hill, which, in spite of the bright interior, is not a difficult feature.

ATLAS.—This, and its companion Hercules on the E., form under oblique illumination a very beautiful pair, scarcely surpassed by any other similar objects on the first quadrant. Its lofty rampart, 55 miles in diameter, is surmounted by peaks, which on the N. tower to an altitude of nearly 11,000 feet. It exhibits an approach to a polygonal outline, the lineal character of the border being especially well marked on the N. The detail on the somewhat dark interior will repay careful scrutiny with high powers. There is a small but distinct central mountain, south of which stands a number of smaller hills, forming with the first a circular arrangement, suggestive of the idea that they represent the relics of a large central crater. Several clefts may be seen on the floor under suitable illumination, among them a forked cleft on the N.E. quarter, and two others, originating at a

dusky pit of irregular form situated near the foot of the S.E. wall, one of which runs W. of the central hills, and the other on the opposite side. A ridge, at times resembling a light marking, extends from the central mountain to the N. border. During the years 1870 and 1871 I bestowed some attention on the dusky pit, and was led to suspect that both it and the surrounding area vary considerably in tone from time to time. Professor W. H. Pickering, observing the formation in 1891 with a 13-inch telescope under the favourable atmospheric conditions which prevail at Arequipa, Peru, confirmed this supposition, and has discovered some very interesting and suggestive facts relating to these variations, which, it is hoped, will soon be made public. On the plain a short distance beyond the foot of the *glacis* of the S.E. wall, I have frequently noted a second dusky spot, from which proceeds, towards the E., a long rill-like marking. On the N. there is a large formation enclosed by rectilineal ridges. The outer slopes of the rampart of Atlas are very noteworthy under a low sun.

HERCULES.—The eastern companion of Atlas, a fine ring-plain, about 46 miles in diameter, with a complex border, rising some 11,000 feet above a depressed floor. There are few formations of its class and size which display so much detail in the shape of terraces, apparent landslips, and variation in brightness. In the interior, S.E. of the centre, is a very conspicuous crater, which is visible as a bright spot when the formation itself is hardly traceable, two large craterlets slightly N. of the centre, and several faint little spots on the east of them. The latter, detected some years ago by Herr Hückel of Stuttgart, are arranged in the form of a horse-shoe. There are two small contiguous craters on the S.E. wall, one of which, a difficult object, was recently detected by Mr. W. H. Maw, F.R.A.S. The well-known wedge-shaped protuberance on the S. wall is due to a large irregular depression. On the bright inner slope of the N. wall are manifest indications of a landslip.

ENDYMION.—A large walled-plain, 78 miles in diameter, enclosed by a lofty, broad, bright border, surmounted in places by peaks which attain a height of more than 10,000 feet above the interior, one on the W. measuring more than 15,000 feet. The walls are much terraced and exhibit two or three breaks. The dark floor appears to be devoid of detail. Schmidt, however, draws two large irregular mounds E. of the centre, and shows four narrow light streaks crossing the interior nearly parallel to the longer axis of the formation.

DE LA RUE.—Notwithstanding its great extent, this formation hardly deserves a distinctive name, as from the lowness of its border it is scarcely traceable in its entirety except under very oblique light. Schmidt, nevertheless, draws it with very definite walls, and shows several ridges and small rings in the interior. Among these objects, a little E. of the centre, there is a prominent peak.

STRABO.—A small walled-plain, 32 miles in diameter, connected with the N. border of the last.

THALES.—A bright formation, also associated with the N. side of De la Rue, adjoining Strabo on the N.E. Schmidt shows a minute hill in the interior.

There are several unnamed formations, large and small, between De la Rue and the limb, some of which are well worthy of examination.

#### WEST LONGITUDE $40^{\circ}$ TO $20^{\circ}$ .

MASKELYNE.—A regular ring-plain, 19 miles in diameter, standing almost isolated in the Mare Tranquilitatis. The floor, which includes a central mountain, is depressed some 3000 feet below the surrounding surface. There are prominent terraces on the inner slope of the walls. Schmidt shows no craters upon them, but Mädler draws a small one on the E., the existence of which I can confirm.

MANNERS.—A brilliant little ring-plain, 11 miles in diameter, on the S.E. side of the Mare Tranquilitatis. There appears to be no detail whatever in connection with its wall. It has a distinct central mountain. About three diameters distant on the S.W. there is a bright crater, omitted by Mädler and Neison.

ARAGO.—A much larger formation, 18 miles in diameter, N. of the last, with a small crater on its N. border, and exhibiting two or three spurs from the wall on the opposite side. The inner slopes are terraced, and there is a small central mountain. There are two curious circular protuberances on the Mare E. of Arago, which are well seen when the W. longitude of the morning terminator is about  $19^{\circ}$ , and a long cleft, passing about midway between them, and extending from the foot of the E. wall to a small crater on the edge of the Mare near Sosigenes. Another cleft, also terminating at this crater, runs towards Arago and the more northerly of the protuberances.

CAUCHY.—A bright little crater, not more than 7 or 8 miles in diameter, on the W. side of the Mare Tranquilitatis, N.E. of

Taruntius. It has a peak on its W. rim considerably loftier than the rest of the wall, which is visible as a brilliant spot at sunrise long before the rest of the rampart is illuminated. On the S. there are two bright longitudinal ridges ranging from N.E. to S.W. These stand in the position where Neison draws two straight clefts. The Cauchy cleft, however, lies N. of these, and terminates, as shown by Schmidt, among the mountains N.E. of Taruntius. I have seen it thus on many occasions, and it is so represented in a drawing by M. E. Stuvaert (*Dessins de la Lune*). There is a number of minute craters and mounds standing on the S. side of this cleft, and many others in the vicinity.

JANSEN.—Owing to its comparatively low border, this is not a very conspicuous object. It is chiefly remarkable for the curious arrangement of the mountains and ridges on the S. and W. of it. There is a bright little crater on the S. side of the floor, and many noteworthy objects of the same class in the neighbourhood. The mountain arm running S., and ultimately bending E., forms a large incomplete hook-shaped formation terminating at a ring-plain, Jansen B. The ridges in the Mare Tranquilitatis between Jansen B. and the region E. of Maskelyne display under a low sun foldings and wrinklins of a very extraordinary kind.

MACLEAR.—A conspicuous ring-plain about 16 miles in diameter. The dark floor includes, according to Mädler, a delicate central hill which Schmidt does not show. Neison, however, saw a faint greyish mark, and an undoubted peak has been subsequently recorded. I have not succeeded in seeing any detail within the border, which in shape resembles a triangle with curved sides.

ROSS.—A somewhat larger ring-plain of irregular form, on the N.W. of the last. There are gaps on the bright S.W. border and a crater on the S.E. wall. The central mountain is an easy feature.

PLINIUS.—This magnificent object reminds one at sunrise of a great fortress or redoubt erected to command the passage between the Mare Tranquilitatis and the Mare Serenitatis. It is 32 miles in diameter, and is encompassed by a very massive rampart, rising at one peak on the E. to more than 6000 feet above the interior, and displaying, especially on the S.E., and N., many spurs and buttresses. The exterior slopes at sunrise, and even when the sun is more than  $10^{\circ}$  above the horizon, are seen to be traversed by wide and deep valleys. The S. *glacis* is especially broad, extending to a distance of 10 or 12 miles before it runs down to the level of the plain. The shape of the circumvallation,

when it is fully illuminated, approximates very closely to that of an equilateral triangle with curved sides. There are two bright little craters on the outer slope, just below the summit ridge on the S.E., and another, larger, on the N. wall, in which it makes a prominent gap. The interior is considerably brighter than the surface of the surrounding Mare, and, a little S. of the centre, includes two crater-like objects with broken rims. These assume different aspects under different conditions of illumination, and it is only when the floor is lighted by a comparatively low morning sun, that their true character is apparent. On the N.W. quarter of the interior are two smaller distinct craters, and a square arrangement of ridges. On the N.E. there are some hillocks and minor elevations. The Plinius rills form an especially interesting system, and under favourable conditions may be seen in their entirety with a good 4-inch refractor, about the time when the morning terminator passes through Julius Cæsar. They consist of three long fissures, originating amid the Hæmus highlands, on the S. side of the Mare Serenitatis, and diverging towards the W. The most southerly commences S.S.E. of the Acherusian promontory (a great headland, 5000 feet high, at the W. termination of the Hæmus range), and, following a somewhat undulating course, runs up to the N. side of Dawes. Under a low evening sun, I have remarked many inequalities in the width of that portion of it immediately N. of Plinius, which appear to indicate that it is here made up of rows of inosculating craters. The cleft north of this originates very near it, passes a little S. of the promontory, and runs to the E. edge of the plateau surrounding Dawes. The third and most northerly cleft begins at a point immediately N. of the promontory, cuts through the S. end of the well-known Serpentine ridge on the Mare Serenitatis, and, after following a course slightly concave to the N., dies out on the N. side of the plateau. This cleft forms the line of demarcation between the dark tone of the Mare Serenitatis and the light hue of the Mare Tranquilitatis, traceable under nearly every condition of illumination, and prominent in all good photographs.

DAWES.—A ring-plain 14 miles in diameter, situated N.W. of Plinius, on a nearly circular light area. Its bright border rises to a height of 2000 feet above the Mare, and includes a central mountain, a white marking on the E., and a ridge running from the mountain to the S. wall. There are two closely parallel clefts on the N. side of the plateau running from E. to W., that nearer Dawes being the longer, and having a craterlet standing

upon it about midway between its extremities. At its W. termination there is a crater-row running at right angles to it. The light area appears to be bounded on the E. by a low curved bank.

VITRUVIUS.—A ring-plain 19 miles in diameter with bright but not very lofty walls, situated among the mountains near the S.W. side of the Mare Serenitatis. It is surrounded by a region remarkable for its great variability in brightness. There is a large bright ring-plain on the W., with a less conspicuous companion on the S. of it.

MARALDI.—A deep but rather inconspicuous formation, bounded on the W. by a polygonal border. A small ring-plain with a central mountain is connected with the S.W. wall; and, running in a N. direction from this, is a short mountain arm which joins a large circular enclosure with a low broken border standing on the N. side of the Mare Tranquilitatis.

LITTRON.—A peculiar ring-plain, rather smaller than the last, some distance N. of Vitruvius, on the rocky W. border of the Mare Serenitatis. It is shaped like the letter D, the straight side facing the W. There is a distinct crater on the N. wall. On the N.W. it is flanked by three irregular ring-planes, and on the S.E. by a fourth. Neison shows two small mountains on the floor, but Schmidt, whose drawing is very true to nature, has no detail whatever. A fine cleft may be traced from near the foot of the E. wall to Mount Argæus, passing S. of a bright crater on the Mare E. of Littrow. It extends towards the Plinius system, and is probably connected with it.

MOUNT ARGÆUS.—There are few objects on the moon's visible surface which afford a more striking and beautiful picture than this mountain and its surrounding heights with their shadows a few hours after sunrise. It attains an altitude of more than 8000 feet above the Mare, and at a certain phase resembles a bright spear-head or dagger. There is a well-defined rimmed depression abutting on its southern point.

RÖMER.—A prominent formation of irregular outline, 24 miles in diameter, situated in the midst of the Taurus highlands. It has a very large central mountain, a crater on the N. side of the floor, and terraced inner slopes. Some distance on the N. is another ring, nearly as large, with a crater on its S. rim, and between this and Posidonius is another with a wide gap on the S. and a crater on its N. border. One of the most remarkable crater-rills on the moon runs from the E. side of Römer through

this latter ring, and then northwards on to the plain W. of Posidonius. Under suitable conditions, it can be seen as such in a 4-inch achromatic. It is easily traceable as a rill in a photograph of the N. polar region of the moon taken by MM. Henry at the Paris Observatory, and recently published in *Knowledge*.

LE MONNIER.—A great inflection or bay on the W. border of the Mare Serenitatis S. of Posidonius. Like many other similar formations on the edges of the Maria, it appears at one time or other to have had a continuous rampart, which on the side facing the "sea" has been destroyed. In this, as in most of the other cases, relics of the ruin are traceable under oblique light. A fine crescent-shaped mountain, 3000 feet high, stands near the S. side of the gap, and probably represents a portion of a once lofty wall. It will repay the observer to watch the progress of sunrise on the whole of the W. coast-line of the Mare up to Mount Argæus.

POSIDONIUS.—This magnificent ring-plain is justly regarded as one of the finest telescopic objects in the first quadrant. Its narrow bright wall with its serrated shadow, the conspicuous crater, the clefts and ridges and other details on the floor, together with the beautiful group of objects on the neighbouring plain, and the great Serpentine ridge on the E., never fail to excite the interest of the observer. The circumvallation, which is far from being perfectly regular, is about 62 miles in diameter, and, considering its size, is not remarkable for its altitude, as it nowhere exceeds 6000 feet above the interior, which is depressed about 2000 feet below the surrounding plain. Its continuity, especially on the E., is interrupted by gaps. On the N., the wall is notably deformed. It is broader and more regular on the W., where it includes a large longitudinal depression, and on the N.W. section stand two bright little ring-plains. On the floor, which shines with a glittering lustre, are the well-marked remains of a second ring, nearly concentric with the principal rampart, and separated from it by an interval of nine or ten miles. The most prominent object, however, is the bright crater a little E. of the centre. This is partially surrounded on the W. by three or four small bright mountains, through which runs in a meridional direction a rill-valley, not easily traced as a whole, except under a low sun. There is another cleft on the N.E. side of the interior, which is an apparent extension of part of the inner ring, a transverse rill-valley on the N., a fourth *quasi* rill on the N.W., and a fifth short cleft on the S. part of the floor.

Between the principal crater and the S.E. wall are two smaller craters, which are easy objects. Beyond the border on the N., in addition to Daniell, are four conspicuous craters and many ridges.

CHACORNAC.—This object, connected with Posidonius on the S.W., is remarkable for the brilliancy of its border and the peculiarity of its shape, which is very clearly that of an irregular pentagon with linear sides. I always find the detail within very difficult to make out. Two or more low ridges, traversing the floor from N. to S., and a small crater, are, however, clearly visible under oblique illumination. Schmidt draws a crater-rill, and Neison two parallel rills on the floor,—the former extends in a southerly direction to the W. side of Le Monnier.

DANIELL.—A bright little ring-plain N. of Posidonius. It is connected with a smaller ring-plain on the N.W. wall of the latter by a low ridge.

BOND, G. P.—A small bright ring-plain 12 miles in diameter, W. of Posidonius. Neison shows a crater both on the N. and S. rim. Schmidt omits these.

MAURY.—A bright deep little ring-plain, about 12 miles in diameter, on the W. border of the Lacus Somniorum. It is the centre of four prominent hill ranges.

GROVE.—A bright deep ring-plain, 15 miles in diameter, in the Lacus Somniorum, with a border rising 7000 feet above a greatly depressed floor, which includes a prominent mountain.

MASON.—The more westerly of two remarkable ring-planes, situated in the highlands on the S. side of the Lacus Mortis. It is 14 miles in diameter, has a distinct crater on its S. wall, and, according to Schmidt, a crater on the E. side of the floor.

PLANA.—A formation 23 miles in diameter, closely associated with the last. Neison states that the floor is convex and higher than the surrounding region. It has a triangular-shaped central mountain, a crater, and at least three other depressions on the S.W. wall where it joins Mason.

BURG.—A noteworthy formation, 28 miles in diameter, on the Mare, N. of Plana. The floor is concave, and includes a very large bright mountain, which occupies a great portion of it. The interior slopes are prominently terraced, and there are several spurs associated with the *glacis* on the S. and N.E. A distinct cleft runs from the N. side of the formation to the S.E. border of the Lacus Somniorum, which is crossed by another winding cleft running from a crater E. of Plana towards the N.E.



BAILY.—A small ring-plain, N. of Burg, flanked by mountains, with a large bright crater on the W. The group of mountains standing about midway between it and Burg are very noteworthy.

GÄRTNER.—A very large walled-plain with a low incomplete border on the E., but defined on the W. by a lofty wall. Schmidt shows a curved crater-row on the W. side of the floor.

DEMOCRITUS.—A deep regular ring-plain, about 25 miles in diameter, with a bright central mountain and lofty terraced walls.

ARNOLD.—A great enclosure, bounded, like so many other formations hereabouts, by straight parallel walls. There is a somewhat smaller walled-plain adjoining it on the W.

MOIGNO.—A ring-plain with a dark floor, adjoining the last on the N.E. There is a conspicuous little crater in the interior.

EUCTEMON.—This object is so close to the limb that very little can be made of its details under the most favourable conditions. According to Neison, there is a peak on the N. wall 11,000 feet in height.

METON.—A peculiarly-shaped walled-plain of great size, exhibiting considerable parallelism. The floor is seen to be very rugged under oblique illumination.

#### WEST LONGITUDE 20° TO 0°.

SABINE.—The more westerly of a remarkable pair of ring-planes, of which Ritter is the other member, situated on the E. side of the Mare Tranquillitatis a little N. of the lunar equator. It is about 18 miles in diameter, and has a low continuous border, which includes a central mountain on a bright floor. From a mountain arm extending from the S. wall, run in a westerly direction two nearly parallel clefts skirting the edge of the Mare. The more southerly of these terminates near a depression on a rocky headland projecting from the coast-line, and the other stops a few miles short of this. A third cleft, commencing at a point N.E. of the headland, runs in the same direction up to a small crater near the N. end of another cape-like projection. At 8h. on April 9, 1886, when the morning terminator bisected Sabine, I traced it still farther in the same direction. All these clefts exhibit considerable variations in width, but become narrower as they proceed westwards.

RITTER is very similar in every respect to the last. A curved rill mentioned by Neison is on the N.E. side of the

floor and is concentric with the wall. On the N. side of this ring-plain are three conspicuous craters, the two nearer being equal in size and the third much smaller.

SCHMIDT.—A bright crater at the foot of the S. slope of Ritter.

DIONYSIUS.—This crater, 13 miles in diameter, is one of the brightest spots on the lunar surface. It stands on the E. border of the Mare, about 30 miles E.N.E. of Ritter. A distinct crater-row runs round its outer border on the W., and ultimately, as a delicate cleft, strikes across the Mare to the E. side of Ritter. Both crater-row and cleft are easy objects in a 4-inch achromatic under morning illumination.

ARIADÆUS.—A bright little crater of polygonal shape, with another crater of about one-third the area adjoining it on the N.W., situated on the rocky E. margin of the Mare Tranquilitatis, N.E. of Ritter. A short cleft runs from it towards the latter, but dies out about midway. A second cleft begins near its termination, and runs up to the N.E. wall of Ritter. E. of this pair a third distinct cleft, originating at a point on the coast-line about midway between Ariadæus and Dionysius, ends near the same place on the border. There is a fourth cleft extending from the N. side of a little bay N. of Ariadæus across the Mare to a point N.W. of the more northerly of the three craters N. of Ritter. At a small crater on the S. flank of the mountains bordering the little bay N. of Ariadæus originates one of the longest and most noteworthy clefts on the moon's visible surface, discovered more than a century ago by Schröter of Lilienthal. It varies considerably in breadth and depth, but throughout its course over the plain, between Ariadæus and Silberschlag, it can be followed without difficulty in a very small telescope. E. of the latter formation, towards Hyginus (with which rill-system it is connected), it is generally more difficult. A few miles E. of Ariadæus it sends out a short branch, running in a S.W. direction, which can be traced as a fine white line under a moderately high sun. It is interesting to follow the course of the principal cleft across the plain, and to note its progress through the ridges and mountain groups it encounters. In the great Lick telescope it is seen to traverse some old crater-rings which have not been revealed in smaller instruments. About midway between Ariadæus and Silberschlag it exhibits a duplication for a short distance, first detected by Webb.

DE MORGAN.—A brilliant little crater, 4 miles in diameter, on the plain S. of the Ariadæus cleft.

CAYLEY.—A very deep bright crater, with a dark interior, N. of the last, and more than double its diameter. There is a second crater between this and the cleft.

WHEWELL.—Another bright little ring, about 3 miles in diameter, some distance to the E. of De Morgan and Cayley.

SOSIGENES.—A small circular ring-plain, 14 miles in diameter, with narrow walls, a central mountain, and a minute crater outside the wall on the E.; situated on the E. side of the Mare Tranquilitatis, W. of Julius Cæsar. There is another crater, about half its diameter, on the S., connected with it by a low mound. This has a still smaller crater on the W. of it.

JULIUS CÆSAR.—A large incomplete formation of irregular shape. The wall on the E. is much terraced, and forms a flat "S" curve. The summit ridge is especially bright, and has a conspicuous little crater upon it. On the W. is a number of narrow longitudinal valleys trending from N. to S., included by a wide valley which constitutes the boundary on this side. The border on the S. consists of a number of low rounded banks, those immediately E. of Sosigenes being traversed by several shallow valleys, which look as if they had been shaped by alluvial action. There is a brilliant little hill at the end of one of these valleys, a few miles E. of Sosigenes. The floor of Julius Cæsar is uneven in tone, becoming gradually duskier from S. to N., the northern end ranking among the darkest areas on the lunar surface. There are at least three large circular swellings in the interior. A long low mound, with two or three depressions upon it, bounds the wide valley on the E. side.

GODIN.—A square-shaped ring-plain, 28 miles in diameter, with rounded corners. The bright rampart is everywhere lofty, except on the S., is much terraced, and includes a central mountain. On the S. a curious trumpet-shaped valley, extending some distance towards the S.W., and bounded by bright walls, is a noteworthy feature at sunrise. There are other longitudinal valleys with associated ridges on this side of the formation, all running in the same direction. There is a large bright crater outside the border on the N.E., and, between it and the wall, another, smaller, which is readily seen under a high sun.

AGRIPPA.—A ring-plain 28 miles in diameter on the N. of the last, with a terraced border rising to a height of between 7000 and 8000 feet above the floor, which contains a large bright central mountain and two craters on the S. The shape of this formation deviates very considerably from circularity, the N. wall, on which

stands a small crater, being almost lineal. On the W., at a distance of a few miles, runs the prominent mountain range, extending northwards nearly up to the E. flank of Julius Cæsar, which bounds the E. side of the great Ariadæus plain. Between this rocky barrier and Agrippa is a very noteworthy enclosure containing much minute detail and a long straight ridge resembling a cleft. A few miles N. of Agrippa stands a small crater; at a point W. of which the Hyginus cleft originates.

SILBERSCHLAG.—A very brilliant crater, 8 or 9 miles in diameter, connected with the great mountain range just referred to. The Ariadæus cleft cuts through the range a few miles N. of it. This neighbourhood at sunrise presents a grand spectacle. With high powers under good atmospheric conditions, the plain E. of the mountains is seen to be traversed by a number of shallow winding valleys, trending towards Agrippa, and separated by low rounded hills which have all the appearance of having been moulded by the action of water.

BOSCOVICH.—This is not a very striking telescopic object under any phase, on account of its broken, irregular, and generally ill-defined border. It is, however, remarkable as being one of the darkest spots on the visible surface: in this respect a fit companion to Julius Cæsar, its neighbour on the W. Schmidt shows some ridges within it.

RHÆTICUS.—A very interesting formation, about 25 miles in diameter, situated near the lunar equator, with a border intersected by many passes. A deep rill-like valley winds round its eastern *glacis*, commencing on the S. at a small circular enclosure standing at the end of a spur from the wall; and, after crossing a ridge W. of a bright little crater on the N. of the formation, apparently joins the most easterly cleft of the Triesnecker system. A cleft traverses the N. side of the floor of Rhæticus, and extends across the plain on the E. as far as the N. side of Réaumur.

TRIESNECKER.—Apart from being the centre of one of the most remarkable rill-systems on the moon, this ring-plain, though only about 14 miles in diameter, is an object especially worthy of examination under every phase. At sunrise, and for some time afterwards, owing to the superior altitude of the N.W. section of the wall, a considerable portion of the border on the N. and N.E. is masked by its shadow, which thus appears to destroy its continuity. On more than one occasion, friends, to whom I have shown this object under these conditions, have likened it to a breached volcanic cone, a comparison which at a later stage is seen to be

very inappropriate. The rampart is terraced within, and exhibits many spurs and buttresses without, especially on the N.W. The central mountain is small and not conspicuous. The rill-system is far too complicated to be intelligibly described in words. It lies on the W. side of the meridian passing through the formation, and extends from the N. side of Rhæticus to the mountain-land lying between Ukert and Hyginus on the N. Birt likened these rills to "an inverted river system," a comparison which will commend itself to most observers who have seen them on a good night, for in many instances they appear to become wider and deeper as they approach higher ground. Published maps are all more or less defective in their representations of them, especially as regards that portion of the system lying N. of Triesnecker.

HYGINUS.—A deep depression, rather less than 4 miles across, with a low rim of varying altitude, having a crater on its N. edge. This formation is remarkable for the great cleft which traverses it, discovered by Schröter in 1788. The coarser parts of this object are easily visible in small telescopes, and may be glimpsed under suitable conditions with a 2-inch achromatic. Commencing a little W. of a small crater N. of Agrippa, it crosses, as a very delicate object, a plain abounding in low ridges and shallow valleys, and runs nearly parallel to the eastern extension of the Ariadæus rill. As it approaches Hyginus it becomes gradually coarser, and exhibits many expansions and contractions, the former in many cases evidently representing craters. When the phase is favourable, it can be followed across the floor of Hyginus, and I have frequently seen the banks with which it appears to be bounded (at any rate within the formation), standing out as fine bright parallel lines amid the shadow. On reaching the E. wall, it turns somewhat more to the N., becomes still coarser and more irregular in breadth, and ultimately expands into a wide valley on the N.E. It is connected with the Ariadæus cleft by a branch which leaves the latter at an acute angle on the plain E. of Silberschlag, and joins it about midway between its origin N. of Agrippa and Hyginus. It is also probably joined to the Triesnecker system by one or more branches E. of Hyginus.

On May 27, 1877, Dr. Hermann Klein of Cologne discovered, with a 5½-inch Plösel dialyte telescope, a dark apparent depression without a rim in the Mare Vaporum, a few miles N.W. of Hyginus, which, from twelve years' acquaintance with the region, he was certain had not been visible during that period. On the announcement of this discovery in the *Wochenschrift für Astronomie*

in March of the following year, the existence of the object described by Dr. Klein was confirmed, and it was sedulously scrutinised under various solar altitudes. To most observers it appeared as an ill-defined object with a somewhat nebulous border, standing on an irregularly-shaped dusky area, with two or more small dark craters and many low ridges in its vicinity. A little E. of it stands a curious spiral mountain called the Schneckenberg. The question as to whether Hyginus N. (as the dusky spot is called) is a new object or not, cannot be definitely determined, as, in spite of a strong case in favour of it being so, there remains a residuum of doubt and uncertainty that can never be entirely cleared away. After weighing, however, all that can be said "for and against," the hypothesis of change seems to be the most probable.

UKERT.—This bright crater, 14 miles in diameter, situated in the region N.E. of Triesnecker, is surrounded by a very complicated arrangement of mountains; and on the N. and W. is flanked by other enclosures. It has a distinct central mountain. Its most noteworthy feature is the great valley, more than 80 miles long, which extends from N.E. to S.W. on the E. side of it. This gorge is at least six miles in breadth, of great depth, and is only comparable in magnitude with the well-known valley which cuts through the Alps, W. of Plato. A delicate cleft, not very clearly traceable as a whole, begins near its N. end, and terminates amid the ramifications of the Apennines S. of Marco Polo.

TAQUET.—A conspicuous little crater on the S. border of the Mare Serenitatis at the foot of the Hæmus Mountains. A branch of the great Serpentine ridge, which traverses the W. side of this plain and other lesser elevations, run towards it.

MENELAUS.—A conspicuously bright regular ring-plain, about 20 miles in diameter, situated on the S. coast-line of the Mare Serenitatis, and closely associated with the Hæmus range. It has a brilliant central mountain, but no visible detail on the walls. On the edge of the Mare, S.W. of it, there is a curious square formation. The bright streak traversing the Mare from N. to S., which is so prominently displayed in old maps of the moon, passes through this formation.

SULPICIOUS GALLUS.—Another brilliant object on the south edge of the Mare Serenitatis, some distance E. of the last. It is a deep circular crater about 8 miles in diameter, rising to a considerable height above the surface. Its shadow under a low morning sun is prominently jagged. On the E. are two bright mounds,

and S. of that which is nearer the border of the Mare, commences a cleft which, following the curvature of the coast-line, terminates at a point in W. long.  $9^{\circ}$ . This object varies considerably in width and depth. Another shorter and coarser cleft runs S. of this across an irregularly shaped bay or inflexion in the border of the Mare.

MANILIUS.—This, one of the most brilliant objects in the first quadrant, is about 25 miles in diameter, with walls nearly 8000 feet above the floor, which includes a bright central mountain. The inner slope of the border on the E. is much terraced and contains some depressions. There is a small isolated bright mountain 2000 feet high on the Mare Vaporum, some distance to the E.

BESSEL.—A bright circular crater, 14 miles in diameter, on the S. half of the Mare Serenitatis, and the largest object of its class thereon. Its floor is depressed some 2000 feet below the surrounding surface, while the walls, rising nearly 1600 feet above the plain, have peaks both on the N. and S. about 200 feet higher. The shadows of these features, noted by Schröter in 1797, and by many subsequent observers, are very noteworthy. I have seen the shadow of a third peak about midway between the two. One may faintly imagine the magnificent prospect of the coast-line of the Mare with the Hæmus range, which would be obtained were it possible to stand on the summit of one of these elevations. It is doubtful whether Bessel has a central mountain. Neither Mädler nor Schmidt have seen one, though Webb noted a peak on two occasions. I fail to see anything within the crater. The bright streak crossing the Mare from N. to S. passes through Bessel.

LINNÉ.—A formation on the E. side of the Mare Serenitatis, described by Lohrmann and Mädler as a deep crater, but which in 1866 was found by Schmidt to have lost all the appearance of one. The announcement of this apparent change led to a critical examination of the object by most of the leading observers, and to a controversy which, if it had no other result, tended to awaken an interest in selenography that has been maintained ever since. According to Mädler, the crater was more than 6 miles in diameter in his time, and very conspicuous under a low sun, a description to which it certainly did not answer in 1867 or at any subsequent epoch. It is anything but an easy object to see well, as there is a want of definiteness about it under the best conditions, though the minute crater, the low ridges, and the nebulous whiteness described by Schmidt and noted by Webb and others, are traceable at the proper phase. As in the case of Hyginus N, there are still many sceptics as regards actual change,

despite the records of Lohrmann and Mädler; but the evidence in favour of it seems to preponderate.

CONON.—A bright little crater, 11 miles in diameter, situated among the intricacies of the Apennines, S. of Mount Bradley. It has a central hill, which is not a difficult object.

ARATUS.—One of the most brilliant objects on the visible surface of the moon, a crater 7 miles in diameter, S. of Mount Hadley, surrounded by the lofty mountain arms and towering heights of the Apennines. A peak close by on the N. is more than 10,000 feet, and another farther removed towards the N.W. is over 14,000 feet in altitude.

AUTOLYCUS.—A ring-plain 23 miles in diameter, deviating considerably from circularity, W. of Archimedes, on the Mare Imbrium, or rather on that part of it termed the Palus Putredinis. Its floor, which contains an inconspicuous central mountain, is depressed some 4000 feet below the surrounding country. With a power of 150 on a  $4\frac{5}{8}$  achromatic, Dr. Sheldon of Macclesfield has seen two shallow crateriform depressions in the interior, one nearly central, and the other about midway between it and the N. wall. The wall is terraced within, and has a crater just below its crest on the W., which, when the opposite border is on the morning terminator, is seen as a distinct notch. Autolycus is the centre of a minor ray-system.

ARISTILLUS.—A larger and much more elaborate ring-plain, 34 miles in diameter, N. of Autolycus. Its complex wall, with its terraces within, and its buttresses, radiating spurs, and gullies without, forms a grand telescopic object under a low sun on a good night. It rises on the east 11,000 feet above the Mare, and is about 2000 feet lower on the W., while the interior is depressed some 3000 feet. Its massive central mountain, surmounted by many peaks, occupies a considerable area on the floor, and exhibits a digitated outline at the base. On the S. and W. a number of deep valleys radiate from the foot of the border, some of them extending nearly as far as Autolycus. Shallower but more numerous and regular features of the same class radiate towards the N.E. from the foot of the opposite wall. On the N.W. are several curved ridges, all trending towards Theætetus. On the S.E. the surface is trenched by a number of crossed gullies, well seen when the E. wall is on the morning terminator. Just beyond the N. *glacis* is a large irregular dusky enclosure with a central mound, and another smaller low ring adjoining it on the S.E. The visibility of these objects is very ephemeral, as they



disappear soon after sunrise. Aristillus is also the centre of a bright ray system.

THEÆTETUS.—A conspicuous ring-plain, about 16 miles in diameter, in the Palus Nebularum, N.W. of Aristillus. It is remarkable for its great depth, the floor sinking nearly 5000 feet below the surface. Its walls, 7000 feet high on the W., are devoid of detail. The *glacis* on the S.W. has a gentle slope, and extends for a great distance before it runs down to the level of the plain. Not far from the foot of the wall on the N. is a row of seven or eight bright little hills, near the eastern side of which originates a distinct cleft that crosses the Palus in a N.W. direction, and terminates among mountains between Cassini and Calippus. I have seen this object easily with a 4-inch achromatic.

CALIPPUS.—A bright ring-plain 17 miles in diameter, situated in the midst of the intricate Caucasus Mountain range. On the E. is a brilliant peak rising more than 13,000 feet above the Palus Nebularum, and nearer the border, on the N.E., is a second, more than 500 feet higher, with many others nearly as lofty in the vicinity. Calippus has not apparently a central peak or any other features on the floor.

CASSINI.—This remarkable ring-plain, about 36 miles in diameter, is very similar in character to Posidonius. It has a very narrow wall, nowhere more than 4000 feet in height, and falling on the E. to 1500 feet. Though a prominent and beautiful object under a low sun, its attenuated border and the tone of the floor, which scarcely differs from that of the surrounding surface, render it difficult to trace under a high angle of illumination, and perhaps accounts for the fact that it escaped the notice of Hevel and Riccioli; though it is certainly strange that a formation which is thrown into such strong relief at sunrise and sunset should have been overlooked, while others hardly more prominent at these times have been drawn and described. The outline of Cassini is clearly polygonal, being made up of several rectilineal sections. The interior, nearly at the same level as the outside country, includes a large bright ring-plain, A, 9 miles in diameter and 2600 feet in depth, which has a good-sized crater on the S. edge of a great bank which extends from the S.W. side of this ring-plain to the wall. On the E. side of the floor, close to the inner foot of the border, is a bright deep crater about two-thirds of the diameter of A, and between it and the latter Brenner has seen three small hills. The outer slope of Cassini includes much detail. On the S.W. is a row of shallow depressions

just below the crest of the wall, and near the foot of the slope is a large circular shallow depression associated with a valley which runs partly round it. The shape of the *glacis* on the W is especially noteworthy, the S W and N W sides meeting at a slightly acute angle at a point 10 or 12 miles W. of the summit of the ring. On the outer E slope is a curious elongated depression, and on the N slope two large dusky rings, well shown by Schmidt, but omitted in other maps. Most of these details are well within the scope of moderate apertures. Perhaps the most striking view of Cassini and its surroundings is obtained when the morning terminator is on the central meridian.

ALEXANDER — A large irregularly shaped plain, at least 60 miles in longest diameter, enclosed by the Caucasus Mountains. On the S W and N W the border is lineal. It has a dark level floor on which there is a great number of low hills.

EUDOXUS — A bright deep ring-plain, about 40 miles in diameter, in the hilly region between the Mare Serenitatis and the Mare Frigoris, with a border much broken by passes, and deviating considerably from circularity. Its massive walls, rising more than 11,000 feet above the floor on the W, and about 10,000 feet on the opposite side, are prominently terraced, and include crater-rows in the intervening valleys, while their outer slopes present a complicated system of spurs and buttresses. There is a bright crater on the N *glacis*, and some distance beyond the wall on the N.W. is a small ring-plain, and on the S E another, with a conspicuous crater between it and the wall. Neison draws attention to an area of about 1400 square miles on the N.E. which is covered with a great multitude of low hills. E. of Eudoxus are two short crossed clefts, and on the N. a long cleft of considerable delicacy running from N E to S W. It was in connection with this formation that Trouvelot, on February 20, 1877, when the terminator passed through Aristillus and Alphonsus, saw a very narrow thread of light crossing the S part of the interior and extending from border to border. He noted also similar appearances elsewhere, and termed them *Murs enigmatiques*.

ARISTOTELES — A magnificent ring-plain, 60 miles in diameter, with a complex border, surmounted by peaks, rising to nearly 11,000 feet above the floor, one of which on the W., pertaining to a terrace, stands out as a brilliant spot in the midst of shadow when the interior is filled with shadow. The formation presents its most striking aspect at sunrise, when the shadow of the W. wall just covers the floor, and the brilliant inner slope of the

E wall with the little crater\* on its crest is fully illuminated. At this phase the details of the terraces are seen to the best advantage. The arrangement of the parallel ridges and rows of hills on the N.E. and S.W. is likewise better seen at this time than under an evening sun. A bright and deep ring-plain, about 10 miles in diameter, with a distinct central mountain, is connected with the W wall.

EGEDE —A lozenge-shaped formation, about 18 miles from corner to corner, bounded by walls scarcely more than 400 feet in height. It is consequently only traceable under very oblique illumination.

THE GREAT ALPINE VALLEY.—A great wedge-shaped depression, cutting through the Alps W. of Plato, from W.N.W. to E.S.E. It is more than 80 miles in length, and varies in breadth from 6 miles on the S. to less than 4 miles on the N, where it approaches the S border of the Mare Frigoris. For a greater part of its extent it is bounded on the S.W. side by a precipitous linear cliff, which, under a low evening sun, is seen to be fringed by a row of bright little hills. These are traceable up to one of the great mountain masses of the Alps, forming the S.W. side of the great oval-shaped expansion of the valley, whose shape has been appropriately compared to that of a Florence oil-flask, and which Webb terms "a grand amphitheatre." On the opposite or N.E. side, the boundary of the valley is less regular, following a more or less undulating line up to a point opposite, and a little N of, the great mountain mass, where it abuts on a shallow *quasi* enclosure with lofty walls, which, projecting westwards, considerably diminish the width of the valley. South of this lies another curved mountain ring, which still farther narrows it. This curtailment in width represents the neck of the flask, and is apparently about 16 or 17 miles in length, and from 3 to 4 miles in breadth, forming a gorge, bordered on the W. by nearly vertical cliffs, towering thousands of feet above the bottom of the valley, and on the E by many peaked mountains of still greater altitude. At the entrance to the "amphitheatre," the actual distance between the colossal rocks which flank the defile is certainly not much more than 2 miles. From this standpoint the view across the level interior of the elliptical plain would be of extraordinary magnificence. Towards the S., but more than 12 miles distant, the outlook of an observer would be limited by some of the loftiest peaks of the Alps, whose flanks form the boundary of the enclosure, through which,

however, by at least three narrow passes he might perchance get a glimpse of the Mare Imbrium beyond. The broadest of these aligns with the axis of the valley. It is hardly more than a mile wide at its commencement on the S. border of the "amphitheatre," but expands rapidly into a trumpet-shaped gorge, flanked on either side by the towering heights of the Alps as it opens out on to the Mare. The bottom, both of the "amphitheatre" and of the long wedge-shaped valley, appears to be perfectly level, and, as regards the central portion of the latter, without visible detail. Under morning illumination I have, however, frequently seen something resembling a ridge partially crossing "the neck," and, near sunset, a tongue of rock jutting out from the E. flank of the constriction, and extending nearly from side to side. At the base of the cliff bordering the valley on the S.W., five or six little circular pits have been noted, some of which appear to have rims. They were seen very perfectly with powers of 350 and 400 on an  $8\frac{1}{2}$ -inch Calver reflector at 8 h. on January 25, 1885, and have been observed, but less perfectly, on subsequent occasions. The most northerly is about 10 miles from the N.W. end of the formation, and the rest occur at nearly regular intervals between it and "the neck." In the neighbourhood of the valley, on either side, there are several bright craters. Three stand near the N.E. edge, and one of considerable size near the N.W. end on the opposite side. A winding cleft crosses the valley about midway, which, strange to say, is not shown in the maps, though it may be seen in a 4-inch achromatic. It originates apparently at a bright triangular mountain on the plain S.W. of the valley, and, after crossing the latter somewhat obliquely, is lost amid the mountains on the opposite side. That portion of it on the bottom of the valley is easily traceable under a high light as a white line. The region N. of the Alps on the S.W. side of the valley presents many details worthy of examination. Among them, parallel rows of little hills, all extending from N.W. to S.E. There is also a number of still smaller objects of the same type on the E. side. The great Alpine valley, though first described by Schröter, is said to have been discovered on September 22, 1727, by Bianchini, but it is very unlikely that an object which is so prominent when near the terminator was not often remarked before this.

ARCHYTAS.—A bright ring-plain, 21 miles in diameter, on the edge of the Mare Frigoris, due N. of the Alpine Valley, with regular walls rising about 5000 feet above the interior on the N.W., and about 4000 feet on the opposite side. It has a very

bright central mountain. Several spurs radiate from the wall on the S., and a wide valley, flanked by lofty heights, forming the S.W. boundary of W. C. Bond, originates on the N. side. There is also a crater-rill running towards the N.W. On the Mare, S.W. of Archytas, is a somewhat smaller ring-plain, Archytas A (called by Schmidt, PROTAGORAS), with lofty walls and a central hill.

CHRISTIAN MAYER.—A prominent rhomboidal-shaped ring-plain, 18 miles in diameter, associated on every side, except the N., with a number of irregular inconspicuous enclosures. It has a central peak. Mädler discovered two delicate short clefts, both running from N.W. to S.E., one on the W. and the other on the E. of this formation.

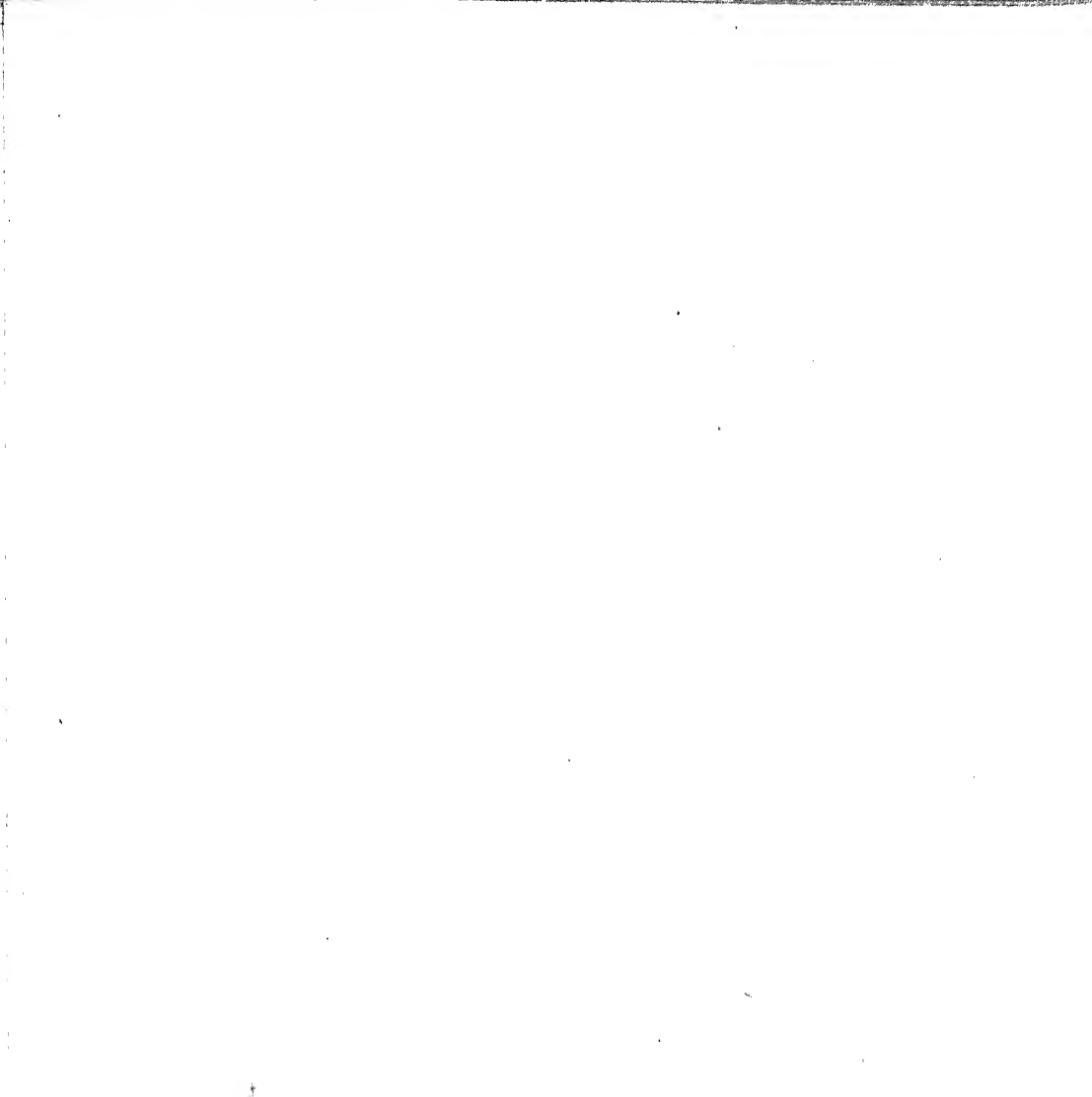
W. C. BOND.—A great enclosed plain of rhomboidal shape on the N. of Archytas, the bright ring-plain Timæus standing near its E. corner, and another conspicuous but much smaller enclosure with a smaller crater W. of it on the floor at the opposite angle. The interior, which is covered with rows of hillocks, is very noteworthy at sunrise.

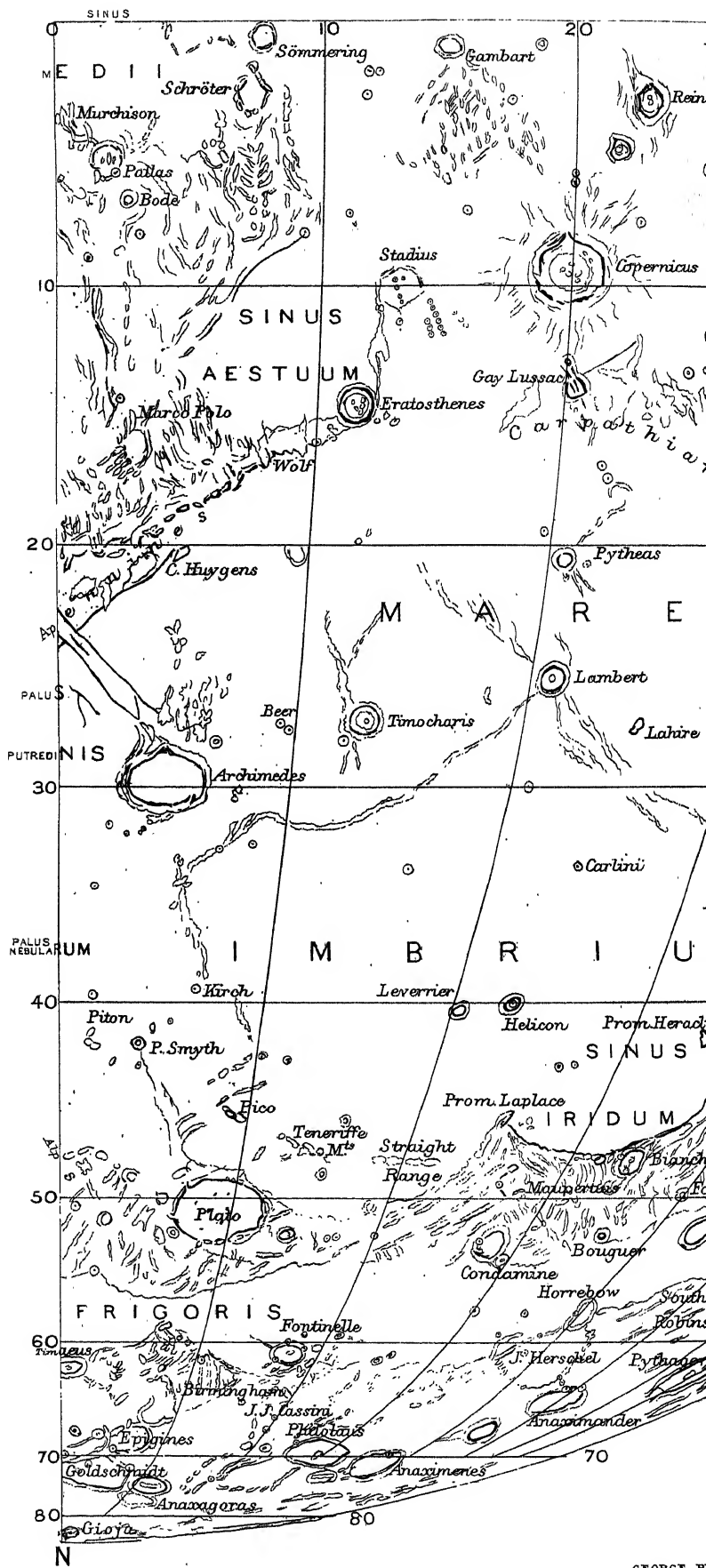
BARROW.—There are few more striking or beautiful objects at sunrise than this, mainly because of the peculiar shape of its brilliant border and the remarkable shadows of the lofty peaks on its western wall. There is a notable narrow gap in the rampart on the W., which appears to extend to the level of the floor. The walls, especially on the S., are very irregular, and include two large deep craters and some minor depressions. If the formation is observed when its E. wall is on the morning terminator, a fine view is obtained of the remarkable crater-row which winds round the N. side of Goldschmidt. Barrow is about 40 miles in diameter. According to Schmidt, there is one crater in the interior, a little S.E. of the centre.

SCORESBY.—A much fore-shortened deep ring-plain, 36 miles in diameter, between Barrow and the limb. It has a central mountain with two peaks, which are very difficult to detect.

CHALLIS.—A ring-plain adjoining Scoresby on the N.E. It is of about the same size and shape.

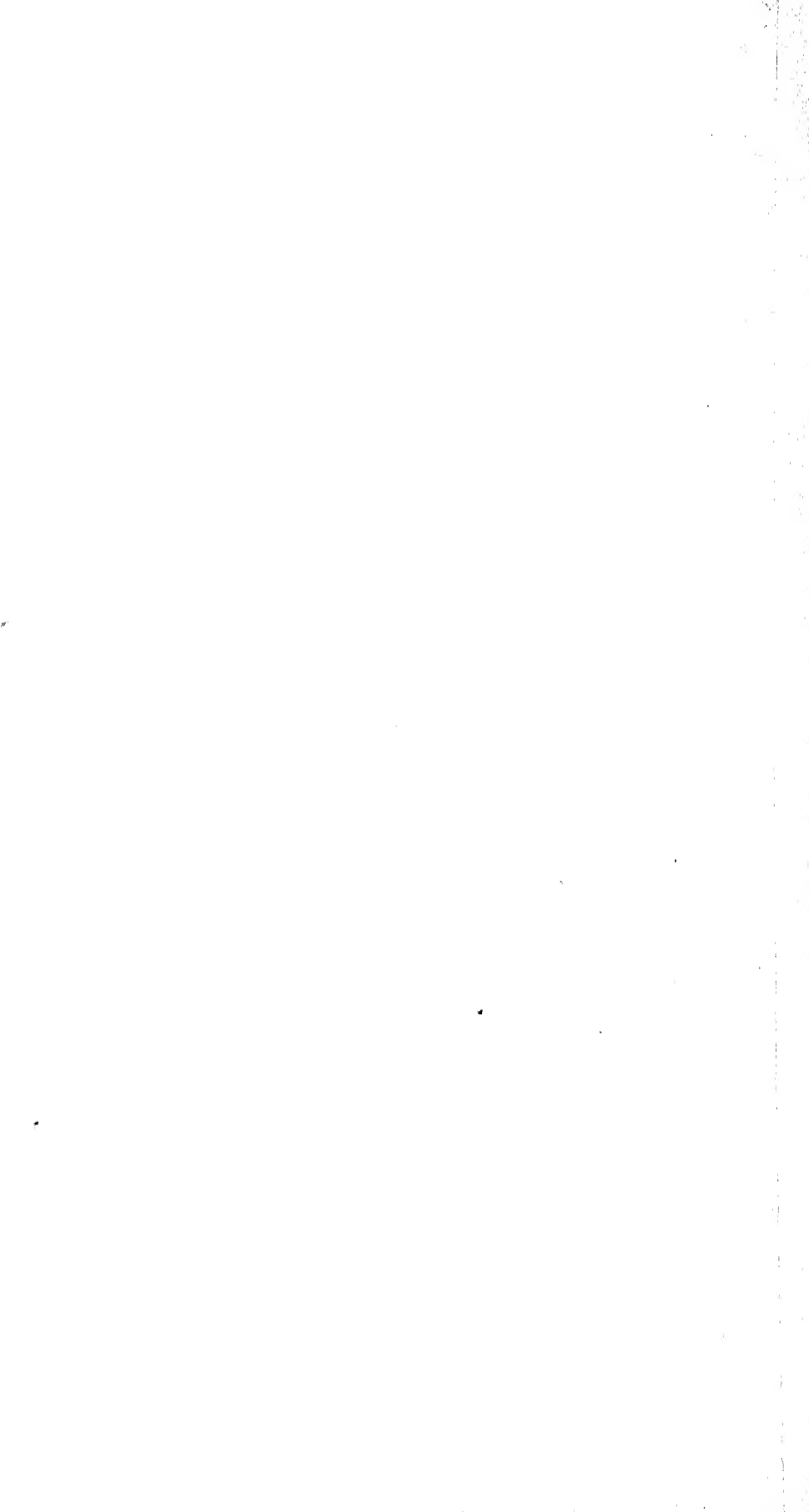
MAIN.—A very similar formation, on the N. of the last, much too near the limb to be well observed.











## SECOND QUADRANT

EAST LONGITUDE  $0^{\circ}$  TO  $20^{\circ}$

MURCHISON.—A considerable ring-plain about 35 miles across on the E., where it abuts on Pallas. It is a pear-shaped formation, bounded on the N. by a mountainous region, and gradually diminishes in width towards the S.E., on which side it is open to the plain. The walls are of no great altitude, but, except on the N.W., are very bright. At the S. termination of the W. wall there is an exceedingly brilliant crater, Murchison A, five miles in diameter and some 3000 feet deep; adjoining which on the N.W. is an oval depression and a curious forked projection from the border. The only objects visible in the interior are a few low ridges on the E. side, and a number of long spurs running out from the wall on the N. towards the centre of the floor. Murchison A is named CHLADNI by Lohrmann.

PALLAS.—A fine ring-plain, about 32 miles in diameter, forming with Murchison an especially beautiful telescopic object under suitable illumination. Its brilliant border, broken by gaps on the W., where it abuts on Murchison, has a bright crater on the N.E., from which, following the curvature of the wall, and just below its crest, runs a valley in an easterly direction. There is a large bright central mountain on the floor, with a smaller elevation to the S. of it, and a ridge extending from the N. wall to near the centre. On the W., a section of the border is continued in a N. direction far beyond the limits of the formation; and on the S. it is connected with a small incomplete ring; on the E. of which, near the foot of the wall, is a somewhat smaller and much duskier enclosure.

BODE.—A brilliant ring-plain, 9 miles in diameter, situated on the N. side of Pallas. Its walls rise about 5000 feet above the interior, which is considerably depressed, and includes, according to Schmidt and Webb, a mountain or ridge. There are two parallel valleys on the W., which are well worth examination.

SÖMMERING.—An incomplete ring-plain, 17 miles in diameter,

situated on the lunar equator. It has rather low broken walls and a dark interior.

SCHRÖTER.—A somewhat larger formation, with a border wanting on the S. Schmidt draws a considerable crater on the S.W. side of the floor. It was in the region north of this object, which abounds in little hills and low ridges, that in the year 1822 Gruithuisen discovered a very remarkable formation consisting of a number of parallel rows of hills branching out (like the veins of a leaf from the midrib) from a central valley at an angle of  $45^\circ$ , represented by a depression between two long ridges running from north to south. The regularly arranged hollows between the hills and the longitudinal valley suggested to his fertile imagination that he had at last found a veritable city in the moon—possibly the metropolis of Kepler's *Subvolvani*, who were supposed to dwell on that hemisphere of our satellite which faces the earth. At any rate, he was firmly convinced that it was the work of intelligent beings, and not due to natural causes. This curious arrangement of ridges and furrows, which, according to Webb, measures about 23 miles both in length and breadth, is, owing to the shallowness of the component hills and valleys, a very difficult object to see in its entirety, as it must be viewed when close to the terminator, and even then the sun's azimuth and good definition do not always combine to afford a satisfactory glimpse of its ramifications. M. Gaudibert has given a drawing of it in the *English Mechanic*, vol. xviii. p. 638.

GAMBART.—A regular ring-plain, 16 miles in diameter, with a low border and without visible detail within; situated nearly on the lunar equator, about 130 miles S.S.W. of Copernicus, at the N.W. edge of a very hilly region. A prominent pear-shaped mountain, with a small crater upon it, stands a short distance on the S.W., and further in the same direction, a large bright crater with two much smaller craters on the N. of it. The rough hilly district about midway between Copernicus and Gambart is remarkable for its peculiar dusky tone and for certain small dark spots, first seen by Schmidt, and subsequently carefully observed by Dr. Klein. The noteworthy region where these peculiar features are found represents an area of many thousand square miles, and must resemble a veritable *Malpais*, covered probably with an incalculable number of craters, vents, cones, and pits, filled with volcanic *débris*. It is among details of this character that the true analogues of some terrestrial volcanoes must be looked for. Under a low angle of illumination the surface pre-

sents an extraordinarily rough aspect, well worthy of examination, but the dusky areas and the black spots can only be satisfactorily distinguished under a somewhat high sun. I have, however, seen them fairly well when the W. wall of Reinhold was on the morning terminator.

MARCO POLO.—A small and very irregularly-shaped enclosure (difficult to see satisfactorily) on the S. flank of the Apennines. It is hemmed in on every side by mountains.

ERATOSTHENES.—A noble ring-plain, 38 miles in diameter; a worthy termination of the Apennines. The best view of it is obtained under morning illumination when the interior is about half-filled with shadow. At this phase the many irregular terraces on the inner slope of the E. wall (which rises at one peak 16,000 feet above an interior depressed 8000 feet below the Mare Imbrium) are seen to the best advantage. The central mountain is made up of two principal peaks, nearly central, from which two bright curved hills extend nearly up to the N.W. wall,—the whole forming a V-shaped arrangement. On the S. there is a narrow break in the wall, and the S.W. section of it seems to overlap and extend some distance beyond the S.E. section. The border on the S.W. is remarkable for the great width of its *glacis*. Eratosthenes exhibits a marked departure from circularity, especially on the E., where the wall consists of two well-marked linear sections, with an intermediate portion where the crest for 20 miles or more bends inwards or towards the centre. From the S.E. flank of this formation extends towards the W. side of Stadius one of the grandest mountain arms on the moon's visible surface, rising at one place 9000 feet, and in two others 5000 and 3000 feet respectively above the Mare Imbrium. If this magnificent object is observed when the morning terminator falls a little E. of Stadius, it affords a spectacle not easily forgotten. I have often seen it at this phase when its broad mass of shadow extended across the well-known crater-row W. of Copernicus, some of the component craters appearing between the spires of shade representing the loftiest peaks on the mountain arm. There is a prominent little crater on the crest of the arm between two of the peaks, and another on the plain to the west.

STADIUS.—An inconspicuous though a very interesting formation, 43 miles in diameter, W. of Copernicus, with a border scarcely exceeding 200 feet in height. Hence it is not surprising that it was for a long time altogether overlooked by Mädler. Except as a known object, it is only traceable under very oblique

illumination, and even then some attention is required before its very attenuated wall can be followed all round. It is most prominent on the W., where it apparently consists of a S. extension of the Eratosthenes mountain-arm, and is associated with a number of little craters and pits. This is succeeded on the S.W. by a narrow strip of bright wall, and on the S. by a section made up of a piece of straight wall and a strip curving inwards, forming the S. side. On the E. the border assumes a very ghostly character, and appears to be mainly defined by rows of small depressions and mounds. On the N.E., N., and N.W. it is still lower and narrower; so much so, that it is only for an hour or so after sunrise or before sunset that it can be traced at all. On every side, with the exception of the curved piece on the S., the wall consists of linear sections. The interior contains a great number of little craters and very low longitudinal mounds. Ten craters are shown in Beer and Mädler's map. Schmidt only draws fifteen, though in the text accompanying his chart he says that he once counted fifty. In the monograph published in the *Journal* of the Liverpool Astronomical Society (vol. v. part 8), forty-one are represented. They appear to be rather more numerous on the S. half of the floor than elsewhere. Just beyond the limits of the border on the N., is a bright crater with a much larger obscure depression on the W. of it. The former is surrounded by a multitude of minute craters and crater-cones, which are easily seen under a low sun. Though almost every trace of Stadius disappears under a high light, I have had little difficulty in seeing portions of the border and some of the included details when the morning terminator had advanced as far as the E. wall of Herodotus, and the site was traversed by innumerable light streaks radiating from Copernicus. At this phase the bright crater, just mentioned, on the N. edge of the border was tolerably distinct.

COPERNICUS.—This is without question the grandest object, not only on the second Quadrant, but on the whole visible superficies of the moon. It undoubtedly owes its supremacy partly to its comparative isolation on the surface of a vast plain, where there are no neighbouring formations to vie with it in size and magnificence, but partly also to its favourable position, which is such, that, though not central, is sufficiently removed from the limb to allow all its manifold details to be critically examined without much foreshortening. There are some other formations, Langrenus and Petavius, for example, which, if they were equally

well situated, would probably be fully as striking; but, as we see it, Copernicus is *par excellence* the monarch of the lunar ring-mountains. Schmidt remarks that this incomparable object combines nearly all the characteristics of the other ring-plains, and that careful study directed to its unequalled beauties and magnificent form is of much more value than that devoted to a hundred other objects of the same class. It is fully 56 miles in diameter, and, though generally described as nearly circular, exhibits very distinctly under high powers a polygonal outline, approximating very closely to an equilateral hexagon. There are, however, two sections of the crest of the border on the N.E. which are inflected slightly towards the centre, a peculiarity already noticed in the case of Eratosthenes. The walls, tolerably uniform in height, are surmounted by a great number of peaks, one of which on the W., according to Neison, stands 11,000 feet above the floor, and a second on the opposite side is nearly as high. Both the inner and outer slopes of this gigantic rampart are very broad, each being fully 10 miles in width. The outer slope, especially on the E., is a fine object at sunrise, when its rugged surface, traversed by deep gullies, is seen to the best advantage. The terraces and other features on the bright inner declivities on this side may be well observed when the sun's altitude is about  $6^{\circ}$ . Schmidt, whose measures differ from those of Neison, estimates the height of the wall on the E. to be 12,000 feet, and states that the interior slopes vary from  $60^{\circ}$  to  $50^{\circ}$  above, to from  $10^{\circ}$  to  $2^{\circ}$  at the base. The first inclination of  $50^{\circ}$ , and in some cases of  $60^{\circ}$ , is confined to the loftiest steep crests and to the flanks of the terraces. There are apparently five bright little mountains on the floor, the most easterly being rather the largest, and a great number of minute hillocks on the S.E. quarter. S.W. of the centre is a little crater, and on the same side of the interior a curious hook-shaped ridge, projecting from the foot of the wall, and extending nearly half-way across the floor. The region surrounding Copernicus is one of the most remarkable on the moon, being everywhere traversed by low ridges, enclosing irregular areas, which are covered with innumerable craterlets, hillocks, and other minute features, and by a labyrinth of bright streaks, extending for hundreds of miles on every side, and varying considerably both in width and brilliancy.

The notable crater-row on the W., often utilised by observers for testing the steadiness of the air and the definition of their telescopes, should be examined when it is on the morning ter-

minator, at which time Webb's homely comparison, "a mole-run with holes in it," will be appreciated, and its evident connection with the E. side of Stadius clearly made out. There is another much more delicate row running closely parallel to this object; it lies a little W. of it, and extends farther in a northerly direction.

ARCHIMEDES.—Next to Plato the finest object on the Mare Imbrium. It is about 50 miles in diameter. The average height of its massive border is about 4000 feet above the interior, which is only depressed some 500 or 600 feet below the Mare, the highest peak (about 7000 feet) being on the S.E. The walls are terraced, and include much detail, both within and without. The most noteworthy features in connection with this formation are the crater-cones, craterlets, pits, white spots, and light streaks which figure on the otherwise smooth interior. Mr. T. P. Gray, F.R.A.S., of Bedford, who, with praiseworthy assiduity, has devoted more than ten years to the close scrutiny of these features, Mr. Stanley Williams, and others, have detected four crater-cones on the E. half of the floor, and about fifty minute craters and white spots, also probably volcanic vents, and a very curious and interesting series of light streaks, mostly traversing the formation from E. to W. A little E. of the centre is a dusky oval area about 6 miles across, and S.W. of this is another, much smaller. Under some conditions of illumination the two principal light markings may be traced over the W. wall, and for some distance on the plain beyond.

On the southern side of Archimedes is a very rugged mountain region, extending for more than 100 miles towards the south: on the W. of this originates a remarkable rill-system, best seen under evening illumination. The two principal clefts follow a nearly parallel course up to the face of the Apennines near Mount Bradley, crossing in their way, almost at right angles, other clefts which run at no great distance from the E. foot of this range and ramify among the outlying hills. Archimedes A is a brilliant little ring-plain on the S.E. of Archimedes. It casts an extraordinary shadow at sunrise, and has a well-marked crater-row on the E. of it, and two long narrow valleys, one of which appears to be a southerly extension of the row.

BEER.—A very bright little crater, with an unnamed formation of about the same size adjoining it on the N., with which is associated a curious winding ridge that appears to traverse a gap in its N. wall.

TIMOCHARIS.—A fine ring-plain, 23 miles in diameter (the centre of a minor ray-system). It stands isolated on the Mare Imbrium (below the level of which it is depressed some 3000 feet), about midway between Archimedes and Lambert. Its walls, rising about 7000 feet above the floor, are conspicuously terraced, and on their W. outer slopes exhibit some remarkable depressions. There is a distinct break on the N., and a bright little crater on the N.W., connected with the foot of the *glacis* by a prominent ridge. On the bright central mountain, Schmidt, in 1842, detected a crater, which is easily seen under a moderately high light. Timocharis and the neighbourhood, especially the peculiar shape of the terminator on the E. of the formation, is well worth examination at sunrise.

PIAZZI SMYTH.—A conspicuous little ring-plain, 5 or 6 miles in diameter, depressed about 1500 feet below the Mare Imbrium, with a border rising about 2000 feet above it. With the curious arrangement of ridges, of which it is the apparent centre, it is a striking object under a low sun.

KIRCH.—A rather smaller object of the same class on the S.E.

PLATO.—This beautiful walled-plain, 60 miles in diameter, with its bright border and dark steel-grey floor, has, from the time of Hevelius to the present, been one of the most familiar objects to lunar observers. In the rude maps of the seventeenth century it figures as the "Lacus Niger Major," an appellation which not inaptly describes its appearance under a high sun, when the sombre tone of its apparently smooth interior is in striking contrast to that of the isthmus on which the formation stands. It will repay observation under every phase, and though during the last thirty years no portion of the moon has been more diligently scrutinised than the floor; the neighbourhood includes a very great number of objects of every kind, which, not having received so much attention, will afford ample employment to the possessor of a good telescope during many lunations.

The border of Plato, varying in height from 3000 to 4000 feet above the interior, is crowned by several lofty peaks, the highest (7400 feet) standing on the N. side of the curious little triangular formation on the E. wall. Those on the W., three in number, reckoning from N. to S., are respectively about 5000, 6000, and 7000 feet in altitude above the floor. The circumvallation being very much broken and intersected by passes, exhibits many distinct breaches of continuity, especially on the S. There is a remarkable valley on the S.W., which, cutting through the border



at a wide angle, suddenly turns towards the S.E., and descends the slope of the *glacis* in a more attenuated form. Another but shorter valley is traceable at sunrise on the W. On the N.W., the rampart is visibly dislocated, and the gap occupied by an intrusive mountain mass. This dislocation is not confined to the wall, but, under favourable conditions, may be traced across the floor to the broken S.E. border. It is probably a true "fault." On the N.E., the inner slope of the wall is very broad, and affords a fine example of a vast landslip.

The spots and faint light markings on the floor are of a particularly interesting character. During the years 1869 to 1871 they were systematically observed and discussed under the auspices of the Lunar Committee of the British Association. Among the forty or more spots recorded, six were found to be crater-cones. The remainder—or at least most of them—are extremely delicate objects, which vary in visibility in a way that is clearly independent of libration or solar altitude; and, what is also very suggestive, they are always found closely associated with the light markings,—standing either upon the surface of these features or close to their edges. Recent observations of these spots with a 13-inch telescope by Professor W. H. Pickering, under the exceptionally good conditions which prevail at Arequipa, Peru, have revived interest in the subject, for they tend to show that visible changes have taken place in the aspect of the principal crater-cones and of some of the other spots since they were so carefully and zealously scrutinised nearly a quarter of a century ago. The gradual darkening of the floor of Plato as the sun's altitude increases from  $20^{\circ}$  till after full moon may be regarded as an established fact, though no feasible hypothesis has been advanced to account for it.

On the N.E. of Plato is a large bright crater, A; and, extending in a line from this towards the E., is a number of smaller rings, the whole group being well worth examination. On the N. there is a winding cleft, and some short crossed clefts in the rugged surface just beyond the foot of the wall, which I have seen with a 4-inch achromatic. The region on the W., imperfectly shown in the maps, includes much unrecorded detail. On the Mare Imbrium S. of Plato is a large area enclosed by low ridges, to which Schröter gave the name "Newton." It suggests the idea that it represents the ruin of a once imposing enclosure, of which the conspicuous mountain Pico formed a part.

TIMÆUS.—A very bright ring-plain, 22 miles in diameter, with

walls about 4500 feet in height, on the coast-line of the Mare Frigoris, and associated with the E. side of the great enclosed plain W. C. Bond. Schmidt shows a double hill, nearly central, and Neison a crater on the S.W. wall.

BIRMINGHAM.—A large rhomboidal-shaped enclosure, defined by mountain chains and traversed by a number of very remarkable parallel ridges. It is situated nearly due N. of Plato on the N. edge of the Mare Frigoris, and lies on the S.E. side of W. C. Bond, to which it bears a certain resemblance. This region is characterised by the parallelism displayed by many formations, large and small. It is more apparent hereabouts than in any other part of the moon's visible surface. When favourably placed under a low morning sun, Birmingham is a striking telescopic object.

FONTINELLE.—A fine ring-plain, 23 miles in diameter, on the N. margin of the Mare Frigoris, N.N.E. of Plato, with a wall rising on the E., 6000 feet above a bright interior. I find its border indistinct and nebulous, excepting under very oblique light, though three of the little craters upon it are bright and prominent. One stands on the S., another on the N.W., and a third on the E. Schmidt shows only the first of these, and Neison none of them. Fontinelle has a low central mountain which is easily distinguished. Fontinelle A, an isolated mountain on the S., is more than 3000 feet high. On the N. there is a curious mountain group, also of considerable altitude, and on the W. an irregular depression surrounded by a dusky area. North of Fontinelle, extending towards Goldschmidt and the limb, Schröter discovered a very wide irregular valley which he named "J. J. Cassini." It is really nothing more than a great plain bounded by ridges. At 9 h. October 15, 1888, when Philolaus was on the morning terminator, I had a fine view of it, and, as regards its general shape, found that it agreed very closely with Schröter's drawing.

EPIGENES.—A remarkable ring-plain, about 26 miles in diameter, abutting on a mountain ridge running parallel to the E. flank of W. C. Bond. It is a notable object under a low morning sun. There are several elevations on the floor.

GOLDSCHMIDT.—A great abnormally-shaped enclosure with lofty walls between Epigenes and the limb. Neison mentions only two crater-pits within. I have seen the rimmed crater shown by Schmidt on the W. side and three or four other objects of a doubtful kind.

ANAXAGORAS.—A brilliant ring-plain of regular form, 32 miles in diameter, adjoining Goldschmidt on the E. It is a prominent centre of light streaks, some of which traverse the interior of Goldschmidt. On the north a peak rises to the height of 10,000 feet. There is a long ridge on the floor, running from E. to W.

GIOJA.—A ring-plain about 26 miles in diameter, near the north pole.

#### EAST LONGITUDE $20^{\circ}$ TO $40^{\circ}$ .

REINHOLD.—A prominent ring-plain, 31 miles in diameter, with a lofty border, rising at a peak on the W. to more than 9000 feet above the floor. Its shape on the W. is clearly polygonal, the wall consisting of three rectilineal sections, and on the E. it is made up of two straight sections connected by a curved section. The inner slope includes a remarkably distinct and regular terrace, the E. portion of which is well seen when the interior is about half illuminated by the rising sun. At this phase also the great extent of the *glacis* on the S.W., and the deep wide gullies traversing it on the E. are observed to the best advantage. The central mountain, though of considerable size, is not prominent. Close to Reinhold on the N.W. stands a noteworthy little formation with a low and partially lineal wall, exhibiting a gap on the north. There is a distinct crater on the S. side of its floor.

GAY-LUSSAC.—A very interesting ring-plain, 15 miles in diameter, situated in the midst of the Carpathian Highlands N. of Copernicus, with a smaller but brighter and deeper formation (Gay-Lussac A) on the S.W. of it, and a conspicuous little crater, not more than 2 or 3 miles in diameter, between the two. The interior of Gay-Lussac is traversed by two coarse clefts, lying nearly in a meridional direction. The more easterly runs from the foot of the S. wall, near the little crater just mentioned, across the floor to the low N. border, which it apparently cuts through, and extends for some distance beyond, terminating in a great oval expansion. The other, which is not shown in the maps, is closely parallel to it, and can be traced up to the N. border, but not farther. Schmidt represents the first as a crater-row, which it probably is, as it varies considerably in width. From the S.E. side of the formation extends a long cleft, termi-

inating at the end of a prominent spur from the S. side of the Carpathians. There are also two remarkable rill-like valleys, commencing on the N. of Gay-Lussac A, which curve round the W. side of Gay-Lussac.

HORTENSIVS.—This brilliant crater, about 10 miles in diameter, is remarkable for its depth, and as being a ray-centre surrounded by a nimbus of light. It has a central mountain, and Schmidt shows a minute crater on the outer slope of the S. wall. The former is a test object.

MILICHIUS.—Is situated on the N.N.E. of Hortensius. It is fully as bright, but rather smaller. Its floor, apparently devoid of detail, is considerably depressed below the surrounding surface.

TOBIAS MAYER.—Like Gay-Lussac, a noteworthy ring-plain associated with the Carpathian Mountains. It is 22 miles in diameter, and has a wall which rises on the W. to a height of nearly 10,000 feet above the floor; on the latter there is a conspicuous central mountain, and on the E. side a crater, and some little hills. Schmidt shows a smaller crater on the W. side, which I have not seen. Adjoining the formation on the W. is a ring-plain of about one-fourth its area, which is a bright object. Tobias Mayer and the neighbouring Carpathians form an especially beautiful telescopic picture at sunrise.

KUNOWSKY.—An inconspicuous ring-plain, about 11 miles in diameter, standing in a barren region in the Mare Procellarum, W.S.W. of Encke. The central mountain is tolerably distinct.

ENCKE.—A regular ring-plain, 20 miles in diameter, with a comparatively low border, nowhere rising more than 1800 feet above the interior, which is depressed some 1000 feet below the surrounding Oceanus Procellarum. A lofty ridge traverses the floor from S. to N., bifurcating before it reaches the N. wall. There is a bright crater on the W. wall, and a depression on the opposite wall, neither of which, strange to say, is shown on the maps. Encke is encircled by ridges, which, when it is on the morning terminator, combine to make it resemble a large crater surrounded by a vast mountain ring.

KEPLER.—One of the most brilliant objects in the second quadrant,—a ring-plain about 22 miles in diameter, with a lofty border; a peak on the E. attaining an altitude of 10,000 feet above the surface. The wall is much terraced, especially the outer slope on the W., where a narrow valley is easily traceable. Though omitted from the maps, there is a prominent circular depression on the W. border, which forms a distinct notch,

thereon at sunrise. On the N., the wall exhibits a conspicuous gap. There is a central hill on the floor. Immediately E. of Kepler is a bright plateau, bounded on the N. by a very straight border, with two small craters on its edge. Both these objects are incomplete on the N., as if they had been deformed by a "fault," which has apparently affected the N. end of Kepler also. Kepler is the centre of one of the most extended systems of bright streaks on the moon's visible surface.

BESSARION.—A bright little ring-plain, about 6 miles in diameter, in the Oceanus Procellarum N. of Kepler. There is a smaller and still brighter companion on the N. (Bessarion E), standing on a light area. Bessarion has a minute central hill, difficult to detect.

PYTHEAS.—A small rhomboidal-shaped ring-plain, 12 miles in diameter, standing in an isolated position on the Mare Imbrium between Lambert and Gay-Lussac. Its bright walls, rising about 2500 feet above the Mare, are much terraced within, especially on the E. There is a bright little crater on the N. outer slope, with a short serpentine ridge running up to it from the region S. of Lambert, and another winding ridge extending from the S. wall to the E. of two conspicuous craters, standing about midway between Pytheas and Gay-Lussac. The former bears a great resemblance to the ridge N. of Mädler, and, like this, appears to traverse the N. border. The interior of Pytheas, which is depressed more than 2000 feet below the Mare, includes a brilliant central peak.

LAMBERT.—A ring-plain, 17 miles in diameter, presenting many noteworthy features. The crest of its border stands about 2000 feet above the Mare Imbrium, and more than double this height above the interior. The wall is prominently terraced both within and without; the outer slope on the W. exhibiting at sunrise a nearly continuous valley running round it. When near the morning terminator, the region on the N. is seen to be traversed by some very remarkable ridges and markings; one cutting across the N. wall appears to represent a "fault." On the S. is a large polygonal enclosure formed by low ridges. On the W., towards Timocharis, is a brilliant mountain 3000 feet high, a beautiful little object under a low sun.

LEVERRIER.—The more westerly of a pair of little ring-plain on the N. side of the Mare Imbrium, and S.W. of the Laplace promontory. It is about 10 miles in diameter, with walls rising some 1500 feet above the Mare, and more than 6000 feet above

the interior, which seems to be without a central mountain or other features. Schmidt shows the crater on the N. rim and another on the S.E. slope, both of which are omitted by Neison, though they are easy objects when Helicon is on the morning terminator. About 20 miles on the S.E. there is a very bright little crater on a faint light area.

HELICON.—The companion ring-plain on the E. It is 13 miles in diameter, and is very similar, though not quite so deep. There is a crater on the S.E. wall, and, according to Neison, another on the outer slope of the N. border. Webb records a central crater. If Helicon is observed when on the morning terminator, it will be seen to be traversed by a curved ridge which cuts through the walls, and runs up to a bright crater S.E. of Leverrier. It appears to be a "fault," whose "downthrow," though slight, is clearly indicated by an area of lower ground on the E. There is a great number of small craters in the neighbourhood of this formation.

EULER.—The most easterly of the row of great ring-plain, which, beginning on the W. with Autolycus, and followed by Archimedes, Timocharis, and Lambert, extends almost in a great circle from the N.W. to the S.E. side of the Mare Imbrium. It is about 19 miles in diameter, and is surrounded by terraced walls, which, though of no great height above the Mare, rise 6000 feet above the floor. There is a distinct little gap in the S. wall, easily glimpsed when it is close to the morning terminator, which probably represents a small crater. Euler has a bright central mountain, and is a centre of white silvery streaks.

BRAYLEY.—A very conspicuous little ring-plain E.S.E. of Euler, with two smaller but equally brilliant objects of the same class situated respectively E. and W. of it.

DIOPHANTUS.—Forms with Delisle, its companion on the N., a noteworthy object. It is about 13 miles in diameter, with a wall, which has a distinct break in its continuity on the N., rising about 2500 feet above the Mare. A rill-valley runs from the E. side of the ring towards the W. face of a triangular-shaped mountain on the E. of a line joining the formation with Delisle. North are three bright little craters in a line, the middle one being much the largest. From the most easterly of these objects a light streak may be traced under a high sun, extending for many miles to another small crater on the N.W. of Diophantus, and expanding at a point due N. of the formation into a spindle-shaped marking. At sunrise, the W. portion of the streak has all the appearance of

a cleft, with a branch about midway running to the S. side of Delisle. Under the same phase a broad band of shadow extends from the N.E. wall to the triangular mountain just mentioned, representing a very sudden drop in the surface—resembling on a small scale the well-known “railroad” E. of Thebit. Diophantus has no central mountain.

DELISLE.—A larger and more irregularly-shaped object than the last, 16 miles in diameter, with loftier and more massive walls, and an extensive but ill-defined central hill. There is an evident break in the northern border. A triangular mountain on the S.E. and a winding ridge running up to the N. wall are prominent features at sunrise, as are also the brilliant summits of a group of hills some distance to the E.N.E.

CARLINI.—A small but prominent and deep little crater about 5 miles in diameter on the Mare Imbrium about midway between Lambert and the Sinus Iridum. There are many faint light streaks in the vicinity, one of which extends from Carlini to Bianchini, on the edge of the Sinus,—a distance of 300 miles. Schmidt shows a central peak.

CAROLINE HERSCHEL.—A bright and very deep ring-plain about 8 miles in diameter on the Mare Imbrium, some distance E.N.E. of the last. On the S.E. lies a larger crater, Delisle B, which has a small but obvious crater on its N. rim, and casts a very prominent shadow at sunrise. Caroline Herschel stands on a long curved ridge running N.E. from Lambert towards the region E. of Helicon, and, according to Schmidt, has a central peak. On the E. is a bright mountain with two peaks; some distance N. of which is a large ill-defined white spot, with another spot of a similar kind on the W. of it, nearly due N. of Caroline Herschel.

GRUITHUISEN.—This ring-plain, 10 miles in diameter, is situated on the Mare Imbrium on the N.E. of Delisle. It is associated with a number of ridges trending towards the region N. of Aristarchus and Herodotus.

THE LAPLACE PROMONTORY.—A magnificent headland marking the extreme western extremity of the finest bay on the moon’s visible surface, the Sinus Iridum; above which it towers to a height of 9000 feet or more, projecting considerably in front of the line of massive cliffs which define the border of the Sinus, and presenting a long straight face to the S.E. Near its summit are two large but shallow depressions, the more easterly having a very bright interior. At a lower level, almost directly below the last, is a third depression. All three are easy objects under a

low sun. The best view of the promontory and its surroundings is obtained when the E. side of the bay is on the morning terminator. Its prominent shadow is traceable for many days after sunrise.

**THE HERACLIDES PROMONTORY.**—The less lofty but still very imposing headland at the E. end of the Sinus Iridum, rising more than 4000 feet above it. It consists of a number of distinct mountains, forming a triangular-shaped group running out to a point at the S.W. extremity of the bay, and projecting considerably beyond the shore-line. There is a considerable crater on the E. side of the headland, not visible till a late stage of sunrise. It is among the mountains composing this promontory that some ingenuity and imagination have been expended in endeavouring to trace the lineaments of a female face, termed the "Moon-maiden."

**BIANCHINI.**—A fine ring-plain, about 18 miles in diameter, on the N.E. side of the Sinus Iridum, surrounded by the lofty mountains defining the border of the bay. Its walls, which are prominently terraced within, rise about 7000 feet on the E., and about 8000 feet on the W. above the floor, which includes a prominent ridge and a conspicuous central mountain. There is a distinct crater on the S. wall, not shown in the maps. Between this side of the formation and the bay is a number of hills running parallel to the shore-line: these, with the intervening valleys, will repay examination at sunrise.

**MAUPERTUIS.**—A great mountain enclosure of irregular shape, about 20 miles in diameter, in the midst of the Sinus Iridum highlands, N. of Laplace. The walls are much broken by passes, and the interior includes many hills and ridges.

**CONDAMINE.**—A rhomboidal-shaped ring-plain, about 23 miles in diameter, N. of Maupertuis, with lofty walls, especially on the E., where they rise some 4000 feet above the interior. There are three large depressions on the outer N.W. slope, and at least three minute craters on the crest of the wall just above. Though neither Neison nor Schmidt draw any detail thereon, there is a prominent ridge on the N. side of the floor, and a low circular hill on the S. On the S.E. four long ridges or spurs radiate from the wall, and on the N.E. are three remarkable square-shaped enclosures. On the edge of the Mare Frigoris, N.W. of Condamine, are many little craters with bright rims and a distinct short cleft, running parallel to the coast-line.

The winding valleys in the region bordering the Sinus Iridum,



and other curious details, render this portion of the moon's surface almost unique.

BOUGUER.—A bright regular little ring-plain, about 8 miles in diameter, N. of Bianchini.

J. F. W. HERSCHEL.—A vast enclosed plain, about 90 miles across, bounded on the W. by a mountain range, which here defines the E. side of the Mare Frigoris, on the S. by massive mountains, and on the other sides by a lofty but much broken wall, intersected by many passes. Within is a large ring-plain, nearly central, and a large number of little craters and crater-pits. The floor is traversed longitudinally by many low ridges, lying very close together, which at sunrise resemble fine grooves or scratches of irregular width and depth.

HORREBOW.—A ring-plain of remarkable shape, resembling the figure  $\infty$ , standing at the S. end of the mountain range bounding J. F. W. Herschel on the W. Schmidt shows a crater on the W. wall, near the constriction on this side, and a second at the foot of the slope of the E. wall.

PHILOLAUS.—A ring-plain 46 miles in diameter, on the N.E. of Fontinelle. Its bright walls rise on the W. to a height of nearly 12,000 feet above the floor (on which there is a conspicuous central mountain), and exhibit many prominent terraces. Philolaus is partially encircled, at no great distance, by a curved ridge, on which will be found a number of small craters.

ANAXIMINES.—A much foreshortened ring-plain, about 66 miles in diameter, on the E. of Philolaus. One peak on the E. is nearly 8000 feet in height. Schmidt shows four craters on the W. side of the floor, and a fifth on the S.E. side. There is a bright streak in the interior, which extends southwards for some distance across the Mare Frigoris.

#### EAST LONGITUDE $40^{\circ}$ TO $60^{\circ}$ .

REINER.—A regular ring-plain, 21 miles in diameter, in the Mare Procellarum, S.S.E. of Marius, with a very lofty border terraced without and within, and a minute but conspicuous mountain standing at the N. end of a ridge which traverses the uniformly dark floor in a meridional direction. A long ridge extends some way towards the S. from the foot of the S. wall, and at some distance in the same direction lie six ill-defined white spots of doubtful nature. On the E.N.E. there is a large

white marking, resembling a "Jew's harp" in shape, and farther on, towards the E., a number of very remarkable ridges. On the W. will be found many bright little craterlets. A ray from Kepler extends almost up to the W. wall of Reiner.

MARIUS.—A very noteworthy ring-plain, 27 miles in diameter, in the Oceanus Procellarum, E.N.E. of Kepler, with a bright border rising about 4000 feet above the interior, which is of an uneven tone. The rampart exhibits some breaks, especially on the S. The outer slope on the W. is traversed by a fine deep valley, distinctly marked when the opposite side is on the morning terminator. It originates on the S.W. at a prominent crater situated a little below the crest of the wall, and, following its curvature, runs out on to the plain near a large mountain just beyond the foot of the N. border. In addition to the crater just mentioned, there are two smaller ones below the summit of the S. wall, and a small circular depression on the S.E. wall. Mr. W. H. Maw, F.R.A.S., has seen, with a 6-inch Cooke refractor, a bright marking at the N. extremity of the ring, which, when examined with a Dawes' eyepiece, resembled an imperfect crater. The floor includes at least four objects—(1) A crater on the N.W., standing on a circular light area; (2) a white spot a little S. of the centre; (3) a smaller white spot S.E. of this; (4) another, near the inner foot of the S.W. wall. Marius is an imposing object under oblique illumination, mainly because of the number of ridges by which it is surrounded. I have frequently remarked at sunrise that the surface on the W., and especially the outer slope of the rampart, is of a decided brown or sepia tint, similar to that which has already been noticed with respect to Geminus and its vicinity, viewed under like conditions. Schmidt in 1862 discovered a long serpentine cleft some distance N. of Marius, which has not been seen since.

ARISTARCHUS.—The brightest object on the moon, forming with Herodotus (a companion ring-plain on the E.), and its remarkable surroundings, one of the most striking objects which the telescope has revealed on the visible surface, and one requiring much patient observation before its manifold details can be fully noted and duly appreciated. Its border rises 2000 feet above the outer surface on the W., but towers to more than double this height above the glistening floor. No lunar object of its moderate dimensions (it is only about 29 miles in diameter) has such conspicuously terraced walls, or a greater number of spurs and buttresses; which are especially prominent on the S. A valley runs

round the outer slope of the W. wall, very similar to that found in a similar position round Marius. There is also a distinct valley on the brilliant inner slope of the E. wall, below its crest. It originates at a bright little crater, and is traceable round the greater portion of the declivity. Under a moderately high sun, an oval area, nearly as large and fully as brilliant as the central mountain, is seen on this inner slope. It is bordered on either side by bands of a duskier hue, which probably represent shallow transverse valleys. From its dazzling brilliancy it is very difficult to observe the interior satisfactorily. In addition, however, to the central mountain, there is a crater on the N.W. side of the floor. On the S. side of Aristarchus is a large dusky ring some 10 miles in diameter, connected by ridges with the spurs from the wall, and on the S.E., close to the foot of the slope, is another smaller ring of a like kind.

HERODOTUS.—This far less brilliant but equally interesting object is about 23 miles in diameter, and is not so regular in shape as Aristarchus. Its W. wall rises at one point more than 4000 feet above the very dusky floor. Except on the S.W. and N.E., the border is devoid of detail. On the S.W. three little notches may be detected on its summit, which probably represent small craters, while on the opposite side, on the inner slope, a little below the crest, is a large crater, easily seen. Both the E. and W. sections of the wall are prolonged towards the S. far beyond the limits of the formation. These rocky masses, with an intermediate wall, are very conspicuous under oblique illumination, that on the S.W. being especially brilliant. On the N. there is a gap through which the well-known Serpentine cleft passes on to the floor. Between the N.W. side of Herodotus and Aristarchus is a large plateau, seen to the best advantage when the morning terminator lies a little distance E. of the former. It is traversed by a T-shaped cleft which communicates with the great serpentine cleft and extends towards the S. end of Aristarchus, till it meets a second cleft (forming the upper part of the T) running from the S.E. side of this formation along the W. side of Herodotus. The great serpentine cleft, discovered by Schröter, October 7, 1787, is in many respects the most interesting object of its class. It commences at the N. end of a short wide valley, traversing mountains some distance N.E. of Herodotus, as a comparatively delicate cleft. After following a somewhat irregular course towards the N.W. for about 50 miles, and becoming gradually wider and deeper, it makes a sudden turn and runs for about 10 miles

in a S.W. direction. It then changes its course as abruptly to the N.W. again for 3 or 4 miles, once more turns to the S.W., and, as a much coarser chasm, maintains this direction for about 20 miles, till it reaches the S.E. edge of a great mountain plateau N. of Aristarchus, when it swerves slightly towards the S., becoming wider and wider, up to a place a few miles N. of Herodotus, where it expands into a broad valley; and then, somewhat suddenly contracting in width, and becoming less coarse, enters the ring-plain through a gap in the N. wall, as before mentioned. I always find that portion of the valley in the neighbourhood of Herodotus more or less indistinct, though it is broad and deep. This part of it, unless it is observed at a late stage of sunrise, is obscured by the shadow of the mountains on the border of the plateau. Gruithuisen suspected a cleft crossing the region embraced by the serpentine valley, forming a connection between its coarse southern extremity and the long straight section. This has been often searched for, but never found. It may exist, nevertheless, for in many instances Gruithuisen's discoveries, though for a long time discredited, have been confirmed. The mountain plateau N. of Aristarchus deserves careful scrutiny, as it abounds in detail and includes many short clefts.

**HARBINGER MOUNTAINS.**—A remarkable group of moderate height, mostly extending from the N.W. towards Aristarchus. They include a large incomplete walled-plain about 30 miles in diameter, defined on the W. by a lofty border, forming part of a mountain chain, and open to the south. This curious formation has many depressions in connection with its N.W. edge. On the N. of it there is a crater-row and a very peculiar zig-zag cleft. The region should be observed when the E. longitude of the morning terminator is about  $45^{\circ}$ .

**SCHIAPARELLI.**—A conspicuous formation, about 16 miles in diameter, between Herodotus and the N.E. limb, with a border rising nearly 2000 feet above the Mare, and about 1000 more above the floor, on which Schmidt shows a central hill.

**WOLLASTON.**—A small bright crater on the Mare N. of the Harbinger Mountains, surpassed in interest by a remarkable formation a few miles S. of it, Wollaston B, an object of about the same size, but which is associated with a much larger enclosure, resembling a walled-plain, lying on the N. side of it. This formation has a lofty border on the W., surmounted by two small craters. The wall is lower on the E. and exhibits

a gap. There is a central hill, only visible under a low sun. About midway between Wollaston and this enclosure stands a small isolated triangular mountain. From a hill on the E. runs a rill valley to the more westerly of a pair of craters, connected by a ridge, on the S.E. of Wollaston B.

MAIRAN.—A bright ring-plain of irregular shape, 25 miles in diameter, on the E. of the Heraclides promontory. The border, especially on the E., varies considerably in altitude, as is evident from its shadow at sunrise; at one peak on the W. it is said to attain a height of more than 15,000 feet above the interior. There is a very minute crater on the crest of the S. wall, down the inner slope of which runs a rill-like valley. About half-way down the inner face of the E. wall are two other small craters, connected together by a winding valley. These features may be seen under morning illumination, when about one-fourth of the floor is in sunlight. Schröter is the only selenographer who gives Mairan a central mountain. In this he is right. I have seen without difficulty on several occasions a low hill near the centre. The formation is surrounded by a number of conspicuous craters and crater-pits. On the N. there is a short rill-like valley, and another, much coarser, on the S.

SHARP.—A ring-plain somewhat smaller than the last, on the E. of the Sinus Iridum, from the coast-line of which it is separated by lofty mountains. There is a distinct crater at the foot of its N.E. wall, and a bright central mountain on the floor. On the N. is a prominent enclosure, nearly as large as Sharp itself; and on the N.E. a brilliant little ring-plain, A, about 8 miles in diameter, connected with Sharp, as Mädler shows, by a wide valley.

LOUVILLE.—A triangular-shaped formation on the E. of a line joining Mairan and Sharp. It is hemmed in by mountains, one of which towers 5000 feet above its dusky floor.

FOUCAULT.—A bright deep ring-plain, about 10 miles in diameter, lying E. of the mountains fringing the Sinus Iridum, between Bianchini and Harpalus. A very lofty peak rises near its N. border, and, according to Neison, it has a distinct central mountain, though neither Mädler or Schmidt show any detail within.

HARPALUS.—A conspicuous ring-plain, about 14 miles in diameter, on the N.E. of the last, with a floor sinking 13,000 feet below the surrounding surface. As the cubic contents of the border and *glacis* are quite inadequate to account for it, we

may ask, what has become of the material which presumably once filled this vast depression? Harpalus has a bright central mountain.

**SOUTH.**—On the W. and S., the boundaries of this extensive enclosure are merely indicated by ridges, which nowhere attain the dignity of a wall. On the N., the edge of a tableland intersected by a number of valleys define its limits, and on the E. a border forming also the W. side of Babbage. The interior is traversed by a number of longitudinal hills, and includes two bright little heights, drawn by Schmidt as craters.

**BABBAGE.**—A still larger enclosed area, adjoining South on the E., and containing a considerable ring-plain near its W. border. It is a fine telescopic object at sunrise, the interior being crossed by a number of transverse markings representing ridges. These are very similar in character (but much coarser) to those found on the floor of J. F. W. Herschel. The curious detail on the E. wall is also worth examination at this phase.

**ROBINSON.**—A bright and very deep little ring-plain, about 12 miles in diameter, on a plateau N. of South. Schmidt shows a crater on the W. border, and two others at the foot of the N. and E. borders respectively.

**ANAXIMANDER.**—A fine but much foreshortened ring-plain, 39 miles in diameter, abutting on the E. side of J. F. W. Herschel. It has a large crater on its W. border, which is common to the two formations, and a very prominent crater, both on the S. and N. The barrier on the S.W. rises to a height of nearly 10,000 feet. Schmidt shows a crater and other details on the floor.

#### EAST LONGITUDE 60° TO 90°.

**LOHRMANN.**—This ring-plain, with Hevel and Cavalerius on the N. of it, is a member of a linear group, which, but for its propinquity to the limb, would be one of the most imposing on the moon's surface. Lohrmann, about 28 miles in diameter, is surrounded by a bright wall, which, to all appearance, is devoid of detail. Two prominent ridges, with a fine intervening valley, connect it with the N. end of Grimaldi. It has a large but not conspicuous central mountain. On the rugged surface, between the ring-plain and the E. edge of the Oceanus Procellarum, lies a very interesting group of crossed clefts, some of which run from N.E. to S.W., and others from N.W. to S.E. Three of the latter

proceed from different points in a coarse valley extending from W. to E., and cross the ridges just mentioned. They follow a parallel course, and terminate on the S. side of a crater-row, consisting of three bright craters ranging in a line parallel to the coarse valley. On the N. side of these objects, and tangential to them, is another cleft, which traverses the W. and E. walls of Lohrmann, and, crossing the region between it and Riccioli, terminates apparently at the W. wall of the latter formation. No map shows this cleft, though it is obvious enough; and, when the E. wall of Hevel is on the morning terminator, the notches made by it in the border of Lohrmann are easily detected. Capt. Noble, F.R.A.S., aptly compares two of the crossed clefts to a pair of scissors, the craters at which they terminate representing the oval handles. On the grey surface of the Mare W. of Lohrmann is the bright crater Lohrmann A, from which, running N., proceeds a rill-like valley ending at a large white spot, which has a glistening lustre under a high light.

HEVEL.—A great walled-plain, 71 miles in diameter, adjoining Lohrmann on the N., with a broad western rampart, rising at one peak to a height above the interior of nearly 6000 feet and presenting a steep bright face to the Oceanus Procellarum. There are three prominent craters near its crest, and one or two breaks in its continuity. It is not so lofty and is more broken on the E., where three conspicuous craters stand on its inner slope. The floor is slightly convex, and includes a triangular central mountain, on which there is a small crater. The S. half of the interior is crossed by four clefts: (1) running from a little crater N. of the central mountain, on the W. side of it, to a hill at the foot of the S.W. wall; (2) originating near the most southerly of the three craters on the inner slope of the E. wall, and crossing 1, terminates at the foot of the W. wall; (3) has the same origin as 2, crosses 1, and, passing over a craterlet W. of the central mountain, also runs up to the W. wall at a point considerably N. of that where 2 joins the latter; (4) runs from the craterlet just mentioned to the W. end of 2.

CAVALERIUS.—The most northerly member of the linear chain, a ring-plain, 41 miles in diameter, with terraced walls rising about 10,000 feet above the floor. Within there is a long central mountain with three peaks. Under a high light the region on the W. is seen to be crossed by broad light streaks.

OLBERS.—A large ring-plain, 41 miles in diameter, near the limb, N.E. of Cavalerius. Though a very distinct formation, it is

difficult to see its details except under favourable conditions of libration. It has a large crater on its W. wall, a smaller one on the E., and a third on the N. The floor includes a central mountain, and, according to Schmidt, four craters. He also shows a crater-rill on the W. wall, N. of the large crater thereon. Olbers is the origin of a fine system of light rays.

GALILEO.—A ring-plain, about 9 miles in diameter, N.E. of Reiner, associated with ridges, some of which extend to the “Jew’s Harp” marking referred to under this formation.

CARDANUS.—A fine regular ring-plain, about 32 miles in diameter, near the limb N. of Olbers. Its bright walls, rising about 4000 feet above the light grey floor, are clearly terraced, and exhibit, especially on the S.E., several spurs and buttresses. There is a fine valley on the outer W. slope, a large bright crater on the Mare just beyond its foot, and a conspicuous mountain in the same position farther north. I have not succeeded in seeing the faint central hill nor the crater N. of it shown by Schmidt, but there is a brilliant white circular spot on the floor at the inner foot of the N.E. wall which he does not show.

KRAFFT.—A very similar object on the N., of about the same dimensions; with a central peak, and a large crater on the dark floor abutting on the S.W. wall, and another of about half the size on the outer side of the W. border. From this crater a very remarkable cleft runs to the N. wall of Cardanus: it is bordered on either side by a bright bank, and cuts through the N.W. border of the latter formation. It is best seen when the E. wall of Cardanus is on the morning terminator.

VASCO DE GAMA.—A bright enclosure, 51 miles in diameter, with a small central mountain. It is associated on the N. with a number of enclosed areas of a similar class, all too near the limb to be well seen.

SELEUCUS.—A considerable ring-plain, 32 miles in diameter, with lofty terraced walls, rising 10,000 feet above a dark floor which includes an inconspicuous central hill. This formation stands on a ridge extending from near Briggs to the W. side of Cardanus.

OTTO STRUVE.—An enormous enclosure, bounded on the E. by the Hercynian Mountains, and on the W. by a mountain chain of considerable altitude, surmounted by three or more bright little rings. On the W. side of the uneven-toned interior, which, according to Mädler, includes an area of more than 26,000 square miles, stand four craters, several little hills, and light spots. On the W. is the much more regular and almost as large formation,



Otto Struve A, the W. border of Otto Struve forming its E. wall. This enclosure is bounded elsewhere by a very low, broken, and attenuated barrier. At sunrise the E. and W. walls, with the mountain mass at the N. end, which they join, resemble a pair of partially-opened calipers. There is one conspicuous little crater on the W. side of the floor; and, at or near full moon, four or five white spots, nearly central, are prominently visible.

BRIGGS.—This bright regular ring-plain, 33 miles in diameter, is situated a short distance N. of Otto Struve A. A long ridge traverses the interior from N. to S. On the E. is another large enclosure, communicating with Otto Struve on the S., and really forming a N. extension of this formation. It has a large and very deep crater, 12 miles in diameter, on its W. border.

LICHTENBERG.—A conspicuous little ring-plain, about 12 miles in diameter, in an isolated position on the Mare, some distance N. of Briggs. It was here that Mädler records having occasionally noticed a pale reddish tint, which, though often searched for, has not been subsequently seen.

ULUGH BEIGH.—A good-sized ring-plain, E. of the last, with a bright border and central mountain. Too near the limb for observation.

LAVOISIER.—A small bright walled-plain N. of Ulugh Beigh. It has a somewhat dark interior. West of it is Lavoisier A, a ring-plain about 14 miles in diameter. Both are too near the limb for useful observation.

GÉRARD.—A large enclosure close to the limb, still farther N., containing a long ridge and a crater.

HARDING.—A small ring-plain W. of Gerard, remarkable for the peculiar form of its shadow at sunrise, and for the ridges in its vicinity.

REPSOLD.—The largest of a group of walled enclosures, close to the limb, on the E. side of the Sinus Roris.

XENOPHANES.—But for its position, this deep walled-plain, 185 miles in diameter, would be a fine telescopic object, with its lofty walls, large central mountain, and other details.

CENOPIDES.—A large and tolerably regular walled-plain, 43 miles in diameter, on the W. of the last. The depressions on the W. wall are worth examination at sunrise. There is apparently no detail whatever on the floor.

CLEOSTRATUS.—A small ring-plain, N. of Xenophanes, surrounded by a number of similar objects, all too near the limb for observation.

---

PYTHAGORAS.—A noble walled-plain, 95 miles in diameter, which no one who observes it fails to lament is not nearer the centre of the disc, as it would then undoubtedly rank among the most imposing objects of its class. Even under all the disadvantages of position, it is by far the most striking formation in the neighbourhood. Its rampart rises, at one point on the N., to a height of nearly 17,000 feet above the floor, on which stands a magnificent central mountain, familiar to most observers.

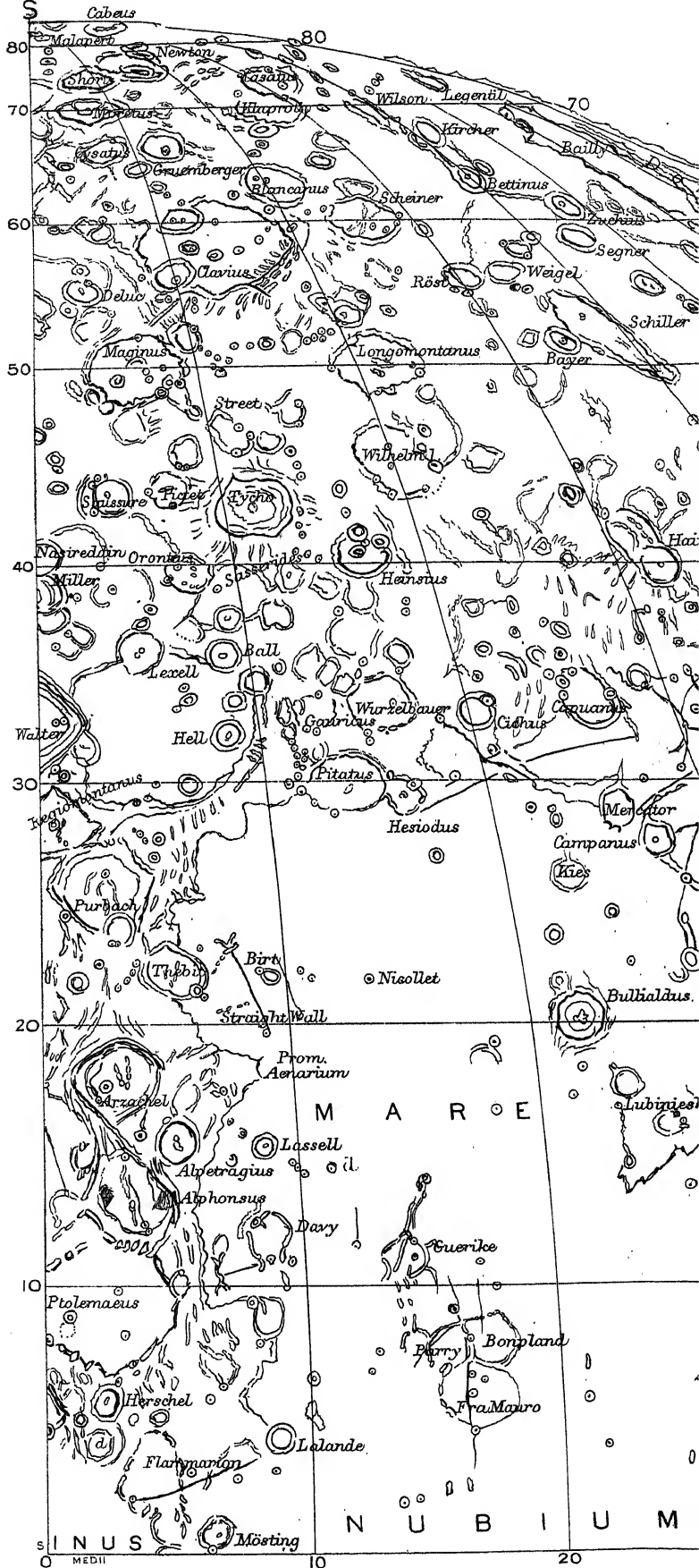
EAST LONGITUDE  $0^{\circ}$  TO  $20^{\circ}$ 

MÖSTING.—A very deep ring-plain, 15 miles in diameter, near the moon's equator, and about  $6^{\circ}$  E. of the first meridian. There is a crater on the N. side of its otherwise unbroken bright border, an inconspicuous central mountain, and, according to Neison, a dark spot on the S. side of the floor. At some distance on the S.S.W., stands the bright crater, Mösting A, one of the most brilliant objects on the moon's visible surface.

RÉAUMUR.—A large pentagonal enclosure, about 30 miles in diameter, with a greatly broken border, exhibiting many wide gaps, situated on the E. side of the Sinus Medii, N.W. of Herschel. The walls are loftiest on the S. and S.W., where several small craters are associated with them. A ridge connects the formation with the great deep crater Réaumur A, and a second large enclosure lying on the W. side of the well-known valley W. of Herschel. At the end of a spur on the S. side of the great crater originates a cleft, which I have often traced to the N.W. wall of Ptolemæus, and across the N. side of the floor of this formation to a crater on the N.E. quarter of it, Ptolemæus *d*. There is a short cleft on the W. side of the floor of Réaumur, running from N. to S.

HERSCHEL.—A typical ring-plain, situated just outside the N. border of Ptolemæus, with a lofty wall rising nearly 10,000 feet above a somewhat dusky floor, which includes a prominent central mountain. Its bright border is clearly terraced both within and without, the terraces on the inner slope of the W. wall being beautifully distinct even under a high light, and on the outer slope are some curious irregular depressions. On the S.S.E. is a large oblong deep crater, close to the rocky margin of Ptolemæus, and a little beyond the foot of the wall on the N.W. is a smaller and more regular rimmed depression, *b*, standing near the E. border of the great valley, more than 80 miles long, and in places fully 10 miles wide, which runs from S.S.W. to N.N.E. on the W. side of Herschel, and bears a close resemblance to the well-known



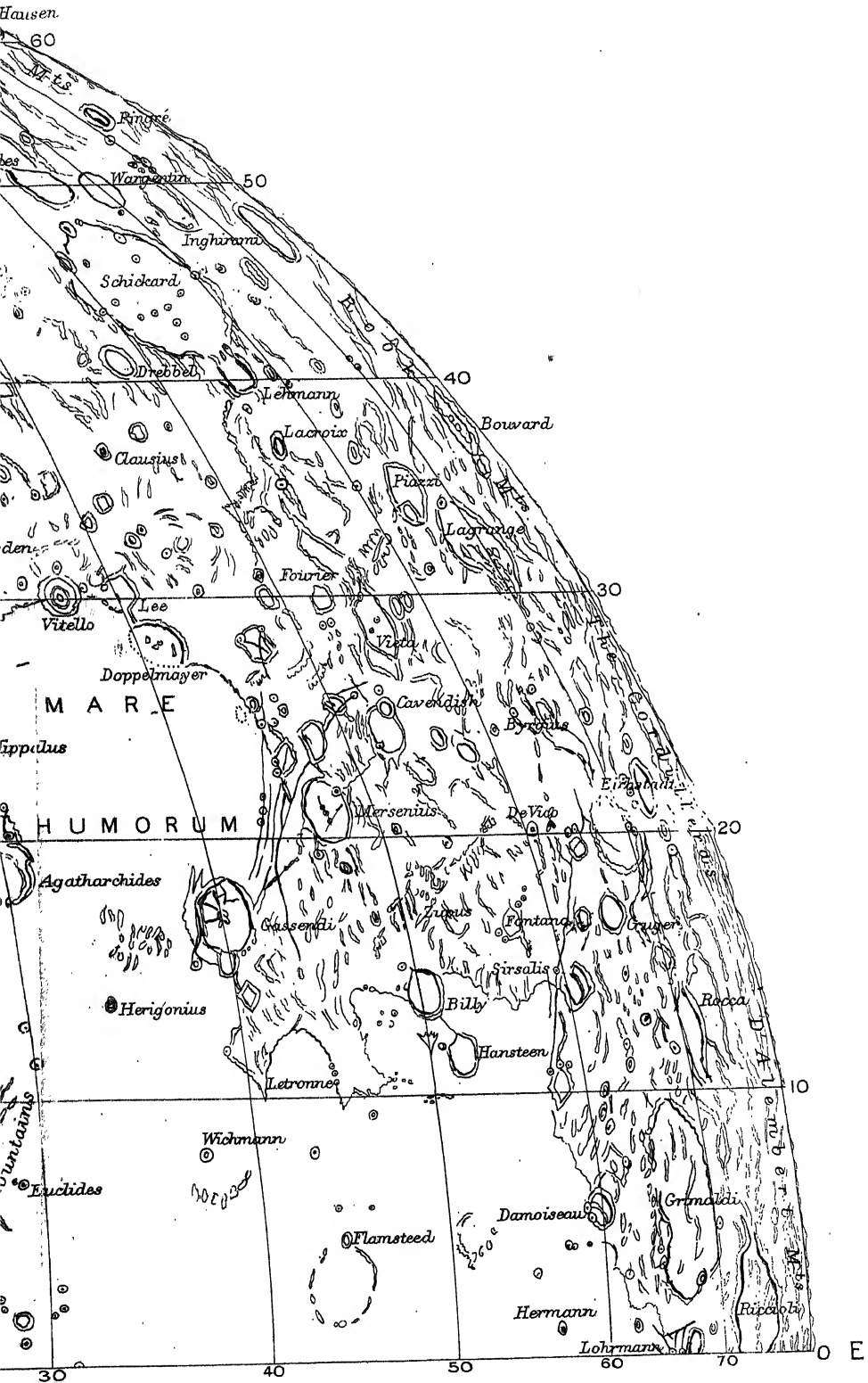


# Map of the Moon

by

T. GWYN ELGER, F.R.A.S.

THIRD QUADRANT.





Ukert Valley. Herschel *d* is a large but shallow ring-plain on the E. of Herschel, with a brilliant but smaller crater on the W. of it.

North of Herschel, on a plateau concentric with its outline, stands the large polygonal ring-plain Herschel *a*, a formation of a very interesting character, with a low broken wall, exhibiting many gaps, and including some craters of a minute class. The largest of these stands on the S.W. wall. Mr. W. H. Maw has detected some of these objects on the N. side, both in connection with the border and beyond it.

FLAMMARION.—A large incomplete walled-plain N.E. of Herschel, open towards the N., with a border rising about 3000 feet above the floor. The brilliant crater, Mösting *A*, stands just outside the wall on the E.

PTOLEMÆUS.—Taking its very favourable position into account, this is undoubtedly the most perfect example of a walled-plain on the moon's visible superficies. It is the largest and most northerly component of the fine linear chain of great enclosures, which extend southwards, in a nearly unbroken line, to Walter. It exhibits a very marked departure from circularity, the outline of the border approximating in form to a hexagon with nearly straight sides. It includes an area of about 9000 square miles, the greatest distance from side to side being about 115 miles. It is, in fact, about equal in size to the counties of York, Lancashire, and Westmorland combined; and were it possible for one to stand near the centre of its vast floor, he might easily suppose that he was stationed on a boundless plain; for, except towards the west, not a peak, or other indication of the existence of the massive rampart would be discernible; and even in this direction he would only see the upper portion of a great mountain on the wall.

The border is much broken by gaps and intersected by passes, especially E. and S., where there are several valleys connecting the interior with that of Alphonsus. The loftiest portion of the wall, which includes many crateriform depressions, is on the W., where one peak rises to nearly 9000 feet. Another on the N.E. is about 6000 feet above the interior. On the N.W. is a remarkable crater-row, called, from its discoverer, "Webb's furrow," running from a point a little N. of a depression on the border to a larger crateriform depression on the S. of Hipparchus *K*. Birt terms it "a very fugitive and delicate lunar feature." As regards the vast superficies enclosed by this irregular border, it is chiefly remarkable for the number of large saucer-shaped hollows which are revealed on its surface under a low sun. They are mostly



found on the eastern quarter of the floor. Some of them appear to have very slight rims, and in two or three instances small craters may be detected within them. Owing to their shallowness, they are very evanescent, and can only be glimpsed for an hour or so about sunrise or sunset. The large bright crater A, about 4 miles in diameter on the N.W. side of the interior, is by far the most conspicuous object upon it. Adjoining it on the N. is a large ring with a low border, and N. of this again is another, extending to the wall. Mr. Maw and Mr. Mee have seen minute craters on the borders of these obscure formations. In addition to the objects just specified, there is a fairly conspicuous crater, *d*, on the N.E. quarter of the floor, and a very large number of others distributed on its surface, which is also traversed by a network of light streaks, that have recently been carefully recorded by Mr. A. S. Williams. A cleft, from near Réaumur A, traverses the N. side of the floor, and runs up to Ptolemæus *d*.

ALPHONSUS.—A large walled-plain, 83 miles in diameter, with a massive irregular border abutting on the S.S.E. side of Ptolemæus, and rising at one place on the N.W. to a height of 7000 feet above the interior. The floor presents many features of interest. It includes a bright central peak, forming part of a longitudinal ridge, on either side of which runs a winding cleft, originating at a crater-row on the N. side of the interior. There is a third cleft on the N.W. side, and a fourth near the foot of the E. wall. There are also three peculiar dark areas within the circumvallation; two, some distance apart, abutting on the W. wall, and a third, triangular in shape, at the foot of the E. wall. The last-mentioned cleft traverses this patch. These dusky spots are easily recognised in good photographs of the moon.

ALPETRAGIUS.—A fine object, 27 miles in diameter, closely connected with the S.E. side of Alphonsus. It has peaks on the W. towering 12,000 feet above the floor, on which there is an immense central mountain, which in extent, complexity, and altitude surpasses many terrestrial mountain systems—as, for example, the Snowdonian group. The massive barrier between Alpetragius and Alphonsus deserves careful scrutiny, and should be examined under a moderately low morning sun. On the E., towards Lassell, stands a brilliant light-surrounded crater.

ARZACHEL.—Another magnificent object, associated on the N. with Alphonsus, about 66 miles in diameter, and encircled by a massive complex rampart, rising at one point more than 13,000 feet above a depressed floor. It presents some very suggestive

examples of terraces and large depressions, the latter especially well seen on the S.E. The bright interior includes a large central mountain with a digitated base on the S.E., some smaller hills on the S. of it, a deep crater W. of it (with small craters N. and S.), and, between the crater and the foot of the W. wall, a very curious winding cleft.

LASSELL.—This ring-plain, some 14 miles in diameter, is irregular both as regards its outline and the width of its rampart. There is a crater on the crest of the N.W. wall, just above a notable break in its continuity through which a ridge from the N.W. passes. There is another crater on the opposite side. The central mountain is small and difficult to see. About 20 miles N.E. of Lassell is a remarkable mountain group associated with a bright crater, and further on in the same direction is a light oval area, about 10 miles across, with a crater (*Alpetragius d*) on its S. edge. Mädler described this area as a bright crater, 5 miles in diameter, which now it certainly is not.

LALANDE.—A very deep ring-plain, about 14 miles in diameter, N.E. of Ptolemæus, with bright terraced walls, some 6000 feet above the floor, which contains a low central mountain. On the N. is the long cleft running, with some interruptions, in a W.N.W. direction towards Réaumur.

DAVY.—A deep irregular ring-plain, 23 miles across, on the Mare E. of Alphonsus. There is a deep crater with a bright rim on its S.W. wall, and E. of this a notable gap. There is also a wide opening on the N. The E. wall is of the linear type. A cleft crosses the interior.

GUERIKÉ.—The most southerly member of a remarkable group of partially destroyed walled-plains, standing in an isolated position in the Mare Nubium. Its border, on the W. and N. especially, is much broken, and never rises much more than 2000 feet above the Mare, except at one place on the N., where there is a mountain about 1000 feet higher. The E. wall is tolerably continuous, but is of a very abnormal shape. On the S. there is a peculiar  $\Delta$ -shaped gap (with a bright crater, and another less prominent on the E. side of it), the narrowest part of which opens into a long wide winding valley, bounded by low hills, extending to the W. side of a bright ring-plain, Gueriké B, on the S.E. A crater-chain occupies the centre of this valley. There is much detail within Gueriké. A large deep bright crater stands under the E. border on a mound, which, gradually narrowing in width, extends to the N. wall; and a rill-like valley runs from the

N. border towards the E. side of the  $\Delta$ -shaped gap. In addition to these features, there is a shallow rimmed crater, about midway between the extremities of the rill-valley, and several minor elevations on the floor.

On the broken N. flank of Gueriké is a number of incomplete little rings, all open to the N.; and E. of these commences a linear group of lofty isolated mountain masses extending towards the W. side of Parry, and prolonged for 30 miles or more towards the north. They are arranged in parallel rows, and remind one of a Druidical avenue of gigantic monoliths viewed from above. They terminate on the S. side of a large bright incomplete ring (with a lofty W. wall), connected with the W. side of Parry.

PARRY.—A more complete formation than Gueriké. It is about 25 miles in diameter, and is encompassed by a bright border, which, at a point on the E., is nearly 5000 feet in height. It is intersected on the N. by passes communicating with the interior of Fra Mauro. There is a crater, nearly central, on the dusky interior, which, under a low sun, when the shadows of the serrated crest of the W. wall reach about half-way across the floor, appears to be the centre of three or four concentric ridges, which at this phase are traceable on the E. side of it. There is a conspicuous crater on the E. wall, below which originates a distinct cleft. This object skirts the inner foot of the E. border, and after traversing the N. wall, strikes across the wide expanse of Fra Mauro, and is ultimately lost in the region N. of this formation. Parry A, S. of Parry, is a very deep brilliant crater with a central hill and surrounded by a glistening halo. A cleft, originating at a mountain arm connected with the E. side of Gueriké, runs to the S. flank of this object, and is probably connected with that which skirts the floor of Parry on the E.

BONPLAND.—A ruined walled-plain with a low and much broken wall, which on the S.W. appears to be an attenuated prolongation of that of Parry. It is of the linear type, the formation approximating in shape to that of a pentagon. The floor is crossed from N. to S. by a fine cleft which originates at a crater beyond the S. wall, and is visible as a light streak under a high light. Schmidt shows a short cleft on the W. of this.

FRA MAURO.—A large enclosure of irregular shape, at least 50 miles from side to side, abutting on Parry and Bonpland. In addition to the cleft which crosses it, the floor is traversed by a great number of ridges, and includes at least seven craters.

THEBIT.—A fine ring-plain, 32 miles in diameter, on the

mountainous W. margin of the Mare Nubium, N E. of Purbach. Its irregular rampart is prominently terraced, and its continuity on the N.E. interrupted by a large deep crater (Thebit A), at least 9 miles in diameter, which has in its turn a smaller crater, of about half this size, on its margin, and a small central mountain within, which was once considered a good optical test, though it is not a difficult object in a 4-inch achromatic, if it is looked for at a favourable phase. The border of Thebit rises at one place on the N W to a height of nearly 10,000 feet above the interior, which includes much detail. The E. wall of Thebit A attains the same height above its floor, which is depressed more than 5000 feet below the Mare.

BIRT —This ring-plain, about 12 miles in diameter, is situated on the Mare Nubium, some distance due E of Thebit. It has a brilliant border, surmounted by peaks rising more than 2000 feet above the Mare, and a very depressed floor, which does not appear to contain any visible detail. A bright crater adjoins it on the S.W., the wall of which at the point of junction is clearly very low, so that under oblique light the two interiors appear to communicate by a narrow pass or neck filled with shadow. I have frequently seen a break in the N.W. wall of Birt, which seems to indicate the presence of a crater. There is a noteworthy cleft on the E, which can be traced from the foot of the E wall to the hills on the N E. It is a fine telescopic object, and, under some conditions, the wider portion of it resembles a railway cutting traversing rising ground, seen from above. It is visible as a white line under a high light.

THE STRAIGHT WALL,—Sometimes called "the railroad," is a remarkable and almost unique formation on the W. side of Birt, extending for about 65 miles from N E to S W in a nearly straight line, terminating on the south at a very peculiar mountain group, the shape of which has been compared to a stag's horn, but which perhaps more closely resembles a sword-handle,—the wall representing the blade. When examined under suitable conditions, the latter is seen to be slightly curved, the S. half bending to the west, and the remainder the opposite way. The formation is not a ridge, but is clearly due to a sudden change in the level of the surface, and thus has the outward characteristics of a "fault." Along the upper edge of this gigantic cliff (which, though measures differ, cannot be anywhere much less than 500 feet high) I have seen at different times many small craterlets and mounds. Near its N. end is a large crater, and on the W. is a row of hillocks, running

at right angles to the cliff. No observer should fail to examine the wall under a setting sun when the nearly perpendicular E. face of the cliff is brilliantly illuminated.

NICOLLET.—A conspicuous little ring-plain on the E. of Birt, and somewhat smaller. Between the two is a still smaller crater, from near which runs a low mountain range, nearly parallel to the straight wall, to the region S.E. of the Stag's Horn Mountains. Here will be found three small light-surrounded craters arranged in a triangle, with a somewhat larger crater in the middle.

PURBACH.—An immense enclosure of irregular shape, approximating to that of a rhomboid with slightly curved sides. It is fully 60 miles across, and the walls in places exceed 8000 feet in altitude, and include many depressions, large and small. On the E. inner slope are some fine terraces and several craters. The continuity of the circumvallation is broken on the N. by a great ring-plain, on the floor of which I have seen a prominent cleft and a crater near the S. side. There is a large bright crater in the interior of Purbach, S. of the centre, two others on the W. half of the floor, and a few ridges.

REGIOMONTANUS.—A still more irregular walled-plain, of about the same area, closely associated with the S. flank of Purbach, having a rampart of a similar complex type, traversed by passes, longitudinal valleys, and other depressions. Schmidt alone shows the especially fine example of a crater-row, which is not a difficult object, in connection with the S.E. wall. Excepting one crater, nearly central, and some inconspicuous ridges, I have seen no detail on the floor. Schmidt, however, records many features.

WALTER.—A great rhomboidal walled-plain, 100 miles in diameter, with a considerably depressed floor, enclosed by a rampart of a very complex kind, crowned by numerous peaks, one of which, on the W., rises 10,000 feet above the interior. If the formation is observed when it is close to the morning terminator, say, when the latter lies from  $1^{\circ}$  to  $2^{\circ}$  E. of the centre of the floor, it is one of the most striking and beautiful objects which the lunar observer can scrutinize. The inner slope of the border which abuts on Regiomontanus, examined at this phase under a high power, is seen to be pitted with an inconceivable number of minute craters; and the summit ridge, and the region towards Werner, scalloped in a very extraordinary way, the engrailing (to use an heraldic term) being due to the presence of a row of big depressions. The floor at this phase is sufficiently illuminated to disclose some of its

most noteworthy features. Taking its area to be about 8000 square miles, at least 1200 square miles of it is occupied by the central mountain group and its adjuncts, the highest peak rising to a height of nearly 5000 feet (or nearly 600 feet higher than Ben Nevis), above the interior, and throwing a fine spire of shadow thereon. In the midst of this central boss are two deep craters, one being about 10 miles in diameter, and a number of shallower depressions. In association with the loftiest peak, I noted at 8 h., March 9, 1889, two brilliant little craters, which presumably are not far from the summit. Near the E. corner of the floor there is another large deep crater, and, ranging in a line from the centre to the S.E. wall, three smaller craters.

LEXELL.—On the E. of Walter extends an immense plain of irregular outline, which is at least equal to it in area. Though no large formation is found thereon; many ridges, short crater-rows, and ordinary craters figure on its rugged superficies; and on its borders stand some very noteworthy objects, among them, on the S., the walled-plain Lexell, about 32 miles in diameter, which presents many points of interest. Its irregular wall, rising, at one point on the S.W., to a height of nearly 8000 feet, is on the N.W. almost completely wanting, only very faint indications of its site being traceable, even under a low morning sun. On the opposite side it is boldly terraced, and has a large crater on its summit. The interior, the tone of which is conspicuously darker than that of the region outside, contains a small central hill, with two craters connected with it. The low N.W. margin is traversed by a delicate valley, which, originating on the N. side of the great plain, crosses the W. quarter of Lexell and terminates apparently on the S.W. side of the floor.

HELL.—A prominent ring-plain, about 18 miles in diameter, on the E. side of the great plain. There is a central mountain and many ridges within.

BALL.—A somewhat smaller ring-plain on the S.E. edge of the great plain, with a lofty terraced border and a central mountain more than 2000 feet high. There are two large irregular depressions on the W. of the formation, a crater on the S., and a smaller one on the N. wall.

PITATUS.—This remarkable object, 58 miles in diameter, with Hesiodus, its companion on the E., situated at the extreme S. end of the Mare Nubium, afford good examples of a class of formations which exhibit undoubted signs of partial destruction, from some unknown cause, on that side of them which faces the Mare.

On every side but the N., Pitatus is a walled plain of an especially massive type, the border on the S.E. furnishing one of the finest examples of terraces to be found on the visible surface. On the S.W., two parallel rows of large crateriform depressions, perhaps the most remarkable of their kind, extend for 60 miles or more to the W. flank of Gauricus. On the N.W., the rampart includes many curious irregular depressions and craters, and gradually diminishes in height, till, for a space of about 12 miles on the N., there can hardly be said to be any border at all, its site being marked by some inconsiderable mounds and shallow hollows. There is a small bright central mountain on the floor, and, S. of it, two larger but lower elevations. A distinct straight cleft traverses the N.W. side of the interior very near the wall, to which it forms an apparent chord, and a second cleft occupies a similar position with respect to the bright N.E. border. A narrow pass forms a communication with the interior of Hesiodus.

HESIODUS.—This walled-plain, little more than half the diameter of the last, has an irregular outline, and for the most part linear walls, which on the S. are massive and lofty (4000 feet), but on the N. very low, and broken by gaps. There is a fine deep crater on the S. border, and a small but distinct crater on the floor, nearly central, the only object thereon which I have seen, though Schmidt draws a smaller one on the W. of it.

A mountain abutting on the N.E. side of Hesiodus is the W. origin of one of the longest clefts on the moon. Running in a E.S.E. direction, it traverses the Mare to a crater near the W. face of the Cichus mountain arm, reappears on the E. side of this object, and is finally lost amid the hills on the N. of Capuanus. The W. section of this cleft is coarser and much more distinct than that lying E. of the mountain arm.

GAURICUS.—A large walled-plain S. of Pitatus, about 40 miles in diameter. The border is very irregular, and, according to Neison, consists on the E. of a precipitous cliff more than 9000 feet high. It is surrounded by a number of large rings on the S., and has several considerable small depressions on its N. border. There is apparently no prominent detail on the floor. Schmidt shows some ridges and craterlets.

WURZELBAUR.—Another irregular walled-plain, about 50 miles in diameter, on the S.E. of Pitatus, with a very complex border, in connection with which, on the S.W., is a group of fine depressions, and on the S.E. a large crater. There is much detail on the very uneven floor.

MILLER.—One of a group of three moderately large ring-plains, of which Nasireddin is a member, near the central meridian in S. latitude  $39^{\circ}$ . Its massive border rises nearly 11,000 feet above the floor, on which stands a central peak. Miller is about 36 miles in diameter.

NASIREDDIN.—A somewhat smaller ring-plain on the S. of the last, and of a very similar type. It contains a central peak and several minor elevations. Between its N.W. border and the S.W. flank of Miller is a smaller ring-plain of about half the size of Nasireddin, and on the S.E. a large enclosure named HUGGINS.

ORONTIUS.—Huggins has encroached on the W. side of this irregular ring-plain and overlaps it. It is of considerable size. The floor includes much detail and a prominent crater.

SASSERIDES.—A formation of irregular shape, with very lofty walls, situated amid the confusion of ring-plains, craters, crater-pits, &c., in the region N. of Tycho, some of which are fully as deserving of a distinct name.

HEINSIUS.—A very curious formation on the N.E. of Tycho: a fine telescopic object under oblique illumination. It has an irregular but continuous border, except on the S., where two large ring-plains have encroached upon it, and a third, N. of a line joining their centres, occupies no inconsiderable portion of the floor. Heinsius is nearly 50 miles across, and the border on the W., is nearly 9000 feet above the interior, which includes, at least, three small craters. The walls of the intrusive ring-plains have craters on their summits; the more westerly has two on the W., and its companion, one on the S.W. The ring-plain on the floor has a crater on its E. wall. Schmidt shows a small crater between the ring-plains on the S. border.

SAUSSURE.—A ring-plain W. of Tycho, 28 miles in diameter, with bright lofty terraced walls and a somewhat dark interior, on which there is a crater, W. of the centre, and some crater-pits. There are several large depressions on the S.W. wall. It is surrounded by formations which, though nearly as prominent as itself, have not, with the exception of Pictet on the E., and one on the N.W., called Huggins by Schmidt, received distinctive names. The region W. of Saussure abounds in craterlets, some of which are of the minutest type. One of the Tycho streaks is manifestly deflected from its course by this formation, and another is faintly traceable on the floor.

PICTET.—A walled-plain of irregular shape, about 30 miles across, between Saussure and Tycho, with a border broken on the



S. by a large conspicuous ring-plain, which is at least 10 miles in diameter, and, according to Schmidt, has a central mountain. Schmidt draws the S.E. border of Pictet as broken by ridges extending on to the floor. He also shows several craters and minor elevations thereon.

TYCHO.—As the centre from which the principal bright ray-system of the moon radiates, and the most conspicuous object in the southern hemisphere, this noble ring-plain may justly claim the pre-eminent title of “the Metropolitan crater.” It is more than 54 miles in diameter, and its massive border, everywhere traversed by terraces and variegated by depressions within and without, is surmounted by peaks rising both on the E. and W. to a height of about 17,000 feet above the bright interior, on which stands a magnificent central mountain at least 5000 feet in altitude. Were it not somewhat foreshortened, Tycho would be seen to deviate considerably from what is deemed to be the normal shape. On the S. and W. especially, the wall approximates to the linear type, no signs of curvature being apparent where these sections meet. The crest on the S. and S.E. exhibits many breaks and irregularities; and it is through a narrow gap on the S. that a rill-like valley, originating at a small depression near the foot of the S.W. *glacis*, passes, and, descending the inner slope of the S.E. wall obliquely, terminates near its foot. There is a distinct crater on the summit ridge on the S.E., and another below the crest on the outer S.W. slope. On the S. inner slope I have often remarked a number of bright oval objects, which, for the lack of a better word, may be termed “mounds,” though they represent masses of material many miles in length and breadth. The outer slope of Tycho, exhibiting under a high light a grey nimbus encircling the wall, includes—craters, crater-pits, shallow valleys, spurs and buttresses—in short, almost every variety of lunar feature is represented. Excepting the central mountain and a crater on the W. of it, I have not seen any object on the floor, which, for some unexplained reason, is never very distinct. Schmidt shows several low ridges on the N.E. side. In a paper recently published in the *Astronomische Nachrichten*, Professor W. H. Pickering, describing his observations of the Tycho streaks made at Arequipa, Peru, with a 13-inch achromatic, asserts that they do not radiate from the centre of Tycho, but from a multitude of minute craters on its S.E. or N. rim. (See Introduction.)

MAGNUS.—An immense partially ruined enclosure, at least

100 miles from side to side, on the S.W. of Tycho, from which it is separated by a region covered with a confused mass of ring-plains and craters. On almost every part of its broken border stand large ring-plains, many of which, if they were isolated, or situated in a less disturbed region, would rank as objects of importance; but among such a multitude of features they pass unnoticed. The largest of them occupies no inconsiderable part of the S.E. wall, and is quite 30 miles in diameter, its own border being also much broken by depressions, as, indeed, are those of almost all the six or more large ring-plains which define the N. limits of Maginus. The loftiest portion of what remains of a true border rises at one place to more than 14,000 feet. On the floor, which is traversed by some of the Tycho rays, there is a mountain group associated with a crater, nearly central, and several large rings on the N. side. Though the formation is very difficult to detect under a high sun, Mädler's dictum that "the full moon knows no Maginus" is not strictly true.

**STREET.**—A walled-plain between Tycho and Maginus, about 28 miles in diameter, with a border of moderate height, broken by depressions on the N. There are some small craters and ridges within; but the surrounding region, with its almost endless variety of abnormally shaped formations, is far more worthy of the observer's attention.

**DELUC.**—The largest and most prominent member of a curious group of ring-plains on the S.W. of Maginus. It is about 28 miles in diameter, and is encircled by a wall some 7000 feet above the interior, which includes a crater. A large ring with a central mountain encroaches on the N. wall, and a smaller object of the same class on the S. wall.

**CLAVIUS.**—There are few lunar observers who have not devoted more or less attention to this beautiful formation, one of the most striking of telescopic objects. However familiar we may consider ourselves to be with its features, there is always something fresh to note and to admire as often as we examine its apparently inexhaustible details. It is 142 miles from side to side, and includes an area of at least 16,000 square miles within its irregular circumvallation, which is only comparatively slightly elevated above the bright plateau on the W., though it stands at least 12,000 feet above the depressed floor. At a point on the S.W. a peak rises nearly 17,000 feet above the interior, while on the E. the cliffs are almost as lofty. There are two remarkable ring-plains, each about 25 miles in diameter, associated, one with the N., and the

other with the S. wall, the floors of both abounding in detail. The latter, however, is the most noteworthy on account of the curious corrugations visible soon after sunrise on the outer N. slope of its wall, resembling the ribbed flanks of some of the Java volcanoes. There are five large craters on the floor of Clavius, following a curve convex to the N., and diminishing in size from W. to E. The most westerly stands nearly midway between the two large ring-plains on the walls, the second (about two-thirds its area) is associated with a complex group of hills and smaller craters. Both these objects have central mountains. In addition to this prominent chain, there are innumerable craters of a smaller type on the floor, but they are more plentiful on the S. half than elsewhere. On the S.E. wall are three very large depressions. On the broad massive N.E. border, the bright summit ridge and the many transverse valleys running down from it to the floor, are especially interesting features. There are very clear indications of "faulting" on a vast scale where this broad section of the wall abuts on the N. side of the formation.

CYSATUS.—A regular walled-plain, apparently about 28 miles in diameter, forming the most northerly member of a chain of formations, of which Newton, Short, and Moretus, extending towards the S. limb, form a part. Its border rises nearly 13,000 feet above a floor devoid of prominent detail.

GRUEMBERGER.—A much larger and more irregular ring-plain, nearly 40 miles from wall to wall, on the E. side of Cysatus. Its W. border rises nearly 14,000 feet above the interior, which includes an abnormally deep crater, the bottom of which is 20,000 feet below the crest of the W. wall, and several small depressions and ridges. The inner E. slope is finely terraced.

MORETUS.—A magnificent object, 78 miles in diameter, but foreshortened into a flat ellipse. Its beautifully terraced walls and magnificent central mountain, nearly 7000 feet high, are very conspicuous under suitable conditions. The rampart on the E. is more than 15,000 feet above the floor, while on the opposite side it is about 5000 feet lower.

SHORT.—A fine but foreshortened ring-plain of oblong shape, squeezed in between Moretus and Newton. It is about 30 miles in diameter, and on the S.E., where its border and that of Newton are in common, it rises nearly 17,000 feet above the interior, which includes, according to Neison, a small central hill. Schmidt shows a crater on the N. side of the floor.

NEWTON.—Is situated on the S.E. side of Short, and is the

deepest walled-plain on the visible surface. It is of irregular form and about 143 miles in extreme length. One gigantic peak on the E. rises to nearly 24,000 feet above the floor, the greater part of which is always immersed in shadow, so that neither the earth or sun can at any time be seen from it.

MALAPERT.—A ring-plain situated far too near the limb for useful observation. Between it and Newton is a number of abnormally shaped enclosures.

CABEUS.—Another object out of the range of satisfactory scrutiny. Mädler considered that it is as deep as Newton. According to Neison, a central peak and two craters can be seen within under favourable conditions. Schmidt draws a long row of great depressions on the N. side of it.

#### EAST LONGITUDE 20° TO 40°.

LANDSBERG.—A ring-plain, about 28 miles in diameter, situated in Mare Nubium, S.E. of Reinhold, which in many respects it resembles. Its regular massive border is everywhere continuous. Only a solitary crater breaks the uniformity of its crest, that rises on the W. to nearly 10,000 feet, and on the E. to about 7000 feet above the floor, which is depressed about 7000 feet below the surrounding surface. The inner slopes exhibit some fine terraces, and on the broad W. *glacis* is a curious winding valley, which runs up the slope from the S.W. side to the crater just mentioned, then, bending downwards, joins the plain at the foot of the N. wall. Neither this nor the crater is shown in the maps. The large compound central peak is apparently the sole object in the interior. At 8 h. 25 m. on January 23, 1888, when observing the progress of sunrise on this formation with a 8½-inch Calver-reflector charged with different eyepieces, I noticed, when about three-fourths of the floor was in shadow, that the illuminated portion of it was of a dark chocolate hue, strongly contrasting with the grey tone of the surrounding district. This appearance lasted till the interior was more than half illuminated, gradually becoming less pronounced as the sun rose higher on the ring. E. and S.E. of Landsberg is a number of ring-plains and craters well worthy of careful examination. Five of the largest are surrounded by a glistening halo, and one (that nearest to the formation) and another (the largest of the group) have each a minute crater on their N. wall.

EUCLIDES.—One of the most brilliant objects on the moon; a crater 7 miles in diameter, standing on a large bright area in the Mare Procellarum, E. of the Riphæan Mountains. Its E. rim rises nearly 2000 feet above the bright depressed floor; on the W. there is a bright little unrecorded crater.

WICHMANN.—This bright crater, about 5 miles in diameter, stands on a light area in Oceanus Procellarum, N.N.W. of Letronne and nearly due E. of Euclides. Some distance on the N.E. are the relics of what appears once to have been a large enclosure, represented now by a few isolated mountains.

HERIGONIUS.—A ring-plain, about 7 miles in diameter, in the Mare Procellarum, N.W. of Gassendi. There is a small crater a few miles S.E. of it, among the bright little mountains which flank this formation. Herigonius has a small central mountain, which is a good test for moderate apertures.

GASSENDI.—One of the most beautiful telescopic objects on the moon's visible surface, and structurally one of the most interesting and suggestive. It is a walled-plain, 55 miles in diameter, of a distinctly polygonal type, the N.W. and S.W. sections being practically straight, while the intermediate W. section exhibits a slightly convex curvature, or bulging in towards the interior. There is also much angularity about the E. side, which is evident at an early stage of sunrise. The wall on the N. is broken through and almost completely wrecked by the great ring-plain Gassendi A. The bright eastern section of the border is in places very lofty, rising at one peak, N. of the well-known triangular depression upon it, to 9000 feet, and at other peaks on the same side still higher. It is very low on the S., being only about 500 feet above the surface. The floor, however, on the N. stands 2000 feet above the Mare Humorum. On the W. there is a peak towering 4000 feet above the wall, which is here about 5000 feet above the floor, and 8000 feet above the Mare Nubium. A very notable feature in connection with this formation is the little bright plain bounding it on the N.W., and separated from it by merely a narrow strip of wall. This enclosure is flanked on the N.E. by Gassendi A, and on the S.W. and N.W. by a coarse winding ridge, running from the W. wall and terminating at a large irregular dusky depression. Gaudibert has detected a crater near the S.E. edge of this bright plain, which includes also some oval mounds. The interior of Gassendi is without question unrivalled for the variety of its details, and, after Plato, has perhaps received more attention from observers than any other object.

The bright central mountain, or rather mountains, for it consists of a number of grouped masses crowned by peaks, of which the loftiest is about 4000 feet, is one of the finest on the moon. It was carefully studied with a 6½-inch Cooke-achromatic by the late Professor Phillips, the geologist, who compared it to the dolomitic or trachytic mountains of the earth. The buttresses and spurs which it throws out give its base a digitated outline, easily seen under suitable illumination. There are between 30 and 40 clefts in the interior, the majority being confined to the S.W. quarter of the floor. Those most easily seen pertain to the group which radiates from the central mountain towards the S.W. wall. They are all more or less difficult objects, requiring exceptionally favourable weather and high powers. A fine mountain range, the Percy Mountains, is connected with the E. flank of Gassendi, extending in a S.E. direction towards Mersenius, and defining the N.E. side of the Mare Humorum.

**BULLIALDUS.**—A noble object, 38 miles in diameter, forming with its surroundings by far the most notable formation on the surface of the Mare Nubium, and one of the most characteristic ring-plains on the moon. It should be observed about the time when the morning terminator lies on the W. border of the Mare Humorum, as at this phase the best view is obtained of the two deep parallel terrace valleys which run round the bright inner slope of the E. wall, of the crater-row against which they abut on the S.E., and of the massive W. *glacis*, with its spurs and depressions. The S. border of Bullialdus has been manifestly modified by the presence of the great ring-plain A, a deep irregular formation with linear walls, which is connected with it by a shallow valley. The rampart of Bullialdus rises about 8000 feet above a concave floor, which sinks some 4000 feet below the Mare on the E. With the exception of the fine compound central mountain, 3000 feet high, there are few details in the interior. On the S., is the fine ring-plain B, connected with the S.E. wall near the crater-row by a well-marked valley, and nearly due E. of B is another, a square-shaped enclosure, C, with a very lofty little mountain on the E. side of it, and a crater on its S. wall. In addition to these features, there are many ridges and surface inequalities, very prominent under oblique illumination.

**LUBINIEZKY.**—A regular enclosure, about 23 miles in diameter, N.E. of Bullialdus, with a low attenuated border, which is nowhere more than 1000 feet in height. It is tolerably continuous, except

on the S., where there are two or three breaks. Its level dark interior presents no details to vary its monotony. Close under the N.W. wall is a small crater connected with it by a ridge, and E. of this a very rugged area, traversed in every direction by narrow shallow valleys, which are well worth looking at when close to the morning terminator. A bright spur projects from the N. wall of Lubiniezky.

KIES.—A somewhat similar formation, S. of Bullialdus, about 25 miles in diameter, also encircled by a border of insignificant dimensions, attaining an altitude of 2400 feet at only one point on the S.E., while elsewhere it is scarcely higher than that of Lubiniezky. It is clearly polygonal, approximating to the hexagonal type. On the more distinct S. section a bright spur projects from it. On the N. its continuity is broken by a distinct little crater. It is traversed by a remarkable white streak, extending in a S.W. direction from Bullialdus c (where it is very wide), across the interior, to the more westerly of two craters S.W. of Mercator. Another streak branches out from it near the centre of the floor, and runs to the W. wall. The principal streak, so far as the portion within Kies is concerned, represents a cleft. On the Mare E. of Kies is a curious circular mound, and farther towards Campanus two prominent little mountains. On the N.W. is a large obscure ring and a wide shallow valley bordered by ridges.

AGATHARCHIDES.—A very irregular complex ring-plain, about 28 miles in diameter, forming part of the N.W. side of the Mare Humorum. It must be observed under many phases before one can clearly comprehend its distinctive features. The wall is very deficient on the N., but is represented in places by bright mountain masses. The formation is flanked on the E. by a double rampart, which is at one place more than 5000 feet in height, with a deep intervening valley. The S. wall is traversed by a number of parallel valleys, all trending towards Hippalus. These are included in a much wider and longer chasm, which, gradually diminishing in breadth, extends up to the N. wall of the latter.

HIPPALUS.—A partially ruined walled-plain, about 38 miles in diameter, on the W. side of the Mare Humorum, S. of Agatharchides. At least one-third of the border is wanting on the S.E., but under a low sun its site can be distinguished by a faint marking and the obvious difference in tone between the dark interior and the lighter-coloured plain. The rest of the wall is bright and continuous, except at a place on the W.,

where what appears to be the segment of a large ring has encroached upon it. There are two craters in the interior of Hippalus, and a row of parallel ridges, running obliquely from the S.W. wall up to a cleft which traverses the floor from N. to S. W. of Hippalus stands a bright crater, Hippalus A, with an incomplete little ring-plain adjoining it on the N.W.; and N.E. of it a much larger obscure ring containing two little hills. The Hippalus rill-system is a very interesting one, and the greater part of it can, moreover, be easily traced in a good 4-inch achromatic. It originates in the rugged region E. of Campanus, from which five nearly parallel curved clefts extend up to the rocky barrier, connecting the N. side of this formation with the S.W. side of Hippalus. The most westerly of these furrows is interrupted by a crater on this wall, but reappears on the N. side of it, and, after making a detour towards the W. to avoid a little mountain in its path, runs partially round the E. flank of Hippalus A, and then, continuing its northerly course, terminates amid the mountains W. of Agatharchides. (A short parallel cleft runs E. of this from the little mountain to the E. side of A.) The most easterly member of the system, originating N. of Ramsden, enters Hippalus at the S. side of the great gap in the border, and, after traversing the floor at the W. foot of a ridge thereon, also extends towards the mountains W. of Agatharchides. Between these clefts are three intermediate furrows, one of which runs N. from the N. side of the encroaching ring already referred to, on the W. wall of Hippalus.

CAMPANUS.—A ring-plain, 30 miles in diameter, on the rocky barrier, extending in nearly a straight line from Hippalus to Cichus. Its terraced walls, which rise on the E. more than 6000 feet above the floor, are broken on the S. by a narrow valley, and on the E. by a small crater. A small central mountain is apparently the only object on a very dark interior.

MERCATOR.—A more irregular ring-plain of about the same area, adjoining Campanus on the S.W. Its rampart is somewhat lower, and is partially broken on the N. by two semi-rings, and on the S. by a gap. The E. wall extends on the S. far beyond the limits of the formation, and terminates in a brilliant mountain mass 6000 feet in height. There is a bright crater on the crest of both the E. and W. border. On the plain E. of Mercator is a remarkable little crater standing on a light area, and, just under the wall, a dusky pit connected with it by a rill-like marking.



These objects are of a very doubtful nature, and should be carefully observed. The floor of Mercator is much lighter than that of Campanus, and appears to be devoid of detail.

**CICHUS.**—A conspicuous ring-plain, about 20 miles in diameter, with a prominent deep crater about 6 miles across on its E. rim. It is situated on a curious boot-shaped plateau, near the S. end of the rocky mountain barrier associated with the last two formations. Its walls rise about 9000 feet above a sunken floor, on which there is some faint detail, but apparently nothing deserving the distinction of a central mountain. The plateau on the N. is cut through by a fine broad valley, which has obviously interfered with a large crateriform depression on its southern edge. A cleft runs from a small crater W. of the plateau up to this valley, and extends beyond to the W. wall of Capuanus. There is also a delicate cleft crossing the region S. of Cichus to the group of complicated formations S.W. of Capuanus. As already mentioned, the great Hesiodus cleft is associated with the Cichus plateau.

**CAPUANUS.**—A large ring-plain, about 34 miles in diameter, E. of Cichus, with a border especially remarkable on the E., where it rises more than 8000 feet above the outside country, and includes a large brilliant shallow crater. It is broken on the N.W. by a small but noteworthy double crater; and on the S. its continuity is destroyed for many miles by a number of big circular and sub-circular depressions and prominent deep valleys, far too numerous and complicated to describe. The level dusky interior contains only a low mound on the S., but is crossed by some light streaks running from N. to S.

**RAMSDEN.**—This ring-plain, 12 miles in diameter, derives its importance from the remarkable rill-system with which it is so closely associated. Its border, about 1800 feet on the W. above the outside surface, is slightly terraced within on the E., where there is an unrecorded bright crater on the slope. The two principal clefts on the S. originate among the hills E. of Capuanus. The more easterly begins at a crater on the N. edge of these objects, and runs N. to the E. side of Ramsden; the other originates at a larger crater, and proceeds in a N. direction up to a bright little mountain S.W. of Ramsden; when, swerving to the N.E., it ends at the W. wall of this formation. This mountain is a centre or node from which three other more delicate branches radiate. On the N., three of the shortest clefts pertaining to the system are easily traceable from neighbouring mountains up to the N. wall, which they apparently partially cut through. The

E. pair have a common origin, but open out as they approach the border of Ramsden.

VITELLO.—A very peculiar ring-plain, 28 miles in diameter, on the S. side of the Mare Humorum, remarkable for having another nearly concentric ring-plain, of considerably less altitude within it, and a large bright central boss, overlooking the inner wall, 1700 feet in height. The outer wall is somewhat irregular, and is broken by gaps and valleys on the S. and N.W. It rises on the E. about 5000 feet above the Mare, but only about 2000 above the interior, which includes a crater on its N. side, and some low ridges.

HAINZEL.—This remarkable formation, which is about 55 miles in greatest length, but is hardly half so broad, derives its abnormal shape from the partial coalescence of two nearly equal ring-plains, the walls of both being very lofty,—more than 10,000 feet. It ought to be observed under a morning sun when the floor is about half illuminated. At this phase the extension of the broad bright terraced E. border across a portion of the interior is very apparent, and the true structural character of the formation clearly revealed. The floor abounds in detail, among which, on the S., are some large craters and a bright longitudinal ridge. Hainzel is flanked on the W. and S.W. by a broad plateau, W. of which stand two ring-plains about 15 miles in diameter, both having prominent central mountains and bright interiors.

WILHELM I.—A large irregular formation, about 50 miles across, S.E. of Heinsius, with walls varying very considerably in height, rising more than 11,000 feet on the E., but only about 7000 feet on the opposite side. The border is everywhere crowded with depressions, large and small. Three ring-plains, not less than 6 miles in diameter, stand upon the S. wall, the most westerly overlapping its shallower neighbour on the E., which projects beyond the wall on to the floor. The interior has a very rugged and uneven surface, upon the N. side of which are two very distinct craters, and a short crater-row on the W. of them. It is traversed from W. to E. by three bright streaks from Tycho, two on the N. being very prominent under a high light.

LONGOMONTANUS.—A much larger walled-plain, S. of the last. It is 90 miles in diameter, with a border much broken by depressions, especially on the N.E. At one peak on this side it rises to the tremendous altitude of 13,000 feet above the floor, and at peaks on the W. more than 1000 feet higher. There is a crowd of ring-plains on the N.E. quarter of the interior, and some hills

and craterlets in other parts of it. It is also crossed by rays from Tycho.

SCHILLER.—A fine lozenge-shaped enclosure, with a continuous but somewhat irregular border. It is about 112 miles in extreme length, and rather more than half this in breadth. The loftiest section of the wall is on the W., where it rises 13,000 feet above a considerably depressed interior. There is a bright crater on this side and some terraces. On the broad inner slope of the E. border, the summit ridge of which is especially well-marked, there is a large shallow depression. The floor contains scarcely any detail, except some ridges on the N. side and a few craterlets. The great bright plain E. of Schiller and the region on the S.E. are especially worthy of scrutiny under a low morning sun.

BAYER.—This object, 29 miles in diameter, with a terraced border rising on the W. to a height of 8000 feet above the floor, is so closely associated with Schiller, that it may almost be regarded as forming part of it. A long lofty mountain arm, apparently connected with the W. wall of the latter, runs from the E. side of Bayer towards the N.W. There is a crater on the E. side of the interior.

RÖST.—An oblong-shaped ring-plain, 30 miles in diameter, on the S.W. of Schiller, with moderately high walls, and, according to Neison, a shallow depression within, nearly central. I have seen a crater shown by Schmidt on the E. side of the floor. A valley runs from the E. side of Röst to the S. of Schiller.

WEIGEL.—A not very conspicuous ring-plain on the S. of Schiller, with a crater on its N.W. rim, and a larger ring adjoining it on the S.E. A prominent curved mountain arm from the E. wall of Schiller runs towards the N. side of this formation.

BLANCANUS.—A formation, 50 miles in diameter, on the S.E. side of Clavius, whose surpassing beauties tend to render the less remarkable features of this magnificent ring-plain and those of its neighbour Scheiner less attractive than they otherwise would be. The crest of its finely terraced wall, which at one peak on the E. rises to 18,000 feet, is at least 12,000 feet above the interior. Krieger saw twenty craters on the floor (1894, Sept. 21, 13h.), most of them situated on the S. quarter.

SCHEINER.—A still larger object, being nearly 70 miles in diameter, with a prominently terraced wall, fully as lofty as that of Blancanus. There is a large crater, nearly central, two others on the N.E. side of the floor, and a fourth at the inner foot of the E. wall. There is also a shallow ring on the N.E. slope.

Schmidt shows, but far too prominently, two straight ridges crossing each other on the S. side of the central crater.

CASATUS.—A large walled-plain, about 50 miles in diameter, S.E. of Blancanus, near the limb, remarkable for having one of the loftiest ramparts of all known lunar objects; it rises at one peak on the S.W. to the great height of 22,285 feet above the floor, while there are other peaks nearly as high on the N. and S. The wall is broken on the E. by a fine crater. There is also a crater on the N.W. side of the very depressed floor, together with some craterlets.

KLAPROTH.—Casatus partially overlaps this still larger but less massive formation on its S.E. flank. The walls of Klaproth are much lower and very irregular and broken, especially on the W. There are some ridges on the floor. The neighbouring region is covered with unnamed objects, large and small.

#### EAST LONGITUDE $40^{\circ}$ TO $60^{\circ}$ .

FLAMSTEED.—A bright ring-plain, 9 miles in diameter, in a barren region in the Oceanus Procellarum, N.E. of Wichmann. It has a regular border (broken at one place on the N. by a gap, which probably represents a crater), rising to a height of about 1400 feet above the surrounding plain. A great enclosure, 60 miles in diameter, lies on the N. of Flamsteed. It is defined by low ridges which exhibit many breaks, though under a high light the ring is apparently continuous. Within are several small craters and two considerable hills, nearly central.

HERMANN.—A ring-plain, about 10 miles in diameter, in the Oceanus Procellarum, W. of Lohrmann. It is associated with a group of long ridges, running in a meridional direction and roughly parallel to the coast-line.

LETRONNE.—A magnificent bay or inflexion in the coast-line of the Oceanus Procellarum, N.N.E. of Gassendi, presenting an opening towards the N. of nearly 50 miles, and bounded on the S. and S.W. by the lofty Gassendi highlands. Its border on the W., about 3000 feet high, is crowned with innumerable small depressions. The interior includes four bright little mountains, nearly central (three of them forming a triangle), a bright crater on the W. side, and several minor elevations and ridges. On the plain N. of the bay, is a large bright crater, from which a fine curved ridge runs to the central mountains. If Letronne is

observed under oblique illumination, the low mounds and ridges on the Mare outside impress one with the idea that they represent the remains of a once complete N. wall.

BILLY.—A ring-plain, 31 miles in diameter, S.E. of Letronne, with a very dark floor, depressed about 1000 feet below the grey surface on the W., and a regular border, rising more than 3000 feet above it. There is a narrow gap on the S., and indications of a crater on the N.W. rim. Two small craters stand on the S. half of the interior. The formation is flanked on the S.W. by highlands.

HANSTEEN.—A somewhat larger ring-plain, with a lower and more irregular rampart, rising on the W. to nearly 3000 feet above the floor, which is depressed to about the same extent as that of Billy. Both the inner and outer slopes are terraced on the E., where the *glacis* is traversed by a short, delicate, rill-like valley. There are some bright curved ridges on the floor. On the W. of Billy and Hansteen is a wide inlet of the Oceanus Procellarum, bounded by the Letronne region on the W., and on the S. by lofty highlands. On the surface, not far from the S.W. border of Hansteen, is a curious triangular-shaped mountain mass, with a digitated outline on the S., and including a small bright crater on its area. Between this and the ring-plain is a large but somewhat obscure depression, N. of which lies a rill-like object extending from the N. point of the triangular mountain to the W. wall. At the bottom of a gently sloping valley between Billy and Hansteen is a delicate marking, which seems to represent a cleft connecting the two formations.

ZUPUS.—A formation about 12 miles in diameter with a dark floor, situated in the hilly region N.E. of Mersenius.

FONTANA.—A noteworthy ring-plain, about 20 miles in diameter, E.N.E. of Zupus, with a bright border, exhibiting a narrow gap on the S. and two large contiguous craters on the N.W. The faint central mountain stands on a dusky interior. On the N. is a large peculiar depressed plain with a gently sloping wall, within which are three short rill-like valleys and a crater.

MERSENIUS.—With its extensive rill-system and interesting surroundings, one of the most notable ring-plain in the third quadrant. It is 41 miles in diameter, and is encircled by a fine rampart, which on the side fronting the Mare Humorum rises 7000 feet above the floor, which is distinctly convex, and is depressed 3000 feet below the region on the E., though it stands considerably above the level of the Mare. The prominently terraced border is tolerably regular on the N.W., but on the

S. and S.E. is much broken by craters and depressions, the largest and most conspicuous interrupting the continuity of its summit-ridge on the latter side. A fine crater-row traverses the central part of the interior, nearly axially, and a delicate cleft crosses the N. half of the floor from the inner foot of the N.E. wall to a crater not far from the opposite side. I detected another cleft on November 11, 1883, also crossing the N. side of the floor.

South of Mersenius is the fine ring-plain Mersenius *d*, about 20 miles in diameter, situated on the border of the Mare; and, extending in a line from this towards Vieta are two others (*a*, and Cavendish *d*), somewhat larger, but otherwise similar; the more easterly being connected with Cavendish by a mountain arm. One of the principal clefts of the system (all of which run roughly parallel to the N.E. side of the Mare, and extend to the Percy Mountains E. of Gassendi) crosses the floor of *d*, and, I believe, partially cuts into its W. wall. Another, the coarsest, abuts on a mountain arm connecting *d* with Mersenius, and, reappearing on the E. side, runs up to the N.W. wall of the other ring-plain, *a*, and, again reappearing on the E. of this, strikes across the rugged ground between *a* and Cavendish *d*, traversing its floor and border, as does also another cleft to the N. of it. Cavendish *d* includes a coarse cleft on its floor, running from N. to S., which I have frequently glimpsed with a 4-inch achromatic. There are two other delicate clefts running from the Gassendi region to the S.W. side of Mersenius, which are in part crater-rills.

CAVENDISH.—A notable ring-plain, 32 miles in diameter, S.E. of Mersenius, with a prominently terraced border, rising at one point on the S. to a height of 6000 feet above the interior, on which are a few low ridges. A large bright ring-plain (*e*), about 12 miles in diameter, breaks the continuity of the S.E. wall, and adjoining this, but beyond the limits of the formation, is another smaller ring with a central hill. There is also a bright crater on the N.W. border. The W. *glacis* is very broad, and includes two large shallow depressions. An especially fine valley runs up to the N. wall, to the W. side of *e*.

VIETA.—One of the finest objects in the third quadrant; a ring-plain 51 miles in diameter, with broad lofty walls, a peak on the west rising to nearly 11,000 feet, and another N. of it to considerably more than 14,000 feet above the interior. It is bounded by a linear border, approximating very closely to an hexagonal shape, which is broken by many gaps and cross-valleys. On

the S., the S.W. and S.E. sections of the wall do not meet, being separated by a wide valley flanked on the W. by a fine crater, which has broken down the rampart at this place. The N. border is likewise intersected by valleys and by a crater-row. The inner slopes are conspicuously terraced. There is a very inconspicuous central mountain and several large craters on the floor, some of them double. Ten have been counted on the N. half of the interior. On the S.E. of Vieta are two fine overlapping ring-plains, with a crater on the wall common to both.

DE VICO.—A conspicuous little ring-plain, about 9 miles in diameter, with a lofty border, some distance E. of Mersenius.

LEE.—An incomplete walled-plain, about 28 miles in diameter, on the S. side of the Mare Humorum, E. of Vitello, from which it is separated by another partial enclosure, with a striking valley, not shown in the published maps, running round its W. side. If viewed when its E. wall is on the morning terminator, some isolated relics of the wrecked N.W. wall of Lee are prominent, in the shape of a number of attenuated bright elevations separated by gaps. Within are three or four conspicuous hills.

DOPPELMAYER.—Under a high sun this large ring-plain, 40 miles in diameter, resembles a great bay open to the N.W., without a trace of detail to break the monotony of the surface on the side facing the Mare Humorum. When, however, it is viewed under oblique morning illumination, a low broad ridge is easily traceable, extending across the opening, indicating the site of a ruined wall. There is an isolated mountain at the S.W. end of this, which casts a fine spire of shadow across the floor at sunrise. The interior contains a massive bright central mountain and several little hills. The crest of the wall on the E. is much broken.

FOURIER.—A large ring-plain, 30 miles in diameter, S.W. of Vieta, with a border rising at a peak on the W. more than 9000 feet above the floor. There are two craters on the outer slope of the N.W. wall, a prominent crater on the S. wall, and (according to Schmidt) a small central crater on the floor, which I have not seen. In the region between Fourier and Vieta there are three ring-plains, two (the more westerly) standing side by side, and on the W., towards the Mare, are two others much larger, that nearer to Fourier being traversed by one cleft, and the other by two clefts, crossing near the centre of the floor.

CLAUSIUS.—A small bright ring-plain in an isolated position N.W. of Schickard, with a crater both on its N. and S. rim, and a faint central hill.

LACROIX.—A ring-plain 20 miles in diameter, N. of Schickard. It has a prominent central mountain.

SCHICKARD.—One of the largest wall-surrounded plains on the visible surface of the moon, extending about 134 miles from N. to S., and about the same from E. to W., enclosing a nearly level area, abounding in detail. Its border, to a great extent linear, is very irregular, and much broken by the interposition of small ring-plains and craters, and on the N. by cross-valleys. Its general height is about 4000 feet, the loftiest peak on the W. wall rising to more than 9000 feet above the floor. The inner slopes of this vast rampart are very complex, especially on the E., where many terraces and depressions may be seen under suitable illumination. There are three large ring-plains in the interior, all of them S. of the centre; and at least five smaller ones near the inner foot of the E. wall, which can only be well observed when libration is favourable. The two more easterly of the large ring-plains are connected by a cleft, and there are several short clefts and crater-rows associated with the smaller ring-plains. On the N. side of the area is a number of minute craters. The floor is diversified by two large dark markings—an oblong patch on the S.W. side, abutting on the wall, being the more remarkable; and a dusky area, occupying a great portion of the N. part of the floor, and extending up to the N. border. This is traversed by a light streak running from N. to S., which is the site of a row of minute craters.

LEHMANN.—A ring-plain, about 28 miles in length, on the N. of Schickard, with which it is connected by a number of cross-valleys.

DREBBEL.—A bright ring-plain, 18 miles in diameter, on the N.W. of Schickard, with a lofty irregular border (especially on the W.), exhibiting a well-marked terrace on the E., a distinct gap on the N., and a small crater on the S.E. rim. On a dusky area between it and Schickard stand three prominent deep craters.

PHOCYLIDES.—This extraordinary walled plain, with its neighbouring enclosures, is structurally very remarkable and suggestive. It consists of a large irregular formation, with a lofty wall, flanked on the N. by a smaller and still more irregular enclosure (*b*), the floor of which is 1500 feet above that of Phocylides, the line of partition being a high cliff, probably representing a "fault," whose shadow under a low sun is very striking. Phocylides is about 80 miles in maximum length,



or, if we reckon the small enclosure *b* to form a part of it, more than 120 miles. The loftiest peak, nearly 9000 feet, is on the W border, near the partition wall. The continuity of the rampart is broken on the S. by a large crater. There is a bright ring-plain on the W. side of the floor, and a few small craters. Phocylides *b* has only a solitary crater within it. Phocylides *c*, abutting on the W flank of Phocylides, is about 26 miles in diameter. Its somewhat dusky interior is devoid of detail, but the outer slope of its W. wall is crowded with a number of minute craters, which, under good conditions, may be utilised as tests of the defining power of the telescope used. Phocylides *A*, on the bright S.W. plain, is a large deep crater with a fine crater-row flanking it on the W.

**WARGENTIN**—A most remarkable member of the Phocylides group, flanking the S.E. side of Schickard. Unlike the majority of lunar formations, its floor is raised considerably above the surrounding region, so that it resembles a shallow oval dish turned upside down. It is 54 miles in diameter, and, except on the S.W. (where it abuts on Phocylides *b*, and for some distance is bounded by its wall), it has only a border of very moderate dimensions. On the N.E. slope of this ghostly rampart I have seen a distinct little crater, and two much larger depressions on the N.W. slope. There are some low ridges on the floor, radiating from a nearly central point, which have been aptly compared to a bird's foot.

**SEGNER**—A fine ring-plain, 46 miles in diameter, on the S.E. side of Schiller, with a linear border on every side except the N. At a peak on the W, whose shadow is very remarkable, it rises to a height of more than 8000 feet above the outer surface. There is a crater on the S.W. wall, another on the N.W. wall, and several depressions on the outer slope on this side. The central mountain is small but conspicuous. A large unnamed enclosure extends N. of Segner; it is larger than Schiller, and is surrounded by a lofty barrier. The bright plain between this and the latter is worth examination under a low sun.

**ZUCHIUS**—Is situated on the S.E. of Segner, which it slightly overlaps. It is very similar in size and general character, and has a lofty terraced wall, rising at one place on the W to nearly 11,000 feet above the floor. A very fine chain of craters, well seen when the opposite border is on the morning terminator, runs round the outer W slope of the wall. There is a bright crater beyond this on the S.W. Zuchius has a central peak.

BETTINUS.—Another ring-plain of the same type and size, some distance S. of the last, with a massive border, terraced within, and rising on the W. more than 13,000 feet above the floor, on which stands a grand central mountain, whose brilliant summit is in sunlight a long time before a ray reaches any part of the deep interior.

KIRCHER.—A ring-plain, about 45 miles in diameter, S. of Bettinus, remarkable also for its very lofty rampart, which on the S. attains the tremendous height of nearly 18,000 feet above the floor, which appears to be devoid of detail.

WILSON.—The most southerly of the chain of five massive ring-planes, extending in an almost unbroken line from Segner and differing only very slightly in size. It is about 40 miles in diameter, and has a somewhat irregular border, both as regards shape and height, rising at one peak on the S.W. to nearly 14,000 feet above a level interior, which apparently contains no conspicuous features.

#### EAST LONGITUDE 60° to 90°.

GRIMALDI.—This ranks among the largest wall-surrounded plains on the moon, and is perhaps the darkest. It extends 148 miles from N. to S. and 129 miles from E. to W., enclosing an area of some 14,000 square miles, or nearly double that of the principality of Wales. This vast dusky surface is bounded on the E. by a tolerably regular border, having an average height of about 4000 feet, while on the opposite side it is much broken, and in places considerably loftier, rising at one peak on the S.W. to an altitude of 9000 feet. About midway, also, this western rampart attains a great height, as may be seen by any one who observes at sunrise the magnificent shadow of it, and its many peaks thrown across the bluish-grey interior. On the S. the wall is broken by a large irregular depression, on the W. of which is a very curious V-shaped rill valley. On the N.W. it is comparatively low, and in places discontinuous; and even to a greater extent than on the S.W., intersected by passes. At the extreme N. end, a number of wide valleys cut through the wall and trend towards Lohrmann. There is a considerable ring-plain at the inner foot of the N.E. wall, but, except this and a few longitudinal ridges, just visible under a very low sun, there is apparently no other objects to vary the monotony of this great expanse.

DAMOISEAU.—Consists of a complex arrangement of rings, an

enclosure 23 miles in diameter, with a somewhat smaller enclosure placed excentrically within it (the N. side of both abutting on a bright plateau), with two large depressions intervening between their W. borders. This peculiarity, almost unique, renders the formation an especially interesting object. Damoiseau is situated on the W. side of Grimaldi, on the E. coast-line of the Oceanus Procellarum, from which the S.W. border rises at a gentle inclination. On the N.W. there is a curious curved inflexion of the Mare, bounded by a bright cliff, representing probably the E. side of a destroyed ring, a supposition which is strengthened by the existence of a faint scar on the surface of the sea, extending in a curve from one extremity of the bay to the other, and thus indicating the position of the remainder of the ring. A conspicuous little crater stands at the S. end of it, and two others some distance to the W. The smaller component of Damoiseau contains a low central ridge.

**RICCIOLI.**—An immense enclosure, near the limb, N.E. of Grimaldi, bounded by a rampart which is very irregular both in form and height, though nowhere of great altitude, and much broken by narrow gaps. It is especially low and attenuated on the N., where a number of ridges with intervening valleys traverse it. On the S. also a wide valley cuts through it. With the exception of a few low rounded hills and ridges, a short crater-row under the S.E. wall, and two small craters on the S.W., there are no details on the floor, which, however, is otherwise remarkable for the dusky tone of its surface, especially on the N. This dark patch occupies the whole of the N.E. side of the interior, and is bounded on the S. by an irregular outline, extending at one point nearly to the centre, and on the W. by a curved edge. The W. side is much darker than the rest. It is, in fact, as dark, if not darker, than any part of the floor of Grimaldi. Riccioli extends 106 miles from N. to S., and is nearly as broad. It includes an area of 9000 square miles.

**ROCCA.**—An irregular formation, 60 miles in length, near the limb S.E. of Grimaldi, consisting of a depression partially enclosed by mountain arms.

**SIRSALIS.**—The more westerly of a conspicuous pair of ring-plains about 20 miles in diameter, in the disturbed mountain region some distance S.W. of Grimaldi. It has lofty bright walls, rising to a great height above a depressed floor, on which there is a prominent central mountain. The E. border encroaches considerably on the somewhat larger companion, which is, however, scarcely a third so deep.

One of the longest clefts on the visible surface runs immediately W. of this formation. Commencing at a minute crater on the N. of it, it grazes the foot of the W. *glacis*; then, passing a pair of small overlapping craters (resembling *Sirsalis* and its companion in miniature), it runs through a very rugged country to a ring-plain E. of De Vico (De Vico *a*), which it traverses, and, still following a southerly course, extends towards Byrgius, in the neighbourhood of which it is apparently lost at a ridge, though Schmidt and Gaudibert have traced it still farther in the same direction. It is at least 300 miles in length, and varies much in width and character, consisting in places of distinct crater-rows.

CRÜGER.—A regular ring-plain E. of Fontana, 30 miles in diameter, with a dark floor, without detail, and comparatively low bright walls. There is a smaller but very conspicuous ring-plain (Crüger *a*) on the W. of it, to which runs a branch of the great *Sirsalis* cleft.

EICHSTÄDT.—A ring-plain, 32 miles in diameter, near the E. limb, S. of Rocca. It is the largest and most southerly of three nearly circular enclosures, without central mountains or any other details of interest. On the W. lies a great walled-plain with a very irregular border, containing several ring-plains and craters, and a crater-rill. Schmidt has named this formation DARWIN.

BYRGIVS.—A very irregular enclosure, about 40 miles in diameter, between Cavendish and the E. limb, with a lofty and discontinuous border, rising at one point on the E. to a height of 7000 feet above the floor. There are wide openings both in the N. and S. wall, and some ridges within. The border is broken on the E. by a crater, and on the W. by the well-known crater Byrgius A, from which a number of bright streaks radiate, mostly towards the E. One on the W. extends to Cavendish, and another to Mersenius, traversing the ring-plain Cavendish c. North-east of Byrgius there is a mountain arm which includes a peak 13,000 feet in height.

PIAZZI.—A walled-plain, about 90 miles in length, some distance S.E. of Vieta, with a complex broken border, including several depressions on the N.W., rising to about 7000 feet above a rather dark interior, on which there is a prominent central mountain.

LAGRANGE.—A larger but similar formation, 100 miles in diameter, associated with the last on the N.E., with a complex terraced border, including peaks of 9000 feet, a bright crater on

the W., and a ring-plain on the N.W. The inner slope of the E. wall is a fine object at sunrise, when libration is favourable. The floor is dark and devoid of detail.

BOUVARD.—A great irregular enclosure, which appears to be still larger than Lagrange, S.E. of Piazzzi, and close to the limb. It is bounded by a very lofty rampart, rising at a peak on the W. to 10,000 feet. It has a fine central mountain.

INGHIRAMI.—A very remarkable ring-plain, 60 miles in diameter, E. of Schickard, with a bright, broad, and nearly continuous border, terraced within, and intersected on the N.E. by narrow valleys, one of which is prolonged over the floor and extends to the central mountain. There are two curious dark spots on the N. side of the interior. Beyond the foot of the *glacis* on the S. a distinct cleft runs from a dusky spot to a group of small craters E. of Wargentín. There is a fine regular ring-plain with a small central mount W. of Inghirami.

PINGRÉ.—A ring-plain, about 18 miles in diameter, between Phocylides and the limb.

HAUSEN.—A ring-plain, close to the limb, N. of Bailly, which, but for its position, would be a fine object. It is, however, never sufficiently well placed for observation.

BAILLY.—One of the largest wall-surrounded plains on the moon, almost a "sea" in miniature, extending 150 miles from N. to S., and fully as much from W. to E. When caught at a favourable phase, it is, despite its position, especially worthy of scrutiny. The rampart on the W., of the linear type, is broken by several bright craters. On the S.W. two considerable overlapping ring-plains interfere with its continuity. On the S.E. several very remarkable parallel curved valleys traverse the border. The E. wall, which at one point attains a height of nearly 15,000 feet, is beautifully terraced. The floor on the eastern side includes several ring-plains (some of which are of a very abnormal type), many ridges, and two delicate dark lines, crossing each other near the S. end, probably representing clefts.

LEGENTIL.—A large walled-plain, close to the limb, S. of Bailly.



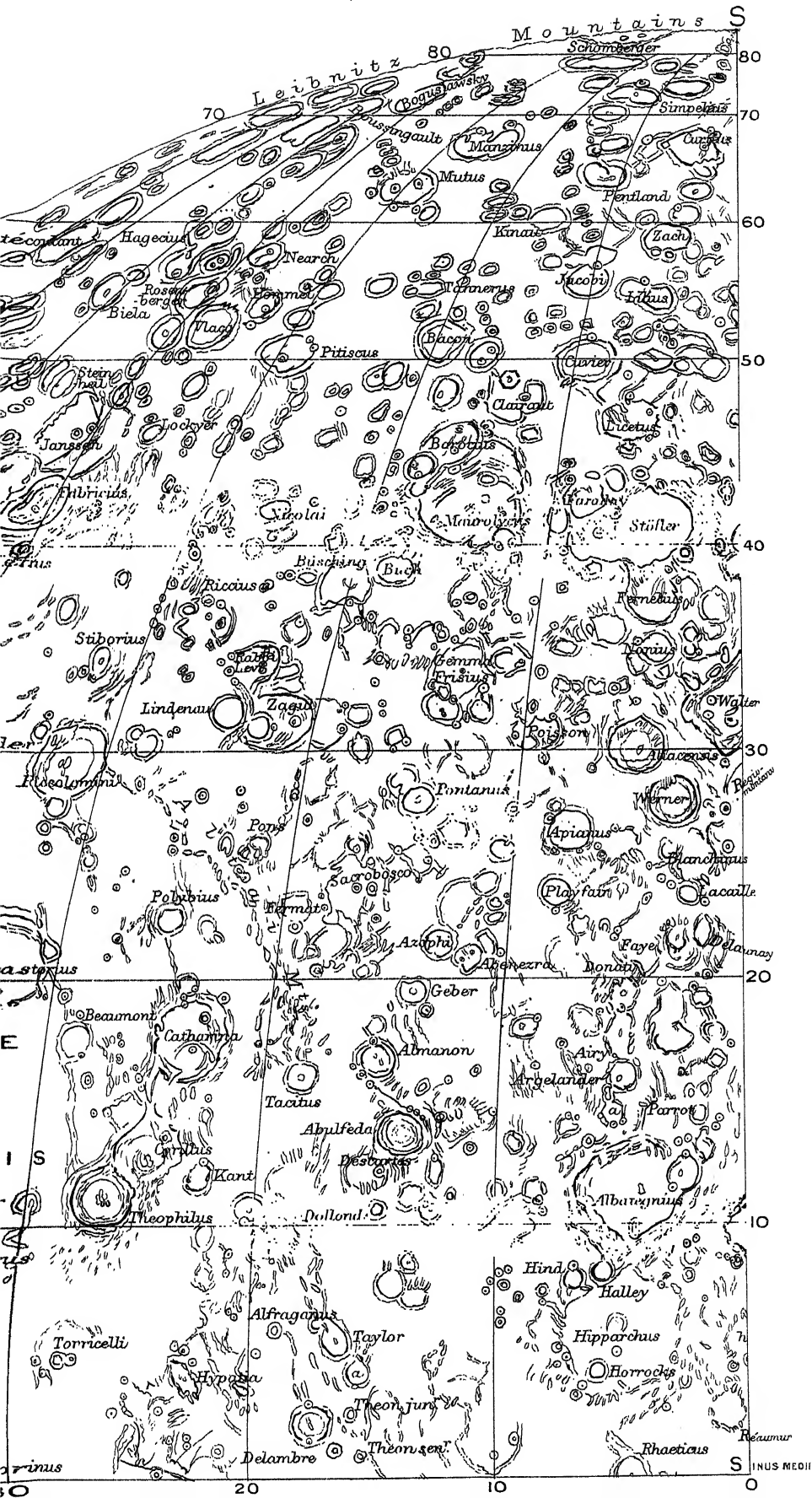
# Map of the Moon

by

T. GWYN ELGER, F.R.A.S.

**FOURTH QUADRANT.**









## FOURTH QUADRANT

WEST LONGITUDE  $90^{\circ}$  to  $60^{\circ}$

KÄSTNER.—A large walled-plain at the S. end of the Mare Smythii, too near the limb for satisfactory observation.

MACLAURIN.—The principal member of a group of irregular ring-plains on the W. side of the Mare Fœcunditatis, a little S. of the lunar equator. Schmidt shows no details within it, except a small crater on the E. side of the floor.

WEBB.—A ring-plain E. of Macclaurin, about 14 miles in diameter, with a dusky floor, enclosed by a bright rim, on the N.E. side of which there is a small crater. Schmidt seems to have overlooked the central hill.

LANGRENUS.—This noble circumvallation, the most northerly of the meridional chain of immense walled-plains, extending for more than 600 miles from near the equator to S. lat.  $40^{\circ}$ , would, but for its propinquity to the limb, rank with Copernicus (which in many respects it resembles) among the most striking objects on the surface of the moon. Its length is about 90 miles from N. to S., and its breadth fully as much. In shape it approximates very closely to that of a foreshortened regular hexagon. The walls, which at one point on the E. rise to an altitude of nearly 10,000 feet, are continuous, except on this side, where they are broken by the interference of an irregular depression, and on the extreme S., where they are intersected by cross-valleys. Within, the terraces are remarkably distinct, and the intervening valleys strongly marked. The brilliant compound central mountain rises at its loftiest peak to a height of more than 3000 feet. On the N. of it is an obscure circular ring, which may possibly merely represent a fortuitous combination of ridges, though it has all the appearance of a modified ring-plain. On the Mare, some distance N.E. of the formation, is a group of three ring-plains, with two small craters (associated with a ridge) on the N. of them. Two of the more westerly of these objects have prominent central mountains, and the third a very dark interior. At least

three bright streaks originate on the E. flank of Langrenus, which, diverging widely, traverse the Mare Fœcunditatis.<sup>1</sup>

**VENDELINUS.**—The second great enclosure pertaining to the meridional chain—a magnificent walled-plain of about the same dimensions as the last. It is bounded by a very irregular rampart, which, under evening illumination, is especially noteworthy though nowhere approaching the altitude of that of Langrenus. Its continuity on the W. is broken by the great ring-plain Vendelinus c, about 50 miles in diameter, a formation resembling Langrenus in miniature. This is hexagonal in shape, and has many rings and depressions on its W. wall. South of Vendelinus c, the wall of Vendelinus runs up in a bold curve to the fine terraced ring-plain Vendelinus b, and is surmounted by a bright serpentine crest, and traversed by several valleys running down the slope to the floor. b has a small crater on its N. wall, and another in the interior. There is a wide gap in the S. border of Vendelinus, which is partially occupied by another somewhat smaller ring-plain, bounded by a southerly extension of the E. wall, which includes on its outer slope many craters and other depressions, and abuts near its N. end on the large ring-plain Vendelinus a, which has a prominently terraced wall and a large bright central mountain. Between a and c extends a plateau that may be regarded as the N. limit of the formation, including, among other minor details, a fine cleft, which traverses it from N. to S., and ultimately extends to a group of craters on the floor. On the S. side of the interior is one large ring-plain, flanked on the W. by two small craters. Near the N. end are many bright little craters, many of them unrecorded. Vendelinus c is bordered on the E. by two large semicircular formations with low walls extending on to the floor. Mr. W. H. Maw and others have detected many minute depressions in connection with these curious objects; and N. of them, on the outer slope of c, where it runs out to the level of the plateau, I have seen the surface at sunset riddled like a sieve with craterlets and little pits. There is an irregular ring-plain N. of a, with linear walls, and another, much smaller and brighter, on the N. of this, standing a little beyond the N. limits of Langrenus.

**LA PEYROUSE.**—A much foreshortened walled-plain, 41 miles

<sup>1</sup> **FLATTENINGS ON THE MOON'S WESTERN LIMB.**—About thirty years ago, the Rev. Henry Cooper Key drew attention to certain flattenings which he had noted on the W. limb, which are very apparent under favourable conditions of libration. Their position cannot be closely defined, but the principal deviation from circularity extends from about S. lat.  $10^{\circ}$  to the region on the limb opposite the S. border of the Mare Crisium.

in diameter, close to the limb, S.W. of Langrenus. There is a longitudinal ridge on the floor. Between it and Langrenus are two large ring-plains with central mountains, and on the N.E., La Peyrouse A, a bright crater, adjoining which is La Peyrouse Δ, one of the most brilliant spots on the moon.

ANSGARIUS.—A ring-plain, 50 miles in diameter, still nearer to the limb than the last.

BEHAIM.—A great ring-plain, 65 miles in diameter, S. of Ansgarius, and connected with it by ridges. It has lofty walls and a central mountain.

HECATÆUS.—An immense walled-plain, 115 miles in length, on the S.W. of Vendelinus, with a very irregular rampart and a conspicuous central mountain. It is flanked E. and W. by other large enclosures, which can only be seen to advantage when libration is favourable.

W. HUMBOLDT.—Though close to the limb, this enormous wall-surrounded plain, some 130 miles in extreme length, and estimated to have an area of 12,000 square miles, is well worth observing under suitable conditions. It ranks among the largest formations of its class, and in many respects resembles Bailly on the S.E. limb. At one point on the E. a peak rises to 16,000 feet, and on the opposite side there are peaks nearly as high. The floor contains some detail—a crater, nearly central, associated with ridges, and two dark spots, one at the S. and the other at the N. end.

PHILLIPS.—Abuts on the E. side of W. Humboldt. It is a walled-plain, about 80 miles in length, with a border much broken on the E., and terraced within on the opposite side. There are many hills and ridges on the floor.

LEGENDRE.—A fine ring-plain, 46 miles in diameter, on the S.E. of the last. According to Schmidt, there is a crater on the S. side of the floor. There is a small ring-plain, ADAMS, on the S.

PETAVIUS.—The third member of the great meridional chain: a noble walled-plain, with a complex rampart, extending nearly 100 miles from N. to S., which encloses a very rugged convex floor, traversed by many shallow valleys, and includes a massive central mountain and one of the most remarkable clefts on the visible surface. To observe these features to the best advantage, the formation should be viewed when its W. wall is on the evening terminator. At this phase a considerable portion of the interior on the N. is obscured by the shadow of the rampart, but the principal features on the S. half of the floor, and on the broad gently-shelving slope of the W. wall, are seen better than under

any other conditions. The border is loftiest on the E., where the ring-plain Wrottesley abuts on it. It rises at this point to nearly 11,000 feet, while on the opposite side it nowhere greatly exceeds 6000 feet above the interior. The terraces, however, on the W. are much more numerous, and, with the associated valleys, render this section of the wall one of the most striking objects of its class. The N. border is conspicuously broken by the many valleys from the region S. of Vendelinus, which run up to and traverse it. On the S., also, it is intersected by gaps, and in one place interrupted by a large crater. There is a remarkable bifurcation of the border S. of Wrottesley. A lower section separates from the main rampart and, extending to a considerable distance S.E. of it, encloses a wide and comparatively level area which is crossed by two short clefts. The central mountains of Petavius, rising at one peak to a height of nearly 6000 feet above the floor, form a noble group, exceeding in height those in Gassendi by more than 2000 feet. The convexity of the interior is such that the centre of it is about 800 feet higher than the margin, under the walls; a protuberance which would, nevertheless, be scarcely remarked *in situ*, as it represents no steeper gradient than about 1 in 300 on any portion of its superficies. The great cleft, extending from the central mountains to the S.E. wall, and perhaps beyond, was discovered by Schröter on September 16, 1788, and can be seen in a 2-inch achromatic. In larger instruments it is found to be in places bordered by raised banks.

WROTTESELEY.—A formation, about 25 miles in diameter, closely associated with the E. wall of Petavius, the shape of which it has clearly modified. Its border on the E., of the linear type, rises nearly 9000 feet above a light interior, where there is a small bright central mountain and some mounds. There is a prominent valley running along the inner slope of the W. wall.

PALITZSCH.—If this extraordinary formation is observed when the moon is about three days old, it resembles a great trough, or deep elongated gorge flanking the W. wall of Petavius, though it is a true ring-plain, albeit of a very abnormal type, about 60 miles in length and 20 miles in breadth, with a somewhat dusky interior. On the outer slope of its W. wall is a bright ring-plain with a lofty border and a central mountain.

HASE.—An irregular formation, about 50 miles in diameter, on the S.W. of Petavius, with which it is connected by extensions of the W. and E. walls of the latter. Its rampart, some 7000 feet above the floor, is broken by depressions on the W.; and on the S. is bounded by a smaller ring-plain with still loftier walls.

Schmidt shows a large crater and three smaller ones on the W. side of the floor.

MARINUS.—A ring-plain on the N.E. side of the Mare Australe, between Furnerius and the limb.

FURNERIUS.—The fourth and most southerly component of the great meridional chain of walled-plains, commencing on the N. with Langrenus: a fine but irregular enclosure, about 80 miles in extreme length and much more in breadth. Its rampart is very lofty, and tolerably continuous on the N. and W., but on the other sides is interrupted by small craters and depressions. At peaks on the E. it attains a height of more than 11,00 feet above the interior, and there are other peaks rising nearly as high. There is a ring-plain (Furnerius B) with a central hill, on the E. side of the floor, and numerous craters and crater-pits in other parts of it. On the N.W. side of B there is a short cleft, on the W., a well-marked crater-row, and on the E. a long rill-valley. The very brilliant crater (Furnerius A) on the N.E. *glacis* is the origin of two fine light streaks, one extending S. for more than 100 miles, and the other in the opposite direction for a great distance.

FRAUNHOFER.—A ring-plain, S. of Furnerius, about 30 miles in diameter, with a regular border rising about 5000 feet above the floor. A smaller ring-plain abuts on the N.E. side of it, which has slightly disturbed its wall.

OKEN.—A large enclosure in S. lat.  $43^{\circ}$  with broken irregular walls. It is too near the limb for observation.

VEGA.—Schmidt represents this peculiar formation, situated S.E. of Oken, as having a regular curved unbroken rampart on the E., while the opposite border is occupied by four large partially overlapping ring-plains, two of which contain small craters. The floor is devoid of detail.

PONTÉCOULANT.—A great irregular walled plain, about 100 miles in length, near the S.W. limb, with a border rising in places to a height of 6000 feet above the floor.

HANNO.—A smaller and more regular enclosure, adjoining Pontécoulant on the N.W., and still nearer the limb.

#### WEST LONGITUDE $60^{\circ}$ TO $40^{\circ}$ .

MESSIER.—The more westerly of a remarkable pair of bright craters, about 9 miles in diameter, standing in an isolated position in the Mare Fecunditatis just S. of the Equator. Mädler represents them as similar in every respect, but Webb, observing them

in 1855 and 1856 with a  $3\frac{7}{10}$  achromatic, found them very distinctly different,—Messier, the more westerly, being not only clearly smaller than its companion, but longer from W. to E. than from N. to S., as it undoubtedly is at the present time. Messier A, however, as the companion is termed, though larger, is certainly not circular, as sometimes shown, but triangular with curved sides. It is just possible that change may have occurred here, for Mädler carefully observed these objects more than three hundred times, and, it may be presumed, under very different phases. Messier A is the origin of two slightly divergent light streaks, resembling a comet's tail, which extend over the Mare towards its E. border N. of Lubbock, and are crossed obliquely by a narrower streak. Messier and Messier A stand near the S. and narrowest end of a tapering curved light area. There is a number of craterlets and minute pits in the neighbourhood, and under a high light two round dusky spots are traceable in connection with the "comet" marking, one just beyond its northern, and the other beyond its southern border, near its E. extremity.

LUBBOCK.—A brilliant little crater, about 4 or 5 miles in diameter, near the E. coast-line of the Mare Fœcunditatis. The region E. of this object is particularly well worthy of scrutiny under a low sun, on account of the variety of detail it includes. On the S.E. run three fine parallel clefts, originating near the N. end of the Pyrenees.

GUTTEMBERG.—A very fine ring-plain of peculiar shape, about 45 miles in width, with a lofty wall, broken on the N.W. by another ring-plain some 14 miles in diameter, and on the S.E. by a small but distinct crater. The border presents a wide opening towards the S., which is traversed by a number of longitudinal valleys, both the E. and W. sections of the wall being prolonged in this direction. A fine crater-row runs round the outer slope of the E. wall, from the crater just mentioned to the N. side of the formation. It is best seen when the W. wall is on the evening terminator. There is also a broad valley on the S. prolongation of the W. wall. The central mountain is bright but not large. A cleft crosses the N.W. side of the floor. North of Guttemberg there is a curious oblong formation with low walls, connected with the N.E. border by a ridge, and with the N. border by a remarkable row of depressions, situated on a mound; and beyond this object on the E. are three parallel clefts running towards the N.E. On the W. will be found some of the clefts belonging to the Goclenius rill-system. In the rugged region S.E.

of the formation is a peculiar low ring with a very uneven floor and a large central hill. The E. wall of Guttemberg may be regarded as forming a portion of the Pyrenees Mountains.

GOELENUS.—A ring-plain, about 28 miles in diameter, bearing much resemblance to Plinius in form and size, and, like this formation, associated with a fine system of clefts. The lofty rampart, tolerably continuous on the W., is broken on the S.W. by a bright crater, and on the N.W. by a remarkable triangular depression. It is also traversed by a delicate valley extending from the crater on the S.W. to another on the N.W. border; and at a point a little W. of the first crater is dislocated by an intrusive mass of rock. There are several gaps on the E. and many spurs and irregularities in outline both within and without. A great portion of the N. wall is linear, and joins the E. section nearly at right angles. West of the triangular depression it appears to be partially wrecked, indications of the destruction being very evident if it be observed when the E. wall is near the morning terminator. The small bright central mountain is remarkable for its curious oblong shadow. Two clefts traverse the interior of Goelenius. (1) Originates at the S. wall, E. of the crater, and runs E. of the central mountain to the N. wall; (2) crosses the *débris* of the ruined N.W. border, runs parallel to the first, and extends nearly to the centre of the floor. (1) Reappears at the foot of a mound outside the N. wall, and, after crossing the outer W. slope of the great ring-plain on the N.W. wall of Guttemberg, runs to the W. side of an oblong formation N. of it. There are two other clefts, closely parallel and W. of this, traversing the Mare, and terminating among the mountains on the N.W. These are crossed at right angles by what appears to be a "fault," running in a N.W. direction from the W. side of Guttemberg.

MACCLURE.—One of a curious group of formations situated in the Mare Fœcunditatis some distance S.W. of Goelenius. It is a bright ring-plain, about 15 miles in diameter, with a narrow gap in the N.E. wall and a small central hill. A prominent ridge runs up to the N. border; and on the S.W. a rill-valley may be traced, extending S. to a bright deep little crater W. of Cook.

CROZIER.—A conspicuous ring-plain a few miles N.N.W. of MacClure, and of about the same size. It has a faint central hill. Neison refers to two long straight streaks extending from Crozier towards Messier.

BELLOT.—A brilliant little ring-plain N.E. of Crozier.



COOK.—A ring-plain, about 25 miles in diameter, on the E. side of the Mare Fœcunditatis in S. lat.  $17^{\circ}$ , with low and (except on the S.E.) very narrow walls. There is a small circular depression on the S. border, and a prominent crater on the W. side of the dark interior. On the S.S.E. is the curiously shaped enclosure Cook  $d$ , with very bright broad lofty walls and a fine central mountain. On the plain W. of Cook is a conspicuous crater-row, consisting of six or seven craters, diminishing in size in both directions from the centre.

COLOMBO.—A fine ring-plain, about 50 miles in diameter, situated in the highlands separating the Mare Fœcunditatis and the Mare Nectaris. The wall, rising at one place to a height of 8000 feet above the floor, is very complicated and irregular, being traversed within by many terraces, and almost everywhere by cross-valleys. Its shape is greatly distorted by the large ring-plain  $\alpha$ , which abuts on its N.E. flank. It loses its individuality altogether on the S., its place being occupied by two large depressions, and lofty mountains trending towards the S.E. In the centre there are several distinct bright elevations.

MAGELHAENS.—The more northerly and the larger of a pair of ring-plain between Colombo and Goclenius, with a bright and somewhat irregular though continuous border. The dark interior includes a small central mountain. Its companion on the S.W., Magelhaens  $\alpha$ , slightly overlaps it. This also has a central hill, and a crater on the outer slope of its E. wall.

SANTBECH.—A very prominent ring-plain, 46 miles in diameter, on the S.E. side of the Mare Fœcunditatis, W. of Fracastorius. The continuity of its fine lofty rampart is broken on the W., where it rises nearly 10,000 feet above the floor, by a brilliant little crater just below the crest, and by a narrow gap on the S. The wall on the E. towers to a height of 15,000 feet above the interior. On its broad outer slope, near the summit, there is a fine crater, and S. of this running obliquely down the slope a distinct valley. On the N.E., where the *glacis* runs down to the level of the surrounding plain, there is a large crateriform object with a broken N. border, and a small crater opposite the opening. A long coarse valley runs from this latter object in a N.E. direction to the region W. of Bohnenberger. Santbech contains a prominent central peak.

BIOT.—A brilliant little ring-plain, scarcely more than 7 miles in diameter, standing in an isolated position in the Mare Fœcunditatis N.E. of Wrottesley. There is a number of

bright streaks in its neighbourhood; and a few miles E. of it, in the hilly region W. of Santbech, another conspicuous crater of about the same size.

BORDA.—A ring-plain about 25 miles in diameter, S.S.W. of Santbech, with a rampart low on the N. and S., but elsewhere of considerable height, and a very conspicuous central mountain. A wide deep valley flanked by lofty mountains extends from the N. wall for many miles towards the N.W. It is an especially noteworthy object when the W. wall of Santbech is on the evening terminator, as its somewhat winding course, indicated by the bright summit-ridges of the bordering mountains, can be followed some hours before either the interior of the valley or the region between it and Santbech are in sunlight. Among the mountains W. of Borda there is a peak more than 11,000 feet in height.

SNELLIUS.—A very fine ring-plain, 50 miles in diameter, S.E. of Petavius, with terraced walls, considerably broken on the S.E. by craters, &c. It rises on the E. nearly 7000 feet above a dark floor, which contains a central mountain. N.E. of Snellius is a smaller ring-plain (*Snellius a*), and due E. a curious rough plateau, bordered on the N. and S. by a number of small craters.

STEVINUS.—A somewhat larger ring-plain, S. of Snellius, with a border rising on the S. to more than 11,000 feet above a dark interior, which includes a bright central mountain.

REICHENBACH.—A very abnormally-shaped ring-plain, about 30 miles in diameter, with a rampart nearly 12,000 feet high. The border is broken on the W., S., and E. by craters and depressions, and on the N. is flanked by two overlapping ring-planes, *a* and *b*. On the S.W. lies a magnificent serpentine valley, fully 100 miles in length and about 12 miles in breadth at the N. end, but gradually diminishing as it runs southwards, till it reaches a depression N. of Rheita, where it terminates: here is scarcely more than 4 miles wide.

RHEITA.—A formation, about 35 miles in diameter, S. of Reichenbach, with regular lofty walls, rising at a peak on the N.E. to a height of more than 14,000 feet above the interior, on which there is a small but prominent central mountain, a smaller elevation W. of the centre, and two adjoining craters at the foot of the S. wall. On the E. originates another fine valley, very similar to that already mentioned in connection with Reichenbach. It runs in a S.S.W. direction, is about 100 miles in length, and, in its widest part, is about 12 miles across. Like the Reichenbach valley, it terminates at a small crater-like object,

which has a border broken down on the side facing the valley, and a small central hill. About midway between its extremities, this great gorge is crossed by a wall of rock, like a narrow bridge.

JANSSEN.—An immense irregular enclosure, reminding one of the very similar area, bordered by Walter, Lexell, Hell, &c., in the third quadrant. It extends about 150 miles from E. to W., and more than 100 from N. to S., its limits on the N. being rather indefinite. Its very rugged humpy surface includes one great central mountain, and innumerable minor hills and ridges, craters, and crater-pits; but the principal feature is the magnificent curved rill-valley running from the S. side of Fabricius across the rough expanse to the S. side. This fine object, very coarse on the N., passes the central mountain on the E. side, and becomes gradually narrower as it approaches the border; before reaching which, another finer cleft branches from it on the W., and also runs to the S. side of the plain.

LOCKYER.—A prominent deep ring-plain, 32 miles in diameter, with massive bright lofty walls, standing just outside the S.E. border of Janssen. Schmidt shows a minute crater on the S. rim. I have seen a crater within, at the inner foot of the W. wall, and a central peak.

FABRICIUS.—A ring-plain, 55 miles in diameter, with a lofty terraced border, rising on the S.W. to a height of nearly 10,000 feet above the interior. It is partially included by the rampart of Janssen, and the great rill-valley on the floor of the latter appears to cut through its S. wall. There is a long central mountain on the floor, with a prominent ridge extending along the E. side of it. W. of Fabricius (between it and the border of Janssen) lies a very irregular enclosure, with three distinct craters within it; and on the E., running from the wall to the E. side of Janssen, is a straight narrow valley. Both Fabricius and Janssen should be viewed under a low morning sun.

STEINHEIL.—A double ring-plain, W. of Janssen, 27 miles in diameter. The more easterly formation sinks to a depth of nearly 12,000 feet below the summit of the border.

METIUS.—This ring-plain, of about the same size as Fabricius, but with a still loftier barrier, abuts on the N. wall of this formation, and has caused a very obvious deformation in its contour. It is prominently terraced internally, and on the W. the wall rises at one peak to a height of 13,000 feet above the floor, which contains a deep crater on the W. of the centre, and many ridges.

BIELA.—A considerable ring-plain, about 55 miles in diameter,

S.W. of Janssen, with a wall broken on the N.W., S., and E. by rings and large enclosures. There is a central mountain, but apparently no other details on the floor.

ROSENBERGER.—This formation, about 50 miles in diameter, is one of the remarkable group of large rings to which Vlacq, Hommel, Pitiscus, &c., belong. Its walls, though of only moderate altitude, are distinctly terraced. In addition to a prominent central mountain (E. of which Schmidt shows two craters), there is a large crater on the S. side of the floor, and many smaller craters and crater-pits.

HAGECIUS.—The most westerly member of the Vlacq group of formations. It is situated on the S.W. of Rosenberger, and is about 50 miles in diameter. The rampart on the E. is continuous and of the normal type, but on the opposite side is broken by a number of smaller rings.

#### WEST LONGITUDE $40^{\circ}$ TO $20^{\circ}$ .

CENSORINUS.—A brilliant little crater, with very bright surroundings, in the Mare Tranquilitatis, nearly on the moon's equator, in W. long.  $32^{\circ} 23'$ . Another smaller but less conspicuous crater adjoins it on the W. On the Mare to the S. extends a delicate cleft which trends towards the Sabine and Ritter rill system.

CAPELLA.—Forms with Isodorus, its companion on the E. (which it partially overlaps), a very noteworthy object. It is about 30 miles in diameter, with finely terraced walls, broken on the S.W. by broad intrusive rill-valleys. The rampart on the N.E. is also cut through by a magnificent valley, which extends for many miles beyond the limits of the formation. There is a fine central mountain, on which M. Gaudibert discovered a crater, the existence of which has been subsequently verified by Professor Weinek on a Lick observatory negative.

ISODORUS.—The rampart of this fine ring-plain, which is of about the same size as Capella, rises at a peak on the W. to a height of more than 13,000 feet above the interior, which, except a small bright crater at the foot of the E. wall and a smaller one adjoining it on the N., contains no detail. The region between Isodorus and the equator includes many interesting objects, among them Isodorus *b*, an irregular formation open towards the N., and containing several craters.

BOHNENBERGER.—A ring-plain about 22 miles in diameter, situated on the W. side of the Mare Nectaris, under the precipitous flanks of the Pyrenees, whose prominent shadows partially conceal it for many hours after sunrise. The circular border is comparatively low, and, except on the N., continuous. Here there is a gap, and on the W. of it an intrusive mass of rock. From its very peculiar shadow at sunrise, the wall on the E. appears to be very irregular. The club-shaped central mountain is of considerable size, but not conspicuous. S. of Bohnenberger stands the very attenuated ring, Bohnenberger A. It is of about the same diameter, has a large deep crater on its N. rim, and a smaller one, distinguished with difficulty, on its S.E. rim. On the N. of Bohnenberger there is a bright little ring-plain connected with the formation by a lofty ridge, under the E. flank of which Schmidt shows a crater-chain. An especially fine cleft originates on the E. side of this crater, which, following an undulating course over the Mare Nectaris, terminates at Rosse, N. of Fracastorius.

TORRICELLI.—A remarkable little formation in the Mare Tranquilitatis, N. of Theophilus, consisting of two unequal contiguous craters ranging from W. to E., whose partition wall has nearly disappeared, so that, under a low sun, when the interior of both is filled with shadow, the pair resemble the head of a javelin. The larger, western, ring is about 10 miles in diameter, and the other about half this size. There is a gap in the W. wall of the first, and a long spur projecting from its S. side; and a minute crater on the S. border of the smaller object. Torricelli is partially enclosed on the S. by a circular arrangement of ridges. There is a delicate cleft running in a meridional direction on the Mare, E. of the formation, and another on the N., running from W. to E.

HYPATIA.—A ring-plain, about 30 miles in extreme length, of very abnormal shape, on the E. side of the Mare, N.N.E. of Theophilus, with a wall rising at a peak on the E. to a height of more than 7000 feet above a dusky floor, which does not apparently contain any detail. A small crater breaks the uniformity of the border on the W. Beyond the wall on the S.E. lies the fine bright crater Hypatia A, with another less prominent adjoining it on the S.W.

THEOPHILUS.—The most northerly of three of the noblest ring-mountains on the visible surface of the moon, situated on the N.E. side of the Mare Nectaris. It is nearly 64 miles in diameter, and is enclosed by a mighty rampart towering above the floor at one peak on the W. to the height of 18,000 feet,

and at two other peaks on the opposite side to nearly 16,000 and 14,000. The border, though appearing nearly circular with low powers, is seen, under greater magnification, to be made up of several more or less linear sections, which give it a polygonal outline. It is prominently terraced within, the loftier terraces on the W. rising nearly to the height of the crest of the wall, and including several craters and elongated depressions. On the W. *glacis* is a row of large inosculating craters; and near its foot, S.E. of Mädler, a short unrecorded rill-valley. The magnificent bright central mountain is composed of many distinct masses surmounted by lofty peaks, one of which is about 6000 feet above the floor, and covers an area of at least 300 square miles. Except a distinct crater on the S.W. quarter, this appears to be the only object within the ring.

CYRILLUS.—The massive border of Theophilus partially overlaps the N.W. side of this great walled-plain, which is even more complex than that of its neighbour, and far more irregular in form, exhibiting many linear sections. Its crest on the S.E. is clearly inflected towards the interior, a peculiarity that has already been noticed in connection with Copernicus and some other objects. On the inner slope of this wall there is a large bright crater, in connection with which have been detected two delicate rills extending to the summit. I have not seen these, but one of the crater-rows shown by Schmidt, between this crater and the crest, has often been noted. The N.E. wall is very remarkable. It appears to be partially wrecked. If observed at an early stage of sunrise, a great number of undulating ridges and rows of hillocks will be seen crossing the region E. of Theophilus. They resemble a consolidated stream of "ropy" lava which has flowed through and over the wall and down the *glacis*. The arrangement of the ridges within Cyrillus is very noteworthy, as is also the triple mountain near the centre of the floor. The fine curved cleft thereon traverses the W. side, sweeping round the central mountains, and then turning to the south. I have only occasionally seen it in its entirety. There are also two oblong dark patches on the S. side of the interior. The S. wall of Cyrillus is broken by a narrow pass opening out into a valley situated on the plateau which bounds the W. side of the oblong formation lying between it and Catherina, and overlooking a curious shallow square-shaped enclosure abutting on the S.W. side of Cyrillus.

CATHERINA.—The largest of the three great formations: a ring-plain with a very irregular outline, extending more than 70

miles in a meridional direction, and of still greater width. The wall is comparatively narrow and low on the N.E. (8000 feet above the floor), but on the N.W. it rises to more than double this height, and is broken by some large depressions. The inner slope on the S.E. is very gentle, and includes two bright craters, but exhibits only slight indications of terraces. The most remarkable features on an otherwise even interior are the large low narrow ring (with a crater within it), occupying fully a third of the area of the floor, and a large ring-plain on the S. side.

MÄDLER.—The interest attaching to this formation is not to be measured by its size, for it is only about 20 miles in diameter, but by the remarkable character of its surroundings. Its bright regular wall, rising 6000 feet on the E. and only about half as much on the W., above a rather dark interior, is everywhere continuous, except at one place on the N. Here there is a narrow gap (flanked on the E. by a somewhat obscure little crater) through which a curious bent ridge coming up from the N. passes, and, extending on to the floor, expands into something resembling a central mountain. Under a high sun Mädler has a very peculiar appearance. The lofty E. wall is barely perceptible, while the much lower W. border is conspicuously brilliant; and the E. half of the floor is dark, while the remainder, with two objects representing the loftier portions of the intrusive ridge, is prominently white. Under an evening sun, with the terminator lying some distance to the W., a very remarkable obscure ring with a low border, a valley running round it on the W. side, and two large central mounds, may be easily traced. This object is connected with Mädler by what appears to be under a higher sun a bright elbow-shaped marking, in connection with which I have often suspected a delicate cleft. Between the obtuse-angled bend of this object and the W. wall of Mädler, two large circular dark spots may be seen under a high sun; and on the surface of the Mare N. of it, a great number of delicate white spots.

BEAUMONT.—A ring-plain about 30 miles in diameter, on the S.E. side of the Mare Nectaris, midway between Theophilus and Fracastorius, with the N.E. side of which it is connected by a chain of large depressions. Its border is lofty, regular, and continuous on the S. and E., but on the W. it is low, and on the N. sinks to such a very inconsiderable height that it is often scarcely traceable. It exhibits two breaks on the S.W., through one of which passes a coarse valley that ultimately runs on the E. side of the depres-

sions just referred to. The interior is pitted with many craters, one on the W. side being shallow but of considerable size. I once counted twenty with a 4-inch Cooke achromatic, and Dr. Sheldon of Macclesfield subsequently noted many more. A ridge, prominent under oblique light, follows a winding course from the N.W. side of Beaumont to the W. side of Theophilus, and there is another lower ridge E. of it. Between them is included a region covered with minute hillocks and asperities. Among these objects are certain dusky little crater-cones, which Dr. Klein of Cologne regards as true analogues of some terrestrial volcanoes. They are very similar in character to those, already alluded to, in the dusky area between Copernicus and Gambart.

KANT.—A conspicuous ring-plain, 23 miles in diameter, situated in a mountainous district E. of Theophilus, with lofty terraced walls and a bright central peak. Adjoining it on the W. is a mountain mass, projecting from the coast-line of the Mare, on which there is a peak rising to more than 14,000 feet above the surface.

FRACASTORIUS.—This great bay or inflexion at the extreme S. end of the Mare Nectaris, about 60 miles in diameter, is one of the largest and most suggestive examples of a partially destroyed formation to be found on the visible surface. The W. section of the rampart is practically complete and unbroken, rising at one peak to a height of 6000 feet above the interior. It is very broad at its S. end, and its inner slope descends with a gentle gradient to the floor. Towards the N., however, it rapidly decreases in width, but apparently not in altitude, till near its bright pointed N. extremity. Under a low sun, some long deformed crateriform depressions may be seen on the slope, and a bright little crater on the crest of the border near its N. end. The southern rampart is broken by three large craters, and a fine valley, running some distance in a S. direction, which diminishes gradually in width till it ultimately resembles a cleft, and terminates at a small crater. The E. border is very lofty and irregular, rising at the N. corner of the large triangular formation, which is such a prominent feature upon it, to a height of 7000 feet, and at a point on the S.E. to considerably more than 8000 feet above the floor. N. of the former peak it becomes much lower and narrower, and is finally only represented by a very attenuated strip of wall, hardly more prominent than the brighter portions of the border of Stadium at sunrise, terminating at an obscure semi-ring-



plain. Between this and the pointed N. termination of the W. border there is a wide gap, open to the north for a space of about 30 miles, appearing, except under very oblique illumination, as smooth and as devoid of detail as the grey surface of the Mare Nectaris itself. If, however, this interval is observed at sunrise or sunset, it is seen to be not quite so structureless as it appears under different conditions, for a number of mounds and large humpy swellings, with low hills and craterlets, extend across it, and occupy a position which we are justified in regarding as the site of a section of the rampart, which, from some cause or other, has been completely destroyed and overlaid with the material, whatever this may be, of the Mare Nectaris. The floor of Fracastorius is, as regards the light streaks and other features upon it, only second in interest to those of Plato and Archimedes, and will repay systematic observation. Between thirty and forty light spots and craters have been recorded on its surface, most of them, as in these formations, being situated either on or at the edges of the light streaks. On the higher portion of the interior (near the centre) is a curious object consisting apparently of four light spots, arranged in a square, with a craterlet in the middle, all of which undergo (as I have pointed out elsewhere) notable changes of aspect under different phases. There are at least two distinct clefts on the floor, one running from the W. wall towards the centre, and another on the S.E. side of the interior. The last throws out two branches towards the S.W.

ROSSE.—A fine bright deep crater in the Mare Nectaris, N. of the pointed termination of the W. wall of Fracastorius, with which it is connected by a bold curved ridge, with a crater upon it. A ray from Tycho, striking along the E. wall of Fracastorius passes near this object. A rill from near Bohnenberger terminates at this crater.

POLYBIUS.—A ring-plain, about 17 miles in diameter, in the hilly region S.E. of Fracastorius. The border is unbroken, except on the N., where it is interrupted by a group of depressions. There is a long valley on the S.W., at the bottom of which Schmidt shows a crater-chain.

NEANDER.—This ring-plain, 34 miles in diameter, a short distance W.S.W. of Piccolomini, has a somewhat deformed rampart, which, however, except on the N., where there is a narrow gap occupied by a small crater, is continuous. It rises on the E. nearly 8000 feet above the floor, on which there is a central mountain about 2500 feet high. Schmidt shows some minor hills,

large crater on the N.E. side, and three smaller craters in the interior

PICCOLOMINI.—A ring-plain of a very massive type, about 7 miles in diameter, S of Fracastorius, with complex and prominently terraced walls, surmounted by very many peaks, one of which on the E. attains a height of 14,000 feet, and another, N of it, on the same side, an altitude of 15,000 feet above the interior. The crest of this grand rampart is tolerably continuous, except on the S W, where, for a distance of twenty miles or more, its character as regards form and brightness is entirely changed. Under a low sun, instead of a continuous bright border, we note a wide gap occupied by a dusky rugged plateau, which falls with a gentle gradient to the floor, and is traversed by three or four parallel shallow valleys running towards the S. I can recall no lunar formation which presents an appearance at all like this: one is impressed with the idea that it has resulted from the collapse of the upper portion of the wall, and the flow of some viscous material over the wreck and down the inner slope. The difference between the reflective power of this matter, whatever may be its nature, and the broad bright declivities of the inner slopes, are beautifully displayed at sunset. The cross-valleys are more easily traced under low morning illumination; but to appreciate the actual structure of the wall, it should be observed under both phases. The N.W. section of the border includes many "pockets," or long elliptical depressions, which at an early stage of sunrise give a scalloped appearance to the crest. Except the great bright central mountain with its numerous peaks, there does not appear to be any prominent detail on the floor. There is a large ring-plain beyond the foot of the *glacis* on the W. with two craters on the E. side of it, another on the S., and a fine rill-valley running up to its N. side from near the crest of the W. wall. On the N. side of Piccolomini is a remarkable group of deformed and overlapping enclosures, mingled with numberless craters and little depressions. The plain on the N.E. is crossed by a fine cleft.

PONS.—A complete formation of irregular shape, about 20 miles in greatest diameter, on the S.E. side of the Altai range, in W. long.  $21^{\circ}$ . It consists of a crowd of rings and craters enclosed by a narrow wall.

STIBORIUS.—An elongated ring-plain, about 22 miles in diameter, S. of Piccolomini, with a lofty wall, broken in one place on the N. by a very conspicuous crater. Schmidt shows a distinct

crater in the centre of the floor. I have only seen a central mountain in this position. There is a large crater on the N.W., a ring-plain on the S.W. side, and a multitude of little craters on the surrounding plain.

**RICCIUS.**—A ring-plain, 51 miles in diameter, of a very irregular type, S.E. of the last. It is enclosed by a complex wall (which is in places double), broken by large rings on the S. The very conspicuous little ring-plain Riccius A is situated on the N. of it, and other less prominent features. The interior includes a bright crater and some smaller objects of the same class.

**ZAGUT.**—The most easterly of a group of closely associated irregular walled-plains, of which Lindenau and Rabbi Levi are the other members, all evidently deformed and modified in shape by their proximity. It is about 45 miles in diameter, and is enclosed by a wall which on the S.W. attains a height of about 9500 feet, and is much broken on the N. by a number of depressions. A large ring-plain, some 20 miles in diameter, occupies a considerable portion of the W. side of the interior; E. of which, and nearly central, there is a large bright crater, but apparently no other conspicuous details. On the S.E. side of Zagut lies an elliptical ring-plain, about 28 miles in diameter, named by Schmidt **CELSIUS**. The border of this is open on the N., the gap being occupied by a large crater, whose S. wall is wanting, so that the interiors of both formations are in communication.

**LINDENAU.**—This formation, about 35 miles in diameter, is bounded on the W. by a regular unbroken wall nearly 8600 feet in height; but which on the E. and N.E. is far loftier and more complex, rising to about 12,000 feet above the floor, consisting of four or more distinct ramparts, separated by deep valleys, and extending towards Rabbi Levi. Neison points out that under a high light Lindenau appears to have a bright uniform single wall. There is a small central mountain and some minor inequalities in the interior.

**RABBI LEVI.**—A larger but less obvious formation than either of its neighbours, Zagut and Lindenau, abutting on the S. side of them. It is about 55 miles in diameter, and is enclosed by a border somewhat difficult to trace in its entirety, except under oblique light. There are some large craters within it, of which one on the N. side of the floor is especially prominent.

**NICOLAI.**—A tolerably regular ring-plain, 18 miles in diameter, S. of Riccius, with a border, rising more than 6000 feet above a level floor, on the N. side of which Schmidt shows a

minute crater. The bright plain surrounding this formation abounds in small craters; and on the W. is a number of curious enclosures, many of them overlapping.

VLACQ.—A member of a magnificent group of closely associated formations situated on the greatly disturbed area between W. long.  $30^{\circ}$  and  $45^{\circ}$  and S. lat.  $50^{\circ}$  and  $60^{\circ}$ . It is 57 miles in diameter, and is enclosed by terraced walls, rising on the W. about 8000 feet, and on the E. more than 10,000 feet above the floor. They are broken on the S. by a fine crater. In addition to a conspicuous central peak, there are several small craters, and low short ridges in the interior.

HOMMEL.—Adjoins Vlacq on the S. It is a somewhat larger and a far more irregular formation. On every side except the W., where the border is unbroken, and descends with a gentle slope to the dark interior; ring-plains and smaller depressions encroach on its outline, perhaps the most remarkable being Hommel *a* on the N., which has an especially brilliant wall, that includes a conspicuous central mountain, a large crater, and other details. The best phase for observing Hommel and its surroundings is when the W. wall is just within the evening terminator.

PITISCUS.—The most regular of the Vlacq group. It is situated on the N.E. of Hommel (a curious oblong-shaped enclosure, Hommel *b*, with a very attenuated E. wall, and a large crater on a floor, standing at a higher level than that of Pitiscus, intervening). It is 52 miles in diameter, and is surrounded by an apparently continuous rampart, except on the E., where there is a crater, and on the S.W., where it abuts on Hommel *b*. Here there is a wide gap crossed by what has every appearance of being a "fault," resembling that in Phocylides on a smaller scale. There is a fine crater on the N. side of the interior connected with the S. wall by a bright ridge. Just beyond the E. border there is a shallow ring-plain of a very extraordinary shape.

NEARCH.—A ring-plain, about 35 miles in diameter, on the S.W. of Hommel, forming part of the Vlacq group.

TANNERUS.—A ring-plain, about 19 miles in diameter, between Mutus and Bacon. It has a central mountain.

MUTUS.—A fine but foreshortened walled plain, 51 miles in diameter. There are two ring-plains of about equal size on the floor, one on the N., and the other on the S. side. The wall on the W. rises to nearly 14,000 feet above the interior.

MANZINUS.—A walled plain, nearly 62 miles in diameter, with

a terraced rampart rising to a height of more than 14,500 feet above the interior. Schmidt shows three craterlets on the floor, but no traces of the small central peak which is said to stand thereon, but to be only visible in large telescopes.

SCHOMBERGER.—A large walled-plain adjoining Simpelius on the S.W. Too near the limb for satisfactory observation.

## WEST LONGITUDE $20^{\circ}$ TO $0^{\circ}$ .

DELAMBRE.—A conspicuous ring-plain, 32 miles in diameter, a little S. of the equator, in W. long.  $17^{\circ} 30'$ , with a massive polygonal border, terraced within, rising on the W. to the great height of 15,000 feet above the interior, but to little more than half this on the opposite side. Its outline approximates to that of a pentagon with slightly curved sides. A section on the S.E. exhibits an inflexion towards the centre. The crest is everywhere continuous except on the N., where it is broken by a deep crater with a bright rim. The north-easterly trend of the ridges and hillocks on the E. is especially noteworthy. The central peak is not prominent, but close under it on the E. is a deep fissure, extending from near the centre, and dying out before it reaches the S. border. At the foot of the N.E. *glacis* there are traces of a ring with low walls.

THEON, SEN.—A brilliant little ring-plain, E.N.E. of Delambre, 11 miles in diameter, and of great depth, with a regular and perfectly unbroken wall. North of it is a bright little crater.

THEON, JUN.—A ring-plain similar in size and in other respects to the last, situated about 23 miles S. of it on a somewhat dusky surface. Between the pair is a curious oblong-shaped mountain mass; and on the E. a long cliff (of no great altitude, but falling steeply on the E. side) extending S. towards Taylor *a*. Just below the escarpment, I find a brilliant little pair of craterlets, of which Neison only shows one.

ALFRAGANUS.—A large bright crater, about 9 miles in diameter, with very steep walls, some distance S.S.W. of Delambre, and standing on the W. edge of a large but very shallow and irregular depression W. of Taylor. There is a remarkable chain of craters on the W. of it. Alfraganus is the centre of a system of light streaks radiating in all directions, one ray extending through Cyrillus to Fracastorius.

TAYLOR.—A deep spindle-shaped ring-plain, S. of Delambre, about 22 miles in length. The wall appears to be everywhere continuous, except at the extreme N. and S. ends, where there are small craters. The outer slopes, both on the E. and W., are very broad and prominent, but apparently not terraced. There is an inconspicuous central hill. On the W. is the irregular enclosure, already referred to under Alfraganus. Three or four short winding valleys traverse the N. edge of this formation, and descend to the dark floor. On the N.E. is the remarkable ring-plain Taylor *a*, 18 miles in diameter, rising, at an almost isolated mountain mass on the E. border, to a height of 7000 feet above the interior. The more regular and W. section of this formation is not so lofty, and falls with a gentle slope to the dark uneven floor, on which there is some detail in the shape of small bright ridges and mounds. On the surface, N.W. of Taylor *a*, is a curious linear row of bright little hills. Taylor and the vicinity is better seen under low evening illumination than under morning light.

HIPPARCHUS.—Except under a low sun, this immense walled-plain is by no means so striking an object as a glance at its representation on a chart of the moon would lead one to expect; for the border, in nearly every part of it, bears unmistakable evidence of wreck and ruin, its continuity being interrupted by depressions, transverse valleys, and gaps, and it nowhere attains a great altitude. This imperfect enclosure extends 97 miles from N. to S., and about 88 miles from E. to W., and in shape approximates to that of a rhombus with curved sides. One of the most prominent bright craters on its border is Hipparchus G, on the W. Another, of about the same size, is Hipparchus E, on the N. of Horrocks. On the E. there is a moderately bright crater, Hipparchus F; and S. of this, on the same side, two others, K and I. The interior is crossed by many ridges, and near the centre includes the relics of a low ring, traversed by a narrow rill-like valley. Schmidt shows a cleft running from F across the floor to the S. border.<sup>1</sup>

HORROCKS.—This fine ring-plain, 18 miles in diameter, stands on the N. side of the interior of Hipparchus, close to the border. It has a continuous wall, rising on the E. to a height of nearly 8000 feet above the interior, and a distinct central mountain.

HALLEY.—A ring-plain, 21 miles in diameter, on the S.W. border of Hipparchus, with a bright wall, rising at one point on

<sup>1</sup> A valuable monograph of Hipparchus, by Mr. W. R. Birt, was published in 1870.

the E. to a height of 7500 feet above the floor, which is depressed about 4000 feet below the surface. Two craterlets on the floor, one discovered by Birt on Rutherford's photogram of 1865, and the other by Gaudibert, raised a suspicion of recent lunar activity within this ring. A magnificent valley, shown in part by Schmidt as a crater-row, runs from the S. of Halley to the W. side of Albategnius.

HIND.—A ring-plain, 16 miles in diameter, a few miles W. of Halley, with a peak on its E. wall 10,000 feet above the floor. The border is broken both on the S.E. and N.E. by small craters.

[Horrocks, Halley, and Hind may be regarded as strictly belonging to Hipparchus.]

ALBATEGNIUS.—A magnificent walled-plain, 65 miles in diameter, adjoining Hipparchus on the S., surrounded by a massive complex rampart, prominently terraced, including many depressions, and crossed by several valleys. It is surmounted by very lofty peaks, one of which on the N.E. stands nearly 15,000 feet above the floor. The great ring-plain Albategnius A, 28 miles in diameter, intrudes far within the limits of the formation on the E., and its towering crest rises more than 10,000 feet above its floor, on which there is a small central mountain. The central mountain of Albategnius is more than 4000 feet high, and, with the exception of a few minor elevations, is the only prominent feature in the interior, though there are many small craters. Schmidt counted forty with the Berlin refractor, among them 12 on the E. side, arranged like a string of pearls.

PARROT.—An irregularly-shaped formation, 41 miles in diameter, S. of Albategnius, with a very discontinuous margin, interrupted on every side by gaps and depressions, large and small; the most considerable of which is the regular ring-plain Parrot *a*, on the E. An especially fine valley, shown by Schmidt to consist in part of large inosculating craters, cuts through the wall on the S.W., and runs on the E. side of Argelander towards Airy. The floor of Parrot is very rugged.

DESCARTES.—This object, about 30 miles in diameter, situated N.W. of Abulfeda, is bounded by ill-defined, broken, and comparatively low walls; interrupted on the S.E. by a fine crater, Descartes A, and on the S.W. by another, smaller. There is also a brilliant crater outside on the N.W. Schmidt shows a crater-row on the floor, which I have seen as a cleft.

DOLLOND.—A bright crater, about 6 miles in diameter, on

the N.E. side of Descartes. Between it and the latter there is a rill-valley.

**TACITUS**—A bright ring-plain, about 28 miles in diameter, a few miles E. of Catherina, with a lofty wall rising both on the E. and W. to more than 11,000 feet above the floor. Its continuity is broken on the N. by a gap occupied by a depression, and there is a conspicuous crater below the crest on the S.W. The central mountain is connected with the N. wall by a ridge, recalling the same arrangement within Madler. A range of lofty hills, an offshoot of the Altai range, extends from Tacitus towards Fermat.

**ALMANON**.—This ring-plain, with its companion Abulfeda on the N.E., is a very interesting telescopic object. It is about 36 miles in diameter, and is surrounded by an irregular border of polygonal shape, the greatest altitude of which is about 6000 feet above the floor on the W. It is slightly terraced, and is broken on the S. by a deep crater pertaining to the bright and large formation Tacitus *b*, the E. border of which casts a fine double-peaked shadow at sunrise. On the N.W. there is another bright crater, the largest of the row, running in a W.S.W. direction, and forming a W. extension of the remarkable crater-chain tangential to the borders of Almanon and Abulfeda. The only objects on the floor are three little hills, in a line, near the centre, a winding ridge on the W. side of it, and two or three other low elevations.

**ABULFEDA**.—A larger and more massive formation than Almanon, 39 miles in diameter, the E. wall rising about 10,000 feet above the interior, which is depressed more than 3000 feet. It is continuous on the W., but much broken by transverse valleys on the S.E., and by little depressions on the N. On the S.E. originates the very curious bright crater-row which runs in a straight line to the N.W. wall of Almanon, crossing for the first few miles the lofty table-land lying on the S.E. side of the border. With the exception of a low central mountain, the interior of Abulfeda contains no visible detail. The rampart is finely terraced on the E. and W. The E. *glacis* is very rugged.

**ARGELANDER**—This conspicuous ring-plain, about 20 miles in diameter, is, if we except two smaller inosculating rings on the S.W. flank of Albategnius, the most northerly of a remarkable serpentine chain of seven moderately-sized formations, extending for nearly 180 miles from the S.W. of Parrot to the N. side of Blanchinus. Its border is lofty, slightly terraced within, and includes a central peak.



AIRY.—About 22 miles in diameter, connected with Argelander by a depression bounded by linear walls. Its border, double on the S.E., is broken on the S. by a prominent crater, with a smaller companion on the W. of it; and again on the N.E. by another not so conspicuous. It has a central peak. The next link in the chain of ring-plains is Airy *c*, a very irregular object, somewhat larger, and with, for the most part, linear walls.

DONATI.—A ring-plain on the S. of Airy *c*, about 22 miles in greatest length. It is very irregular in outline, with a lofty broken border, especially on the N. and S., where there are wide gaps. There is another ring on the S.E.

FAYE.—The direction of the chain swerves considerably towards the E. at this formation, which resembles Donati both in size and in irregularity of outline. The wall, where it is not broken, is slightly terraced. There is a craterlet on the S. rim and a central crater in the interior.

DELAUNAY.—Adjoins Faye on the S.E., and is a larger and more complex object, of irregular form, with very lofty peaks on its border. A prominent ridge of great height traverses the formation from N. to S., abutting on the W. border of Lacaille. Delaunay is the last link in the chain commencing with Argelander.

LACAILLE.—An oblong enclosure situated on the N. side of Blanchinus, and apparently about 30 miles in greatest diameter. The border is to a great extent linear and continuous on the N., but elsewhere abounds in depressions. Two large inosculating ring-plains are associated with the N.E. wall.

BLANCHINUS.—A large walled-plain on the W. of Purbach and abutting on the S. side of Lacaille. It much resembles Purbach in shape, but has lower walls. Schmidt shows a crater on the N. side of the floor, which I have seen, and a number of parallel ridges which have not been noted, probably because they are only visible under very oblique light.

GEBER.—A bright ring-plain, 25 miles in diameter, S. of Almanon, with a regular border, rising to a height on the W. of nearly 9000 feet above the floor. There is a small crater on the crest of the S. wall, and another on the N. A ring-plain about 8 miles in diameter adjoins the formation on the N.E. According to Neison, there is a feeble central hill, which, however, is not shown by Schmidt.

SACROBOSCO.—This is one of those extremely abnormal formations which are almost peculiar to certain regions in the fourth

quadrant. It is about 50 miles in greatest diameter, and is enclosed by a rampart of unequal height, rising on the E. to 12,000 feet above the floor, but sinking in places to a very moderate altitude. On the N. its contour is, if possible, rendered still more irregular by the intrusion of a smaller ring-plain. On the N.E. side of the floor stands a very bright little crater and two others on the S. of the centre, each with central mountains.

FERMAT.—An irregular ring-plain 25 miles in diameter on the W. of Sacrobosco. Its partially terraced wall is broken on the N. by a gap which communicates with the interior of a smaller formation. There are some low hills on the floor, which is depressed 6000 feet below the crest of the border.

AZOPHI.—A prominent ring-plain, 30 miles in diameter, E.N.E. of Sacrobosco, its lofty barrier towering nearly 11,000 feet above a somewhat dusky interior, which includes some light spots. A massive curved mountain arm runs from the S. side of this formation to a small ring-plain W. of Playfair.

ABENEZRA.—When observed near the morning terminator, this noteworthy ring-plain, 27 miles in diameter, seems to be divided into two by a curved ridge which traverses the formation from N. to S., and extends beyond its limits. The irregular border rises on the W. to a height of more than 14,000 feet above the deeply-sunken floor, which includes several craters, hills, and ridges.

APIANUS.—A magnificent ring-plain, 38 miles in diameter, N.W. of Aliacensis, with lofty terraced walls, rising on the N.E. to about 9000 feet above the interior, and crowned on the W. by three large conspicuous craters. The border is broken on the N. by a smaller depression and a large ring with low walls. The dark-grey floor appears to be devoid of conspicuous detail.

PLAYFAIR.—A ring-plain, 28 miles in diameter, with massive walls. It is situated on the N. of Playfair, and is connected with it by a mountain arm. The rampart is tolerably continuous, but varies considerably in altitude, rising on the S. to a height of more than 8000 feet above the interior. On the W., extending towards Blanchinus, is a magnificent unnamed formation, bounded on the E. by a broad lofty rampart flanking Blanchinus, Lacaille, Delaunay, and Faye; and on the W. by Playfair and the mountain arm just mentioned. It is fully 60 miles in length from N. to S. Sunrise on this region affords a fine spectacle to the observer with a large telescope. The best phase is when the morning terminator intersects Aliacensis, as at this time the long jagged shadows

of the E. wall of Playfair and of the mountain arm are very prominent on the smooth, greyish-blue surface of this immense enclosure.

PONTANUS.—An irregular ring-plain, 28 miles in diameter, S.S.W. of Azophi, with a low broken border, interrupted on the S.W. by a smaller ring-plain, which forms one of a group extending towards the S.W. The dark floor includes a central mountain.

ALIACENSIS.—This ring-plain, 53 miles in diameter, with its neighbour Werner on the N.E., are beautiful telescopic objects under a low sun. Its lofty terraced border rises at one peak on the E. to the tremendous height of 16,500 feet, and at another on the opposite side to nearly 12,000 feet above the floor. The wall on the S. is broken by a crater, and on the W. traversed by narrow passes. There is also a prominent crater on the inner slope of the N.E. wall. The floor includes a small mountain, several little hills, and a crater.

WERNER.—A ring-plain, 45 miles in diameter, with a massive rampart crowned by peaks almost as lofty as any on that of Aliacensis, and with terraces fully as conspicuous. It has a magnificent central mountain, 4500 feet high. At the foot of the N.E. wall Mädler observed a small area, which he describes as rivalling the central peak of Aristarchus in brilliancy. Webb, however, was unable to confirm this estimate, though he noted it as very bright, and saw a minute black pit and narrow ravine within it. Neison subsequently found that the black pit is a crater-cone. It would perhaps be rash, with our limited knowledge of minute lunar detail, to assert that Mädler over-estimated the brightness of this area, which may have been due to a *recent* deposit round the orifice of the crater-cone.

POISSON.—An irregular formation on the W. of Aliacensis, extending about 50 miles from W. to E., but much less in a meridional direction. Its N. limits are marked by a number of overlapping ring-plains and craters, and it is much broken elsewhere by smaller depressions. The E. wall is about 7000 feet in height.

GEMMA FRISIUS.—A great composite walled-plain, 80 miles or more in length from N. to S., with a wall rising at one place nearly 14,000 feet above the floor. It is broken on the N. by two fine ring-plains, each about 20 miles in diameter, and on the E. by a third open to the E. There is a central mountain, and several small craters on the floor, especially on the W. side.

BÜSCHING.—A ring-plain S. of Zagut, about 36 miles in diameter, with a moderately high but irregular wall. There are several craterlets within and some low hills.

BUCH.—Adjoins Büsching on the S.E. It is about 31 miles in diameter, and has a less broken barrier. There is a large crater on the E. wall, and another smaller one on the S.W. Schmidt shows nothing on the floor, but Neison noted two minute crater-cones.

MAUROLYCUS.—This unquestionably ranks as one of the grandest walled-plains on the moon's visible surface, and when viewed under a low sun presents a spectacle which is not easily effaced from the mind. Like so many of the great enclosures in the fourth quadrant, it impresses one with the notion that we have here the result of the crowding together of a number of large rings which, when they were in a semi-fluid or viscous condition, mutually deformed each other. It extends fully 150 miles from E. to W., and more from N. to S.; so it may be taken to include an area on the lunar globe which is, roughly speaking, equal to half the superficies of Ireland. This vast space, bounded by one of the loftiest, most massive, and prominently-terraced ramparts, includes ring-plains, craters, crater-rows, and valleys,—in short, almost every type of lunar formation. It towers on the E. to a height of nearly 14,000 feet above the interior, and on the W., according to Schmidt, to a still greater altitude. A fine rill-valley curves round the outer slope of the W. wall, just below its crest, which is an easy object in a 8½-inch reflector when the opposite border is on the morning terminator, and could doubtless be seen in a smaller instrument; and there is an especially brilliant crater on the S. border, which is not visible till a somewhat later stage of sunrise. The central mountain is of great altitude, its loftiest peaks standing out amid the shadow long before a ray of sunlight has reached the lower slopes of the walls. It is associated with a number of smaller elevations. I have seen three considerable craters and several smaller ones in the interior.

BAROCIUS.—A massive formation, about 50 miles in diameter, on the S.W. side of Maurolycus, whose border it overlaps and considerably deforms. Its wall rises on the E. to a height of 12,000 feet above the floor, and is broken on the N.W. by two great ring-plains. On the inner slope of the S.E. border is a curious oblong enclosure. There is nothing remarkable in the interior.

On the dusky grey plain W. of Maurolycus and Barocius there is a number of little formations, many of them being of a very abnormal shape, which are well worthy of examination. I have seen two short unrecorded clefts in connection with these objects.

STOFLE — A grand object, very similar in size and general character to Maurolycus, its neighbour on the W. To view it and its surroundings at the most striking phase, it should be observed when the morning terminator lies a little E. of the W wall. At this time the jagged, clean-cut, shadows of the peaks on Faraday and the W. border, the fine terraces, depressions, and other features on the illuminated section of the gigantic rampart, and the smooth bluish-grey floor, combine to make a most beautiful telescopic picture. At a peak on the NE, the wall attains a height of nearly 12,000 feet, but sinks to a little more than a third of this height on the E. It is apparently loftiest on the N. The most conspicuous of the many craters upon it is the bright deep circular depression E on the S. wall, and another, rather larger and less regular, on the NW, which has a very low rim on the side facing the floor, and a craterlet on either side of the apparent gap. A large lozenge-shaped enclosure abuts on the wall, near the crater E, with a border crowned by a number of little peaks, which at an early stage of sunrise resemble a chaplet of pearls. The floor of Stofler is apparently very level, and in colour recalls the beautiful steel-grey tone of Plato seen under certain conditions. I have noted several distinct little craters on its surface, mostly on the NE side; and on the E side a triangular dark patch, close to the foot of the wall, very similar in size and appearance to those within Alphonsus.

FARADAY — A large ring-plain, about 35 miles in diameter, overlapping the SW. border of Stofler; its own rampart being overlapped in its turn by two smaller ring-plain on the SE, and by two still smaller formations (one of which is square-shaped) on the NW. The wall is broad and very massive on the E and NE, prominently terraced, and includes many brilliant little craters. Schmidt shows a ridge and several craters in the interior.

LICETUS — An irregular formation, about 50 miles in maximum width, on the S. of Stofler, with the flanks of which it is connected by a coarse valley. Neison points out that it consists of a group of ring-plain united into one, owing to the separating walls having been partially destroyed. This seems to be clearly the case, if Licetus is examined under a low sun. On the E. side of

the N. portion of the formation, the wall rises to nearly 13,000 feet.

**FERNELIUS.**—A ring-plain, about 30 miles in diameter, abutting on the N. wall of Stofler. It is overlapped on the E. by another similar formation of about half its size. There are many craters and depressions on the borders of both, and a large crater between the smaller enclosure and the N E outer slope of Stofler. Schmidt shows eight craters on the floor of Fernelius.

**NONIUS**—A ring-plain, about 20 miles in diameter, abutting on the N wall of Fernelius. There is a prominent bright crater on the W. of it, and another on the N, from which a delicate valley runs towards the W. side of Walter.

**CLAIRAUT.**—A very peculiar formation, about 40 miles in diameter, S. of Maurolycus, affording another good example of interference and overlapping. The continuity of its border, nowhere very regular, has been entirely destroyed on the S by the subsequent formation of two large rings, some 10 or 12 miles in diameter, the more easterly of which has, in its turn, been partially wrecked on the N. by a smaller object of the same class. There is also a ring-plain N E of Clairaut, which has very clearly modified the shape of the border on this side. Two craters on the floor of Clairaut are easy objects

**BACON**—A very fine ring-plain, 40 miles in diameter, S W of Clairaut. At one peak on the E the terraced wall rises to nearly 14,000 feet above the interior. It is broken on the S. by three or four craters. On the W there is an irregular inconspicuous enclosure, whose contiguity has apparently modified the shape of the border. There are two large rings on the N. (the more easterly having a central peak), and a third on the E. The floor appears to be devoid of prominent detail.

**CUVIER**—A walled-plain, about 50 miles in diameter, on the S E of Clairaut. The border on the E. rises to 12,000 feet; and on the N W is much broken by depressions. Neison has seen a mound, with a minute crater W. of it, on the otherwise undisturbed interior.

**JACOBI**—A ring-plain S of Cuvier, about 40 miles in diameter, with walls much broken on the N and S, but rising on the E to nearly 10,000 feet. There is a group of craters (nearly central) on the floor. The region S of this formation abounds in large unnamed objects.

**LILIUS**—An irregular ring-plain, 39 miles in diameter, with a rampart on the E. nearly 10,000 feet above the floor. A

smaller ring between it and Jacobi has considerably inflected the wall towards the interior. It has a conspicuous central mountain.

ZACH.—A massive formation, 46 miles in diameter, on the S. of Lilius, with prominently terraced walls, rising on the E. to 13,000 feet above the interior. A small ring-plain, whose wall stands 6000 feet above the floor, is associated with the N. border. Two other rings, on the S.W. and N.E. respectively, have craters on their ramparts and central hills.

PENTLAND.—A fine conspicuous formation under a low sun, even in a region abounding in such objects. It is about 50 miles in diameter, with a border exceeding in places 10,000 feet in height above the floor, which includes an especially fine central mountain.

KINAU.—One of the group of remarkable ring-plains extending in a N.W. direction from Pentland.

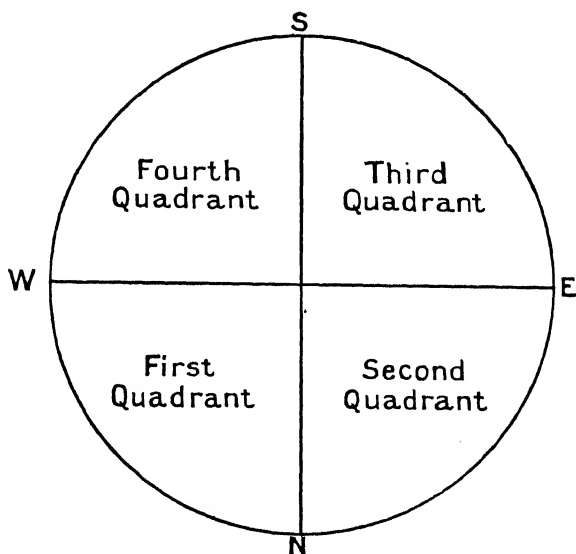
SIMPELIUS.—Another grand circumvallation, almost as large as Pentland, but unfortunately much foreshortened. One of its peaks on the E. rises to a height of more than 12,000 feet above the floor, on which there is a small central mountain. Between Simpelius and Pentland are several ring-plains, most of which appear to have been squeezed and deformed into abnormal shapes.

CURTIUS.—A magnificent formation, about 50 miles in diameter, with one of the loftiest ramparts on the visible surface, rising at a mountain mass on the N.E. to more than 22,000 feet, an altitude which is only surpassed by peaks on the walls of Newton and Casatus. There is a bright crater on the S.E. border and another on the W. The formation is too near the S. limb for satisfactory scrutiny. Between Curtius and Zach is a fine group of unnamed enclosures.


# APPENDIX

## DESCRIPTION OF THE MAP

THE accompanying map, eighteen inches in diameter, represents the moon under mean libration. Meridian lines and parallels of latitude are drawn at every  $10^{\circ}$ , except in the case of the meridians of  $80^{\circ}$  E. and W. longitude, which are omitted to avoid confusion, and as being practically needless. These lines will enable the observer, with the aid of the Tables in the Appendix, to find the position of the



terminator at any time required. As astronomical telescopes exhibit objects inverted, maps of the moon are always drawn upside down, and with the right and left interchanged, as in the diagram above, which also shows how the quadrants are numbered.

This circle , intended to be .15708 in diameter, represents a circle of one degree in diameter at the centre of the map, and as the length of one selenographical degree is 18.871 miles, it represents an area of nearly 280 square miles.



The catalogue is so arranged that, beginning with the W. limb, and referring to the lists under the first and fourth, and the second and third quadrants, all the formations falling within the meridians  $90^{\circ}$  to  $60^{\circ}$ ,  $60^{\circ}$  to  $40^{\circ}$ ,  $40^{\circ}$  to  $20^{\circ}$ ,  $20^{\circ}$  to  $0^{\circ}$  (the central meridian), and from  $0^{\circ}$  to  $20^{\circ}$ , and so on, to the E. limb, will be found in convenient proximity in the text.

*In the Catalogue, N. S. E. W. are used as abbreviations for the cardinal points.*

# LIST OF THE MARIA, OR GREY PLAINS, TERMED "SEAS," &c.

## FIRST QUADRANT.

Mare	Tranquilitatis (nearly the whole), page 5.
"	Fœcunditatis (the N. portion), 5.
"	Serenitatis, 5.
"	Crisium, 6.
"	Frigoris (a portion), 5.
"	Vaporum (nearly the whole), 6.*
"	Humboldtianum, 6.
"	Smythii (a portion), 39.
Lacus	Mortis, 53.
"	Somniorum.
Palus	Somnii.
"	Nebularum (a portion), 62.
"	Putredinis, 61.
Sinus	Medii (a portion), 6.

## SECOND QUADRANT.

Mare	Imbrium, 5.
"	Nubium (the N. portion), 5.
"	Frigoris (a portion), 5.
"	Vaporum (a portion), 6.
Oceanus	Procellarum (the N. portion), 5.

Palus	Nebularum (a portion), p. 62.
Sinus	Iridum, 80.
"	Medii (a portion), 6.
"	Roris, 90.
"	Æstuum.

## THIRD QUADRANT.

Mare	Nubium (the greater portion), 5.
"	Humorum, 6.
Oceanus	Procellarum (the S. portion), 5.
Sinus	Medii (a small portion), 6.

## FOURTH QUADRANT.

Mare	Fœcunditatis (the greater portion), 5.
"	Nectaris, 7.
"	Tranquilitatis (a small portion), 5.
"	Australe, 127.
"	Smythii (a portion), 39.
Sinus	Medii (a portion), 6.

LIST OF SOME OF THE MOST PROMINENT MOUNTAIN  
RANGES, PROMONTORIES, ISOLATED MOUNTAINS,  
AND REMARKABLE HILLS.

FIRST QUADRANT.

*The Alps.* The western portion of the range.

*The Apennines.* The extreme northern part of the range.

*The Caucasus.*

*The Hæmus.*

*The Taurus.*

*The North Polar Range.* On the limb extending from N. lat.  $81^{\circ}$  towards the E.

*The Humboldt Mountains.* On the limb from N. lat.  $72^{\circ}$  to N. lat.  $53^{\circ}$ .

*Mount Argæus.* A mountain mass rising some 8000 feet above the Mare Serenitatis in N. lat.  $20^{\circ}$ , W. long.  $28^{\circ}$ , N.W. of Dawes.

*Prom. Acherusia.* A bright promontory at the W. extremity of the Hæmus range, rising nearly 5000 feet above the Mare Serenitatis. N. lat.  $17^{\circ}$ , W. long.  $22^{\circ}$ .

*Cape Agarum.* The N. end of a projecting headland on the S.W. side of the Mare Crisium, in N. lat.  $14^{\circ}$ , W. long.  $66^{\circ}$ , rising nearly 11,000 feet above the Mare.

*Le Monnier A.* An isolated mountain more than 3000 feet high, standing about midway between the extremities of the bay: probably a relic of a once complete ring.

*Secchi.* South of this formation there is a lofty prominent isolated mountain.

*Manilius A and B.* Two conspicuous mountains N. of Manilius; A, the more westerly, being more than 5000 feet, and B about 2000 feet in height.

*Autolycus A.* A mountain of considerable altitude, S. of this formation.

*Mont Blanc.* Principal peak, N. lat.  $46^{\circ}$ , W. long.  $0^{\circ} 30'$ , nearly 12,000 feet in height.

*Cassini  $\epsilon$  and  $\delta$ .* Two adjoining mountain masses N. of Cassini, more than 5000 feet high.

*Eudoxus.* S.E. of this formation, in N. lat.  $43^{\circ}$ , W. long.  $10^{\circ}$ , are two bright mountain masses, the more southerly rising 7000, and the other 4000 feet above the surface.

*Mount Hadley.* The northern extremity of the Apennines, in N. lat.  $27^{\circ}$  W. long.  $5^{\circ}$ , rising more than 15,000 feet above the Mare.

- Mount Bradley.* A promontory of the Apennines, in N. lat.  $23^{\circ}$ , W. long.  $1^{\circ}$ , nearly 14,000 feet above the Mare Imbrium
- The Silberschlag Range*, running from near the S.E. side of Julius Cæsar to the region W of Agrippa

## SECOND QUADRANT

- The Alps.* The eastern and greater portion
- The Apennines* Nearly the whole of the range
- The Carpathians*
- The Teneriffe Mountains* S E of Plato Highest peak, 8000 feet.
- The Straight Range* East of the last, in N. lat.  $48^{\circ}$ , E long.  $20^{\circ}$
- The Harlinger Mountains* N W. of Aristarchus
- The Hercynian Mountains.* Near the N E limb, E of Otto Struve, N lat.  $25^{\circ}$
- Mount Huygens* A mountain mass projecting from the escarpment of the Apennines, in N lat.  $20^{\circ}$ , E. long.  $3^{\circ}$ , one peak rising to 18,000 feet above the Mare Imbrium.
- Mount Wolf* A great square-shaped mountain mass, near the S E. extremity of the Apennines, in N lat.  $17^{\circ}$ , E long.  $9^{\circ}$ , the loftiest peak rising to nearly 12,000 feet above the Mare Imbrium
- Eratosthenes*  $\iota$  and  $\kappa$  Two isolated mountains N of this formation, in N lat.  $20^{\circ}$ ,  $\kappa$  is 1800 feet in height.
- Pico.* A magnificent isolated mountain, S of Plato, in N lat.  $45^{\circ}$ , E long.  $9^{\circ}$ , rising some 8000 feet above the Mare Imbrium
- Pico B.* A triple-peaked mountain a few miles S. of Pico
- Piton* A bright isolated mountain 7000 feet high, in N. lat.  $1^{\circ}$ , E long.  $1^{\circ}$
- Fontinelle* A A conspicuous isolated mountain about 3000 feet high, S. of Fontinelle
- Archimedes*  $\zeta$ . A triangular-shaped group E. of Archimedes, in N. lat.  $31^{\circ}$ , E. long.  $8^{\circ}$ , the highest of the peaks rising more than 2000 feet
- Caroline Herschel* E of this formation is a double-peaked mountain rising to 1300 feet
- Gruithuisen*  $\delta$  and  $\gamma$  On the N of this bright crater, in N lat.  $36^{\circ}$ , E long.  $40^{\circ}$ , rises a fine mountain,  $\delta$ , nearly 6000 feet in height, and on the N E of it the larger mass  $\gamma$ , almost as lofty
- Manan* There is a group of three bright little mountains, the loftiest about 800 feet above the Mare, some distance E. of this formation
- Euler*  $\beta$  A fine but small mountain group, more than 3600 feet high, on the Mare Imbrium, S.E. of Euler.
- The Laplace Promontory.* A magnificent headland on the N. side of the Sinus Iridum, rising about 9000 feet above the latter, and about 7000 feet above the Mare Imbrium
- Cape Heracles* A fine but less prominent headland on the opposite side of the bay, rising more than 4000 feet above it.

- Lahure* A large bright isolated mountain in the Mare Imbrium, N E of Lambert, in N. lat  $27^{\circ}$ , E long  $25^{\circ}$ . It is, according to Schroter, nearly 5000 feet high.
- Delisle  $\beta$*  A curious club-shaped mountain on the S E of this formation, nearly 4000 feet in height.
- Pytheas  $\beta$*  An isolated mountain, 900 feet high, in N lat.  $20^{\circ}$ , E long.  $23^{\circ}$ .
- Kirch* There is a small isolated hill a few miles N of this formation.
- Kirch  $\Gamma$*  A bright mountain about 700 feet high, in N lat.  $39^{\circ}$ , E long  $3^{\circ}$ .
- Piazzi Smyth  $\beta$*  A small bright isolated mountain on a ridge S. of this, is a noteworthy object under a low sun.
- Lambert  $\Gamma$*  In N. lat.  $26^{\circ}$ , E long  $18^{\circ}$ , a remarkable curved mountain about 3000 feet in height, a brilliant object under a low sun.
- D'Alembert Mountains* A range on the E. limb running S. from N. lat  $12^{\circ}$ .
- Wollaston*. An isolated triangular mountain about midway between this and Wollaston B.

### THIRD QUADRANT.

- The Rhiphaean Mountains* An isolated range S. of Landsberg in S lat  $7^{\circ}$ , E long  $28^{\circ}$ . They run in a meridional direction, and rise at one peak to nearly 3000 feet above the Oceanus Procellarum.
- The Percy Mountains* extend from the eastern flank of Gassendi towards Mersenius, forming the north-eastern border of the Mare Humorum.
- Prom. Aenarium*. A steep bluff situated at the northern end of a plateau, some distance E of Arzachel, in S. lat  $18^{\circ}$ , E. long.  $9^{\circ}$ . It rises some 2000 feet above the Mare Nubium.
- Euclides  $\zeta$  and  $\chi$*  Two mountain masses N. of this formation in S lat  $5^{\circ}$ ,  $\zeta$  rises about 1700 feet above the Mare, both are evidently offshoots from the Rhiphaean range.
- Landsberg  $\Pi$* . An isolated hill in S lat  $4^{\circ}$ , E long  $25^{\circ}$ .
- Niccollet c* SE of Niccollet, in S lat.  $22^{\circ}$ , E long.  $17^{\circ}$ , is hemmed in by a mountain mass rising to more than 2000 feet above the Mare Nubium.
- The Stag's-Horn Mountains* At the S end of the straight wall, or "railroad," in S lat.  $24^{\circ}$ , E. long.  $8^{\circ}$ , a curious mountain mass rising about 2000 feet above the Mare Nubium.
- Lacroix  $\delta$* . A mountain more than 7000 feet high, N. of Lacroix.
- Flamsteed  $\epsilon$*  A mountain of more than 3000 feet in S. lat  $4^{\circ}$ , E long  $51^{\circ}$ .
- D'Alembert Mountains* A very lofty range on the E. limb, extending to S. lat  $11^{\circ}$ .

- The Cordilleras.* Close to the E. limb; they lie between S. lat.  $8^{\circ}$  and S. lat.  $23^{\circ}$ .
- Rook Mountains.* On the E. limb, extending from about S. lat.  $18^{\circ}$  to S. lat.  $35^{\circ}$ . According to Schröter, they attain a height of 25,000 feet.
- Dörfel Mountains.* On the S.E. limb between S. lat.  $57^{\circ}$  and S. lat.  $80^{\circ}$ .
- Leibnitz Mountains.* On the S. limb extending W. from S. lat.  $80^{\circ}$  beyond the Pole on to the Fourth Quadrant. Perhaps the loftiest range on the limb. Mädler's measures give more than 27,000 feet as the height of one peak, and there are several others nearly as high.

## FOURTH QUADRANT.

- The Altai Mountains.* A fine conspicuous serpentine range, extending from the E. side of Piccolomini in a north-easterly direction to the region between Tacitus and Catherina, a length of about 275 miles. The loftiest peak is over 13,000 feet. The average height of the southern portion is about 6000 feet. The region lying on the S.E. of this range is a vast tableland, devoid of prominent objects, rising gradually towards the mountains, which shelve rapidly down to an equally barren expanse on the N.W.
- The Pyrenees.* These mountains, on the E. of Guttemberg, border the western side of the Mare Nectaris. Their loftiest peak, rising nearly to 12,000 feet, is on the S.E. of Guttemberg.

# LIST OF THE PRINCIPAL RAY-SYSTEMS, LIGHT-SURROUNDED CRATERS, AND LIGHT-SPOTS.<sup>1</sup>

## FIRST QUADRANT.

- Autolycus*. Encircled by a delicate nimbus, throwing out four or five prominent rays extending towards Archimedes. Seen best under evening illumination.
- Aristillus*. The centre of a noteworthy system of delicate rays extending W. towards the Caucasus; and on the S. disappearing among the rays of Autolycus. They are traceable on the Mare Nubium near Kirch.
- Theætetus*. A very brilliant group of little hills E. of this formation.
- Eudoxus* A. A light-surrounded crater W. of Eudoxus, with distinct long streaks, one of which extends to the S. wall of Aristoteles.
- Aristoteles* A. A light-surrounded crater in the Mare Frigoris, N.E. of Aristoteles.
- Aratus*. A very conspicuously brilliant crater in the Apennines, with a smaller light-surrounded crater W. of it.
- Sulpicius Gallus*. A light spot near.
- Manilius*. Surrounded by a light halo and streaks.
- Taquet*. Has a prominent nimbus, and indications of very delicate streaks.
- Plinius* A. Is surrounded by a well-marked halo.
- Posidonius*  $\gamma$ . Among the hills E. of this formation a light spot resembling Linné, according to Schmidt. He first saw it in 1867, when it had a delicate black spot in the centre. Dr. Vogel observed and drew it in 1871 with the great refractor at Bothkamp. These observations were confirmed by Schmidt in 1875 with the 14-feet refractor at Berlin.
- Littrow*. A very bright light-spot with streaks, on the site of a little crater and well-known cleft E. of this ring-plain.
- Römer*. A light-surrounded mountain on the E.
- Macrobis*. Two light-surrounded craters on the E. of this formation, the more northerly being the brighter.
- Cleomedes* A. (On the floor.) Surrounded by a nimbus and rays. Large crater, A, on the E. has also a nimbus and rays.

---

<sup>1</sup> In this list, which does claim to be exhaustive, most of the objects noted by Schmidt are incorporated.

- Agrippa.* Exhibits faint rays.
- Godin.* Exhibits faint rays.
- Proclus.* A well-known ray-centre, some of the rays prominent on part of the Mare Crisium.
- Taruntius.* Has a very faint nimbus, with rays, on a dark surface.
- Dionysius.* A brilliant crater with a prominent, bright, excentrically placed nimbus on a dark surface, on which distinct rays are displayed.
- Hypatia B.* A very small bright crater on a dark surface: surrounded by a faint nimbus.
- Apollonius.* Among the hills S. of this, there is a small bright streak system.
- Eimmart.* There is a large white spot N.W. of this.
- Geminus* is associated with a system of very delicate rays.
- Menelaus.* A brilliant object. It is traversed by a long ray from Tycho.

## SECOND QUADRANT.

- Anaxagoras.* The centre of an important ray-system.
- Timocharis* is surrounded by a pale irregular nimbus and faint rays, most prominently developed on the W. side of the formation.
- Copernicus.* Next to Tycho, the most extended ray-centre on the visible surface. Some distance on the E., in E. long.  $25^{\circ}$ , N. lat.  $11^{\circ}$ , lies a very small but conspicuous system, and in E. long.  $22^{\circ}$  N. lat.  $8^{\circ}$  a bright light spot among little hills.
- Gambart A.* A bright crater with large nimbus and rays.
- Landsberg A.* A light-surrounded crater on a dark surface, with companions, referred to under the Third Quadrant.
- Encke.* There is a light-surrounded crater S. of this.
- Kepler.* A noted ray-centre. It is surrounded by an extensive halo, especially well developed on the E., across the Mare Procellarum.
- Bessarion.* Two bright craters: the more northerly is prominently light-surrounded, while its companion is less conspicuously so.
- Aristarchus.*—The most conspicuous bright centre on the moon, the origin of a complicated ray-system.
- Delisle.* S. of this formation there is a tolerably bright spot on the site of some hills.
- Timæus.* A ray-centre.
- Euler.* Feeble halo with streaks.
- Galileo.* Between this and Reiner is a curious bright formation with short rays, referred to in the Catalogue, under Reiner.
- Cavalerius.* A light streak originating in the W. wall, and extending on to the Oceanus Procellarum.
- Olbers.* A considerable ray-system, but seldom distinctly visible.
- Lichtenberg.* Faintly light-surrounded.



## THIRD QUADRANT.

- Tycho*. The largest and best known system on the visible surface.
- Zuchius*. A remarkable ray-system, but one which is only well seen when libration is favourable.
- Bailly*. N. of the centre of this great enclosure are two very distinct radiating streaks.
- Schickard*. Four conspicuous light spots, probably craters, on the S.E.
- Byrgius A*. A brilliant ray-centre, most of the rays trending eastward from a nimbus.
- Hainzel*. There are several bright spots E. of this formation.
- Mersenius*. Two or three light-rays originate from a point on the W. rampart.
- Mersenius C*. A light-surrounded crater with short rays.
- Grimaldi*. There are three bright spots on the W. wall.
- Damoiseau*. A light-surrounded crater W. of Damoiseau, E. long.  $58^\circ$ , S. lat.  $6^\circ$ .
- Flamsteed C*. A light-surrounded crater on a dark surface.
- Lubieniezky A*. Crater with halo on a dark surface.
- Lubieniezky F*. Crater with halo on a dark surface.
- Lubieniezky G*. Crater with halo on a dark surface.
- Birt a*. A light-surrounded crater.
- Landsberg*. E. of Landsberg, four light-surrounded craters, forming with Landsberg A (in the Second Quadrant) an interesting group.
- Lohrmann A*. A light-surrounded crater, with a light area a few miles N. of it. S. lat.  $1^\circ$ , E. long.  $61^\circ$ .
- Euclides*. Has a conspicuous nimbus with traces of rays, a typical example.
- Gueriké*. There is a crater, with nimbus, W. of this, in E. long.  $12^\circ$ , S. lat.  $11^\circ 5'$ .
- Parry*. A very brilliant light-spot in the S. wall.
- Parry A*. Surrounded by a bright nimbus.
- Alpetragius B*. A conspicuous light-surrounded crater, one of the most remarkable on the moon.
- Alpetragius d* (E. long.  $11^\circ$ , S. lat.  $13^\circ 8'$ ). A bright spot, seen by Mädler as a crater, but which, as Schmidt found in 1868, no longer answers to this description.
- Mösting C*. A light-surrounded crater.
- Lalande*. Has a large nimbus and distinct rays.
- Hell*. A large ill-defined spot in E. long.  $4^\circ$ , S. lat.  $33^\circ$ . This is most probably the site of the white cloud seen by Cassini.
- Mercator*. There is a brilliant crater and light area under E. wall.

## FOURTH QUADRANT.

- Stevinus* a. A crater E. of *Stevinus*; it is a centre of wide extending rays.
- Furnerius* A. Prominently light-surrounded, with bright streaks, radiating for a long distance N. and S.
- Messier* A. The well-known "Comet" rays, extending E. of this.
- Langrenus*. Has a large but very pale ray-system. It is best seen under a low evening sun. Three long streaks radiate towards the E. from the foot of the *glacis* of the S.E. wall.
- Censorinus*. A very brilliant crater with faint rays.
- Theophilus*. The central mountain is faintly light-surrounded.
- Müder*. This ring-plain and the neighbourhood on the N. and N.W., include many bright areas and curious streaks.
- Almanon*. About midway between this and *Argelander* is a very brilliant little crater.
- Beaumont*. Between this and *Cyrrillus* stand three considerable craters with nimbi.
- Cyrrillus* A. A prominent light-surrounded crater.
- Alfraganus*. A light-surrounded crater with rays.

# POSITION OF THE LUNAR TERMINATOR

THOUGH the position of the Lunar Terminator is given for mean mid-night throughout the year in that very useful publication the *Companion to the Observatory*, it is frequently important in examining or comparing former drawings and observations to ascertain its position at the times when they were made. For this purpose the subjoined tables (which first appeared in the *Selenographical Journal*) will be found useful, as they give for any day between A.D. 1780 and A.D. 1900 the selenographical longitude of the point where the terminator crosses the moon's equator, which it does very nearly at right angles.

## TABLE I.

*Position of the Moon's Terminator on March 1, noon G.M.T., of each year.*

YEAR.	°	'	YEAR.	°	'	YEAR.	°	'
1780 . . .	145	40	1820 . . .	250	49	1860 . . .	344	7
1781 . . .	26	2	1821 . . .	121	11	1861 . . .	214	30
1782 . . .	246	24	1822 . . .	351	33	1862 . . .	84	52
1783 . . .	116	46	1823 . . .	221	55	1863 . . .	315	15
1784 . . .	334	59	1824 . . .	80	17	1864 . . .	173	26
1785 . . .	205	20	1825 . . .	310	40	1865 . . .	43	49
1786 . . .	75	42	1826 . . .	181	2	1866 . . .	274	11
1787 . . .	305	4	1827 . . .	51	25	1867 . . .	144	33
1788 . . .	164	16	1828 . . .	269	26	1868 . . .	2	45
1789 . . .	34	39	1829 . . .	139	49	1869 . . .	233	7
1790 . . .	265	1	1830 . . .	10	11	1870 . . .	103	29
1791 . . .	135	23	1831 . . .	240	33	1871 . . .	333	52
1792 . . .	353	36	1832 . . .	98	55	1872 . . .	192	3
1793 . . .	223	58	1833 . . .	329	17	1873 . . .	62	26
1794 . . .	94	21	1834 . . .	199	39	1874 . . .	292	48
1795 . . .	324	45	1835 . . .	70	1	1875 . . .	163	11
1796 . . .	182	55	1836 . . .	288	13	1876 . . .	21	23
1797 . . .	53	17	1837 . . .	158	36	1877 . . .	251	45
1798 . . .	283	40	1838 . . .	28	58	1878 . . .	122	8
1799 . . .	154	2	1839 . . .	259	21	1879 . . .	352	30
1800 . . .	24	25	1840 . . .	117	33	1880 . . .	210	43
1801 . . .	254	46	1841 . . .	347	55	1881 . . .	81	4
1802 . . .	125	9	1842 . . .	118	17	1882 . . .	311	26
1803 . . .	355	31	1843 . . .	88	40	1883 . . .	181	48
1804 . . .	213	35	1844 . . .	306	52	1884 . . .	40	1
1805 . . .	83	57	1845 . . .	177	15	1885 . . .	270	23
1806 . . .	314	19	1846 . . .	47	36	1886 . . .	140	45
1807 . . .	184	41	1847 . . .	277	58	1887 . . .	11	7
1808 . . .	43	3	1848 . . .	136	11	1888 . . .	229	20
1809 . . .	273	25	1849 . . .	6	33	1889 . . .	99	42
1810 . . .	143	48	1850 . . .	236	55	1890 . . .	330	5
1811 . . .	14	10	1851 . . .	107	17	1891 . . .	200	26
1812 . . .	232	13	1852 . . .	325	29	1892 . . .	58	39
1813 . . .	102	34	1853 . . .	195	52	1893 . . .	289	1
1814 . . .	332	58	1854 . . .	66	14	1894 . . .	154	24
1815 . . .	203	20	1855 . . .	296	37	1895 . . .	29	46
1816 . . .	61	41	1856 . . .	154	48	1896 . . .	247	57
1817 . . .	292	3	1857 . . .	25	11	1897 . . .	118	19
1818 . . .	162	26	1858 . . .	255	33	1898 . . .	347	40
1819 . . .	32	48	1859 . . .	125	54	1899 . . .	119	2

TABLE II.  
Position of the Moon's Terminator at midnight G.M.T., for each day of the year.

Days	March	April	May	June	July	August	September	October	November	December	January	February
1	6	23	29	48	54	73	92	98	116	121	138	155
2	18	35	41	60	67	86	104	110	128	133	150	167
3	30	48	55	72	79	98	116	122	140	145	162	179
4	42	60	66	84	91	110	129	135	152	157	174	191
5	54	72	78	97	103	129	141	147	164	169	186	203
6	66	84	90	109	116	134	153	159	177	181	198	215
7	79	96	102	121	128	147	165	171	189	194	211	227
8	91	109	115	133	140	159	177	183	201	206	223	240
9	103	121	127	146	152	171	190	195	213	218	235	252
10	115	133	139	158	164	183	202	208	225	230	247	264
11	127	145	151	170	177	196	214	220	237	242	259	276
12	140	157	163	182	189	208	226	232	250	254	271	288
13	152	170	176	194	201	220	238	244	262	267	283	300
14	164	182	188	207	213	232	251	256	274	279	296	313
15	176	194	200	219	226	244	263	269	286	291	308	325
16	188	206	212	231	238	257	275	281	298	303	320	337
17	200	218	224	243	250	269	287	293	310	315	332	349
18	213	231	237	256	262	281	299	305	323	327	344	361
19	225	243	249	268	274	293	312	317	335	340	356	373
20	237	255	261	280	287	305	324	330	347	352	368	385
21	249	267	273	292	299	318	336	342	359	364	380	397
22	261	279	286	304	311	330	348	354	371	376	392	409
23	274	292	298	317	324	342	360	366	383	388	404	421
24	286	304	310	329	336	354	372	378	395	400	416	433
25	298	316	322	341	348	366	384	390	407	412	428	445
26	310	328	335	353	360	378	396	402	419	424	440	457
27	322	340	347	365	372	390	408	414	431	436	452	469
28	334	352	359	377	384	402	420	426	443	448	464	481
29	347	365	372	391	398	416	434	440	457	462	478	495
30	359	377	384	403	410	428	446	452	469	474	490	507
31	371	389	396	415	422	440	458	464	481	486	502	519

*To find the position of the Lunar Terminator on any day in a year  
between 1780 and 1900.*

From Table I. take out the angle opposite the year, supposing the year to begin on March 1; so that, for example, January and February 1829 are to be considered the last two months of 1828. From this quantity subtract the angle opposite the given day in Table II., adding  $360^\circ$ , if necessary, to avoid negative quantities. An angle between  $0^\circ$  and  $360^\circ$  will be obtained, which will come under one of these four cases.

- I. Between  $0^\circ$  and  $90^\circ$ ,—The sum by which it exceeds  $0^\circ$  will be the W. longitude of the Morning Terminator.
- II. Between  $360^\circ$  and  $270^\circ$ ,—The sum by which it falls short of  $360^\circ$  will be the E. longitude of the Morning Terminator.
- III. Between  $270^\circ$  and  $180^\circ$ ,—The sum by which it exceeds  $180^\circ$  will be the W. longitude of the Evening Terminator.
- IV. Between  $180^\circ$  and  $90^\circ$ ,—The sum by which it falls short of  $180^\circ$  will be the E. longitude of the Evening Terminator.

*Example 1.* Required the position of the terminator on August 6, 1875, at midnight.

In Table I., opposite 1875, is the angle . . .  $163^\circ 11'$

In Table II., opposite August 6, is the angle . . .  $134^\circ 55'$

Subtracting . . . . . =  $28^\circ 16'$

which comes under Case I. Therefore the Morning Terminator is in  $28^\circ 16'$  W. longitude.

*Example 2.* Required the position of the terminator on January 23, 1872, at midnight.

In Table I., opposite 1871 (it being January),

is the angle . . . . .  $333^\circ 52'$

In Table II., opposite January 23, is the angle  $45^\circ 34'$

Subtracting . . . . . =  $288^\circ 18'$

which comes under Case II. Therefore, as  $360^\circ - 288^\circ 18' = 71^\circ 42'$ , this is the E. longitude of the Morning Terminator.

*Example 3.* Required the position of the terminator on April 30, 1842, midnight.

In Table I., opposite 1842, is the angle . . .  $118^\circ 17'$

In Table II., opposite April 30, is the angle . . .  $17^\circ 30'$

Subtracting . . . . . =  $100^\circ 47'$

which comes under Case IV. Therefore, as  $180^\circ - 100^\circ 47' = 79^\circ 13'$ , this is the E. longitude of the Evening Terminator, or it is a day before New Moon.

If it is required to find the position of the terminator for some time before or after midnight, it is only necessary to make a corresponding alteration in the angle opposite the day in Table II. Thus, for April 30, 9 P.M., the quantity  $17^{\circ} 30'$  opposite April 30 must be diminished by  $\frac{3}{24}$  or  $\frac{1}{8}$  of the difference ( $17^{\circ} 30' - 5^{\circ} 17' = 12^{\circ} 13'$ ) between the values for April 29 and April 30, or nearly  $1^{\circ} 32'$ . It will be, therefore,  $15^{\circ} 58'$ , instead of  $17^{\circ} 30'$ . Without material error, it may be supposed that the terminator travels towards the E. at the rate of  $30' 5$  per hour, and its position computed by adding or subtracting this amount, multiplied by the number of hours it is past or before midnight.

## LUNAR ELEMENTS

Moon's mean apparent diameter, . . .	31' 8".
Moon's maximum apparent diameter, . . .	33' 33".20.
Moon's minimum apparent diameter, . . .	29' 23".65.
Moon's diameter, in miles, . . .	2163 miles.
Volume (earth's = 1), . . .	$\frac{1}{49.20}$ or 0.02033.
Mass (earth's = 1), . . .	$\frac{1}{81.40}$ or 0.0128.
Density (earth's = 1), . . .	$\left\{ \begin{array}{l} 0.60419, \text{ or } 3.444 \text{ the} \\ \text{density of water} \\ \text{(water being unity).} \end{array} \right.$
Surface area, about 14,600,000 square miles (earth's surface area, 196,870,000 miles);	
Earth's surface area = 1, moon's = . . .	About $\frac{2}{37}$ or 0.07407.
Action of gravity at surface, . . .	$\left\{ \begin{array}{l} 0.16489 \text{ or } \frac{1}{6.088} \text{ of the} \\ \text{earth's.} \end{array} \right.$
Surface of moon never seen, . . .	0.4100.
Surface of moon seen at one time or another, . . .	0.5900.
Synodical revolution, or interval from new moon to new moon (commonly called a lunation), . . .	$\left\{ \begin{array}{l} 29\text{d. } 12\text{h. } 44\text{m. } 2.684\text{s.} \\ 29.5305887 \text{ days.} \end{array} \right.$
Sidereal revolution, or time taken in passing from one star to the same star again, . . .	$\left\{ \begin{array}{l} 27\text{d. } 7\text{h. } 43\text{m. } 11.545\text{s.} \\ 27.3216614 \text{ days.} \end{array} \right.$
Tropical revolution, or time taken in passing from "the first point of Aries" to the same point again, . . .	$\left\{ \begin{array}{l} 27\text{d. } 7\text{h. } 43\text{m. } 4.68\text{s.} \\ 27.321582 \text{ days.} \end{array} \right.$
Anomalistic revolution, or time taken in pass- ing from perigee to perigee, . . .	$\left\{ \begin{array}{l} 27\text{d. } 13\text{h. } 18\text{m. } 37.44\text{s.} \\ 27.55460 \text{ days.} \end{array} \right.$
Nodical revolution, or time taken in passing from rising node to rising node, . . .	$\left\{ \begin{array}{l} 27\text{d. } 5\text{h. } 5\text{m. } 35.81\text{s.} \\ 27.21222 \text{ days.} \end{array} \right.$
Distance (mean) in terms of the equatorial radius of the earth, . . .	$\left\{ \begin{array}{l} 60.27. \end{array} \right.$
Distance in miles (mean), . . .	238,840 miles.
Distance, maximum, . . .	252,972 miles.
Distance, minimum, . . .	221,614 miles.
Mean excentricity of moon's orbit, . . .	0.05490807.
Inclination of moon's orbit to the ecliptic (mean), . . .	$\left\{ \begin{array}{l} 5^\circ 8' 39''.96. \end{array} \right.$
Inclination of moon's axis to the ecliptic, . . .	87° 27' 51".
Inclination of moon's equator to the ecliptic, . . .	1° 32' 9".

---

Maximum libration in latitude, .	6° 44'
Maximum libration in longitude,	7° 45'
Maximum total libration from earth's centre,	10° 16'
Maximum diurnal libration, .	1° 1' 28" 8
Angle subtended by one degree of seleno- graphical latitude and longitude at the centre of the moon's disc, when at its mean distance, .	16" 566
Length of a degree under these conditions, .	18 871 miles
Selenographical arc at the centre of the moon's surface, subtending an angle of one second of arc, .	3' 37" 31.
* Miles at the centre of the moon's disc, sub- tending an angle of one second of arc,	1 139.
Period of similar phase.	59d 1h 28m = 2 luna- tions
Or, more accurately,	442d 23h = 15 luna- tions

---

\* It must be remembered that this value is *increased*, in departing from the centre, in the proportion of the secants of the angular distance from the centre



# ALPHABETICAL LIST OF FORMATIONS

ABENEZRA, 147.	Azophi, 147.	Bouguer, 82.
Abulfeda, 145.	Azout, 39.	Boussingault, 133.
Adams, 125.		Bouvard, 122.
Agatharchides, 108.	BABBAGE, 87.	Bradley, Mt., 157.
Agrippa, 56.	Bacon, 151.	Brayley, 79.
Airy, 146.	Bailly, 122.	Briggs, 90.
Albategnius, 144.	Baily, 54.	Buch, 149.
Alexander, 63.	Ball, 99.	Bullialdus, 107.
Alfraganus, 142.	Barocius, 149.	Burckhardt, 44.
Alhazen, 40.	Barrow, 66.	Burg, 53.
Aliacensis, 148.	Bayer, 112.	Büsching, 149.
Almanon, 145.	Beaumont, 136.	Byrgius, 121.
Alpetragius, 94.	Beer, 72.	
Alphonsus, 94.	Behaim, 125.	CABEUS, 105.
Alpine Valley, 64.	Bellot, 129.	Calippus, 62.
Alps, 17.	Bernouilli, 44.	Campanus, 109.
Altai Mts., 19.	Berosus, 40.	Capella, 133.
Anaxagoras, 76.	Berzelius, 45.	Capuanus, 110.
Anaximander, 87.	Bessarion, 78.	Cardanus, 89.
Anaximines, 82.	Bessel, 60.	Carlini, 80.
Ansgarius, 125.	Bettinus, 119.	Carpathian Mts., 18.
Apennines, 17.	Bianchini, 81.	Carrington, 41.
Apianus, 147.	Biela, 132.	Casatus, 113.
Apollonius, 39.	Billy, 114.	Cassini, 62.
Arago, 48.	Biot, 130.	Cassini, J. J., 75.
Aratus, 61.	Birmingham, 75.	Catherina, 135.
Archimedes, 72.	Birt, 97.	Caucasus Mts., 17.
Archytas, 65.	Blanc, Mt., 156.	Cauchy, 48.
Argæus, Mt., 51.	Blancanus, 112.	Cavalerius, 88.
Argelander, 145.	Blanchinus, 146.	Cavendish, 115.
Ariadæus, 55.	Bode, 67.	Cayley, 56.
Aristarchus, 83.	Boguslawsky, 133.	Celsius, 140.
Aristillus, 61.	Bohnenberger, 134.	Censorinus, 133.
Aristoteles, 63.	Bond, G. P., 53.	Cepheus, 46.
Arnold, 54.	Bond, W. C., 66.	Chacornac, 53.
Arzachel, 94.	Bonpland, 96.	Challis, 66.
Atlas, 46.	Borda, 131.	Chevallier, 46.
Autolycus, 61.	Boscovich, 57.	Chladni, 67.

- 
- |                      |                     |                         |
|----------------------|---------------------|-------------------------|
| Christian Mayer, 66. | Encke, 77.          | Gueriké, 95.            |
| Cichus, 110.         | Endymion, 47.       | Guttemberg, 128.        |
| Clairaut, 151.       | Epigenes, 75.       | HADLEY, Mt., 156.       |
| Clausius, 116.       | Eratosthenes, 69.   | Hæmus Mts., 50.         |
| Clavius, 103.        | Euclides, 106.      | Hagecius, 133.          |
| Cleomedes, 43.       | Euctemon, 54.       | Hahn, 40.               |
| Cleostratus, 90.     | Eudoxus, 63.        | Hainzel, 111.           |
| Colombo, 130.        | Euler, 79.          | Halley, 143.            |
| Condamine, 81.       |                     | Hanno, 127.             |
| Condorcet, 39.       | FABRICIUS, 132.     | Hansen, 39.             |
| Conon, 61.           | Faraday, 150.       | Hansteen, 114.          |
| Cook, 130.           | Faye, 146.          | Harbinger Mts., 85.     |
| Copernicus, 70.      | Fermat, 147.        | Harding, 90.            |
| Cordilleras, 20.     | Fernelius, 151.     | Harpalus, 86.           |
| Crozier, 129.        | Firmicus, 39.       | Hase, 126.              |
| Crüger, 121.         | Flammarion, 93.     | Hausen, 122.            |
| Curtius, 152.        | Flamsteed, 113.     | Hecateus, 125.          |
| Cuvier, 151.         | Fontana, 114.       | Heinsius, 101.          |
| Cyrrillus, 135.      | Fontinelle, 75.     | Helicon, 79.            |
| Cysatus, 104.        | Foucault, 86.       | Hell, 99.               |
|                      | Fourier, 116.       | Hercynian Mts., 19.     |
| D'ALEMBERT Mts., 20. | Fracastorius, 137.  | Hercules, 47.           |
| Damoiseau, 119.      | Fra Mauro, 96.      | Herigonius, 106.        |
| Daniell, 53.         | Franklin, 46.       | Hermann, 113.           |
| Davy, 95.            | Fraunhofer, 127.    | Herodotus, 84.          |
| Dawes, 50.           | Furnerius, 127.     | Herschel, 92.           |
| Delambre, 142.       |                     | Herschel, J. F. W., 82. |
| De la Rue, 48.       | GALILEO, 89.        | Herschel, Caroline, 80. |
| Delaunay, 146.       | Gambart, 68.        | Hesiodus, 100.          |
| Delisle, 80.         | Gärtner, 54.        | Hevel, 88.              |
| Deluc, 103.          | Gassendi, 106.      | Hind, 144.              |
| Democritus, 54.      | Gauricus, 100.      | Hippalus, 108.          |
| De Morgan, 55.       | Gauss, 41.          | Hipparchus, 143.        |
| Descartes, 144.      | Gay Lussac, 76.     | Hommel, 141.            |
| De Vico, 116.        | Geber, 146.         | Hooke, 45.              |
| Dionysius, 55.       | Geminus, 44.        | Horrebow, 82.           |
| Diophantus, 79.      | Gemma Frisius, 148. | Horrocks, 143.          |
| Dollond, 144.        | Gérard, 90.         | Hortensius, 77.         |
| Donati, 146.         | Gioja, 76.          | Huggins, 101.           |
| Doppelmayr, 116.     | Goclenius, 129.     | Humboldt Mts., 156.     |
| Dürfel Mts., 20.     | Godin, 56.          | Huygens, Mt., 157.      |
| Drebbel, 117.        | Goldschmidt, 75.    | Hyginus, 58.            |
|                      | Grimaldi, 119.      | Hypatia, 134.           |
| EGEDE, 64.           | Grove, 53.          |                         |
| Eichstädt, 121.      | Gruemberger, 104.   | INGHIRAMI, 122.         |
| Eimmart, 40.         | Gruithuisen, 80.    | Isodorus, 133.          |

- JACOBI, 151.  
 Jansen, 49.  
 Janssen, 132.  
 Julius Cæsar, 56.  
  
 KANT, 137.  
 Kästner, 123.  
 Kepler, 77.  
 Kies, 108.  
 Kinau, 152.  
 Kirch, 73.  
 Kircher, 119.  
 Klaproth, 113.  
 Krafft, 89.  
 Kunowsky, 77.  
  
 LA CAILLE, 146.  
 Lacroix, 117.  
 Lagrange, 121.  
 La Hire, 158.  
 Lalande, 95.  
 Lambert, 78.  
 Landsberg, 105.  
 Langrenus, 123.  
 Lapeyrouse, 124.  
 Lassell, 95.  
 Lavoisier, 90.  
 Lee, 116.  
 Legendre, 125.  
 Le Gentil, 122.  
 Lehmann, 117.  
 Leibnitz Mts., 159.  
 Le Monnier, 52.  
 Letronne, 113.  
 Le Verrier, 78.  
 Lexell, 99.  
 Licetus, 150.  
 Lichtenberg, 90.  
 Lilius, 151.  
 Lindenau, 140.  
 Linné, 60.  
 Littrow, 51.  
 Lockyer, 132.  
 Lohrmann, 87.  
 Longomontanus, 111.  
 Louville, 86.  
  
 Lubbock, 128.  
 Lubiniecky, 107.  
  
 MACLAURIN, 123.  
 Maclear, 49.  
 McClure, 129.  
 Macrobius, 43.  
 Mädler, 136.  
 Magelhaens, 130.  
 Maginus, 102.  
 Main, 66.  
 Mairan, 86.  
 Malapert, 105.  
 Manilius, 60.  
 Manners, 48.  
 Manzinus, 141.  
 Maraldi, 51.  
 Marco Polo, 69.  
 Marinus, 127.  
 Marius, 83.  
 Maskelyne, 48.  
 Mason, 53.  
 Maupertuis, 81.  
 Maurolycus, 149.  
 Maury, 53.  
 Menelaus, 59.  
 Mercator, 109.  
 Mercurius, 41.  
 Mersenius, 114.  
 Messala, 45.  
 Messier, 127.  
 Metius, 132.  
 Meton, 54.  
 Milichius, 77.  
 Miller, 101.  
 Moigno, 54.  
 Moretus, 104.  
 Mösting, 92.  
 Murchison, 67.  
 Mutus, 141.  
  
 NASIREDDIN, 101.  
 Neander, 138.  
 Nearch, 141.  
 Neper, 39.  
 Newcomb, 45.  
 Newton, 104.  
  
 Nicolai, 140.  
 Nicollet, 98.  
 Nonius, 151.  
 North Polar Range,  
     156.  
  
 CENOPIDES, 90.  
 Oersted, 46.  
 Oken, 127.  
 Olbers, 88.  
 Oriani, 40.  
 Orontius, 101.  
  
 PALITZSCH, 126.  
 Pallas, 67.  
 Parrot, 144.  
 Parry, 96.  
 Peirce, 42.  
 Pentland, 152.  
 Percy Mts., 19.  
 Petavius, 125.  
 Peters, 54.  
 Phillips, 125.  
 Philolaus, 82.  
 Phocylides, 117.  
 Piazzzi, 121.  
 Picard, 42.  
 Pico, 157.  
 Piccolomini, 139.  
 Pictet, 101.  
 Pingré, 122.  
 Pitatus, 99.  
 Pitiscus, 141.  
 Piton, 157.  
 Plana, 53.  
 Plato, 73.  
 Playfair, 147.  
 Plinius, 49.  
 Plutarch, 40.  
 Poisson, 148.  
 Polybius, 138.  
 Pons, 139.  
 Pontanus, 148.  
 Pontécoulant, 127.  
 Posidonius, 52.  
 Proclus, 43.  
 Prom. Acherusia, 156.

- Prom. Ananiam, 158  
 Prom Agarum, 156  
 Prom Herachdes, 81  
 Prom. Laplace, 80  
 Protagoras, 66  
 Ptolemæus, 93  
 Purbach, 98  
 Pyrenees Mts, 19  
 Pythagoras, 91  
 Pytheas, 78  
  
 RABBI LEVI, 140  
 Ramsden, 110.  
 Réaumur, 92.  
 Regiomontanus, 98  
 Reichenbach, 131  
 Reiner, 82.  
 Reinhold, 76  
 Repsold, 90  
 Rhæticus, 57  
 Rheita, 131  
 Riccioli, 120  
 Riccius, 140  
 Riphæan Mts, 19  
 Ritter, 54  
 Robinson, 87  
 Rocca, 120  
 Romer, 51.  
 Rook Mts., 20  
 Rosenberger, 133  
 Ross, 49  
 Rosse, 138  
 Rost, 112  
  
 SABINE, 54.  
 Sacrobosco, 146.  
 Santbech, 130  
 Sasserides, 101  
 Saussure, 101.  
 Scheiner, 112  
 Schiaparelli, 85  
 Schickard, 117  
 Schiller, 112  
 Schmidt, 55  
  
 Schomberger, 142  
 Schroter, 68.  
 Schubert, 39  
 Schumacher, 45  
 Scoresby, 66  
 Secchi, 42  
 Segner, 118  
 Seleucus, 89  
 Seneca, 40  
 Sharp, 86  
 Short, 104  
 Shuckburgh, 45.  
 Silberschlag, 57  
 Silberschlag Range,  
     157  
 Simpelius, 152.  
 Sirsalis, 120  
 Smyth, Piazza, 73.  
 Snellius, 131  
 Sommering, 67  
 Sosigenes, 56  
 South, 87  
 Stadius, 69  
 Stag's Horn Mts, 158.  
 Steinheil, 132  
 Stevinus, 131.  
 Stiborius, 139.  
 Stoffer, 150  
 Strabo, 48  
 Straight Range, 18  
 Straight Wall, 97  
 Street, 103.  
 Struve, 41  
 Struve, Otto, 89  
 Sulpicius Gallus, 59.  
  
 TACITUS, 145  
 Tannerus, 141  
 Taquet, 59  
 Taruntius, 42.  
 Taurus Mts, 18  
 Taylor, 143.  
 Teneriffe Mts, 18  
 Thales, 48  
  
 Theætetus, 62  
 Thebit, 96.  
 Theon, sen. 142  
 Theon, jun., 142  
 Theophilus, 134  
 Timæus, 74  
 Timocharis, 73  
 Tobias Mayer, 77  
 Torricelli, 134  
 Tralles, 44  
 Triesnecker, 57  
 Tycho, 102  
  
 UKERT, 59  
 Ulugh Beigh, 90.  
  
 VASCO DE GAMA, 89  
 Vega, 127  
 Vendelinus, 124.  
 Vieta, 115.  
 Vitello, 111  
 Vitruvius, 51.  
 Vlacq, 141  
  
 WALTER, 98  
 Wargentín 118  
 Webb, 123  
 Weigel, 112  
 Werner, 148  
 Whewell, 56  
 Wichmann, 106  
 Wilhelm Humboldt,  
     125.  
 Wilhelm I., 111.  
 Wilson, 119  
 Wolf Mt, 157  
 Wollaston, 85  
 Wrottesley, 126  
 Wurzelbauer, 100  
  
 XENOPHANES, 90.  
  
 ZACH, 152  
 Zagut, 140.  
 Zuchius, 118  
 Zupus, 114



## IMPORTANT NEW ASTRONOMICAL WORK

By SIR ROBERT S. BALL, LL.D., F.R.S.,

LOWNDEAN PROFESSOR OF ASTRONOMY AND GEOMETRY IN THE UNIVERSITY OF  
CAMBRIDGE,

*Author of "The Story of the Heavens," "Starland," "In Starry Realms," &c*

# AN ATLAS OF ASTRONOMY

A SERIES OF SEVENTY-TWO PLATES

WITH INTRODUCTION AND INDEX

---

Small 4to, cloth, gilt edges, price 15s

---

### OPINIONS OF THE PRESS

"The high reputation of Sir Robert Ball, as a writer on Astronomy at once popular and scientific, is in itself a more than sufficient recommendation of his newly published 'Atlas of Astronomy.' The plates are clear and well arranged, and those of them which represent the more striking aspects of the more important of the heavenly bodies are very beautifully executed. The introduction is written with all Sir Robert Ball's well known lucidity and simplicity of exposition, and, altogether, the atlas is admirably adapted to meet the needs and smooth the difficulties of young and inexperienced students of astronomy, as well as materially to assist the researches of those who are more advanced."—*Times*

"These plates, which are large enough to be pre-eminently clear and legible, and yet small enough to make the book a volume of handy size, are fully indexed, and accompanied by an introduction, which thoroughly explains their construction and use. For one commencing the study of the heavenly bodies, the book is so useful as to be practically indispensable, while it will form, at the same time, a very serviceable work of reference to those who have gone so far as to make independent observations. The extent of the Atlas and certain original features give it a place of its own among works of the kind. Long-continued use alone can finally determine the value of such a book as this, but it requires no very close examination to show that it will at once take a foremost place among works of its kind, and will form a valuable acquisition to the library of any student of the stars."—*Scotsman*

"Just as an atlas is the first requisite to the study of geography, so is it to the study of the geography of the heavens, and to meet this very general requirement Sir Robert Ball has prepared an admirable 'Atlas of Astronomy,' which alone, with its clear explanatory details, is a complete introduction to the study of the science. It is convenient in size, but not too small to be clear. . . . Indeed, the whole thing is admirably carried out."—*Graphic*

"Sir Robert Ball has always found time to do very much for the amateur astronomer besides his more serious work, but it is doubtful whether any of the very many of the books which bear his name will rival in popularity and utility the latest. . . . Small in size, it is yet admirable in detail, and so clear, well arranged, and comprehensive, that not only the beginner, but the far more advanced student will find it of extreme value."—*Daily Graphic*

"Sir Robert Stawell Ball, l'un des astronomes anglais contemporains les plus lus et les plus appréciés, vient de publier à Londres un élégant atlas astronomique . . . C'est assurément l'un des atlas les plus complets et les plus utiles qui aient paru jusqu'ici, et nous nous empressons de le signaler aux lecteurs de *L'Astronomie*."—M. C. FLAMMARION in *L'Astronomie*, Paris

"Cannot fail to be exceedingly useful to students and amateurs of astronomy"  
—*Athenæum*.

---

GEORGE PHILIP AND SON, LONDON AND LIVERPOOL

"A marvel of clearness and accuracy."—THE SPEAKER.

## A COMPLETE PHYSICAL AND POLITICAL ATLAS.

EDITED BY

J. SCOTT KELTIE, H. J. MACKINDER, M.A., and E. G. RAVENSTEIN, F.R.G.S.

# PHILIP'S SYSTEMATIC ATLAS.

Containing over 250 Maps and Diagrams in Fifty-two Plates, with an Explanatory Introduction and Complete Index of over 12,000 Names. Imperial 4to, handsomely bound in cloth, or Maps folded in 8vo, price 15s. net.

### CLASSIFIED SUMMARY OF CONTENTS.

	No. of Maps and Diagrams.		No. of Maps and Diagrams.
<b>I. MATHEMATICAL GEOGRAPHY AND ASTRONOMY</b>	13	<b>II. PHYSICAL GEOGRAPHY</b> (con-	
		<i>tinued</i> )—	
<b>I. PHYSICAL GEOGRAPHY—</b>		Geographical Distribution of	
General Maps	7	Plants	12
Contoured Maps	16	Geographical Distribution of	
Sections	10	Animals	17
River Basins	2	<b>III. POLITICAL GEOGRAPHY—</b>	
Geological Maps	4	General Maps	3
Volcanoes	4	Languages and Religion	9
Ocean Currents	5	Density of Population	12
Co-Tidal Lines	2	Parts of Europe	63
Temperature of the Ocean	3	" Asia	13
Salinity of the Sea	1	" Africa	10
Climatology	10	" Australasia and the	
Magnetic Phenomena	3	Pacific	9
		" America	27

#### WHAT WE SAY

1. **The Systematic Atlas** is intended to meet the requirements of those for whom neither the ordinary School Atlas nor the general Reference Atlas is entirely adequate.

2. **Title.**—By the Title which we have given it we claim that, unlike many "New" Atlases, this is not an indiscriminate collection of Maps and fragments of maps which have for years done duty in other Atlases, but that it has been built upon a carefully considered system, and that every Map has been specially constructed to take its place in the general plan.

3. **Scope.**—So far as limits of space would allow, we have endeavored to select all departments of Geography, but more especially of Physical Geography, which is the foundation of every other branch of the subject, and indispensable to a thorough mastery of its Political and Commercial divisions.

4. **British Empire.**—In planning the Atlas care has been taken to give the pre-eminence to those countries and regions specially interesting to British students.

5. **Scale.**—In order to enable a comparison to be made of the areas of different countries, we have largely employed equivalent projections, and have also drawn as many Maps as possible on the same scale or in multiples or sub-multiples of that Scale.

6. **Names.**—The names introduced have been selected with the greatest care; nothing has been left out likely to be wanted by teacher or student. The Spelling adopted has been in the main that recommended by the Royal Geographical Society, and followed by most public departments.

7. **Index.**—A special feature of the Atlas is an Index containing over 12,000 names.

8. **The Introduction** deals with the various projections used in the Atlas which are explained by means of diagrams. Detailed instructions are also given for measuring distances on Maps, together with notes on the physical and political Maps.

9. **The General Idea** which has governed the compilation of this Atlas has been to provide a body of matter so ordered that those contrasts and comparisons which make of Geography a study of high disciplinary value may be easily and clearly demonstrated.

#### WHAT OTHERS SAY

1. **J. M. D. MEIKLEJOHN, M.A.**, Professor of the Theory, History, and Practice of Education in the University of St. Andrews.—"It is in every respect an admirable work. It possesses all the best features of the best German and French Atlases. The clearness and beauty of the get-up speak for themselves."

2. **THE DAILY TELEGRAPH.**—"Prepared on a carefully considered system."

3. **A. W. CLAYDEN, M.A., F.G.S.**, Principal of the Exeter Technical and University Extension College.—"Admirable both in design and in execution; while, considering the amount of information it contains, it is remarkably cheap."

4. **The Right Hon. JAMES BRYCE, D.C.L.**—"Extremely well planned and worked out."

5. **C. R. MARKHAM, Esq., C.B., F.R.S.**, President of the Royal Geographical Society.—"Arranged with very great care and ability, and admirably executed."

6. **THE ATHENÆUM.**—"Mr. Ravenstein has compressed a wonderful amount of information into the fifty-two plates of his Atlas. The Spelling of the names themselves seems faultless, and we have failed to find any flaw in the index."

7. **THE STANDARD.**—"Special attention appears to have been given to the geographical aspects of Politics and Commerce, and the value of the Atlas as a practical work of reference is increased by a clear and well-arranged index of twelve thousand places."

8. **Dr. H. R. MILL, F.R.S.E.**, Librarian Royal Geographical Society.—"The Physical Maps are remarkably clear, and the letterpress contains information which I have never before seen in a connected form, or in any form so clearly and concisely put."

9. **THE OBSERVER.**—"It required a certain amount of courage to plan an Atlas which should be reasonable in price and, at the same time, should contain no old work. The Atlas is what it purports to be—a serious contribution to the efforts which are being made to raise Geography from its low estate."

*A Sheet showing Specimen Map of the Atlas, printed in Colours, together with a Detailed List of the Maps, sent Gratis on Application.*

GEORGE PHILIP AND SON, LONDON AND LIVERPOOL.

Aligned groups of such cones in the Jordan Valley volcanics, Oregon and at Lakagígur, south central Iceland, are shown in Figs. 16 and 17, respectively. These crater alignments are similar to those on the Moon particularly



FIG. 16. Spatter cone alignment, Jordan Valley.

in the relationship of an alignment of small craters to a large one. Figure 18 illustrates the relationship of crater alignments *tangential* to a parent crater. In the Ludent crater area in Iceland, and in many other places on Earth, this relationship is quite normal inasmuch as volcanic craters and calderas are localized by fractures which are often tangential to the crater outline. In other words, fractures often serve to define a polygonal plate which is subsequently engulfed or otherwise fragmented by volcanic activity. The fractures may subsequently provide zones of weakness along which extrusives may issue.

Thus, a fracture that formed the boundary of a large crater could also provide a locus for an alignment of smaller craters which would be tangential to the parent. An excellent example on the Moon is the crater row forming



the boundary of Müller and extending into the northern segment of the walled plain Ptolemaeus. The tangential alignment of craters on the Moon is a feature in strong support of the volcanic origin of the lunar surface and the attendant terrain and mineralization advantages. For a review of lunar crater alignments see Boneff [15-18].



FIG. 17. Crater cone alignment in Lakagígar.

The most important groups of surface structures that might serve as natural installation sites on the lunar maria are lava tubes and caves. Figure 19(a) illustrates a classic example of a cave in basaltic lava in the Dimmuborgir region of Iceland. The cave diameter is 5 m. The roof of this cave is not excessively fractured (Fig. 19b) and could easily be sealed. One such sealant might be a natural waterless cement sulfur. Sulfur is the most abundant volcanic sublimate. Granting an adequate power and gas source, the plasmatron might also be used in vacuum to spray molten rock to fill fractures in natural rock cavities. Caves and lava tubes could thus be used as pressurized chambers which would afford protection against micro-meteorites and temperature, pressure and radiation extremes.

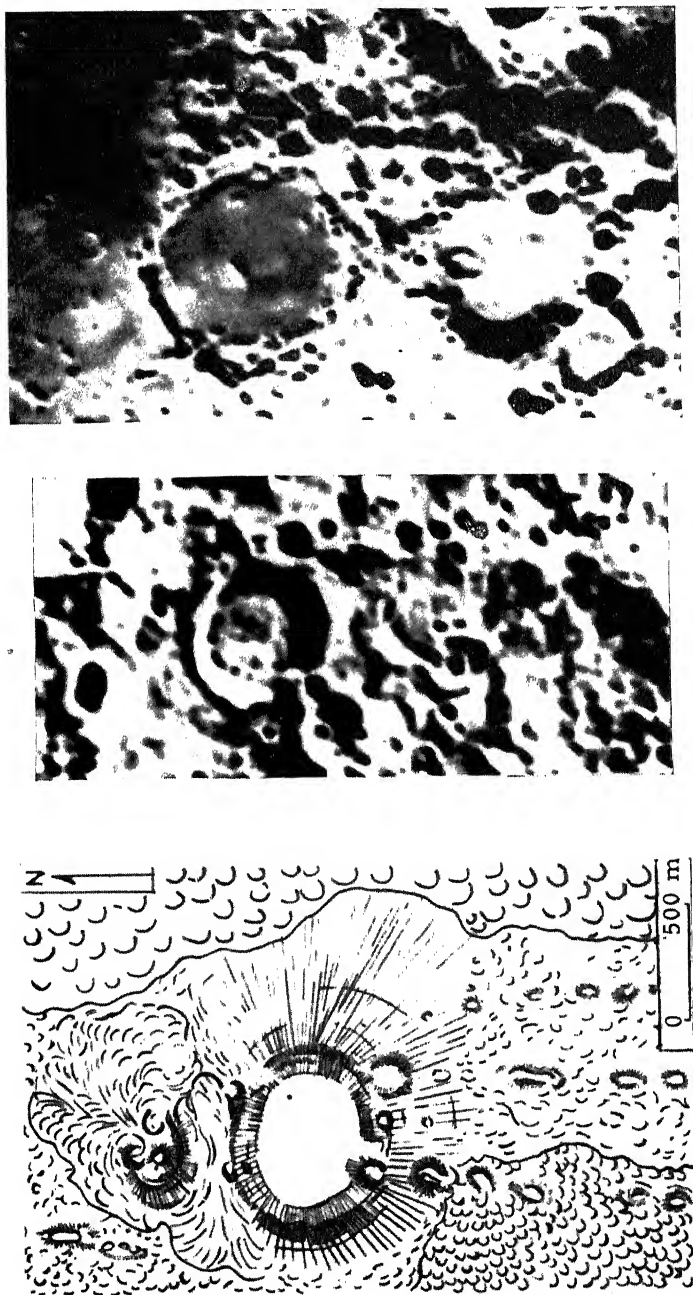


FIG. 18. Comparison of tangential crater alignments on Earth and on the Moon. (a) Iceland (volcanic crater), (b) Albufeda, (c) Pitatus. Courtesy of Dr. S. Thorarinsson.



FIG. 19(a). Basaltic lava cave, Dimmuborgir region of Iceland.

The most imposing features of the non-mare areas are the craters, clefts and valleys. Each of these offers terrain benefits in varying degrees of significance depending on their method of origin. Even if only a small proportion of lunar craters are found to be volcanic, it is still of high importance to seek them out. Features observed in and around lunar craters, which are suggestive of a volcanic origin, are given in Table 3.

The use of high-resolution altitude television scanning techniques will undoubtedly resolve many of the questions regarding lunar craters. For example, the fusion area of lunar craters deserves more scrutiny. Similar features in the Nejapa area, Nicaragua, have been studied by McBirney [19]. The fracture pattern in controlling crater distribution may also be defined by an altitude television survey. On Earth these patterns aid in regional interpretations of, say, distribution of calderas or in local tectonic analyses of arrangements of spatter cones within calderas [20-23].

Other features deserving study include the mud volcanoes that are secondary phenomena of solfataras [24], radiating dikes and ring fissures [25], certain odd-shaped pit craters [26], lava deltas [27], and flow patterns of nuées ardentes [28]. Details of morphology of a polygenetic volcano, such

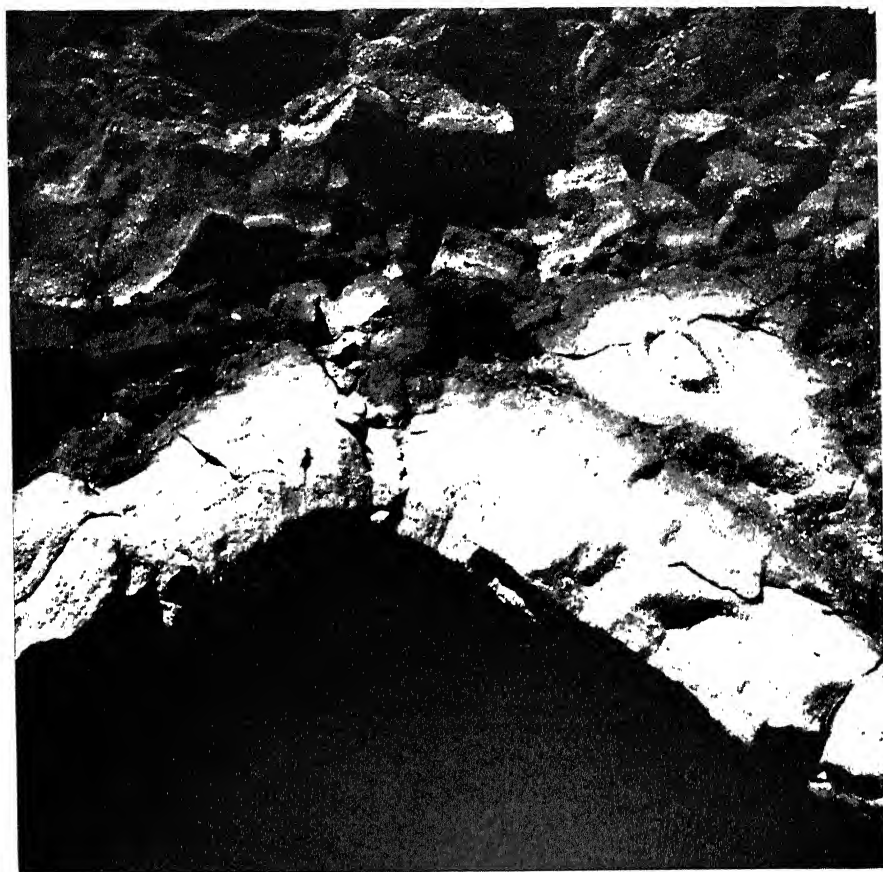
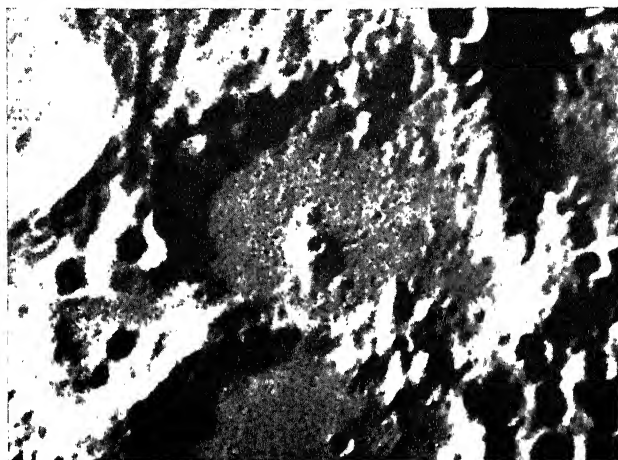


FIG. 19(b). Detail of cave roof.

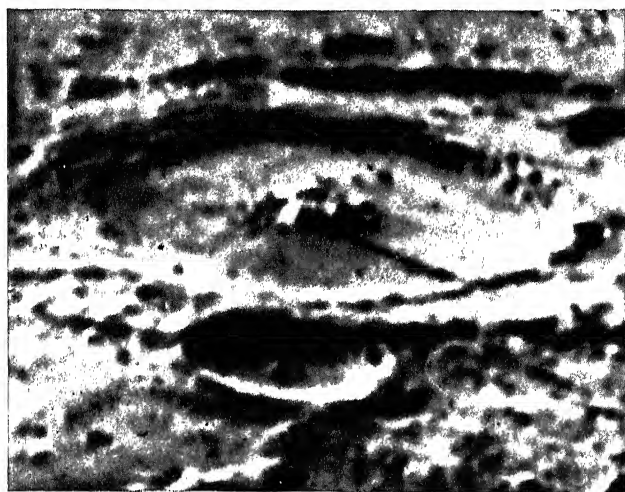
TABLE 3. Caldera Features Found in Lunar Craters

<i>Feature</i>	<i>Number observed</i>
Polygonal shape	25
Central mountain	234
Central crater	43
Median ridge	26
Pressure ridge	48
Dark floor	32
Rim "dikes" and radiating structures	20
Internal faulting (incl. terracing)	250
Breaching	40
Lava infilling	19
Changes (e.g. mist, lava flow, eruption)	15
Alignments	180†

† Each entry includes alignment of many craters.

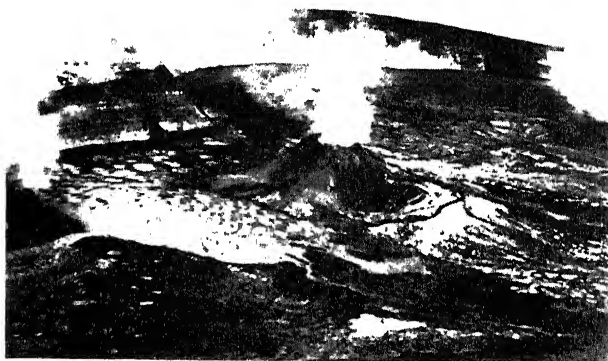


(a)



(b)

FIG. 20. Morphological features of mountains in lunar craters compared with volcanoes in terrestrial calderas. (a) Noncentral mountain in Regiomontanus A (Photo courtesy of Dr. Z. Kopal, Pic-du-Midi Observatory). (b) Central mountain in Petavius (Photo courtesy of Dr. A. Dollfus, Pic-du-Midi Observatory).



(c)



(d)

FIG. 20. (c) Noncentral cinder cone of Mokuaweoweo Caldera, Hawaii in 1940 (Photo courtesy of *National Geographic Magazine*). (d) Central mountain, Awoe Caldera, Java (Photo courtesy of Dr. R. W. van Bemmelen).

as Shiveluch in Kamchatka, are most germane in defining volcanic forms on the Moon [29].

Central volcanoes in calderas also have specific features potentially identifiable by a television surface survey. Baldwin ([30], p. 147) states that lunar central mountains do not look like volcanoes within calderas; however, such is not the case. The lunar central mountains are not always central, as illustrated by Regiomontanus A in Fig. 20. In addition, the shapes of the central mountain within lunar craters range from the crisp centrally pitted volcano-like mountains (also demonstrated in Regiomontanus A) to the irregular non-descript accumulations in craters such as Petavius. This range in form is duplicated on Earth within calderas (Fig. 20). With the variety of rock types in volcanic terrains, the complexity of fracture patterns and the variables involved in volcanic activity, this range in size, shape and disposition is quite normal.

Studies of central cones in the Aso crater, Japan, show them to be of two types: (1) distorted diamond shaped, presumed to have been formed in an early period of activity; and (2) elliptical, formed in a later period of activity. Another Japanese volcano, Ō-Shima, warrants study in the light of future surface examination of the Moon. Within the main caldera of Ō-Shima are numerous cones and craters arranged roughly in three narrow zones radiating from the center of the main body to the north-west. This geometry is similar to that of Cleomedes on the Moon.

Terracing can conceivably be characteristic of both impact and volcanic crater types, although the horizontally floored terraces are good arguments for lava withdrawal processes rather than gravity slump of impact blocks. Photographic evidence of lava draining back into a parent fissure [31] stresses the validity of the magma withdrawal processes at depth. Escher [32] believes that the multiple concentric rim seen in terrestrial calderas is a key volcanic feature in lunar craters.

Finally, the ratios of crater depth to width, the central peak height to crater depth, and the central peak height to crater width would do much to support or refute the Baldwin approach to problems involving origin of lunar craters [30, 33]. Data plotted for these parameters from telescopic observational data are ambiguous. The scatter of points may represent (1) later volcanism in earlier formed calderas, which would tend to shallow them; or (2) unreliable lunar altitude data, which mask a diameter depth relationship indicative of the impact mechanism of origin.

In the field of tectonics, present astronomic resolution cannot define the discrete fracture patterns that conceivably may bound many lunar craters. However, lunar surface television scanning could possibly provide this structural detail, which could be compared with the structural geology of terrestrial calderas. For example, the main volcanic vents of the Azores on Earth, including the Aqua-de-Pau on San Miguel, Cino Picos on Terceira, and Fayal, are calderas which lie in the center of a spiderweb fracture pattern formed by the combination of radial and concentric features [20]. There is a suggestion of radial and concentric features surrounding many lunar craters, and the pattern is certainly present on the borders of most maria [34].

Tectonic activity could have produced the lunar rays. Recent horizontal movement could expose silicic ash in a tangential or radial pattern to craters. Structural movements along zones of weakness could also incur volcanic

activity along these zones which would produce linear and discontinuous ash deposits. The kinetics of ash formation on the Moon may be quite different from those on Earth in view of the difference in depth and rapidity of bubble nucleation. Verhoogen [35] has stressed this point in explaining the differences in terrestrial volcanic ash formation. Natural barriers such as pressure ridges would also control the distribution of volcanic ash possibly produced by lunar craters as first elaborated on by Spurr [36]. Rays composed of debris ejected over tremendous distances by impact, and yet coincident with the statistically abundant on-ray craters, are difficult to understand. Surface television scanning of rays would do much to determine their origin.

The question of folded mountain systems versus block faulted ranges [37, 38] could possibly be resolved by lunar altitude television techniques. High-resolution altitude surveying may also be applied to differentiating meteor gouge valleys from rift valleys associated with volcanic apparatuses [39]. Probably the presence of rhyolite domes, as exemplified by the Hlidarfjall dome in Iceland, could be verified by high-resolution surveys.

Again in these non-mare surface features, natural protection against the elements would be provided by overhangs and caves associated with at least five structures: (1) central cones within calderas; (2) pressure ridges on caldera floors; (3) major and minor faults attending localization of calderas; and (4) the major rift systems such as the Hyginus, the Triesnecker or the Sirsalis.

#### METEORITIC TERRAIN FEATURES

On the other hand, a terrain that has been impacted shows none of the features discussed above. Figure 21 of the Meteor Crater, Arizona, illustrates the flat floor typical of all terrestrial meteor craters and the absence of

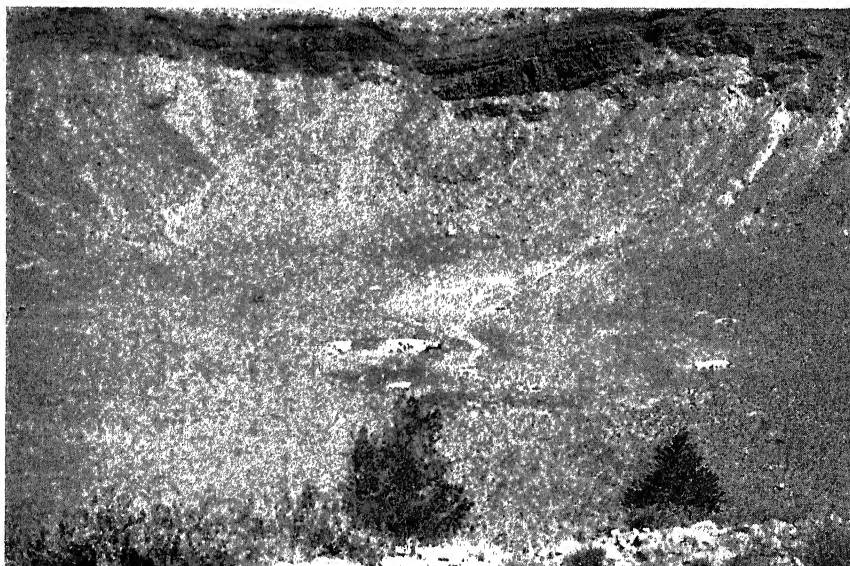


FIG. 21. Interior view of Meteor Crater, Arizona.



terracing. Radial or tangential features are absent. There are no large fissures or spatter cones available for installation sites in impact craters.

However, steep dips and overturns of sedimentary strata bordering Meteor Crater provide natural overhangs (Fig. 22) which if developed on the Moon would be useful against radiation and micrometeorite infall. Large rubble blocks ejected during impact could also provide this protection. Erosional processes have removed most of the large blocks at Meteor Crater. A thorough treatment of the geology of this terrestrial impact crater is given by Shoemaker [40].

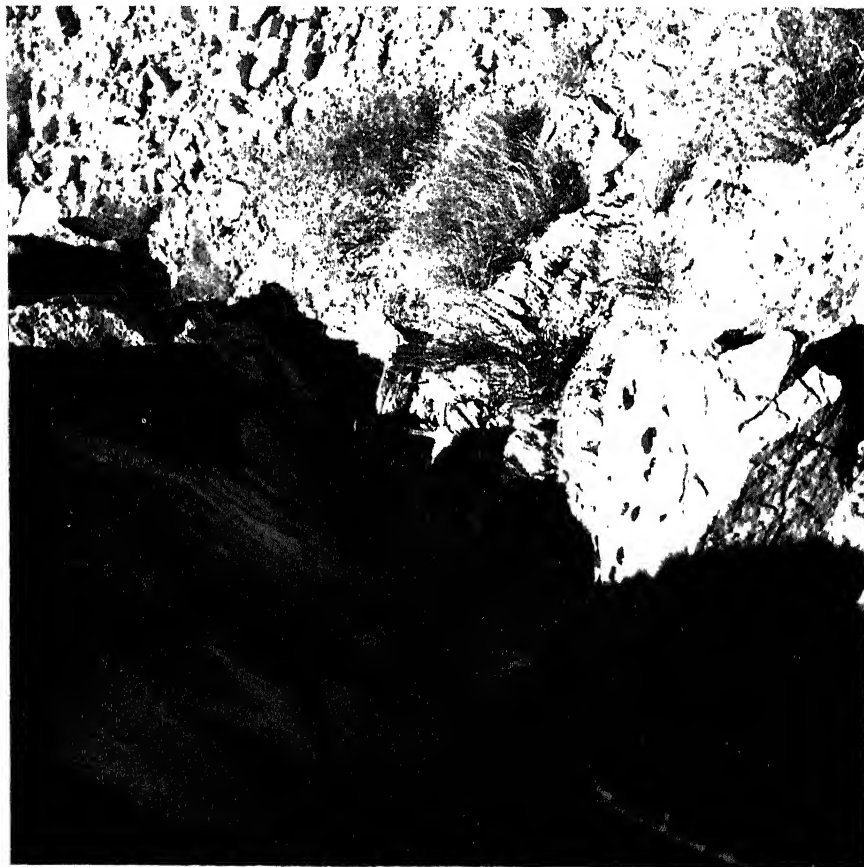


FIG. 22. Steep dips in rim sediments produced by impact of Meteor Crater, Arizona.

Caution must be exercised in appealing to the lunar surface television scan to solve unambiguously the volcanic versus impact mechanisms of origin. In Fig. 21, for example, an internal view of Meteor Crater, while admittedly lacking the internal morphology of a caldera, also fails to disclose the rim reversal of strata and peripheral breccia zones that can only be observed by "high resolution" inspection [40].

## ROCKS AND DUST

## (A) INFALL AND VOLCANIC DUST

Polarization studies by Wright [41] verified that the surface of the lunar maria is covered with dust. However, various estimates of the depth of this dust layer have been proposed. In a model based on the radio-astronomy techniques of Dicke and Beringer [42] and others, a thin dust layer is assumed. Whipple ([43], p. 270) assumes the covering to be less than a few meters thick.

On the other hand, Gold [44], Gilvarry [45] and Wesselink [46] favor a very thick dust layer. Gold explains the smooth maria surface by an erosion process that creates dust in the highlands, coupled with a transport mechanism which deposits it in the lower maria. As possible physical agents for dust transport, Gold suggests an evaporation-condensation cycle, electrostatic forces, and, in particular, bombardment by meteorites and micrometeorites. The latter mechanism was advocated by See [47]. Metallic, stony and icy meteorites producing this dust would provide a type of erosion not found on Earth. The amount of such erosion of the Moon is as yet unknown.

Gold further suggests that the dark color of the maria surface is due to damage by solar X-ray, ultraviolet, and corpuscular radiation. He attributes the light color of the lunar highlands to continual denudation.

Because no polar homogenization of lunar surface details can be demonstrated, however, the concept of a thin dust layer appears more reasonable. Impact dust would presumably be rich in iron-nickel, similar to the particulate matter dredged from the ocean floor or pulverized chondritic material. Such iron-rich cosmic infall material could be used in smelting operations to make conductors, castings and structural components for a lunar base.

Proponents of lunar volcanism contend that varying quantities of dust would be produced by volcanoes. This is because of the sustained evolution of dust during the eruption cycle which often varies in duration. The amount of dust resulting from impact would probably be less by comparison.

In the absence of a lunar atmosphere, layering of any type of dust would be more poorly defined than on Earth because both coarse and fine material would settle equally as fast. Marked heterogeneity would be common in accumulations of both pyroclastics or meteoritic rubble. However, if volcanism were the dominant source of lunar ejectamenta, intercalations of fine ash and dust would be formed during those periods when only this ash or dust was being expelled from volcanic vents. Therefore, from the recurrence and periodicity of volcanism within a given caldera, volcanic strata could be distinguished from impact rubble strata. Because of the absence of erosional processes in the vicinity of lunar craters a higher degree of continuity of either impact or volcanic strata should be evidenced in these areas.

Local accumulation of thick dust layers is possible in the non-mare areas according to the volcanic theory. Such accumulations are common on Earth, for example at Parícutin, Mexico (Fig. 23). Thin dust layers, thickening in topographic basins near post-mare craters, are predicted for mare areas. In explaining either the impact or volcanic hypothesis, the author assumes that the maria are basaltic. The impact mechanism of crater origin would produce a thicker dust layer on the crater floor than on the crater flank, which is quite the opposite effect in volcanism. Again, the maria would have a thinner dust cover if basaltic rocks were formed by melting of

impacted material. However, creation of basalt by impact melting cannot be demonstrated on Earth.

Finally, temperature cycling from 134 to  $-150^{\circ}\text{C}$  would produce surface dust from exposed rocks by spallation processes. The spallation mechanism is self-limiting, and consequently this also requires that the dust layer be thin.

The use of this volcanic dust in various technological processes will be detailed in a later section.

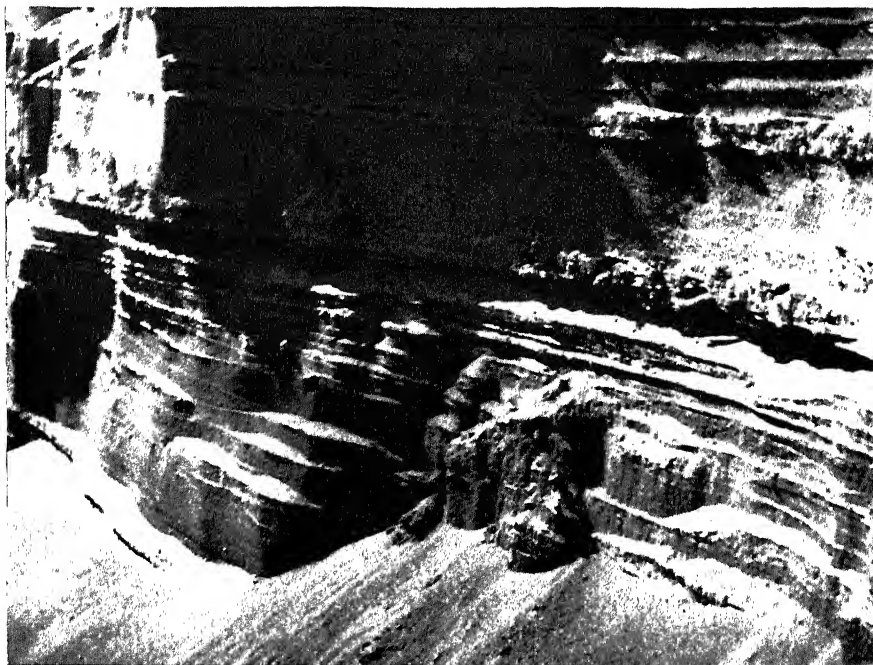


FIG. 23. Detail of basaltic dust, ash, and lapilli layering, Parícutin, Mexico.

### (B) VOLCANIC ROCKS

Many volcanologists believe the black portions of the Moon are basaltic and the white portions are silicic. The specific rock names ultimately to be applied to these great areas on the Moon will undoubtedly be many. Basaltic rocks could include basalt, tholeiite, diabase, dolerite, tephrite, basanite, and tachylite; the particular name assigned would depend on mineralogy and texture. They are, in general, fine-grained, dark-colored rocks, poor or lacking in quartz, rich in calcic plagioclase feldspar and with varying amounts of olivine, pyroxene and, in some varieties, feldspathoids.

Silicic extrusive rocks would be named in a similar manner; a simplified classification of these light-colored, fine-grained rocks being as follows:

	<i>Much quartz    Minor quartz</i>	
K feldspars abundant:	rhyolite	trachyte
Ca feldspars abundant:	dacite	andesite

Photometric and spectrophotometric studies by Barabashev and Chekirda [48] indicate that pyroclastics and other volcanic rocks make up the lunar surface. The lunar spectra were compared with those from terrestrial rocks. Comparisons were made relative to (1) brightness of integral light, (2) reflection coefficients for different regions of the spectrum, (3) the energy distribution on the spectrum, (4) a "smoothness" factor, (5) variation of the degree of polarization as a function of the angle of incidence and reflection and phase angles, and (6) thermal conductivity. Additional comparisons were made with terrestrial rocks of varying grain size which were irradiated by ultraviolet rays, X-rays and protons in vacuum and fused at atmospheric pressure and vacuum.

Certain volcanic rocks tested by Ahrens, *et al.* and reported in Brun-schwig *et al.* [49] have relative permittivities (dielectric constants) approaching those obtained for the lunar surface based on electromagnetic surveys conducted by the University of Michigan Radiation Laboratory. The relative permittivity of the lunar surface is found to be 1.08; that of rhyolitic pumice from Millard County, Utah, is 2.29. This value is the lowest recorded by Brun-schwig *et al.* ([49], p. 56) and is much lower than values obtained for meteorites.

The volcanic nature of the lunar rocks has been upheld by volcanologists for decades. The appeal to mechanisms such as electrostatic winds, which have no counterpart on Earth—but even more critical, the frequent neglect of generally operative geological processes that do occur on Earth—is difficult to understand. Production of basalt by passive extrusion through fractures created by internal stresses can be demonstrated for almost all basalt basins on Earth. Spurr [36] wished to create the lunar maria by the wholesale foundering of a portion of silicic crust in a basaltic substratum. However, many other volcanologists, including von Wolff and Bülow, propose the formation of the lunar maria by upwelling of basalt through fissure and fracture systems that localize the mare basins.

The lunar maria are assumed to be basaltic or a variety of basalt, because it is the most abundant dark-colored volcanic extrusive on Earth. Moreover, basaltic lava is among the most fluid of rock-melts. The viscosity approximates 100 poises at 1300° C. However, the flow mechanism is usually non-uniform. A single lava flow may consist of several flow units, and lava may flow in a series of spurts rather than at a constant velocity ([50], p. 315). A few hours or days after the lava front ceases to move and is consolidated, more liquid from the same flow may bury the lava that has already stopped. This process may be repeated several times and what is called a "single" eruption is actually composed of several flow units [51].

Individual flows may differ greatly in size. Some are only a few meters thick, and flows more than 90 m thick are rare. For example, the average thickness of lava flows in the Columbia Plateau of north-western United States is probably less than 15 m; in India, basaltic flows average less than 18 m; and in Iceland, the average flow is 4 to 9 m thick. The area may be a few acres or many square miles. In Iceland, single flows covering more than 259 square kilometers are known, and one flow is said to encompass 1040 square kilometers.

One of the paradoxes of volcanic phenomena is the diversity of products resulting from the consolidation of a megascopically uniform lava. Two distinctive forms, known by their Hawaiian names as pahoehoe and aa

(Figs. 24 and 25), are important to consider from the standpoint of lunar vehicle landings. The most obvious characteristics of pahoehoe lava are a low gas content, high viscosity and surface continuity (when solidified). The aa lava has a high gas content, low viscosity, mobility and a broken surface (when solidified).

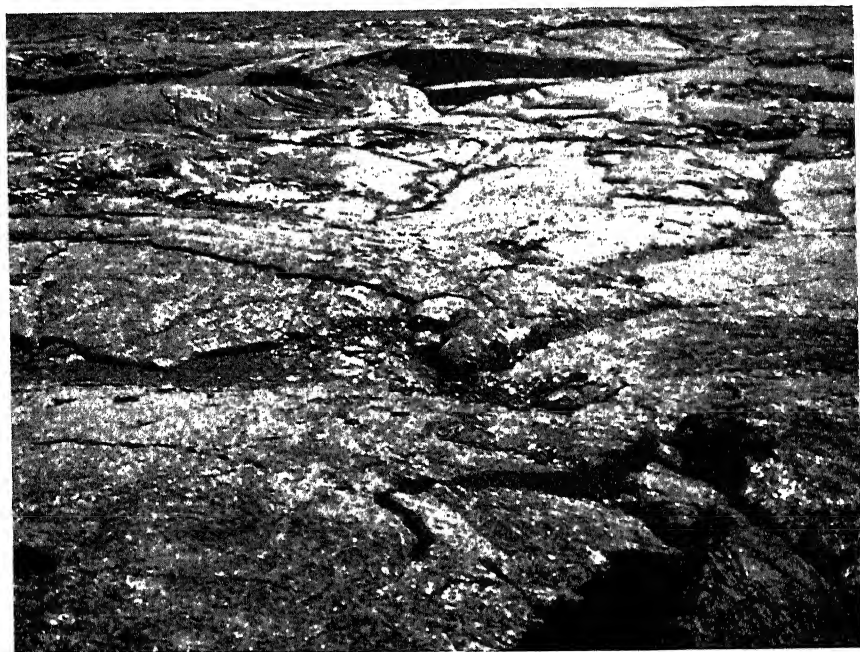


FIG. 24. Pahoehoe lava, Jordan Valley.

The term "surface continuity" does not mean flatness, but rather a continuously overfolded globular, ropy or flat formation which prevents radiation from the hot interior and maintains its fluidity. A flat level area may result from laking and crusting. In cross-section, the pahoehoe crust tends to have a three-fold structure: (1) an upper vitreous surface layer resulting from rapid cooling; (2) a crystalline layer below this; and (3) in areas of subsequent subsurface drainage, a stalactitic lower zone. Sometimes the pahoehoe lava presents a fractured mosaic surface such as that in the Vesuvius area ([52], p. 50).

The characteristic features of aa lava are its greater fluidity and lower temperature. These two factors promote the crystallization of rock-forming minerals. Feldspar, mostly labradorite, crystallizes out first and enriches the melt in more mafic constituents. This tends to increase further the fluidity of the lava. The increased fluidity promotes internal molecular mobility, inducing even more crystallization. The production of crystals provides nuclei for the formation of bubbles. The bubbles tend to coalesce at the angular corners and points of crystals, thus creating large vesicles typical of lava. Pahoehoe lava, on the other hand, is not characterized by feldspar or augite phenocrysts; it is more glassy. This characteristic is confirmed by

thin-section petrography, a higher ferrous/ferrie ratio, and a lower density than the more crystalline aa lava.

A second factor favoring the high fluidity of aa lava is its slower cooling rate. This effect is produced by the increase in temperature due to the latent heat of crystallization of mineral phases. The increase of temperature thus produced tends to diminish the slope of the cooling gradient ([53], p. 402).

The very generation of a crystalline phase increases the relative concentration of the gas phase which promotes a low matrix viscosity of the crystallized aa blocks. These conclusions are supported by field observations. The high gas content of aa lava produces a flow similar to a "moving stone wall" accompanied by loud roaring and hissing sounds. Numerous flames play on the advancing front and top surfaces; noxious fumes are also present. On the other hand, pahoehoe although it is fairly fluid on extrusion, increases in viscosity rapidly with increasing distance of flow.

If pahoehoe lava contains much gas other than that in tiny vesicles, the gas will emerge, agitate the lava liquid and prevent the formation of the

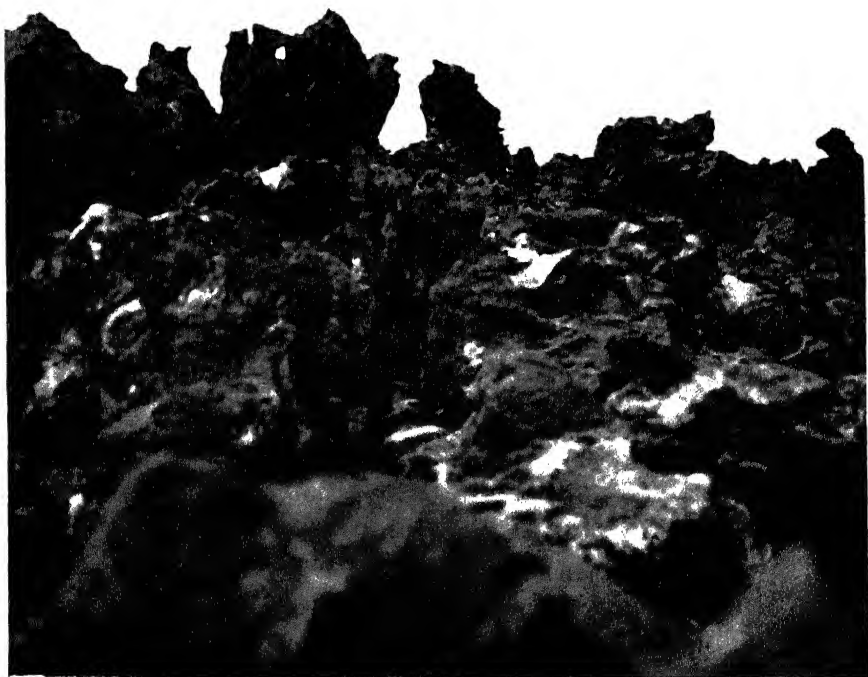


FIG. 25. Andesitic aa lava field, San Benedicto Island, Pacific Ocean.

typical pahoehoe skin (Fig. 26). For example, during the July 1911 lava eruption in Halemaumau, Hawaii, gases escaped in lava fountains, resulting in gas-impooverished lavas so that pahoehoe surface structures were formed. On the other hand, gas-charged lava at Vesuvius produced aa lava. The rapid supply and escape of gas from such a lava enhance exothermic crystallization and produce rigid blocks, even though the lava stream moves quickly.



FIG. 26. Ropy surface typical of pahoehoe lava near Herdubreidarlindir, central Iceland.

If the great expanse of dark-colored rock on the Moon is basaltic, it might indicate a lava of high fluidity typical of the blocky aa type. The variation of external temperatures would probably influence cooling rates only to a trivial degree. However, frothing would be enhanced by the lesser gravity and external vacuum.

Chemical composition does not appear to influence the texture of lava because pahoehoe forms easily from ultramafic Hawaiian lavas. From mafic Vesuvian lavas, it forms less easily but nevertheless does form. It is even

produced in the more viscous basalts of Etna and in the andesites of Sakurashima. Two other features of aa lava include a central core that remains intact until the lava mass disintegrates on cooling and a greater topographic elevation as compared with pahoehoe ([52], p. 54).

#### (C) ROCK FROTHS

Inasmuch as extrusion of a silicate into vacuum would tend to produce surficial high gas activity, the blocky, rough surface aa lava may possibly represent the more dominant form of surface lava on the Moon. A larger vesicle size and a general dominance of rock froths in and on the aa lava flows are also considered more likely on the Moon. This is because molten silicates intumescence and become frothy when extruded into a vacuum. "On the moon, with an essential vacuum at the surface, the unit bubbles of the escaping gases would be greatly inflated and enlarged, so that the mare surface would be honeycombed on a scale foreign to our experience; thus the absorption or lack of reflection of sunlight becomes clearer." ([36], I, p. 258.)

Rock froths would be common products of such explosive eruptions. They can produce either in the laboratory or in the field by extrusion of gas-charged melts into environments of low pressure. It is believed that the vesicle size of rock froths on the Moon would be a function of the amount of gas present in the lava, the lesser gravity, and the viscosity of the lava at the temperature of chilling. Consideration of all these factors leads to a prediction of a much greater abundance of rock froths on the lunar surface than on Earth and a larger vesicle size in any given extrusive.

The crushing strengths of rock froths are poorly documented in the literature. An average crushing strength for pumice is  $140 \text{ kg/cm}^2$ , but the range varies from 14 to  $840 \text{ kg/cm}^2$ . Lunar silicic froths may have very low strengths. One must bear in mind, however, that a mass which exerts, say,  $14 \text{ kg/cm}^2$  on Earth will be six times heavier to exert this same force on the Moon. The crushing strength for basalt ranges from 1250 to  $3100 \text{ kg/cm}^2$ . Thus, 18 000 psi may be a more realistic value for lunar scoriae. Certain types of scoria (Fig. 27), such as threadlace scoria or reticulite, may have crushing strengths below  $10.5 \text{ kg/cm}^2$ . Hence, we may be faced with a paradox that, for certain areas on the Moon, the shear strength of the rock froth layer may be less than the dust layer overlaying it.

Rock froths could be utilized as insulation and as a possible source of atmospheric gases. Because of their cellular structure, they may be easily worked to provide building or cap materials for installation sites. Their extremely high porosity, which can exceed 25%, may supply a source of nitrogen or carbon dioxide by simple mechanical crushing of these rocks. As mentioned above, their crushing strengths are low. Gas extraction for the manufacture of an artificial atmosphere is qualitatively simpler than the dissociation of the bulk rock into cations and anions using high-energy and fluid-consuming techniques such as the plasma flame provides.

#### (D) CAST BASALT

The use of basalt in the Czechoslovak Glass Institute at Hradec Králové has been the subject of several recent publications. Voldán [54] cites the use of specific basalt types, particularly the pyroxene-rich varieties, in the manufacture of structural components—even pipes and castings (Fig. 28). The technology of casting basalt has been summarized by Vlček [55]. Basalt



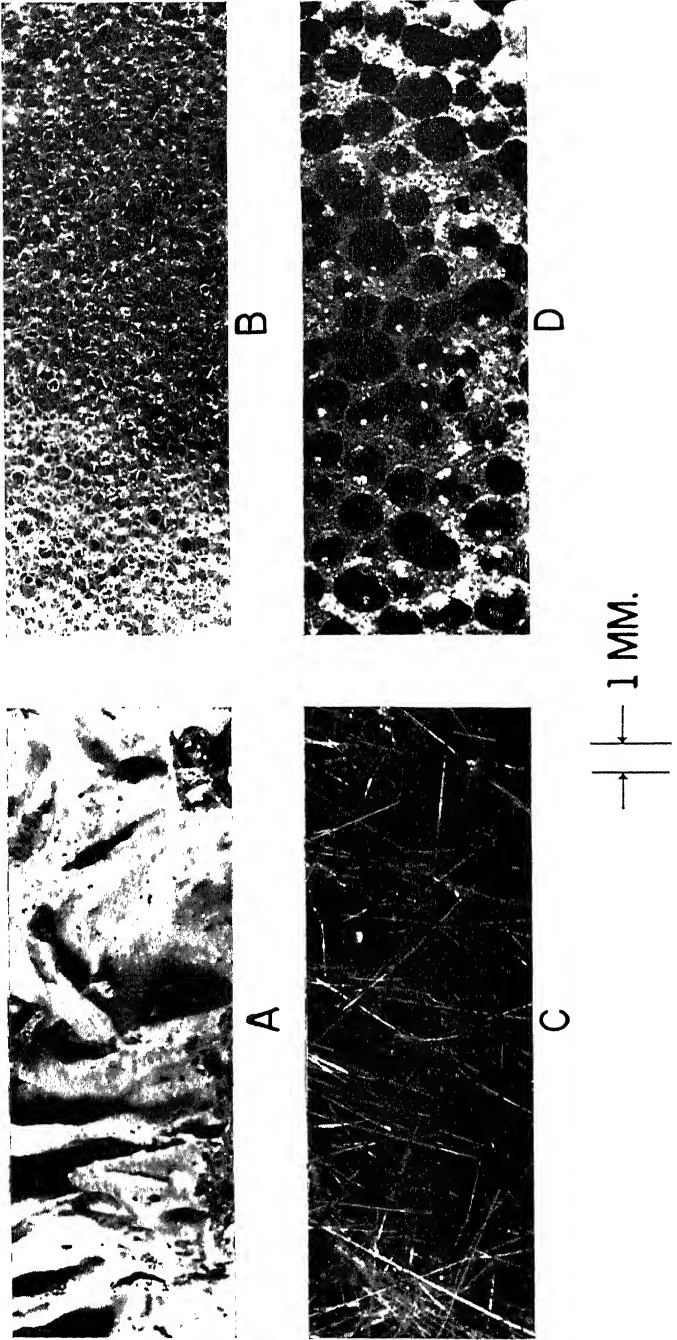


FIG. 27. Basaltic rock froths.



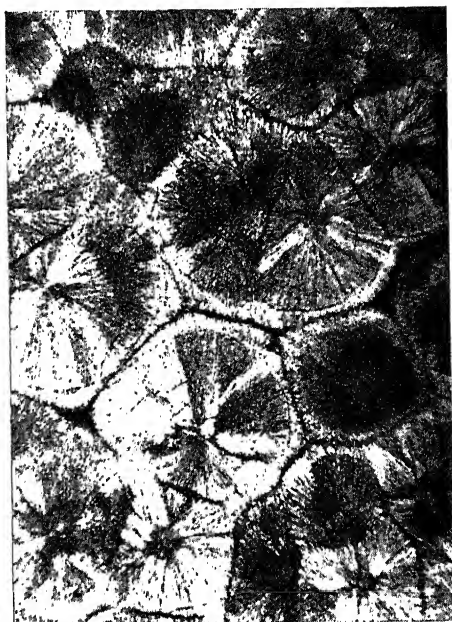
(c)



(d)



(a)



(b)

FIG. 28. Cast Basalt. (a) Columnar basalt, Kamenický Šenov, Bohemia, used as raw material. (b) Recrystallized cast basalt. Radiating pyroxene crystals in a matrix of magnetite pigmented glass. (c) Cast basalt pipes and tiles. (d) Cast basalt sorting bar.

aggregate, 8 to 15 mm mesh, is used as raw material. This is melted at 1300 to 1350° C in shaft furnaces fired with producer gas, similar to the open-hearth furnaces commonly used in steel works. The molten material is then channeled into a homogenizer drum. Here, with slightly reduced and controlled temperature, crystallization begins. The casting process which follows is similar to that used in metallurgical production, with certain differences required by the greater viscosity of the material and the need to prevent vitreous solidification.

Centrifugal casting of basalt in metal molds rotating at speeds up to 900 rpm has resulted in products of superior quality. Pipes, milling balls, mill linings, and other articles requiring high density may be produced by this method. The chief valuable quality of cast basalt is its outstanding resistance to abrasion. A synopsis of the proposed National Standard for cast basalt in Czechoslovakia is presented in Table 4.

TABLE 4. Czechoslovak Proposed National Standard for Cast Basalt†

<i>Oxide</i>	<i>Chemical analysis (%)</i>	<i>Oxide</i>	<i>Chemical analysis (%)</i>
SiO <sub>2</sub>	43.5–47.0	MnO	0.2–0.3
TiO <sub>2</sub>	2.0–3.0	CaO	10.0–12.0
Al <sub>2</sub> O <sub>3</sub>	11.0–13.0	Na <sub>2</sub> O	2.0–3.0
Fe <sub>2</sub> O <sub>3</sub>	4.0–7.0	K <sub>2</sub> O	2.0–3.0
FeO	0.5–8.0	H <sub>2</sub> O	1.0–2.0
MgO	8.0–11.0	P <sub>2</sub> O <sub>5</sub>	0.5–1.0

<i>Physical property of statistically or dynamically made crystallized castings</i>	<i>Obligatory minimum</i>	<i>Average</i>
Density (g/cu cm).		2.90–2.96
Hygroscopicity (%)		0.1
Tensile strength (kg/sq cm)	280	360
Compressive strength (kg/sq cm)	4500	5500
Bending strength (kg/sq cm)	400	460
Moh's hardness		8.5
Grinding hardness (sq cm/cu cm)	1900	2200
Young's modulus (kg/mm)		11000
Specific heat (kcal/kg °C)		0.2
Heat conductivity (kcal/sq m/hr °C)		0.7
Linear thermal expansion coefficient		
0–100 °C; 1/°C		77·10 <sup>-7</sup>
0–400 °C; 1/°C		86·10 <sup>-7</sup>
Thermal shock resistance (°C)		150
Surface resistivity (ohm-sq cm/cm)		1 × 10 <sup>12</sup>
Internal resistivity (ohm-sq cm/cm)		1 × 10 <sup>11</sup>

† Taken from Vlček [55].

**(E) METEORITIC MATERIALS**

A vast literature exists on meteorites [56, 57]. According to Kennedy ([58], p. 261), meteorites are classified into five major groups. These groups are the irons, pallasites, the meso-siderites, chondrites, and achondrites. However, many meteorites contain iron sulfide (troilite). Troilite meteorites may be considered a sixth group of meteorites, while ice meteorites could conceivably constitute group seven. The siderites or iron meteorites are made up of approximately 90% metallic iron and about 8.5% nickel, similar in composition to low-grade stainless steel. Pallasites are predominantly metallic iron and the common rock-forming mineral olivine, a magnesium iron silicate. Meso-siderites contain two other rock-forming minerals, pyroxene and feldspar. Chondrites and achondrites are termed the stony meteorites even though chondrites contain about 14% nickel-iron and achondrites about 2% nickel-iron. Both types are essentially silicates of calcium, magnesium and iron. The chondrites are characterized by a peculiar textural feature—the chondrule—which is a rounded grain or aggregate of olivine or enstatite. Other differences also exist between the chondrites and achondrites.

Sytinskaya [59] proposes a volcanic slag on the Moon created by meteoritic impact. The resulting slag material would be dark colored due to the decomposition of silicates, such as olivine, and the formation of black iron oxides. Sytinskaya further states that the slag is darker on the lunar maria because the original rocks there contained more iron than those in the non-mare areas. This hypothesis is based on photometric, colorimetric, and polarimetric investigations. In an impacted lunar terrain, therefore, one would expect to find large quantities of nickel-iron which would of course be useful in lunar base technology. According to H. C. Urey, the ratio of abundances of iron, sulfide and stony meteorites is 10:6:7:100. On this basis considerably more meteoritic iron debris would be present on the light-colored (cratered) highland areas of the Moon if these craters have been formed by impact.

If the lunar surface were completely lacking in volcanic rocks, chondrites could possibly be used as an alternate source of oxygen. Kaiser and Komárek are conducting studies on this subject at New York University. Using a hydrogen reduction technique at 1000° C they have found that 3 to 4 kg of oxygen may be obtained from each 100 kg of chondritic or other stony meteorites. It has also been estimated that, at 1800°C, each 100 kg of meteoritic material would yield 15 kg of oxygen. Unfortunately, this technique depends on a substantial source of hydrogen for oxygen extraction. Compared with the rock froth crushing method discussed above, much larger quantities of energy would also be required.

**MINERALIZATION****(A) VOLCANIC MINERALIZATION**

If it exists on the Moon, volcanic mineralization would probably involve the same elements which are concentrated in sea water on Earth. This reasoning is based on the defluidization process endorsed by Rubey [60] and Poldervaart [61]. The defluidization hypothesis maintains that submarine volcanism on Earth has enriched certain elements in sea water and has even supplied part of the water. Water resulting from an analogous defluidization

process in the lunar interior has obviously escaped. However, one might ask what has become of the elements that could have been similarly enriched in volcanic vapors contributing to a pre-existent lunar hydrosphere.

In order of abundance on Earth, the excess volatile materials in the present atmosphere, hydrosphere and sedimentary rocks are  $H_2O$ , C in  $CO_2$ , Cl, N, S, H, and the group B, Br, Ar and F. Of these elements and compounds, those more likely to be found in the sunlit portions of the Moon would include  $H_2O$ ,  $CO_2$ , Cl, N, H, and F. However, because of the small mass of the Moon (1/80th that of the Earth), elements and compounds of high vapor pressure would soon evaporate. The fugacity and photodecomposition of ammonia and methane would also preclude their concentration on the lunar surface. However, the author believes that the elements given in

TABLE 5. Elements Possibly Enriched in the Lunar Surface

<i>Element</i>	<i>Ppm supplied to sea water from igneous rocks</i>	<i>Ppm in sea water</i>	<i>Per cent transfer</i>	<i>Neutron-capture cross-section (barns)</i>
Chlorine	138	19000	13800	33
Bromine	1.1	65	6000	66
Argon	0.024	0.6	2500	0.6
Sulfur	540	900	170	0.49
Selenium	0.006	0.004	67	13
Boron	(1.8)	(4.6)	(256)	755
	7.8	4.8	62	
Iodine	0.24	0.05	21	6.3
Fluorine	396	1.3	0.33	0.010
Antimony	0.2	< 0.0005	< 0.28	5.5
Radon	$4 \times 10^{-12}$	$9 \times 10^{-15}$	0.25	—
Arsenic	1.2	0.003	0.25	4.3
Cadmium	0.078	$1.1 \times 10^{-4}$	0.14	3300
Mercury	0.036	$3 \times 10^{-5}$	0.083	350
Lead	10	0.003	0.03	0.17
Zinc	48	0.01	0.021	1.10

Table 5 will be enriched in the lunar terrain compared to the average sedimentary rock on Earth. Those listed above the solid line in the table form soluble compounds which are greatly enriched in sea water. Those below the horizontal line, although not enriched in sea water, are known to be present in terrestrial volcanic areas.

Four boundary conditions may control lunar mineralization. First, the mineral must be able to form as a sublimate in an environment poor or lacking in oxygen. These would possibly correspond to the "closed-tube" sublimates of determinative mineralogy tests. Such sublimates include sulfur, cinnabar, realgar and many others. The second condition is that if these minerals presumably exist in sunlight, they must not photodecompose.

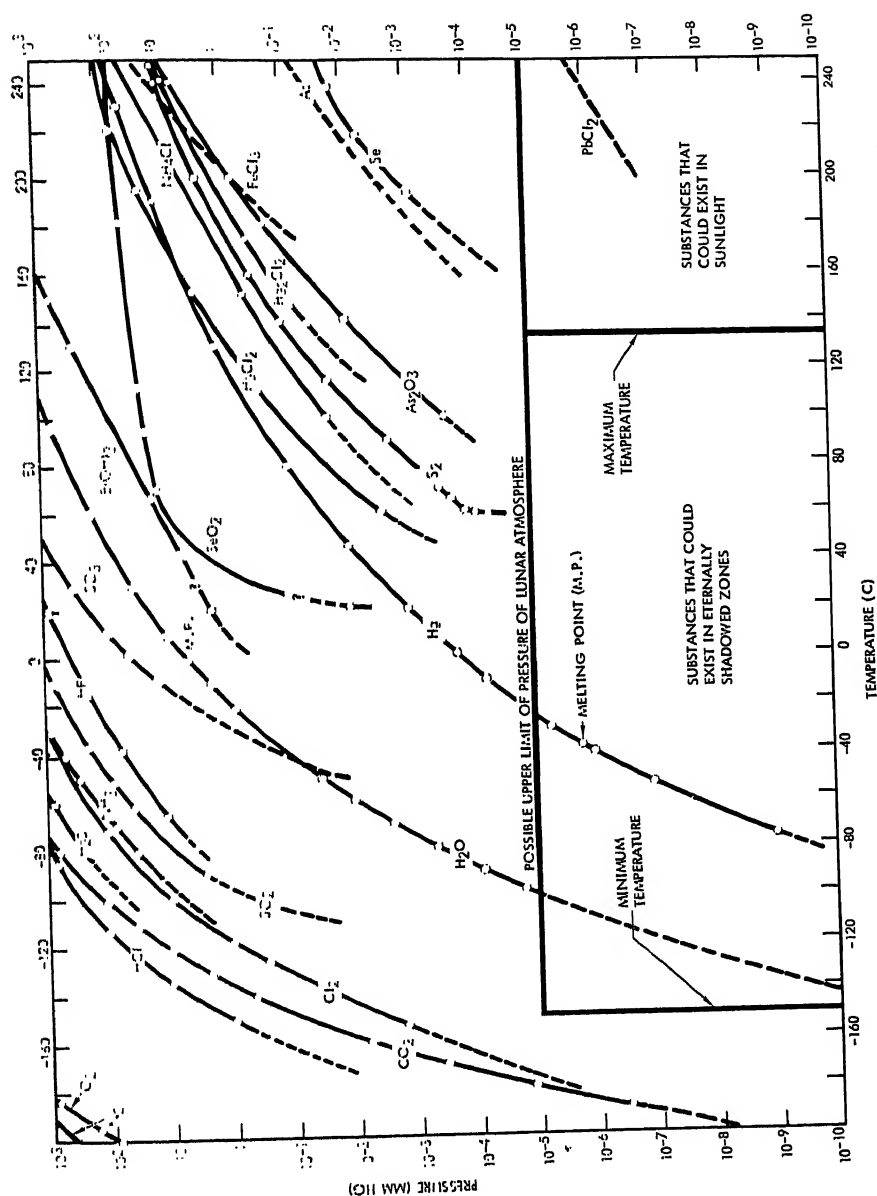


FIG. 29. Pressure-temperature relationships of possible lunar volcanic sublimates and emanations.

Thus, we are obliged to reject realgar (arsenic monosulfide) because it decomposes under sunlight to form orpiment and, if oxygen is available, arsenolite. Thirdly, we should discard the possibility of those minerals that would melt under subsolar temperatures on the Moon. Sulfur may be a borderline case with its melting point of  $125^{\circ}\text{C}$ . However, the ability of vaporized sub-

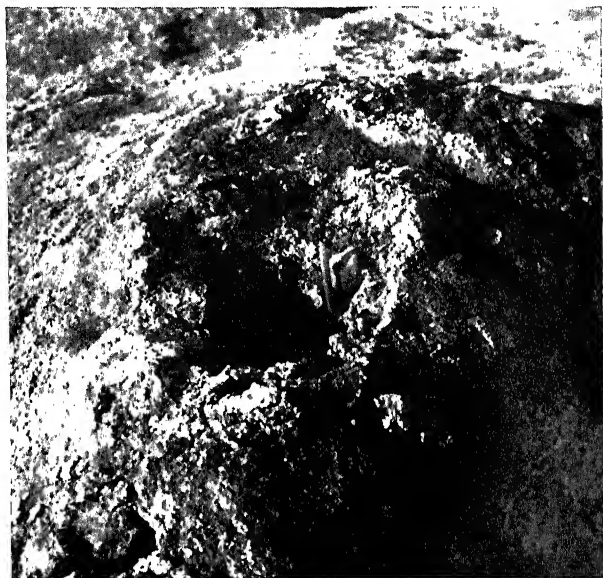


FIG. 30. Sulfur fumarole in Námafjall near Lake Myvatn, Iceland.

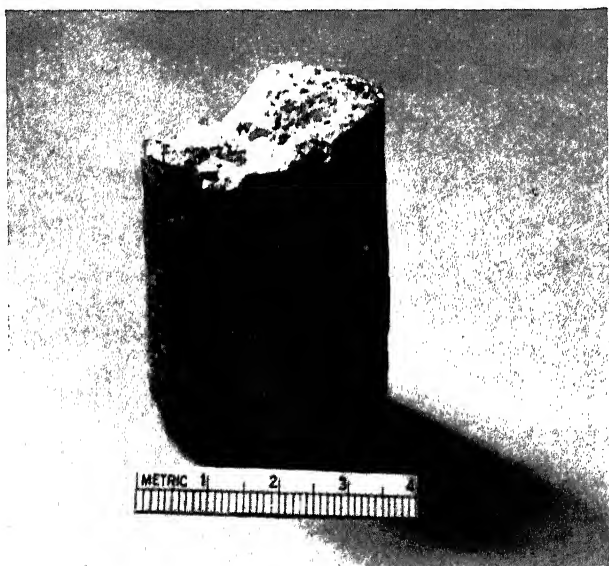


FIG. 31. Core of sealed fracture in basalt, Pisgah Crater area, California

limates to migrate is reason to believe that mineralization may concentrate in the eternally shadowed zones. The final consideration for lunar mineralization is vapor pressure (Fig. 29). One sublimate that could possibly exist in sunlit areas on the Moon is cotunnite ( $\text{PbCl}_2$ ) which, incidentally, is important in age-dating techniques.

The presence of chlorides in eternally shadowed zones would substantially assist in the maintenance of the lunar base. Most of the other minerals that

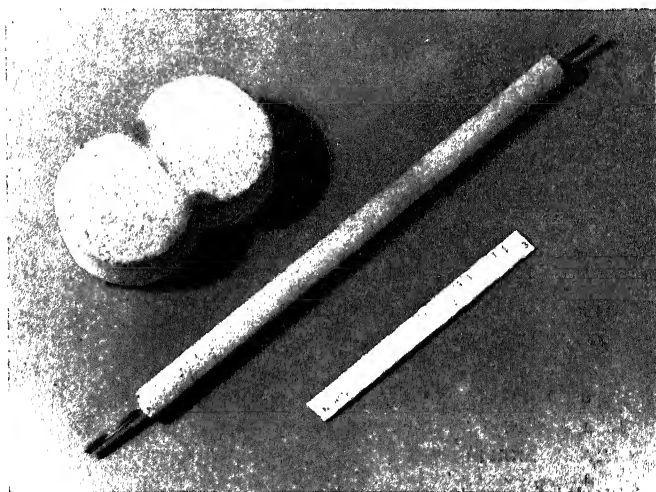


FIG. 32. Sulfur-volcanic ash mixtures illustrating use as structural components and insulation.

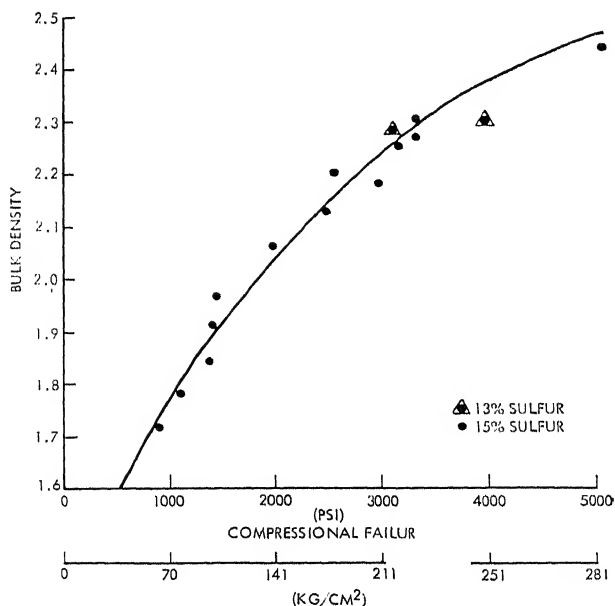


FIG. 33. Compression tests of sulfur-volcanic ash briquettes.



could form in the absence of oxygen have vapor pressures which predict their existence in unknown quantities in eternally shadowed zones (Fig. 29).

One of the most common minerals found in volcanic areas is sulfur (Fig. 30). This mineral fulfils all of the previously mentioned boundary conditions required for possible lunar mineralization. Mixing sulfur with volcanic ash makes for a waterless cement that could be used on the Moon to seal fractures. It has been possible to seal a fracture in a basaltic lava tube in the Pisgah Crater area, California, using only sulfur. Preliminary tests indicate a permeability of less than a millidarcy at the sulfur-basalt interface (Fig. 31). Sulfur and volcanic ash may also be molded into structural forms and insulation (Fig. 32). Briquettes made from 15% sulfur and 85% volcanic ash have rather high crushing strengths of 350 g/cm<sup>2</sup>. On the Moon, these briquettes could sustain a mass that would exert 2100 g/cm<sup>2</sup> (Fig. 33).

#### (B) WATER CONTENT IN LUNAR SURFACE MATERIALS

In the search for critical raw materials on the Moon, no single substance is as important as water. From all standpoints—supply of oxygen and fuels, maintenance of equipment and life support—a source of water is a primary exploration objective. In order of probability of occurrence, the sources of water that may be present on the lunar surface or near-surface include: (1) chemically bound water (H<sub>2</sub>O<sup>+</sup>) present in volcanic extrusives; (2) ice in permanently shadowed zones in volcanic fractures and fissures; (3) water of crystallization in volcanic sublimates; (4) permafrost in dust basins; and (5) water in carbonaceous chondrites and other rock types.

From Fig. 29, we note that the vapor pressure of ice at -150° C, which is the shadow temperature on the Moon, is 10<sup>-11</sup> mm Hg. This means that if lunar atmospheric pressure is above 10<sup>-11</sup> mm Hg, it is possible for ice to accumulate in the eternally shadowed areas. Estimates of the lunar vapor pressure vary from 10<sup>-8</sup> to 10<sup>-13</sup> mm Hg. However, the pressure in the fractures and fissures of a lunar volcanic surface could have considerably higher pressures than on the mountain tops, even from radon gas leakage alone.

From this standpoint, even though the water is derived from surface runoff, the formation of ice in caves is of special interest. The stalactites in the Arco Tunnel at Craters of the Moon National Monument, Idaho (Fig. 34), are a striking example of how ice forms in caves. More significant perhaps is the existence of ice under an 1885 pumice fall in the Askja caldera in Iceland (Fig. 35). Although it would be extremely optimistic to predict similar conditions on the Moon, the existence of ice is not entirely impossible.

More realistic is the use of rocks to supply water. Three guesses concerning the nature of the rocks that make up the surface of the Moon are (1) meteoritic materials, (2) volcanic extrusives, and (3) ultrabasic rocks, including serpentines. The water content of these rock groups differs considerably, and even within a single group there is considerable range of water content. Although this discussion is in terms of weight per cent, it should be noted that 5% by weight of water in the rock types considered is equivalent to 130 liters per cubic meter of rock.

Figure 36 illustrates the water content in the three classes of rocks. The water percentages are for H<sub>2</sub>O at +110° C; this being the water given off at temperatures ranging from 110 to 1000° C. In general, the water content of meteorites is on the order of a 0.1%, with the exception of carbonaceous chondrites which contain as much as 10% of water. However, even if the

Moon's surface were heavily impacted, this variety of chondrite would be a valuable but rare find. The fine degree of fragmentation suffered by impacting meteorites, particularly those which are already internally fragmented, must be considered.

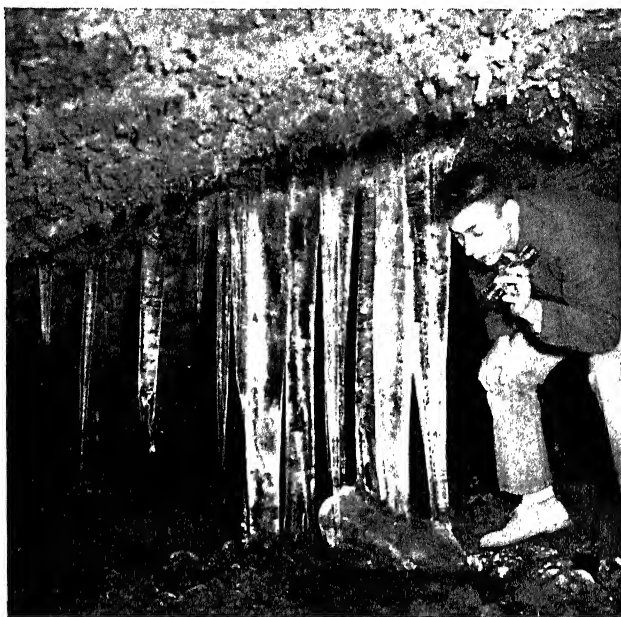


FIG. 34. Ice stalactites in Arco tunnel, Craters of Moon National Monument, Idaho.

The volcanic extrusives listed in Fig. 36 show a wide range in water content. The " $\text{H}_2\text{O}^+$  average" approximates 1% if abundances based on areal distributions are applied for the rock types included. For example, pitchstones are volumetrically uncommon. Whether pitchstones are more common among volcanic extrusives than are carbonaceous chondrites among stony meteorites on the Moon is not known. However, our knowledge of occurrences of pitchstones on Earth should be helpful in prospecting for this rock type on the Moon.

Space Sciences Laboratory of North American Aviation has conducted a more thorough study, on an areal basis, of the distribution of water in volcanic extrusives. Of the 2432 analyses that were compiled, 451 were rejected because of alteration effects that could be deduced from the analysis itself or the rock description. The remaining 1981 superior analyses were divided into 625 geographical groups and five lithologic groups (based on the  $\text{Na} + \text{K} / \text{Ca} + \text{Na} + \text{K}$  ratio). The overall water content of screened volcanic extrusives is 1.1% by weight with a standard deviation of 0.33.

In Fig. 36, the category marked "other" consists of ultramafic rocks which approximate 0.1% available water and a metamorphic equivalent (serpentine) which contains 12.7%. The argument for ultramafic rocks on the Moon is based on the hypothesis that a silicic lunar crust did not develop and that highly magnesium ultramafic rocks are light-colored. As more evidence of a volcanic origin of lunar surface features accrues, the more a

1% value should be favored as the predicted water content of lunar surface rocks.

One might speculate on the possibility of the presence of liquid water at depth on the Moon. If water does exist in the lunar crust, water or permafrost might reach its greatest concentration near the surface at the end of the lunar night. Moreover, the search for water on the Moon might be most



FIG. 35. Ice under 1885 pumice fall, Askja Caldera, central Iceland.

favorable at those times when the Moon is farthest from the Earth. This concept is a lunar extrapolation of Lambert's observations ([68], p. 18). Lambert indicated that the water level in certain water wells decreases during the Moon's transit. According to Dr. C. L. Pekeris of M.I.T. (cited by Lambert, [68], p. 23), dilational effects in the Earth produced by the Moon

are believed to be the cause of this phenomenon. Because the Earth exerts greater tidal effects on the Moon than the Moon on the Earth, lunar dilational effects might be intensified at perigee of the Moon. Conversely, tidal effects may result in compressional effects at apogee. Therefore, water may be forced closer to the lunar surface during apogee.

TABLE 6. Mineralogy of Meteorites

<i>Mineral</i>	<i>Weight (per cent) in</i>		
	<i>Iron</i>	<i>Achondrite</i>	<i>Chondrite</i>
Albite		5.8	7.4
Anorthite		13.2	3.3
Apatite			0.7
Chromite†		0.7	0.7
Cohenite (Fe, Ni, Co, C)†	0.4		
Iron-nickel†	98.3	1.6	10.6
Olivine		12.8	42.3
Orthoclase		1.7	1.1
Pyroxenes		62.3	28.9
Schreibersite (Fe, Ni, P)†	1.1	0.4	
Troilite (FeS)†	0.1	1.5	5.0

† Of technological importance if in large quantities.

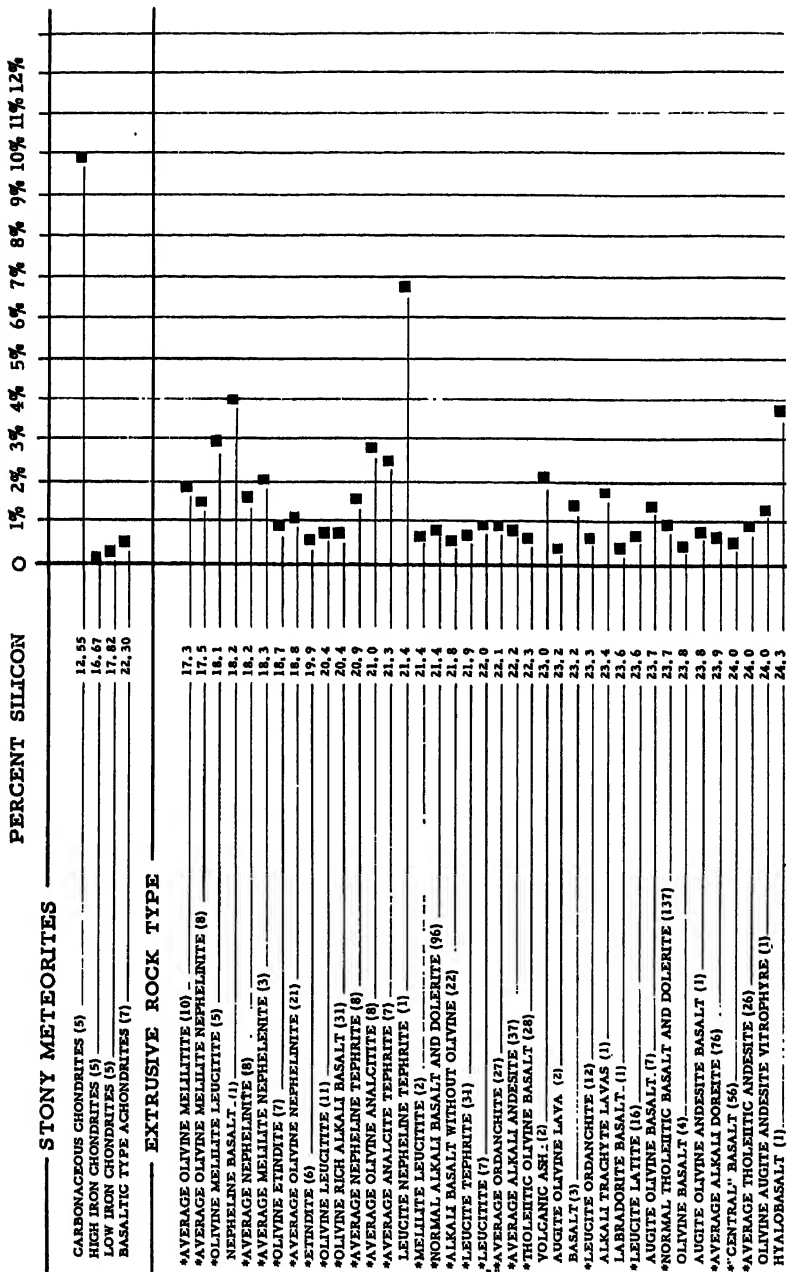
#### (c) METEORITIC MINERALIZATION

Meteorites contain a large number of minerals as indicated in Table 6 but they are volumetrically insignificant. Aside from nickel-iron, meteorites that have hit the Earth are almost devoid of useful minerals. However, meteorites that have hit the Moon may be relatively enriched in minerals that decompose in terrestrial environments; lawrencite, for example. Also, on the Moon larger concentrations of troilite may be present. Possibly its scarcity on Earth may be due to its ablation in passing through the atmosphere.

The occurrence of minerals produced by shock waves such as coesite [12] or diamonds [69] is also a rarity on Earth. According to information released by the United States Geological Survey, coesite, the high temperature modification of quartz, was found by X-ray diffractometry in the strongly sheared Coconino sandstone from drillings in the floor of Meteor Crater. Coesite is extremely refractory and has been suggested as a suitable nosecone material. However, it is doubtful if coesite would occur in sufficient quantities on the lunar surface—even assuming frequent impact—because highly silicic rock types are required to produce coesite.

#### LUNAR THERMAL SOURCES

Numerous changes have been observed on the lunar surface and at least three craters—Linné, Plato and Alphonsus—have a long history of reported changes. Unfortunately, such changes are difficult to document, although the spectrogram obtained by Kozyrev [70] has offered more direct evidence. Available data on these and other craters are listed in Table 7.



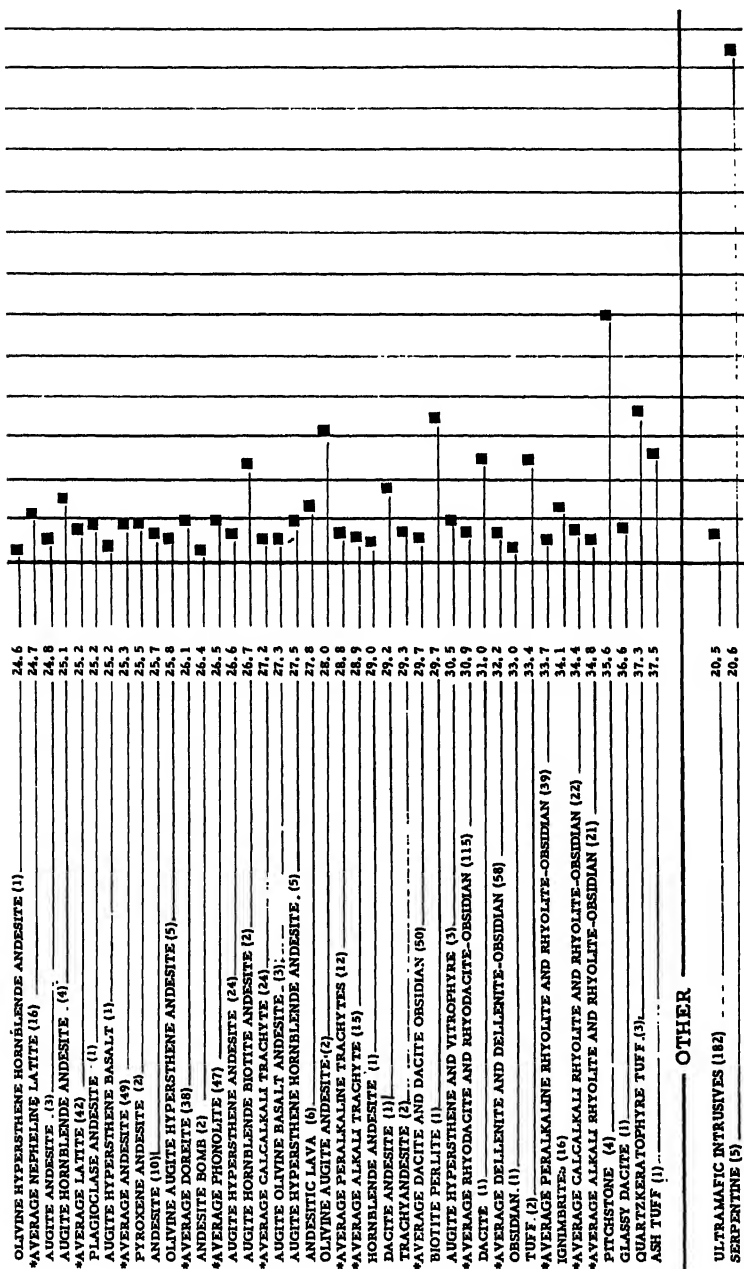


Fig. 36. Water content in rocks. Meteorite analysis is taken from Urey and Craig [62], carbonaceous chondrite data from Wiik [63] and ignimbrite data are from Steiner [64] pp. 330-331. Asterisked volcanic extrusive data are from Nockolds [65]; all others except pitchstone average from Tilley [66] are from an undated compilation by Van Bemmelen. Serpentine average is from Nagy and Faust [67]. Numbers in parentheses indicate the number of individual analyses involved in determining the average.

TABLE 7. Reported Changes in Lunar Features

<i>Feature</i>	<i>Nature of change</i>	<i>Date</i>	<i>Duration</i>	<i>Observer</i>	<i>Location and telescope aperture</i>
Apennine Mountains	Cloud-like features along face	Several occasions		W. H. Pickering	Mandeville, Jamaica
Agarum Promontory	Mist-like appearance	18 Nov 1958		H. P. Wilkins,	Moudon, France
		22:00		P. Moore	33 inches
Alpetragius	Portion of shadow replaced by lighter shade	26 Oct 1937	5 min	R. J. Stein	Newark Museum, N.J.
Alphonsus	Milky floor				4 inches
	Rills obscured in blue-violet plates more than in infra-red	26 Oct 1956		D. Alter	Lick Observatory, Calif.
	Reddish cloud, then whitening of central peak; spectrograms show Swan emission bands	3 Nov 1958	1 hr 30 min	N. A. Kozyrev	36 inches
	Bright cloud obscuring central peak	03:30			Mt. Wilson, Calif.
	Faint reddish patch, 2 miles in diameter, south of bright central mountain	18 Nov 1958		H. F. Poppendiek,	60 inches
	Dusty patch near central mountain	20:00	30 min	W. H. Bond	San Diego, Calif.
	Reddish spot near central mountain	19 Nov 1958		H. P. Wilkins	6 inches
	Radial bands evidence increase in visibility in past 50 years	Dec 1958			Kent, England
Aristarchus				J. Wall,	15½ inches
				F. D. Brewin	England
				G. A. Hole	12 inches
				R. Barker	Brighton, England
					24 inches
					Cheshunt, Hertfordshire
					12½ inches (reflector)

TABLE 7—continued

<i>Feature</i>	<i>Nature of change</i>	<i>Date</i>	<i>Duration</i>	<i>Observer</i>	<i>Location and telescope aperture</i>
Bartlett	"Crosses" reported before chief wall, Zeta, do not appear on modern maps			W. H. Wilkins	Kent, England 15½ inches
Kant	Mist-like appearance inside crater	4 Jan 1873		E. Trouvelot	
Kepler	Whitish glow near Earth-lit rim	2 Feb 1942 18:20	55 min	Y. W. I. Fisher	Brussels, Belgium
Lichtenberg	Reddish tint in area	1830-1840		J. H. Mädler	Berlin, Germany 3½ inches
	Reddish tint	1940		D. P. Barcroft, W. H. Haas	Las Cruces, New Mexico 6 inch (reflector)
	Reddish glow	21 Jan 1952		R. M. Baum	Chester, England 6 inch (reflector)
	Deep distinct crater	1842		W. Beer, J. H. Mädler, W. Lohrman	Berlin, Germany 3½ inches Dresden, Germany 4½ inch (reflector)
Linné	Crater	1840-1843		J. Schmidt	Athens, Greece 7 inches
	Whitish patch with mound	1866		J. Schmidt	
	Mountain in center of mound	1867		J. Schmidt	
	Shallow depression in center of mound ½ mile in diameter	1868		Knott, Buckingham Key	
	Craterlet in whitish patch	1868		A. Secchi	
	Low dome in white nimbus with deep, minute summit pit	1951		F. H. Thornton	Northwich, England 18 inch (reflector)



If volcanism is now occurring in certain places on the Moon, as Kozyrev's data indicate, these areas should be of great value as sources of heat and power. Volcanic structures offer much higher thermal and power potential than impact craters. In addition, the subsurface of volcanic regions would presumably be warmer than in impacted meteoritic regions.

Some believe that meteoritic impact may have created the system of rays on the Moon while others propose that expansion and contraction processes could have caused them. If the first theory is correct, streamers of material given off by the impact would not produce deep-seated thermal effects. Hence, no sustained heat flow anomalies would be expected from the Moon's interior. In fact, the extreme brilliancy of the rays would produce a linear anomaly of low heat flow because of reflection of most of the incident heat. On the other hand, defluidization and consequent tectonic activity would produce profound faults and more than normal heat flow might be expected along these zones of weakness.

The heat flow of the Earth per year is estimated to be  $10^{30}$  ergs [71]. If one assumes only a fraction of this value to represent the heat flow from the Moon, the possibility exists for appreciable localization of this heat along major deep-seated lunar fractures. Rejuvenated fractures are also potential loci for hot-spring activity. Fracture intersections and rejuvenated fractures may be heat sources convenient in maintaining a lunar base. Bülow [34] has made an extended study of the tectonics of lunar surface fracture patterns and he has also mapped the major fracture systems, exclusive of ray patterns. Bülow's maps give evidence of hundreds of fracture intersections; close inspection will undoubtedly reveal thousands more.

Infrared surveying techniques may indicate once-active volcanoes on the Moon. The heat flow from the Alphonsus eruption must have been considerable [70, 72]. In 1953, ground surveys at Vesuvius recorded a hot spot 91.5 m below the present rim [73]. Similar surveys have proven effective in predicting volcanic activity at Kagoshima [74] and Usu [75]. Other surface heat flow measurements of areas of possible geothermal power have been made in New Zealand [76] and the Kurile Islands [77].

Gross lithologic types are also identifiable by heat flow techniques. The maria would be expected to absorb more heat than, say, the ray systems, just as basalt absorbs more infrared radiation than does pumiceous ash. A survey of the lunar surface to determine thermal anomalies would also be valuable from a mineralization standpoint. Hot springs, fumaroles and solfataras—often mineralized—are known to occur in volcanic terrains and at fracture intersections on Earth [78].

Finally, infrared techniques may be the simplest means of distinguishing among not only the main rock types but also major mineral accumulations, including ice and sulfur.

During the lunar eclipse of 12 and 13 March 1960, Shorthill [79] made a bolometric survey of lunar infrared radiation at the Newtonian focus of the 72-in. reflector of the Dominion Astrophysical Observatory. The measurements were made with a thermistor-bolometer detector with a KRS-5 window which limited the spectral bandpass to 0.5 to  $40\mu$ . The dimensions of the sensitive surface of the thermistor were 0.3 by 0.3 mm subtending a field of 7 sec of arc at the f/5 Newtonian focus. This corresponds to a linear dimension of about 12 km at the lunar surface. A filter wheel with a microscope cover glass, a germanium disk and open positions was used. The cover

glass provided a wavelength cutoff at about  $5\mu$  and the germanium pass-band extended from about  $1.8$  to  $15\mu$ . The r.m.s. noise level of the device corresponded to a radiation flux of  $3 \times 10^{-9}$  Watts for a 10 cps bandwidth, approximately that due to a lunar temperature change of 20 K in the background temperature of  $180^\circ$  K. A restricted scan program was selected using Aristarchus as a starting point as shown in Fig. 37.

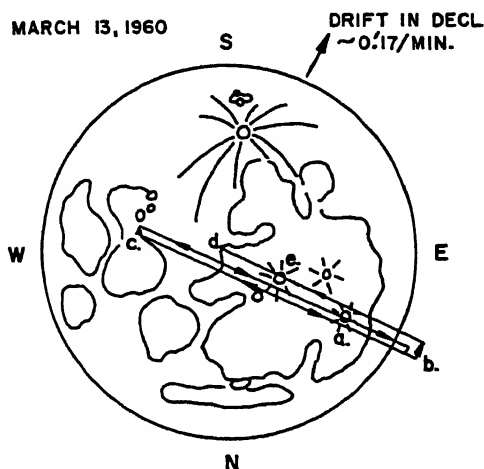


FIG. 37. Scan cycle with Aristarchus as a starting point. (a) Aristarchus. (b) End of scan off east limit. (c) End of scan near Sea of Nectar. (d) Center of disk, end of 14.5 minute scan cycle. (e) Copernicus. (After Shorthill *et al.* [79].)

The rapid cooling of the lunar surface during a lunar eclipse from  $370$  down to  $180^\circ$  K measured by Pettit and Nicholson [80] was verified by Shorthill, *et al.* Alphonsus evidenced no temperature anomaly indicating that its temperature was within  $20^\circ$  K of the general lunar background. The most remarkable result of the survey was the marked high-temperature anomaly associated with the rayed craters examined (Tycho, Aristarchus and Copernicus). A traverse across Tycho (Fig. 38) shows a temperature rise twice that of the background at the south rim. A maximum of  $60^\circ$  K above background was reached at one point during the traverse. Shorthill *et al.*, believe the data are in agreement with the theory that the rayed craters are among the more recent lunar features. The observation that a temperature rise is associated with the rayed craters does not conflict with the reasoning a rayed crater is a caldera bounded by rejuvenated fractures. It may be especially true for tangential rays such as those bounding Tycho.

The presence of a thinner dust layer in the rayed crater areas would not tend to produce a temperature anomaly in a stony meteoritic crust. Moreover, the rayed craters are bright and would tend to reflect incident heat. Therefore, the heat may possibly be internal. Heat associated with volcanism and tectonic activity is thought to be of a sustained nature and magnitude to create the temperature anomalies measured. Heat generated by impact would migrate concentrically beyond crater boundaries or be dissipated by radiation. The survey indicated that the anomaly is confined to the crater area for Copernicus, Aristarchus and Tycho. The temperature profile of

Tycho is asymmetrical which may possibly be related to the crater's well-developed ray system. Linear temperature anomalies apparently exist on certain sides of Tycho, possibly corresponding to the position of tangential rays. (See plates D7-c and D7-d in the lunar atlas compiled by Kuiper [81].) Further work on lunar temperature anomalies using Shorthill's technique is in progress. The assumption that the temperature anomaly is caused by a thinner dust cover resulting from recent impact of the rayed craters is difficult to accept because the impact mechanism itself produces dust. The crater floors if impact produced would be filled with rock flour—an insulator. This author rejects impact as being the origin of the temperature anomalies of the rayed craters.

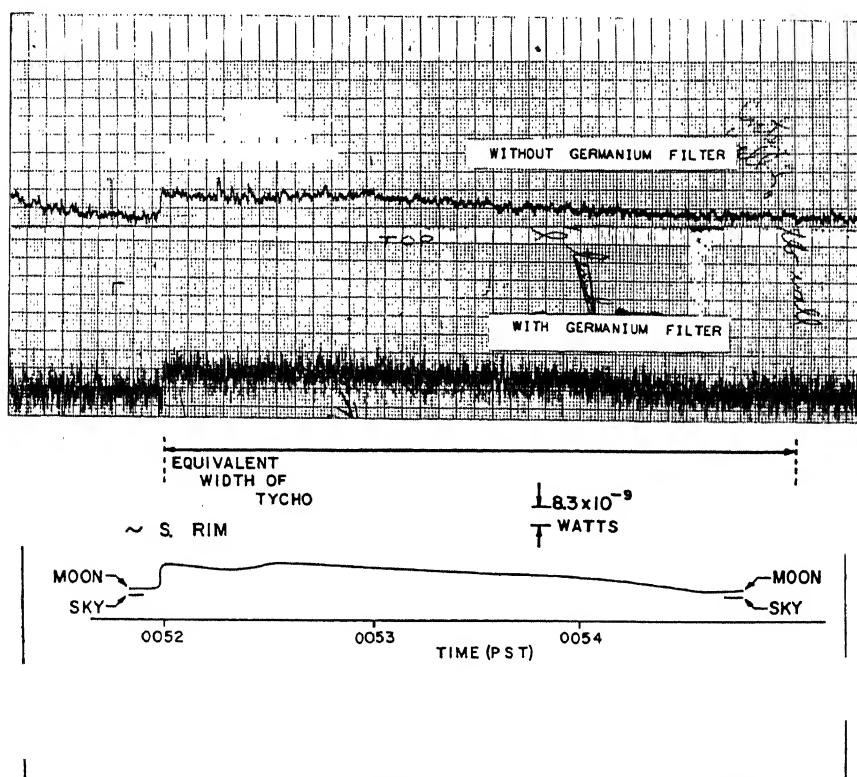


FIG. 38. Temperature profile across the crater Tycho (after Shorthill *et al.* [79]).

A quantitative test of the assumption that the lunar surface is chondritic could be made using infrared surveys. The average heat production of a chondritic Moon is  $2.3 \times 10^{-7}$  cal/cm<sup>2</sup>/sec [82]. On this basis and if a conductivity of  $2 \times 10^{-4}$  is assumed, the subsurface temperature is calculated to be 3° C. Fremlin [83], however, points out that this calculation must be in error because low subsurface temperatures could not give rise to the volcanic eruption reported by Kozyrev [70]. Thus, the assumption that the lunar surface is chondritic is thought to be incorrect because chondrites cannot supply the amount of heat necessary to induce volcanism. The abundances of uranium, thorium and potassium in basalt and rhyolites on Earth are

much higher than in chondrites and may be sufficient to initiate near-surface melting. It is unnecessary to appeal to abnormally high radioactive elemental abundances in rocks to produce melting [84].

Internal heat produced by radioactivity decay of isotopes of uranium, thorium, potassium, and rubidium would be at least an order of magnitude greater from volcanic rocks than from stony meteorites as the abundance data in Table 8 indicate. One can calculate that a thermally insulated silicic rock, with the quantities of radioactive elements shown, will heat up  $40^{\circ}\text{C}$  in 1 million years; a basalt would heat up about  $6^{\circ}\text{C}$ . During the same time period an insulated stony meteorite with the abundances shown would heat up less than  $0.5^{\circ}\text{C}$ . The table also indicates the heat rise per million years in these insulated rock types 3 billion years ago when potassium was much more abundant. Again chondrites would heat up only a degree or so in contrast to the volcanic rock types.

One of the important consequences of the higher uranium content of volcanics, as compared with chondrites, is the greater production of radon. The atmospheric pressure in a volcanic fissure should be greater than that in a fissured chondritic terrain. Argon would also be produced by radioactive decay, but the relative thermal velocities of argon and radon indicate that radon would be retained longer on the lunar surface. At craters of the Moon National Monument in Idaho, large rifts exist which locally exhibit radioactivity anomalies presumably due to radon. Anomalies greater than 0.05 microroentgens are observable in some of the fissures. For this reason, the large rift systems on Earth, such as the Eldgjá and Grjótagja (Figs. 39 and 40) in Iceland and the Dead Sea rift deserve closer scrutiny from the standpoint of the thermal sources and radon leakage.

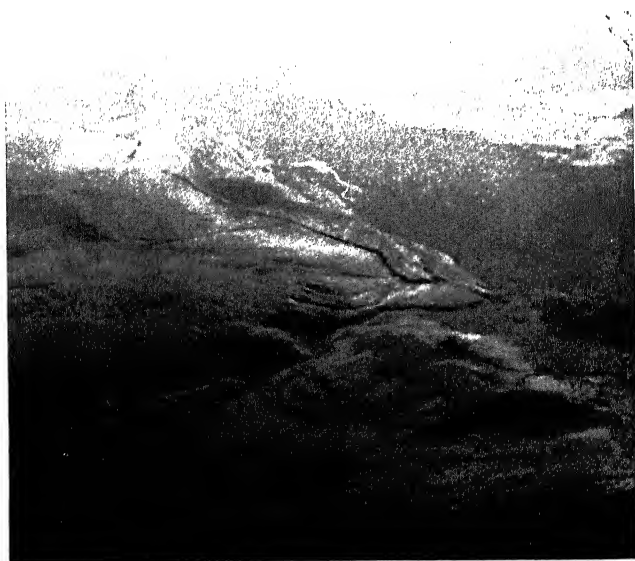


FIG. 39. Eldgjá rift, south-central Iceland.

The discovery of the radiogenic isotope xenon-129 in the Richardton chondrite by Reynolds [85] is of significance; it establishes the presence of some iodine-129 of 17 million years of half-life during an early period of the solar system. This means that other now-extinct radionuclides may also have been present in this period. Such radionuclides are of interest because they could have provided the additional heat source necessary for intense defluidization and volcanism during the Moon's early history. However, as noted in Table 7, the heat contributed by  $I^{129}$  would be negligible because of the time span between 4.5 and 3 billion years.

The low content of radioactive elements would produce a much lower

TABLE 8. Temperature Increase in Insulated Lunar Materials

Element	Annual rate of heat generation (cal/g)	Abundance (ppm)	Heat produced per 10 <sup>6</sup> year (cal/g)	
			During last 10 <sup>6</sup> years	3 × 10 <sup>9</sup> years ago
<i>Silicic rocks (rhyolite-granite clan)</i>				
Uranium	0.75	4	3.00	7.17
Thorium	0.203	20	4.06	4.71
Potassium	27 × 10 <sup>-6</sup>	40 000	1.08	5.16
Rubidium	38.9 × 10 <sup>-6</sup>	200	0.008	—
Samarium	342.5 × 10 <sup>-6</sup>	6	0.000	—
Iodine	?	?	—	—
Total			8.1	17.0
Temperature rise (°C) per 10 <sup>6</sup> years				
During last 10 <sup>6</sup> years			40.5	
3 × 10 <sup>9</sup> years ago				85.0
<i>Mafic rocks (basalt-gabbro clan)</i>				
Uranium	0.75	0.5	0.375	1.207
Thorium	0.203	3	0.608	0.704
Potassium	27 × 10 <sup>-6</sup>	5000	0.135	0.645
Rubidium	38.9 × 10 <sup>-6</sup>	20	0.001	—
Samarium	342.5 × 10 <sup>-6</sup>	2	0.000	—
Iodine	?	?	—	—
Total			1.12	2.56
Temperature rise (°C) per 10 <sup>6</sup> years				
During last 10 <sup>6</sup> years			5.6	
3 × 10 <sup>9</sup> years ago				12.8

TABLE 8—*continued*. Temperature Increase in Insulated Lunar Materials  
*Chondritic rocks (high and low iron groups)*

Uranium	0.75	0.01	0.0075	0.0245
Thorium	0.203	0.02	0.004	0.0046
Potassium	$27 \times 10^{-6}$	850	0.023	0.110
Rubidium	$38.9 \times 10^{-6}$	5	0.000	—
Samarium	$342.5 \times 10^{-6}$	1	0.000	—
Iodine	?	?	—	—
Total			0.035	0.14

Temperature rise (°C) per $10^6$ years	
During last $10^6$ years	0.17–0.35
$3 \times 10^9$ years ago	0.7–1.40

$K^{40} = 0.0119\%$  of K;  $Rb^{87} = 28\%$  of Rb;  $Sm^{147} = 15\%$  of Sm.

Heat capacities for silicic and mafic rocks taken at 0.2. Two heat capacities taken for chondrites at 0.2 and 0.1; true value probably lies between these values.

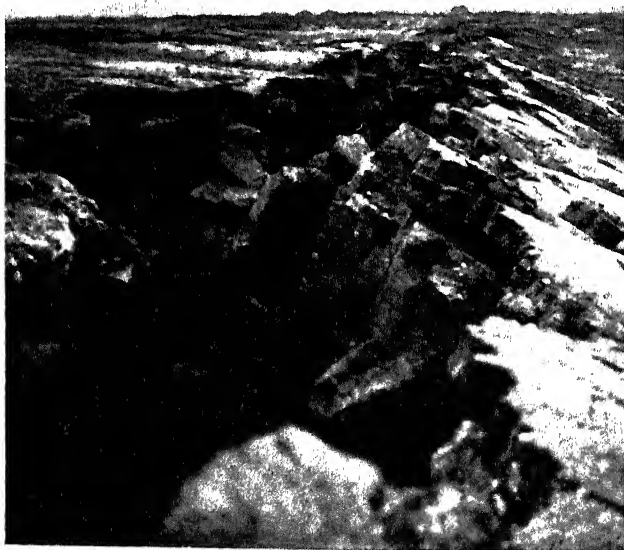


FIG. 40. Grjótagja rift, north-central Iceland.

heat flow from fractures in a chondritic terrain than in a volcanic terrain. Similarly, the heat generated by impact of large meteorites would have been dissipated very rapidly. This would also be true for the radial gouge zones from the so-called impact center in Mare Imbrium, if their origin were due

to ejected meteoritic fragments. Inspection of these gouges makes this geologically exotic mechanism of origin highly unlikely. In addition, micro-meteorites are of extremely small mass. Hence, the heat generation by their impact on the Moon would not produce a realistic heat source, particularly since they would be randomly located and unpredictable either in time or place.

Let us assume for the moment that radiogenic heat cannot provide the heat required to differentiate a lunar crust. There may be an auxiliary process—tidal heat. The same Earth-induced tidal forces that may have served to disrupt and fracture the lunar surface may have been sufficient in the geological past to flex the chondritic mantle of the Moon every few days. These internal stresses would generate heat; possibly even more heat than the lunar tides create in the Earth. If Earth-induced tides in the lunar mantle have served to accumulate heat in the Moon, we may follow Zotov, *et al.* [86] in their arguments on terrestrial heat-up by lunar tides. Zotov, assumes that the Moon was closer to the Earth in the geological past and induced greater tides in the Earth which travelled at higher speeds than at present because of an increased rate of terrestrial rotation. According to Zotov, assuming that the Earth has increased its period of rotation from 4 to 24 hr and that its mass and moment of inertia have remained the same, the amount of heat generated up to the present time should be  $1.04 \times 10^{36}$  ergs, less a potential energy of about 15% stored in the removed Moon. This would produce  $2.17 \times 10^{30}$  calories of heat which is 11 billion times the heat ( $2.0 \times 10^{20}$  calories per year) released by the Earth per year.

Taking the specific heat of the Earth at 0.2 calories per gram degree, the above calculated quantity of energy according to Zotov could heat the entire Earth from 0° C to 1800° C. This tidal heat is found to equal two-thirds of the radiogenic heat generated in the Earth in 5 billion years. The tidal heat so formed and accumulated during the cosmic history of the Earth is considered to participate in the tectonic and volcanic processes in the Earth. The present author believes that a similar but possibly intensified tidal effect may have been induced in the Moon by the Earth perhaps to the degree where rotation was stopped altogether. Therefore the tidal heat induced in the Moon falls into two periods. The first and most intense when lunar rotation was being slowed down to a stop, and the second now operative of tidal crustal and mantle flexing produced by the eccentricity of the lunar orbit.

## GEOLOGICAL TOOLS

### (A) RANGE OF EXPLORATION SYSTEMS

One's philosophy of approach to a lunar exploration program is easily influenced by the sequence of phases used in terrestrial exploration for oil and ore. Here, an aerial survey first outlines gross features and areas of interest; then, a ground survey examines those areas of interest for tectonic and alteration features. Finally, subsurface examination by geological, geophysical or geochemical means is initiated at specific points based on the aerial and ground surveys. This sequence, with some modifications, is proposed in this paper for lunar exploration. The modifications of a terrestrial exploration program arise from four differences in objectives and implementation:

1. The lunar survey is not primarily directed to detection of materials that are presently of economic importance.

2. The sampling grid must be crude because of the limitation of the number of instrumented probes that can be implanted.
3. The choice of site for inspection or analysis will vary with the information to be obtained.
4. The guidance to this site will not be precise.

The scope of the measurements that could be made from the hovering and surface vehicles is outlined in Table 9. Many of the instruments specified for the altitude surveys are also applicable to the surface traverses. As this table shows, a great proportion of the tools suitable for lunar exploration could be modified or redesigned logging devices used in the oil industry. Table 10 outlines a group of logging tools already in use or in development and their applicability to lunar exploration.

The logs that require fluid—often an electrically conducting fluid—between the sonde and the borehole wall are the self-potential, resistivity,

TABLE 9. Geophysical Surveys and Well Logging Devices  
Applied to Lunar Exploration

<i>Type of survey or measurement</i>	<i>Parameter measured</i>
Hovering or lunar surface vehicle: modified or redesigned aerial and ground geophysical surveys	
Television	Topography, terrain, mineralization and surface structure
Infrared	Surface structure
Magnetic	Lithology and subsurface structure
Radiometric	Lithology and gas emission
Gravity	Subsurface structure
Mass spectrometric	Gas emission
Lunar surface vehicle: modified or redesigned well logging devices†	
Self-potential	Porosity and/or water content
Resistivity	Surface structure, porosity and/or water content
Velocity	Lithology, surface structure, poro- sity and/or water content
Sonic geophone	Subsurface structure
Density	Lithology, surface structure, poro- sity and/or water content
Neutron-neutron	Porosity and/or water content
Discriminated gamma	Lithology and gas emission
Temperature	Surface and subsurface structure
Nuclear spectroscopy	Mineralization and lithology
Magnetic susceptibility	Lithology and surface structure
Inclinometric	Topography, terrain and surface structure

† Includes measurements that may be made from a surface vehicle.



induction, sonic velocity, nuclear magnetism and mud logs. Tools which require a hydrous environment are probably not applicable to lunar exploration. Therefore, the logging devices discussed below are the dry-hole resistivity, conventional gamma, discriminated gamma, conventional neutron, neutron-neutron, density and magnetic susceptibility.

A major breakdown of the measurements to be obtained by these potentially important logging devices, if modified for horizontal or in-place surface usage, might consist of three categories: solid, liquid and gas (Table 10). Each of these may be further divided. For example, under solids, the lithologic types shown in Table 11 may possibly be present in extra-terrestrial environments. Admittedly, this classification is extremely elementary, but it does represent a group of rocks that in theory could be distinguished by adaptation of present-day logging devices. On the Moon, only meteoritic rock types and the extrusive varieties of igneous rocks may be present.

In addition to lithology, we are interested in sublimate and meteoritic mineralization. For completeness, cements in sedimentary rocks and skarn minerals of metamorphic rocks are included; however, they are regarded as highly unlikely rock groups on the Moon. Common mineral cements, sublimates and metamorphic minerals are also included in Table 11.

Many rocks may be grouped into chemical or mineralogical assemblages which are diagnostic of environment at any particular time or place. Such facies or assemblages are included in Table 11. Then, because alteration tends to obscure parent lithologies (the convergence principle of Schwartz), there are a group of alteration products common to most rock types. These include kaolinite, montmorillonite-illite, alunite, jarosite, zeolite, chlorite, epidote, palagonite and chert (opal).

A family of physical parameters may also be included under the heading of solids because of the expression of the parameter in the rock matrix. These properties are of considerable interest to the petroleum industry because of the use of logging devices in evaluating rock formations. Almost all of the following entries are considered valuable for space exploration.

<i>Formation Evaluation</i>	<i>Miscellaneous</i>
<i>Parameters</i>	<i>Factors</i>
Permeability	Bed orientation
Fracturing	Magnetic susceptibility
Porosity	Temperature
Density	Hardness
Sonic velocity	Grain size
Bed thickness	Grain shape
Formation resistivity	Rock fabric
Mud cake thickness	

Liquids, the second major category in Table 10, are likewise of significance to man's existence on the Moon. However, of the numerous formation evaluation parameters, only the detection of water, formation water salinity and water saturation are considered important to the exploration of space.

The third major class of substances potentially measurable by logging tools is that of gases. However, many gas determinations are made only as a consequence of the dilution of borehole fluids by gas which produces variations in the log readings. Of the three pertinent entries—methane, oxygen and nitrogen—only the last two are of interest.

TABLE 10. Well Logging Devices for Lunar Exploration

Parameter measured	Conventional well logs			New well logs			
	Dry-hole resistivity	Neutron-neutron	Gamma	Discriminated gamma	Density	Sonic velocity	Accelerator types susceptibility magnetism
Solids							
Lithology			†	§			++
Mineralization			†	§			+
Cementation			†				+
Provenance			†	++			++
assemblages							
facies							
Alteration, weathering			†	++	†	†	+
Physical properties	++	†			§	§	§
Liquids							
H-bearing Properties	++	†	§			§	++
			†			§	+
Gases							
Composition							++

The following conventional logging devices require a hydrous environment in which to function and are therefore not considered here: self-potential, resistivity (including well resistivity), induction and mud logs.

† Limited or specific isolated applications in extraterrestrial environments.

++ Useful or applicable

§ Highest potential in space exploration problems.

TABLE 11. Possible Rock and Mineral Types in Extraterrestrial Environments

<i>Sedimentary</i>	<i>Igneous</i>	<i>Metamorphic</i>	<i>Meteoritic</i>
<i>Lithologic types</i>			
Sandstone	Ultramafic	Serpentine	Stony
Shale-clay	Gabbro	Eclogite	Stony-iron
Arkose	Basalt	Slate	Iron
Graywacke	Tachylite	Marble	
Limestone	Andesite	Schist	
Dolomite	Granite	Gneiss	
Anhydrite-gypsum	Rhyolite		
Halite	Pumice		
	Obsidian		
	Pitchstone		
<i>Common mineral cements, sublimates, and metamorphic minerals</i>			
Quartz	Sulfur	Chlorite	Lawrencite
Calcite-dolomite	Halite	Talc	Magnetite
Hematite	Molybite	Garnet	Osbornite
Siderite	Sassaolite	Staurolite	Graphite
Pyrite	Borax	Zeolites	Troilite
Chert	Alum	Graphite	Oldhamite
Anhydrite-gypsum	Gypsum	Spinel	Schreibersite
Apatite	Hydrated minerals		
<i>Chemical and mineralogical assemblages</i>			
Carbonate	Olivine-free	Diabasic	High total iron
Evaporate	Olivine-bearing	Hornfels	Low total iron
Marine	Feldspathoid-rich	Amphibolite	Chondritic
Non-marine	Alkalic	Green schist	Hydrous varieties
	Mafic	Granulite	
	Silicic	Eclogite	
		Glaucophane	

## (B) DRY HOLE RESISTIVITY LOG

According to Casey, Scott and Westcott [87], the number of variables involved in dry hole logging, although fewer than in wet hole logging, are less easily controlled. For landing pad instrumentation, the dry hole resistivity log is possibly well-suited for lunar surface exploration. The tool is designed for use in arid-regions on Earth where water is scarce or expensive to obtain. Two types of dry hole type resistivity logs are either available or under development—the single-electrode and the multiple-electrode sondes. In single-point logging, the resistivity of the Earth in the immediate vicinity

of the electrodes is measured; in multiple-electrode logging, the resistivity of a larger volume of Earth is measured; i.e. the depth of penetration is deeper. Multiple-electrode dry hole logging has the advantage of minimizing spurious electrode-contact resistance fluctuations.

The superiority of the dry hole resistivity log to the wet hole log is shown in Fig. 41. The dry hole sonde gives much better definition of thin-bedded

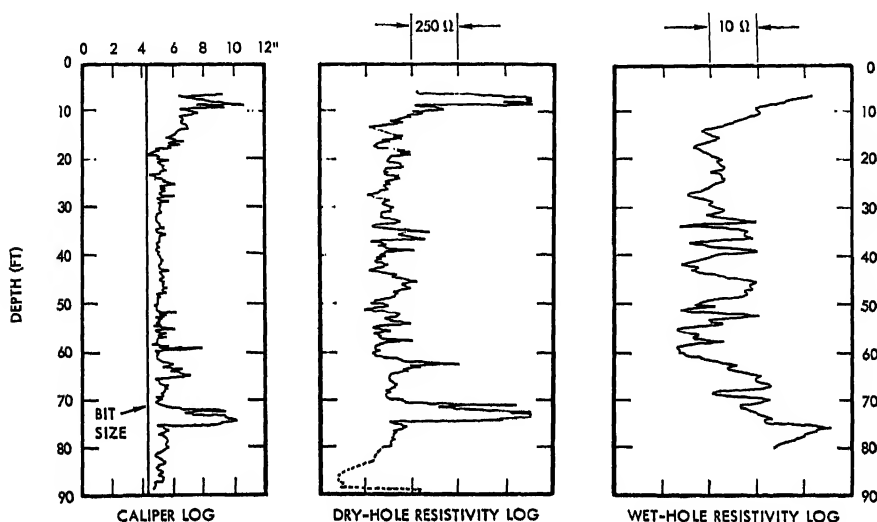


FIG. 41. Comparison of caliper, dry-hole resistivity, and wet-hole resistivity logs. (After Casey *et al.* [87], p. 58)

strata than the other device. (Volcanic tuffs and flows are often thin-bedded.) The zone from 72 to 75 ft shows extremely high resistivity in the dry hole log because the electrodes were not in contact with the formation walls; i.e. the walls have caved away as shown by the caliper log. However, if fluids were present, the response might resemble that of the wet hole log because fluid, especially water containing salts, would drastically lower the formation resistivity. Because this Fig. 41 does not actually show how one might interpret a resistivity measurement of traverse on the lunar surface, license has been taken to add a dashed line continuing the dry hole log from 80 ft to a greater depth. This was done to illustrate what might be the case if a stratum were encountered containing saline water in an otherwise dry lithologic column.

Conventional well logs through igneous rocks are rarely made. The most comprehensive study involving the application of resistivity, self-potential, induction, gamma ray, pulse transient and magnetic susceptibility logging was made in mineralized igneous rocks of the Lake Superior region by the U.S. Geological Survey [88]. However, fluids are required between the sonde and the borehole for most of these logs. A self-potential and resistivity log through solid basalt and associated pyroclastics of Clatsop County, Oregon, is shown in Fig. 42. Here, the resistivity of a non-vesicular Eocene age basalt is greater than 600 ohm-meters; the decrease in fluid content is reflected in a deflection in the self-potential curve.

Many problems must be solved before lunar resistivity surveys can be made. Emphasis should be placed on the importance of the electrical resistivity data in defining steam areas, as has been done in Italy [89] and New Zealand [90]. Factors that complicate interpretations of resistivity surveys in basalt, such as weathering variations [91], would be absent on

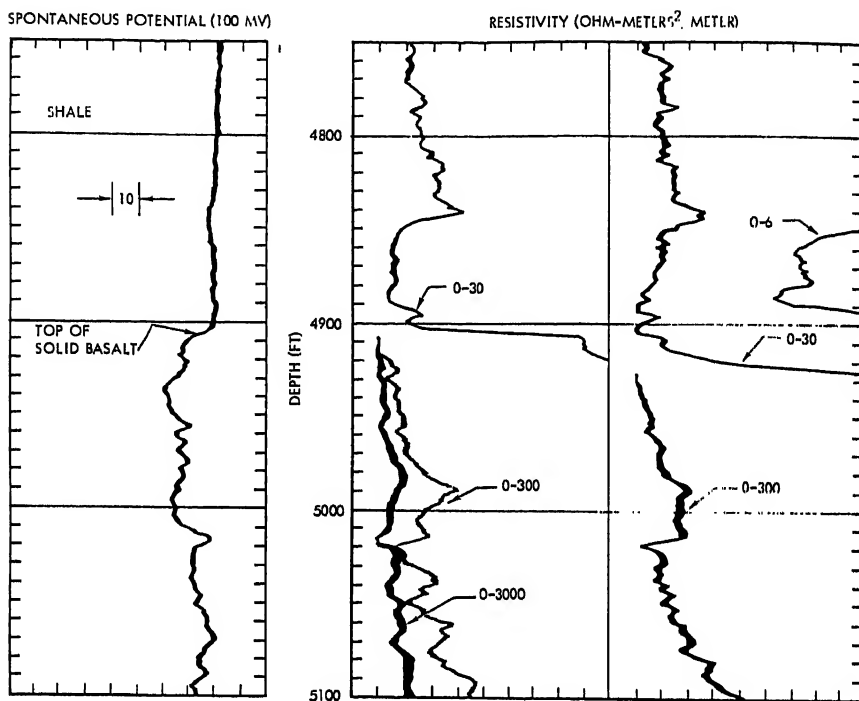


FIG. 42. Resistivity profile through solid basalt underlying shale in Standard of California Hoagland Unit No. 1, Clatsop County, Oregon.

the Moon. On the other hand if the lunar surface is covered with a bed of iron-rich cosmic infall material and if this conducting layer is not blown away by rocket blast, resistivity measurements may be impractical for determination of hydrous zones or permafrost. For this reason, a desirable landing site might be in the Aristarchus area, whose luminescence spectrum rules out the presence of iron [70].

#### *Neutron-Resistivity Log Interpretation*

One technique that may be used to define the nature of the lunar surface is the combination of resistivity and neutron responses as a function of temperature change. A detailed treatment of the neutron log is given below. For the purpose of this discussion, however, it is considered in conjunction with the resistivity log. Briefly, an increase in resistivity occurs with decrease in temperature in most naturally occurring silicates such as volcanics and in most dielectrics such as the most common volcanic mineral, sulfur. Iron, which would compose the bulk of cosmic infall material, shows a decrease in

resistivity with decrease in temperature. Thus, in Fig. 43 an increase in resistivity is shown with passing of the shadow zone over a lunar resistivity probe in an assumed dry sulfur-rich, volcanic surface dust. This shadow zone could be artificially produced by the shadow of the vehicle itself or by the normal passage of a lunar shadow every 14 days.

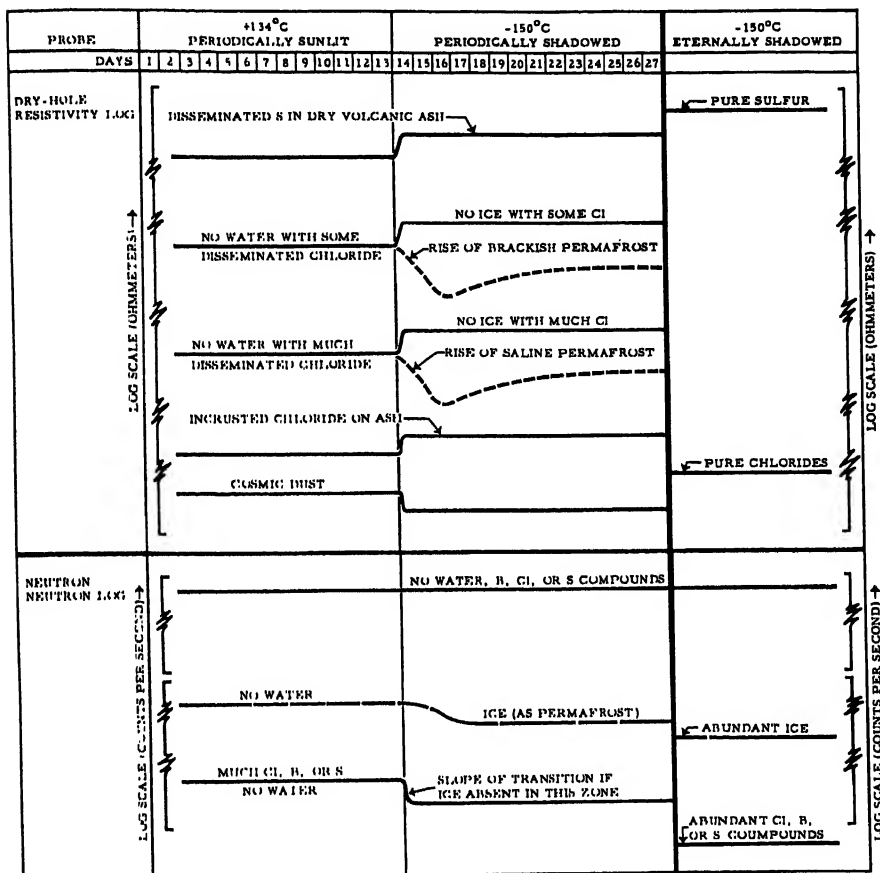


FIG. 43. Changes in resistivity and radioactivity in periodically sunlit versus shadowed zones of the Moon.

Under sunlight, the existence of water on the lunar surface would be impossible; however, in shadow there is a possibility of the rise of a permafrost layer in the lunar dust. If the permafrost is saline, the resistivity of the permafrost will be much lower than if the permafrost layer were brackish or pure. Furthermore, the change in resistivity would be gradual at the onset of shadow if there is a slow rise of the permafrost layer as a function of time. In the eternally shadowed zones, one might predict ice. If so, there should be a marked drop in resistivity in the transition from a dry volcanic dust to an ice layer.

According to Ananyan [92], electrical conductivity in finely dispersed frozen rocks is governed by the progressive advance of the not-yet-frozen

portion of the water. The electrical conductivity of such rocks is determined by the phase relations of the water. The smaller the amount of ice and the larger the amount of unfrozen water, the higher the electrical conductivity. The electrical conductivity of frozen rocks reaches its maximum when the moisture content approaches the lower limit of plasticity.

An extremely high resistivity should be expected if sulfur has accumulated in eternally shadowed zones, and an extremely low resistivity should be expected if chlorides have accumulated there. Figure 44 illustrates the changes in resistivity for sulfur, volcanic tuff, halite, saline water and iron. The positive slope of iron with respect to the other constituents may be of importance in interpreting resistivity data from lunar probes with passage of a shadow zone over lunar surface materials.

For a further aid in the interpretation of the resistivity probe as a function of temperature, one might also simultaneously observe the neutron log (Fig. 44). On the basis of the response of the neutron log, which is in counts per second, one could expect high absorption of neutron energy if hydrogen nuclei were present. Water or ice on the lunar surface would be dispelled under subsolar conditions, and any response of the neutron-neutron device would therefore be a function of the boron, chlorine or sulfur content in the surface dust or rock. If water as permafrost is present, it would tend to approach the lunar surface during the lunar night. Therefore, for the case in which only sulfur is disseminated on the lunar surface, the reading would be low during the lunar day with perhaps a small short-time decrease in cps at the onset of night because of reprecipitation of vapor in the colder environment.

If a near-surface permafrost layer is present, there would be a gradual decrease in the count rate as the fast neutrons encounter more and more hydrogen nuclei with rise of permafrost. There is more likelihood of drastic degrees of neutron absorption in the eternally shadowed zones where, in the manner of a cold trap, larger concentrations of ice, boron, sulfur and the halogens could accrue faster than they would be evaporated. A distinction among each of these substances of high neutron-capture cross section would be most competently handled by nuclear prospecting techniques.

On the other hand the neutron log, showing a high and uniform counts-per-second spectrum both in sun and shadow (Fig. 44) would tend to negate the possibility of both water and volcanic mineralization on the lunar surface. Such a pattern would be expected if the lunar surface were composed of stony meteorites.

In the neutron sonde technique, the log is obtained by moving a source of neutrons and a radiation detector along the well bore. The source and detector are separated by a fixed distance of approximately 51 cm. Polonium-beryllium or plutonium-beryllium provides a 3- to 10-curie source. The average minimum thickness of bed that can give a diagnostic recording of what the tool measures is 46 cm. The radioactivity detector is a scintillation counter about 1.1 m long.

In the original neutron curve process, which remains the most widely used, the detector is sensitive to gamma radiation. Because the method involves bombardment of the rock by neutrons and detection of the induced gamma rays, it is described as a neutron-gamma process. Neutron-gamma radiation is influenced primarily by the amount of hydrogen present in the vicinity of the instrument, and this in turn is a function of the fluid content

of the rock. By using the sufficiently strong source of neutrons, the induced gamma radiation intensity is made so large that the effects of variations of the natural radioactivity are completely obscured. However, the neutron sources also emit gamma radiation which must be shielded from the detector.

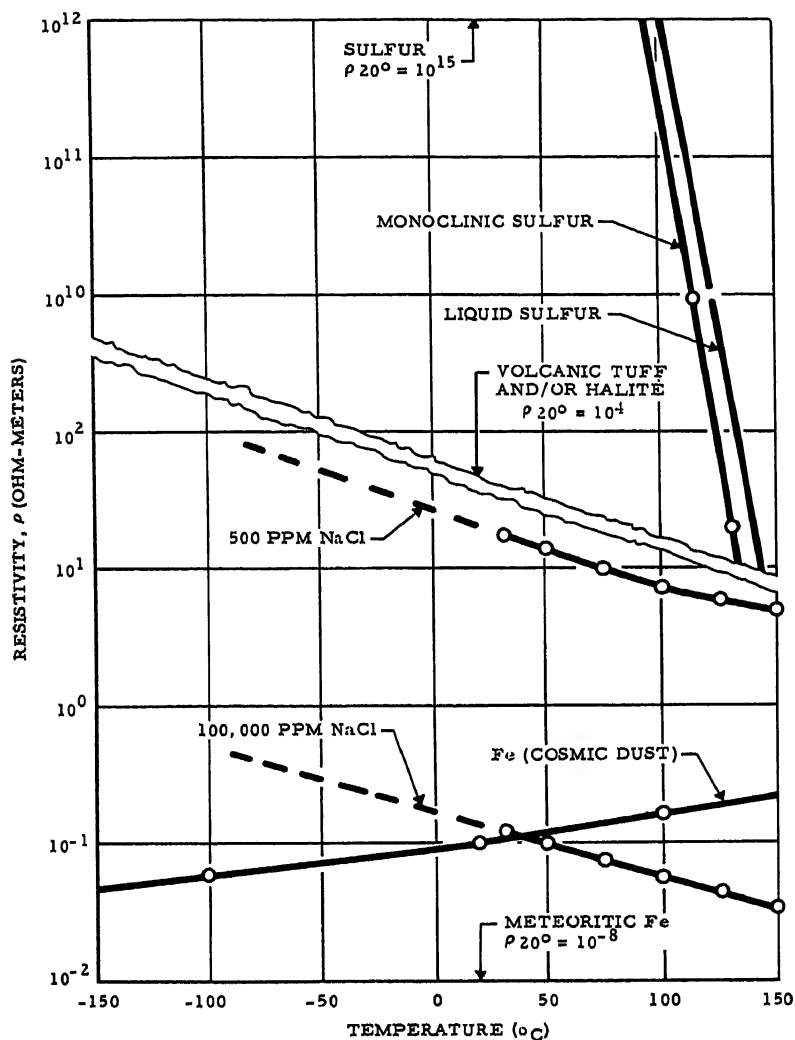


FIG. 44. Resistivity as a function of temperature for possible lunar surface materials.

For lunar exploration, the neutron log used in horizontal traverses or stationary on landing pads would not significantly contribute to an understanding of the surface lithologies. However, it would be of value in defining water-filled (or hydrocarbon-filled) vesicular rocks. The neutron log might also be definitive in distinguishing ice from dry rock.



*Neutron-Neutron Log*

Another neutron logging method, which is commercially available, avoids the effects of scattered gamma radiation. This method involves the use of a slow neutron detector instead of a gamma ray detector. Fast neutrons emitted by the source are recorded by the instrument after being slowed by the wall rocks. The instrument responds only to slow neutrons; it is not affected by the gamma rays of capture or any other gamma rays which may be present in the source. The slowing down of the fast neutrons emitted by the source is essentially proportional to the number of hydrogen nuclei present in the formation. According to Castel [83], the neutron-neutron log is a direct method of evaluating the amount of hydrogen contained in the formation.

In a formation of high water content, high-energy neutrons emitted by the source are quickly slowed down. Only a small number of them reach the counter, which results in a low reading. In a formation containing little or no hydrogen-bearing fluid, however, the fast neutrons emitted by the source have little chance to be slowed down or captured. Hence, a large number of them reach the counter to result in a high reading.

In oil fields, the neutron-neutron log has been used with considerable success in defining porous zones filled either with water or oil. On the Moon, a neutron-neutron device would be of value in locating ice or permafrost. The advantages of this log for lunar exploration are twofold. First, the response of the tool is independent of density changes in the rock. From the standpoint of the possibility of surface rock froths, a device designed for the detection of hydrogen should be insensitive to this parameter for accurate evaluation of the lunar hydrology. Secondly, the neutron-neutron log is not sensitive to radioactivity. If one wishes to associate radioactivity with hot-spring activity, as is justified in some instances on Earth, one would again prescribe a tool that would not confuse water content with radioactivity.

The disadvantage of the neutron-neutron log is that it will respond to elements of high neutron-capture cross-section, such as sulfur, chlorine and boron. These substances could conceivably be present in local accumulations or disseminated in volcanic ash, if wholesale defluidization of the lunar mantle occurred with a resulting enrichment of these elements on the surface.

*Discriminated Gamma Log*

Discriminated gamma logging, either horizontal or vertical, on the lunar surface is another valuable tool if indeed it is able to determine the quantitative distribution of uranium, thorium and potassium. As indicated in Table 8, these three elements will immediately distinguish mantle rocks (stony meteorites) from crustal rocks (rhyolites and basalts). The differences in radioactive element abundances are as much as two orders of magnitude apart. More importantly, however, discriminated gamma spectroscopy can provide information on the subtleties of lithologic composition of a lunar surface. Discriminated gamma analysis may provide data on the nature of the ray systems, because if they are silicic volcanic ash, they would certainly be enriched in potassium. If evaporates are present on a local scale, again potassium would be enriched. If fumarolic centers exist or once existed, they may be slightly radioactive in uranium salts. All of these possibilities warrant the use of a device that will distinguish uranium from thorium and potassium.

*Density Log*

Another logging device applicable to lunar exploration is the density log. As indicated in the range of densities in common rock types listed in Table 12, the density range in volcanic extrusives is the most extreme. By modifying the radioactivity logging sonde with a source of gamma radiation instead of neutron radiation, curves (sometimes called photon curves) are obtained that indicate the density of the strata traversed. This tool uses a collimated source of medium-energy gamma rays and a collimated scintillation crystal detector [94].

TABLE 12. Density Range of Common Rock Types

<i>Rock Type</i>	<i>Density Range</i>
Intrusive rocks	
Granite, quartz-diorite	2.5-2.9
Diorite-gabbro	2.7-3.1
Peridotite-dunite	3.2-3.4
Volcanic rocks	
Obsidian, pitchstone, rhyolite, dacite†	2.2-2.7
Pumice†	0.9-1.4
Andesite†	2.4-2.8
Basaltic glass† (one sample)	1.9
Basalt†	2.7-3.0
Sedimentary rocks	
Carbonates	1.8-2.9
Shale	1.6-2.9
Sandstone	2.0-3.2
Salt (halite)	2.1-2.3
Anhydrite-gypsum	2.2-3.0
Meteorites	
Nickel-iron†	7.6-8.05
Chondrites†	3.4-3.9
Metamorphic rocks	
Serpentine to dunite	2.45-3.34

† Considered most likely to exist on the Moon.

The scintillation counter has two advantages over the geiger counter or ionization chamber. First, the scintillation counter has a much higher sensitivity and therefore permits shorter time constants or greater logging speed. Second, the use of integral biasing makes the tool less sensitive to the chemical composition of the formation. The density log may be an ideal tool for the detection of lunar rock froths of widely differing rock types.

TABLE 13. Nuclear Methods of Lunar Surface Analysis

<i>Reaction</i>	<i>Advantages</i>	<i>Disadvantages</i>
<i>From 14-MEV neutron source</i>		
<i>Prompt gamma emission†</i>	From 10 to 20 cm of penetration; diagnostic for many elements	Shielding required
Neutron, elastic and inelastic Multiple particle emission Neutron albedo; neutron relaxation Induced radioactivity	Simplicity	Ambiguity of interpretation Not diagnostic of elemental species Not diagnostic of elemental species Severe scattering, shallow depth and penetration Not diagnostic of elemental species Not suitable for identification of light elements Ambiguity of interpretation
Proton and alpha emission Fission fragmentation Delayed gamma emission		
<i>From 14-MEV proton source</i>		
<i>Neutron emission†</i> <i>Delayed radioactivities†</i> Elastic and inelastic scattering of protons Inelastic gamma rays	Little shielding, low scattering Clean spectrum Ease of collimation, no pulsing required	Shallow (1 mm) depth of penetration Shallow (1 mm) depth of penetration Shallow (1 mm) depth of penetration Complex spectrum. requires magnetic analyzer

† Considered most important in lunar exploration. Modified from Martina and Schrader [100].

Gamma radiation is permitted to leave the source only in a conically shaped beam by using a tungsten collimator. For stationary surface use on the Moon, a gamma source might be placed in one leg of a stationary vehicle and a detector in another leg; for mobile surface use, a hemispherical shape would be required.

The principle of the density log operation is not complicated. Assuming that single Compton scattering is the dominant process, rock density governs the response of the detector. For very low densities or very penetrating radiation, the counting rate increases with increasing density.

### *Magnetic Susceptibility Log*

The magnetic susceptibility log has received very limited use in petroleum exploration. Possibly this is due to highly specific applications—for example, stratigraphic correlation of iron-rich beds. The application of this logging device in sediments is discussed in detail by Veshev *et al.* [95], Karus and Zuckernik [96], and Broding *et al.* [97]. Magnetic susceptibility is perhaps a more valuable parameter in identifying igneous rocks. Most basalts have a higher magnetic susceptibility than other extrusive types (Fig. 45). There are some interesting exploration aspects of locating iron-nickel meteorite

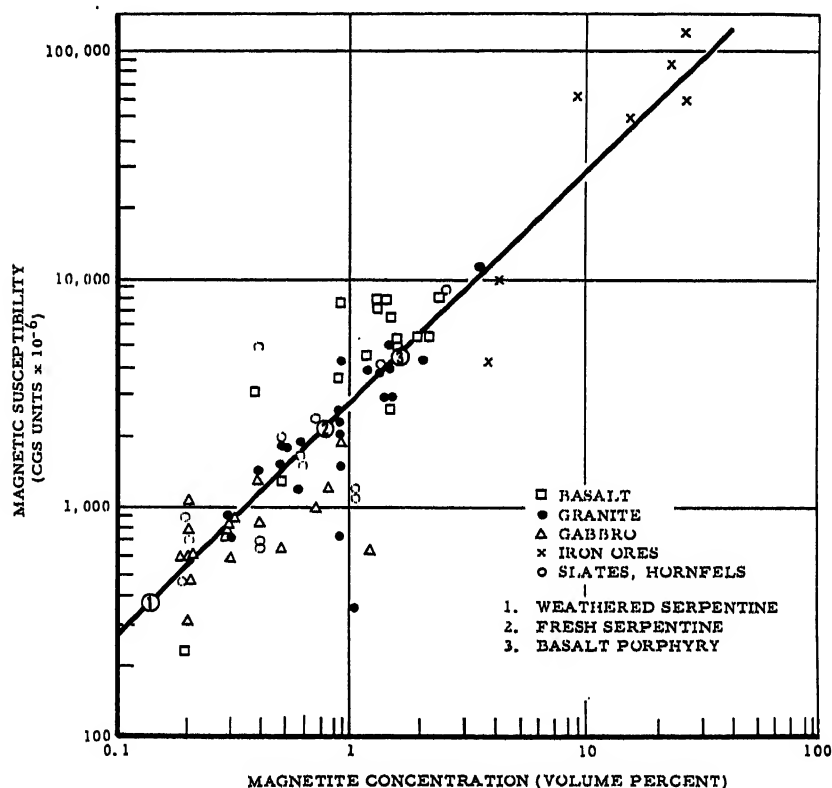


FIG. 45. Magnetic susceptibility of igneous rocks versus magnetite concentration (After Mooney and Bleifuss [101]; Broding *et al.* [97]; Nagata [102].)

masses by a device of this type. A sizable literature exists on other magnetic dredges specific for meteorites ([98], pp. 258-64).

One might speculate on the intensity of magnetic susceptibility as a function of the distance from an eruptive center. Also, hydrothermal alteration in volcanics (as may exist in colored areas such as Aristarchus on the Moon) drastically reduces magnetic susceptibility by alteration of magnetite to pyrite.

The Soviet lunar probe indicated the magnetic field of the Moon to be less than 50 gammas. Therefore, because the induced magnetization is affected by the strength and direction of the applied magnetic field, magnetic susceptibilities of lunar rocks would be lower than their terrestrial equivalents. The relative differences in susceptibility will remain the same, however. The magnetic susceptibility log of Broding *et al.* [97] is an alternating current induction device with a sensitivity of  $1 \times 10^{-6}$  cgs units. This log is analogous to the gamma log in that it measures a natural property of the rock which is not necessarily specific to the rock type. For example, some tuffs are highly magnetic while others are only weakly so. Magnetic susceptibility is reduced and coercive force is increased with a decrease in grain size. These variations could be important considerations in interpreting magnetic variations in cosmic infall material which could be extremely fine-grained (in the  $1 \mu$  diameter range). In contrast, marked uniformity may be the rule for lunar welded tuffs if they exist, and if we may extrapolate to the Moon the data obtained by Hatherton [99] on the Whakamaru welded tuffs of New Zealand.

## (B) NUCLEAR SPECTROSCOPIC TECHNIQUES

Volcanism is a surficial result of a more fundamental process called defluidization, which is the release of volatiles from the interior of a cosmic body at any given rate and at any time. For example, the enrichment of chlorine in sea water is thought to be the result of its addition to the hydrosphere from volcanic sources over geologic time. A part of the volume of the seas is also thought to have evolved by defluidization of the Earth's mantle. The majority of elements released to the surface by the defluidization processes have high thermal neutron-capture cross-sections. This means that such elements and their compounds may be easily detected by nuclear prospecting techniques.

Therefore, the degree of importance of lunar nuclear spectroscopy is based on the particular mechanism which has formed the surface of the Moon. If the mechanism is volcanic, nuclear prospecting assumes importance because elements such as sulfur, boron and the halogens (except fluorine) may easily be detected by this technique, even under dust. On the other hand, if impact is considered the dominant mechanism, there will be no mineralization diagnostic of volcanism, and nuclear prospecting is not as important. However, this should not be interpreted as cause for eliminating nuclear tools on the Moon. The most abundant metallic elements in an impacted terrain—iron, nickel and chromium—have high thermal neutron-capture cross-sections (2.5, 4.6 and 2.9 barns, respectively).

An outstanding merit of the neutron gamma reaction is its ability to analyze a volume of material, not a surface layer. It could thus analyze through a thin surface cosmic infall layer. The pulsed deuterium-tritium

accelerator described by Martina and Schrader [100] has a depth of penetration of neutrons of some 10 to 20 cm of Earth materials in contrast to the 1 mm depth of penetration of protons. The advantages and disadvantages of the proton-gamma and neutron-gamma systems are outlined in Table 13 together with other nuclear techniques suggested by Martina and Schrader. The neutron-gamma system prescribed by these authors includes a pulsed DT accelerator source, pulse height analyzer and data display system.

The Moon represents an area on which the nuclear spectroscopy log may prove itself superior to surface measuring devices. A spectrum of sulfur that is achieved by a nuclear log, employing a polonium-beryllium neutron source, is shown in Fig. 46. Chlorine, another element of much interest and of wide-

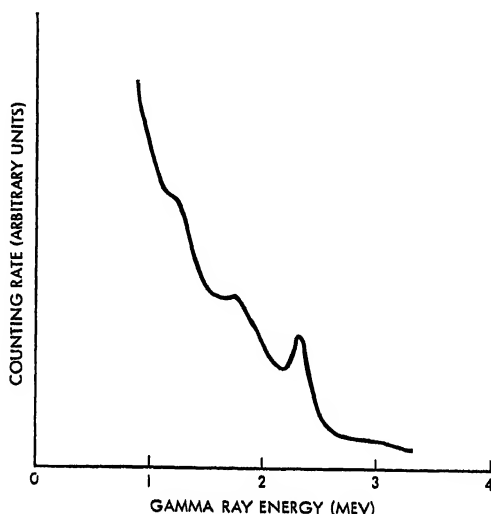


Fig. 46. Counting rate versus gamma ray energy (showing sulfur peak) (After Caldwell and Sippel [94]).

spread abundance on Earth and possibly on the Moon, may be detected in a silica matrix using nuclear spectroscopy techniques (Fig. 47).

#### *Detection Limits*

Figures 46 and 47 show that mineralization can be identified in rock matrices. According to information released by California Research Corporation detectable limits for elements that have been found in artificial formation in the laboratory using nuclear spectroscopy techniques (Dr. P. E. Baker, personal communications) are: hydrogen, 0.6%; silicon, 7%; calcium, 3.6%; chlorine, 0.3%; aluminum, 12%; iron, 1.4%; magnesium, 15%; and sulfur, 2.4%. The minimum detectable limits for other elements (not included in artificial laboratory formations but based on thermal neutron capture cross-sections) are: potassium, 4.2%; manganese, 15%; and sodium, 5.9%. These figures are based on sedimentary rock matrices, and some uncertainty must be realized in extrapolating these minimum detection limits to igneous rock and meteorite matrices. These limits vary, depending upon

the concentration of associated compounds whose elements may compete in neutron absorption with a reference element. These limits are graphed in Figs. 48 to 51, assuming that no interfering effects are present. Certain detection limits will probably be lowered with refinements in instrumentation.

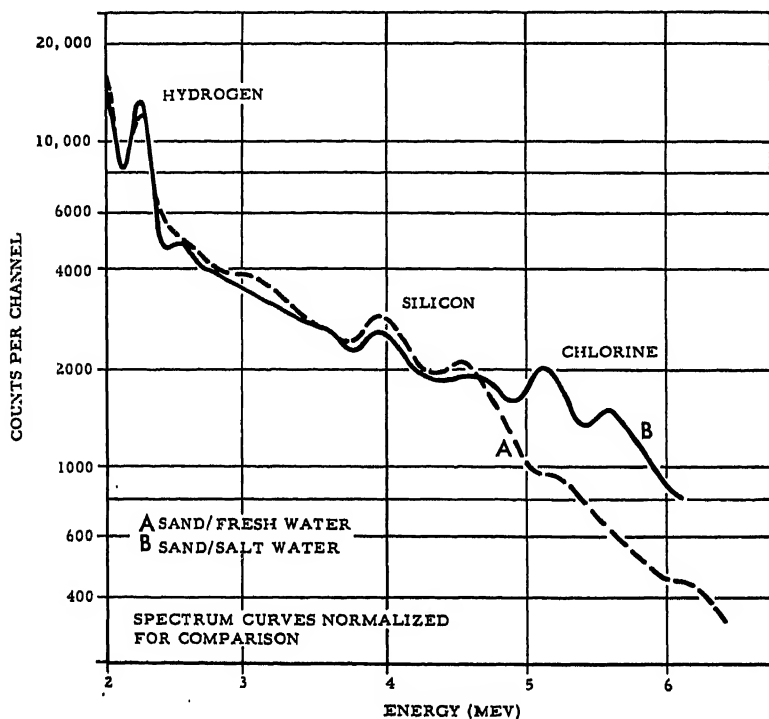


FIG. 47. Counting rate versus gamma ray energy (showing hydrogen, silicon and chlorine peaks) (After Baker [103]).

The minimum nuclear log limits are based on neutron-gamma reactions of elements of neutron capture-cross-sections given in Table 14. The elements are grouped in categories of lunar significance.

Silicon, although of low thermal neutron-capture cross-section (0.13 barns), is so abundant in all rock types that its concentrations is well within the minimum detectable limit of 7% (Fig. 48). All rock types could thus be analyzed by neutron-gamma techniques for silicon variations. The prospect of adequately defining aluminum by such reactions is not good, even with considerable lowering of the minimum detection limit. However, other techniques such as induced radioactivities are quite suitable for aluminum analysis by nuclear methods.

Iron, on the other hand, is amenable to the neutron-gamma analysis methods. Almost all rock types—cnstatite chondrite, anorthosite and serpentine excluded—are above the assumed minimum detectable limit of 1.4% (Fig. 49). Nickel-iron meteorites are not shown; they have iron contents of about 91%. Manganese concentrations are too low in common

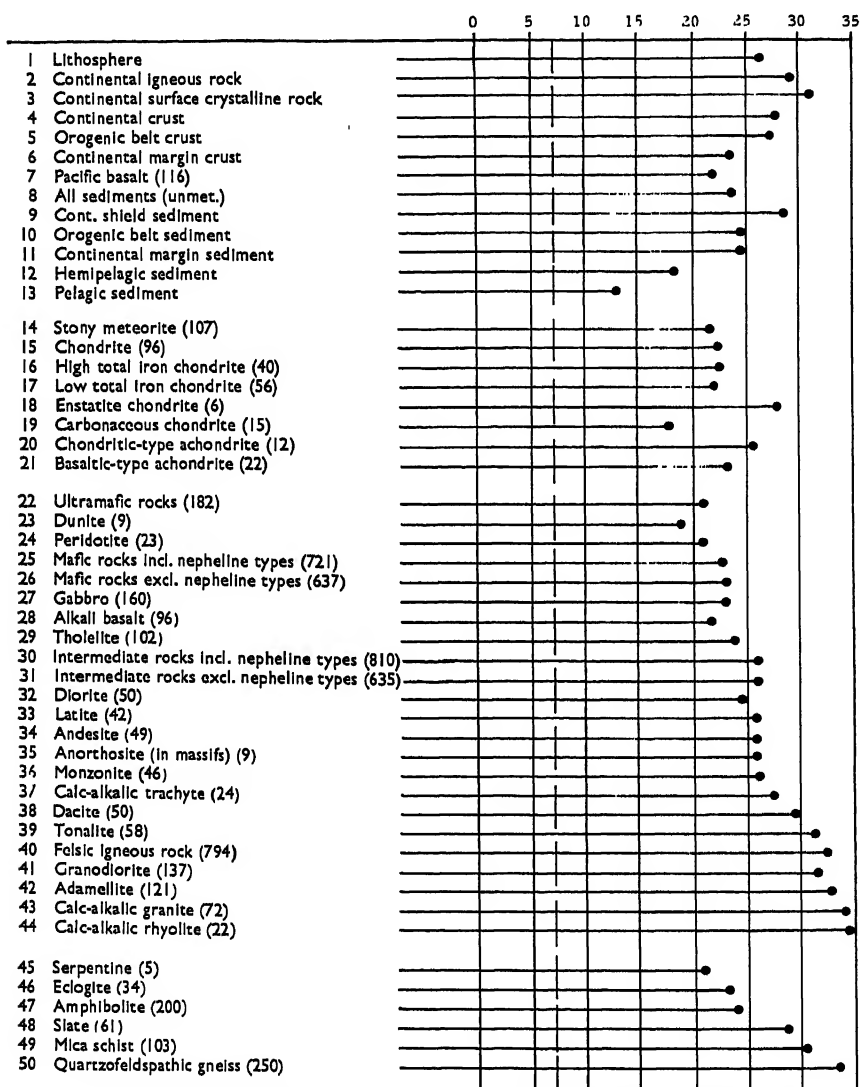
TABLE 14. Significant Elements in Lunar Spectroscopy

<i>Element</i>	<i>Thermal Neutron-capture cross-section (barns)</i>	<i>Element</i>	<i>Thermal Neutron-capture cross-section (barns)</i>
Non-maria volcanic rocks		Meteorites (chondritic and iron)	
Silicon	0.13	Iron	2.5
Aluminum	0.23	Chromium	3.1
Sodium	0.53	Nickel	4.6
Potassium	2.0		
Maria volcanic rocks		Other major silicate elements	
Magnesium	0.063	Oxygen	0.0002
Calcium	0.43	Carbon	0.0032
Iron	2.5	Phosphorus	0.20
		Titanium	6.0
		Manganese	13.3
Volcanic mineralization		Significant trace elements	
Hydrogen	0.33	Strontium	1.3
Sulfur	0.49	Copper	3.7
Iodine	6.3	Vanadium	4.9
Bromine	6.6	Lead	8.0
Chlorine	33	Lithium	71
Boron	755	Cadmium	3300
		Gadolinium	38000



rock types to be detected by the nuclear prospecting system endorsed. The lack of character to the abundance data of manganese would indicate that if manganese were detected, it could be interpreted as being manganese mineralization regardless of the nature of the host lithology. However, magnesium concentrations show a wide range (Fig. 50). Certain groups, such as the chondrites, the ultramafic rocks and serpentines, are above the minimum detectable limit.

If the detection limit of calcium in an igneous rock matrix is 3.6 as

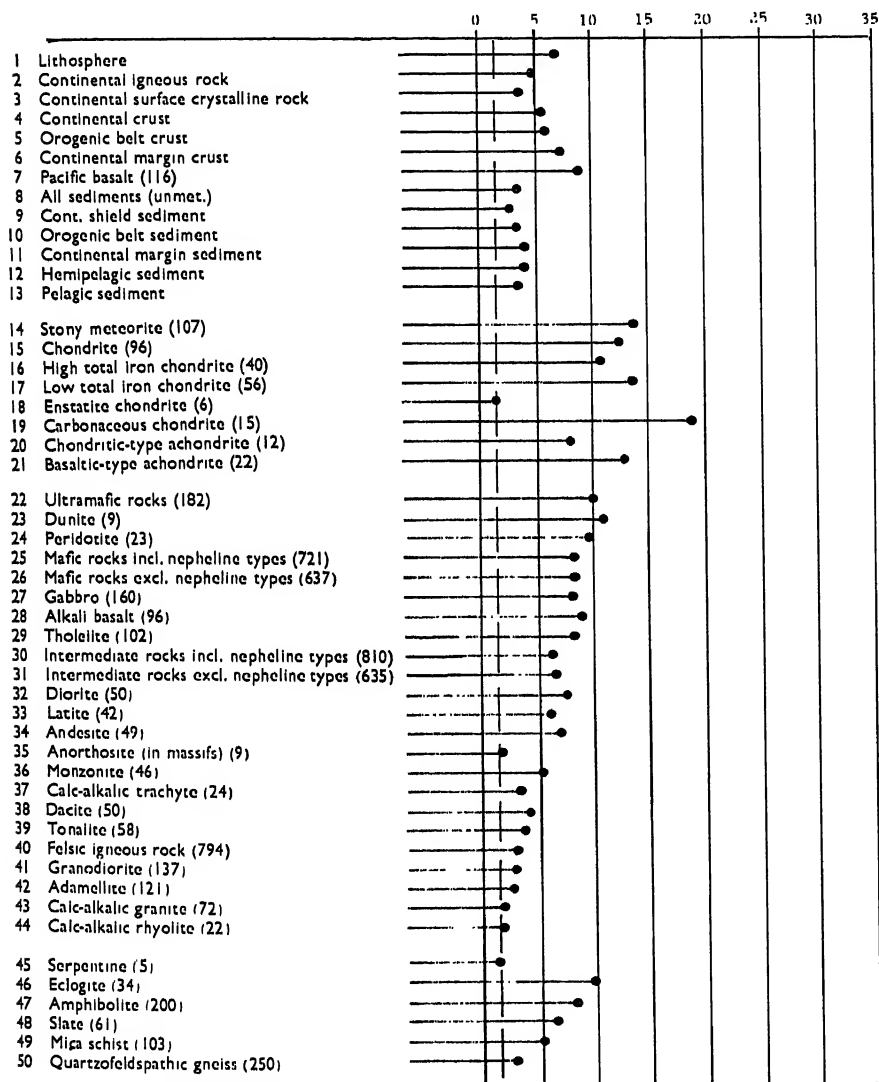


Numbers in parentheses indicate the number of individual analyses involved in determining the average.

FIG. 48. Silicon content in rocks.

assumed, this element falls in between chondrites and most ultramafic and mafic rocks (Fig. 51). One might conceivably distinguish between gross rock types on a yes-no basis by setting the instrument on critical concentration detection levels. On the Moon, high calcium contents would be improbable unless travertine dikes, as associated with certain South African and Arizona diatremes, are abnormally abundant.

The capabilities of the neutron-gamma nuclear log are poor as far as sodium detection is concerned. Even the most alkalic igneous rock falls well

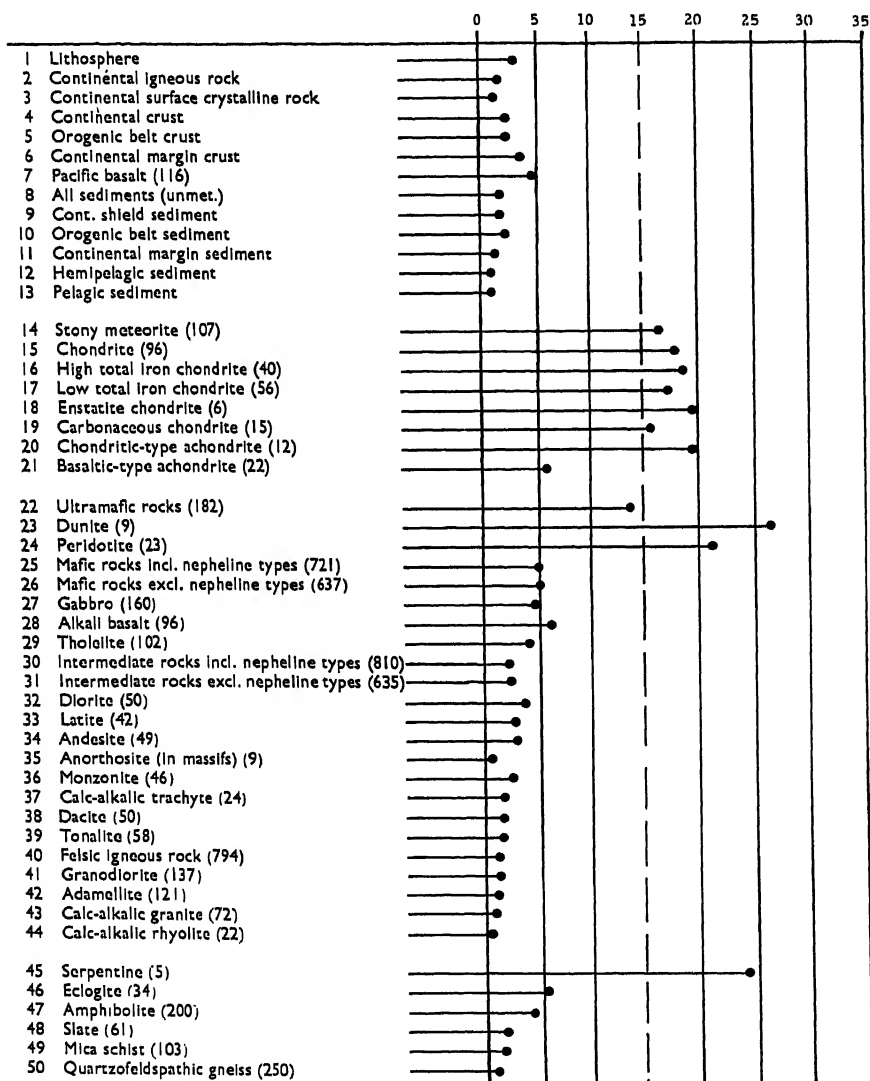


Numbers in parentheses indicate the number of individual analyses involved in determining the average.

FIG. 49. Iron content in rocks.

below the assumed minimum detection limit of 5.9%. One might possibly detect potassium in these alkalic rock types. Doubtless, phosphorus is almost impossible to detect when present in normal concentrations in rocks since its cross-section is only 0.19 barns. Chromium, on the other hand, has a larger cross-section of 2.9 barns. No data are available as to what the minimum detection limit of this element might be in iron meteorites.

Because sedimentary processes are considered unlikely on the Moon, the presence of carbon is also improbable. However, high-energy accelerator neutron sources have been used on an experimental basis to detect organic

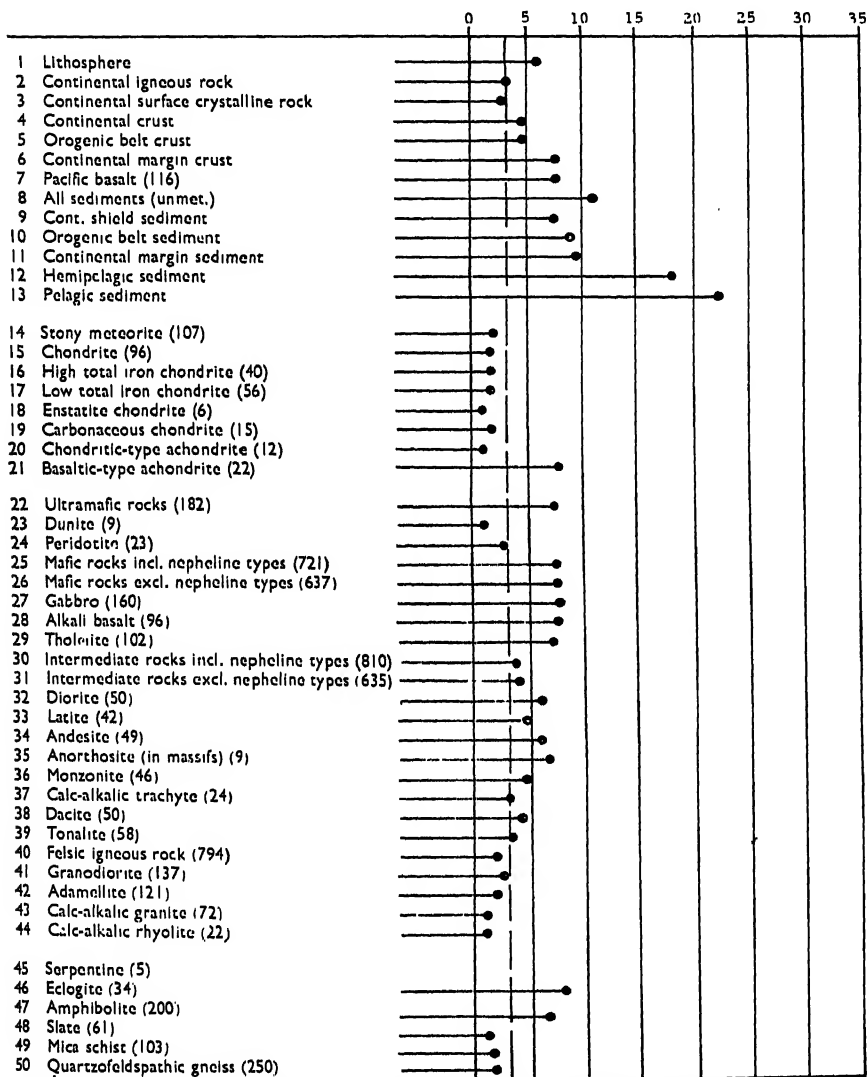


Numbers in parentheses indicate the number of individual analyses involved in determining the average.

FIG. 50. Magnesium content in rocks.

carbon in the borehole [104]. Probably carbonaceous chondrites could also be detected by this technique. Titanium, with small range and low concentration in rocks, is not considered a likely element for lunar prospecting in spite of its high neutron-capture cross-section of 5.6 barns.

From the preceding discussion, we may conclude that silicon, iron, magnesium and calcium are suitable elements for lithologic analysis of the lunar surface of the Moon using neutron-gamma reactions with a DT accelerator source. For detection of volcanic mineralization, Table 14 shows that sulfur,



Numbers in parentheses indicate the number of individual analyses involved in determining the average.

FIG. 51. Calcium content in rocks.

chlorine, boron, iodine and bromine all have high thermal neutron capture cross-sections. The abundant elements in impacted terrains (iron, nickel and chromium) are also of high cross-section. The depth beyond 10 to 20 cm to which iron-nickel debris might exist on the Moon could, however, be best detected by a two-curve magnetometer.

Both the neutron-gamma and the proton-gamma systems of the type outlined by Martina and Schrader [100] are endorsed for incorporation in a more sophisticated lunar vehicle for the reasons outlined below:

<i>Source</i>	<i>Weight of system</i>	<i>Depth of analysis</i>	<i>Material analyzed</i>
14 mev neutron source from DT accelerator	25 kg	10-20 cm	Subsurface volcanic mineralization, host lithologies, and permafrost (?)
14-mev proton source from accelerator	25 kg	1 mm	Cosmic infall layer, surface lithologies, and surface-induced radioactivities by external solar and cosmic radiation

The risk of discounting one hypothesis and instrumenting lunar probes on the basis of the other is too great to consider at this stage of space exploration. Volcanism offers: (1) better prospects of water in various forms, (2) mineralization that would prove vital in maintaining a scientific base, (3) terrain advantages for protection and concealment, and (4) easily manipulated building materials. Therefore, consideration of the best tools to interpret a volcanic surface is at least as important as interpreting an impacted lunar surface. Prospecting for elements of high neutron-capture cross-section by nuclear spectroscopic techniques has been recommended [105]. In particular, the pulsed DT accelerator neutron-gamma technique suggested by Martina and Schrader [100], has been proposed.

#### (c) GEOPHYSICAL TRAVERSES

Of the numerous geophysical tools that might be applied to the lunar surface, four in addition to the geophone deserve mention. These are the magnetometer, bolometer, gravimeter and scintillometer. Four important geophysical traverses involving these instruments, across an invaded lunar crater of meteoritic impact origin and across one of volcanic origin, are shown in Fig. 52. For both the impact and volcanic crater, invasion by basalt on the seaward side is assumed. The letter *f* in the volcanic crater denotes an active fumarole. Numbers at the top of the diagram will be referred to for correlating the curves with surface features. This figure is applicable both to altitude and surface surveys with the exception of the two-curve magnetometer. For the purposes of this discussion, the near surface curve will be considered the one applicable for the lunar surface magnetometer traverse.

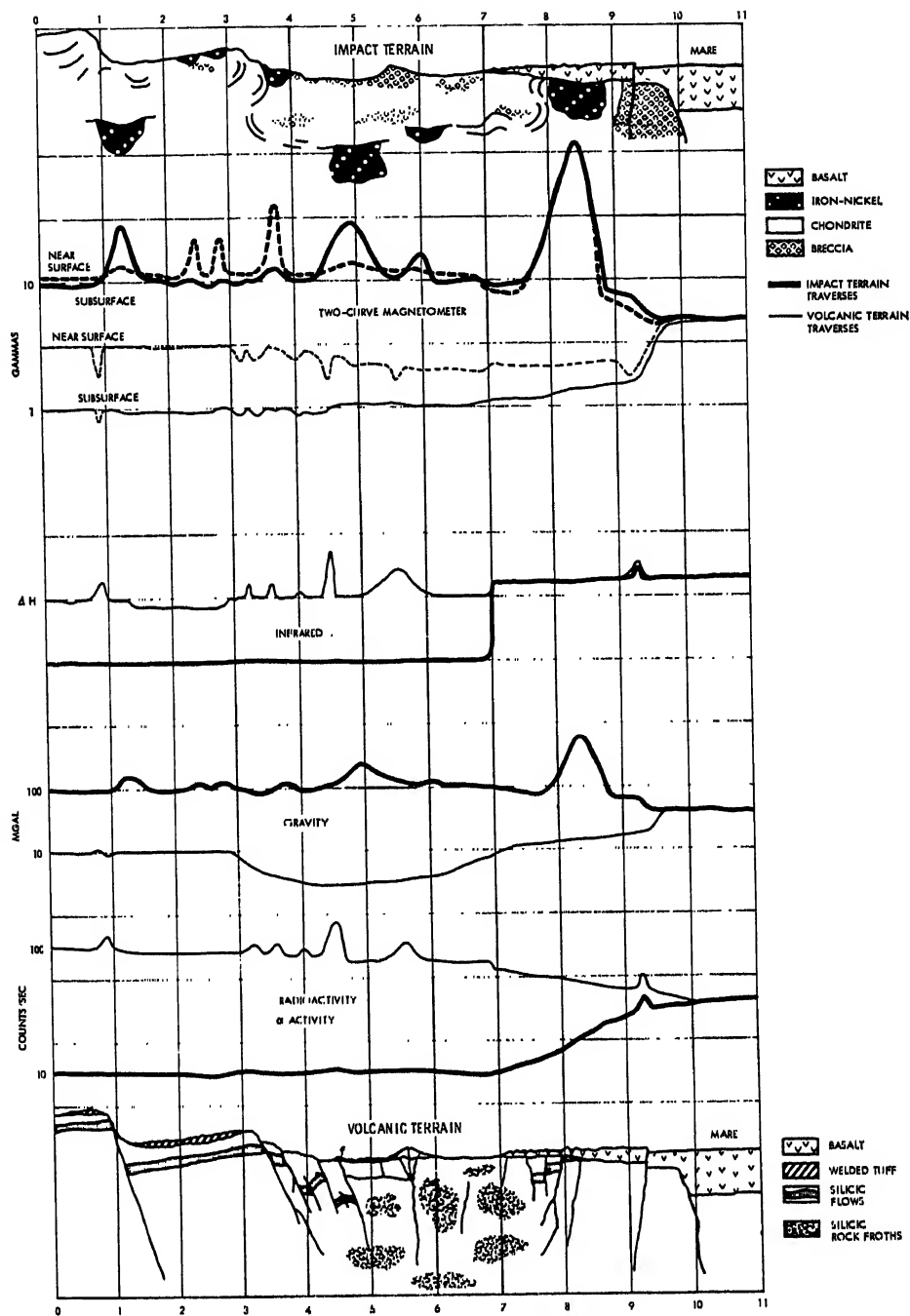


FIG. 52. Geophysical surface and altitude surveys across invaded lunar crater.

The gross difference between the near-surface magnetometer profile across an impacted terrain and that of a volcanic terrain reflects the order of magnitude difference between the magnetic susceptibilities of volcanic and chondritic material. This difference would exist even in the weak magnetic field present on the Moon. Theoretically, the near-surface curve of the magnetometer traversed on an impacted terrain would be in contrast in other ways with that of a traverse across a volcanic terrain. For example, to the left of point 1 on the volcanic terrain, surface expression of a normal fault could be reflected because of two possible mechanisms. The first is that faulting is sometimes accompanied by hydrothermal alteration and the production of minerals of lower magnetic susceptibility than the original minerals. The second mechanism would be the disruption of the surface layer of magnetic cosmic infall material thereby exposing the less magnetic volcanic ash or breccia.

On the other hand, the impacted terrain to the right of point 1 (Fig. 52) illustrates a deeply buried but large iron-nickel mass or its fragments. The near-surface curve, although not reflecting this mass as strongly as if it were closer to the surface, shows an anomaly in an opposite sense to that illustrated by the curve representing the traverse across the volcanic crater. More distinct anomalies in the impact terrain are indicated along the near surface magnetometer curve at points 2.5, 2.8 and 3.7. The fairly even magnetometer profile from 1 to 3 across the volcanic terrain is possible if the data by Gerard and Lawrie [95] may be extrapolated from welded tuffs in New Zealand to lunar crater flanks in non-mare areas. This is so because many welded tuffs have a remarkably uniform magnetic susceptibility.

Inasmuch as the internal features of calderas on Earth originate at a later time than the caldera walls and flanks themselves, one might expect fresher surfaces of silicic material and correspondingly thinner accumulations of cosmic infall material on the caldera floors. The fractures on the caldera floor may therefore be more recent than the one at point 1. The fumarole *f* is also shown as being free of cosmic infall material. The most recent large-scale event illustrated is the invasion of the crater by basalt. A slight increase in the near-surface curve from 7 to 9 reflects the greater magnetic susceptibility of the basaltic rock type. The curve rises in response to an increasing thickness of basalt seaward, with the exception of a slight dip reflecting the fault intersection at 9.3.

On the basis of the previous discussion concerning the infrared characteristics of meteoritic and volcanic materials, it is possible to obtain the pattern shown by the infrared response curves. However, the anomalies along the curve representing the volcanic terrain deserve amplification. Near point 1, a positive anomaly indicates an above-normal heat flow from a fault. The volcanic crater floor may possibly be warmer than the crater flanks because of numerous rim fractures, as at 3.2 and 3.5, and a central extinct volcano. Volcanoes, even if not active, commonly exhibit hot-spots. The sharpest anomaly at 4.5 (marked by *f* on the volcanic terrain) indicates a fumarole. Many of the dark spots in the crater Alphonsus are thought by some to represent fumarolic activity. From 7 onward, a slight increase in infrared activity over that of the welded tuff on the crater flanks is indicated because of the greater percentage of absorption of heat in the darker basalt. However, this is not to be confused with heat generating potential. Silicic rocks, such

as rhyolite or tuff, have a higher concentration of uranium, thorium, and potassium, than basalt.

A slight positive anomaly at 9.2 reflects a fault cutting the basalt. In the infrared curve representing the traverse across the impacted terrain, the low and uniform radioactive element content of chondrites accounts for the low heat flow as compared with the volcanic infrared curve. The anomaly at 9.3 is lower than over the volcanic terrain. This is because the heat flow from buried chondritic rocks is lower than that from the buried silicic rocks.

With regard to the gravity pattern over an impacted terrain, some of the large buried masses of metallic meteorites, as at 1.2, 5 and 8.3, would create anomalies: the larger and more shallow the buried meteoritic mass, the greater the gravity anomaly. The overall greater density of stony meteorites would cause the gravity profile to be above that of the volcanic traverse, particularly if rock froths contribute to the lunar surface rocks. A gravity low is predicted across the volcanic crater (Fig. 52) if results from the Kuttayaro gravity survey in eastern Hokkaido, Japan, can be extrapolated as a general case, and if we assume the volcanic crater shown to a caldera of the Krakatoa type.

In Hokkaido, Japan, a gravity survey made in March 1958, on the frozen surface of the lake filling the caldera showed a low Bouguer anomaly of about 46 milligals concentrated in the center of the caldera [107]. Analysis of the distribution of anomalies shows that low-density material (pumice), about 0.3 to 0.5 g/cc less dense than the surroundings, has accumulated to a depth of 3 to 4 km beneath the lake. In calderas formed by the subsidence of rock masses without eruption of pumice (the Glencoe type), higher Bouguer anomalies should be observed. This has actually been observed in a caldera of this type; the Mihara caldera shows a high of about 15 milligals in the crater center [108].

With the exception of the magnetometer traverse, most of the geophysical curves over meteoritic terrains may possibly be more monotonous than over a volcanic terrain. This may best be illustrated by the radioactivity traverses. Over a meteoritic landscape, the abundances of the radioactive elements giving rise to alpha activity are orders of magnitude lower than these elements in volcanic rocks. The gradual increase in radioactivity in the meteoritic traverse from 7 to 9 reflects the increasing thickness of basalt. Regarding the volcanic terrain profile, blips in the curve at 1, 3.2 and 3.5 reflect radon leakage along faults bordering the caldera. The large anomaly at 3.5 is ascribable to radon leakage from a fumarole.

Additional geophysical traverses could also be plotted on a diagram of this type, and other features of both an impact and volcanic nature could be incorporated into the sketches. Geophysical techniques may prove to be decisive in analyzing lunar surface and subsurface structures.

More geophysical traverses over volcanic and meteoritic craters on Earth are required so that lunar return data can be more fully interpreted. An excellent example of a terrestrial study of this type is that given by Nemoto *et al.* [75] who performed numerous geophysical traverses across the Usu (Shōwa-Shinzan) volcano in south-western Hokkaido, Japan. Gravity, seismic, magnetic, electrical, and radioactivity surveys and temperature measurements were made to study underground structures and surface phenomena.



## CONCLUSIONS

The application of the geo-sciences to manned lunar exploration may be divided into five groups: terrain, rocks, minerals, power and tools. By understanding the processes which formed certain features on Earth, we will be more capable of realizing the advantages of impacted and volcanic terrains on the Moon. A lunar terrain would offer more natural protection to man. Volcanic rocks would also be more useful to the lunar astronaut than meteoritic rock because of the adaptability of certain volcanic materials for insulation and because their water content is much higher (approximating 1% by weight).

Moreover, water in the form of ice is more likely to be found in the eternally shadowed zones of a volcanic surface than an impacted one. Sulfur may also be a valuable raw volcanic material for use as waterless cement. The uses of cosmic infall dust, if ferrous, are obvious. Heat produced by impact would tend to be dissipated rapidly in contrast to internal heat developed in tectonic zones of weakness. In this case, possible fumarolic activity or radon leakage may exist in these fracture zones.

The tools best-suited for a study of these features depend on the predicted range of environmental and surface conditions. For example, inspection of possible surface vesiculation of melts extruded into vacuum would favor the application of a density log. The geophone would also be valuable in determining whether surface or subsurface noise were the dominant expression of energy release. Geochemical investigation of the subsurface would require a form of nuclear prospecting device. The prompt gamma emission technique may be used to analyze for elements of high neutron-capture cross-section common to both impact and volcanic terrains.

These analytical methods of lunar exploration would yield information not only concerning the lunar crust but also regarding the origin and development of the Earth's crust, such as the origin of continents and the permanency of the ocean basins. The presence of water in any form on the Moon, particularly as ice in the shadowed zones, could provide data on the nature of pre-life sea water on Earth. Finally, the nature of the lunar craters would be a logical preliminary step in the interpretation of the surface features of other cosmic bodies.

## ACKNOWLEDGMENTS

The writer is indebted to Drs. C. Amstutz, K. von Bülow, P. D. Lowman, A. Poldervaart, E. Roedder, E. M. Shoemaker, H. C. Urey and many others for discussion of arguments presented here. Few of these people fully agree with the author on the major premise of volcanism, but all have stimulated thought and creative controversy. Portions of this paper are based on a North American Aviation S&ID report prepared by the author and entitled "Geophysics as Applied to Lunar Exploration" (AFCLR Document No. AFCLR-TR-60-409).

## REFERENCES

1. Morey, G. W. *J. Wash. Acad. Sci.* **12**, 219-30 (1922).
2. Williams, H. *Univ. Calif. Publ. Geol. Sci.* **32**, 239-346 (1941).
3. Bemmelen, R. W. van. *De Mijnningenieur* no. 4 (1949).
4. Miyamoto, S. *Contr. Inst. Astrophys. Kyoto. Univ.* no. 96, 6 pp. (1960).
5. Turner, F. J. and Verhoogen, J. "Igneous and Metamorphic Petrology". McGraw-Hill Book Co., New York, 602 pp. (1951).

6. Verhoogen, J. Thermodynamics of a magmatic gas phase: *Univ. Calif. Publ. Geol. Sci.* **28**, 91-136 (1949).
7. Gilbert, G. K. *Bull. Phil. Soc. Wash.* **12**, 241-92 (1893).
8. Williams, H. *Quart. J. Geol. Soc. Lond.* **109**, 311-32 (1954).
9. Minakami, T. *Bull. Earthq. Res. Inst. Tokyo*, **20** Pt. I, 65-92 (1942).
10. Yoder, H. S., Jr. *J. Geol.* **60**, 364-74 (1952).
11. Uffen, R. J. *J. Geophys. Res.* **64**, 117-22 (1959).
12. Chao, E. C. T., Shoemaker, E. M. and Madson, B. M. *Science* **132**, 220-22 (1960).
13. Proctor, R. A. "The Moon", second edition 160 pp. (1878).
14. Nichols, R. L. *Trans. Amer. Geophys. Un. Pt. 3*, 432-33 (1939).
15. Boneff, N. *Ast. Nachr.* **260**, 422-26 (1936).
16. Boneff, N. *Annu. Univ. Sof. (Faculté des Sciences)* **44**, (1947-1948), Livre I: Math. et Phys., 67-82 (1948).
17. Boneff, N. *Annu. Univ. Sof. (Faculté des Sciences)* **50**, 1955-56, Livre I: Math. et Phys., pt. I, 177-81 (1957).
18. Boneff, N. *Annu. Univ. Sof. (Faculté des Sciences)* **50**, 1955-1956, Livre I: Math. et Phys., pt. II, 121-28 (1958).
19. McBirney, A. F. *Bull. volcan., Ser. 2*, **17**, 145-54 (1955).
20. Machado, F. *Bull. volcan., Ser. 2*, **17**, 119-25 (1955).
21. Kuno, H. *Internat. Geol. Rev.* **1**, 48-59 (1959).
22. Vlodavets, V. I. *Akad. Nauk S.S.S.R. Lab. vulkanol. Byull. vulkanol. stantsii*, no. 23, pp. 38-46 (1954).
23. Namba, M. and Murota, T. *Kumamoto J. Sci., Ser. A*, **1**, 66-73 (1952).
24. Sicardi, L. *Bull. volcan., Ser. 2*, **18**, 151-58 (1956).
25. Kuno, H. *Trans. Amer. geophys. Un.* **34**, 269-80 (1953).
26. Roux, J. *C.R. Soc. geol. Fr.* **13**, 318-19 (1958).
27. Richards, A. F. *Volcano Lett., Hawaii* **7**, p. 519 (1953).
28. MacDonald, F. A. and Alcaraz, A. *Bull. volcan., Ser. 2*, **18**, 169-78 (1956).
29. Monyaylov, A. A. *Akad. Nauk. S.S.S.R., Lab. vulkanol. Trudy* **8**, 115-25 (1954).
30. Baldwin R. B. "The Face of the Moon", Chicago University Press, 239 (1949).
31. MacDonald, G. A. and Eaton, J. P. *Volcano Lett. Hawaii* no. 524, 1-9 (1954).
32. Escher, B. G. *Bull. volcan., Ser. 2*, **16**, 55-70 (1955).
33. Green J. *Prop. Lunar and Planet. Explor. Coll.* **1**, 1-18 (1959).
34. Bülow, K. von. *Geologie* **6**, 565-609 (1957).
35. Verhoogen, J. *Amer. J. Sci.* **249**, 729-30 (1951).
36. Spurr, J. E. "Geology as Applied to Selenology" Science Press (1945).
37. Barth, T. F. W., 1952, *Schweiz. min. petrog. Mitt.* **32**, 354-60.
38. Chamberlin, R. T. *J. Geol.* **53**, 361-73 (1954).
39. Escher, B. G. *Bull. volcan., Ser. 2*, **12**, 33-47 (1952).
40. Shoemaker, E. M. "Impact Mechanism at Meteor Crater, Arizona" (AEC report), 55 pp. (1959).
41. Wright, F. E. "Cooperation in Scientific Research", Carnegie Institution, Washington, 59-74 (1938).
42. Dicke, R. H. and Beringer, R. *Astrophys. J.* **103**, 375-76 (1946).
43. Whipple, F. L. "Vistas in Astronautics: II Annual Astron. Symp". Pergamon Press, 2, 267-72 (1959).
44. Gold, T. "Vistas in Astronautics: II Annual Astron. Symp". Pergamon Press, 261-66 (1959).
45. Gilvarry, J. J., *Nature, Lond.* **181**, 751-62 (1958).
46. Wesselink, A. M. *Bull. Astron. Inst. Netherlands* **10**, 351 (1948).
47. See, T. J. J. *Publ. astr. Soc. Pacif.* **22**, 13-20 (1910).
48. Barabushov, N. P. and Chokirda, A. T. *Astr. Zhurn.*, **36**, 851-55 (1959).
49. Brunsehwig, M., et al. *Rep. Univ. Mich.* **3544-1-F**, 81 pp. (1960).
50. Billings, M. P. "Structural Geology," Prentice-Hall, New York, 473 pp. (1942).
51. Nichols, R. L. *J. Geol.* **44**, 617-30 (1936).
52. Perrot, F. A. *Publ. Carneg. Instn.* no. 549, 162 (1950).
53. Washington, H. S. *Amer. J. Sci. Ser. 5*, **6**, 409-23 (1923).
54. Voldán, J. *Reports of the Glass Res. Inst. Hradec Králové, CSR, Silikatechnik* **7**, Heft 2, 48-53 (1956).
55. Vlček, O. S. *Tech. Digest* (Prague) (1960).
56. Brown, H. "A Bibliography on Meteorites", Chicago University Press, Chicago 686 (1953).

57. Krinov, E. L. "International Series of Monographs on Earth Sciences", Pergamon Press, Oxford 7 (1960).
58. Kennedy, G. C. "Modern Chemistry for the Engineer and Scientist", McGraw-Hill Book Co., New York 256-75 (1957).
59. Sytinskaya, N. N. *Astron. Zhurn.* 36, 315-21 (1959).
60. Rubey, W. W. *Geol. Soc. Amer. Special Paper No. 62*, 631-50 (1955).
61. Poldervaart, A. *Geol. Soc. Amer. Special Paper no. 62*, pp. 119-44 (1955).
62. Urey, H. C. and Craig, H. *Geochim. et cosmochim. acta* 4, 36-82 (1953).
63. Wiik, H. B. *Geochim. et cosmochim. acta* 9, 279-89 (1956).
64. Steiner, A. *New Zealand J. Geol. Geophys.* 1, 325-63 (1958).
65. Nockolds, S. R. *Bull. Amer. geol. Soc.* 65, 1007-32 (1954).
66. Tilley, C. E. E. *Geol. Mag.* 94, 329-33 (1957).
67. Nagy, B. and Faust, G. T. *Amer. Min.* 41, 817-38 (1956).
68. Lambert, W. D. "Coast and Geogetic Survey", Spec. Pub., no. 223 (Washington) (1940).
69. Lipschutz, M. E. and Anders, E. "The Record in the Meteorites" (AEC Contract No. AT(11-1)-382), Pt. IV (submitted to *Geochim. et cosmoch. acta*) (1960).
70. Kozyrev, N. A. *Sky and Telosc.* 18, 184 (1959).
71. Lyustikh, Y. N. *Akad. Nauk SSSR. Bull. Geophys. Series.* no. 1, 92-94 (1956).
72. Dolezal, E. *Universum* 14, 167-70 (1959).
73. Bullard, F. M., *Volcano Lett. Hawaii* no. 521, 1-5 (1953).
74. Yoshimura, J. *Quart. J. Seismology* 21, 35-43 (1957).
75. Nemoto, T., Hayakawa, M., Takahashi, K. and Oana, S. *Rep. Geol. Surv. Japan* no. 170, 149 pp. (1957).
76. Healy, J. *VIII Congr. Proc. N.Z. Pacific Sci. Ass.* 2, 27-30 (1956).
77. Makarenko, F. A. *Priroda*, 2, 89-91 (1958).
78. Banfield, A. F., Behre, C. H. Jr. and St. Clair, D. *Bull. Geol. Soc. Amer.* 67, 2, 215-34 (1956).
79. Shorthill, R. W., Borough, H. C. and Conley, J. M. *Publ. Astr. Soc. Pacif.* (in press).
80. Pettit, E., and Nicholson, S. B. *Astrophys. J.* 71, 102-35 (1930).
81. Kuiper, G. P. (ed.), "Photographic Lunar Atlas", Chicago University Press, Chicago.
82. Jaeger, J. C. *Nature, Lond.* 183, 1316-17 (1959).
83. Fremlin, J. H. *Nature, Lond.* 183, 239 (1959).
84. Baranov, V. I., and Serdyukova, A. S. *Priroda*, 3, 29-34 (1959).
85. Reynolds, J. *Phys. Rev. Letters* 4, 351-54 (1960).
86. Zotov, P. P. *et al. Priroda* 3, 122-4 (1960).
87. Casey, R. D., Scott, J. H. and Westcott, E. M. Multipurpose logging equipment for uranium exploration and evaluation of deposits: *Proc. 11 Internat. Conf. on Peaceful Uses of Atomic Energy* 3, 54-59 (1958).
88. Zablocki, C. J. and Keller, G. V. *VII Annual Drilling Sym. on Explor. Drilling, Minnesota Univ.*, 15-24 (1957).
89. Mazzoni, A. and Breusse, J. J. *XIX Internat. Geol. Congress, Algiers, Comptes rendus Sec.* 15, 17, 161-68 (1954).
90. McKellar, I. C. and Collins, B. W. *VII Congr. Proc. Pacific Sci. Ass.* 2, 129, 1949 (1953).
91. Deshpande, B. G. and Sen Gupta, S. N. *Bull. geol. Surv. India Series B*, no. 8, 27 pp. (1956).
92. Ananyan, A. A. *Akad. Nauk. SSSR, Bull. Geophys. Series*, 1958, no. 12, 878-81 (in translation) (1960).
93. Castel, J. H. *Symposium sur les Mesures Effectuées dans les Sondages X*, no. 11, 1402-1405 (1955).
94. Caldwell, R. L. and Sippel, R. F. *Bull. Amer. Ass. Petrol. Geol.* 42, 159-72 (1958).
95. Veshev, A. V., Meyer, V. A., Larionov, L. V. and Barkhatov, D. P. *Vses. Nauchno-Issled. Inst. Razved. Geofiz. Voprosy Rudnov Geofiz., Sbornik, Statev* 1, 69-78 (1957).
96. Karus, Y. V. and Zuchernik, V. B. *Akad. Nauk SSSR Bull., Geophys. Series*, no. 11, 755-61 (in translation) (1959).
97. Broding, R. A., Zimmerman, C. W., Somers, E. V., Wilhelm, E. S. and Stripling, A. A. *Geophysics* 17, 1-26 (1952).

98. Lapaz, L. In Vol. 4, Lansberg, H. E. and Van Mieghem, J. (ed.) "Advances in Geophysics", Academic Press, New York, 218-350 (1958).
99. Hatherton, T. *N.Z. J. Sci. Tech. sec. B* 35, no. 5, 421-32 (1954).
100. Martina, E. F. and Schrader, C. D. *Report STR/RT* 60-0000-00078: *UCLRL-5916*, Space Technology Lab., Inc., Univ. Calif. Lawrence Radiation Lab. 31 pp. (1960).
101. Mooney, H. M. and Blofuss, R. *Geophysics* 18, 383-93 (1953).
102. Nagata, T. "Rock Magnetism". Tokyo Maruzen Co., Ltd. 232 pp. (1953).
103. Baker, P. E. *Petrol. Tech.* 9, 97-101 (1957).
104. Martin, P. W. "An Atom Smasher for Well Logging", presented at joint meeting of Rocky Mountain Petrol. Sections and Amer. Inst. of Mining and Metallurgical Engr., 17-18 May 1956 (unpublished paper No. 657-G) (1956).
105. Green, J. *Bull. geol. Soc. Amer.* 70, 1127-84 (1959).
106. Gerard, V. B. and Lawrie, J. A. *Geophys. Mem.* no. 3 (New Zealand Dept. of Science and Industry Research), 20 pp. (1955).
107. Yokoyama, I. *J. Phys. Earth* 6, 75-9 (1958).
108. Yokoyama, I. and Tajima, H. *Nature, Lond.* 183, 730-40 (1959).
109. Bemmelen, R. W. "Rock Analyses of Indonesia" (unpublished).
110. Birch, F., Schairer, J. F. and Spicer, H. C. *Geol. Soc. Amer. Special Paper* no. 36, 325 pp. (1942).
111. Firsoff, V. A. *J. Brit. astr. Ass.* 69, 153-155 (1959).
112. Bonhoff, N. *Proc. IX Internat. Astron. Congress*, 1958 Springer-Verlag, pp. 557-61 (1959).
113. Brown, O. D. R., Finn, J. C., Jr. and Green, J. Certain Biological and Geological Advantages of a Polar Lunar Base (submitted to *Astronautica*) (1962).
114. Gibson, J. E. *Naval Res. Lab., Report No.* 49 84 *ALD-143403*, 11-12 (1957).
115. Henderson, E. P. and Perry, S. H. *Geochim. et cosmoch. acta* 6, 221-40 (1954).
116. Herring, J. R. and Licht, A. L. *Science* 130, 266 (1959).
117. Jaeger, J. C. and Harper, A. F. A. *Nature, Lond.* 166, 1026 (1950).
118. Kennedy, G. C. *Amer. J. Sci.* 246, 529-48 (1948).
119. Kozyrev, N. A. *Izvestia Crimean Astrophys. Obs.* 16, 148 (1956).
120. Lyot, B. and Dollfus, A. *C.R. Acad. Sci., Paris* 229, 1277 (1949).
121. Piddington, J. H. and Minnett, H. C. *Aust. J. sci. Res. Ser A* 2, 63-77 (1949).
122. Poldervaart, A. and Green, J. *Geotimes* 3, 25-26 (1959).
123. Rankama, K. "Isotope Geology". McGraw-Hill Book Co., New York, and Pergamon Press, Ltd., London (1954).
124. Rankama, K. and Sahama, T. G. "Geochemistry", Chicago University Press, Chicago, 911 pp. (1950).
125. Vinogradov, A. P. *Geokhimiya* no. 1, 6-52 (1956).
126. Green, J. *Ann. N.Y. Acad. Sci.* The Geology of the Lunar Base. (In press, 1962.)



# ON MOON VOLCANISM

N. BONEV

*Astronomical Institute, University of Sofia, Bulgaria*

1. THE Moon craters grew out of Moon volcanism in the remote past. N. A. Kozyrev observed a volcanic eruption at the beginning of November 1958. In the remote past this activity was probably much more intense. The distribution of the craters over the eastern and the western halves of the Moon disk does not support the meteoritic hypothesis of the origin of the Moon craters. We ascertained this in 1955 and 1956 by means of some theorems from the field of continued probabilities bearing on the hemisphere and on the polygon†. The eastern hemisphere of the Moon is continually undergoing a meteoritic bombardment to an even greater degree than the western one, yet no adequate effect is to be observed. It is true that nowadays the orbital velocity of the Moon about the Earth is slow in respect to the annual motion of the Earth about the Sun. However, according to the theory of probability, the slight advantage of the eastern over the western hemisphere would certainly have become apparent after a sufficiently large number (say several hundreds of millions) of years.

The eastern and the western hemispheres of the Moon happened to play a game of chance, an unfair one, of course. The gambling house, say that of Monte Carlo, exists and will exist. Why? Because the odds favour the house. If the game were a fair one, the gambling house would become bankrupt. However slight the unfairness of the game, it ensures the very existence of the gambling house *in the course of time*.

Moreover, one should bear in mind that in the remote past the Moon was much nearer to the Earth and its orbital velocity sensibly higher. According to G. H. Darwin, the Moon—in its initial state—revolved round the Earth in  $5\frac{1}{2}$  hours; at that time it was at a distance of  $2\frac{1}{2}$  earth-radii from it. Yet, it is not necessary to go so far into the remote past.

The fundamental theorems of continued probabilities, as mentioned above, are as follows:

(1) The probability  $p$  that the angular distance of two points, taken arbitrarily on the surface of a hemisphere, is to be smaller than  $\alpha$  is

$$p = 1 - \cos \alpha, (\alpha \text{ small}).$$

(2) The probability  $p$  that the linear distance of two points, taken arbitrarily within a flat polygon, is to be smaller than a given length  $\epsilon$  is

$$p = \frac{1}{S^2} \left\{ \pi S \epsilon^2 - \frac{2}{3} L \epsilon^3 + \frac{\epsilon^4}{8} \sum [(\pi - A) \cot A + 1] \right\}$$

In this formula  $S$  and  $L$  are the area and the perimeter of the polygon respectively;  $\Sigma$  is the sum of all such angles [2].

† We dealt with this matter first in 1936 (See ref. [1]).

It should be noted that we take into consideration the influence of the deformation, when making an orthographic projection of the Moon surface on a plane, which is perpendicular with respect to a line from the Moon's centre.

When we were working in 1956 with the visible craters of the Moon only, we forbore from making any hypothesis whatever as to the distribution of the craters over the invisible surface of the Moon and availed ourselves of the second formula as given above. The findings were the same as those of our investigation in 1955 (first formula), when we reached the conclusive hypothesis that the distribution of the craters on both the parts of the Moon, the visible and the invisible, is the same (i.e. the same number of craters, characterized by the same minimum distance). What does this result mean? The meteoritic hypothesis of the origin of the Moon craters does not correspond to the facts. What accounts for the similarity of both results? The fact that both these investigations were founded on the visible craters. *The quantity of craters on the first quarter is greater than that on the last quarter.* The very essence of our argument against the meteoritic hypothesis lies in this cardinal fact on which our computations are based. (The minimum distance between the craters is of importance as well. A large minimum distance characterizes very straggling craters.)

On the latest map of the reverse of the Moon, as presented by Professor A. A. Mikhailov to the Stockholm Astronautical Congress in August 1960, one can see immediately that the right half of this reverse side, *upon which a greater number of meteorites falls*, contains fewer craters than the left half. This is a further confirmation of our argument against the meteoritic hypothesis.

We refer, of course, to the more considerable craters, i.e. those to be seen on ordinary scale maps. The smaller craters are not so interesting. They may have grown out of different causes, including meteorite fall.

2. This conclusion, founded on close examination of the natural satellite of the Earth, is of very great importance to astronautics. If the majority of Moon craters were really of meteoritic origin, this would have clouded the horizon and darkened the outlook for astronautics†. The observations by Soviet artificial satellites (from 1958 onwards) have also shown more exactly that the surrounding space is comparatively "clean".

3. The volcanism has been exceedingly intense on the Moon in the remotest past. It may be that its volcanism has caused the very existence of the Moon as an Earth satellite.

The Moon is a particularly anomalous satellite in many respects. When compared with the other satellites, it has a very great mass in respect to its primary body (planet). Its moment of revolution is considerably greater than the rotation moment of the Earth. It looks a rather "unreliable" satellite of the Earth. If we could stop the Earth in its revolution round the Sun, the Moon would separate from the Earth and would become a planet of the Sun. The case is quite different with the satellites of Mars and the other planets (the motion of a point by Newtonian attraction from two fixed centres). After all, the occurrence of large craters as on the Moon is such as can be observed nowhere else.

† Cf. my lectures delivered to the astronautical congresses in Amsterdam (August 1958) and London (September 1959) [3].

All this suggests the idea that primarily the Moon was, perhaps, a stranger to the Earth and that its orbit was very close to that of the Earth (planet of the Sun)†. It “came in orbit” round the Earth and became its “artificial satellite” by a corresponding change of its velocity due to a huge volcanic eruption. To all appearances, it had initially an enormous internal energy like the planet Phaëthon which even burst, thus giving rise to the asteroids and the meteorites. The Moon is the “last stage” of a “multi-step” spherical rocket. It has lost a considerable part of its initially very large mass, nearly equal, perhaps, to that of Phaëthon (0.07–0.1 of the mass of the Earth).

May be the approach of the *planet* Moon to the Earth (we mentioned that the orbits of both these celestial bodies had been initially very close) has given rise to that tremendous volcanic eruption on the Moon, just as the approach of Phaëthon to Jupiter, along an orbit very close to that of the latter, has caused Phaëthon to burst [cf. 4].

Why should we assume that Nature has realized rocket motions only in the organic world (sepia, medusa, the insect dragon-fly during the aquatic phase of its life)? Nature has realized such motions in the inorganic world as well, e.g. in the catching of the Moon by the Earth.

Cosmogony does not today distinguish any essential difference between stars and planets in respect to their origin or to their internal energies. Just as stars exist with enormous internal energies, so also can planets exist having considerable internal energies.

Tsiolkovski's equation shows that it is preferable to increase the velocity of the ejected gases in order to obtain high speeds in rocket propulsion, and then to aim at increasing the mass ratio of the rocket.

Perhaps Nature did just this with the Moon. In this respect Nature shows her exceedingly large capabilities.

Let us take Tsiolkovski's equation outside of the field of attraction

$$V = \frac{u}{\lambda} \log \frac{M_0}{M},$$

where  $V$  is the velocity at an instant when the mass of the rocket is  $M$ ;  $M_0$  is the initial mass, and  $u$  is the velocity of the stream of exhaust gases. The logarithm is to the base 10;  $\lambda = 0.434$ . . . .

Let a given volcano on the Moon become active. After a series (I) of eruptions the Moon's centre will have the velocity  $V_1$ . If  $u$  is the speed of the stream of gases,  $M_0$  and  $M_1$  the initial and the remaining mass of the Moon, respectively, then

$$V_1 = \frac{u}{\lambda} \log \frac{M_0}{M_1};$$

in another volcano which becomes active *after* the first one, at the same speed  $u$ , at the end of the new series (II) of eruptions, when the Moon mass has become  $M_2$  and the new velocity communicated to the Moon centre is  $V_2$ , we shall have

$$V_2 = \frac{u}{\lambda} \log \frac{M_1}{M_2}.$$

† Even nowadays the Moon orbit, in respect to the Sun, is fully concave (with a slight change of the curvature—it is somewhat less at new Moon than in full Moon).



After  $n$  such series of eruptions we shall have

$$V_n = \frac{u}{\lambda} \log \frac{M_{n-1}}{M_n}.$$

If we take the sum of all these velocities, we shall get

$$V_1 + V_2 + \dots + V_n = \frac{u}{\lambda} \log \frac{M_0}{M_n}.$$

Therefore, in this case again, only the ratio of the initial and the final masses is of importance. The intermediate masses and their ratios, respectively, would be of importance only if the velocities of the gases from the different volcanoes were different.

The sum of the left side of the latter equation  $V_1 + V_2 + \dots + V_n$  is a geometric one.

For this sum to be large, it is necessary: (1) that the individual terms correspond to eruptions *nearly in the same direction* (this has been assumed in our deviation), (2) that  $M_0/M_n$  be large, and (3) that  $u$  also be large, which is the most important condition.

With the value of the mass as admitted above for the "planet" Moon  $M_0/M$  makes approximately 10 and the sum of the left-hand side of the last equation is nearly equal to  $2.34u$ .

Taking into consideration the velocities possible in Nature, one can understand that the velocity  $V_1 + V_2 + \dots + V_n$  may easily become sufficient for the Moon's catching by the Earth to prove possible, viz. that the Moon becomes an "artificial" satellite of the Earth, even if the quotient  $M_0/M_n$  were considerably less.

#### REFERENCES

1. Bonev, N. Les probabilités des causes et l'origine des cratères lunaires, *Astr. Nachr.* 260, no. 6239 (1936).
- Bonev, N. La distribution des cratères lunaires en rapport à leur origine. Un argument nouveau contre l'hypothèse météorique. *Ann. Univ. Sofia* 50, livre I, première partie (1955-56).
- Bonev, N. La distribution des cratères lunaires en rapport à leur origine. Un nouveau argument contre l'hypothèse météorique (suite). *Ann. Univ. Sofia* 50, livre I, deuxième partie (1955-56).
- Bonev, N. On the meteoritic hypothesis of the origin of the Moon craters (in Russian) *Meteoritica* fasc. XVI (1958).
- Bonev, N. Recherches nouvelles sur la distribution des formations sur la surface lunaire, *Ann. Univ. Sofia* 44, livre I (1948-49).
- Bonev, N. La théorie des marées et l'origine des formations lunaires et des régions sismiques terrestres. *Ann. Univ. Sofia* 44, livre II (1948-1949).
2. Borel, E. "Les Principes de la Théorie des Probabilités" 1, fasc. I, 84-87. Paris (1925).
3. Bonev, N. Sur le danger météorique en astronautique, "Proceedings of the Ninth International Astronautical Congress, Amsterdam" (1958).
- Bonev, N. Sur le danger météorique en astronautique (II). "Proceedings of the Tenth International Astronautical Congress, London" (1959).
4. Bonev, N. On the origin of the asteroids and meteorites, (in Russian). *Meteoritica*, fasc. XVIII (1960).

# SPECTROSCOPIC PROOFS FOR EXISTENCE OF VOLCANIC PROCESSES ON THE MOON

N. A. KOZYREV

*Pulkovo Observatory, Leningrad, U.S.S.R.*

A CONCEPT of the Moon devoid of internal energy, sufficient for volcanic and mountain-forming processes, is widely accepted at the present time. Therefore, it is generally assumed that the relief formation of the Moon is due to external actions on its surface. However, such a viewpoint is not sufficiently substantiated. In fact, the history of Earth's relief shows that the period of telescopic observations of the Moon is too short to enable us to observe changes in whole sections of the crust. Catastrophic changes, apart from actions of water and atmosphere, occur on the Earth only in a very restricted area, and the size does not exceed a few kilometres. Therefore, we must not expect on the Moon any sudden changes over an area exceeding appreciably one square second. The reality of such minute effects in the relief could hardly be established on the basis of available cartographic data.

Whereas it is impossible to establish morphologically in exact manner the consequences of mountain-forming processes, we may attempt to detect the existence of these processes from the accompanying physical phenomena. The luminescence of gases escaping from the lunar interior may constitute an example of such a phenomenon. A flame, i.e. the luminescence of the gases themselves, can hardly be observed because of the absence of atmosphere and free oxygen on the Moon. However, a luminescence of gases must occur under the action of solar radiation. After the observations had proved the fluorescence of rocks constituting the lunar surface, it became evident that the fluorescence of gaseous cloud should be observable much more distinctly near the terminator—due to the geometric effect of illumination—than the fluorescence of the surface; indeed, it should even produce the effects of atmospheric mist, veiling the lunar surface. From general concepts of light absorption on the photodissociation of molecules, we may assume that  $10^{15}$  molecules above  $\text{cm}^2$  of the surface should be sufficient for a complete absorption of the short-wave solar radiation and, consequently, for obtaining the maximum luminosity of fluorescence. The temporary existence of such a local atmosphere of pressure, smaller than one-billionth of the terrestrial atmosphere, is quite possible.

The American astronomer, D. Alter, was the first to secure an objective proof attesting to the temporary appearance of the mist which can obscure certain regions of the lunar surface. On the basis of a comparison of photographs taken in violet and infrared rays, Alter arrived at the conclusion that he had observed a blurring of the features in the crater Alphonsus. However, only the spectral analysis can provide a direct and rigorous proof of the existence of such physical processes on the Moon. Only by this method can we establish and investigate additional spectral peculiarities, which the physical phenomenon on the Moon adds to the usual solar spectrum reflected from the lunar surface.

We must not expect the number of active regions on the Moon to be great. Therefore, to solve the problem of lunar activity, it is quite sufficient to prove the existence of just one active area. In these spectral investigations it is important that the width of spectrograph slit be not greater than one second of arc with a sufficient focal-ratio of telescope. The 50-in. reflector of the Crimean Astrophysical Observatory with the scale of 8" per mm fully satisfies these requirements.

Beginning in 1955 up to the present, I have conducted spectral examinations of many sections of the lunar surface by means of this reflector. In 1958, after D. Alter had published his interesting photographs of Alphonsus, I decided to pay particular attention to this crater.

On 3 November 1958, with exposure lasting from 3 hr 00 min to 3 hr 30 min (UT), a spectrogram was obtained, showing the luminescence of gases escaping from the central peak of Alphonsus. During the time of exposure the central peak on the spectrograph slit appeared to be brighter and whiter than usual. Suddenly, the brightness of this peak dropped to normal during the time on the order of tens of seconds. Then I terminated the exposure immediately and started a new one lasting from 3 hr 30 min to 3 hr 40 min with the same position of the slit. This spectrogram confirmed the reality of the visual impression; it showed the spectrum of the quite normal state of the crater. In addition to these pictures, I obtained during the same night, at about 1 hr (UT), one more spectrogram through clouds; this spectrogram was also completely devoid of any symptoms of gaseous emission.

I pointed out in my preliminary reports that the central peak on this spectrogram appears to be noticeably weaker in violet rays, and that this phenomenon can be explained by the ejection of dust, i.e. volcanic ashes. However, a detailed study of this spectrum, carried out at Pulkovo by Miss Polozhentseva, proved that this report was not correct. It can be concluded from the above data that the duration of the gas-escape process was longer than 30 min and shorter than 2 hr 30 min. During the next night, 3-4 November, I managed to obtain two further spectrograms of Alphonsus. These spectrograms showed that the state of the crater remained normal.

Figure 1 illustrates the position of the spectrograph slit during the exposure of the spectrogram with gaseous emission. The height of the Sun above the horizon of the crater was equal to  $18^\circ$ . The next picture (Fig. 2) reproduces two spectrograms of Alphonsus, obtained one after another from 3 hr 00 min to 3 hr. 40 min (UT) with the indicated slit position. These spectrograms show clearly the spectra of eastern and western walls of the crater and the spectrum of the central peak with its shadow.

An additional emission, superimposed on the normal spectrum of the central peak, constitutes a striking feature of the first spectrogram. The most characteristic peculiarity of this additional emission consists of a band with a comparatively sharp red edge of about  $4740 \text{ \AA}$ . The brightness of this band attains 40% of the normal brightness of the peak at the same wavelengths. This band is characteristic of the spectra of cometary heads. It is beyond any doubt a band of Swan resonance series of carbon molecule  $C_2$ . A system of weak bands with maximum of about  $4400 \text{ \AA}$  is noticeable towards the violet. The blurring of the Fraunhofer line at  $4384 \text{ \AA}$  confirms the existence of emission there. Two bands with maxima of  $5470 \text{ \AA}$  are seen on the long-wave side. It is possible that the last band also constitutes a Swan band.

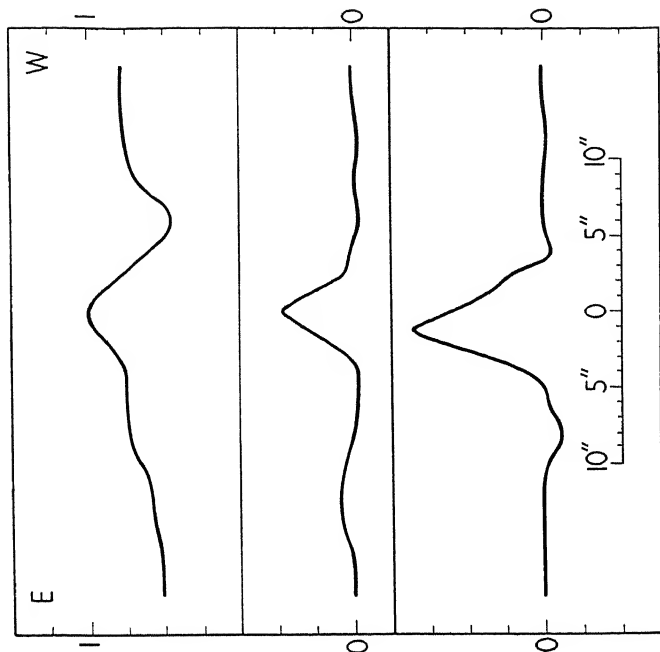


FIG. 2. Profiles of the intensity of the central peak of Alphonsus and the additional emission along the slit of the spectrograph. The top curve gives the profile of the peak in its normal state. The curve at the centre shows a section of weak additional emission ( $\lambda$  4620, 4580 Å); and the bottom curve, a section of the additional emission in the bright part of the  $\lambda$  4740 Å band (the average of sections in the light of  $\lambda$  4740, 4730, and 4660 Å bands). The unit of intensity is the maximum intensity of the central peak.

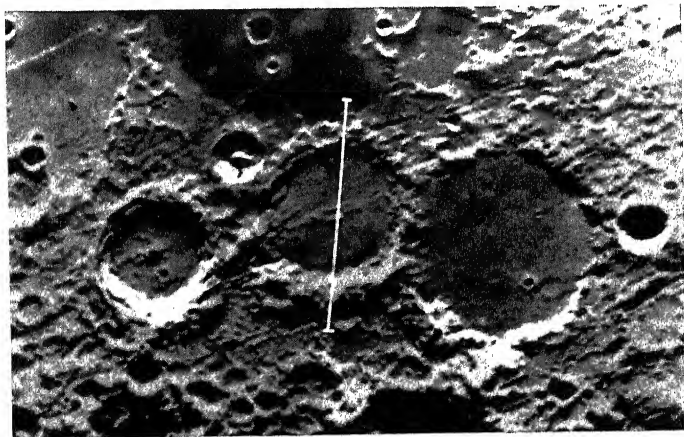


FIG. 1. Photograph of a group of craters, Ptolemy, Alphonsus and Arzachel, showing the position of the slit during the author's spectrographic observations on 3 November 1958.

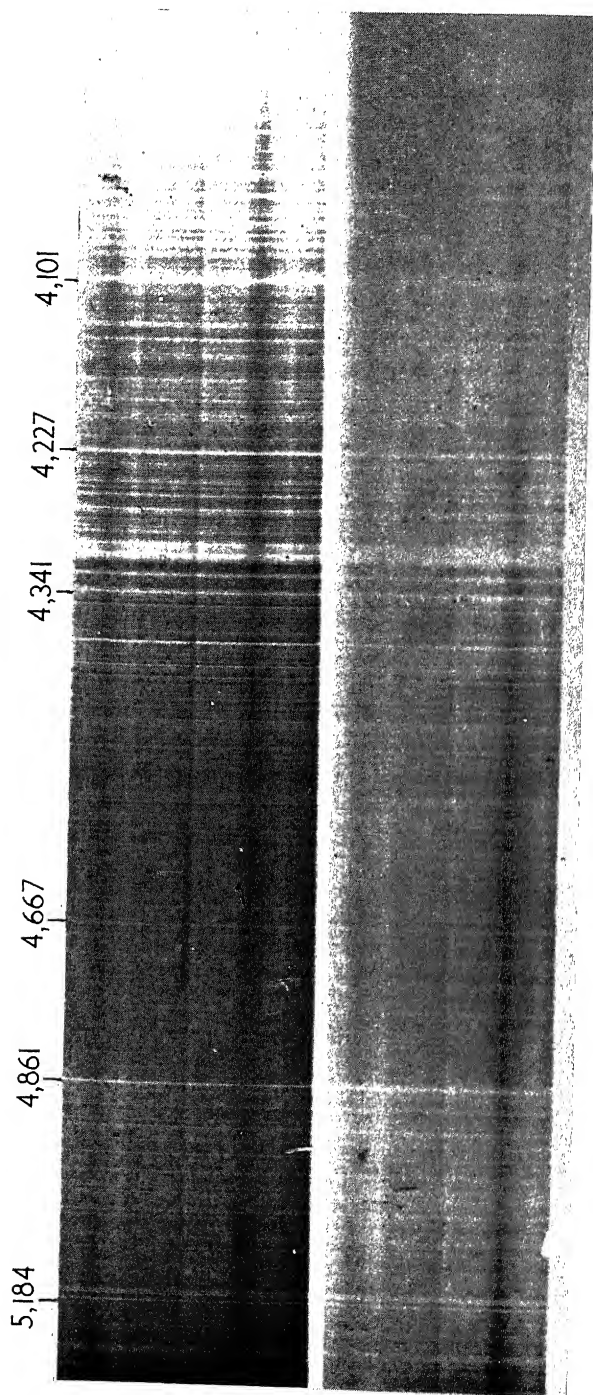


Fig. 3. Spectrograms of the crater Alphonsus, taken on 3 November 1958. The upper spectrum, exposed between 3 hr 00 min and 3 hr 30 min UT, shows an additional emission in the spectrum of the central peak. The one below, exposed between 3 hr 30 min and 3 hr 40 min, shows the crater in its normal state.

The emission spectrum of the central peak was studied thoroughly by A. A. Kalinyak at the Pulkovo Observatory with the aid of a microphotometer. He will publish a special report on this research. I would like to discuss only certain essential peculiarities of the spectrum. The measurements demonstrate that the band at  $4740 \text{ \AA}$  had a distinct structure, which confirms the gaseous nature of this emission. A number of maxima of the band structure coincide with vibration transitions of  $\text{C}_2$  molecule. However, the entire band is much more complex, its extension along the spectrum is almost twice as great as the normal extension of this band, and its maxima are strongly washed out. It is very important, for clarification of these circumstances, that the entire bright portion of the band from  $4640 \text{ \AA}$  is shifted toward the Sun away from the central peak and the position of weak bands. This shift is conspicuous on the spectrogram, and is confirmed by measurements perpendicular to the dispersion. The results of measurements are presented in Fig. 2. The upper curve on this diagram gives the normal profile of the central peak, obtained from measurements in the region  $\lambda 4740 - H_\beta$ , where the emission is clearly absent. The middle curve, obtained by subtracting brightnesses of the normal profile from brightnesses of the peak in region  $\lambda 4575 - 4610 \text{ \AA}$ , gives the profile of a weak emission. The emission band of  $4740 \text{ \AA}$ , based on three cross-sections on borders of the band and in its centre, is shown on the lower curve of the diagram. This curve gives the same shift of brightness maximum toward the Sun by  $1''2$ , i.e. by 2 km.

The following conclusions can be drawn from these data. The gases consisting of complex molecules, producing a weak emission, escaped from the central peak of Alphonsus. This circumstance must not be regarded as accidental. Assuredly, the peak of this formation has a funnel, i.e. constitutes a genuine volcano. Hence we can conjecture that the central peaks of lunar craters may be of a similar origin to the cones of terrestrial volcanoes and are, consequently, gradually accumulated formations. The outer craters themselves may be similar to calderas of terrestrial volcanoes, formed by subsidence due to the depletion of magmatic seat. A large diameter of lunar craters, exceeding by nearly one order of magnitude the size of terrestrial calderas, can be explained by the fact that the gravity on the Moon amounts to one-sixth of the gravity on the Earth surface; and, as a result, an arch may have an appreciably greater diameter without collapsing.

The complex molecules, escaping from the funnel of the central peak, had to disintegrate under the action of the short-wave radiation of the Sun. The radical  $\text{C}_2$  could be produced only in this way. In the presence of a sufficiently great number of primary molecules the short-wave radiation of the Sun, which caused the photodissociation, could not penetrate far into the gaseous cloud. Therefore, the molecules of  $\text{C}_2$  could be produced only on the border of the cloud facing the Sun. The shift of brightness maximum of  $4740 \text{ \AA}$  band may be due to this fact. This should make it possible to draw a very simple estimate of the amount of gas escaping from the central peak. The non-transparency of the cloud shows that no less than  $10^{15}$  molecules should have been present in a column with the base of  $1 \text{ cm}^2$  in the path of solar rays. In order to obtain the actual amount, this number should be probably increased by one order. It is obvious from the photometric cross-sections, introduced earlier, that the observed part of the gaseous cloud had a diameter of about 3-5 km. Therefore, assuming the cross-section area of the cloud as  $10^{11} \text{ cm}^2$ , we find for the total number of molecules the value of

the order of  $10^{27}$ . The gas density is of the order of  $10^{11}$  particles per  $\text{cm}^3$ . At such a density the mean free path should be about 1 km, which ensures the dispersion of particles without collisions. The rates of gas discharge should not differ appreciably from thermal velocity, i.e. several hundreds of m/sec. Therefore, on termination of gas discharge, the cloud should scatter in several minutes; and this was noted during the observations. It is evident that  $10^{27}$  molecules should be released during this time at a steady state of the cloud. In 1 hr,  $10^{30}$  molecules yielding  $\text{C}_2$  should have been released. We will probably obtain a correct estimate of the total amount of all molecules if we increase this figure by one more order. Thus, during the process under observation, the Moon's interior released about 1 million  $\text{m}^3$  of gas, at terrestrial pressure. We must note that this quantity is small by comparison with cubic kilometres of gases escaping during violent eruptions of terrestrial volcanoes. This comparison shows a low intensity of the process, at which appreciable changes in the relief could hardly occur.

The entire band of 4740 Å showed the same shift in the direction toward the Sun. Therefore, in spite of an unusually great extension along the spectrum, the entire band must be of the same chemical nature, i.e. constitute the band of  $\text{C}_2$  molecule. Another peculiarity of our carbon spectrum consists in the fact that, according to measurements of Kalinyak, the band of 5165 Å is missing in the spectrum altogether. These peculiarities prove that conditions of excitation of  $\text{C}_2$  molecule occurred under quite unusual circumstances. To understand these conditions, it is important to bear in mind that the amount of photons, capable of exciting the luminescence of 4740 band, is very small (or the order of  $10^{15}$  photons per  $1 \text{ cm}^2$ ). On the other hand, the absorption coefficient in this band per one molecule equals  $10^{-16}$ , or even less. Thus, the probability of molecule excitation per second equals  $1/10$ . The velocities of  $\text{C}_2$  molecules, obtained on photo-dissociation, should be the same as in cometary heads, i.e. on the order of 1 km/sec. Therefore, the overwhelming majority of  $\text{C}_2$  molecules should escape without giving rise to luminescence beyond the limits of the gaseous cloud under observation. Consequently, only one act of excitation could have been observed for each molecule. This excitation occurred most probably at the moment of photo-dissociation of a complex primary molecule. At such an excitation, the population of levels in  $\text{C}_2$  molecule could have been quite unusual. Apart from that, the energy levels of  $\text{C}_2$  molecules in the state of nascence could have been shifted by the field of molecular residue. By virtue of these considerations, the emission spectrum thus obtained should be similar to the spectrum of a cometary nucleus, rather than to that of a head.

In 1959, I obtained twelve spectrograms of Alphonsus. All these spectrograms show the usual solar spectrum. However, on 23 October 1959, one more spectrum of a particular state of Alphonsus was obtained under very good conditions from 2 hr 10 min to 2 hr 25 min (UT). Unfortunately, no peculiarities in the appearance of the crater were noted in guiding, and the exposure was not repeated. The next night was cloudy; and on 25 October the crater was no longer accessible for observations.

At the time of the exposure, the Sun was setting for Alphonsus at a height of  $19^\circ$ . The orientation of the slit differed only by  $4^\circ$  from that in the 1958 observations, being more closely perpendicular to the axial crest of the crater. In order not to disturb the current programme of stellar observations in 1959, we had to take photographs with an additional prism installed at the

collimator immediately behind the slit. This prism halved the working part of the slit and turned the image with respect to the direction of dispersion. Owing to the reduced height of the slit, we obtained on spectrograms only the wall of the crater illuminated by the Sun, and the floor almost exactly up to the shadow of the eastern wall. In the centre appeared the spectrum of the region near the central peak with its shadow. A special characteristic of the spectrum of this region is that the red part of the spectrum, behind the triplet of magnesium of 5184 Å, is conspicuous. Particularly noticeable is a bright feature of small cross-section ( $1''^2$ ), which is invisible in the blue of spectrum. This feature is located at a distance of 6'' (i.e. 11 km from the shadow toward the Sun) toward the east. The shadow in this part of the spectrum is very short; it is preceded from the side of the Sun only by a small increment in brightness of the central peak. It is interesting to compare directly the violet and red regions of this spectrum with that of 1958. The narrow feature of the red region of the 1959 spectrum is evidence of very good images during which this spectrum has been obtained. At the same time, the region of the central peak with its shadow is wider in the violet part of spectrum than in the 1958 spectrum. Thus, the spectrum of 1959 is anomalous also in the short-wave region.

The interpretation of this complex spectrum must begin naturally with measurements of the brightness of the narrow red feature in relation to the brightness of the crater floor on the side of the Sun, where no appreciable anomalies are present. The results of measurements are presented in the diagram (Fig. 4), where the ratios of red-feature brightness to crater-floor brightness are plotted on Y-axis. Irregularities of contrast, obviously due to emission bands, appear towards the blue. These bands continue farther toward shorter wavelengths and occupy the whole area of the lunar surface from the red feature to the shadow. On the other hand, beginning with

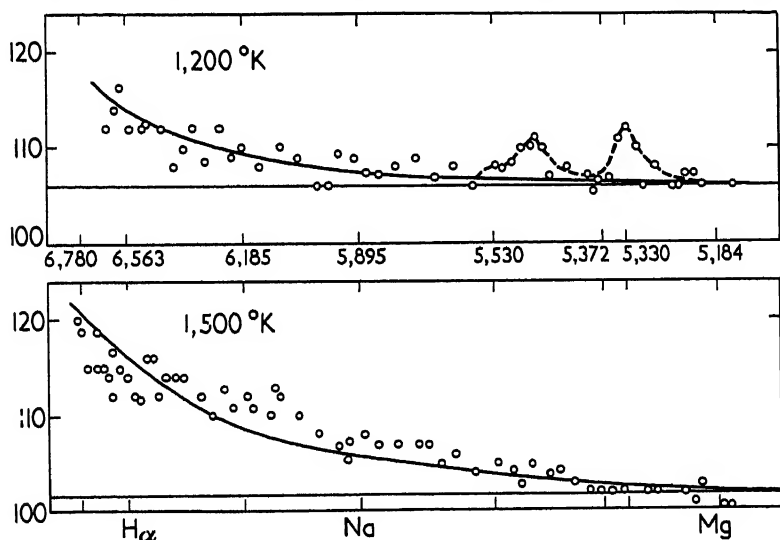


FIG. 4. Intensity distribution in the spectrum of the red glow observed in Alphonsus on 23 October 1959. The upper curve gives the intensity distribution with respect to that at the floor of the crater; and the bottom curve gives the same distribution in comparison with that prevailing in the shadow.



wave lengths of 5300–5400 Å, a monotonic increase in contrast becomes apparent, which may be traced on our photograph up to 6600 Å. It is possible that a weak monotonic increase in contrast is due to thermal radiation. In this section, the brightness of solar spectrum decreases toward the red by 20%, and is, in all probability, compensated fully by the increase in albedo of the lunar surface. Therefore, we may assume that the brightness of the comparison spectrum is identical for the entire region under consideration. Then, as indicated by the curve plotted on diagram, the monotonic trend of contrast corresponds fully to the radiation of black body at the temperature of 1200° K.

The explanation of the red feature by thermal radiation can be verified by calculation of temperature according to the absolute value of the radiant energy. Introducing  $x = 1.44/\lambda T$ , we have

$$e^{-x} \zeta = 2.1 \times 10^{-5} A_{h_{\odot}} \cdot K[(e^{x\zeta} - 1)^{-1}].$$

The numerical coefficient in this equation constitutes the factor of dilution of solar radiation at the distance of the Moon;  $A_{h_{\odot}}$  is the albedo of the floor of the crater at the elevation  $h_{\odot}$  of the Sun, and  $K$  is the contrast of the detail in the selected wave length. We shall carry out the calculation for  $\lambda = 6500$  Å and  $T_{\odot} = 6700^{\circ}$ . According to the diagram of contrast,  $K = 0.08$ . Finally, at  $h_{\odot} = 19^{\circ}$ , the albedo of the crater floor in the red should be taken as  $A_{h_{\odot}} = 0.015$ . As a result of the calculations, we find that  $x\zeta = 20.7$  and, consequently,  $T_{\zeta} = 1080^{\circ}$  K. This value of temperature is in good agreement with the colour temperature of 1200° determined above.

In fact, the unsteadiness of images and the guiding errors should reduce the contrast of the details, which would cause a decrease in the energy temperature. Since the factor reducing the contrast range does not depend on the wavelength, the colour temperature is obtained correctly. To obtain the energy temperature of 1200°, the contrast range should be reduced to 1/8. Consequently, the true extension of the red feature was not equal to 2 km, but was on the order of 300 m. In all probability, the slit of the spectrograph may have crossed a lava flow of this width. The lava of terrestrial volcanoes retains its plasticity up to 1000° K. On the other hand, at the outlet from volcano, the lava has a temperature of about 1400° K. The value of 1200° K inferred above for the red feature on the Moon agrees so well with these data that the correctness of identification of this feature with a lava stream is strongly indicated.

The calculations show that 1 km<sup>2</sup> of the Moon's surface, heated up to 1200° K, should radiate in infrared light (8000 Å) as a fourth or fifth magnitude G spectral type star. On 26 October, we took direct photographs of the Moon, showing crater Alphonsus, on infrared plates. The conditions were such that a record of an object of the above-indicated brightness should have been easily secured. The result of observations was negative. We must assume that the processes of the lava flow had ended already on 26 October.

The short shadow in the red part of spectrum, and the small contrast range of the elevation producing this shadow, indicate that the slit did not pass through the central peak. The brightest object of the crater center was set on the middle part of the slit for guiding. Such an object in our case was a gaseous cloud emitting at wavelengths shorter than 5500 Å. The probable position of the slit can be seen on the beautiful photograph by Alter. The slit passed most probably near the foot of the central peak from the south,

where elevations of the axial crest of Alphonsus produced a noticeable (though short) shadow. Some 11 km from the edge of the shadow in the direction of the slit we located the position of the red feature near a small conical hill on the eastern ridge of a branch of the axial crest. It appears that the axial crest of Alphonsus is now in the formative stage, and that this hill is a volcano producing lava flows. The liberation of emission-producing gases occurred above the lava stream and above the entire valley formed by the fork of the axial crest. The emission bands are packed so closely that they give an impression of a continuous spectrum. Unfortunately, the spectrum does not show such distinct signs of emission as the  $C_2$  band. This is connected, in all probability, with a different chemical composition of gases. In fact, the liberation of gases in this case may have been of a fumaroli type. On the Earth, however, fumaroles have a different chemical composition from that of gases escaping from the craters of active volcanoes.

The spectrum of 1958 appears to be more significant only because of the presence of the 4740 Å band. In reality, however, an appreciably more active volcanic process took place on 23 October 1959 in the crater Alphonsus; this process was tantamount in its magnitude to great eruptions of terrestrial volcanoes.

All these observations reveal that, even in our time, the Moon has an internal energy sufficient for mountain-forming processes. This result shows directly that the history of formation of the Moon's relief is a history of internal processes of the cosmic life of the Moon. The external actions constituted circumstances of secondary importance, and the role of meteorites was hardly greater than the role which they had played in creating the face of the Earth.



# MICROPHOTOMETRIC ANALYSIS OF THE EMISSION FLARE IN THE REGION OF THE CENTRAL PEAK OF THE CRATER ALPHONSUS ON 3 NOVEMBER 1958

A. A. KALINYAK, L. A. KAMIONKO

*Pulkovo Observatory, Leningrad, U.S.S.R.*

A MICROPHOTOMETRIC analysis of the spectrum of the emission flare in the region of the central peak of the crater Alphonsus, obtained by N. A. Kozyrev and V. I. Ezersky on 3 November 1958, leads to a conclusion that the escape of gas from the depths of the Moon had a purely fluorescent character. By the character of the intensity distribution, the spectrum of the flare is similar to the emission spectra observed in the heads of comets. Some maxima of the intensity of curve can be identified with the Swan molecular bands of  $C_2$ . No continuous radiation of thermal character was observed.

On 3 November 1958 Kozyrev with the help of Ezersky obtained a spectrogram of an emission flare, observed in the region of the central peak of the crater Alphonsus [1]. The observations were made at the Crimean Astrophysical Observatory on the 50-in. reflector with a prism spectrograph with dispersion of  $33\text{\AA}/\text{mm}$  at  $H_\beta$ . In view of the unique scientific value of the negative, supplemental evaluation of it was entrusted to the authors of this article by the Central Astronomical Observatory of the Academy of Sciences of the U.S.S.R. and the Planetary Commission of the Astronomical Council of the Academy of Sciences of the U.S.S.R.

## GENERAL DESCRIPTION OF THE SPECTRUM

On the general background of the spectrum (Fig. 1) obtained by Kozyrev and Ezersky in observing the lunar crater Alphonsus, we can note quite distinctly an increase of brightness extending in the form of a strip, sharply limited on the red side at about  $\lambda 4740\text{ \AA}$ , reaching its maximum at  $\lambda 4660\text{ \AA}$ , and fading to zero at  $\lambda 4540\text{ \AA}$ . A second increase of brightness, considerably less pronounced, exhibits a very gently sloping maximum near  $\lambda 4400\text{ \AA}$ . This second increase in brightness of the continuous spectrum cannot be reliably seen with the eye, but is revealed quite distinctly by micro-densitometric measurement. In the direction perpendicular to that of dispersion (i.e. vertical) the dimension of the strip of the spectrum exhibiting increased brightness is found to be of the order of  $0.22\text{ mm}$ . Translating this into angular measurement and scale on the surface of the Moon, the height of the strip corresponds to 2 seconds of arc or a linear distance of about  $3\text{ km}$ .

In the region of the steep decrease in brightness near  $\lambda 4700\text{ \AA}$  details in the structure of the spectrum are observed in the form of extended beads protruding upward beyond the limits of the strip. A characteristic peculiarity also is the non-coincidence of the direction of the strip of increased brightness with the direction of the dispersion. This effect in a more revealing form is shown as breaks in the strip at its red end.

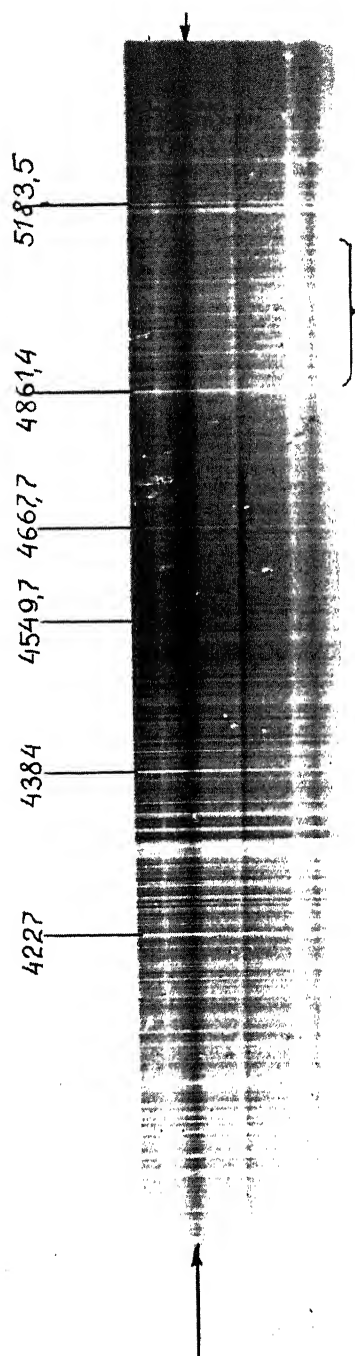


FIGURE 1.

## MICROPHOTOMETRIC ANALYSIS OF THE SPECTROGRAM

The microphotometric evaluation of the spectrogram was performed with the aid of a MF-2 microphotometer converted into a self-recording instrument by the attachment of a special drive and photo-multiplier with a recording electronic potentiometer EPPV-51. In order to eliminate errors arising from the inconstancy of the speed of movement of the tape and inertia of the recording device, the shifting of the negative was done in steps with stops at every 0.02 mm. The dimensions of the slit of the microphotometer on the negative corresponded to a rectangular area of a height of 0.18 mm and width of 0.08 mm. This size is equivalent, on the average, to a spectral interval of 2.5 Å being singled out for measurement.

As a result of the microphotometric measurements, the spectral distribution of the brightness in the radiation of the flare observed in the region of the central peak was determined. These data were obtained by subtracting the brightness of the comparison area from the total brightness of the spectrum of the central peak. The comparison area was chosen on the basis of the equality of its density and that of the spectrum of the central peak in the spectral interval from  $H_\beta$  to 5050 Å where the radiation of the flash was practically unobservable.

In Fig. 1 the place of the illuminated slope of the crater on which the choice of a comparison area was made is indicated by arrows.

## RESULTS OF THE MICROPHOTOMETRIC ANALYSIS

The curves of the intensity of the radiation produced at the central peak itself are shown in Figs. 2, 3, 4 and 5, obtained as a result of several recordings at different positions as to height of the spectrum of the central peak on

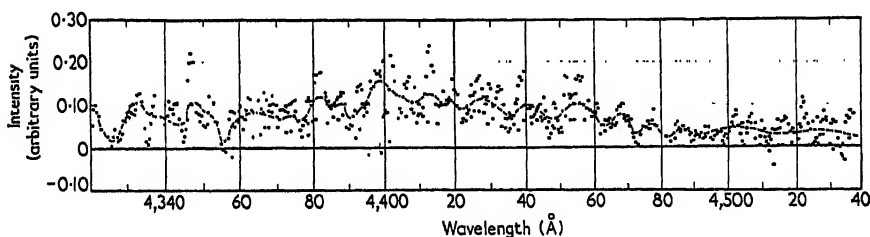


FIGURE 2.

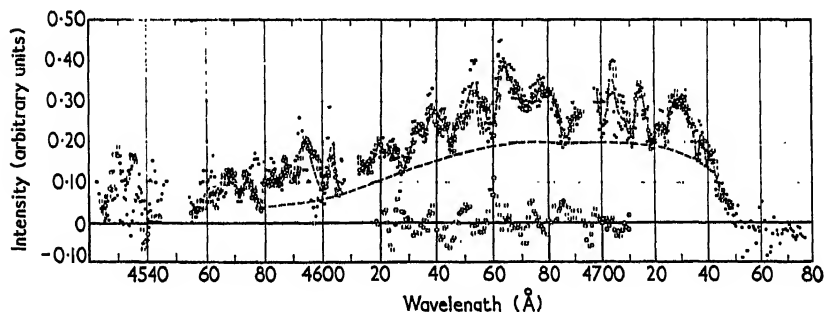


FIGURE 3.

the slit of the microphotometer. The brightness of the spectrum of the photometric comparison area at places free of absorption lines in accordance with Minnaert's Atlas [3] was taken as the unit of light. Because of the coarse-grain emulsion (the spectrum was obtained on Kodak plates 103-A), the presence of defects, and also the need for making photometric measurements with a small section of the light spot, the dispersion of the points in

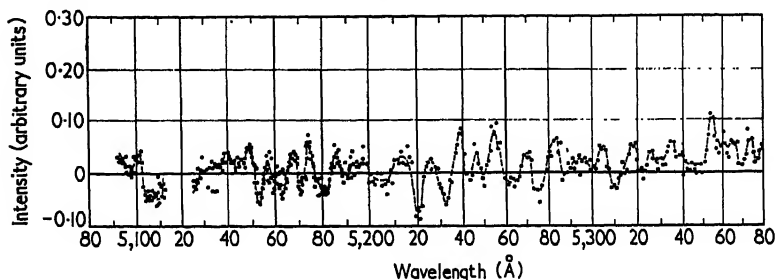


FIGURE 4.

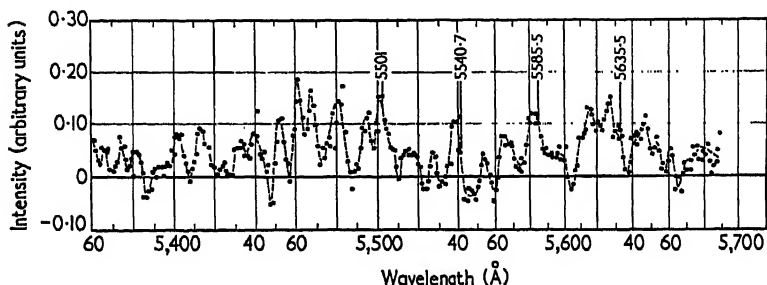


FIGURE 5.

a number of places on the spectrum turned out to be quite considerable. As regards the reliability of the photometric data, the spectral region corresponding to the section of the curve on Fig. 3 proves to be the most valuable. In other spectral regions the results of measurements are affected by considerable errors, resulting from an insignificantly low or, on the contrary, too high density of the negative, plate defects and other unfavourable factors. For evaluating the magnitude of the error in the measurements in Fig. 3, points are plotted which were obtained as a result of photometric deduction for two arbitrary spectral regions outside the region of the central peak.

The results of the spectrophotometric analysis as presented in Figs. 2, 3 and 4 reveal a large number of details in the spectrum of the flare of the central peak of the crater Alphonsus. A number of very reliable maxima of the spectral curve of intensity distribution correspond without doubt to the real structure of the spectrum of the flare, and can probably be ascribed to molecular emission. In Table 1 a list is given of the most reliable intensity maxima, their wavelength and intensity in units of the Moon's brightness.

One should note that at  $\lambda$  4695 Å there is doubtless a maximum of intensity, the precise position and magnitude of which cannot be determined on account of a defect on the negative at that particular place.

TABLE 1

<i>Numbered in order</i>	<i><math>\lambda</math> in Å</i>	<i>Total intensity</i>
1	4737	0.23
2	4730	0.31
3	4714	0.34
4	4703	0.40
5	4677	0.35
6	4663	0.40
7	4653	0.35
8	4638	0.29
9	4622	0.20
10	4602	0.20
11	4594	0.20

## CONCLUSIONS

From the character of the structure of the spectrum as revealed by microphotometric analysis we conclude that the effect of the flare of the central peak of the crater Alphonsus, recorded by Kozyrev and Ezersky, was due to the fluorescence of a gaseous plasma ejected from the Moon's interior. The absence of complete coincidence between the direction of the strip of the spectrum and the direction of the dispersion, which we mentioned above, can be explained by the nonhomogeneity of the chemical composition of the gaseous medium within the volume occupied by it.

In the general form of the intensity distribution of the flare spectrum its great similarity to the spectra of the heads of comets at a given stage of development of their nucleus proves to be very characteristic. In the general case the spectrum of the system of Swan bands is observed in a cometary head on the background of a relatively intense continuous spectrum of diffuse solar light, and probably non-quantum electron transitions in molecules. However, under certain conditions the continuous spectrum is greatly weakened and remains in the form of a constant component mainly in the area of the sequence  $\Delta\nu = +1$  of the Swan band system.

In the monograph by Bobrovnikoff [2], devoted to the study of Halley's comet, a number of microphotograms are presented which relate to spectra with successive weakening of the continuous radiation component. On the negative obtained on 2 June 1910 two maxima of intensity in the spectral interval from  $\lambda$  4200 Å to  $\lambda$  4750 Å are observed. The first, considerably more intense, increase in brightness begins on the shortwave side near  $\lambda$  4500 Å. It reaches a maximum near  $\lambda$  4737 Å with a following sharp drop in brightness towards the red. The second rise in intensity in the shorter-wave region of the spectrum is characterized by a very weakly expressed maximum near  $\lambda$  4400 Å. The intensity distribution of the flare spectrum discovered on the Moon, as was shown above, has the same character. On the basis of this similarity one can assume that according to the character of optical excitation and chemical composition, the flare on the Moon was very similar to cometary emission.



## IDENTIFICATION OF THE SPECTRUM

The character of the intensity distribution in the emission spectrum of the flare observed on the Moon, necessitates first of all an explanation of the nature of the phenomenon from the viewpoint of the molecular structure of the spectrum observed. However, the question of identification of the spectra of the luminescence of gaseous media of celestial objects cannot be solved, as Swings [4] particularly emphasizes, by a simple comparison of the wavelengths of the observed intensity maxima with molecular bands obtained under laboratory conditions.

The causes of the luminescence of gaseous media in space in a number of cases cannot be simulated in the laboratory, because of the impossibility of reproducing all the physical-chemical conditions prevailing in space. This should explain the manifold deviations in the structure of the molecular bands and relative intensities which are revealed in comparisons with the customary laboratory spectra. Without enumerating such irregularities in the structure of molecular spectra of celestial objects, and also the causes leading to such anomalies, we note that, in the analysis and identification of spectra of cosmic origin, one often has to be guided by indirect indications following from the general principles valid for phenomena of this kind. Such indirect indications can be insufficient for the analysis of spectra obtained in the laboratory, and may even be completely lacking.

Numerous spectroscopic data obtained as a result of the observation of comets convince us that the intensive fluorescence of gases emitted by solid mineral bodies always shows the spectrum of the molecules of carbon and its compounds. The most characteristic in this case is the presence of the intense electron system  $A^3\Pi_g-X^3\Pi_u$  of the Swan bands, with vibrational quantum number differences  $\Delta v = -1, 0, +1$ . The most intense are the two last sequences, with main bands  $\lambda 5165.2 \text{ \AA}$  for the sequence  $\Delta v = 0$  and  $\lambda 4737.1 \text{ \AA}$  for the sequence  $\Delta v = +1$ . The sequences with higher absolute values of  $\Delta v$  are not very intense and can serve only as secondary indications in identification.

In Fig. 3 the intensity distribution in the maximum of emission in the region  $\lambda 4737 \text{ \AA}$ , discovered on the Moon, is very probably due mainly to the sequence  $\Delta v = +1$  of the Swan band system. The argument in favour of this view is not only the general form of the intensity distribution with a sudden drop in intensity at  $\lambda 4737 \text{ \AA}$  to the presence of the red, as occurs in the case of the spectra of comets, but also the presence of two clearly expressed maxima at  $\lambda 4714 \text{ \AA}$  and  $\lambda 4677 \text{ \AA}$ , which can be compared with the corresponding bands of the sequence  $\Delta v = +1$ . In Table 2 the wavelengths of the observed maxima and the heads of the corresponding band of the sequence  $\Delta v + 1$  are given. Special reference will be made further on with regard to the presence of the band (1—0).

Of the five maxima of sequence  $\Delta v = +1$ , three have been detected. The absence of the maximum (3—2) is probably due to a defect in the negative. As regards the maxima (4—3) and (5—4), they in general are difficult to resolve at the given dispersion and grain of the 103- $\text{\AA}$  emulsion, and probably appear as one maximum at  $\lambda 4677 \text{ \AA}$ . Besides the resolution of microphotometric measurements was too low on account of the small height of the spectrum.

In comparing Fig. 3 with the microphotometric recording of the spectrum of the comet of 1948 XI (Fig. 6) shown in Swings's Atlas [5], one detects in

a number of cases a repetition of details in the structure of the intensity maxima. In particular, one notices in both cases the presence of a step in the red slope of the maximum at  $\lambda 4715 \text{ \AA}$ . The maximum of the bands (4—3) and (5—4) in both cases proves to be very broad, but in the spectrum of the flare on the Moon the small decrease in intensity between these two molecular bands is absent.

TABLE 2

$v-v$	$\lambda$ in $\text{\AA}$ for Observed maximum	$\lambda$ in $\text{\AA}$ for head of band	Measured central intensity	Intensity of band by Swings
1—0	4737	4737.1		20
2—1	4714	4715.2	30	30
3—2		4697.6	Band is missing on account of defect	
4—3	4677	4684.8	33	15
5—4		46778.6		15

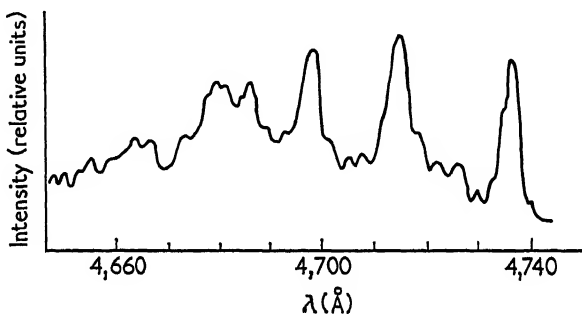


FIGURE 6.

The relative intensities at the maxima in these cases can be evaluated only approximately, because of the impossibility of a correct reduction for the influence of the extraneous maxima of intensity, unrelated to the Swan band system, and also the effect of the background of the continuous spectrum probably of molecular origin. Nevertheless, if one adopts for the level of the background the dotted curve (Fig. 3), and if one interprets the distance from the maximum to the level of the continuous spectrum as the intensity of the band, the ratio of the intensity of the band (2—1) to the total intensity of the bands (4—3) and (5—4) is in good agreement with Swings's data. For the total intensity of the bands (4—3) and (5—4) we take its maximum at  $\lambda 4677 \text{ \AA}$ .

In order to confirm the correctness of identification of the maxima of intensity with the Swan bands, it is necessary to establish the causes of the observed anomalies in the intensities of the bands of the flare spectrum. The absence of the basic band (0—0), the head of which is at  $\lambda 5165.2 \text{ \AA}$ , proves to be the most difficult to explain. The data of microphotometric analysis of the region of the magnesium triplet, shown in Fig. 7 show that, within the limits of observational errors, there are no signs of emission at  $\lambda 5165 \text{ \AA}$ .

Judging by the photometric data of the band (3—2), the equivalent width of which can be estimated to be of the order of  $0.4 \text{ \AA}$  of the brightness of the background of the Moon, one may assume that the photometric effect from the band (0—0) should not be less than in the first case, and also not less than the effect of the group of absorption bands (Fig. 7) at  $\lambda 5193 \text{ \AA}$ ; the total equivalent width of which, according to Minnaert's Atlas [3], is equal to about  $0.5 \text{ \AA}$ . An effect of such a magnitude could not be overlooked in the process of photometric measurements. Doubtless, the observed fluorescence over the central peak of the crater Alphonsus must be interpreted as the result of the superposition of two oppositely directed processes.

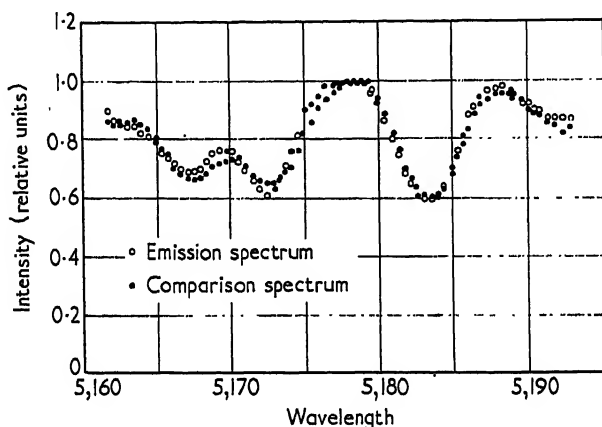


FIGURE 7.

Together with the process of emission occurring as a result of optical excitation under the action of the direct solar rays, we should expect an absorption of light reflected from the surface of the Moon in molecular bands. As will be shown below, the resulting effect can turn out to be positive or negative, and provide a satisfactory explanation of the anomalies in the observed distribution of the relative intensities in the spectrum of the molecular bands.

In this way the problem is reduced, on one hand, to a computation of the decrease in brightness of a beam reflected from the Moon by its passage through a layer of absorbing gas; and, on the other, to a computation of the increase in the brightness of the same beam as a result of the re-emission of light absorbed by the gas illuminated by the Sun both directly and indirectly (i.e. by the diffused light of the Moon). In the general case the problem can be solved with the aid of the equation of transfer; but for the sake of simplicity we shall employ a more elementary method. In order to simplify the computations, we shall assume that the layer of gas is compressed to a thickness of  $1 \text{ cm}$ , and all developments will refer to a beam of light of  $1 \text{ cm}^2$  cross-section.

Since the optical depth of such a layer is small, the decrease in brightness of the rays reflected from the Moon, caused by the absorption of light in the

frequency  $\nu_v''v'$  with the transition from the lower vibrational level  $v''$  to the higher vibrational level  $v'$ , will be equal to

$$\Delta_n K_{\zeta}(\nu_v''v') = K_{\zeta}(\nu_v''v') 2K(\nu_v''v'), \quad (1)$$

where  $K_{\zeta}(\nu_v''v')$  denotes the brightness of the Moon and  $K(\nu_v''v')$  is the coefficient of volume absorption. The factor 2 enters because of the double passage of the rays through the absorption layer. The value  $\Delta_n K_{\zeta}(\nu_v''v')$  is in turn equal to the energy absorbed by two cubic centimeters of gas per second with an aperture of the rays of 1 steradian. Therefore,  $\Delta_n K_{\zeta}(\nu_v''v')$  can be represented with the aid of Einstein's coefficient of absorption in the form:

$$\Delta_n K_{\zeta}(\nu_v''v') = \frac{2}{4\pi} N_{v''} B_{v''v'} K_{\zeta}(\nu_v''v') h \nu_{v''v'}. \quad (2)$$

In the given case  $B_{v''v'}$  is determined as the probability of the transition  $v'' \rightarrow v'$  of a molecule in the field of isotropic radiation with the specific intensity of the rays equal to unity.  $N_{v''}$  is the number of molecules in 1 cm<sup>3</sup> of gas which are at the lower vibrational level  $v''$ .

The light flux  $\varphi(\nu_v''v')$  emitted by 1 cm<sup>3</sup> of gas in all directions, as a result of the re-emission of radiation absorbed from direct sunlight as well as from the diffused light of the surface of the Moon, will be equal to

$$\varphi(\nu_v''v') = \left( \frac{K_{\odot}(\nu_v''v') \Omega_{\odot}}{4\pi} + \frac{\int K_{\zeta}(\nu_v''v') d\omega}{4\pi} \right) \cdot \frac{\sum_{k''=0}^{\infty} N_{k''} B_{k''v'}}{\sum_{k''=0}^{\infty} A_{v'k''}} A_{v'v'} h \nu_{v'v''}. \quad (3)$$

The summation is to be extended for all vibrational levels of the lower electron state  $X^3\Pi_u$  where  $A_{v'v''}$  is the Einstein coefficient of radiation; and  $\Omega_{\odot}$  denotes the solid angle at which the Sun is seen from the surface of the Moon. The second member in parentheses corresponds to the re-emission excited by the diffused light of the Moon. This member may be discarded on account of the fact that at the moment of observation, the region of Alphonsus was near the lunar terminator; and the actual illumination by moonlight was limited to a small area on the slope of the crater.

As is easy to see, the transition from the light flux  $\varphi(\nu_v''v')$  to the surface intensity  $\Delta_e K_{\zeta}(\nu_v''v')$  of the emitting layer of gas, is obtained as the quotient of the division of  $\varphi(\nu_v''v')$  by  $4\pi$ . Thus, the increase in the intensity  $\Delta_e K_{\zeta}(\nu_v''v')$  of the beam of light coming to the observer will be equal to

$$\Delta_e K_{\zeta}(\nu_v''v') = \frac{\varphi(\nu_v''v')}{4\pi} = \frac{K_{\odot}(\nu_v''v') \Omega_{\odot}}{(4\pi)^2} \cdot \frac{\sum_{k''=0}^{\infty} N_{k''} B_{k''v'}}{\sum_{k''=0}^{\infty} A_{v'k''}} A_{v'v'} h \nu_{v'v''}. \quad (4)$$

For a more detailed consideration of the problem it is very interesting to

examine the relationship of  $\Delta_e K_{\mathcal{Q}}(\nu_{v''} v')$  to  $\Delta_n K_{\mathcal{Q}}(\nu_{v''} v')$ , which can be presented in the form:

$$\frac{\Delta_e K_{\mathcal{Q}}(\nu_{v''} v')}{\Delta_n K_{\mathcal{Q}}(\nu_{v''} v')} = \frac{\Omega_{\odot} K_{\odot}(\nu_{v''} v')}{8\pi K_{\mathcal{Q}}(\nu_{v''} v')} \cdot \frac{\sum_{k''=0}^{\infty} \frac{N_{k''}}{N_{v''}} \cdot \frac{B_{k''v'}}{B_{v''v'}}}{\sum_{k''=0}^{\infty} A_{v'k''}} A_{v'v''}. \quad (5)$$

If we assume the absence of degeneracy, the ratio of the coefficients of absorption can be replaced by the ratio of the coefficients of emission, i.e.

$$\frac{B_{k''v'}}{B_{v''v'}} = \frac{A_{v'k''}}{A_{v'v''}}. \quad (6)$$

Consequently,

$$\frac{\Delta_e K_{\mathcal{Q}}(\nu_{v''} v')}{\Delta_n K_{\mathcal{Q}}(\nu_{v''} v')} = \frac{\Omega_{\odot}}{8\pi} \cdot \frac{K_{\odot}(\nu_{v''} v')}{K_{\mathcal{Q}}(\nu_{v''} v')} \cdot \frac{\sum_{k''=0}^{\infty} \frac{N_{k''}}{N_{v''}} A_{v'k''}}{\sum_{k''=0}^{\infty} A_{v'k''}} = \delta(v'' v'). \quad (7)$$

The behaviour of the relationship  $\delta(v'' v')$  becomes very simple if one assumes that  $N_{k''}$  satisfies Boltzmann's distribution. In this case

$$\delta(v'' v') = \frac{\Omega_{\odot} K_{\odot}(\nu_{v''} v')}{8\pi K_{\mathcal{Q}}(\nu_{v''} v')} \times \frac{\exp[G_0(v'')/0.695T] \cdot \sum_{k''=0}^{\infty} \exp[-G_0(k'')/0.695T] A_{v'k''}}{\sum_{k''=0}^{\infty} A_{v'k''}} = C\sigma_1, \quad (8)$$

where

$$\sigma = \frac{\exp[G_0(v'')/0.695T] \cdot \sum_{k''=0}^{\infty} \exp[-G_0(k'')/0.695T] A_{v'k''}}{\sum_{k''=0}^{\infty} A_{v'k''}};$$

$G_0(k'')$  being the term of the  $k''$ th vibration level of the lower electron state reckoned from the zero vibrational energy level.

By the character of the behaviour as a function of the absolute temperature  $T$ , the bands  $v'' = 0$  sharply differ from the bands with  $v'' \neq 0$ . In the first case, with the change of temperature in the whole interval from  $0^\circ \text{K}$  to  $\infty$ , the magnitude  $\sigma$  changes from a few tenths to unity. To be more precise,

$$\sigma \rightarrow \frac{A_{v'0''}}{\sum_{k=0}^{\infty} A_{v'k''}} < 1 \quad \text{when } T \rightarrow 0^\circ \text{K},$$

$$\sigma \rightarrow 1 \quad \text{when } T \rightarrow \infty.$$

For  $v'' \neq 0$  the limits of the change are determined:

$$\left. \begin{aligned} \sigma' \rightarrow \infty: & \quad T \rightarrow 0^\circ \text{K}, \\ \sigma \rightarrow 1: & \quad T \rightarrow \infty. \end{aligned} \right\} \quad (9)$$

Two sub-cases arise, depending on whether the expression

$$\sum_{k''=0}^{\infty} A_{v'k''} \left[ \exp\left(\frac{G_0(v') - G_0(k'')}{0.695T}\right) - 1 \right]$$

remains positive in the whole range of temperature from  $0^\circ \text{K}$  to  $\infty$ , or whether it changes sign from plus to minus, with the increase in temperature, beginning at some value for it. Two cases should be distinguished:

$$\left. \begin{aligned} (a), & \quad \infty \geq \sigma \geq 1 & 0^\circ \text{K} \leq T \leq \infty \\ (b) & \quad \infty \geq \sigma \geq 1 & 0^\circ \text{K} \leq T \leq T^* \\ & \quad 1 \geq \sigma & T^* \leq T \leq \infty \end{aligned} \right\} \quad (10)$$

The presence of the sub-cases (a) and (b) basically depends on the rate of decrease of  $A_{v'k''}$  as a function of  $k''$ .

Figure 8 shows all the considered modes of behaviour of the function  $\sigma$

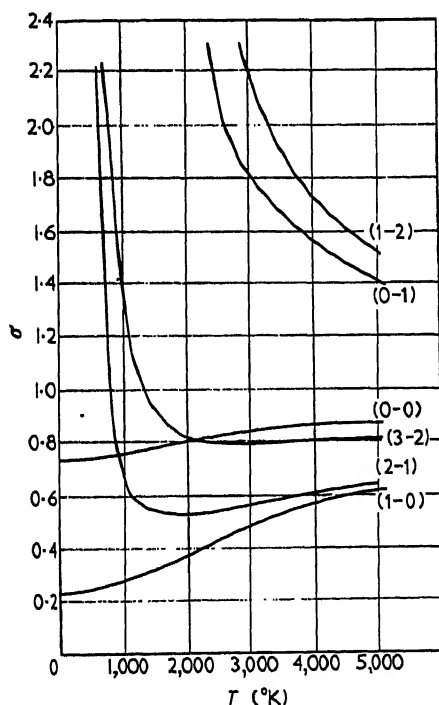


FIGURE 8.

under discussion, which were computed on the basis of the relative transition probabilities given in Swing's Atlas of the spectra of comets [5]. Case (a) occurs for bands of the sequence with  $\Delta v = -1$ . Case (b) is observed

for the sequence with  $\Delta v = +1$ , while  $\sigma$  indicates the minimum located in the region of 2000° K for the band (2—1).

From this analysis it follows that the contrast of the molecular bands in emission depends on the absolute brightness of the Moon and  $\sigma$ , which, in turn, is a function of the temperature.

By introducing into equation (11) the expression

$$\delta(0''0') = \frac{\Omega_{\odot}}{8\pi} \frac{K_{\odot}(\nu_0''0')}{K_{\zeta}(\nu_0''0')} \sigma = 1, \quad (11)$$

the two values  $\sigma = 0.735$  at  $T = 0^\circ \text{ K}$  and  $\sigma = 1$  at  $T = \infty$ , and  $\Omega_{\odot}$ , we get two values for  $K_{\zeta}(\nu_0''0')$ , i.e.  $K_{\zeta}(\nu_0''0') = 1.82 \cdot 10^{-6} K_{\odot}(\nu_0''0')$  and  $K_{\zeta}(\nu_0''0') = 2.37 \cdot 10^{-6} K_{\odot}(\nu_0''0')$ , respectively.

Hence, it follows that the brightness of the Moon obtained from mutual compensation of the absorption and the emission in the band (0—0) proves to be in good agreement with the values directly measured. Therefore the explanation of the absence of the band (0—0) by mutual compensation of absorption and emission can be considered as very justified.

The values for the brightness of the Moon as calculated from the condition of compensation were obtained in a very indirect way and, therefore, may serve basically as a criterion for the estimation of the method adopted by the authors for explaining the anomalies found in the spectrum of flare. Among the formations on the surface of the Moon, according to data presented in the book by N. N. Sytinskaya [6], there are a considerable number of details the brightness of which equals, and even exceeds, the computed values. Nevertheless, one should keep in mind possible variations of the degrees of brightness of the Moon due to our incomplete knowledge of the relative transition probabilities, the deviations from precise compensation, and also the incompleteness of the knowledge of the reflecting capacity of the micro-relief on the Moon.

On the basis of the intensity distribution curve, Fig. 3, the presence of a maximum at the position of the band (1—0) cannot be established with complete confidence, on account of the considerable dispersion of points. Therefore, it remains an open question as to which one of the two bands (0—0) or (1—0) fulfils best the condition of compensation between absorption and re-emission. Under full compensation for the band (1—0) the brightness of the Moon for the extreme values of temperature  $0^\circ \text{ K}$  and  $\infty^\circ \text{ K}$  of a gas will be equal to  $5 \cdot 10^{-7} \text{ K}$  and  $2.37 \cdot 10^{-6} \text{ K}_{\odot}$ , respectively.

The true value of surface brightness of the slope of the peak on which the emission flare was observed was, apparently, considerably above average for flat areas, because of its inclination to incident sunlight. The determination of the true value of the brightness of the central peak by means of a comparison with the floor of the crater cannot be reliable, since the turbulence in the terrestrial atmosphere can lower considerably the brightness of details having dimensions of not more than 1" or 2"—and the central peak of the crater Alphonsus belongs to this category.

The uncertainty of the computed brightness of the central peak is increased by our incomplete knowledge of the values of the coefficients of the relative transition probabilities which enter into the expression for  $\sigma$ . In Table 3 are given the values of  $\sigma$  at  $T = 0^\circ \text{ K}$  for the band (0—0) and the

corresponding values for the brightness of the Moon, computed on the basis of theoretical and experimental data by different authors [7].

The data given in Table 3 indicate that a complete absence of the bands (0-0) and (1-0) or their partial weakening can be explained as a result of the mutual compensation of absorption and re-emission in the beam reflected from the surface of the Moon in the direction of the observer. Microphotometric analysis of the band (1-1) cannot be made on account of the presence of a plate defect near it, which is marked by a break in the photometric curve in Fig. 4.

TABLE 3

<i>Author</i>	$\sigma$ for the band (0-0) with $T = 0^\circ \text{ K}$	<i>Brightness of the Moon in units of the brightness of the Sun</i>
King	0.77	$1.82 \times 10^{-6}$
Johnson and Tawde	0.57	$1.35 \times 10^{-6}$
Tawde and Patel	0.60	$1.43 \times 10^{-6}$
Pillow	0.75	$1.79 \times 10^{-6}$
Tawde and Patel	0.72	$1.72 \times 10^{-6}$
McKeller and Buscombe	0.71	$1.71 \times 10^{-6}$
Average		$1.64 \times 10^{-6}$

The definite presence of emission in the region of sequence with  $\Delta v = -1$  can probably serve as an additional confirmation of the explanation stated above. A number of the maxima of intensity which are found in this area can be identified with the molecular bands of the sequence  $\Delta v = -1$ . In the spectra of comets, this sequence usually turns out to be less intense in comparison with the sequence  $\Delta v = +1$  and, therefore, one may expect its absence in an emission flare on the Moon. The indications of its presence on the spectrogram of Kozyrev and Ezersky can be explained by the large value of  $\sigma$  for the bands of this sequence in a rather wide temperature interval from zero to a thousand degrees Kelvin.

The leading role played by the band (2-1) in the identification of the emission spectrum follows directly from the magnitude, form, and position of its maximum on the wave-length scale. In the light of theoretical considerations, this band determines the upper limit of the temperature which makes it possible to observe the bands of sequence  $\Delta v = +1$ . On the basis of the graphs shown in Fig. 8, the limiting value of the temperature is about 700 to 750° K. Any further increase of the temperature would necessarily bring about a gradual disappearance of the sequence with  $\Delta v = +1$ , with the subsequent appearance of a relatively weak band of absorption (2-1) at a temperature near 2000° K.

The considerations in favour that the temperature of the plasma of the emission flare on the Moon was relatively low seem in contradiction to the suggestion expressed earlier about a close similarity between the flare spectrum and those of the luminescence of cometary heads, since the molecule  $\text{C}_2$  in the spectra of comets invariably reveals a high-temperature distribution within the limits from 1500° K to 3000° K, with the vibrational levels in the lower electron state. Due to the homonuclear structure of the molecule  $\text{C}_2$



and, consequently, the equality to zero of the permanent electrical moment in the lower electron state, the high temperature distribution of the molecules of  $C_2$  can be preserved in the atmosphere of a comet for an indefinitely long time because of the low pressure and, consequently, the absence of collision between molecules.

However, the nature of the phenomena which result in the high-temperature distribution of the molecules of  $C_2$  remains unsolved. Since the formation of gaseous plasma containing  $C_2$  and other radicals of carbon apparently took place under the action of sunlight as a result of the decomposition of the parent molecule of a complex carbon compound, the distribution at the vibrational levels of the lower electron state can be occasioned by the process of photochemical reaction of decomposition, without interference of the gas-kinetic properties of the plasma at high-vacuum conditions. In this case the distribution of the molecules at different energy levels cannot be connected in any way with the kinetic temperature of the surrounding medium, and the value of the temperature associated with it has only conventional significance.

The general resemblance of the spectrum of the emission flare, observed in the region of the central peak of the crater Alphonsus with the spectra of comets, suggests that the physico-chemical processes observed in both cases may be closely related. On the other hand, the presence of peculiarities in the spectrum of the central peak can be satisfactorily explained only if the escaping lunar gas was at a considerably lower temperature.

The considerable difference observed in the distribution at the vibrational levels in the case of the comets and of the flare on the Moon can be explained if we assume that the high-temperature distribution originated through a decomposition of the parent molecule by mutual collisions before the phenomena of absorption and fluorescence of the gas came into action.

A very approximate computation, based on the oscillator strengths  $f = 10^{-2}$  for Swan bands, shows that the high-temperature distribution (which is characteristic of the cometary atmospheres) could not appear in the spectrum of the flare on the Moon at a pressure higher than  $10^{-9}$  to  $10^{-8}$  mm Hg. In this way, in spite of the very close postulated affinity of physico-chemical conditions and optical excitation for the gases emitted from the interior of the Moon, and the atmospheres of comets, we are not justified to expect a full identification of the structure of the spectra in both cases, insofar as they depend on the temperature of the gas.

In conclusion, one should note that over the whole area covered by the negative obtained by Kozyrev with the assistance of Ezersky, no thermal emission was detected from a study of the continuous spectrum. On the basis of the microphotometric measurements reported in this article a general description of the spectrum of the emission flare is given, and considerations are presented in favour of the presence of several  $C_2$  molecular emission bands of the Swan system. A more detailed analysis of the microphotometric data for detecting the possible presence of other molecules would constitute a separate problem.

#### CONCLUSIONS

The result of the microphotometric analysis of the spectrum obtained on the 3 November 1958 by Kozyrev and Ezersky when observing the central peak of the crater Alphonsus reveal with certainty that:

1. The emission effect observed by them was produced by a fluorescent gas under the action of solar radiation.

2. The emission was localized in two regions of the spectrum. The first, a more intense region, reveals a maximum of intensity approximately at  $\lambda$  4690 Å, and a very sharp drop in intensity towards the red. The second, a less intense area, is characterized by a broad and flat maximum at  $\lambda$  4400 Å.

3. A number of secondary maxima on the intensity distribution curve are found, agreeing well in position with the molecular bands of the Swan system.

4. The absence of the resonance emission band (0-0) and the uncertain appearance of the band (1-0) can be explained by the presence of the bright background of the surface of the Moon, and the relatively low value of the kinetic temperature of the plasma in which the observed phenomenon occurred.

5. Within the limits of errors of measurement, our microphotometric data do not give evidence of thermal emission in the flare spectrum of the central peak of the Alphonsus crater.

The authors of this article express their sincere thanks to Professor G. Herzberg of the National Research Council of Canada for very valuable suggestions and literature directly bearing on this work.

The modernization of the microphotometer used by us, was done by a collaborator of the Central Astronomical Observatory, S. I. Bulanov. The aid we received made it possible to obtain objective data of high precision, which revealed the magnitude of the observational errors and the degree of reliability of the results of the measurements.

#### REFERENCES

1. Kozyrov, N. A. *Priroda (Nature)* no. 3 (1959).
2. Bobrovnikoff, N. *Publ. Lick Obs.* 17 (1931).
3. Minnaert, M., Mulders, G. F. W. and Houtgast, J. "Photometric Atlas of the Solar Spectrum", Amsterdam (1940).
4. Swings, P. "Vistas in Astronomy", Vol. 2. London; New York (1956).
5. Swings, P. and Huser L. "Atlas of Representative Cometary Spectra", Louvain, A.R.D.C. (1956).
6. Sytinskaya, N. N. "The Moon and Its Observation", State Publishing Office of Technical and Theoretical Literature, Moscow.
7. McKellar, A. and Climenhaga, J. L. "Contributions from the Dominion Astrophysical Observatory". No. 28 (1952).



# STRATIGRAPHIC BASIS FOR A LUNAR TIME SCALE†

EUGENE M. SHOEMAKER, ROBERT J. HACKMAN

*U.S. Geological Survey, Menlo Park, California,  
and Washington, D.C., U.S.A.*

## INTRODUCTION

THE impending exploration of the Moon and geologic mapping of its surface raise the need for an objective lunar time scale. Photogeologic mapping already in progress has made this need immediate, and at the same time furnishes the stratigraphic foundation on which the broad framework of a lunar time scale may be based. This paper is a report of progress in meeting this need. Five major stratigraphic subdivisions will be described which have been adopted for use in detailed photogeologic mapping at a scale of 1 : 1 000 000.

The geological law of superposition is as valid for the Moon as it is for the Earth, but at the present time the application of this law to the Moon is restricted to the study of the relation of surface features as they are seen through the telescope or as they may be photographed from the Earth or a space vehicle. The chronologic relationships of many of the visible features of the lunar surface, nevertheless, can be unambiguously determined.

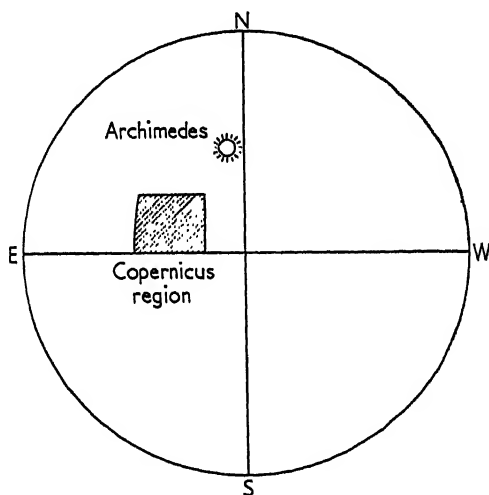


FIG. 1. Index map of the Moon showing location of the Copernicus region.

The lunar surface is locally built up of an intricate and complexly overlapping set of layers of ejecta from craters, material underlying the crater walls and floors, and material that occupies the maria. The composition and

† Prepared on behalf of the National Aeronautics and Space Administration.

thickness of these layers are not known, though reasonable estimates can in some cases be made of the thickness. These are specific problems for future exploration. The existence of the layers, however, can be recognized, and their stratigraphic succession provides the basis for a relative time scale for events in the history of the Moon. Determination of the absolute age of points or events in this time scale, again, is a problem for the future.

A region around the crater Copernicus was selected for initial detailed investigation of the stratigraphy. This region is favorably located near the center of the lunar disk (Fig. 1) and is one where the relative succession of many stratigraphic units can be worked out. For this reason the Copernicus region has become a type area from which we are extending or tracing a number of major units by photogeologic mapping.

#### EJECTA FROM COPERNICUS

Copernicus is a somewhat polygonal crater about 90 km across (Fig. 2), and about 3500 m deep, measured from rim crest to floor; the rim rises about 1000 m above the surrounding lunar surface. The interior walls of the crater comprise a series of terraces, scarps, and irregular sloping surfaces that descend stepwise from the crest to the crater floor, a roughly circular area of generally low relief 50 km in diameter. A few low peaks rise above the floor near the center of the crater.

The outer slopes of the rim are characterized by a distinctive topography. Rounded hills and ridges are combined in a hummocky array that consists of humps and swales near the crest of the rim and passes gradually outward into a system of elongate ridges and depressions with a vague subradial alignment. The relief of the ridges gradually diminishes until it is no longer discernible at a distance of about 80 km from the crest of the rim. Beyond this distance the rim passes gradationally into the ray system.

The ray system, which extends out more than 500 km from Copernicus, consists mainly of arc-like and loop-shaped streaks of relatively highly reflective material on a generally dark part of the Moon's surface. In certain photometric characteristics the rays are essentially an extension of the crater rim and cannot be sharply delimited from it. The major arcs and loops can be locally resolved into an echelon feather-shaped element, ranging from 15 to 50 km in length, with the long axes of the element aligned approximately radially with respect to the center of the crater.

Within the rays, and preponderantly near the concave margins of the major arc and loops, numerous elongated depressions or gouge-like craters in the lunar surface may be seen that range in length from the limit of telescopic resolution to about 8 km (Fig. 3). Visible depressions or gouges lie at the proximal ends of many ray elements, though there is not a correspondence of one gouge for each distinguishable ray element. At very low angles of illumination the Moon's surface along the rays can be seen to be roughened ([1], p. 289, 291). The roughness is due, at least in part, to the presence of the gouge-like craters and very low rims around these craters.

A full explanation of the ray pattern and associated gouge-like craters can be given in terms of the ballistics of material ejected from Copernicus [2]. In this explanation the gouges are formed mainly by impact of individual large fragments or clusters of large fragments ejected from Copernicus and the ray elements are splashes of crushed rock derived chiefly from the impact of these fragments. The ray system may thus be conceived as a discontinuous

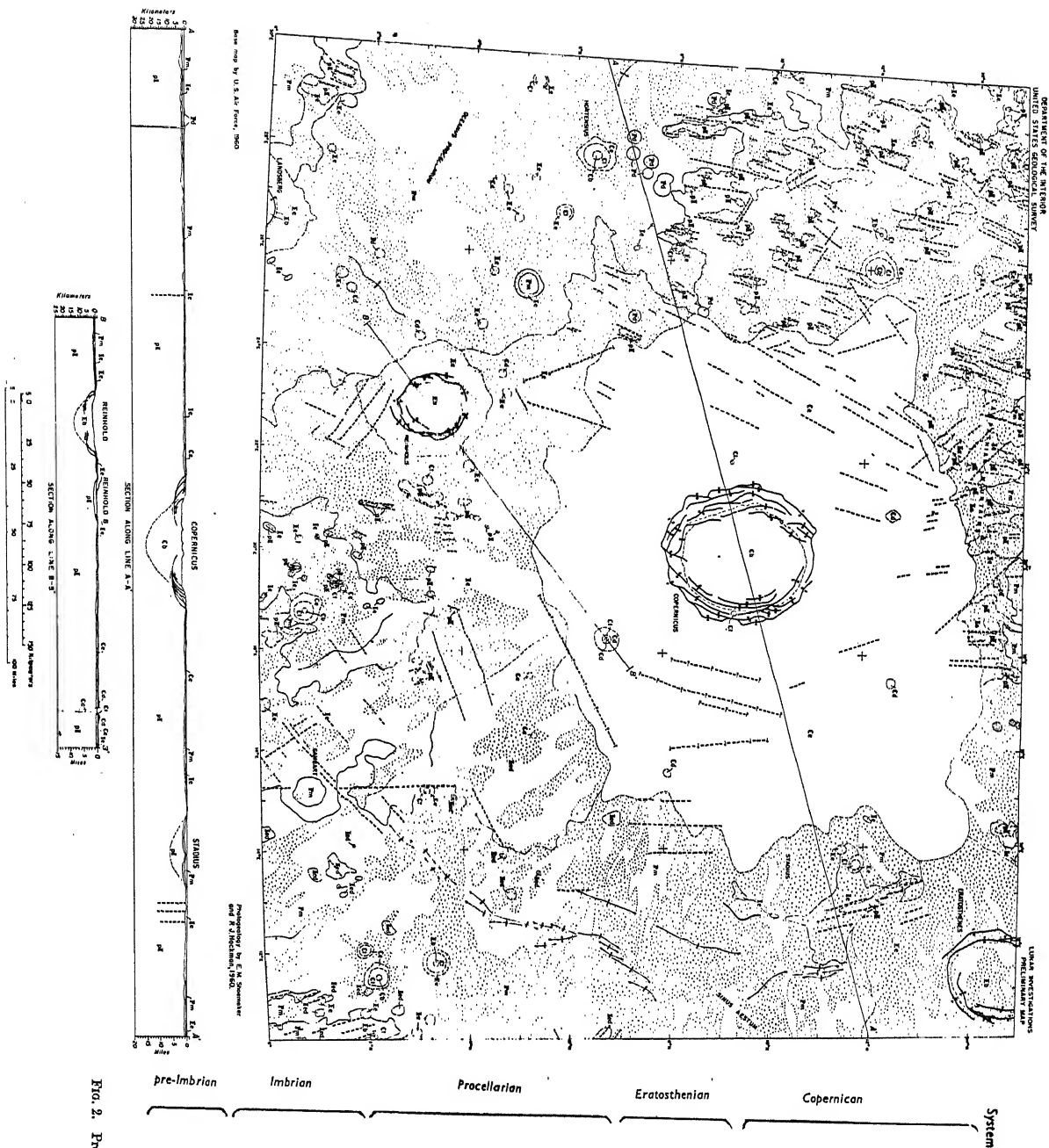


FIG. 2. Preliminary photogeologic map of the Copernicus region of the Moon.

# EXPLANATION

## Stratigraphic Units

**Dark ejecta**  
Probably basaltic or dark colored volcanic ash. Forms layers ranging from a few feet to several hundred feet thick, initial surface probably smooth or the scale of feet and inches.

Cd

**Ejecta blanket**  
Probably chiefly crusted rock with large blocks. Forms locally thin layers ranging from a few feet to about 3000 feet thick around small and large craters. Initial surface probably rough at the scale of feet and inches.

Ce

**Ray material**  
Probably chiefly crusted rock. Forms thin patchy layers, in most cases less than a foot thick. Initial surface probably very rough at the scale of feet and inches.

Ee

**Ejecta blanket**  
Probably chiefly crusted rock with large blocks. Forms hummocky layers ranging from a few feet to about 3000 feet thick around small and large craters. Initial surface probably rough at the scale of feet and inches.

Eb

**Breccia**  
Probably chiefly crusted rock with large blocks. Probably fairly deep masses made from broken fragments of craters. Topography is irregular to smooth. Initial surface probably rough at the scale of feet and inches.

Ci

**Talus**  
Probably partially sorted accumulations of fragments ranging in size from dust to large blocks. Generally forms sheets mantling the surface of craters. Initial surface probably rough at the scale of feet and inches.

Pd

**Dome material**  
Probably chiefly volcanic domes; may include volcanic ash. Common dark color and low relief suggest small craters and a few thousand feet high, generally with summit craters. Initial surface probably rough at the scale of feet and inches.

Pm

**Flow material**  
Great craters and numerous smooth topography suggest older flows. Flows of basaltic and andesitic lava. Initial surface probably smooth or the scale of feet and inches.

Ile

**Ejecta blanket**  
Probably chiefly crusted rock with large blocks. Forms a layer ranging from a few hundred to a few thousand feet thick. Layer is probably of heterogeneous composition because of local alteration. This is thicker than the and locally establishes flow. Green coloration. Initial surface probably rough at scale of feet and inches.

pII

**Pre-Imbrian rocks (undifferentiated)**  
Probably includes breccia, layers of ejecta, and possibly volcanic or other igneous rocks. May in places be covered with a thin mantle of Imbrian ejecta.

## Surface Characteristics

Generally smooth at the scale of miles. Topography controlled by regional and local tectonics. Surface is generally smooth. Among the youngest material on the Moon, the surface is probably largely unmodified. Low reflectivity.

Topography at the scale of miles varies from fairly smooth to hummocky to smooth. Probably rough to very rough at the scale of feet and inches. Initial surface probably smooth or the scale of feet and inches. High to very high reflectivity.

Topography at the scale of miles varies from pitted to hummocky to smooth. Probably smooth to slightly rough at the scale of feet and inches. Initial surface probably smooth or the scale of feet and inches. Low to moderate reflectivity.

Volcano-shaped topographic forms. Probably smooth at the scale of miles. Topography is generally smooth to slightly rough at the scale of feet and inches. Initial surface probably smooth or the scale of feet and inches. Low to moderate reflectivity.

Smooth ridges broken by small depressions and secondary impact craters and craters. Probably smooth at the scale of miles. Topography is generally smooth to slightly rough at the scale of feet and inches. Initial surface probably smooth or the scale of feet and inches. Low reflectivity.

Hilly to locally smooth at the scale of miles. Topography characterized by small depressions and secondary impact craters and craters. Probably smooth at the scale of miles. Topography is generally smooth to slightly rough at the scale of feet and inches. Initial surface probably smooth or the scale of feet and inches. Low to moderate reflectivity.

Not well exposed.



**Rim and chain crater material**  
Probably includes breccia, fault blocks and volcanic rocks or scoria. Age not definitely established but probably chiefly Imbrian.

**Contact**  
Dashed where approximately located  
Indefinite contact

**Fault**  
Dashed where approximately located  
U. upthrown side; D. downthrown side  
Concealed fault or fracture  
Queried where precise

**Anticline**  
showing trace of axial dip and bearing  
showing trace of  $\sigma_2 \approx \sigma_3$   
**Syncline**  
showing trace of  $\sigma_2 \approx \sigma_3$   
**Flow front or monocline**  
showing direction of slope of surface scarp

thin layer of ejecta derived partly from the main central crater and partly from the local gouges.

The radial frequency distribution of gouges shows a sharp mode near 160 km from the center of Copernicus. At greater distances the frequency drops off rapidly, and toward the outer extremity of the ray system the frequency drops gradually to zero. If we come closer to Copernicus from the

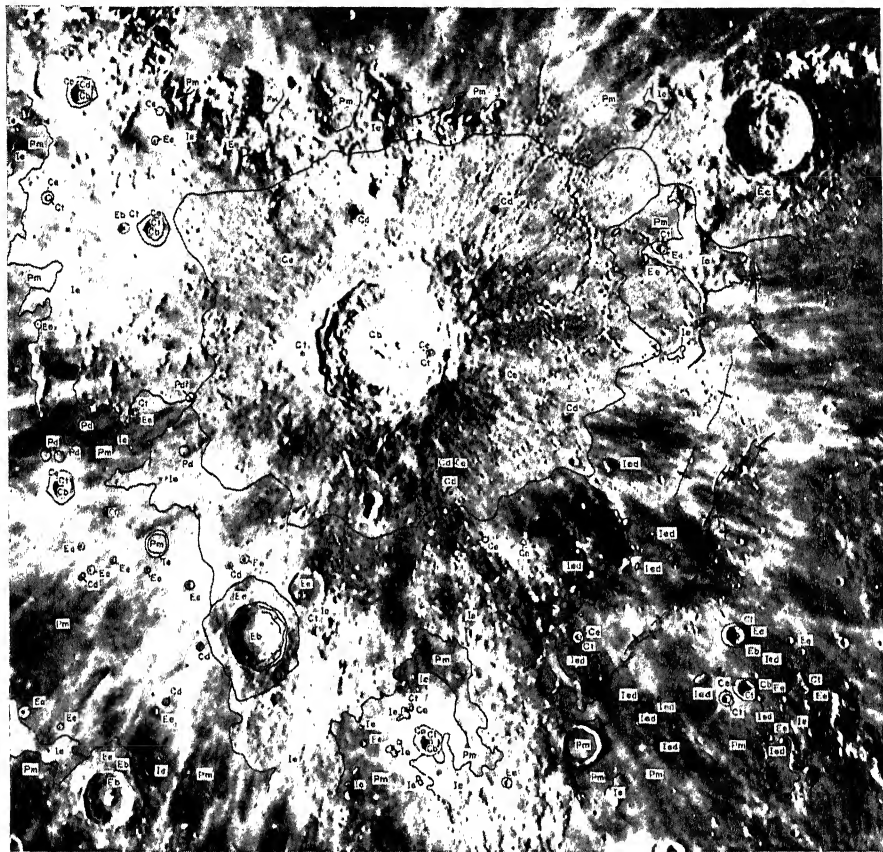


FIG. 3. Annotated photograph of the Copernicus region. Photograph taken by F. G. Pease at the 100-in. Hooker telescope in 1929, Mount Wilson Observatory.

modal distance, the frequency drops off very rapidly, evidently owing chiefly to the fact that toward the main crater the gouges in the pre-existing lunar surface tend to be covered up or smothered under an increasingly thick deposit of material making up the crater rim. The smothering effect begins about 80 km from the edge of the crater, about where the relief of the sub-radial ridges can first be seen, and from this distance inward there is essentially a continuous blanket of ejecta. The thickness of this blanket ranges from a feather edge at its outer extremity, beyond which the pre-existing lunar surface is exposed between the rays, to a maximum that probably does not exceed about 1000 m, the height of the rim.



## EJECTA FROM OTHER CRATERS

Scattered over the lunar disk are many other craters the size of Copernicus and smaller that have similar hummocky rims. In general, the ratio of the width of the hummocky terrain to the diameter of the crater decreases with decreasing size of the crater. Around some craters almost all the rim terrain is made up of a nearly random arrangement of hummocks typical of the rim crest at Copernicus; around others the rim is marked by a strong radial or subradial pattern of low ridges typical of the peripheral zone of the rim of Copernicus. Visible gouges surround the rims of all such craters approaching Copernicus in size. The interior walls of these craters are almost invariably terraced, the floors are irregular, and nearly all have a central peak or peaks.

Many craters with this group of characteristics are the foci of prominent ray patterns, but many others, such as Eratosthenes (Fig. 2) lack rays entirely. Where they are not overlapped by Copernican rays, the rim and floor of Eratosthenes have relatively low reflectivity or albedo. Wherever a rayless crater like Eratosthenes or a crater with very faint rays occurs in an area with bright rays from some other crater, the bright ray pattern is in all cases superimposed on the darker crater or on the faint ray pattern. From this sequence and from the fact that both craters with rays and rayless craters are widely distributed over the surface of the Moon, we infer that some process or combination of processes is at work on the lunar surface that causes fading of the rays and other parts of the Moon's surface with high reflectivity.

It can be shown that the exterior ballistics for a lunar crater, the velocities and angles at which fragments are ejected, are independent of the size of the crater and the volume of material thrown out [2]. A fragment ejected at a given velocity and angle of elevation will go just as far from a small crater as it will from a large crater. A small volume of material ejected from a small crater, therefore, tends to be as widely distributed as a large volume of material from a large crater. But since the smaller volume is distributed over a comparable area, the lateral and vertical dimensions of the continuous layer of ejecta must obey different scaling laws than the dimensions of the crater.

The ratio of maximum thickness of the ejecta layer on the rim to the diameter of the crater and the ratio of the extent of the continuous ejecta layer surrounding the crater to the diameter of the crater should decrease with decreasing size of the crater. There may be a lower limiting size of craters on the Moon around which only scattered fragments and no continuous layer of ejecta will be found. These scaling relations are partly confirmed by the rim heights and the extent of the rim material of the smaller lunar craters. The width of the visible hummocky terrain diminishes rapidly with decreasing crater diameter so that craters of 15 km diameter and smaller are encompassed only by narrow belts of continuous rim deposits generally less than 5 km wide. An example of such a crater is Hortensius (Fig. 2). Major rim deposits are associated only with the larger craters.

## STRATIGRAPHY OF THE COPERNICUS REGION

In the Copernicus region the surface of the Moon is underlain mainly by an overlapping series of deposits surrounding major craters. The materials have been grouped into five stratigraphic subdivisions; from oldest to

youngest these are (1) pre-Imbrian material, (2) the Imbrian system, (3) the Procellarian system, (4) the Eratosthenian system, and (5) the Copernican system. These stratigraphic subdivisions correspond to five intervals of time which we will call periods. A brief description of the stratigraphic relations and surface characteristics of each system is given in the following pages. A more detailed description of each system and its photometric properties will accompany reports on specific regions that are currently being mapped by the U.S. Geological Survey.

#### PRE-IMBRIAN MATERIAL

No material of pre-Imbrian age can definitely be shown to be exposed in the Copernicus region, but pre-Imbrian rocks may crop out on ridges and hills in the Carpathian Mountains and on scattered ridges and hills east†, west, and south of Copernicus in areas indicated on the map (Fig. 2). The overlying Imbrian system, if present on these ridges, appears to be very thin. The Imbrian system can be inferred with high confidence to overlie a surface of complex relief that includes ridges, valleys, and craters. Rocks which underlie the Imbrian probably have diverse origins and a complex history. Because craters are a conspicuous component of the pre-Imbrian terrain, it is likely that the pre-Imbrian includes many crater rim deposits like those associated with craters of younger age. The overlying Imbrian system thins rapidly south of the Copernicus region, and pre-Imbrian material is probably widely exposed in the southern hemisphere of the Moon. Detailed mapping in the southern regions may show that the pre-Imbrian can be divided into many separate mappable stratigraphic units.

#### IMBRIAN SYSTEM

The Imbrian system is the oldest widely exposed stratigraphic unit in the Copernicus region. It is continuously exposed from the Carpathian Mountains southward to a group of hills or low mountains north of Hortensius and in a broad area south of Copernicus between the longitudes of Reinhold and Gambart. The topography developed on the Imbrian is unique. It is a gently rolling surface studded in most places with close-spaced low hills and intervening depressions generally ranging from 1 to 4 km across. Isolated larger hills and elongate ridges occur, but these may, in the main, merely reflect buried pre-Imbrian topography. The numerous small-scale topographic features impart a shagreen appearance to the Imbrian as it is seen through the telescope or on photographs with high resolution at certain angles of illumination.

Most of the Imbrian has an albedo intermediate between the extremes of the range of lunar albedo, but locally, north of Gambart (shown as II ed on the map, Fig. 2) and in isolated exposures in Sinus Aestuum and to the west, the Imbrian has a very low albedo. These areas of low albedo are some of the darkest places on the Moon.

The surface on which the Imbrian rests in the Copernicus region appears to include prominent linear ridges and intervening valleys in the Carpathian Mountains and the area south-east of the Carpathian Mountains and includes a few recognizable pre-Imbrian craters such as Stadius that are nearly filled

† In this report east and west will be used according to astronomical convention as shown in Fig. 1.

with Imbrian and younger strata. In most of the area between Reinhold and Gambart and north of Gambart the pre-Imbrian is apparently so deeply buried that this buried surface has little influence on the topography developed on the Imbrian, except possibly at a few isolated hills. Gambart, a crater north-west of Reinhold (Reinhold B), and a crater north of Copernicus (Gay-Lussac) are partly filled with Imbrian, but it is not clear whether these craters are pre-Imbrian in age or should be assigned to the Imbrian period. Unlike most craters partly filled with Imbrian material the rims of these three craters are not broken or displaced by linear trenches, which are part of a system of linear features referred to by Gilbert ([3], p. 275-279) as Imbrian sculpture, features which characterize part of the pre-Imbrian terrain. The Imbrian may be a few thousand meters thick where it fills or partly fills some of the pre-Imbrian craters and the valleys in the Carpathian Mountains, but it is evidently thin and perhaps locally absent where it covers or laps against the crests of old crater rims and certain high ridges, as indicated by relative sharpness of form of these features.

The Imbrian is extensively exposed in a very large region around the southern margin of Mare Imbrium and is probably related in origin to the great topographic basin which the mare occupies. Essentially the materials of the Imbrian system form an immense sheet partly surrounding Mare Imbrium. Gilbert ([3], p. 274-277), Dietz ([4], p. 373), Baldwin ([5], p. 210-212), Urey ([6], p. 221), and Kuiper ([7], p. 1104; [1], p. 290-295) have interpreted, each in a somewhat different way, part of the material which we recognize as the Imbrian system as ejecta from some place in the region occupied by Mare Imbrium. On the basis of its distribution and surface characteristics we concur with the interpretation of this material as ejecta, but the recognition of the Imbrian system is independent from the problem of its mode of origin and source. It has been named Imbrian for the extensive exposures that partially surround Mare Imbrium.

#### PROCELLARIAN SYSTEM

The Procellarian system in the Copernicus region forms the relatively smooth dark floors of the Oceanus Procellarum, Mare Imbrium, and Sinus Aestuum and rests stratigraphically on the Imbrian system. It is the material which partly fills the topographic depressions of the Oceanus Procellarum and the maria. The name is taken from the Oceanus Procellarum which is by far the largest area of exposure of the Procellarian on the Moon. The albedo of the Procellarian is everywhere relatively low, but is by no means uniform. Determination of the photometric characteristics of the Procellarian in the Copernicus region is complicated by the presence of the superimposed Copernican rays. In areas between the rays the albedo of Procellarian is lowest east of Landsberg and just north of Hortensius and highest in Sinus Aestuum. At no place is the albedo of the Procellarian as low as that of the dark Imbrian material north of Gambart, but in general the Procellarian has a lower albedo than most of the Imbrian system and most of the other stratigraphic units on the Moon.

Relief on the Procellarian is exceptionally low compared to most other parts of the lunar surface, but the surface of the Procellarian is not featureless. Characteristic topographic forms intrinsic to the Procellarian include ridges, some of them probably more than 100 m high, and low conical and

dome-shaped hills up to 100 to 200 m high and 5 to 10 km across. Rarely do the slopes on any of these features exceed about 5°.

Individual ridges are typically 15 to 30 km long and they occur both singly and in complex en echelon systems, such as one extending into Sinus Aestuum that is nearly 200 km long. The ridges have commonly been interpreted as folds by previous investigators and are shown symbolically as anticlines on the map, but the structure of the ridges may be more complex or even entirely different than ordinary anticlines. By telescopic examination Kuiper ([1], p. 302) has found protrusions and fissure-like depressions on their crests.

Many of the low hills, which are referred to in the lunar literature as "domes", have small craters in their summits; within the limits of telescopic resolution some of these features resemble small terrestrial basaltic shield volcanoes and are so interpreted in the cross-sections accompanying the map. The surfaces of many of the "domes", however, unlike most shield volcanoes, are distinctly convex. The margins of the "domes" are topographically distinct and can be readily mapped, but it is not certain whether they are formed of material that is superimposed on the other Procellarian material or whether the domes are merely structural features in the Procellarian. Most of the dome material appears to be photometrically indistinguishable from the rest of the Procellarian.

In the Copernicus region the Procellarian rests nearly everywhere on the Imbrian system, and the surface of contact has considerable relief. Many isolated exposures of Imbrian occur on hills where the Imbrian rises above the level of the Procellarian in the midst of areas generally covered by the Procellarian. Elsewhere the Procellarian extends along comparatively narrow channelways or corridors into areas of general Imbrian exposure. Local completely isolated exposures of the Procellarian occur within craters such as Gambart. The thickness of the Procellarian, as judged from the extent and distribution of partly buried pre-Procellarian features, is probably nowhere greater than a few thousand meters in the Copernicus region. In other regions of the Moon it may be thicker (compare with Marshall [8]).

In the past the Procellarian material has very generally been interpreted to be volcanic, but recently the hypothesis has been advanced (Gold [9]; Gilvarry [10]) that the material referred to here as the Procellarian system is composed entirely of dust or fragmental debris derived by nonvolcanic processes. Except for the volcano-shaped domes, only a few features of form and scale characteristic of terrestrial lava fields have been found on the Procellarian. An irregular extension of the Procellarian between Gambart and Reinhold resembles a large lava flow, and a low scarp near the terminus may be a secondary flow front, possibly indicative of more than one surge of fluid. The exact nature of the scarp is not known however. It is a low rise on the surface of the Procellarian and could be a flow front, a monocline, or related in some way to the ridges that occur elsewhere on the Procellarian. Whatever the origin of the Procellarian system, it can be shown that the Procellarian is definitely older than a large number of strata that are superimposed upon it.

#### ERATOSTHENIAN SYSTEM

The Eratosthenian system comprises the rim deposits surrounding Eratosthenes, Reinhold, Landsberg, and a number of smaller craters and the

material that occupies the floors of these craters. Eratosthenian deposits rest on the Imbrian and Procellarian systems and locally may rest on pre-Imbrian material. Individual deposits surrounding each of the three largest Eratosthenian craters rest on both the Imbrian and the Procellarian. The most extensive of these deposits is associated with the crater Eratosthenes, from which the name for the system is taken. A pattern of numerous gouges in the Procellarian in both Mare Imbrium and Sinus Aestuum on either side of Eratosthenes (Fig. 3) shows conclusively that ejecta from this crater are superimposed on the Procellarian.

Eratosthenian deposits are characterized and can be distinguished photometrically from nearly all stratigraphically higher deposits of the Copernican system by their low to medium albedo. Where it is not overlapped by Copernican rays, the rim of Eratosthenes has a lower albedo than the Procellarian system in the adjacent parts of Mare Imbrium and Sinus Aestuum. The albedo of the rim deposit of Reinhold is about the same as that of the immediately adjacent part of the Procellarian system and distinctly lower than the albedo of the nearby Imbrian system, on which most of the Reinhold ejecta rest. Eratosthenian deposits around Landsberg have nearly the same albedo as nearby Imbrian exposures, which is distinctly higher than the albedo of the adjacent Procellarian.

The topography of the Eratosthenian deposits varies with the size of the individual craters with which they are associated. Upper slopes of the rim of Eratosthenes are irregularly hummocky, but low subradial ridges are present near the outer extremity of the ejecta blanket. The rim deposits of Reinhold and Landsberg are entirely hummocky. Rims of the smaller Eratosthenian craters are narrow and smooth at the scale observable through the telescope. The thicknesses of the rim deposits range from a feather edge to maxima that probably do not exceed the height of the crater rims above the surrounding terrain, about 600 m in the case of Eratosthenes, the largest Eratosthenian crater in the region.

The floors of the larger Eratosthenian craters have small-scale topographic features and photometric characteristics similar in some respects to the rim deposits. The floors have been outlined and designated somewhat arbitrarily as breccia on the map to differentiate the material that underlies the crater floors from the ejecta of the rims, which presumably have been thrown out. In the cross section, which is necessarily speculative, the breccia is interpreted as a deep lens under the crater by analogy with large terrestrial impact craters (Shoemaker [2]).

The deposits around the various craters in the Copernicus region that have been grouped in the Eratosthenian system probably have a wide range in age, but all can be shown to be post-Imbrian and most of the deposits rest partly or entirely on the Procellarian and thus are post-Procellarian. Nearly all of the Eratosthenian deposits are partly overlapped by Copernican rays and are therefore pre-Copernican.

#### COPERNICAN SYSTEM

The Copernican system, the stratigraphically highest system in the Copernicus region, includes several mappable units. The most extensive units of the Copernican system are the rays and rim deposits of the crater Copernicus and the rays of several smaller craters, notably Hortensius and a bright ray crater east of Gambart. Other units in the Copernican system

have been termed breccia, talus, and dark ejecta. As in the Eratosthenian craters, the material that occupies the more or less level floors of the larger Copernican craters has been mapped separately and somewhat arbitrarily as breccia. The term talus has been applied to all material of high albedo on smooth steep slopes. Among the stratigraphically highest units in the region are the dark rim deposits of certain small craters that are superposed on the ejecta blanket and rays of Copernicus. Because of their stratigraphic position these dark deposits have been included in the Copernican system although they contrast photometrically with the other Copernican units. Various units of the Copernican system rest on all the other stratigraphic systems in the Copernicus region.

The albedo of all units of the Copernican system, except for the small dark rim deposits, ranges from medium to high and is higher than the albedo of any of the other stratigraphic system. The wall of the ray crater east of Gambart (Gambart A) is one of the brightest places on the surface of the Moon, but in some places the Copernican units have only slightly higher albedo than adjacent systems. The ejecta blanket around Copernicus is mottled with streaks and patches of lower albedo than the average for the blanket, which is considerably lower than the albedo of the rim deposit of Gambart A.

The rays present a peculiar problem in cartography because they have no well-defined boundaries. Their diffuse margins are probably areas where fragments of Copernican ejecta are scattered individually over the lunar surface and much pre-Copernican material is exposed. The measurable albedo at any place on the rays would therefore contain the integrated effect of Copernican ejecta and whatever pre-Copernican material is present at the surface. The rays have no determinable thickness and their topography is thus the pre-Copernican topography modified locally by the presence of gouges. For these reasons a stipple pattern overprinted on the pre-Copernican units was chosen to represent the ray material on the present map.

Units mapped as talus in the Copernicus region occur only on slopes exceeding 20°. Most such slopes occur on the walls of the smaller craters, and nearly all slopes this steep have a high albedo, regardless of the age of the crater or the albedo of the ejecta surrounding the crater. This correlation between albedo and slope suggests that fresh material of a high albedo is being continuously or intermittently exposed by mass movement on the slopes; hence, it has been termed talus. Similar material probably occurs along steep scarps characterized by higher than average albedo that separate terraces on the walls of Copernicus, but for the sake of clarity of the map have not been shown. The bases of the scarps are indicated by symbols for faults.

The Copernican dark rim deposits, which form small diffuse haloes around craters ranging from 1 to 5 km across, have been tentatively interpreted by us as dark colored volcanic ash [11, 2]. They are unusual features which are peculiar to the Copernicus region and a few other widely separated localities on the Moon. One small crater is present in the southern hemisphere of the Moon (Buch B) around which there are both bright and dark rays. Only for these few deposits and some exceptional dark streaks and haloes in Copernican ejecta blankets does the albedo fail as a criterion for the recognition of Copernican material.

The individual deposits assigned to the Copernican system probably range

widely in age but all are superimposed on pre-Copernican strata or on the ejecta from Copernicus itself. Rays from Copernicus are superimposed at one place or another on all exposures of pre-Copernican units in the Copernicus region except for a few small isolated areas of outcrop of pre-Imbrian, Imbrian, and Eratosthenian material. The rays and rim deposits of two small bright ray craters and from several dark halo craters are, in turn, superimposed on the ejecta blanket of Copernicus. The stratigraphic relations between the rays of Copernicus and bright rays of certain other Copernican craters such as Hortensius and Gambart A have not yet been demonstrated conclusively, but the very bright rays of Gambart A appear to be superimposed on the somewhat darker rays of Copernicus.

#### RILLS AND CHAIN-CRATER MATERIAL

Rills, which are long narrow trenches in the lunar surface, and craters aligned in a chain or a row that passes laterally into a rill, occur in Sinus Aestuum and Mare Imbrium. These features are developed on the Procellarian and are overlapped by Copernican rays and locally by the ejecta blanket. Their age is not definitely established, as they could be either late Procellarian or Eratosthenian or possibly early Copernican. The chain craters have distinct raised rims but the extent of any ejecta that may have been derived from them has not been determined. The material on the floors of these craters and in the rills is shown on the map as a unit separate from the surrounding Procellarian material, but the areas of exposure are so small that it is difficult to discriminate the material photometrically from the Procellarian.

#### THE LUNAR TIME SCALE

Reconnaissance studies indicate that the stratigraphic systems recognized in the Copernicus region can be correlated and mapped over most of the visible hemisphere of the Moon, and the systems have been traced by photogeologic mapping from the Copernicus region into the contiguous regions. A lunar time scale corresponding to the stratigraphic systems described and extending from the beginning of lunar history to the present is therefore proposed as follows:

- Present time
- Copernican period
- Eratosthenian period
- Procellarian period
- Imbrian period
- pre-Imbrian time
- Beginning of lunar history.

The periods are defined as consecutive.

The beginning of the Imbrian period is defined as the moment of deposition of the stratigraphically lowest material in the Imbrian system. This material lies at the base of the great Imbrian sheet extending south of Mare Imbrium. All of lunar history prior to this moment makes up pre-Imbrian time, an historical interval that may be divisible into formal periods in future investigations.

The end of the Imbrian period and beginning of the Procellarian period is the moment of deposition of the stratigraphically lowest material of the

Procellarian system. Considerable evidence indicates that the Imbrian period occupies a significant interval of absolute time in lunar history. The rim deposit around the crater Archimedes (Fig. 1), for example, overlies the Imbrian sheet and is in turn overlain by the Procellarian. Numerous other craters outside the Copernicus region were formed during the Imbrian period, and the ejecta from them are part of the Imbrian system.

The end of the Procellarian period and beginning of the Eratosthenian period is defined as the moment when deposition or emplacement of the stratigraphically highest material in the Procellarian system ended. Statistical studies of the distribution of Eratosthenian and Copernican craters on the Procellarian [12] suggest that the top of the Procellarian system is about the same age wherever the Procellarian occurs on the Moon. The absolute time interval occupied by the Procellarian period is probably relatively short.

The end of the Eratosthenian period is operationally defined as the moment of deposition of the faintest rays that can be discriminated photometrically by their higher albedo. Implicit in this definition is the working hypothesis that the albedo of all rays has decreased with the passage of time, that the rate of decrease is a monotonic function of time and similar for all bright rays, and that the photometric properties of the rays approach those of the material on which they are deposited so that the rays ultimately disappear. A corollary of this working hypothesis is that many or most Eratosthenian craters, such as Eratosthenes, were once the foci of rays that have disappeared. All Eratosthenian craters, are by definition, devoid of rays. The local relative stratigraphic sequence of all Eratosthenian and Copernican craters so far mapped or studied is consistent with this working hypothesis.

The Copernican period is taken as extending to the present. Studies of crater frequency distribution, which will be reported elsewhere, suggest that the Eratosthenian and Copernican periods, taken together, correspond to the greater part of geological time and that the Copernican period represents somewhat less than half of this total interval. If this is so, the earlier periods are comparatively compressed intervals in absolute time, but ones of considerable activity in the development of the lunar surface features.

The deposition of most individual deposits of ejecta probably occurs in extremely small fractions of the total span of lunar history, and the precise position of the type Eratosthenian deposits of the Copernicus region and the type Copernican deposits within the Eratosthenian and Copernican periods, as defined, is not known. The number of small bright ray craters superimposed on the ejecta blanket of Copernicus suggests it was formed in the later third of the Copernican period. Further studies are expected to show that it is possible to subdivide the Copernican period and correlate Copernican ejecta according to the albedo of the rays.

The causes of the fading of the rays are not known, but two processes acting on the lunar surface may be expected to contribute to the lowering of their albedo: (1) solar ultraviolet irradiation and cosmic ray bombardment, and (2) micrometeorite bombardment. High energy radiation is known to lower the albedo of some silicate and other rock-forming materials, and the processes of bombardment by micrometeorites and small meteorites serve to mix the bright ejecta forming the rays with underlying and adjacent materials of the lunar surface.



## REFERENCES

1. Kuiper, G. P. The exploration of the Moon. *In* " Vistas in Astronautics 2nd annual astronautics symposium ", Pergamon Press, New York, 2, 273-312 (1959).
2. Shoemaker, E. M. Interpretation of lunar craters. *In* Kopal, Zdeněk, ed. "Physics and Astronomy of the Moon," Academic Press Inc., New York and London (1962).
3. Gilbert, G. K. *Bull. Phil. Soc. Wash.*, 12, 241-292 (1893).
4. Dietz, R. S. *J. Geol.* 54, 359-375 (1946).
5. Baldwin, R. B. " The Face of the Moon ", Chicago University Press, Chicago, p.239 (1949).
6. Urey, H. C. *Geochim. et Cosmochim. Acta*, 1, 209-277 (1951).
7. Kuiper, G. P. *Proc. Nat. Acad. Sci., Wash.* 40, 1096-1112 (1954).
8. Marshall, C. H. Thickness of the Procellarian System, Letronne region of the Moon. *In* " Short Papers in the Geological Sciences ", U.S. Geol. Survey Prof. Paper 424 (In press.)
9. Gold, Thomas. *Mon. Not. R. Astr. Soc.* 115, 585-604 (1955).
10. Gilvarry, J. J. *Astrophys. J.* 127, 751-762 (1958).
11. Hackman, R. J. Generalized photogeologic map of the Moon. *In* " Engineer Special Study of the Surface of the Moon ", U.S. Army, Office of the Chief of Engineers (1960).
12. Shoemaker, E. M., Hackman, R. J. and Eggleton, R. E. Interplanetary correlation of geologic time. *Proc. Amer. astronaut Soc.*, 7th Annual Meeting. (In press.)

# PHOTOGEOLOGIC STUDY OF THE MOON†

ARNOLD C. MASON‡, ROBERT J. HACKMAN

*U.S. Geological Survey, Washington, D.C., U.S.A.*

A GENERALIZED photogeologic study of the surface of the Moon was prepared for the Office of the Chief of Engineers by the United States Geological Survey, as a part of a joint program with Army Map Service, which meanwhile was making a lunar topographic map. A "Generalized Photogeologic Map of the Moon" and "Physical Divisions of the Moon" were compiled using a photomosaic in orthographic projection at an approximate scale of 1:3 800 000 as a base, prior to the completion of the lunar topographic map. Modified forms of these two maps are presented here, in which details have been simplified appropriate to the smaller scale.

The study presents the interpretations selected as probable or most likely among those possible. In many cases other interpretations have been advanced. In general, statements that appear to be arbitrary are so worded only for brevity, to avoid repetitious qualifications.

In photogeology, as normally applied to areas on the Earth, a pair of photographs having for viewing purposes an effective angular difference averaging about  $30^\circ$  are studied stereoscopically to obtain geologic information. The photogeologist is able to observe features in their relative horizontal and vertical positions. Structures and other geologic relationships are commonly detected which may not be apparent to an observer close to them on the ground. Details such as fine lines or textural differences, not readily seen on single photographs, commonly are discernible in the stereoscopic model. Where not concealed, rock units may in some areas be identified and mapped. Photogeologic interpretations normally are developed from at least some prior knowledge obtained from examination in the field, and results are usually field checked to whatever extent is appropriate.

The study of the Moon was made by applying photogeologic principles to the study of selected libration pairs of lunar photography. Lacking field data, interpretations depended upon analogies to Earth features, allowing for known differences existing on the Moon. The Moon's libration permits selected photographs taken from the Earth to appear as though taken from two stations typically about 50 000 miles apart, equivalent to an angular difference of approximately  $12''$ . Although less than ordinarily used for photogrammetric purposes, this difference provides acceptable stereoscopic vision.

For satisfactory stereoscopic viewing, lunar photographs selected should have sufficient angular difference in libration, have the same scale, include a common area, and have image shadows falling in the same direction. Rarely, opposing shadows enable interpretation of additional details. Use of a number of pairs of photographs of the same area under different solar lighting conditions is desirable to bring out different details.

† Publication authorized by the Director, U.S. Geological Survey.

‡ The editors regret to announce that, while this volume was in the press, Dr. Mason died on 31st October 1961.

Photographic pairs can be positioned approximately by trial and error, but a systematic method of orientation is preferable. In one method the geometric center of the lunar disk for each of a particular pair of photographs is located by geometric construction or by use of a circular template. For each photograph the image point representing the geometric center on one is located on the other, where it is termed the conjugate center. The line connecting the geometric centers and conjugate centers on each photograph is aligned with the "x-direction" (parallel to a line connecting the eyepieces) of the stereoscope, and the pair placed under the stereoscope with proper separation for viewing. The right and left members of the stereoscopic pair must be under the appropriate eyepiece, otherwise image reversal results.

In a quick method, particularly useful to view one photograph with several others having different librations, only the geometric center on each photograph is located. One photograph is flipped up and down over another until image points coincide approximately. The alinement of geometric centers is placed parallel to the "x-direction," and the photographs are separated for viewing under the stereoscope. Libration co-ordinates can also be plotted for positioning to view stereoscopically.

For detailed study, the photographs, obtained from several observatories, were enlarged to a lunar diameter of about 32 in. As this size is too large to be handled under a conventional stereoscope, the photographs were cut into about a dozen hexagons. In a libration pair, the corresponding hexagons were cut to cover identical areas.

Recognition and interpretation of geologic features in the stereoscopic model are based on such elements as size, shape, tone, texture, pattern, and relationship to associated features. Many features on the Moon are probably comparable to those on Earth, allowing for differences in the environment. As on the Earth, younger material generally is superposed on older material. Younger features are "sharper" in appearance than older, which may be partially eroded, destroyed, or buried.

The "Generalized Photogeologic Map of the Moon" (Fig. 1) shows the stratigraphy and structure of the surface in generalized form. The surface materials were assigned to one of three relative ages: (1) Pre-Maria rocks, (2) Maria rocks, and (3) Post-Maria rocks. Additional subdivision is possible with more detailed study of smaller areas.

The oldest are the Pre-Maria rocks composing the crater-pocked lunar highlands, probably consisting of fragmental and comminuted accretionary material with some breccia, layers of ejecta, and volcanic rocks. Impinging upon and interfingering into the highlands are the Maria rocks, probably great lava flows of thick sheets of basalt occupying the lunar lowlands, some of which appear to be basins resulting from very large impacts. The youngest are the Post-Maria rocks which compose little-eroded fresh-appearing features scattered over both the highlands and the lowlands; these rocks probably consist of fragmental and comminuted material from impacts, including layers of unsorted ejecta, breccia, surficial ray material, and some volcanic material, the Rümker Hills in particular being interpreted as extrusive accumulations. The age relationships are based upon overlap of the series of deposits of ejecta and probable lava flows, and the relative freshness in the appearance of the physical features.

The Pre-Maria rocks compose features which generally have been exposed to considerable erosive processes as a result of their greater age. Many

craters are partly eroded, overlapped, or buried, and are cut by fractures extending from impacts forming younger craters. The Pre-Maria rocks appear in places to be overlain by material ejected from some of the maria. Also in some areas they may be mantled with ejecta from Post-Maria impacts; the thickness of this mantle depends upon the local relief, and the number, size, and proximity of the later impacts. Some Pre-Maria craters appear to have formed after the creation of the basin of Mare Imbrium but before the deposition of Maria rocks, as they are structurally unaffected despite their proximity to the basin, yet their flanks are overlapped and their bottoms are partly filled by maria material; Archimedes is an example.

The Maria rocks appear to be occupying basins, and in places to have overflowed low rims. These probable flows appear to have occurred approximately contemporaneously, as their contacts have little contrast, and Post-Maria craters on their surfaces have similar frequency distribution.

Post-Maria craters appear to be more numerous on the highlands than on the lowlands of the maria. This difference probably results from the inclusion of some craters formed after the creation by impact of the basin of Mare Imbrium and before the maria flows, as such craters are difficult to distinguish from strictly Post-Maria craters. The Post-Maria chain craters appear to be volcanic craters. Only the more prominent have been mapped. The domes are probably basaltic shield volcanoes. The chain craters and domes correspond in scale to volcanic features on the Earth.

The major structural features on the Moon relate to the principal impact basins—Mare Imbrium, Mare Serenitatis, Mare Neotaris, Mare Crisium, and Mare Humorum. These tend to have elevated rims comprising ring mountains that consist of radial wedge-shaped fault blocks formed by dilation at time of impact. These blocks tend to be cut by diagonal shear faults, and by circumferential faults. Beyond the elevated rims ring synclines are developed to some extent. The structural trough occupied by the west part of Mare Frigoris is the north sector of a ring syncline that partly encircles Mare Imbrium.

Structural features on the surface of the maria are less pronounced. In some areas the material at the surface forms low ridges which are suggestive of anticlinal folds, many of which are en echelon. Monoclines are numerous, particularly near borders. Some of these suggest downwarping of the material occupying the maria basins.

Crater structures occupy the greater part of the Moon's surface. The various types have been described above.

The study lends support to the suggestion that most visible craters on the Moon are the result of meteoric impact, although some craters and other features are interpreted as volcanic in origin, and are so distinguished where possible on the photogeologic map. Volcanic craters are formed either by accumulation of ejecta around the orifice, or by removal of material around the vent as by gas coring or by explosion (a maar). Large volcanic craters on the Earth, however, are equal in size only to small visible lunar craters. Large basin-shaped volcanic depressions are formed chiefly by subsidence (a caldera). Calderas are much larger, although none approaches in size the largest lunar craters. Large calderas on Earth tend to be irregular in shape, because subsidence tends to be toward a number of collapse areas. As even large lunar craters tend to be circular, it is unlikely they are lunar calderas, and hence, that volcanism has produced other than small lunar craters.

With minor exceptions, volcanoes, even those having subsidence craters, usually show an increase of material around vents. The material around most lunar craters, however, would approximately fill the crater, which would be true for meteoric impacts; the volume of a meteor is negligible with respect to size of the crater created by impact. In volcanoes, a central peak may be either higher or lower than the crater rim, depending upon the extent of the later eruption that produced the central peak. On the Moon, central peaks are lower than the rim. Hence, they likely do not have a volcanic origin, but have probably formed mostly by infall and rebound after the explosion. Volcanoes develop over a period of time; lunar craters seem to have the one-shot characteristics of a meteoric impact. On the Earth, volcanoes occur along belts of structural weakness; the craters of the Moon occur at random, as would be expected of meteoric impact. The radial fractures, ring synclines, and other structures associated with the maria lend support to their origin as resulting from impacts of asteroid size.

The "Physiographic Division of the Moon" (Fig. 2) was compiled to enable description of areas rather than individual features. Areas having similar characteristics were bounded and distinguished from areas having dissimilar characteristics, and the visible surface was divided into major divisions, divisions, provinces, and sections, to which eighty-one terms were applied. These names are derived from those of outstanding features in the region, or are descriptive terms. The location and characteristics of each follows:

## PHYSIOGRAPHIC DIVISIONS

### LUNAR HIGHLANDS

Nearly two-thirds visible surface of Moon, almost completely covered with 30 000 distinguishable and perhaps a million or more other craters, many overlapping and impinging on others; and with small craters superimposed on large craters; diameters from 146 miles (Clavius, 7R, see grid on maps) to below limit of visibility, about  $\frac{1}{2}$  mile; depths vary roughly with diameters and range from 20 000 ft. (Newton, 1T) to probably a few feet; also ejecta-covered, rugged, ring mountains encircling some maria. Rough surface almost entirely in slopes, except many crater bottoms fairly level in whole or part.

### IMBRIUM-SERENITATIS MOUNTAINS

Two large ring mountain systems nearly encircling Mare Imbrium and Mare Serenitatis. Mountain blocks fractured in radial pattern; cut off on maria side by faults nearly encircling the maria. Rough surfaces of ejecta thrown from maria partly or wholly concealing eroded and fractured older surface, but not Post-Maria craters including several prominent ones. Many steep slopes, especially near maria rims where slopes are very steep toward maria, less steep away from maria.

#### *Carpathian Province*

South-west part of ring mountains encircling Mare Imbrium. Radial-wedge-faulted mountains and hills. Generally rough surfaces of ejecta from Mare Imbrium partly concealing eroded and fractured older surface; smoother surfaces on prominent Post-Maria craters of Copernicus and Kepler.

*Carpathians.* Adjacent to Mare Imbrium, in the S.W. part of ring mountains nearly encircling the mare. Radial-wedge-faulted mountains with S.S.W.-trending ridges; promontories, interrupted by embayments of the mare, grade westward to isolated hills rising from floor of mare. Mostly rough surfaces of ejecta partly concealing eroded and fractured older surface.

*Lower Carpathian Section.* Remote from Mare Imbrium in the S.W. part of ring mountains encircling the mare. Radial-wedge-faulted hills trending S.S.W., grading to isolated knobs surrounded probably by lava flows; two prominent Post-Maria craters. Moderately rough surfaces on hills and knobs; fairly smooth surfaces surrounding knobs.

### *Apennines Province*

South part of ring mountains nearly encircling Mare Imbrium, and part of W. border of ring mountains nearly encircling Mare Serenitatis. Mostly rugged, radial-wedge-faulted mountains, with rugged crestline near Mare Imbrium rim; and lower shelf mountains within the rim. Generally rough surfaces of ejecta from Mare Imbrium almost concealing eroded and fractured older surface; smoother surfaces in lower shelf mountains, and on prominent Post-Maria craters of Eratosthenes (8J), Autolycus (9G), and Aristillus (9G).

*Apennines.* Extend 640 miles along S.E. rim of Mare Imbrium and 100 miles along W. side of Mare Serenitatis. Extremely rugged, radial-wedge-faulted mountains with S.E.-trending ridges, in most places terminated abruptly to N.W. by fault around Mare Imbrium rim; peaks above mare rim 12 000 to 18 000 ft. high, tallest in Imbrium-Serenitatis Mountains; elevations decrease to S.E. Generally very rough surfaces of ejecta from Mare Imbrium almost conceal eroded and fractured older surfaces.

*Lower Apennines Section.* Shelf mountains N.W. of Apennines and much lower. Consist of a partly foundered block broken into a higher S.E. mountain group and a lower N.W. mountain group with a low saddle between; cut in two by an embayment of Mare Imbrium trending S.E.; mountains radially faulted trending S.E. and block faulted N.E.-S.W. Generally rough surfaces of ejecta from Mare Imbrium, but smoother in saddle. Slopes steepest in S.E.

### *Haemus Province*

South-west and S. of Mare Serenitatis, W. of Mare Tranquilitatis, separated from Central Crater Province to S. by saddle; grading W. to higher Apennines without sharp boundary. Rim mountains bordering Mare Serenitatis have faint S.W.-trending radial faults on which S.E.-trending radial faults from Mare Imbrium are superimposed; center of province partly invaded by lava floods. Rugged to moderately rugged ridges and isolated valleys trend S.E. and decrease in elevation to S.; ejecta from Mare Imbrium largely to partly conceal eroded and fractured older surfaces, including some craters. Slopes steepest toward Mare Serenitatis and Apennines.

*Haemus Mountains.* South-west and S. rim of Mare Serenitatis, and E. of Apennines. Rugged mountains trending S.E. have dominant radial wedge faults; partly separated by similarly aligned isolated valleys; highest elevation 8000 ft. Rough surface of blocky ejecta from Mare Imbrium, largely conceals eroded and fractured older surfaces, including some craters. Slopes steepest towards Mare Serenitatis and Apennines.

*Lower Haemus Section.* West of Mare Tranquilitatis, N. of Central

Crater Province, and E. of Mare Vaporum. Moderately rugged mountains trend S.E. with dominant radial wedge faults; partly separated by similarly alined valleys. Fairly rough surface of blocky ejecta from Mare Imbrium, partly concealing eroded and fractured older surfaces, including some craters.

### *Taurus Mountains*

Situated between Mare Serenitatis to the W. and Crisium-Fecunditatis Highlands to the E. Mostly moderately rugged, eroded and fractured, older cratered surface partly covered by ejecta; more like a plateau than mountains; large blocks displaced by faulting alined chiefly about N.W.-S.E., some N.E.-S.W.; some S.E.-trending valleys between craters; elevations decrease toward saddle in S. at boundary with Crisium-Fecunditatis Highlands; several dozen fresh Post-Maria impact craters, mostly small. Most craters of moderate height; fairly rough surface from discontinuous layer of blocky ejecta. Slopes decrease toward E. and S.E.

### *Caucasus Province*

East part of ring mountains nearly encircling Mare Imbrium, and N.W. part of ring mountains nearly encircling Mare Serenitatis. Very rugged, radial-wedge-faulted mountains between the two maria; grades N.E. and E. to rugged mountains, then to low tongues irregularly jutting into Lunar Lowlands; two large craters. Generally rough surfaces of ejecta from Mare Imbrium almost conceal eroded fractured older surface in S.W., partly conceal eroded and fractured older surface in S.E., moderately rough surfaces on prominent Post-Maria craters of Aristoteles (11E) and Eudoxus (11F).

*Caucasus Mountains.* Extend S. as tongue between Mare Imbrium to W., and Mare Serenitatis to E. Extremely rugged, radial-wedge-faulted mountains with E.-trending ridges terminated abruptly at rims of both maria; peaks along crestline above maria almost as high in Apennines; elevations decrease at N. and where block has foundered and margins are partly engulfed by lava flows. Generally very rough surfaces of ejecta from Mare Imbrium partly conceal eroded and fractured older surface.

*Lower Caucasus Section.* North rim of Mare Serenitatis. Rugged, radial-wedge-faulted mountains, cross-faulted into hummocky blocks and short valleys; grading W. into higher Caucasus Mountains, and N.E. and E. into prongs of low hills and isolated knobs irregularly jutting into Lowlands where foundered blocks are partly engulfed by lava flows; two large craters. Generally rough surfaces of ejecta from Mare Imbrium overlying ejecta from Mare Serenitatis, together partly concealing eroded and fractured older surfaces; moderately rough surfaces on prominent Post-Maria craters of Aristoteles (11E) and Eudoxus (11F).

### *Alps Province*

North-east part of ring mountains nearly encircling Mare Imbrium. Very rugged, radial-wedge-faulted mountains, highest in middle near mare. Generally very rough surfaces of ejecta from Mare Imbrium concealing eroded and fractured older surface. Slopes steepest facing mare and on sides of Alpine Valley (9E):

*Alps.* Highest part of ring mountains on N.E. side of Mare Imbrium.

Very rugged, radial-wedge-faulted mountains; highest near mare. Mostly rough surfaces of ejecta from Mare Imbrium, concealing eroded and fractured older surface.

*Lower Alps.* Crescent of lower mountains N.E. of and partially encircling adjacent Alps. Rugged, radial-wedge-faulted mountains broken into blocks by cross faulting, forming some short isolated valleys. Generally rough surfaces of ejecta from Mare Imbrium, nearly concealing eroded and fractured older surface.

#### *Jura Mountains*

North-west part of ring mountains nearly encircling Mare Imbrium and between this mare and Mare Frigoris. Generally moderately rugged, radial-wedge-faulted mountains, cross-faulted into blocks with intervening isolated valleys; most rugged in concave arc rimming embayment of Sinus Iridum; elevations decrease toward S.W., N. and E. Several medium and many small Post-Maria craters. Rough to moderately rough surfaces with ejecta from Mare Imbrium partly concealing eroded and fractured older surface, including some craters.

#### CENTRAL AND SOUTHERN HIGHLANDS

Almost one-third visible surface of Moon, in center and S. Densely pocked with contiguous, overlapping, and superimposed impact craters; ranging in diameter from 146 miles (Clavius, 7R) (Bailly, 1R, may be 183 miles in diameter, but on limb and visible only during favorable libration) to below limit of visibility, about  $\frac{1}{2}$  mile; in rim height from 10 500 ft. to a few feet; in depth from 20 000 ft (Newton 1T) to a few feet; includes some mountains on limb (highest, Leibnitz Mountains, 18S, 29 000 ft. high). Rough surfaces almost everywhere of fragmental material from impacts; some crater bottoms smooth. Most surfaces in slopes; some crater bottoms nearly level.

#### *Central Crater Province*

Large area extending S. from center of visible face of Moon. Densely pocked with impact craters, ranging in diameter from about 50 miles to limit of visibility; many traces of nearly destroyed craters; in N.W. many fractures radial from Mare Imbrium, forming some isolated valleys. Rough surfaces almost everywhere, including most crater bottoms. Most surfaces in slopes; level bottoms in a few craters.

#### *Macro-Crater Province*

Extends S. from near center of visible face of Moon, W. of Central Crater Province. Densely pocked with impact craters, many large, and including the largest on Moon; in N. some craters fractured from impact forming Mare Imbrium. Rough surfaces almost everywhere, except for some crater bottoms. Most surfaces in slopes; some crater bottoms nearly level.

#### *Cratered Plain Province*

South-east of Central Crater Province and N.E. of S. pole. Mostly covered with medium to small, mostly eroded craters; many noncontiguous, rising above plainlike surface. Crater surface moderately rough; plain only slightly rough.



*Janssen Crater Province*

Extends from S. pole along E. limb more than halfway to equator. Densely pocked with impact craters, many mostly eroded. Rough surfaces almost everywhere, including most crater bottoms. Most surfaces in slopes; sides of Rheita Valley (15P) steep.

*Nectaris Crater Province*

Nearly half encircling Mare Nectaris from W. to S.E. Moderately to lightly pocked by craters. Tilted block dipping toward mare; near mare elevation changes not abrupt; boundary with mare irregular. A few large, well-preserved Post-Maria craters. Surfaces moderately rough.

*Pyrenees Province*

Between Mare Nectaris and Mare Tranquilitatis to W. and Mare Fecunditatis to E. Medium-sized craters, mostly eroded and fractured, partly covered by ejecta from Mare Nectaris. Surfaces generally rough.

*Pyrenees.* South part of province, between Mare Nectaris and Mare Fecunditatis. Plateaulike upland, about 6000 ft. high, of medium-sized craters, mostly eroded, partly covered by ejecta from Mare Nectaris; many S.E.-trending fractures; some N.E. Surfaces generally rough.

*Lower Pyrenees Section.* North part of province forming peninsula between Mare Tranquilitatis and Mare Fecunditatis. Mostly medium to small craters, forming low plateau; S.E.-N.W. and N.E.-S.W.-trending fractures. Surfaces moderately rough.

*Aestuum Upland*

Nearly isolated upland largely surrounded by Sinus Aestuum, Mare Vaporum, Sinus Medii, and Oceanus Procellarum. Linear hills of impact material from Mare Imbrium, and fractured craters partly covered by impact material. Surfaces mostly very rough; moderately rough in S.

*Schröter Hills.* North-west half of Aestuum Upland. Numerous elongated hills and depressions trending S.S.E.; formed by blocks faulted radially from Mare Imbrium impact, covered by ejecta from Mare Imbrium; some blocks foundered and partly engulfed by lava; Pre-Maria surface largely destroyed and buried by ejecta. Relief several thousand feet, decreases to low relief to W. Surfaces very rough.

*Pallas Section.* South-east half of Aestuum Upland. Faulted and partly destroyed craters, and some linear hills and valleys radially wedge-faulted and fractured S.S.E. from Mare Imbrium impact; some N.-S. fractures also; some blocks foundered and overlapped by Maria lavas; older surface mantled by Mare Imbrium ejecta in N.; mantle thins to S.E. Surfaces very rough in N.; moderately rough in S.E.

*Procellarum Upland*

Upland in S.E. part of, and almost completely surrounded by, Oceanus Procellarum. Elongated hills and valleys in N. formed by structural disturbance and ejecta from Mare Imbrium, grading S. to shattered craters partly buried by this ejecta; marginal blocks partly foundered and engulfed by lava flows; some Post-Maria craters. Surfaces generally rough.

*Parry Section.* South and N.W. part of province. Mostly eroded craters

with walls fractured, broken, or partly missing; partially covered by ejecta from Mare Imbrium and Copernicus, especially in N.; structural blocks in N.-S. alinement radial from Mare Imbrium; some blocks foundered and engulfed at margins by lavas of Oceanus Procellarum; older craters generally flat bottomed, and some partially filled with lava; some Post-Maria craters. Surfaces generally rough.

*Gambart Hills.* North-east part of province. Generally similar to Schröter Hills; mostly elongated hills composed of ejecta thrown from Mare Imbrium and Copernicus, separated by depressions several miles wide; both trending N.-S. radial to Mare Imbrium impact; some faulted blocks foundered and partly engulfed by lavas of Oceanus Procellarum; some Post-Maria craters. Surfaces rough.

#### *Shickard Crater Province*

West of Macro-Crater Province, S. of Mare Nubium and Mare Humorum, and extending to S.W. limb. Densely pocked with older, eroded craters; radial-wedge-faulted high mountains partly encircling Mare Humorum cut at right angles by faults concentric to the mare; scattered small to medium-sized Post-Maria craters; some isolated mare areas in low places. Surfaces generally rough.

#### *Rook Mountains*

On S.W. limb midway between equator and S. pole. Lofty mountains, nature unknown because of position on limb. Surfaces probably rough.

#### *Doerfel Mountains*

On S.W. limb midway between Rook Mountains and S. pole. Lofty mountains, nature unknown because of position on limb; possibly the profile of a ring mountain. Surfaces probably rough.

#### *Leibnitz Mountains*

On S.E. limb near S. pole. Lofty mountains rising 29 000 ft.; among highest on Moon; nature unknown because of position on limb. Surfaces probably rough.

### CRISIUM-FECUNDITATIS HIGHLANDS

Extensive area on E. limb. Densely pocked with eroded and fractured impact craters, including several large ones. Several maria partly interrupt central part, the largest being Mare Crisium. Surrounding Mare Crisium are radial faulted mountains which slope away from mare; shelf mountains and promontories extend into mare. Boundaries with other maria chiefly formed by embayments and are irregular. Some Post-Maria craters. Surfaces generally rough.

### NORTHERN HIGHLANDS

On N. limb, N. of Mare Frigoris. Densely pocked with eroded and fractured impact craters, many with somewhat level bottoms; numerous Pre-Maria and a number of large Post-Maria craters. Several strong fracture patterns, in order of prominence extending N.E.-S.W., N.W.-S.E., N.-S. Surfaces generally rough.

## CORDILLERAS HIGHLANDS

Along W. limb, W. of Oceanus Procellarum. Densely pocked with eroded and much altered old craters. Boundary with Oceanus Procellarum sinuous and poorly defined, with many re-entrants. Some Post-Maria craters. Mountains of uncertain nature along limbs. Surfaces rough to moderately rough.

*Hercynian Mountains*

Along W.N.W. limb, too close to limb to indicate boundary. Nature uncertain because of position; possibly the E.-facing wall of a very large crater, and not of sufficient significance to be a province. Surfaces probably rough.

*D'Alembert Mountains*

Along W.S.W. limb, too close to limb to indicate boundary. Nature uncertain because of position. Surfaces probably rough.

*Cordilleras*

On W.S.W. limb, S. of D'Alembert Mountains. Nature uncertain because of position. Surfaces probably rough.

## LUNAR LOWLANDS

Lowland areas widely distributed on Moon's visible surface, but more in N. than S., the larger areas termed mare. Plains probably of lava which has both occupied large impact areas and flooded adjacent lowlands. The prelava surface forms many islandlike highlands; some of foundered blocks. Plains have low, sinuous lava ridges and moderate differences in elevation from one part to another. Some low domes and hills of extruded lava. Most lava probably cooled after flowing into position, so lava surface probably smooth, but slaggy rough surface possible; probably has many small pits and craters from Post-Maria impacts. Numerous scattered larger craters also formed by Post-Maria impacts. Slopes gentle in plains; steep on craters and included highlands.

## MID-LUNAR LOWLANDS

Group of connected lowland areas occupying about one-third Moon's visible surface, principally in N.W. quadrant, but extending S. and S.E. into the other quadrants. Other characteristics the same as Lunar Lowlands.

*Mare Imbrium*

Approximately circular lowland in N.W. quadrant, about 700 miles diameter and 340 000 sq. miles area. A fairly level inner circle, about 300 miles diameter, including a circle of intermittent ridges 200 to 400 ft. high near perimeter, and isolated highland blocks, as Straight Range (7E), Tenerife Mountains (8E), Pico (8F), Spitzbergen Mountains (9G), and others on perimeter. Inner circle considered lava-filled crater of greatest impact on the Moon's surface. Outer circle, between perimeter of inner circle and rim of Mare Imbrium, a crescent-shaped slump area, only partly lava-flooded. Openings in mare rim and in nearly encircling ring mountains principally W. to Oceanus Procellarum and E. through 25-mile wide break to Mare

Serenitatis. Surface generally smooth except for many small pits and craters, and some larger Post-Maria impact craters; rough in isolated highland blocks. Slopes generally low. The impact elevated and radially fractured and faulted ring mountains, and threw ejecta great distances. At right angles to the radial fractures, relapse created concentric fractures and depressions as Sinus Aestuum, Mare Vaporum, and W. part of Mare Frigoris. Lava flooded these depressions and floors of many craters, some of which formed subsequent to Mare Imbrium impact. Sinus Iridum (6F) probably flooded remnant of nearly concurrent explosion.

#### *Mare Serenitatis*

East of Mare Imbrium and nearly encircled by Imbrium-Serenitatis Mountains; 400 miles N.W.-S.E., 340 miles N.E.-S.W. Probably oldest of mountain-bordered maria; created by second largest impact on Moon's surface. Lava-flooded lowland with numerous low ridges, parallel, en echelon, or randomly arranged. Surface generally smooth except for many small pits and craters, and some larger craters from Post-Maria impacts. Slopes generally low. Structure of ring mountains around rim and encircling depressions, and their mantle of unsorted ejecta, similar to Mare Imbrium, but on a smaller scale.

#### *Lacus Somniorum*

North-east of Mare Serenitatis; boundaries with highlands very irregular. Lowland covered by lava flows from Mare Serenitatis. Downwarp possibly associated with noncontinuous ring of depressions forming great circle around ring mountains rimming Mare Serenitatis. Surfaces and slopes like Mare Serenitatis, but without low ridges.

#### *Mare Tranquilitatis*

Between and contiguous to Mare Serenitatis to N.W. and Mare Nectaris and Mare Fecunditatis to S.E., approximately 500 miles E.-W. Lava-flooded downwarped area with irregular boundaries; in N. isolated emergent highlands, possibly a partially foundered segment of ring mountains encircling Mare Serenitatis. Near S.W. border are minor rilles, probably from contraction and slumping during cooling of lava; S.E.-trending rilles also prominent in E. In W. numerous approximately N.-S. low ridges converge on a circular ridge area, possibly the result of meteoric impact during solidification of lava. Numerous Post-Maria craters, the larger ones mostly in W. Surface generally smooth except for many small pits and craters, and few large Post-Maria impact craters; in isolated highlands rough. Floor generally level; isolated highlands steeper.

#### *Mare Fecunditatis*

South-east of Mare Tranquilitatis. Lava-flooded low area with irregular boundaries, except parts of W. side where bounded by straight fault escarpment. Some low ridges 50 to 300 ft. high trending N.E., N., and N.W. Scattered, small Post-Maria craters. Surfaces and slopes similar to Mare Tranquilitatis.

#### *Mare Nectaris*

South-east of Mare Tranquilitatis and S.W. of Mare Fecunditatis.

Lava-flooded, large, nearly circular, impact area, diameter 170 miles; almost surrounded by ring mountains. Some low ridges trending N. and N.E., and poorly defined circular ridge in center. Few prominent Post-Maria craters. Surfaces and slopes similar to Mare Serenitatis.

### *Mare Vaporum*

South-east of Mare Imbrium and S.W. of Mare Serenitatis; narrow connection with Sinus Medii to S.W., and possibly with Mare Serenitatis. Lava-flooded downwarp, part of interrupted depression encircling Mare Imbrium beyond its ring mountains; probably formed at time of Imbrium impact. Boundaries somewhat straight following structural control, but some irregular embayments. In E., low ridges trending N. and N.W.; in E., W.-sloping monocline. Surfaces and slopes similar to Mare Serenitatis.

### *Sinus Medii*

South-east of Mare Imbrium and S. of Mare Vaporum; includes mean libration center of Moon. Nature, structural relations, and character of boundaries similar to Mare Vaporum. Some conspicuous rilles in E. generally trending N.-S.; N.E. of these is Hyginus Rille (10J). Some Post-Maria craters. Surfaces and slopes similar to Mare Serenitatis except includes several long slopes variously oriented.

### *Oceanus Procellarum*

In W.; largest feature in Mid-Lunar Lowlands. An extensive, lava-flooded lowland with irregular boundaries where lava flows penetrated highlands; open to E. to Mare Imbrium. Islandlike lava-surrounded highland masses, partly submerged crater remnants, Post-Maria craters, and low domes and hills of extruded lava rise above lowland plain. Low, sinuous lava ridges on plain. Surface probably mostly smooth except for many small pits and craters. Slopes mostly low; steep in included highlands and on craters.

*Sinus Roris.* North end of Oceanus Procellarum. Lava-flooded lowland; in E. probably part of the depression encircling Mare Imbrium beyond its ring mountains. Some low ridges trend chiefly N.-S. Some Post-Maria craters and lava hills. Surface generally smooth except for many small pits and craters, and a few large Post-Maria impact craters; in lava hills fairly rough. Slopes generally low; steeper in pits, craters, and lava hills.

*Northern Section.* West of Mare Imbrium. Extensive lava-flooded lowland; includes Harbinger Mountains (5G) and other isolated highland remnants of founded W. rim of Mare Imbrium. Numerous low ridges chiefly trending N.-S. Numerous Post-Maria craters. Surface generally smooth except for many small pits and craters, and some large Post-Maria impact craters; rough in Harbinger Mountains and related isolated highland remnants. Slopes generally low; steeper in pits, craters, and Harbinger Mountains and related highlands.

*Aristarchus Hills.* In N. part of Northern Section, entirely surrounded by Northern Section; extending about 160 miles N.-S. Low hills having rough surfaces of ejecta from Mare Imbrium partially concealing eroded and fractured older surface; also two large Post-Maria craters in S.E. In S. large rille, Schröter's Valley (4G). Surface generally rough, particularly on sides of Schröter's Valley; smoother on lower slopes of the large Post-Maria craters. Slopes steep on sides of Schröter's Valley.

*Milichius Dome Field.* East of Northern Section, and S.W. of lower Carpathian Section. Lava-flooded lowland containing a half-dozen or more small domes 2 to 3 miles in diameter, probably formed from accumulation of lava around a central vent; possibly an end phase of Mare Imbrium flooding after surface of lava hardened but fluid lava underneath still under pressure. Some Post-Maria craters, of which Milichius (6J) is largest. Surfaces moderately rough or pitted. Slopes generally low, except steeper on Post-Maria pits and craters.

*Intermaria Section.* East of Northern Section and S. of Mare Imbrium. Mostly an irregular-shaped, lava-flooded lowland, in part the structural downwarp encircling Mare Imbrium beyond its ring mountains; includes many isolated highland masses. Some low ridges S.E. of Copernicus. Numerous Post-Maria craters. Surfaces on low areas generally smooth except for many small pits and craters, and a few larger craters from Post-Maria impacts; surfaces rough on isolated highlands. Slopes generally low.

*Rhiphaeus Section.* South-west part of Oceanus Procellarum. Lava-flooded lowland, containing numerous isolated islandlike highlands including the Rhiphaeus Mountains (6L) and many partly engulfed older craters. Numerous low ridges, commonly trending N.W. Surface of lowland generally smooth except probably for many small pits and craters, and some larger Post-Maria impact craters; highlands and craters mostly moderately rough.

*Sinus Aestuum.* Reentrant N.E. of Intermaria Section. Oblong lava-flooded lowland, 160 miles long. Intermittent and en echelon low lava ridges parallel S.E. boundary. Surface of lowland generally smooth except probably for many small pits, and some small craters from Post-Maria impacts. Slopes generally low.

### *Mare Nubium*

South of Oceanus Procellarum. Lava-flooded lowland, about 400 miles in greatest dimension, containing numerous isolated islandlike highlands and partly engulfed older craters. E. of Straight Wall (8M) along border are nearly engulfed older craters. Some low lava ridges, most trending N.-S. Surface of lowland generally smooth except probably for many small pits and craters, some larger Post-Maria impact craters, and Straight Wall. Slopes low, except steep in Straight Wall.

### *Mare Humorum*

South of Oceanus Procellarum and W. of Mare Nubium. A lava-flooded, large, impact area, roughly circular about 250 miles diameter; partly rimmed by ring mountains; isolated mare-like areas to S.W. and S. Low lava ridges on E. side. Minor rilles paralleling W. boundary indicate contraction and downwarping of lava after cooling. Surface generally smooth except probably for many small pits and craters from Post-Maria impacts. Slopes generally low.

### *Pulus Epidemiarum*

South-east of Mare Humorum and S.W. of Mare Nubium. Lava-flooded lowland; maximum width 150 miles; boundaries partly controlled by N.W.-S.E. faults; connects with Mare Humorum, but separated from Mare Nubium by narrow highlands. Numerous minor rilles. Surface generally

smooth except for small pits and craters from Post-Maria impacts, and in vicinity of minor rilles. Slopes generally low; minor rilles steeper.

#### NORTHERN LOWLANDS

North and N.E. of Mare Imbrium and Mare Serenitatis. Lava-flooded downwarp depressions, lowlands, and impact craters. Boundaries mostly irregular, in part circular from craters. Some low lava ridges, and Post-Maria craters. Surface generally smooth except for small pits and craters from Post-Maria impacts. Slopes mostly low.

##### *Mare Frigoris*

North of Mare Imbrium and Mare Serenitatis. Lava-flooded lowland trough 1300 miles E.-W.; mostly part of interrupted depressions encircling both Mare Imbrium and Mare Serenitatis beyond their ring mountains. Boundaries generally irregular except for circular boundary of Laeus Mortis (11F). Some low lava ridges. Surface generally smooth except for small pits and craters, and some large Post-Maria impact craters. Slopes generally low.

##### *Mare Humboldtianum*

Near N.E. limb. Lava-flooded, large impact crater, roughly circular, 200 miles diameter. Other smaller lava-flooded areas in vicinity. Because of position near limb, surfaces and slopes undetermined, but probably similar to Mare Humorum.

#### MARGINAL LOWLANDS

Near E. limb. Lava-flooded impact area and lowlands, possibly connected in part. Ring mountains nearly encircle impact area, forming generally circular boundary; most boundaries irregular. Low lava ridges. Surface generally smooth except probably for many small pits and craters from Post-Maria impacts. Slopes generally low; pits and craters steeper.

##### *Mare Crisium*

Near E. limb. Oval-shaped, lava-flooded impact area; 340 miles E.-W. and 260 miles N.-S. Nearly encircled by ring mountains; numerous re-entrants of lava penetrate surrounding highlands along fault rifts; largest at N.E. to Mare Anguis (16H). Low lava ridges, and inward-facing slopes near borders. On N.W. partial slumping forms shelf mountains. Surfaces and slopes similar to Mare Humorum.

##### *Mare Undarum; Mare Spumans; Mare Smythii; Mare Marginis; Mare Novum*

These maria at or near E. limb of Moon. All are lava-flooded lowlands, possibly connected in whole or part. Not easily observed because of position on limb.

#### AUSTRALE LOWLANDS

##### *Mare Australe*

Situated on S.E. limb. Australe Lowlands beyond limb probably includes other maria areas like Mare Australe, a lava-flooded lowland. Surfaces and slopes unknown, but probably similar to Mare Humorum.

## AESTATIS LOWLANDS

*Mare Aestatis; Mare Autumni; Mare Veris*

On W. limb of Moon; Mare Veris beyond limb in libration position. All the maria in this division are lava-flooded lowlands, not easily observed because of position on limb. Surfaces and slopes unknown but probably similar to Mare Humorum.





# SOME SYSTEMATIC VISUAL LUNAR OBSERVATIONS†

D. W. G. ARTHUR

*Lunar and Planetary Laboratory, University of Arizona,  
Tucson, Arizona, U.S.A.*

## INTRODUCTION

SINCE the visual observer obtains a resolution some three times that obtained photographically with the same telescope, justification of this method of getting data on the lunar surface is quite unnecessary. Visual observations have the well-known drawbacks of subjectivity and selectivity and are also positionally inaccurate. These defects can be controlled and their effects reduced by repetition and by appropriate observation routines.

The observations of this paper were made with the 40 in. refractor of the Yerkes Observatory and the 82 in. reflector of the McDonald Observatory. The full apertures were rarely brought into play and the bulk of the observing was performed at 24 in. aperture because of imperfections in the seeing. Even with these reduced apertures the observer may be presented with such intricate masses of detail that he is obliged to be very selective in what he records.

## OBSERVATIONAL TECHNIQUES

In the case of topographic and cartographic research the observations were entered directly on the sheets of the "Photographic Lunar Atlas," thus following the example of Krieger. Slope and shadow observations were used to investigate the detailed topography of craters, rilles and domes.

In shadow observations of small craters, the shadows are estimated as fractions of the diameters of the crater. These estimates are affected by strong subjective errors and can be made only in the very best conditions. In my case, poor seeing has the effect of making the estimated fraction too small, but the effect is reversed for certain other observers. These shadow estimates permit the determination of the depth-diameter ratios and for diameters less than 5 km the results are as trustworthy as micrometric or photographic determinations.

The slope estimates are even more delicate and are perhaps the most difficult of all lunar observations. Here the observer must decide on the moment of transition from black to grey of the lunar shadows. Since this transition is continuous the moment is indeterminate and all one can do is to "box" it between two moments, one corresponding to a definitely grey shadow and the other to a black.

## CARTOGRAPHIC AND TOPOGRAPHIC OBSERVATIONS

These are necessary to supplement the defective resolving power of available photographs. A glance through the "Photographic Lunar Atlas" will soon convince anyone that even with relatively small apertures it is

† Communication, Lunar and Planetary Laboratory, No. 4.

possible, in large areas of the disk, to add to the photographic data. An example of one evening's work is shown for the Aristarchus region (Fig. 1).

The observer starts with the photograph as a base, adds details which are missing and sharpens up those details which are hazy or doubtful in the photographic image. Very often, the photograph will give a faint and vague marking, so that in clarifying this the observer retains much of the positional accuracy of the photograph.

#### CRATER OBSERVATIONS

These were usually limited to establishing general characteristics such as the determinations of the depth-diameter ratio, the external and internal slopes and the nature of the central peak when present.

Examination of the interiors of the smaller craters with large apertures has enforced a change in my opinions. At one time I believed that the interiors of most of these were smooth hemispherical or paraboloidal bowls, but recent work with the 40 in. contradicts this. It now appears that all craters, except the very smallest ( $< 2$  km), have interior forms which are



FIG. 1. Visual observations on Aristarchus area (one evening).

inverted truncated cones, with floors which are somewhat darker than the walls. In the smaller sizes these floors are difficult to detect since they may be no more than a kilometer across. They are most easily seen at full when they appear as dusky spots in the centers of the bright patches of the craters.

One peculiarity of these observations is that a practised observer soon finds that the cast shadows are transparent and that he can look down

through them and see the entire floor, even though most of this is in shadow. Clarity rather than steadiness is the prerequisite for this type of observation, which was aimed at estimating the size of the floor and its cross-section. Very often, when the floor is convex, the illuminated wall will cause a shadow to be thrown in the reverse direction, forming a crescent of shadow along the edge of the floor nearest to the Sun. The concavity or convexity can also be detected by comparing the curvature of the end of the shadow with that of the rim, but this depends on the assumption that the rim is level, which is frequently not the case. The floor diameter is about  $\frac{1}{3}$  of the rim diameter for craters of 15 km in diameter and appreciably less, say about  $\frac{1}{4}$ , for craters of 10 km diameter. These floors tend to be level or concave but examples of convexity were noted.

Most of the depth-diameter ratios for craters in the range 5 to 15 km fall between the limits 0.15 and 0.23. The ratio is not very sensitive to size in this range and indeed this insensitivity is demonstrated by the following averages:

Diameter Range	Average Ratio
5—10 km	0.194
10—15 km	0.193

The individual means for the observed craters are shown in Fig. 2.

The external heights of the rims of smaller craters were also investigated

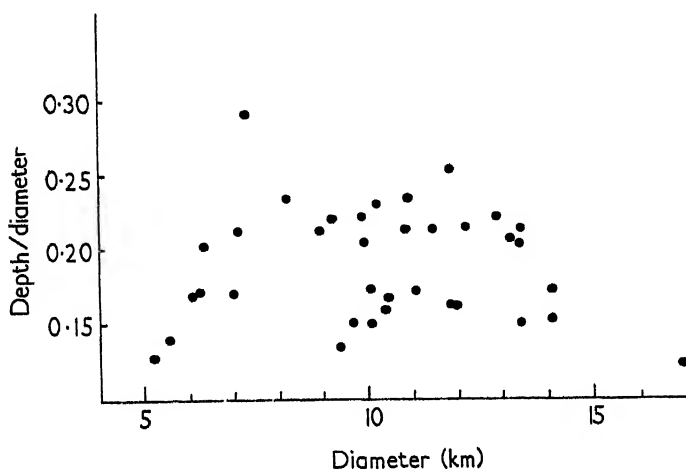


FIG. 2. Depth: diameter ratios for craters between 5 and 15 km.

by means of shadow estimates. Over the range 0 to 20 km there appears to be quite a definite correlation between the diameter and the external height of the rim, the corresponding regression being

$$\text{Rim height (meters)} = 49.416 \text{ Diam} - 68$$

in which the diameter is in kilometers. This regression is illustrated in Fig. 3. The crater Birt deviates from the regression and is exceptional in this respect, as well as others. Its rim rises almost 1000 m above the surrounding plain and is abnormally high.

The slope estimates were aimed at the physical values, not at the average straight-line values obtained by Fauth. Particular attention was given to the inner and outer slopes immediately adjacent to the rim. The inner slopes were found to be quite consistent, lying between  $30^\circ$  and  $40^\circ$ , with  $35^\circ$  as a fair average. This accords with earlier results. In contrast with this, the estimates of the outer slopes did not agree with earlier work. In a large number of cases I noted a very thin crescent of black shadow immediately adjacent to the rim and indicating a brief slope with values lying between  $10^\circ$  and  $20^\circ$ . This contradicts impressions obtained from photographs, but it must be remembered that with any loss of resolution

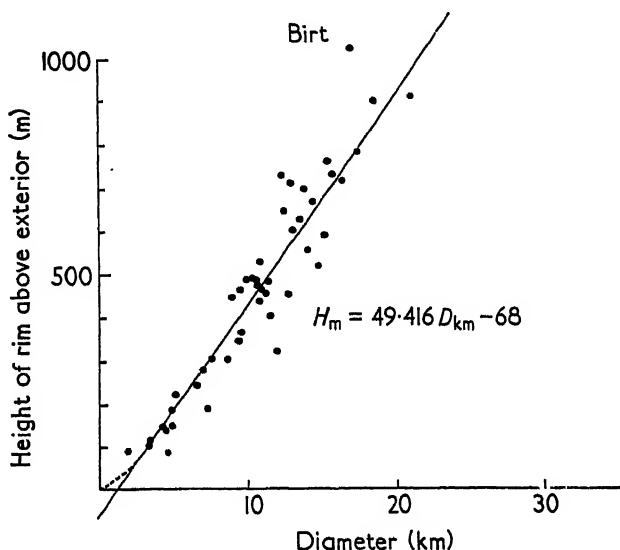


FIG. 3. Height of crater rims above exterior surface.

this thin black band of shadow is smeared into a grey tone. The much lower values of  $3^\circ$  to  $6^\circ$  quoted by other authorities no doubt refer to the average slope from rim to base. The brief steep slopes may correspond to an overturn region immediately adjacent to the rim of the crater.

Observations of the central peaks added nothing of value. These features have a heterogeneity which makes classification and systematization difficult. Craterlets were often noted on the summits of the peaks, as in the case of Albategnius, but with attention they could also be detected on the flanks. Further work in the way of craterlets counts, on the peaks and in their immediate vicinity on the floors, will be necessary to make any headway in this topic.

#### LUNAR RILLES

The rilles were observed in order to improve the picture of their distribution and structure. Unfortunately, it is much easier to detect a narrow rille than to see the details of even the broadest specimens; therefore, most of the new results are additions to the list of known rilles. However, it has been possible to confirm Fielder's median ridge in the Ariadacus Rille

and to detect similar ridges in three other rilles. This median ridge is by no means characteristic of all the broad rilles but it is a peculiarity which will have to be taken into account in any theories concerning the lunar rilles.

The rilles are evidently not a homogeneous group. The Ariadaeus Rille has clear-cut graben features since its floor has dropped between parallel bounding faults. These can be seen as fine dark lines cutting through the overlying blocks whose central portions have subsided with the floor of the rille. This rille is almost alone in that its walls are visible as bright lines at full Moon. Other rilles have graben features, but the Triesnecker rilles appear to be very different. These are shallow and rather blurred grooves with no definite line between wall and floor. The row of brilliant white pits along the interior of the Hyginus Rille are now well-known and are even recorded on one Pic-du-Midi photograph, but this appears to be an exceptional feature. Almost all the broader rilles appear to have nearly level floors (except when the median ridge is present) meeting the walls in quite well-defined lines. At moments of good seeing, one can sometimes detect craterlets and other small features on these floors. The impression is that fusion, or some other leveling agency has acted on these rille-floors as it has undoubtedly done in the interiors of many craters.

Shadow estimates of the depths of both major and minor rilles were made when the shadow occupied one half of the apparent width of the rille. The results were surprisingly uniform and the depth came out at 15 to 20% of the width. These findings do not agree with the deeper estimates of other authorities. Further observations of this sort are therefore necessary.

The study of the distribution of the rilles confirmed the impression that the major systems are associated with the edges of the dark areas, whether these are maria or the interiors of certain large craters. The distribution is illustrated in Fig. 4. Near Marius in Oceanus Procellarum is a long rille with abnormal siting since long rilles are usually absent from the interiors of the maria. This is a serpentine type of rille. Another of this type has been found in the central M. Imbrium and still another near Ictonne.

Associated with rilles are the shadow valleys noticed by Krieger and Goodacre. In plan these are large features perhaps 10 to 15 km wide but their inward slopes towards the V-bottom are so gentle that they can be seen only when close to the terminator. Almost all those seen by the writer have a rille along the center of the valley. An easy specimen runs south from the crater Guericke B.

#### FAULTS

There is a temptation to label all linear features as faults, but the writer has not been able to detect many unmistakable fault features on the lunar surface. Apart from the well-known faults near Cauchy and Birt there is a much-mutilated example running south-east across the south end of Mare Humorum, which appears to be quite independent of the nearby rille system. There is an even weaker example across the south end of Mare Crisium and a well-displayed example with a western downthrow near Lubbock. However, the most extensive system of faults lies in the Apennines. Here there are numerous lines parallel to the frontal scarp with a secondary series at right-angles to this.

Many of the rilles were examined to detect fault characteristics. Not one example of horizontal offsetting was found, but downthrows or vertical displacements turned out to be fairly common. As an example of the close association between rille and fault, the Cauchy fault is extremely interesting. A rille runs along the foot of the fault, perhaps a kilometer or so away, while the fault itself appears to turn into a rille at its east end.

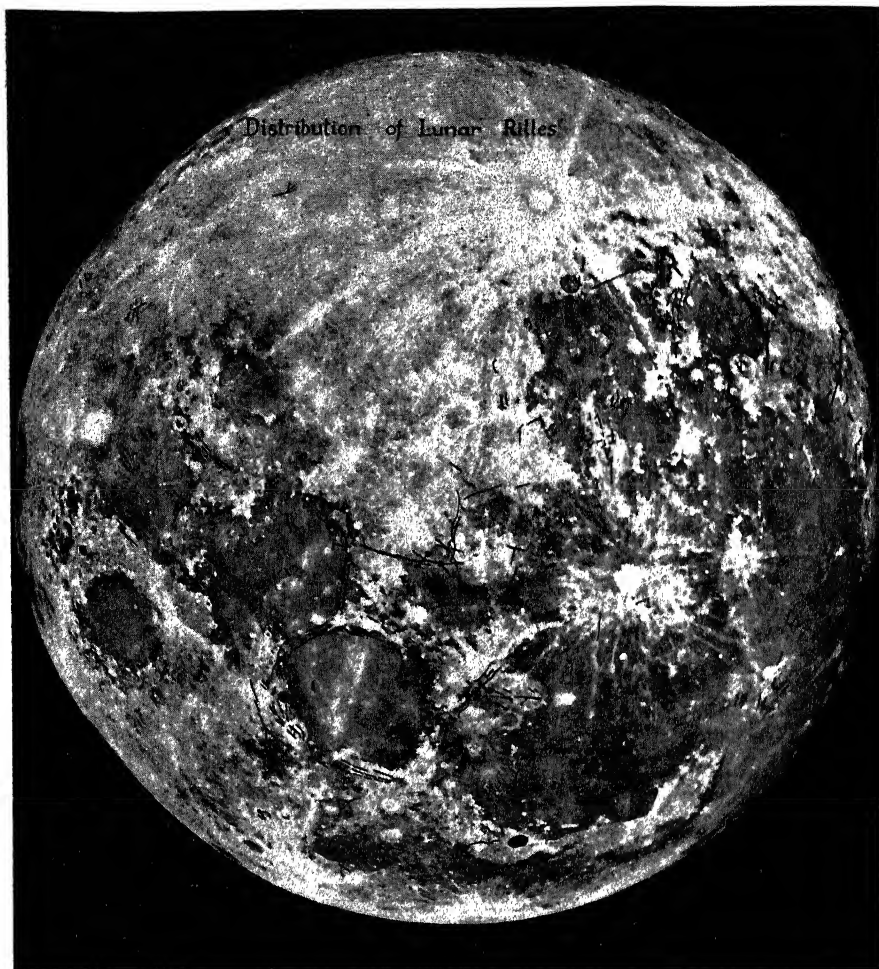


FIG. 4. The distribution of lunar rilles.

#### THE LUNAR DOMES

The distribution of these, based on the observations of G. P. Kuiper, E. A. Whitaker and the writer, as shown in Fig. 5, appears to support the following conclusions: (i) the domes are restricted to the dark areas usually assumed to be lava flows; (ii) the domes are further restricted to areas where one would expect the lava covering to be shallow; (iii) domes usually occur in related groups.

To support these conclusions it may be noted that persistent attempts by the writer to detect domes in Mare Crisium, Mare Nectaris and Mare Humorum have not been successful while the only domes found in Mare Serenitatis and Mare Imbrium are very close to the edges of these maria. The large dome concentrations are found in Mare Nubium, Mare Tranquillitatis and east of Copernicus. In these latter areas, the existence of ghost rings, isolated peaks, and the wrecks of former craters indicate a shallow lava cover.

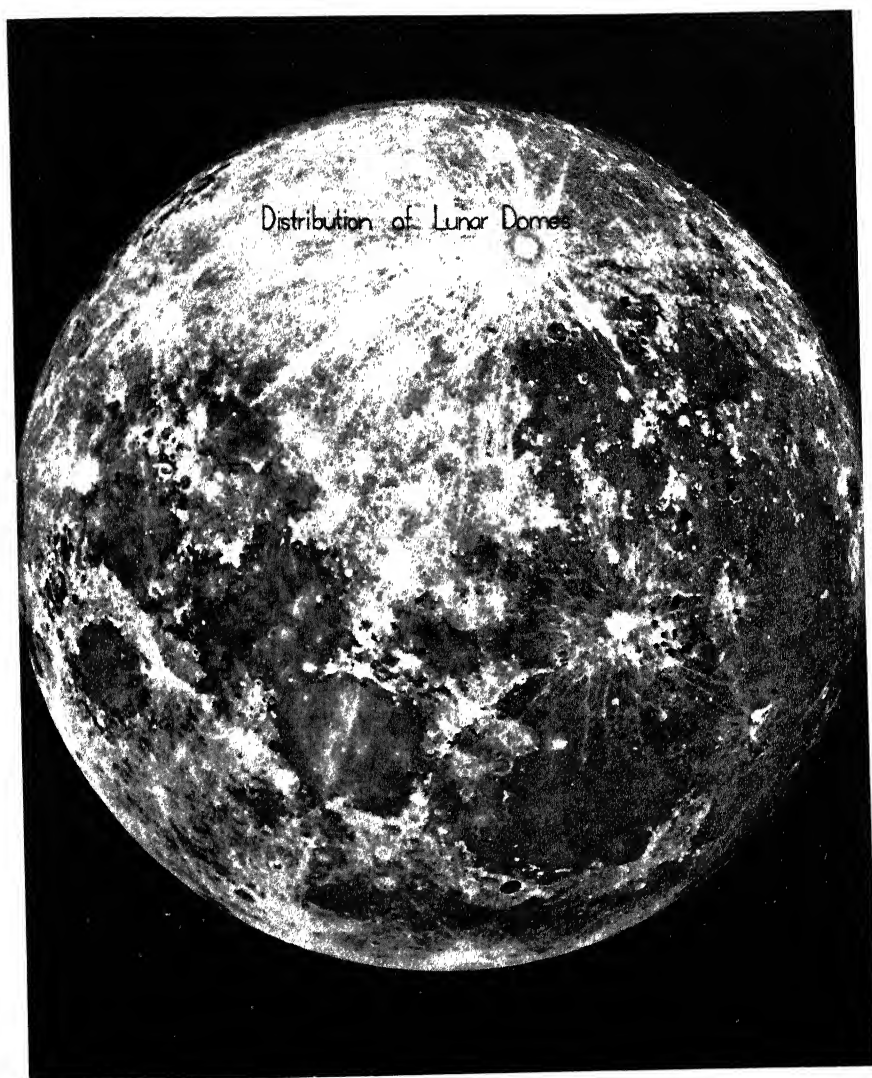


FIG. 5. The distribution of lunar domes.

It is usually accepted that domes have the same tone as the surface on which they stand, but the dome bisected by a rille just north of Menelaus is distinctly darker than the mare and appears as a dark spot at full Moon.



There is considerable variation in the forms of the domes, exemplified by the two near Cauchy. One is a disk-like structure with a central aperture, while the other is conical with a very small bright spine at its summit. Neither of these bears any resemblance to the large complex domes near Arago or the strange complex of swellings which constitutes the feature called Rümker. The disk-type dome near Cauchy and others of the same sort have been observed for height and the typical dimensions of these features are:

base diameter	=	6 km
summit diameter	=	4 km
central aperture	=	1 km
height	=	110 m.

The large dome east of Arago is about 500 m in height. In all cases the heights of the domes came out at 2 or 3% of their base diameters. This very gentle relief is confirmed by the slope estimates, which indicate slopes from  $2^{\circ}$  to  $5^{\circ}30'$  for the flanks of the domes. The smallness of the central orifices makes these features difficult to examine. I was unable to detect rims, but by comparing the glimpsed inner shadows with those of nearby craters, it was possible to establish that their depth-diameter ratios are not much different from those established for normal small craters of the same size.

### MARE RIDGES

In a few cases it was possible to confirm previous observations by G. P. Kuiper that many of these ridges are cracked open with rille-like openings along the summits. In some there is appreciable downthrow. The easiest example is perhaps the broad ridge north of Spitzbergen.

The plaited ridge running across S. Aestuum shows one remarkable feature. Its structural lines are prolonged into the mass of the Apennines and do not stop at the junction of mountain and mare. These lines, as fugitive markings, run some 60 or 70 km into the mountain mass. This may indicate a deeper seating of the forces which caused these ridges than is commonly supposed.

The relations between the mare ridges and submerged structures is still obscure, but a frequent association between these features has been noted. The most prominent examples are at Lamont in the Mare Tranquillitatis and in the very large ring surrounding the Straight Wall. Undoubtedly, the mare ridges tend to follow the lines of submerged objects.

# PHOTOGRAPHIES A GRANDE RESOLUTION DE CERTAINES REGIONS LUNAIRES

AUDOUIN DOLLFUS

*Observatoire de Paris, Section d'Astrophysique,  
Meudon, France*

EN vue d'une étude très détaillée de la surface de la Lune et des planètes B. Lyot avait installé en 1941 un réfracteur de 38 cm à l'Observatoire du Pic-du-Midi. Le but était de mettre à profit les conditions atmosphériques souvent excellentes rencontrées sur ce sommet de 2860 m d'altitude. En 1944 cet instrument fut remplacé par un réfracteur plus puissant dont l'ouverture de 60 cm permettait de tirer un encore meilleur parti des nuits assez fréquentes où la turbulence atmosphérique reste réduite.

L'étude topographique de la surface lunaire fut conduite selon deux procédés.

Des clichés couvrant de grandes portions de la surface lunaire ont été effectués au foyer direct du réfracteur de 60 cm, mesurant 18 m 25 de distance focale. La plupart de ces clichés ont été effectués en 1944 et 1945, par B. Lyot lui-même et par M. Gentili. L'ensemble de la collection recueillie couvre la surface totale de la Lune sous des éclairagements divers, et constitue un atlas complet actuellement en cours d'impression. (Les Editions de Visscher—Bruxelles.)

Un certain nombre d'images de la collection précédente sont d'une finesse inhabituelle et montrent des détails d'une grande délicatesse. Cependant il fut vérifié que la dimensions angulaire de l'image projetée sur la plaque ne permettait pas de tirer le parti maximum de l'extrême finesse de la résolution donnée certaines nuits.

Pour compléter la collection précédente, il parut désirable d'agrandir l'image à l'aide de dispositifs optiques et d'effectuer des clichés complémentaires de certaines régions particulières. Ces régions sont beaucoup moins étendues, mais elles sont soigneusement choisies pour leur topographie caractéristique ou singulière, et montrent une richesse de détails qui souvent n'a pas été égalée.

Ce programme de photographies lunaires à très haute résolution a débuté en 1942. Il s'est prolongé déjà durant 19 ans jusqu'à cette année. Au cours des campagnes d'observations successives des dispositifs optiques et photographiques ont variés. MM. Camichel, Clastre, Dollfus, Gentili, Leroy, ont contribué avec B. Lyot à l'enrichissement de la collection.

La Figure 1 montre le cratère Aristillus. Cette photographie prise par B. Lyot lui-même, en 1945 suggère un caractère explosif; des sillons radiaux labourent le sol vers la droite.

Vu par la tranche, un tel cratère ressemblerait à celui de la Figure 2, bien que de beaucoup plus grande dimension.

La Figure 3 est prise dans les régions claires, au voisinage de Maurolycus. Les cratères y sont répartis d'une manière qui rappelle le hasard. Ils empiètent les uns sur les autres de telle façon qu'il semble difficile de leur attribuer

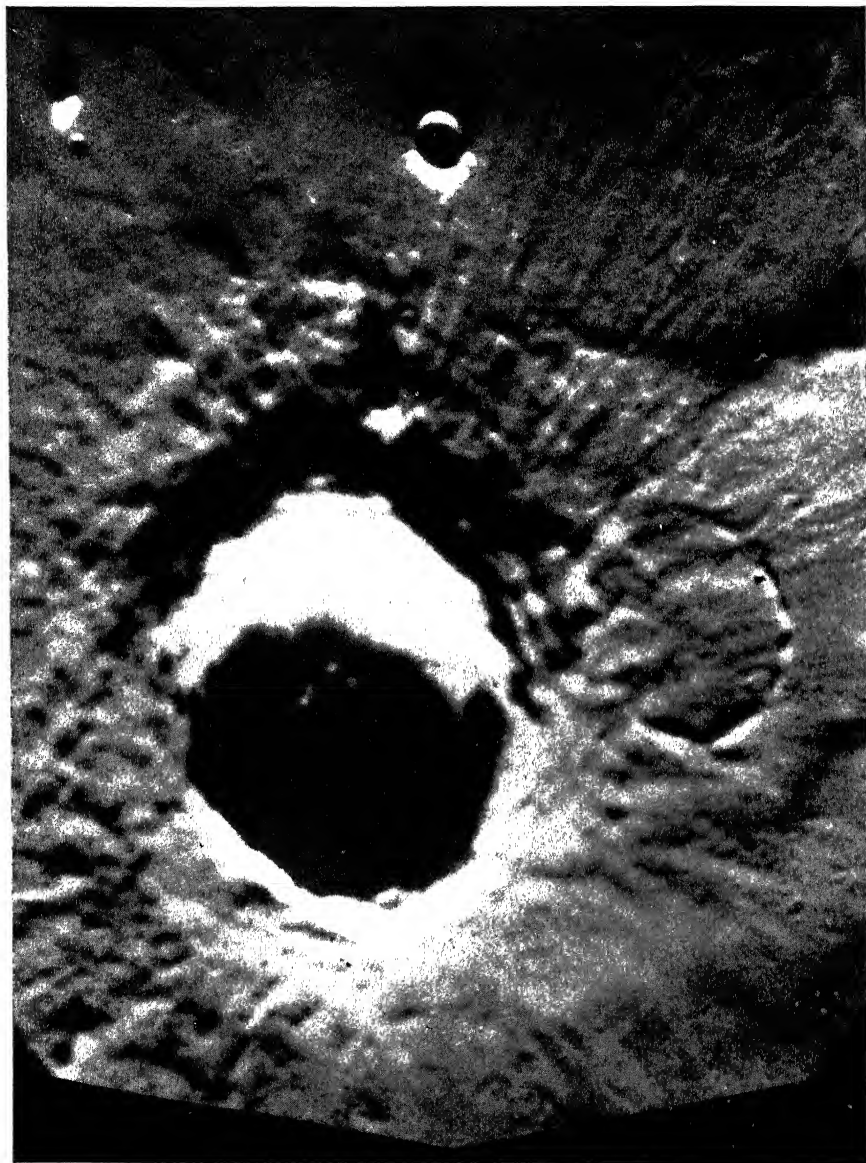


FIG. 1. Aristillus 21 Mars 1945 21<sup>h</sup> 13<sup>m</sup>. Réfracteur de 60 cm. Foyer de 18, 25 mètres allongé à 39 mètres par une lentille divergente. Pose 2 secondes. Le Nord est en bas.

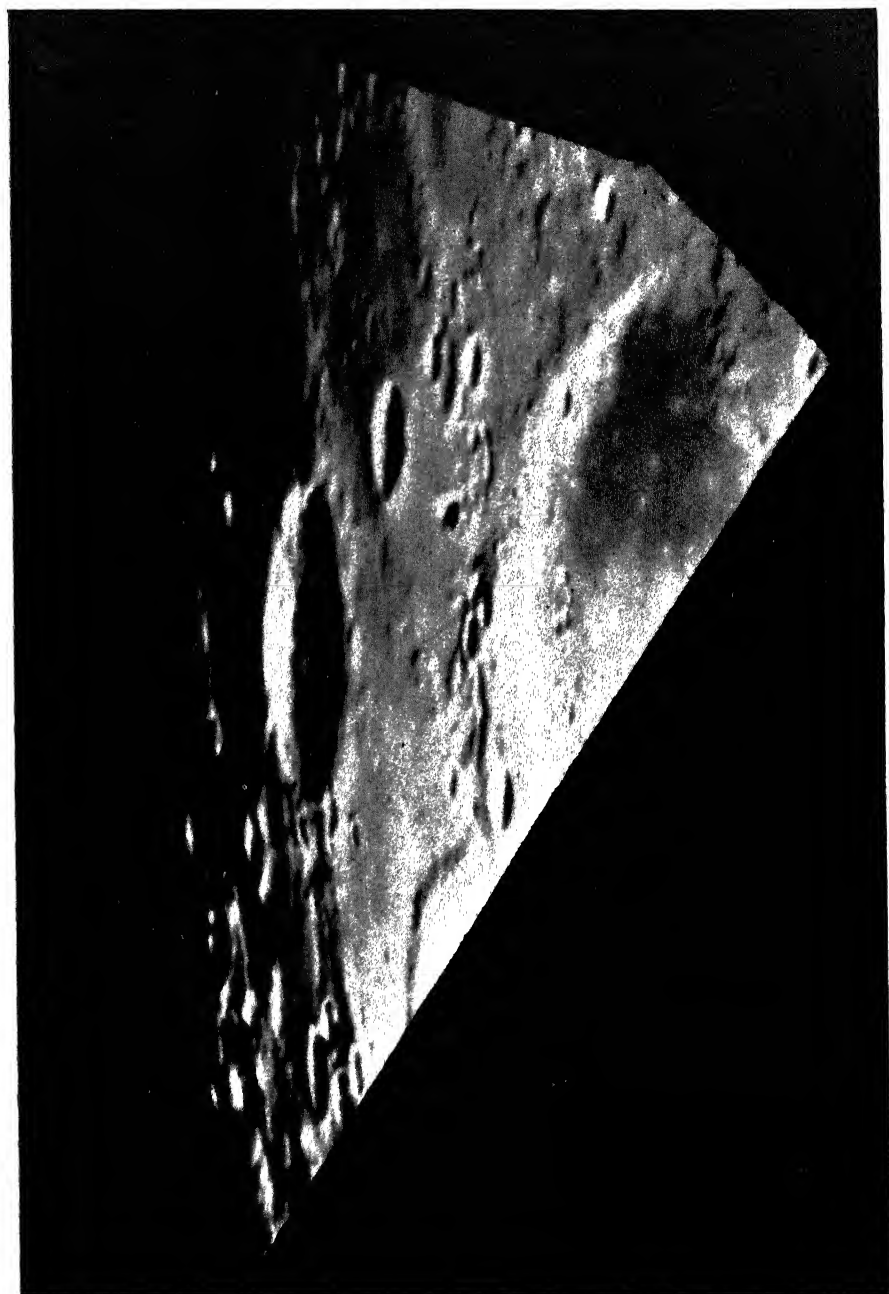


FIG. 2. Inghirami 25 Août 1942. Réfracteur de 38 cm. Le Nord est à droite et le Sud à gauche.

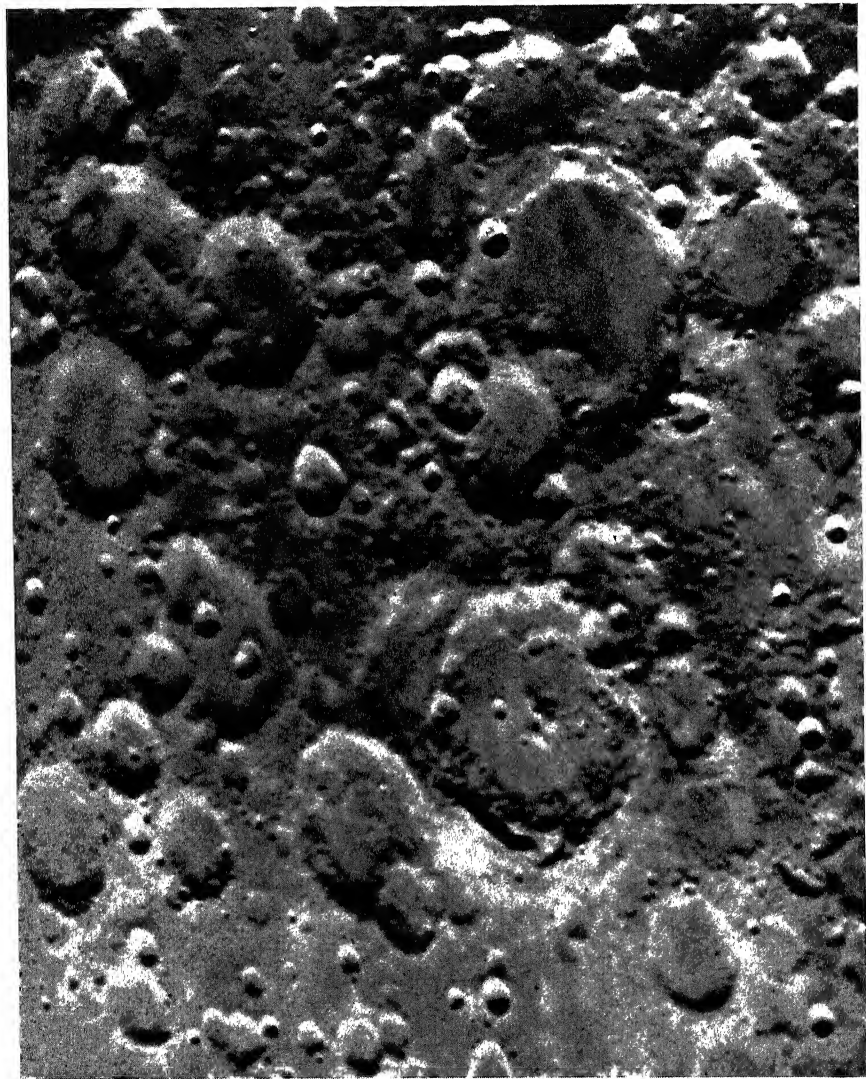


FIG. 3. Région entourant Maurolycus, 1er Mars 1944. Enchevêtrements et empiètements de cratères.

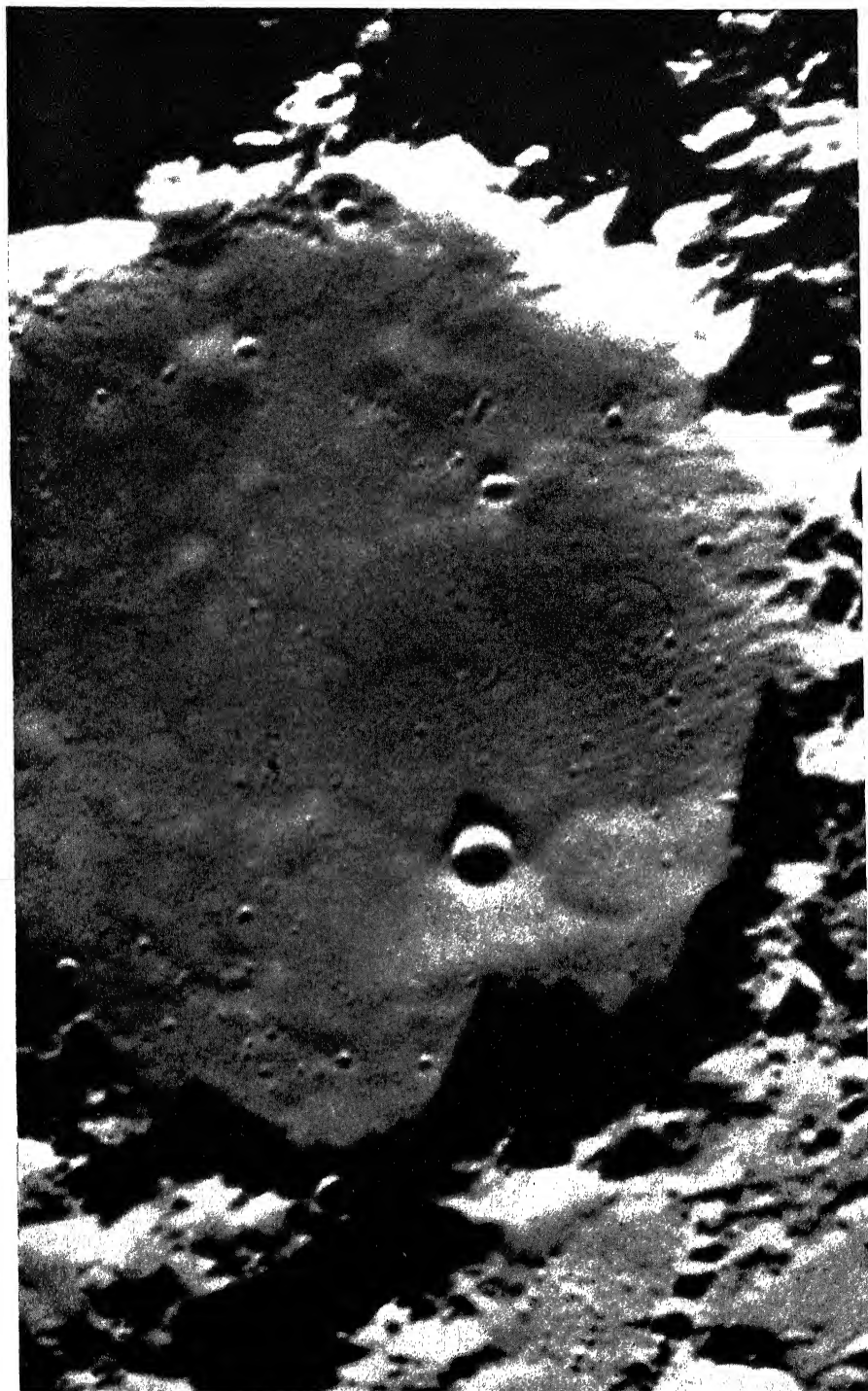


FIG. 4. Ptolemaüs 21 Mars 1945. Réfracteur de 60 cm. Fond du cratère parsemé de nombreux petits cratèrets.

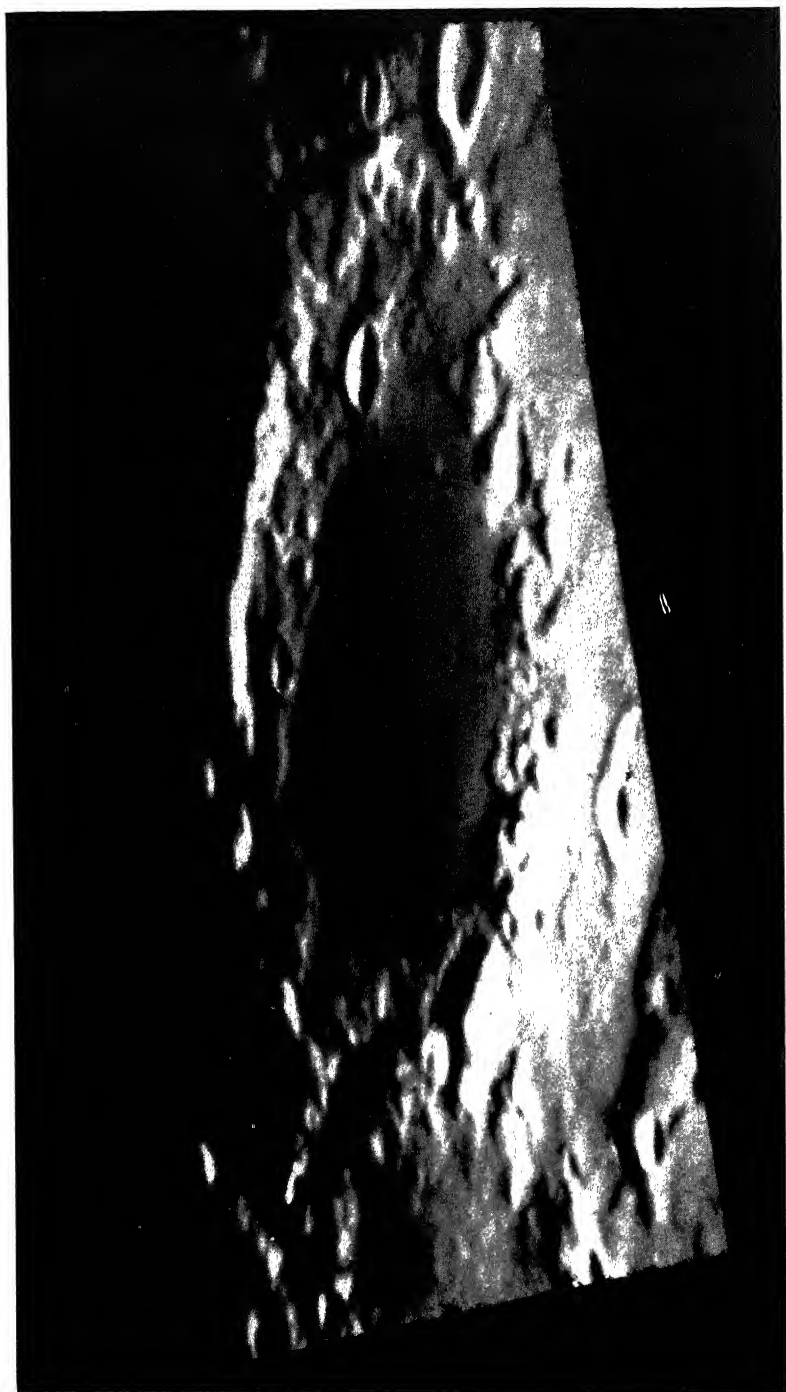


Fig. 5. Grimaldi 25 Août 1942. Réfracteur de 38 cm. Cratère rempli par de la lave. Le Nord est à droite et le Sud à gauche.



une provenance interne. Les impacts de météores donneraient cette répartition. Chaque collision donne lieu à une explosion, et celles ci sont accumulées pendant de très nombreux millénaires. Les empiètements successifs des cratères permettent de les classer par ordre d'apparition. Les plus récents ont des bords nets et des arêtes vives. Les cratères anciens sont généralement émoussés et leurs remparts sont altérés. Cette dégradation pourrait provenir en partie de l'érosion par les petits météores; ceux-ci sont très nombreux et leurs cavités explosives, trop petites pour être observées, pourraient finir par se superposer et altérer le modelé après de très nombreuses années.

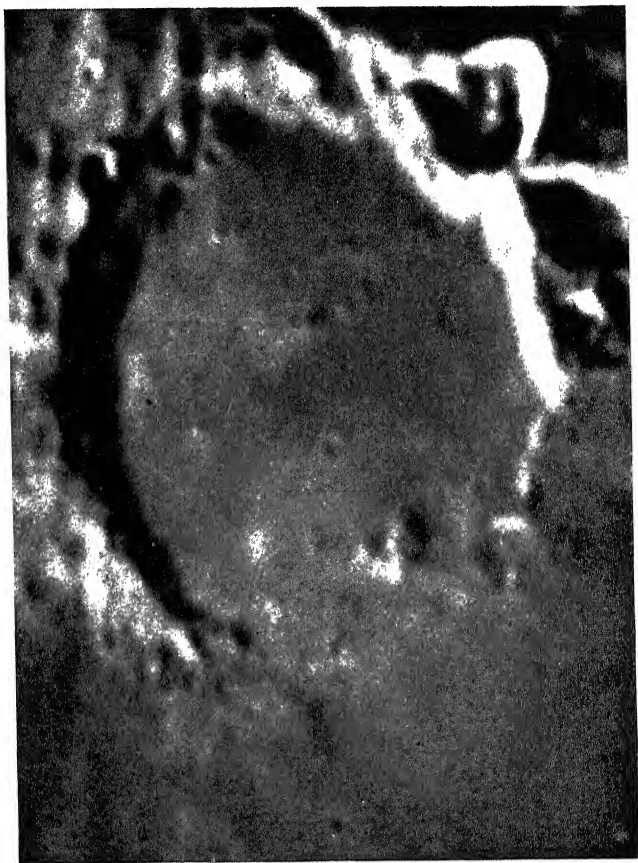


FIG. 6. Fracastorius 20 Février 1961. Réfracteur de 60 cm. Cratère envahi par un épanchement.

Sur la Figure 4 le fond du grand cratère Ptolemaïus paraît rempli par une matière sombre assez lisse. Il semble qu'une étendue liquéfiée se soit épanchée puis ensuite solidifiée. Cette lave a pu provenir de l'intérieur de la Lune, si de grandes étendues liquéfiées ont pu se maintenir sous la surface. Elle peut provenir aussi du choc lui même qui donna naissance au cratère, si la vitesse du gros météore, responsable de la formation du cratère était insuffisante pour dissiper toute l'énergie par volatilisation explosive. L'étendue sombre est apparue à une date beaucoup plus récente que la surface



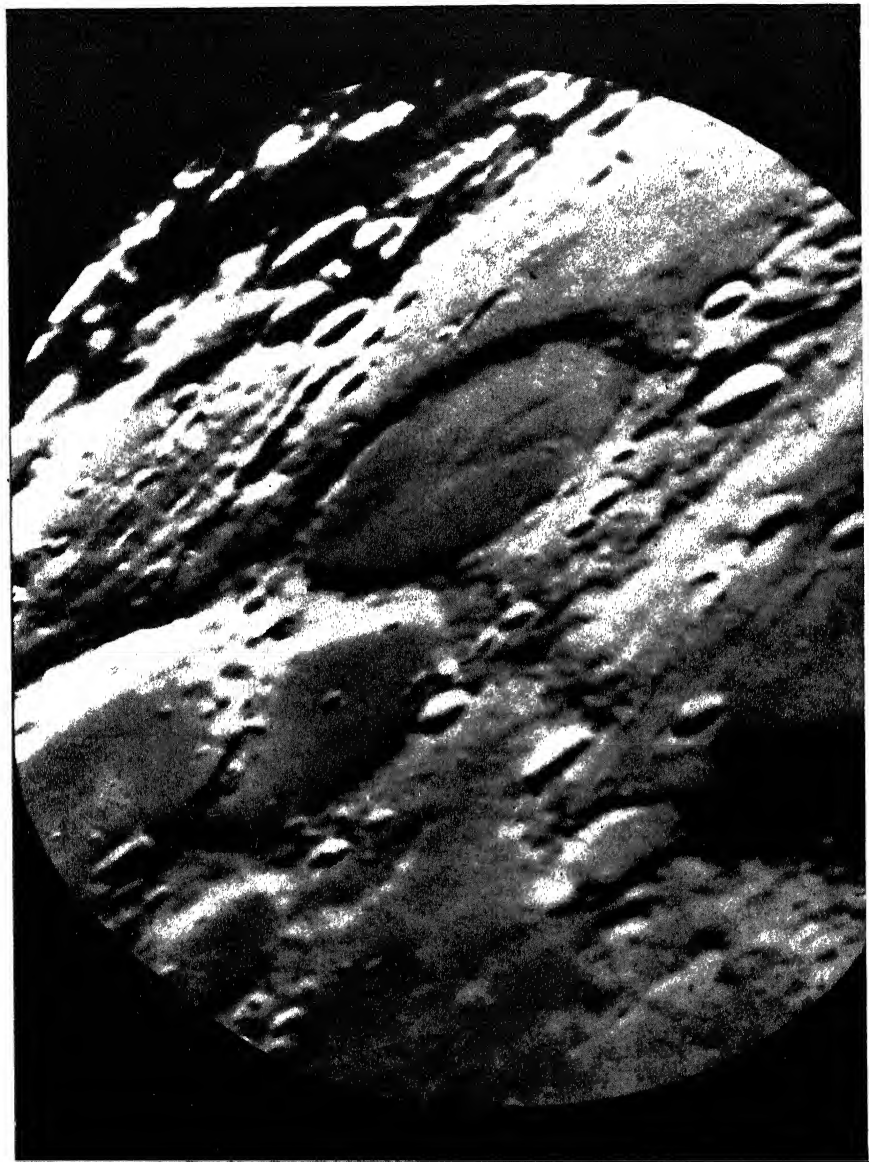


FIG. 7. Wargentin 27 Novembre 1955 à 21<sup>h</sup> 02<sup>m</sup>. Réfracteur de 60 cm. Epanchement de lave débordant du cratère en bas à droite.



FIG. 8. Triesnecker 21 Mars 1945 à 20<sup>h</sup> 45<sup>m</sup>. Lunette de 60 cm. Fracturations du sol probablement attribuables à des séismes.

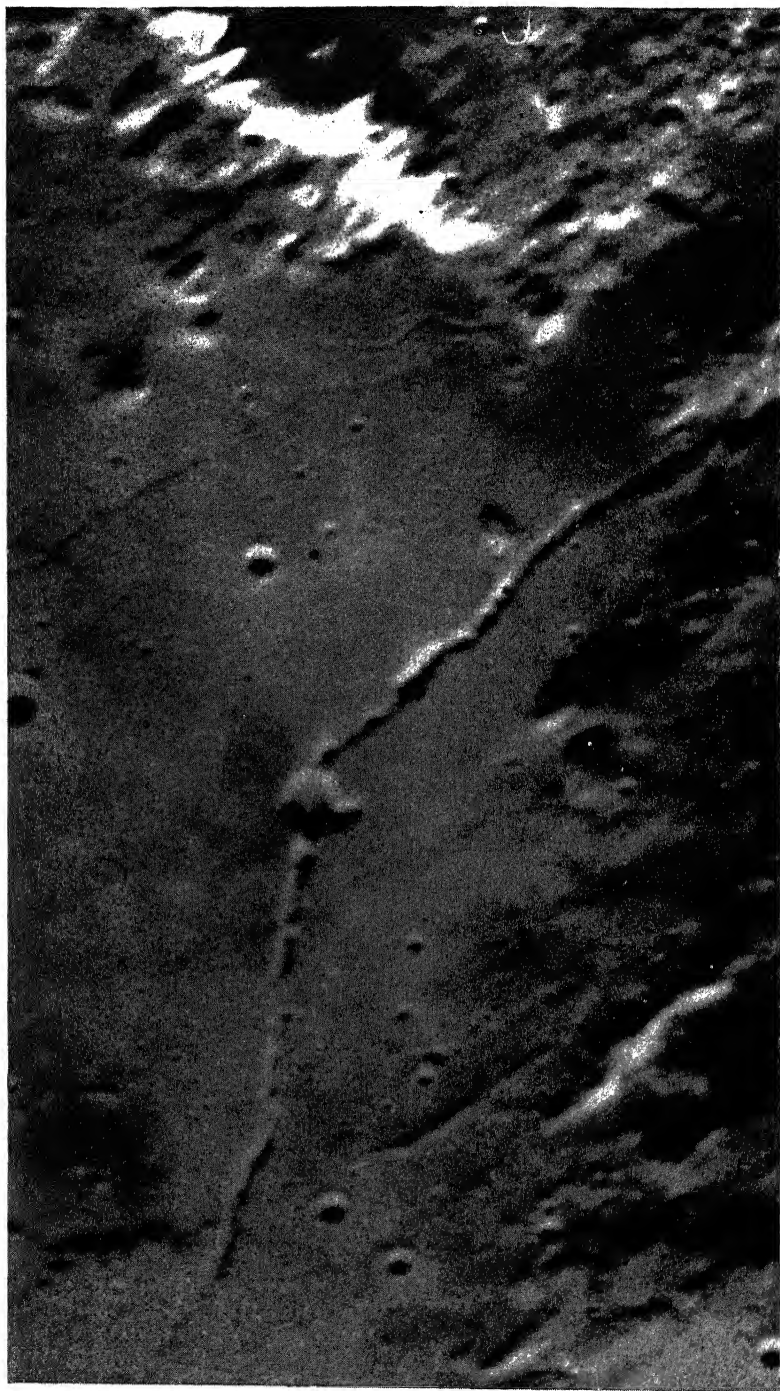


FIG. 9. Hyginus 21 Mars 1945. Rainure large, partiellement comblée.

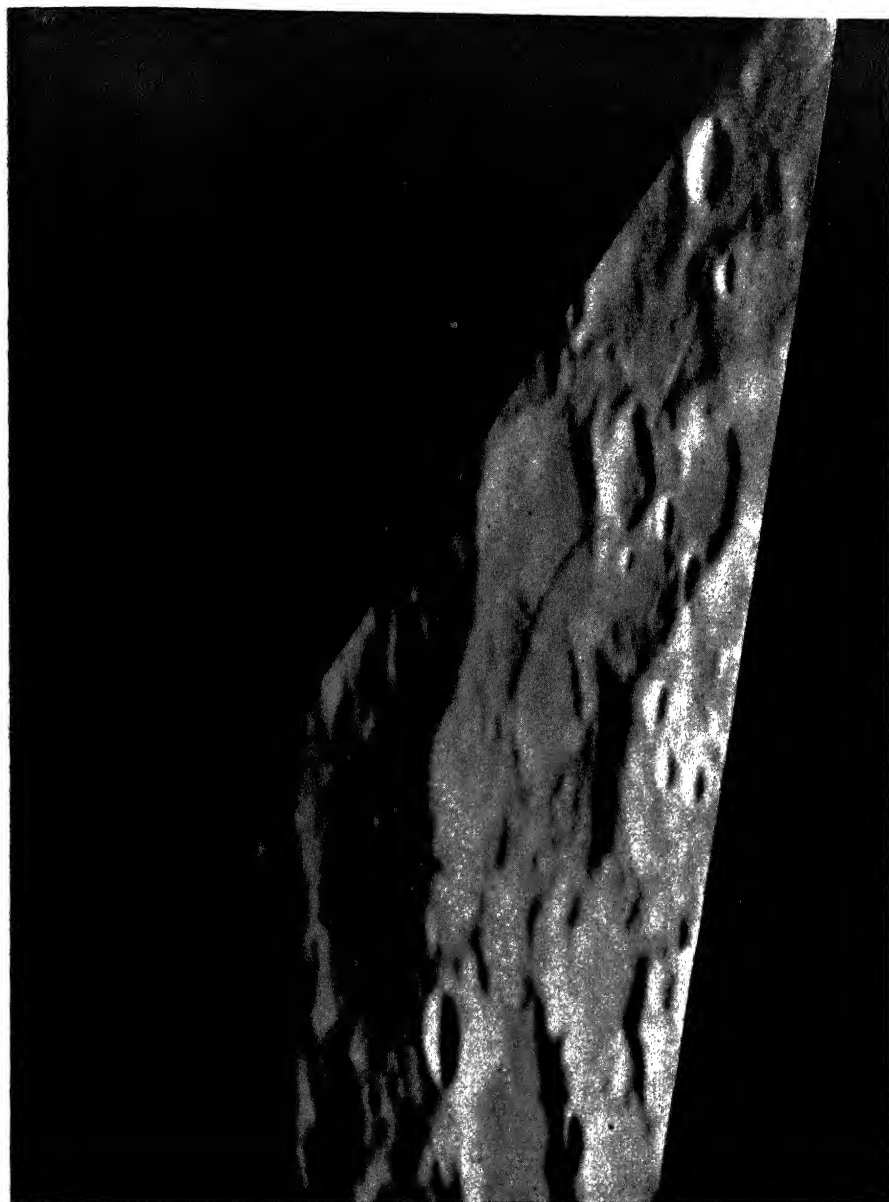


FIG. 10. BYRGÍUS 25 Août 1942. Lunette de 38 cm. Faille rectiligne traversant des formations topographiques diverses.  
Le Nord est à droite et le Sud à gauche.

claire du sol de la Figure 3; par suite elle a accumulé les impacts des météores pendant moins longtemps, et les cratères importants y sont presque inexistants. Mais les très petits cratères restent innombrables; les plus petits décelables sur la figure ont 800 mètres de diamètre; tout laisse penser que leur nombre serait encore bien plus considérables si la résolution du cliché pouvait être encore améliorée.



FIG. 11. Posidonius 20 Février 1961. Lunette de 60 cm. Fond de cratère ancien parcouru de failles et déboité.

Les épanchements de lave ne sont pas rares sur la Lune; en fait toutes les étendues sombres appelées mers semblent pouvoir s'expliquer par de tels processus. Ainsi la Figure 5 nous montre le cratère Grimaldi. L'épanchement parfaitement plan semble avoir recouvert primitivement une surface plus

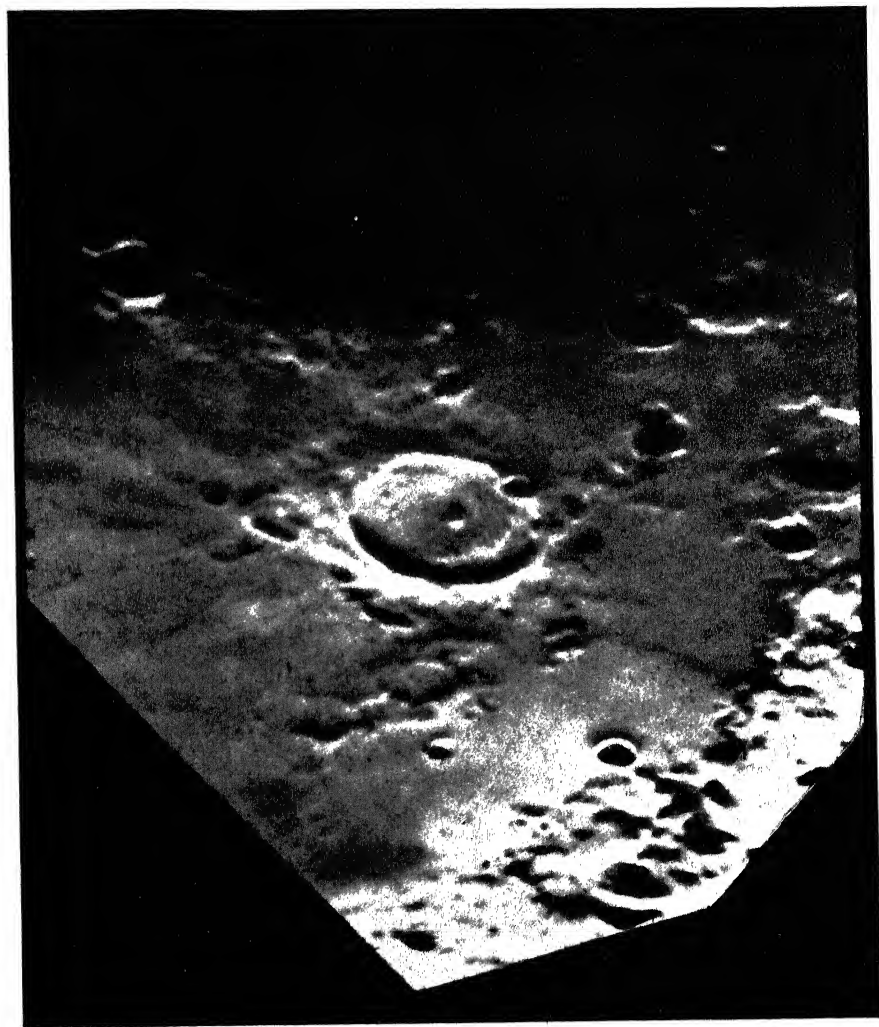


Fig. 12. Tarantius 29 Mars 1960 à 20<sup>h</sup> 10<sup>m</sup>. Réfracteur de 60 cm. Ancien cratère dont le socle entoure d'une faille circulaire à basculé.



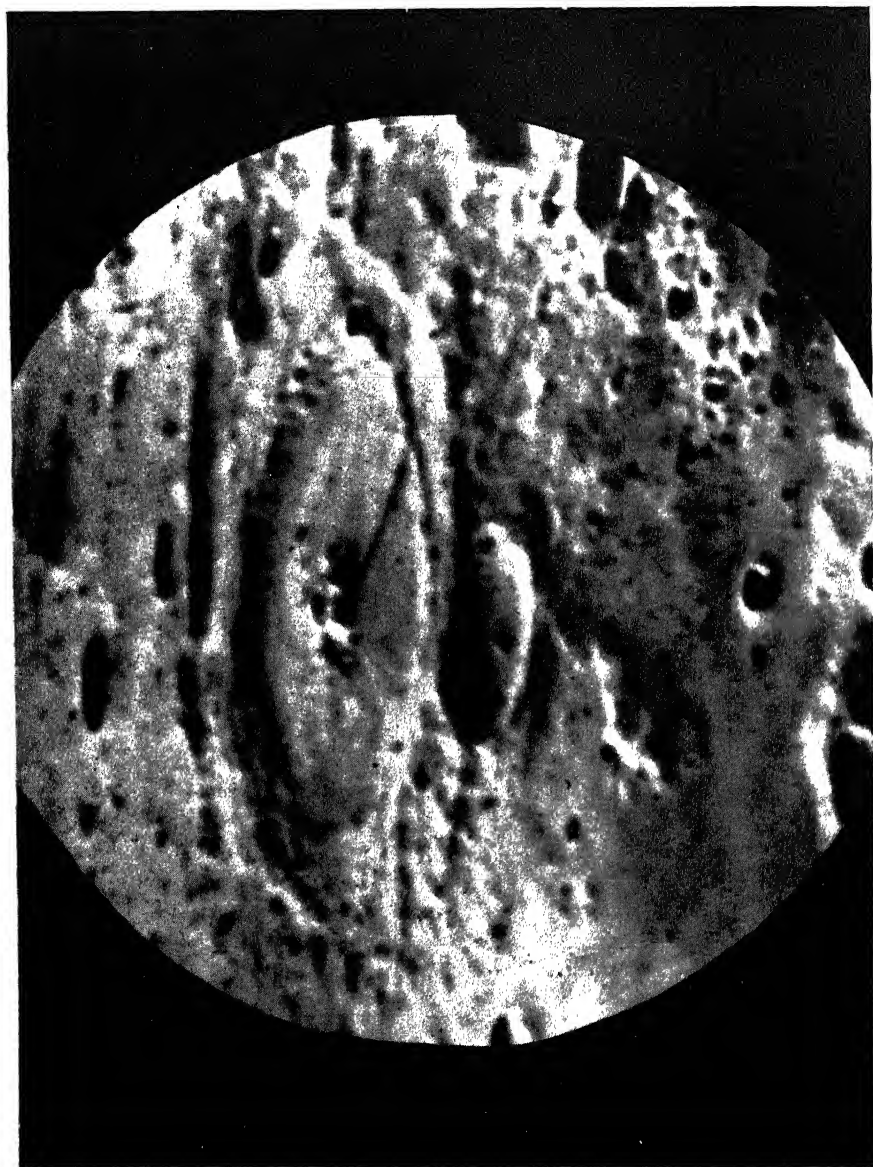


FIG. 13. Petavius 21 Mars 1960 à 20<sup>h</sup> 00<sup>m</sup>. Réfracteur de 60 cm. Cratère très altéré par l'érosion dont le fond est séparé en deux parties égales par une faille et dont les moitiés sont déportées.



Fig. 14. Alphonsus 21 Mars 1945 vers 21<sup>h</sup> 15<sup>m</sup>. Réfracteur de 60 cm. Fond de cratère très tourmenté.





étendue du côté Nord (à droite sur la figure); un retrait a dégagé ces rivages en laissant les accidents du sol partiellement refondus.

La Figure 6 donne l'exemple inverse de l'arène de Fracastorius, envahi par l'épanchement de lave constituant la Mare Nectaris, avec fusion partielle du rempart primitif.

Certains cratères partiellement comblés avec remparts émoussés paraissent avoir pu être remplis de lave à la suite des raz de marées accompagnant la libération cataclysmique locale d'une grande quantité de lave.

Dans le cas différent du cratère Wargentín, Figure 7, l'étendue primitivement liquide occupa un volume supérieur à la contenance du bassin et déversa, en bas à droite, dans le cratère voisin.

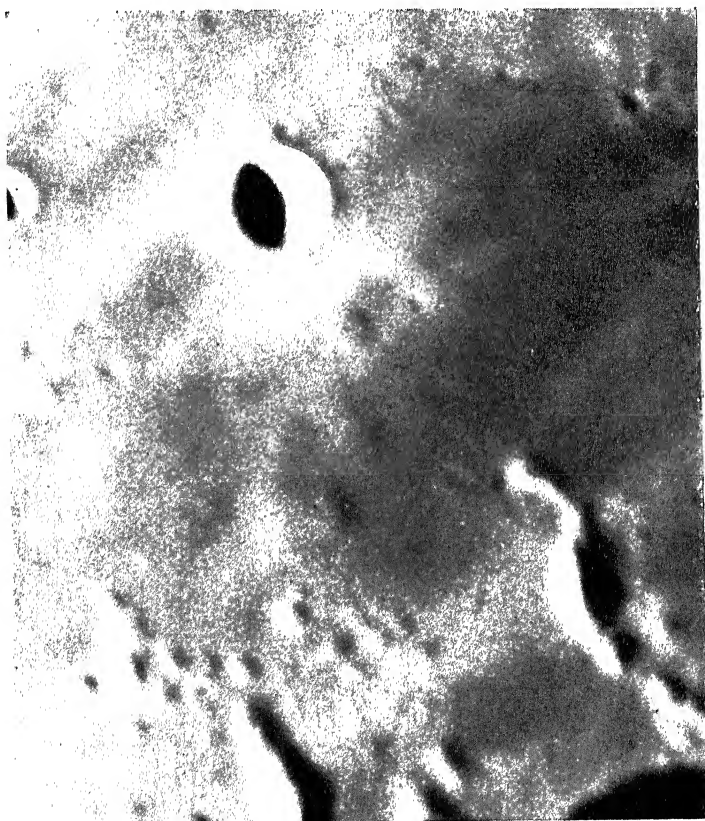


FIG. 16. Hortensius 29 Avril 1958 20<sup>h</sup> 47<sup>m</sup>. Réfracteur de 60 cm. Petites collines avec puit central, attribuables à des volcans.

Les chutes des corps célestes à la surface de la Lune, qui ont donné naissance aux cratères et provoqués les épanchements liquides, ont dû produire également des séismes considérables. Des ébranlements de la croûte lunaire ont provoqué des crevasses et des fissures. La rainure de Triesnecker, Figure 8, mesure de 1 à 3 km de large et elle est accompagnée de craquelures plus fines; le caractère anguleux du tracé et les intersections caractérisent généralement les crevasses résultant de séismes.

Non loin de cette région, la rainure de Hyginus, Figure 9, beaucoup plus large et partiellement comblée, semble s'être ouverte le long de petits cratères préexistants qui ont pu affaiblir localement le sol. On devine sur le tirage original de l'excellent cliché de la Figure 9 des éboulements le long des lèvres de la fracture, peut-être dus aux impacts de petits corps célestes à proximité du bord.

Certaines fractures, souvent parallèles aux contours des mers, semblent s'étirer le long de tracés rectilignes ou sinueux, sans aucun angle vif. Ces trainées traversent sans altération les obstacles topographiques préexistants. La Figure 10, obtenue dans la région de Byrgius, en donne un exemple. La trainée qui prend naissance au centre de l'image traverse successivement une colline confondue avec le rempart d'un cratère, puis le fond du cratère, le rempart opposé, un mamelon à proximité d'un plus petit cratère etc. Ces fractures pourraient être dues non plus à des séismes mais à des tensions superficielles résultant d'échauffements et de refroidissements de l'ensemble de la surface lunaire, ou de certaines régions affectées par les épanchements liquides à haute température.

Certain clichés de la collection sont consacrés aux cratères dont les fonds comblés sont très souvent marqués par des structures très tourmentées. La Figure 11 montre Posidonius. Plusieurs fractures craquelées se croisent tandis que l'arène semble avoir été cassée et soulevée à gauche. Le même phénomène se retrouve dans Taruntius, Figure 12, dont le fond apparaît comme découpé circulairement aux deux tiers de son rayon, et déboité. La Figure 13 montre le fond du très vieux cratère érodé Petavius. Une fracture exactement diamétrale sépare le socle interne en deux parties égales. Les lèvres rejointes ont presque complètement effacé la faille au-delà du piton central, mais les deux moitiés se sont déportées en avant pour constituer une très grande falaise.

La Figure 14 montre le fond d'Alphonsus. Les failles, les rides et les nombreux petits cratères s'y enchevêtrent pour riger une topographie particulièrement tourmentée. Vu de profil, ce cratère ressemblerait à celui de la Figure 15. La bouffée gazeuse observée spectroscopiquement le 3 Novembre 1958 par le Dr Kozyrev s'est produite au centre d'Alphonsus, immédiatement à droite du piton central, dans la région à l'ombre de celui-ci sur la Figure 14. Cette observation indiquerait l'existence de phénomènes volcaniques sur la Lune. Le dernier cliché, Figure 16, reproduit les monticules voisins du cratère Hortensius. Ces mamelons possèdent un petit puits central; ils ont été attribués à des restes d'assez importants volcans.

# CINE PHOTOGRAPHY OF THE MOON FROM PIC-DU-MIDI†

ZDENĚK KOPAL, THOMAS W. RACKHAM

*Department of Astronomy, University of Manchester, England*

THE aim of our present communication should be to give you a brief account of the current photographic work on the Moon which the Manchester astronomers have been carrying out, for some time, from the French high-altitude observatory at Pic-du-Midi under the auspices of the United States Air Force‡. This work, today, includes a variety of lines of lunar studies but since the inception of the entire programme in 1958 our principal aim has been to secure adequate data for extensive three-dimensional topography of the surface of our satellite; and it is this work whose recent developments we should mainly like to describe to you today.

The importance of a closer acquaintance with topographic properties of the lunar surface needs, perhaps, scarcely any additional emphasis at this time. To the astronomer, the surface of the Moon represents both the visible boundary condition and cumulative record of all internal (thermal and stress) processes, as well as an "impact counter" of external events, which our satellite must have undergone since the days of its formation. To the astronaut it represents again a territory through which he may have to find his way in the relatively near future (astronomically speaking). The visible face of the Moon represents indeed a fossil record—unique because of its immutability—of equal value to both; and for these reasons alone its countless details merit closer exploration than has been done so far.

In order to help meeting the anticipated needs for accurate lunar maps in the future, the Department of Astronomy at the University of Manchester, with financial support from the U.S. Air Force, embarked in 1958 on an extended programme of lunar cinematography—aiming to record the sunrise and sunset phenomena over all parts of the lunar surface—in order to secure the data from which three-dimensional lunar coordinates (i.e. not only the latitude  $\beta$  and longitude  $\lambda$  of any particular point, but also its relative height  $h$  above the surrounding landscape) could be determined with sufficient accuracy. The accuracy which one can attain in positional or height measurements depends, in turn, on the resolving power of the telescope employed for such work, that of the detector (i.e. photographic emulsion) as well as the quality of images as influenced by atmospheric seeing at the observing site.

Of the sites which have been conveniently accessible to us, the optimum conditions in respect to all these requirements exist at the Observatoire du Pic-du-Midi in the French Pyrenees, situated at an altitude of 2862 m—14 m

† Astronomical Contributions from the University of Manchester, Series III, No. 87.

‡ Supported under Contracts AF 61(052)-168, 380 and 496 between the University of Manchester, and the Geophysics Research Directorate of the Air Research and Development Command, U.S. Air Force.

below the actual summit of Pic-du-Midi—well above the level of atmospheric dust and sufficiently far from disturbing city lights, yet easily accessible with heavy equipment and provided with excellent facilities (power, living conditions, etc.) for sustained long-range work. And, most important of all, this Observatory possesses a long-focus refractor of 60 cm (24 in.) clear aperture and 18 m focal distance—by far the highest-situated instrument of its size—which, together with its companion photographic doublet, saw its first distinguished tour of duty, in the service of lunar photography, at the hands of Loewy and Puiseux in Paris in the preparation of their famous *Atlas de la Lune*. Seventy years later, in the new location at Pic-du-Midi (where it was removed in 1944) it resumed thus, in our hands, its former calling at a site where the renowned clarity of the atmosphere and steadiness of images repeatedly made history of the annals of observational astronomy since the days of Lyot (see Fig. 1). We are indeed very grateful to Dr. Jean Rösch, Director of the Observatoire du Pic-du-Midi, for allowing us all the valuable privileges of his institution, and for his continued courtesy and cooperation in our work.

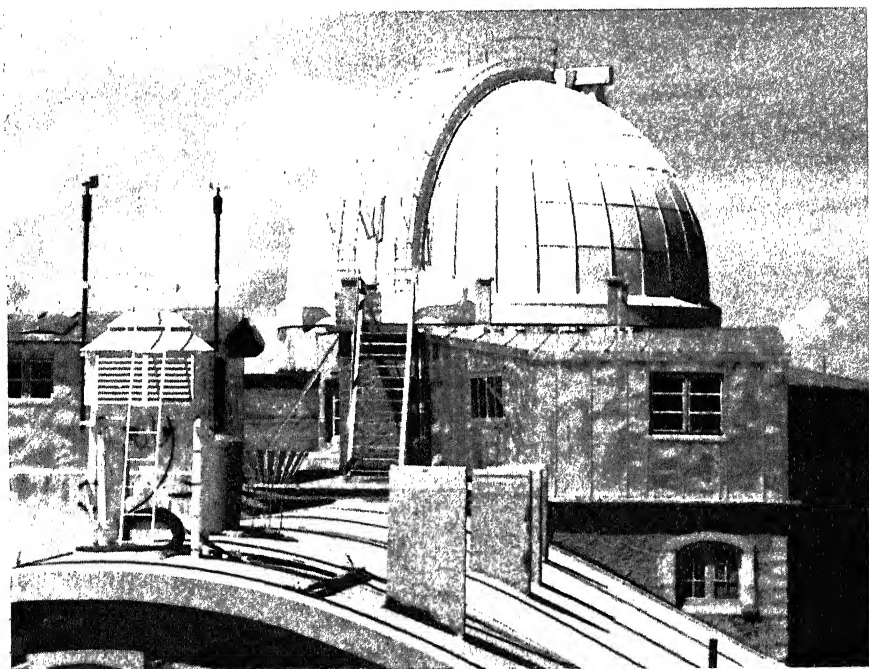


FIG. 1. The large dome housing the 24 in. refractor at Pic-du-Midi, with which all photographic work reported in this paper has been carried out.

The objective of the coudé refractor of Pic-du-Midi is a doublet corrected for visual light; and on account of its long focal length, its depth of focus is considerable. In order to improve its definition, a pass-band of approximately 150 Å in width and centred at  $\lambda = 5\,600\text{ Å}$  was isolated by suitable glass filters—this wave-length being chosen partly because of the characteristics of the films employed in our work (Ilford 5G91, Pan F, or Eastman Kodak

Plus-X) and partly because the secondary spectrum of the objective is such that the longitudinal aberration—zero at  $5850 \text{ \AA}$ —rises steeply towards both shorter and longer wavelengths. The photographs taken in the light of  $\lambda < 5500$  or  $> 6300 \text{ \AA}$  would, therefore, have necessitated the use of filters with even narrower passbands (and, consequently, longer exposures).



FIG. 2. Region of the lunar crater Pythagoras on the north-western limb of the Moon.

The linear scale attained in the focal plane is  $11''.4/\text{mm}$ ; and as (at the mean distance of the Moon from the Earth) one second of arc corresponds to  $1\,864 \text{ m}$  on the lunar surface, it follows that  $1 \text{ mm}$  on our original negatives corresponds to  $21.3 \text{ km}$  on the Moon, and  $1\mu$  to  $21.3 \text{ m}$ . This latter resolution

is, of course, unobtainable on several grounds; the most important one being the fact that the diameter  $1.22(\lambda/D)$  of the first Airy's disk of a lens of aperture  $D = 60$  cm at the effective wave-length of  $5\,600\text{ \AA}$  is equal to  $0''.23$ —corresponding to 430 m on the Moon, or  $20\mu$  in our focal plane. The maximum resolving power of a 24-in. refractor would, therefore, permit us to measure the details on our films with a minimum error of  $\pm 0''.12$ , corresponding to about  $\pm 200$  m of transverse distance on the Moon (corresponding to errors of  $\pm 1$  min of arc in the determination of the selenographic coordinates  $\lambda, \beta$  in the central parts of the apparent disk of the Moon), or about

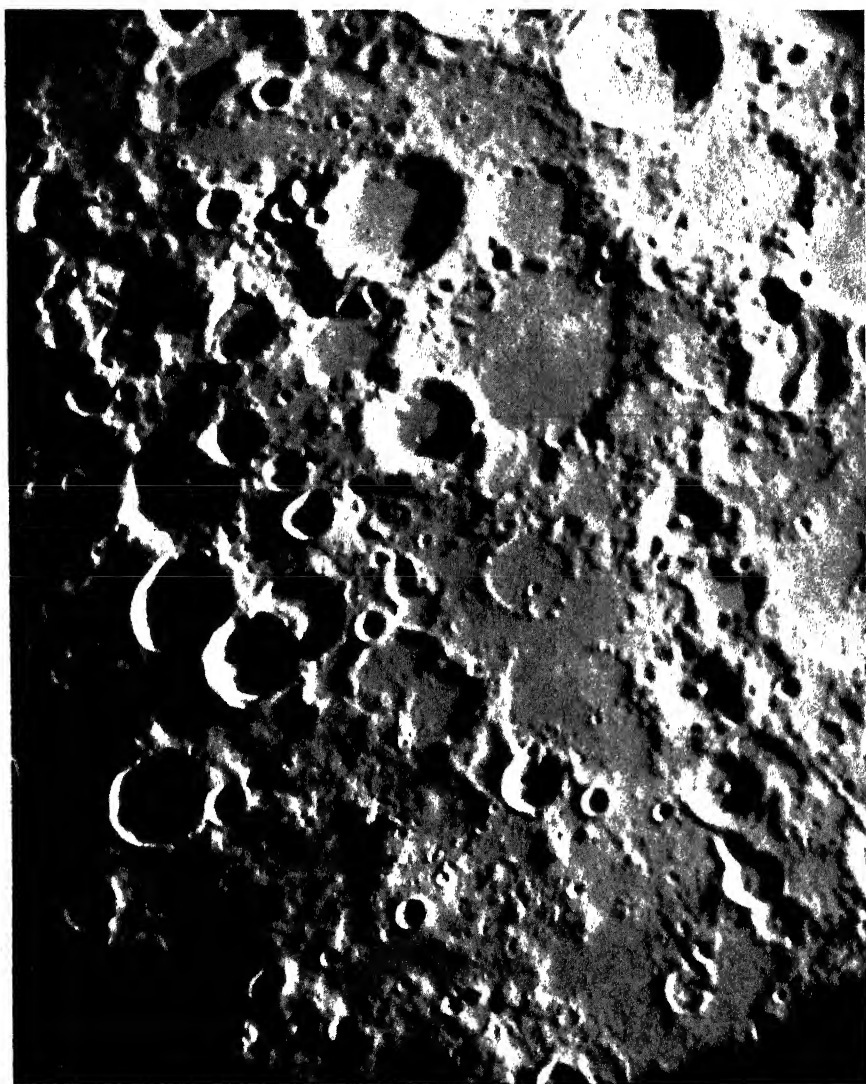


FIG. 3. Part of the Southern Hemisphere of the Moon, showing the surface formation north of Werner.

$\pm 200 \sin \nu$  m in lunar elevations (where  $\nu$  stands for the sight angle of the respective peak as seen from the tip of its shadow on the Moon). At low altitudes of the Sun above the lunar horizon,  $\sin \nu \approx 0.05$ ; so that the errors in relative heights of lunar mountains, as determined from the measured lengths of the shadows cast by them on the surrounding landscape, become of the order of  $\pm 10$  m near the centre of the apparent disk of the Moon. An extensive experience of the past 2 years leads us to conclude that an accuracy of this order is indeed attainable at Pic-du-Midi on approximately 10% of our films.

In order to secure the actual observations, a film camera is attached to the telescope and placed directly in the prime focus of the 60-cm objective. Systematic work began early in 1959, when the astronomers of Manchester University attached to the 60-cm refractor an existing camera using 35-mm film, whose shutter admitted a field of 25 mm in diameter. Before we can



FIG. 4. Sunset over the lunar crater Copernicus.

survey the progress which has been made since that time in our observing techniques, it may be as well to mention two disadvantages of the prototype camera. The first was its inability to record more than approximately one-fiftieth of the visible lunar surface at one exposure; and secondly, the action of the camera was fully automatic so that exposures were obtained at the rate of three per minute regardless of the atmospheric conditions and the



quality of the images. However, considerable amounts of film were exposed and processed in the photographic laboratories of the Observatory, and from the many thousands of negatives a large number were subsequently used for topographic studies of the surface features of the Moon; for their examples, cf. the accompanying Figs. 2, 3 and 4.

Later in 1959 the shutter of the camera was replaced by one which enabled a format area of  $25 \times 90$  mm to be used—25 mm being the maximum usable width of 35-mm film—and this in turn permitted the lunar terminator to be fully covered in two overlapping exposures (cf. Fig. 5). At the same time the mounting was modified so as to allow the camera format to be aligned with any prevailing lunar terminator. Also, the automatic system of shutter operation was discarded in favour of manual control; for while the lunar photographer cannot predict atmospheric observing conditions exactly, the experienced operator can recognize certain patterns and trends and can discriminate against excessively poor conditions. As a result of these modifications, not only were larger areas of the lunar surface recorded on each negative, but the percentage of good negatives showed a marked increase.

In the principal focal plane of the 60-cm refractor at the Pic-du-Midi Observatory the diameter of the lunar image varies between 15.4 cm at apogee to 17.6 cm at perigee. Such an image is large and can be accommodated quite easily on glass photographic plates when only a few negatives are required to justify a night's work. However, the shadow progression technique is far more complicated, for the lunar shadows must be photographed frequently over long periods of time if their individual movements are to be recorded. This involves certainly many hundreds of exposures during the course of one night's operations, and there is scarcely any need to comment on the difficulties that would be engendered by the use of glass plates under such circumstances. On the other hand, large quantities of film, of sufficient width to more than cover the full lunar image, also poses problems, particularly in the processing stage, for such work requires the use of large and expensive apparatus which is not available at the Pic-du-Midi Observatory. Fortunately this problem was solved when our colleagues at the Aeronautical Chart and Information Center of the U.S.A.F. volunteered to process the lunar film in their laboratories in St. Louis.

So much, then, for the processing of the film. The problem which confronted us then was to find a camera which could be suitably converted to astronomical use, which could contain many feet of film in one loading, and which would have a focal-plane shutter of sufficient dimensions to more than cover the full lunar disk.

From several cameras which were suggested, the K-22 Aero Camera came nearest to our specifications (Fig. 6). This camera was designed for aerial mapping and employs a  $9 \times 9$ -in. square format, and possesses removable film magazines with capacities up to 390-ft of 9.5-in. film (smaller standard 180-ft rolls of film are more frequently used so as to reduce the weight on the telescope). The K-22 camera has two interchangeable focal-plane shutters, one for high speeds of the order of  $1/500$  sec, the other for speeds as low as  $1/150$  of a sec. The duration of these exposures is far too short for a telescope possessing a focal ratio of 30; in addition, we must not overlook the effects of the Chance-Pilkington OY2 filter which further reduces the light intensity in the plane of the emulsion. Neither must we forget the film characteristics and sacrifice fine-grain image structure to emulsion speed.

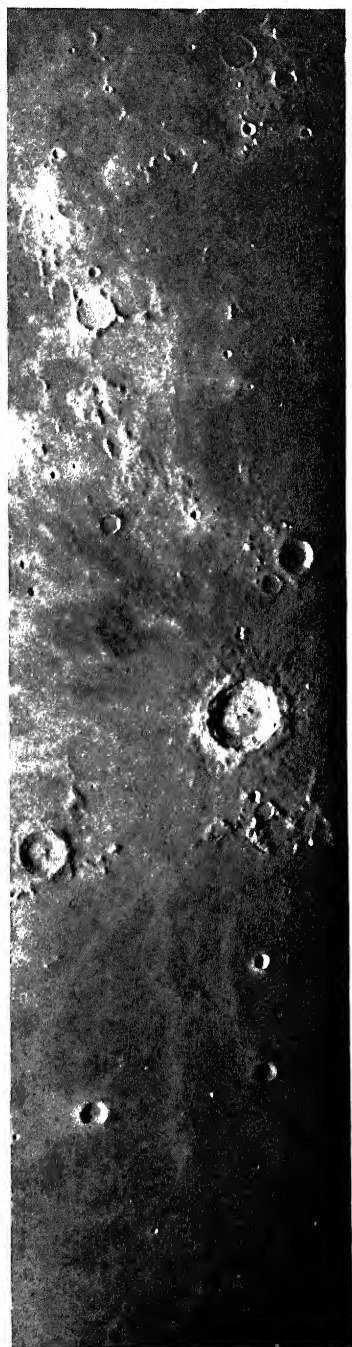


FIG. 5. Sunrise over the eastern planes of Mare Imbrium, with the crater Copernicus.

In view of all these factors the focal-plane shutters were modified and the speeds can now be varied at will from 0.1 sec up to 6 sec. A specially constructed electrical "intervalometer" determines the exposure durations and this is found to be very reliable in operation.

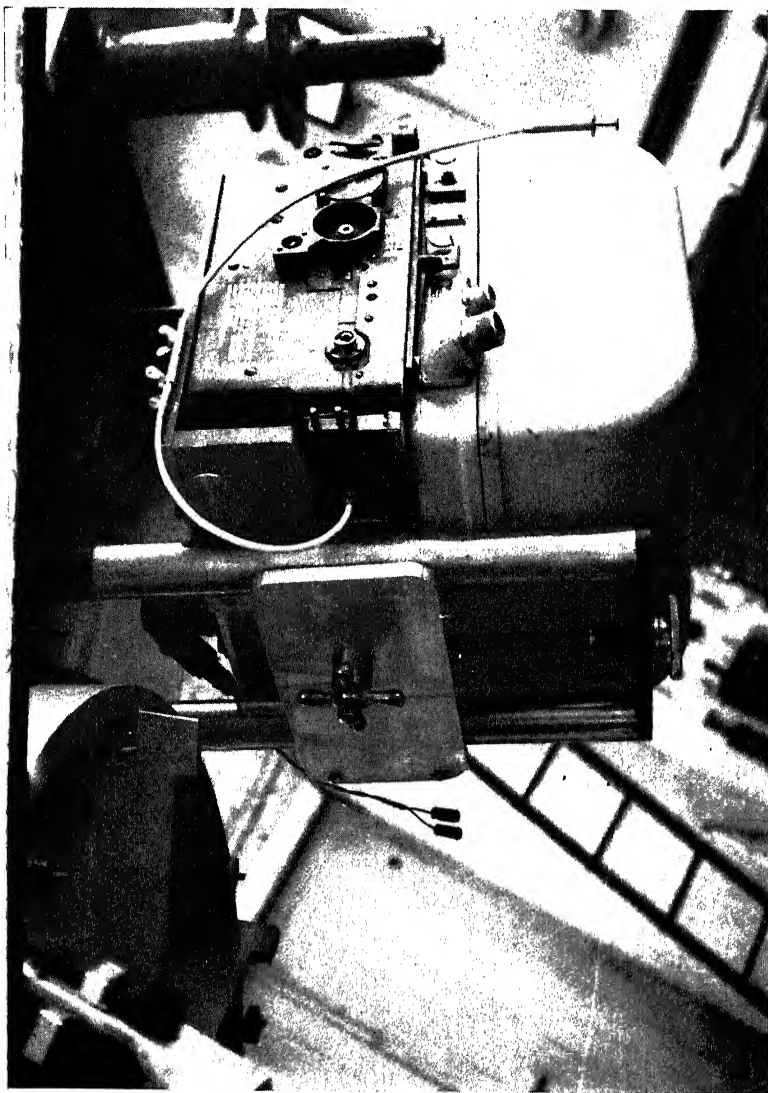


FIG. 6. The K-22 photographic camera mounted at the prime focus of the 24 in. refractor at Pic-du-Midi.

Since its inception in the autumn of 1960 the K-22 camera has already provided several thousands of lunar photographs under widely varied phase angles, the examples of which can be seen on the accompanying Figs. 7-10. Although Manchester astronomers are frequently testing new types of film emulsions in order to achieve optimum results, the film which has been used

mostly is Eastman-Kodak Plus-X emulsion. This has a useful A.S.A. rating of 80, fine-grain characteristics, and possesses a topographical or low shrinkage base which makes it very suitable for all work involving accurate measurements. The Plus-X emulsion characteristic curve is remarkably linear, and there is sufficient latitude to accommodate a fair proportion of the various lighting intensities which prevail upon the lunar surface; but it has been our practice to vary the exposure durations so as to procure complete coverage of the extreme lighting intensities. This, in our opinion, is a practical solution to a problem that would otherwise invoke especially shaped shutter curtains, although later in this paper other techniques will be considered in this connection.

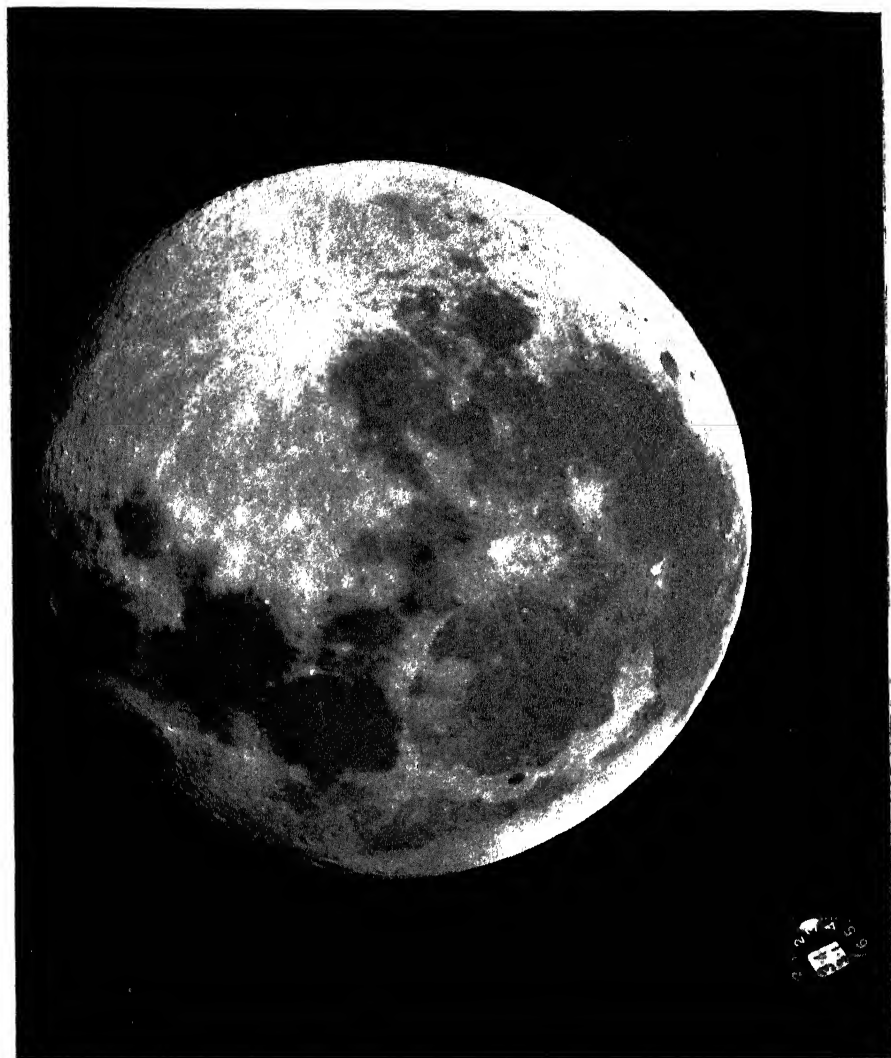


FIG. 7. A photograph of the Moon age 15 days, taken with the K-22 camera in the prime focus of the 24 in.

If a lunar negative is to be used for accurate hypsometric work it is essential to know the exact date and time at which it was exposed at the telescope. To facilitate this, a small optical projector was constructed and fitted to the camera in such a way as to allow an image of a watch to fall in one corner of the format. The watch has a small white plastic disk in the middle of the face on which the date is written, and this too is imprinted on the film when the exposure is made.

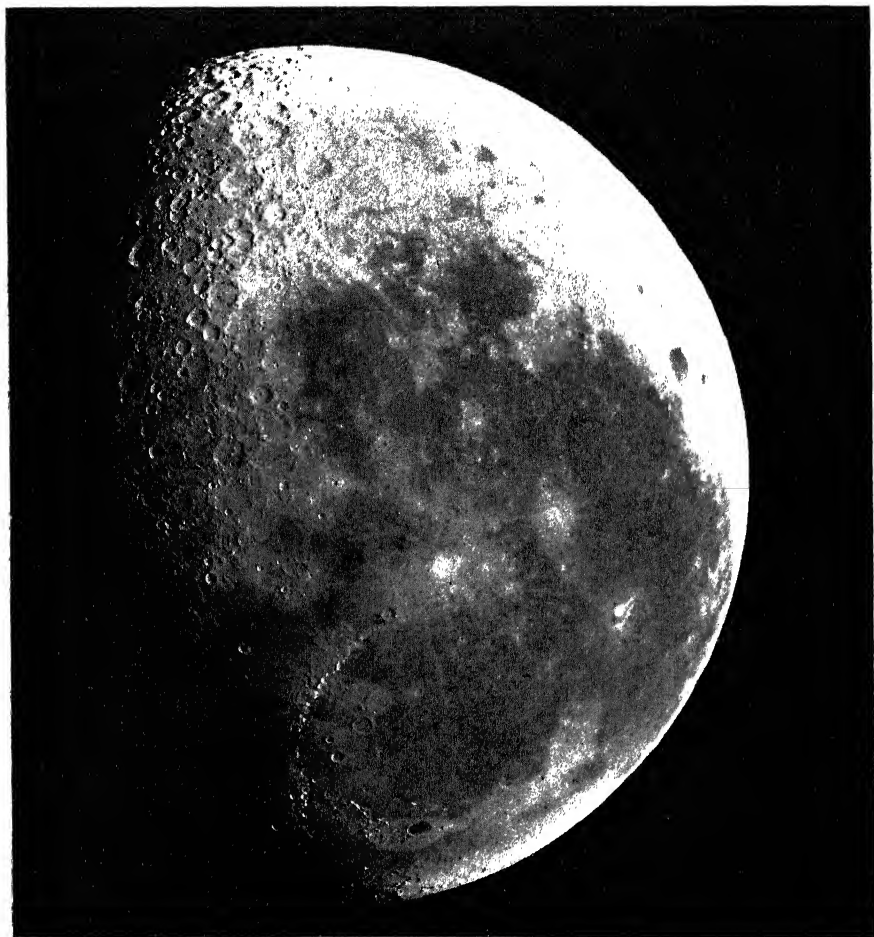


FIG. 8. A photograph of the Moon, age 21 days, taken with the K-22 camera in the prime focus of the 24-in. refractor at Pic-du-Midi.

When the camera magazine is removed from the guides which hold it to the back of the camera it can then be replaced by a ground-glass focusing screen which has an eyepiece fitted to the centre of it. In the centre of the screen a small area of the glass is clear and this allows the observer to focus the eyepiece on to a small cross ruled on the front surface of the glass. Since the front surface of the glass occupies the exact plane of the film emulsion,

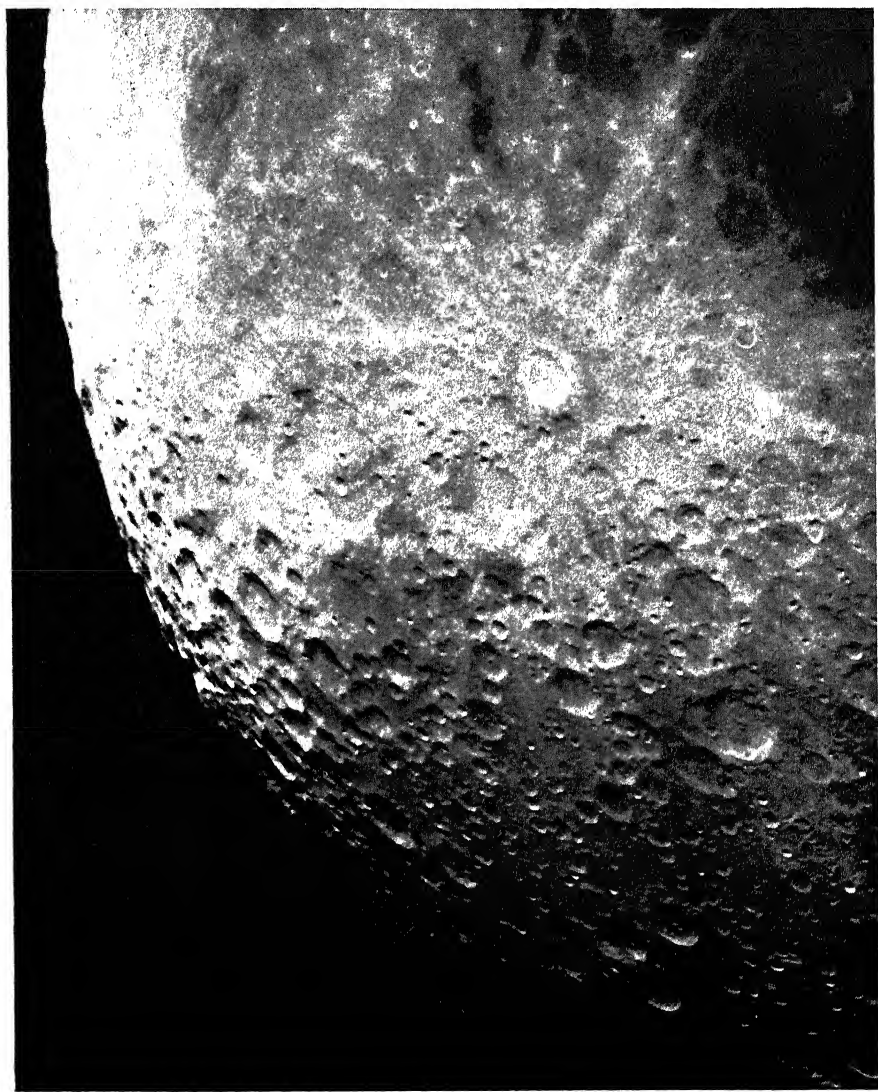


Fig. 9. A photograph of the Moon with the crater Tycho (an enlargement of a K-22 negative secured at Pic-du-Midi).

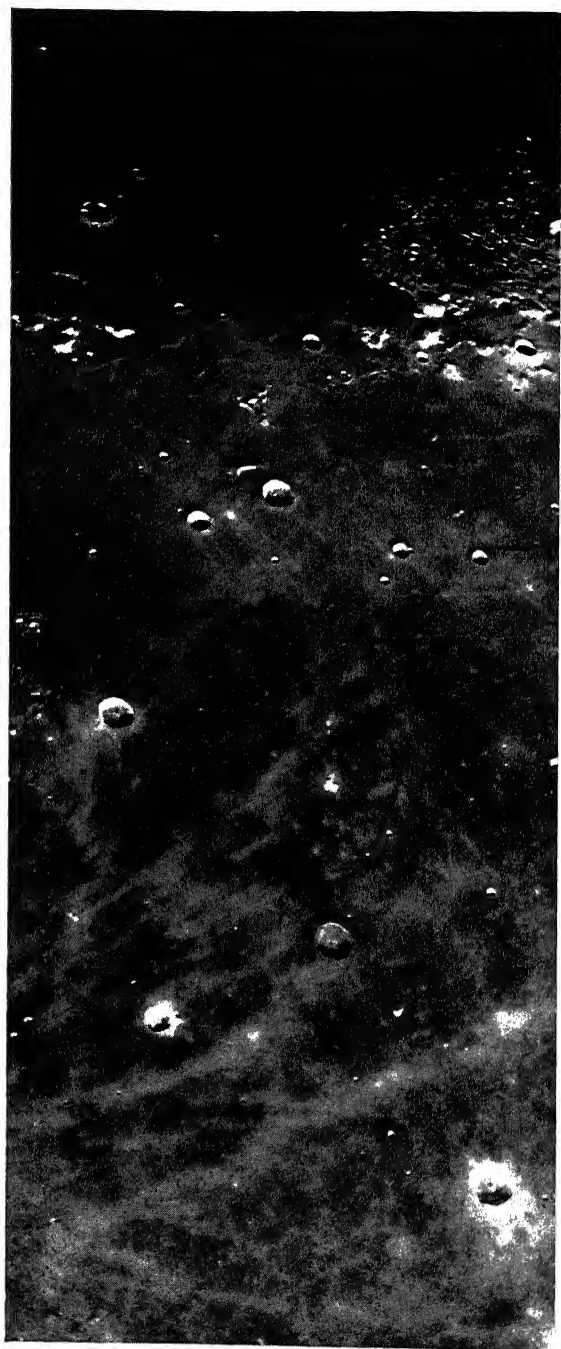


FIG. 10. Enlarged portion of a photograph of the Mare Imbrium region showing the craters Timocharis, Pytheas, Euler as well as narrow serpentine valleys east of Harbinger Mountains. This photograph can be regarded as a sample of the best results obtainable from Pic-du-Midi with the existing equipment; the smallest details measurable on the negatives are approximately 700 m in size.

it is necessary only to rack the complete camera back and forth on its mounting until the image of the lunar limb is seen at its maximum definition. The camera is locked in this position and the R.A. and Declination of the telescope are adjusted until the whole lunar image falls centrally within the area of the focusing screen. The magazine is replaced and the work can then begin. Another interchangeable attachment allows the well-known Foucault knife-edge arrangement to be employed for the same purpose.

The guiding of the 60-cm refractor is controlled by another refractor of 20 cm diameter mounted above it, and with the same instrument, the



FIG. 11(a). Direct photograph of the Moon taken with the K-22 camera at Pic-du-Midi on 5 October 1960.

observer examines the images for the effects of atmospheric turbulence and presses his manual camera control when he judges the images to be good. After a night's work a few of the frames are cut from the roll of negatives and these are processed at the Observatory to provide a check on the work and to monitor the quality of the negatives. The remainder is dispatched to St. Louis for processing with minimum delay.

Using the Eastman-Kodak Plus-X emulsion with the apparatus described



above, not forgetting the OY2 filter, we have found that good lunar negatives were obtained with the following exposures:

<i>Age of Moon</i> (days)	<i>Phase</i>	<i>Exposure Duration</i> (seconds)
3.5 and 24.5	Crescent	0.50
7.0 and 21.0	Dichotomy	0.25
14	Full	0.10

Acceptable full-Moon negatives were exposed with a shutter speed of  $1/25$  sec.

Lunar photography with the aid of a camera imaging the entire face of the Moon on each frame gives rise to certain special problems. Consider,

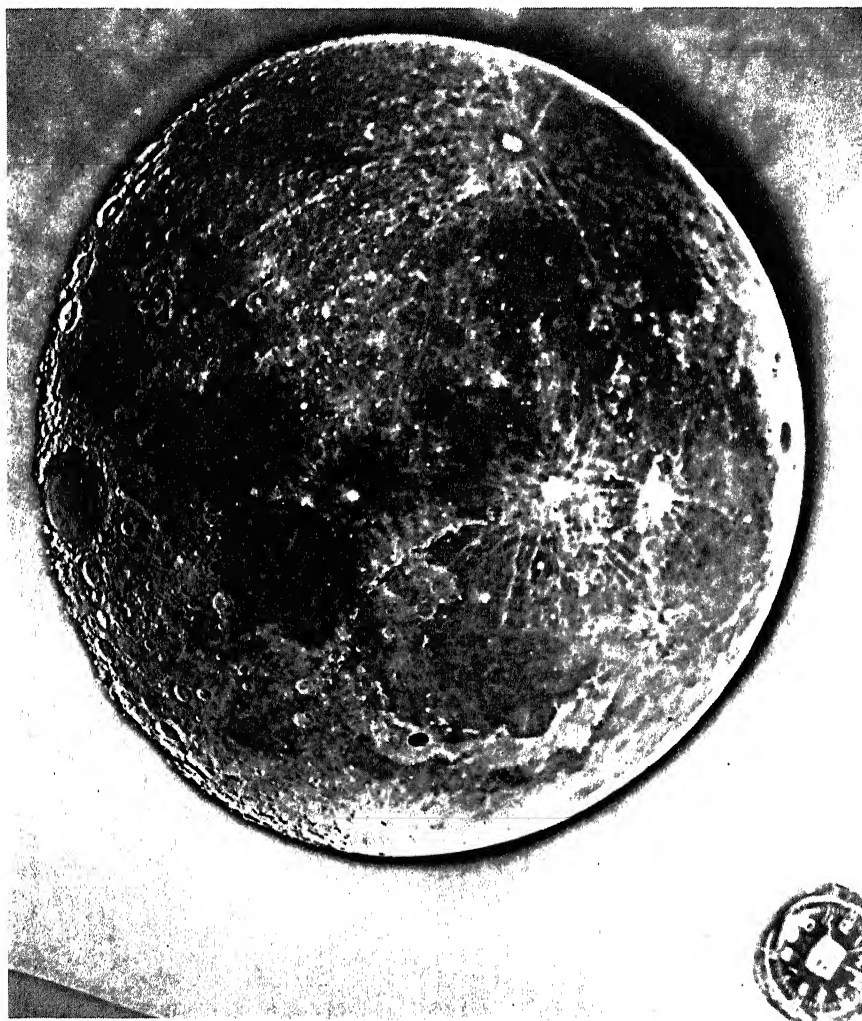


FIG. 11(b). A fluoro-dodged version of a direct lunar photograph reproduced on Fig. 11(a).

for instance, that of the optimum exposure times. It goes without saying that each part of the illuminated surface would call for its own appropriate length of the exposure; and whenever the latter is adjusted to the degree of illumination prevailing on the terminator (where the shadows cast by the lunar mountains are longest—a condition essential for successful hypsometric work) the major part of each image is bound to be overexposed.



FIG. 12(a). Direct photograph (mirror image) of the Moon taken with the K-22 camera at Pic-du-Midi.

How to extract the maximum amount of information from over-exposed parts of the negatives? In an effort to do so, we have experimented so far with two different techniques for photometric “rectification”. One is purely photographic and consists of copying our negatives by “fluorododging” (a process based on the Herschel effect of infra-red light in quenching the fluorescence of an auxiliary screen illuminated by a UV lamp through the original negative [1]); and the other consists of a transcription of the original negative by means of an electron scanning beam.

In order to see the results, compare a direct K-22 negative as seen on Fig. 11*a*—one of several hundred we took in the past few months—with its fluoro-dodged copy (Fig. 11*b*): the gain in information obtained by this process along the bright limb as well as the terminator region is evident at a glance. In fact, one of the defects of conventional photography in exhibiting the “false age” of the Moon can thus be neatly rectified. These pairs of photographs were kindly prepared for us by Father Francis J. Heyden, S.J.,

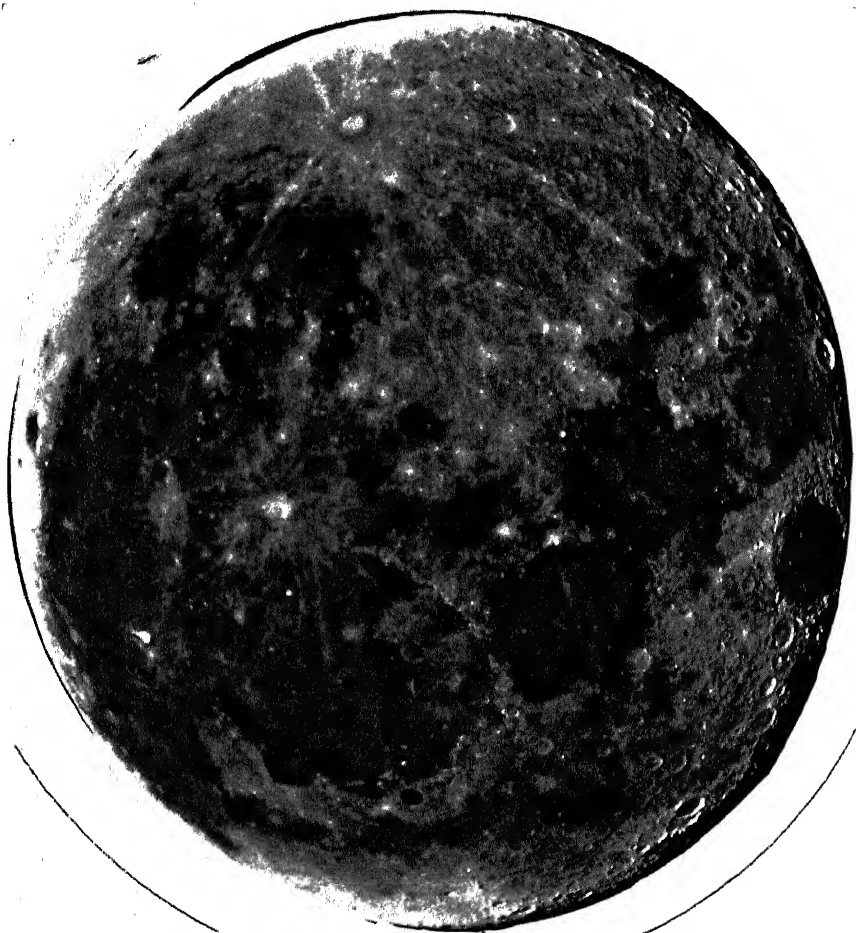


FIG. 12(*b*). Electronic transcription of the photograph shown on Fig. 12(*a*) at E.M.I. Laboratories in Middlesex, England. (By virtue of the method of transcription, a mirror image of the Moon is shown.)

Director of the Georgetown College Observatory; while the pair of photographs on Figs. 12(*a*) and 12(*b*) show the results of an electronic transcription of our negative at the E.M.I. Research Laboratories in England. Preliminary experiments carried out so far in both these directions reveal that both methods are potentially of great usefulness.

The principal aim of our whole programme so far has been to provide new basic information on topographic features of the lunar surface—partly for purposes of selenologic and stratigraphic analysis, and partly to serve as a

basis for the construction of new charts of the lunar surface, on the scale of 1:1 000 000 which are being prepared by the Aeronautical Chart and Information Centre of the United States Air Force. The actual methods of reduction of our topographic data have already been described elsewhere [2] and need not be repeated here. Suffice it to mention that our photographic material should be sufficient for a determination of lunar positions within errors of

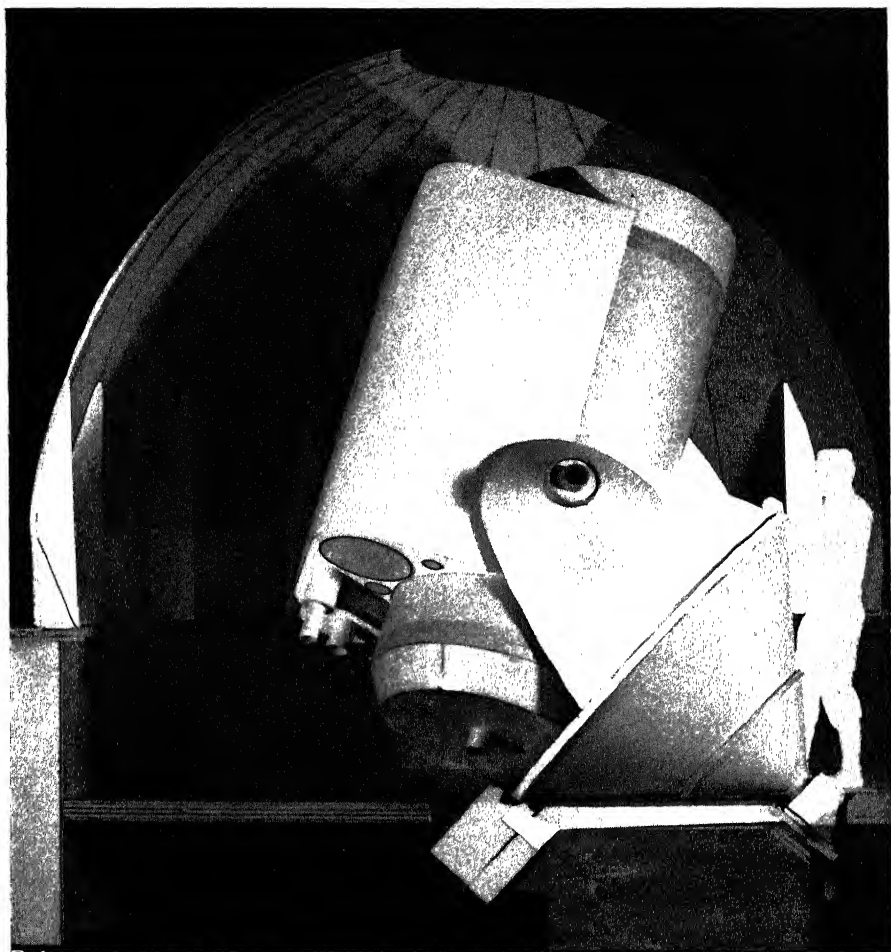


FIG. 13. A model of the new 43 in. reflector of 30 m Cassegrain focal distance, designed by Dr Jean Rösch, which is being built for the Observatoire du Pic-du-Midi for high-resolution lunar and planetary work.

the order of 1' in selenographic latitude or longitude (i.e. rather less than 1 km on the actual lunar surface); while the relative heights of lunar mountains can be determined from the length of the shadows cast on the surrounding landscape within  $\pm 10$  m near the centre of the apparent lunar disk.

Limitations of space render it impossible to go into details of the work we accomplished so far in this field; and it may also be unnecessary to do so, as our main efforts at present are being spent in making all past work

obsolete as rapidly as we can. In the past two-and-a-half years we have taken close to 20 000 new lunar photographs, many of which compare favourably with the best previous work. In the next twelve months we hope, again in collaboration with the U.S. Air Force and Dr. Rösch, to erect on the Pic a considerably larger instrument—namely, a 43-in. reflector of 30 m focal length, to commence its own tour of duty in the service of lunar photography (for its design, cf. the accompanying Fig. 13). When this happens, most of our present work will have to be done over again—and better.

The next logical step in improvement of the quality and resolving power of the lunar photographs should be accomplished by lifting a telescope of comparable optical power to an altitude of 70 000–100 000 ft above some 99% of the atmospheric air masses—a feat not at all impossible by means of the existing balloons—to defeat both the air turbulence and clouds. Moreover, as we all know, the day is not distant when artificial satellites launched by human hand will orbit the Moon to relay to us (by television) the pictures of the lunar landscape viewed from much closer vantage points than any terrestrial base, and affording a correspondingly greater resolution. Ultimately, the quality of the lunar maps based on such observations will be tested by the first interplanetary travellers actually landing on the Moon's surface; but this should also mark the beginning of an entirely new story of lunar exploration than the one with which our ground-based astronomers have so far been concerned.

#### REFERENCES

1. Its description can be obtained from Watson Electronics and Engineering Co., Arlington, Virginia, U.S.A., or the U.S. Radium Corporation in Geneva, Switzerland.
2. Cf., e.g. Kopal, Z. Topography of the Moon. In "Physics and Astronomy of the Moon", Academic Press, New York and London (1962).

# TELEVISION ASTRONOMICAL OBSERVATIONS AT THE PULKOVO OBSERVATORY

N. F. KUPREVICH

*Pulkovo Observatory, Leningrad, U.S.S.R.*

In recent years we witnessed in science and technology a wide application of the methods of television in intensifying the brightness of faint images. The increase in brightness of the image makes it, in turn, possible to shorten considerably the time of exposure. In astronomical observations using photographic techniques this proves to be very important, since it enables us to lessen the adverse effects of the atmospheric disturbance and thereby to bring the resolving power of the telescope closer to its theoretical value. Besides, in the television system the image is converted into a series of electrical signals, one following the other with very high speed. This makes it possible to perform any kind of a manipulation with the video signals—for example, to add them, to subtract them, etc., and to examine the results in the form of an image on the screen of the kinescope. On it, it is possible to view at the same time several images of simultaneous phenomena occurring at different points in space. This characteristic of the television system distinguishes it from other methods and possibilities for electron amplification of the brightness of images used in practice.

In 1958 at the Pulkovo observatory we constructed an experimental television telescope for astronomical observations. In the telescope, the aperture of which is 285 mm, we used the optical reflecting system of Cassegrain, which permits to obtain equivalent focal distances of 9.5, 18.0, 32.0, 56.0 and 125 m [1].

The telescope is mounted on a parallactic stand, and its view with the television camera is shown on Fig. 1. In the camera of simplified construction is fastened the focusing system with a camera tube of the type "Super-orthicon". The focusing of the telescope is accomplished by moving the secondary mirror, with the aid of a screw.

The television camera is connected with units of the apparatus, located elsewhere, by the use of connecting cables. In the apparatus we use the standard 625-line scanning, line-by-line or interlaced, 50 and 25 frames per second respectively. The band of the video frequency passed through the amplifiers without distortion is of the order of 11 Mc/sec. The general appearance of the television apparatus used in the astronomical observations is shown in Fig. 2. The power supply for the equipment is provided by voltage stabilizers and rectifiers 1. The control of the system of the transmitting tube is concentrated in unit 2. The generators of the scanning by lines are located in unit 3 and the generators of the frame frequency in unit 4. The monitor is 5. In photographing the image from the screen of the kinescope one uses electronic synchronous shutter 6, which gives a precisely timed exposure of 1/25 or 1/50 sec. In order to decrease the outside illumination of the screen of the kinescope we use the cone screen 7, at the end of which the photographic camera 8 is fixed.

The television telescope is used for taking experimental photographs of the Moon from the screen of the kinescope. When this is done, one uses a focal distance of 9.5, 18, and 32 m with corresponding relative openings of the optical system of 1:33.3, 1:63 and 1:112. As an illustration, Fig. 3 reproduces a photograph of the Moon from the screen of the kinescope

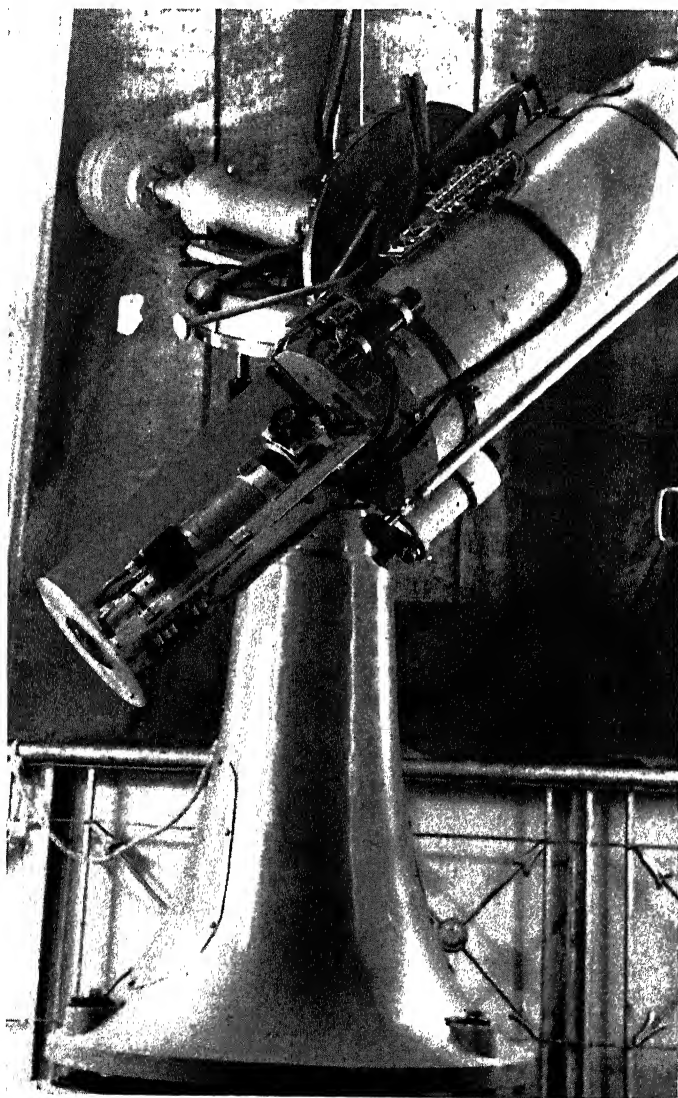


FIG. 1. A view of the experimental television telescope.

obtained with an exposure of  $1/50$  sec. The optical focus of the telescope was 9.5 m. Figure 4 shows a television photograph of another part of the lunar surface, but with the focal length of the telescope being 18 m. In both cases the kinescope screen was photographed with a camera using a  $f/3.5$



objective and a 35-mm moving-picture film with a sensitivity of 90 units according to the Government Standard.

In the published literature one encounters suggestions about the possibility of automatic photography of stellar images (and also of the planets) undistorted by atmospheric turbulence. For this purpose the impulses of the photocurrent of the multiplier, due to the scintillation of the star image, are used for operating the shutter. The latter, which has a speed of  $1/100$  sec, is placed in front of the plate on which the photograph of the celestial object is being taken. It is assumed that the impulses in brightness of the star image and, consequently, in the photocurrent of the photomultiplier, are caused by the formation of the theoretical diffraction image in the focus of the telescope. This should correspond to an instantaneous absence of atmospheric interferences, and momentary attainment of the theoretical resolving power of the astronomical telescope yielding the maximum sharpness of the photographed images.

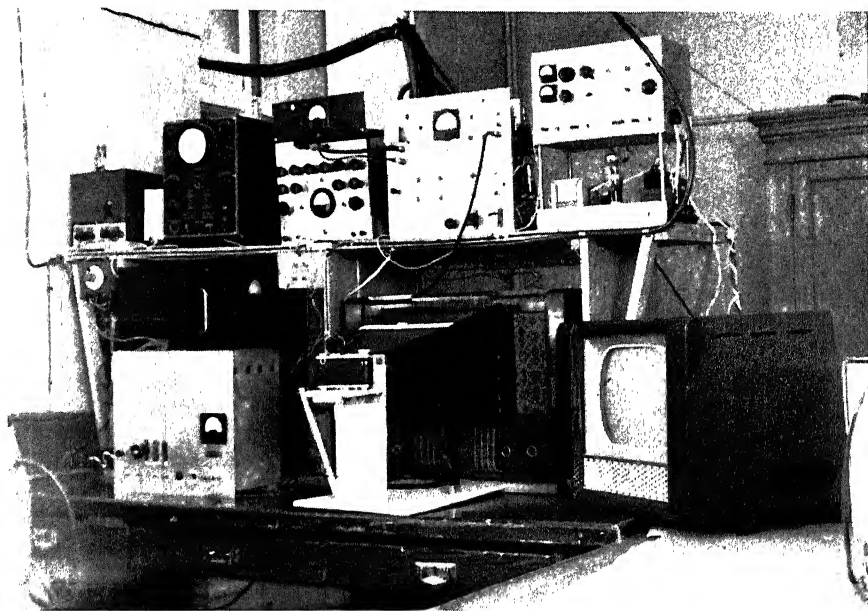


FIG. 2. The television apparatus used in the astronomical observations.

In order to study the changes in form of the stellar image resulting from atmospheric disturbances, instantaneous photographs of these images on a sufficiently large scale prove to be interesting. However, for the solution of this problem it is necessary to use small focal ratios of the telescope, of the order of  $1/300$  or  $1/400$ . This, however, leads to a diminution of brightness of the stellar image which does not permit the obtaining of negatives with normal density with an exposure of  $1/25$  or  $1/50$  of a second. This problem is easy to solve by the television method combined with the usual photographic method.

For studies of the deformation of star images at large magnification with the television telescope one uses the equivalent Cassegrain focus of 56 or



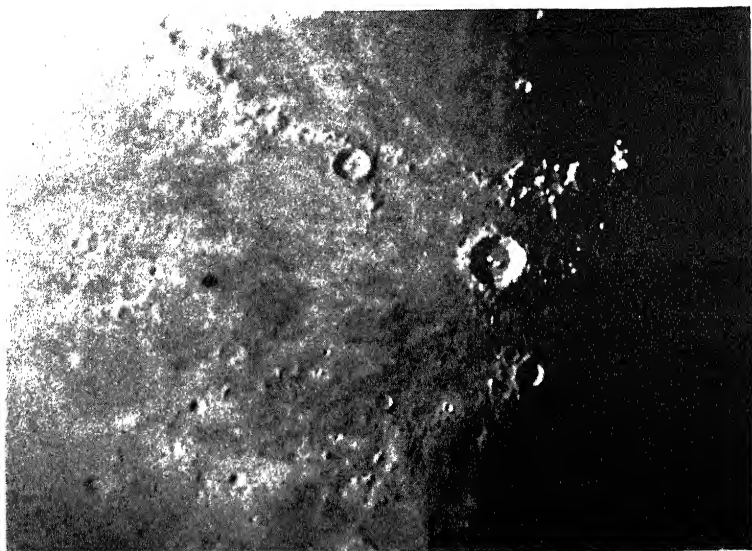


FIG. 3. Photograph of the surface of the Moon on the screen of the kinescope. Focal length: 18 m.

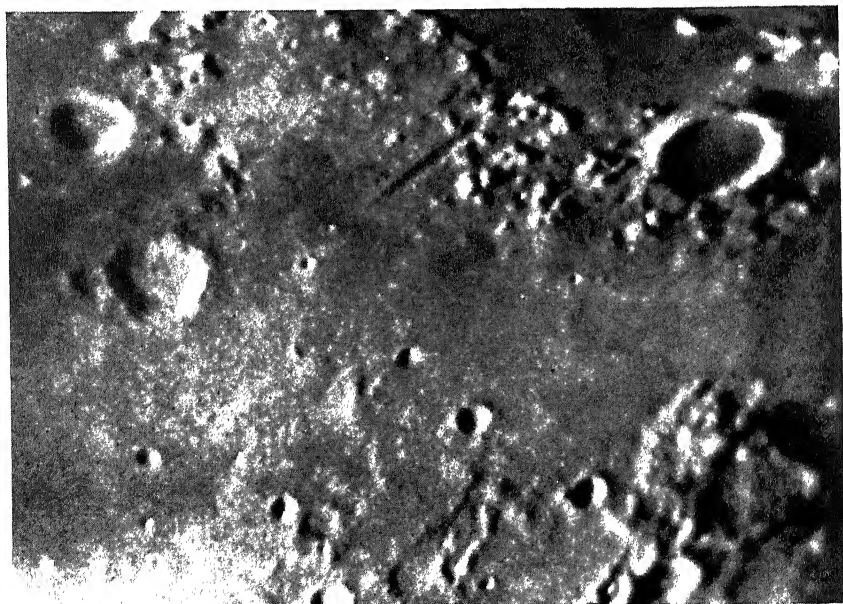


FIG. 4. Photograph of the surface of the Moon on the screen of the kinescope. Focal length: 9.5 m.

125 m. In the latter case the image of the star on the screen of the kinescope is about 15 mm in diameter and corresponds to an image which would be observed by an optical telescope with focal length of 1062 m. This figure is arrived at by the enlargement of the image from the optical focus of 125 m due to its subsequent transmission through the television system by a factor of about 8.5.

Figure 5 shows some separate frames (negative nos. 35, 36, 37, and 38) obtained on the screen of the kinescope with an exposure of 1/50 sec of the

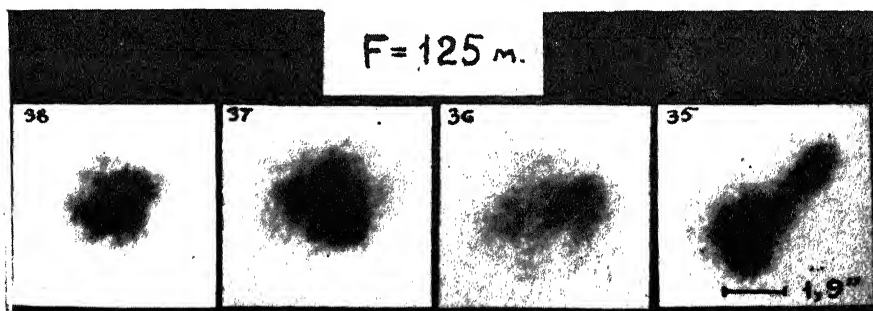


FIG. 5. Image of the star  $\alpha$  Tauri photographed on the screen of the kinescope. Focus of the optical telescope 125 m. Exposure 1/50 sec.

bright star  $\alpha$  Tauri, at zenith distance  $z = 40^\circ$ . The interval of time between the separate frames was on the average from 10 to 20 sec. The optical focus of the telescope was 125 m. One should note that the diameter of the image of the star (frame 38) proved to be larger than the theoretical by a factor of 2.9. These frames fix the instantaneous formation of the complex structure of the image of a star. Large deformations and spots appear on the image of the star. The dimensions of the spots are less than the theoretical diameter of the first maximum in the diffraction image formed by the telescope (for example, frames 36 and 35). This can be explained by the possible break-up of the diffraction image as a result of the atmospheric turbulence.

The next stage of research in this field was an attempt to record simultaneously the form of the image and the light flux of the scintillating star. One should note, however, that attempts to solve this problem by the usual optical methods met with no success, since one cannot simultaneously produce on the photographic plate both the image of the curve of the photocurrent from the screen of the oscillograph and the image of the star itself. However, by using modern electronic techniques it becomes possible not only to increase the brightness of the image, but also to obtain simultaneously on one screen two images regardless of their mutual positions, distance or even brightness.

Starting with these considerations in 1959 and 1960 the television telescope was adapted for simultaneous recording of the light flux as well as of the form of the stellar image during scintillation. For the observation we used the 56-m focus of the telescope and the television apparatus as briefly described above. A commercial television set of the type PTU-3, working also with a camera tube of the type "Superorthicon" was used for transmission of the curve of the photocurrent from the screen of the electron

oscillograph. Figure 6 shows a block-diagram of the whole equipment. The image of the star formed by the telescope 1 falls on the aluminum semi-transparent mirror 2. Fifty per cent of light is passed through the mirror and forms an image on the photocathode of the first "Superorthicon" 3 (basic channel of the television unit). The other 50 per cent of the light is reflected from the mirror and falls on the photocathode of the photomultiplier 6. The spectral characteristics of the photocathodes of the "Superorthicon" and the photomultiplier are approximately identical.

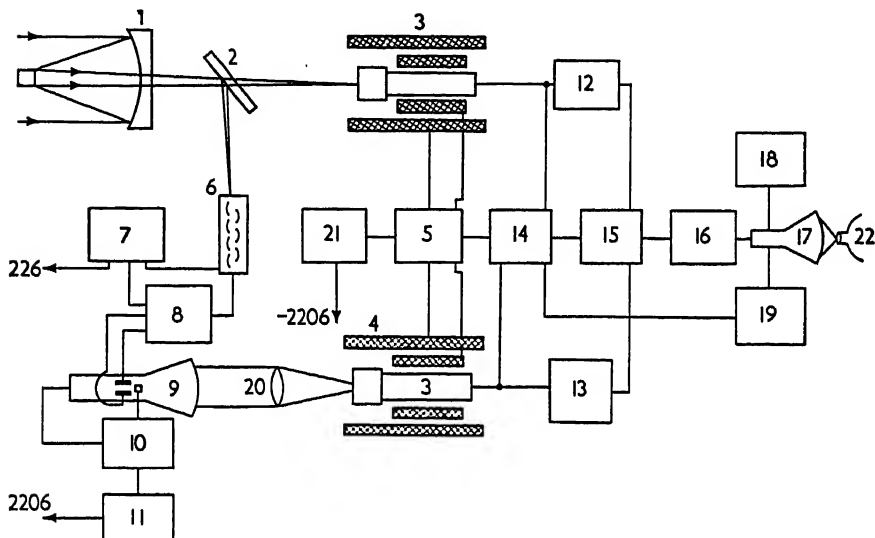


FIG. 6. Block diagram of the television unit for simultaneous recording of the light flux (photocurrent) and the form of the image of the star during its scintillation.

The maximum sensitivity proves to be in the region of 4500 to 5000 Å. The input currents from the photomultiplier pass to the amplifier of the DC 8. The input signals after passing the amplifier pass on to the electron oscillograph 9 (on to the plates of the vertical deflection of the electron beam). The oscillograph is provided with a generator of continuous scanning 10, which works in the system of synchronization with the frequency of the frames of the television system, i.e. 25 or 50 periods per second. The photomultiplier has a voltage supply from the stabilization unit 7, and the electron oscillograph from the unit 11. The image of the oscillogram of the photocurrent from the screen of the oscillograph is projected by the lens 20 on to the photocathode of the second "Superorthicon" 3, installed in the camera of a commercial television set. The two television channels are synchronized with each other. The units 5 and 21 ensure separate control of the mode of working of the camera tubes. During experiments in the television system one uses interlaced or line-by-line scanning. In order to obtain an interlaced raster of 25 frames per sec. one uses a synchronous generator 14 for 625 lines. The output video signals of the amplifiers 12 and 13 pass into the unit of electron commutation of signals 15. With the aid of this unit the images from the two television channels are viewed simultaneously on the screen of the kinescope 17. In this case the image of the basic channel (distorted

star image) occupies the upper half of the kinescope screen. The lower part, however, reproduces the image of the oscillogram of the photocurrents given by the photomultiplier. The image from the screen of the kinescope is photographed by the camera 22. For precise timing of the exposures of  $1/25$  or  $1/50$  sec, we used an electron synchronous generator (synchronous shutter) in the circuit. The units 16 and 18 serve as a supplementary amplifier and power source for the kinescope. The unit of scanning of the kinescope is 19.

Figure 7 shows photographs from the screen of the kinescope obtained by the method described, with an exposure of  $1/25$  sec by interlaced scanning. These are test photographs made on 3 May 1960 at Pulkovo, of the star  $\alpha$  Bootis. The optical focus was 56 m. The interval of time between the separate frames was of the order of 10 to 15 sec. In the upper part of each frame we see the distorted images of the star, averaged for the time intervals of the order of  $1/25$  sec.

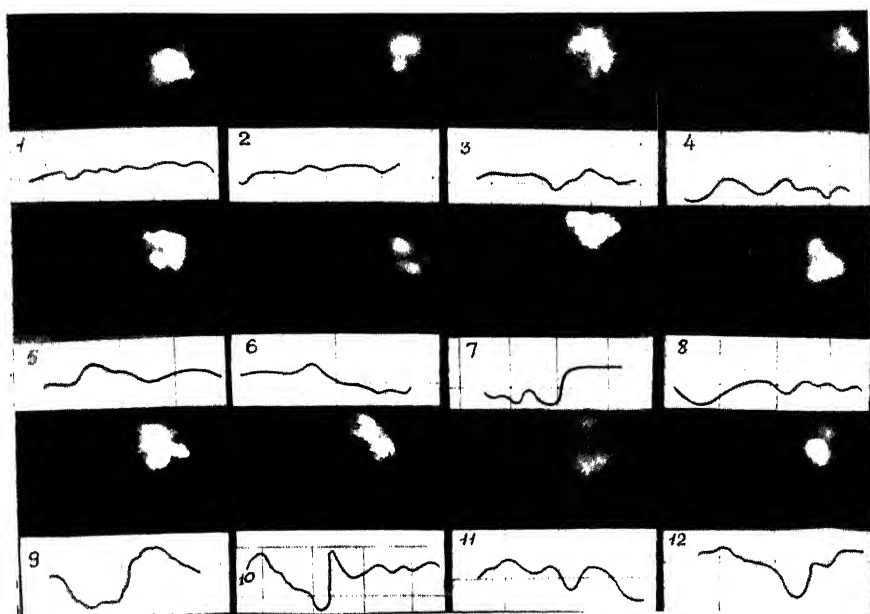


FIG. 7. Photograph of simultaneous television recording of the light flux (photocurrent) and the form of the image of the star  $\alpha$  Bootis during its scintillation. Optical focus of the telescope 56 m.

In the lower part of the frame we see the changes in the photocurrents in the same form as they were observed on the screen of the oscillograph. In the course of the experiments, the scale of the scanning (the magnitude of the horizontal amplification) sometimes changed in the oscillograph; and, as a result, the curves of the photocurrents in some frames are not always identical in length—although the time of the scanning was always  $1/25$  sec. The photocurrent curves were reproduced on the central part of the screen of the oscillograph. The scanning of the oscillograph and the television system was sufficiently linear. Therefore, the geometrical distortions in the

curve of the photocurrent were small, as can be verified from the squares of the coordinate lattice.

The scale of the voltages of the vertical deflection on the screen of the oscillograph corresponds to 18 V per cm, and is equal to the distance between the lines in the coordinate lattice. The horizontal line corresponds to a signal of 36 V. The zero value of the voltage of the signal on the frame is not shown on account of the lack of space.

Distinct from the television image of the star, which is averaged in time during 1/25 sec on the screen of the kinescope, the photocurrent of the photomultiplier is registered continuously during this time by the oscillograph. With the use of a photoelectric device, with a frequency-band higher than 1000 cps, the screen of the oscillograph can record impulses in the photocurrent, the duration of which is less than 0.001 sec (see frame 10, Fig. 7).

In examining the photographs obtained from the screen of the kinescope with an exposure of 1/25 sec, one can note that there exists no correlation between the photocurrent (and consequently, the light flux) and the form of the image of the star. From an examination of the frames 1 and 2 one sees that the photocurrent curves differ from each other very little. The form of the image of the star, however, is different. A comparison of the frames 2 and 12 reveals almost identical structure of the forms of the images although they are turned 180° with respect to each other. The form of the photocurrents is, however, different. The same is true of the images recorded on frames 5 and 6.

On the basis of experimental observations of distortions of stellar images with a television telescope the following preliminary conclusions can be drawn:

1. For speeds of the order of 1/25 and 1/50 sec no noticeable connection between the form of the image and the light flux of the star during its scintillation was detected.

2. It appears, therefore, unlikely that one could design an automatic instrument in which a high-speed shutter controlled by the photocurrent resulting from the scintillation of the star (1/25 or 1/50 sec) is used for separating high-quality images (of a star or planet) that are not distorted by atmospheric turbulences.

3. Rapid deformations in the diffraction image of the star may be the cause of the formation of rapid (of the order of 0.01 sec or less) changes in the intensity of the photocurrent. This, in turn, causes the operation of the high-speed shutter and the recording of distorted images of the star or planet.

#### REFERENCES

1. Kuprevich, N. F. Experimental television telescope of the Pulkovo Observatory. *Bull. astr. Obs. AN. SSSR*, no. 163, pp. 133-160 (1960).

## IV. PHYSICAL STUDIES OF THE LUNAR SURFACE



# PHYSICAL NATURE OF DIFFERENT ZONES OF THE LUNAR SURFACE

A. V. MARKOV

*Pulkovo Observatory, Leningrad, U.S.S.R.*

At the present time a sufficiently objective analysis of the data on the nature of the lunar surface collected by Soviet as well as foreign astronomers [1] has been made. Therefore, it is timely to examine critically the question of the nature of the upper layer of the lunar crust, since it is specially important for the astronaut to know its structure to a depth of from 2 to 5 m.

Information about this can be gathered from data on the lunar topography as a whole, and also from the results of the study of the lunar surface layer by photometric, spectrocoulometric, polarimetric, and thermoelectric methods, as well as from the study of the temperature and structure of the upper layer of the Moon by radio-astronomical observations.

In attempting to solve the problem of the structure of the lunar surface layer, it is necessary to proceed from the formation of the Moon in the past as a celestial body. In a direct examination of the problem of the structure of the lunar surface layer one should note that the conclusions should be made with care. On one hand, the physical characteristics of the surface layer from observations are not very precise; and, on the other hand, the area of the regions examined is small as compared to the whole surface of the Moon. It seems to us that it is precisely because of these facts that there exist such divergencies in the interpretation of the nature of the lunar surface.

Supporters of the volcanic origin of the lunar topography—Khabakov [1] and Fremlin [2], for example—referring to the presence on the Moon of sharply cut mountain ranges, and also regions with abundant cracks with steep sides, consider it possible (by a number of photometric and thermoelectric observations) to establish a basis for the reality of the existence on separate regions of the Moon of outcropping solid rock material. One should add that there is some argument in favour of this view, for the floors of ray craters, in the observations published by Sinton [3] on the crater Copernicus as well as in his report to this symposium on the crater Tycho.

However, in the majority of cases, the conclusions concerning the nature of the lunar surface layer are based on the comparison of average characteristics of large areas of the surface of the Moon, up to some tens of kilometers in diameter, with the same characteristics of small specimens of terrestrial rocks measured in laboratories. More important, it seems to us is the conclusion drawn from photometric investigations that, in contrast to the Earth, there are no areas on the lunar surface with reflecting capacity higher than 0.22. Another assumption about the existence on the surface of the Moon of layers of dust to a depth of hundreds of meters is expressed in a hypothesis by Gold [4]. Even a simple geomorphological study of the structure of the mountain ranges of the Moon and those parts of the lunar "maria" and craters which abound in cracks (zones of the Triesnecker and Ariadeus cracks, the floor of the ring mountain Alphonsus, etc., as well as



the straight wall near the crater Birt) suggests that, in these regions, a deep layer of dust cannot exist because the faults and cracks with steep sides would have been submerged by it. It should be noted that in the last publication of J. J. Gilvarry [5] in which he defends Gold's views one can find hardly any arguments for the existence of "basins" of lunar dust of some tens of meters in depth. Evidence against such conclusions is furnished by the results of Soviet radio observations of lunar eclipses, which give the thickness of the dust layer to be not more than 30 cm.

The concept of Firsoff [6], that the lunar pumice (which must have been formed by the endogenous process at the time of the violent outflow of gases from the hot magma during the hardening of the crust) is more porous than the terrestrial pumice deserves notice. By the same principles, according to Firsoff, it should be less dense than the terrestrial. Firsoff affirms, for example, that monolithic rocks of the type of terrestrial granites and basalts could not have been formed on the lunar surface. He stresses also the need for repetition of measurements of the heat conductivity of terrestrial powders (earlier done by Smolukhovsky), but only in a vacuum close to that on the Moon, since he considers that the measurements of the heat conductivity of powders under terrestrial conditions lead to values which are not comparable with those on the Moon.

The photometric peculiarities of the reflection of light from the lunar surface layer (called in Soviet literature the Barabashev-Markov effect [7]) showed that, with all different assumptions as to the law of reflection of light by the lunar surface, not less than 70% of its elements should form a very large angle with the horizontal plane, and not more than 30% of it is perpendicular to the vertical. This constitutes evidence for the extremely broken-up character of all the regions of lunar crust. The low albedo of lunar details made it possible for astronomers of the Leningrad University to assume a meteor-slag hypothesis for the structure of the lunar surface layer, based on the constant infall of meteors on the surface of the Moon, leveling its original characteristics over the whole lunar sphere to a surface layer some millimeters thick. For the measurements of such fine unevenness in the lunar surface layer it is essential to make use of the methods of radio-astronomy and temperature studies of the Moon, and also the polarization measurements of different regions of the lunar surface.

Temperature measurements of the Moon, conducted earlier in America, have begun at Pulkovo [8]. Such measurements of different areas of the lunar surface (see Fig. 1) have now been completed by Chistyakov. One should note that the results of the measurements of the temperatures on the lunar sphere for phase angles from  $17^\circ$  to  $60^\circ$  fully agree with the data obtained by Pettit and Sinton for the phase angles from  $0^\circ$  to  $57^\circ$  (see Fig. 2). However, although these measurements of temperature on a wave length of  $8\mu$  and polarization measurements (see special report by Kohan) on the wave length  $0.5\mu$  were made for areas with cross-sections ranging from 6 to 120 km, the total area of zones thus studied by the two methods adds up to hardly more than 5% of the fraction of the lunar surface visible to us. Therefore, if the existence of the Barabashev-Markov effect (i.e. of the very rough structure of the whole lunar surface) is confirmed also by the investigations of the phase-curve of the Moon (Zoellner, Fessenkov), then—strictly speaking—the estimates of the absolute dimensions of the roughness by measurement of the temperature and polarization make it possible to scrutinize only

5% of the area of the lunar surface, without any assurance that on the remaining areas of the Moon one may not discover effects similar to those which are characteristic of solid rocks on the Earth. The same can also be said about the results of polarization measures of the Moon, which are not at all similar to those for the fusion crust of meteorites and solid Earth rocks.

However, the value of the degree of negative polarization of details of the Moon, as measured by Kohan at Pulkovo, differs little from estimates of the absolute dimensions of the roughness for terrestrial powderlike materials

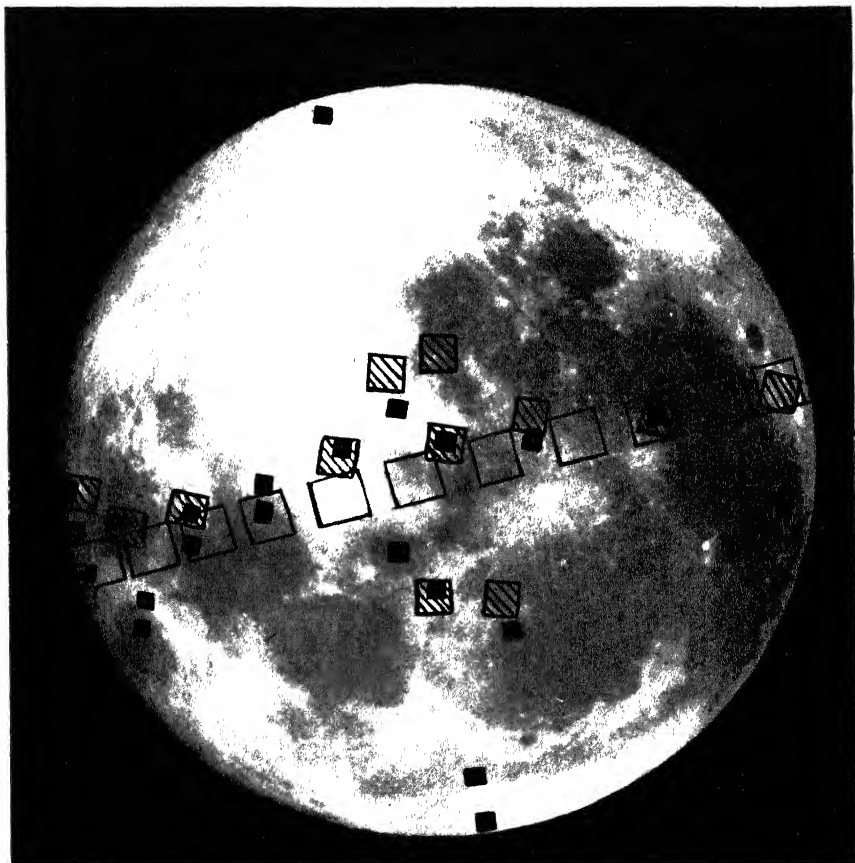


FIG. 1. Separate parts of the lunar surface the temperature of which has been measured.

- ▨ Chistyakov, Abastumani reflector
- Pettit
- Chistyakov, Moscow reflector

according to the measurements by Dollfus. The existing measurements, which are not numerous, but reliable, made by Dollfus in France and Kohan at Pulkovo (among them, measurements of granular minerals, powders and sands of various degrees of fineness), have indicated up to now that the outermost layer of the Moon is made of fine grains. However, the investigations conducted by Kohan in the U.S.S.R. on the rotation of the plane of polarization for thirty-five details of the Moon near full Moon—both

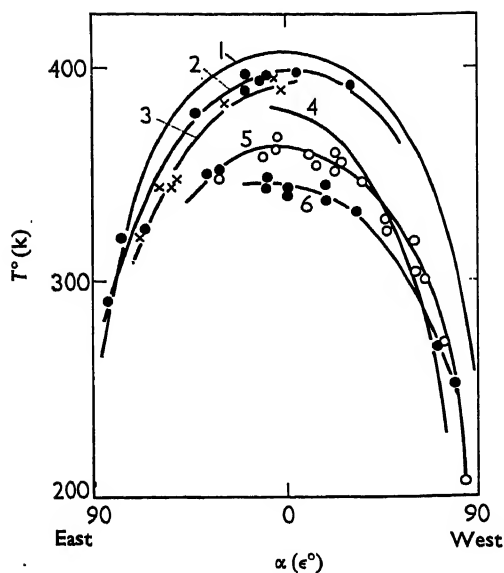


FIG. 2. Temperature distribution over the Moon at different phases  
Curves:

- |                 |                                 |                 |                             |
|-----------------|---------------------------------|-----------------|-----------------------------|
| 1 by Pettit     | $\alpha = 0^\circ$              | 4 by Sinton     | $\alpha = -57^\circ$        |
| 2 by Chistyakov | $\alpha = +17^\circ$ Abastumani | 5 by Chistyakov | $\alpha = -50^\circ$ Moscow |
| 3 by Chistyakov | $\alpha = +54^\circ$ Abastumani | 6 by Chistyakov | $\alpha = -60^\circ$ Moscow |

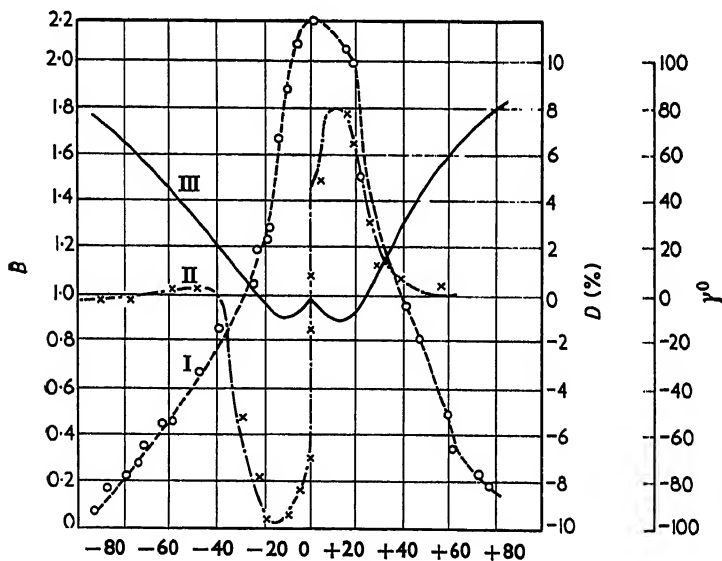


FIG. 3. Floor of Ptolemaeus. Measurements as a function of the phase  
Curve I Brightness  $B$   
Curve II Position angle of plane of polarization  $\gamma^\circ$   
Curve III Degree of polarization  $D$  (%)

in the centre and at the limb of the visible hemisphere—showed a new, unexpected, and very important peculiarity of the lunar surface. In analyzing, for example, the results of the study of the rotation of the plane of polarization for the floor of the crater Ptolemaeus (Fig. 3), the Mare Crisium, and the Sinus Iridum we noticed a gradual rotation of this plane. With the phase angle varying from  $-100^\circ$  to  $-40^\circ$ , the plane of polarization of the light reflected by all areas of the Moon remains perpendicular to the equator of intensity. When the phase angle approaches  $\alpha = -23^\circ$ , and the degree of polarization (which before had a positive sign) passes through zero, the plane of the polarization, rapidly turns around clockwise and forms an angle of the order of  $80^\circ$  with the equator of intensity  $\alpha = -23^\circ$ . With further decrease of the angle of intensity to  $-10^\circ$ , when the degree of polarization of the light reflected by the Moon reaches a maximum negative, the clockwise rotation of the plane of polarization to  $90^\circ$  ceases at the maximum value of its rotation in this direction. With a further decrease of the value of the phase angle within the limits  $-10^\circ < \alpha < -2^\circ$  the rotation of the plane of polarization suddenly reverts to counterclockwise, and moves so rapidly that at  $-2^\circ < \alpha < +2^\circ$  (when the degree of polarization again becomes zero) the prevailing fluctuations of the electrical vector of the light reflected by the Moon again become (just as in the case of  $\alpha < -40^\circ$ ) perpendicular to the plane of the equator of intensity. With further increase in the phase angle (within the limits of  $+2^\circ < \alpha < +10^\circ$ ) the counterclockwise rotation of the angle of polarization continues rapidly. Between the phase angles  $\pm 10^\circ < \alpha < +10^\circ$  the plane of polarization rotates through  $180^\circ$ .

With the value  $\alpha = +10^\circ$ , when the degree of polarization again becomes maximum negative ( $\sim -1.5$ ), the counterclockwise rotation of the plane of polarization stops when the fluctuations of the electrical vector of the reflected light again occur in the plane of the equator of intensity. Afterwards with further increase in the phase angle within the limits  $+10^\circ < \alpha < +40^\circ$ , the plane rapidly turns clockwise again, and at  $\alpha = +40^\circ$  coincides with the equator of intensity. After this, up to the time of the sunset (both in the centre and on the limb of the lunar disk), the position of the plane of the prevailing fluctuations remains the same, but the magnitude of the positive polarization increases.

A similar comparison of the rotation of the plane of polarization with the degree of polarization on one hand, and with the course of the change of the brightness of the details on the other ([1] page 5, 169) is being made for the first time at Pulkovo. It is interesting to note, in this connection, that the beginning and the end of the rapid rotation of the plane of polarization at the phases  $\sim -40^\circ$  and  $+40^\circ$  occur when the brightness of the detail is about half of its maximum brightness at full Moon, and the degree of polarization at the phases near to the full Moon passes through zero. The following fact is also very important and requires explanation: at the moment of full Moon, when there are no shadows on the Moon, and the sunlight penetrates into the deepest cracks, (1) the degree of polarization (for the second time in a lunation) becomes zero, (2) the plane of polarization rotates counterclockwise most rapidly and (3) the brightness of any detail, whether found in the centre or at the limb of the lunar disk, reaches maximum [9]. Further analysis should clear up the cause of the coincidence mentioned in the course of polarization variations and brightness of lunar formations. As yet it should be noted that the coincidence of a rapid rotation of the plane of

polarization with the moment of illumination by the Sun of all the depressions of the lunar surface is very important.

For the limb of the lunar disk, this illumination occurs at large angles between the direction of the incident sunlight and the vertical to the lunar surface; but at the centre of the Moon this illumination strikes the lunar surface vertically. One is, therefore, led to the conclusion that such phenomena can only occur with a porous, spongy microstructure type of surface layer—like the terrestrial pumice—and only with the directions of the outlets of these pores at all possible angles to the vertical. Therefore it may be necessary to reconsider the earlier conclusions [1] concerning a close agreement of the distribution of the negative polarization for the Moon and for the terrestrial powders, along the lines of analysis already initiated by van Diggelen [10].

The hypothesis proposed by the author, postulating depressions everywhere on the lunar surface, and the existence of a layer of dust not only on the floor but also on the walls (inclined at any angle to the vertical), is capable of harmonizing the Pulkovo polarization observations with the earlier conclusions of Dollfus regarding the increase of negative polarization with the pulverization of the powders. If, however, the existence of dust on steep walls of such depressions cannot be proved, one has to consider again the explanation proposed by Öhman [11] that the polarization of moonlight is caused by numerous reflections of light inside lunar pores. The Pulkovo polarization measurements should provide additional material for the verification of Öhman's hypothesis.

It is interesting also to note that analysis of all measurements of thermal radiation of the Moon and the heat conductivity of the outer layers of the lunar crust made with thermoelements and their comparison with the heat conductivity of Earth's powders in a vacuum of  $5 \times 10^{-4}$  (Smolukhovskiy) has until recently been interpreted to mean that the outer part of the crust can consist to the depth of about 15 mm of layers of grains with dimensions of the order of a millimetre and less. However, it is necessary to note that now, besides increasing the number of areas of the Moon with measured polarization and temperature characteristics, laboratory measurements of a great number of specimens of terrestrial rocks, especially of porous pumice and slags should be made. Temperature measurements in a vacuum of the order of  $10^{-8}$  atmosphere are desirable.

Thermoelectric measurements of the lunar surface are characterized by a semiamplitude  $C$  of the fluctuation of its temperature in the course of the lunar month and at the time of lunar eclipses. These quantities were computed for the lunar month by the formula  $F_0 = c(2\pi kPc/\tau)^{1/2}$ , where the thermal conductivity  $k$  is expressed in  $\text{cal cm}^{-2} \text{ min}^{-1}$  and  $\tau = 4.26 \cdot 10^4$  min.

Table 1 shows that the lunar surface cannot consist either of granite or of any small-grained powders. The observations would be better satisfied, for example, if the lunar surface were covered by a layer of quartz-sand with grains of the diameter of the order of 0.3 mm. We shall be able to determine whether the surface of the Moon is covered by pumice with a density of ore of the order of 0.6 to 0.2 only after having measured the conductivity of the latter in a vacuum, as, in the computations, the values of  $k$  for pumice are obtained from density.

It proved more successful to use the values of these heat conductivities

of pumices for checking, with Wessolink ([1], page 192) the theoretical values of the depth  $X$  (in centimetres) of that layer at which the periodical fluctuations of temperature in a homogeneous lunar surface layer are damped out. In accordance with the theory, we should have

$$\xi = \frac{X(\text{cm})}{(4\pi kT/C)^{1/2}} = \frac{X}{l}.$$

TABLE 1. Semiamplitude  $C$  of Variation of the Surface Temperature

		<i>Lunation, <math>F_0 = 0.017</math> Eclipse <math>F_0 = 0.08</math></i>				
<i>Object</i>	<i>State</i>	<i>(kpc)<sup>-1</sup></i>	<i>(<math>2\pi kPc/\tau</math>)<sup>1/2</sup></i>	<i>C</i>	<i>(<math>2\pi kPc/\tau</math>)<sup>1/2</sup></i>	<i>C</i>
<i>A. Laboratory measurements</i>						
Granite	monolith	20	$7.02 \times 10^{-4}$	$\pm 24^\circ$	$7.2 \times 10^{-3}$	$\pm 11^\circ$
Sand†	grain diam. $D = 0.3$ mm	III	$1.03 \times 10^{-4}$	$\pm 167^\circ$	$1.2 \times 10^{-3}$	$\pm 64^\circ$
Quartz	grain diam. $D = 0.1$ mm	189	$7.60 \times 10^{-5}$	$\pm 224^\circ$	$9.7 \times 10^{-4}$	$\pm 83^\circ$
<i>B. Observations of the Moon</i>						
Lunation	centre of disk	120	$1.00 \times 10^{-4}$	$\pm 170^\circ$	$1.2 \times 10^3$	$\pm 70^\circ$
Eclipse	1939	—	—	—	—	$\pm 95^\circ$
Eclipse	1927	—	—	—	—	$\pm 96^\circ$
<i>C. Computation of the effect of the density of the surface layer</i>						
Moon	$P = 2.0$	120	$1.00 \times 10^{-4}$	$\pm 170^\circ$	$1.2 \times 10^{-3}$	$\pm 70^\circ$
Pumice	$P = 0.6$	120	$1.00 \times 10^{-4}$	$\pm 170^\circ$	$1.2 \times 10^{-3}$	$\pm 70^\circ$
Pumice	$P = 0.2$	120	$1.00 \times 10^{-4}$	$\pm 170^\circ$	$1.2 \times 10^{-3}$	$\pm 70^\circ$

† By Smolukhovsky

By substituting for  $\tau$  and  $k$  the values from the preceding table we have:

TABLE 2.

Object	$k$ (in cal/cm <sup>2</sup> min <sup>-1</sup> )	$l$ (in cm)	Depth of the damping layer (in mm)
Real surface (Moon):	$1.7 \times 10^{-4}$	21.6	6.5–13.0
Pumice $\rho = 0.6$ :	$5.8 \times 10^{-4}$	40.0	12.0–24.0
Pumice $\rho = 0.2$ :	$1.7 \times 10^{-3}$	105.0	29.5–59.0
Granite $\rho = 2.0$	$6 \times 10^{-2}$	1210.0	363.0–726.0

Table 2 shows that, even for granite, Wessolink's formula for the depth of penetration of temperature variations leads to a depth of the order of several centimetres.

Recent radar observations of the Moon turned out to be very important.

They showed that more than half of the radar pulse is reflected to the Earth from the lunar region near the centre of the disk—or, to be more exact, from parts of the lunar surface not more than 54 km distance from the centre. It is interesting to note the analogy with the reflection of radar signals from a terrestrial desert. Since the experiments with radar echoes from the Moon were carried out on 10 cm, it can be assumed that such a mirror reflection of these waves from the lunar surface indicates an average dimension of the micro-relief of not more than 5 mm in diameter.

By generalizing what has been discussed so far we come to the following final conclusions about the probable structure of the lunar surface:

1. Gold's hypothesis about the presence on the Moon of layers of dust with a depth up to tens of metres is incorrect, especially in regions of the lunar ranges and planes with numerous cracks and faults.

2. In the regions of lunar mountain ranges outflows onto the surface of the original rocks can exist (Fremlin), and it is very important to check these now by all possible means.

3. The great variations of temperature on the surface of the Moon at the time of eclipses and at different phases, as well as the confirmed presence of some kinds of volcanic action in individual regions, point to the conclusion that in a number of regions of the Moon subjected to such changes (i.e. near its equator) small cracks with a width up to 1 m may be found.

4. In remaining regions of the Moon, and especially the zones of its surface investigated by polarization and thermoelectric measurements, the negative polarization and low thermal conductivity of the surface lead us to assume that the surface is covered with fine-grain material to a depth of not less than 4 cm.

5. If the meteor-slag hypothesis is valid, then the outer layer of lunar rocks is harder than a powder layer.

6. New conclusions about the structure of the upper layer of the lunar crust may be obtained from an investigation of the Moon with the aid of powerful telescopes by polarization, thermoelectric and radio methods, as well as by photographing it on a large scale and compiling new lunar atlases.

7. Considerable refinement of the conclusions on the structure of the upper layer of the lunar crust should come about by the use of some of these methods of investigation on installations operating outside of the Earth's atmosphere—artificial satellites and rockets.

#### REFERENCES

1. Markov, A. V. ed. "The Moon", monograph compendium. State Publishing Office of Physics and Mathematics Literature, Moscow (1960).
2. Fremlin, T. H. *Nature, Lond.* **183**, 1316 (1959).
3. Sinton, W. M. *Sky and Telesc.* **19**, 348 (1960).
4. Gold, T. *Mon. Not. R. astr. Soc.* **115**, 585 (1955).
5. Gilvarry, J. J. *Astrophys. J.* **127**, 751 (1958).
6. Firsoff, V. A. *J. Brit. astr. Ass.* **69**, 153 (1959).
7. Markov, A. V. and Barabashev, N. I. *Astr. Zhurn.* **11**, 55 (1925).
8. Markov, A. V. and Chistyakov, Yu. [N. *Mitt. russ. Hauptstern, Pulkowo*, **21**, 134, no. 163, 166 (1960).
9. Fedorets, V. A. *Ucheni Zap. Kharkov Univ.* **42**, 49 (1952).
10. Van Diggelen, T. *Rech. Astr. Utrecht*, **14**, 2 (1959).
11. Öhman, Y. *Ann. Obs. Stockholm.* **18**, no. 8 (1950).

# THE ROCKS THAT MAY CONSTITUTE THE LUNAR SURFACE

N. P. BARABASHEV

*Kharkov Astronomical Observatory, Kharkov, U.S.S.R.*

In investigating the lunar surface it is necessary to use all possible methods of observation, and draw conclusions on the basis of a simultaneous comparison of the results obtained by different methods. The comparison should be made statistically by making use of a sufficient number of specimens of the rock of each type. The comparison should be made in accordance with the following characteristics and parameters: (a) the light or brightness factor; (b) the law of reflection; (c) the smoothness factor; (d) the spectral distribution of reflectivity; (e) the degree of polarization in dependence on the angle of incidence, reflection and phase in the different spectral regions; (f) heat conductivity; and (g) luminescence. At the Kharkov Astronomical Observatory such a research has basically been completed [1].



FIGURE 1.

The law of reflection was studied with the aid of a photoelectric photometer. The results of the measurements were presented in the form of indices of reflection, and also by the dependence of the brightness on the angle of incidence  $i$  at  $i = \epsilon$  for the case of the incident and reflected ray on the same side of the normal ( $\alpha = 0^\circ$ ), as well as for the case when the



rays lie on different sides of the normal. The factor of smoothness was also computed from these data. Not only different specimens of rock were subjected to such measurements, but also specially prepared models, namely: cylindrical pockets, conical and hemispherical pockets, vertical cracks with different ratios of depth and diameter and different degrees of porosity, and also specimens consisting of irregularly arranged sharp-edged fragments of broken-up tuffs with different dimensions of the grain from 0.1 mm to 10 mm, as well as volcanic slag and volcanic ashes.

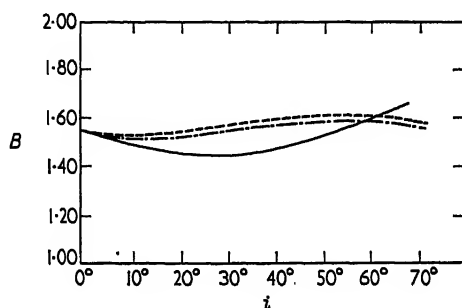


FIG. 2. — Moon (continent)  $i = \epsilon$ ,  
 --- specimen no. 28  $\alpha = 0^\circ$   
 - · - specimen no. 29

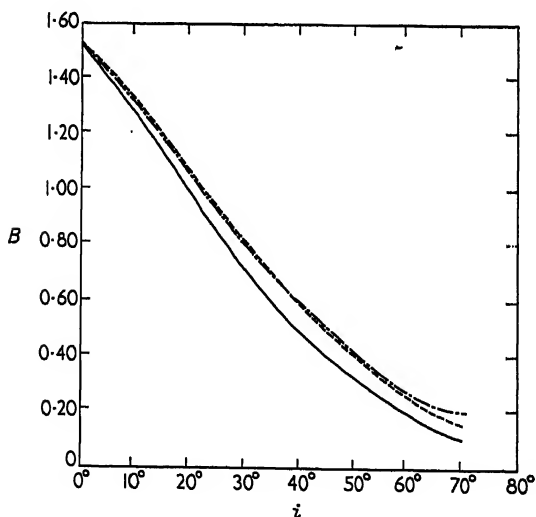


FIG. 3. — Moon (continent)  $i = \epsilon$   
 --- specimen no. 28  $i + \epsilon = \alpha$   
 - · - specimen no. 29

The indices of reflection of lunar continents and maria were determined from data of Fedorets' catalogue [3]. Good agreement resulted from a comparison of the fragmented tuffs with grains with dimensions of 2—3, 3—4, and 4—6 mm. This is well illustrated by Tables 1 and 2 which are given below and by Figs. 2 and 3.

In the case of the broken-up volcanic slag with grain size of 2 to 3 mm,

the course of the dependence of the brightness on  $i = \epsilon$  at  $\alpha = 0^\circ$  agrees poorly with the corresponding data for the Moon, which is possibly due to some specular effects in the volcanic slag.

TABLE 1

$i = \epsilon$	<i>On one side</i>		<i>On different sides</i>	
	<i>Mare</i>	<i>Tuff with grain 2—3 mm</i>	<i>Mare</i>	<i>Tuff with grain 2—3 mm</i>
0°	1.00	1.00	1.00	1.00
10	0.99	1.02	0.75	0.91
20	0.99	1.00	0.57	0.72
30	1.02	0.96	0.43	0.56
40	0.99	0.90	0.31	0.40
50	0.98	0.91	0.21	0.27
60	0.97	—	0.15	0.17
70	0.88	—	0.12	0.09

TABLE 2

$i = \epsilon$	<i>On one side</i>		<i>On different sides</i>	
	<i>Continent</i>	<i>Tuff with grain 6 mm</i>	<i>Continent</i>	<i>Tuff with grain 6 mm</i>
0°	1.56	1.56	1.56	1.56
10	1.50	1.51	1.27	1.36
20	1.47	1.33	1.00	1.03
30	1.40	1.54	0.65	0.80
40	1.47	1.56	0.53	0.58
50	1.51	1.56	0.35	0.44
60	1.55	1.56	0.21	0.28
70	1.62	—	0.12	0.22

The broken-up tuffs match up both for the "maria" and the "continents". Although volcanic ashes do not show as good an agreement as the tuffs, they correspond better to the maria than to the continents. Volcanic slag matches better for the continents, although it does not agree in polarization and spectrophotometric characteristics. Fine sand and dust do not correspond to the "continents" nor to the "maria". From this it follows that great areas of the lunar surface cannot be covered by fine dust or by fused rock. For all the remaining rocks investigated and also for the specimens having a regular geometrical form, sufficiently close correspondence with the lunar data was not found.

In examining the data on the law of reflection of light, one has to conclude that the lunar surface corresponds best to broken-up tuff with sharp-edged irregularities and grains with sizes from 2 to 5 mm.

Spectrophotometric measurements of 220 specimens of volcanic rock were made in the interval between 4000 Å and 7500 Å with the spectrophotometer SF-2 m, which was put at our disposal by the Institute of Geological Sciences of the Academy of Sciences of the Armenian SSR.

In plotting the data obtained on the colour-brightness diagram, it was

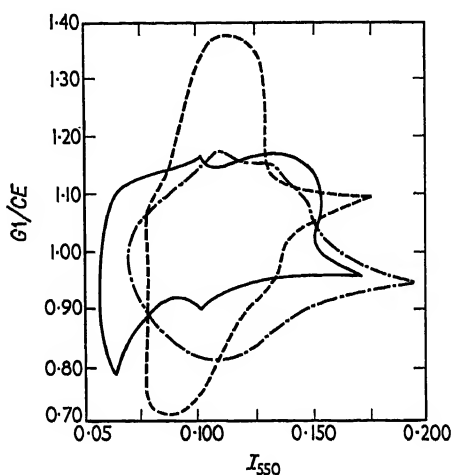


FIG. 4. ——— Lunar area  
 - - - - - Volcanic tuff  
 - · - · - Volcanic slag

found that into the area occupied by the lunar data (according to data of Sytinskaya) there fall:

1. Volcanic slags	60%	of the specimens measured		
2. Volcanic tuffs	60%	" "	" "	" "
3. Andesite-basalt lavas	17%	" "	" "	" "
4. Lava from intermediate rocks	25%	" "	" "	" "
5. Acid magmatic rocks	15%	" "	" "	" "

Values of the gradient

$$\Gamma = \frac{\Delta CI}{\Delta \lg T_{\lambda 550}}$$

were determined for different types of volcanic rocks:

Volcanic tuff	$1.12 \pm 0.2$
Volcanic slag	$1.6 \pm 0.4$
Felsite tuff	$0.70 \pm 0.2$
Tufolava	$0.42 \pm 0.1$

These data are in good agreement with corresponding measurements for the lunar surface, given in [4] and [5].

Volcanic rocks show the same tendency as separate lunar regions: the colour index increases with the brightness. Besides, a comparison was made of the curves of the spectral reflectivity in the interval 4000—6200 Å. For many specimens, and especially for tuffs and tufo-lavas, the laboratory data proved to be sufficiently close to that for the spectral reflectivity of separate areas of the lunar surface. In polarimetric measurements with the

aid of photoelectric equipment, the degree of polarization was determined in dependence on the phase angle, the angles of incidence and reflection in different spectral regions and also on the state of the surface [1].

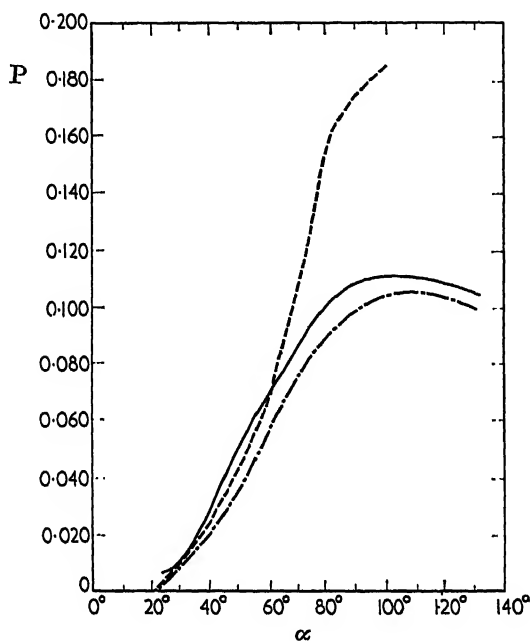


FIG. 5. ——— Mare Crisium  
 - - - - - Uncrushed tuff  
 - · - · - Crushed tuff

Some specimens of tuffs show good agreement with the lunar surface according to these characteristics. The following table contains the values of polarization as a function of the phase angle for one of the samples of the tuffs, in a solid and also crushed pulverized state.

In this, as in other cases, the breaking up of the tuffs into grains of 2 to 4 mm in size results in a noticeable decrease in the degree of polarization, i.e. a closer approach to the data for the lunar surface.

Similarly, the effect on the degree of polarization and other optical characteristics was examined, as well as the effect of its radiation by ultraviolet and X-rays. In this case the degree of polarization and brightness changes insignificantly.

As a result of bombarding the specimens by beams of protons (energy 2.1 Mev) in a vacuum the degree of polarization increased, and the colour index and brightness decreased.

Specimens were fused in a vacuum ( $10^{-4}$  mm of Hg) and under atmospheric pressure at a temperature of the order of  $1200^{\circ}$  C. Measurements of the fused specimens showed that the degree of polarization increases very greatly, considerably exceeding that obtained for the lunar surface. There is also a decrease in the value of the colour index and brightness, and the

intensity distribution in the spectrum is considerably more frequency-independent.

TABLE 3

$\alpha$	<i>Mare Crisium</i> $\rho$	<i>Unbroken tuff</i> $\rho$	<i>Crushed tuff</i> $\rho$
130°	0.103	—	0.095
120	0.107	0.200	0.096
110	0.109	0.192	0.105
* 100	0.109	0.184	0.101
* 90	0.106	0.174	0.091
80	0.100	0.165	0.088
70	0.083	0.095	0.078
60	0.069	0.050	0.045
50	0.052	0.048	0.035
40	0.031	0.039	0.030
30	0.010	0.021	0.020
20	0.006	0.000	0.000

In the case of the fused and then pulverized specimens of tuffs, the degree of polarization continues to be large and noticeably exceeds that of the surface of the Moon. All these data are evidence against the presence of large slag-like and fused material on the Moon.

The values for the density of the specimens were determined. For the tuffs in an uncrushed state these values are within the limits 1.00 and 1.70. For the investigation of pulverized specimens the density was found to be less by a factor of 2 to 3, i.e. 0.4 to 0.8, which corresponds to the latest data for the surface of the Moon from radio-astronomical observations.

On the basis of all the results of investigations presented in this paper the following conclusions can be made. The surface of the Moon is covered, in all probability, by tuff-like rocks in a very broken-up state, with the grain ranging in size from 3 to 10 mm. The surface of the Moon cannot be covered by very fine powder or fine dust, as substances in the form of powder or dust with very fine grains cannot match the observed properties of reflection of light from the surface of the Moon. For substances in the form of dust with grains of the size of 0.06 mm the law of reflection is close to Lambert's law.

According to the character of light reflection, surfaces covered by sharp-edged fragments and rectilinear grooves with vertical and tapered walls correspond best to the lunar surface.

## REFERENCES

1. Barabashev, N. P. and Chekirda, A. T. *Astr. Zhurn.* 36, 851 (1959); *Izv. planet. com.* no. 1 (1960).
2. Barabashev, N. P. and Garazha, V. I. *Circ. astron. Obs. Kharkov Univ.* no. 21 (1960).
3. Fedorets, V. A. *Trans. astron. Obs. Kharkov Univ.* no. 2 (1952).
4. Barabashev, N. P., Ezersky, V. I. and Ezerskaya, V. A. *Astr. Zhurn.* 36, 496 (1959).
5. Teyfel, V. G. *Astr. Zhurn.* 36, 114, 1041 (1959).

# MICRORELIEF OF THE LUNAR SURFACE AND THE PROBABLE WAYS OF ITS FORMATION

V. V. SHARONOV

*Leningrad State University, Leningrad, U.S.S.R.*

ALREADY in the seventeenth century Galileo Galilei [1] had turned his attention to the peculiarity of the reflection of light from the lunar surface, which consisted of the fact that the disk of the full Moon exhibits no darkening towards the limb. Galilei explained this by assuming that, besides the mountainous macrolief on the Moon, which could be observed in the telescope, there existed an ubiquitous microrelief pointing to a very rough structure of the lunar surface. Modern photometric observations have fully confirmed this conclusion and have enabled us to unravel many peculiarities of this microrelief—in particular, the rather unique law of reflection from the lunar surface, expressed by a reflection diagram very elongated in the direction of the Sun. The comparison with the laboratory measurements carried out by Orlova [2] showed that the elements of this relief should possess vertical, or very steep, walls and sharp broken-off edges reminding one by their structure of laced volcanic slags and lapilli. At the same time the dimensions of these irregularities are found to be small—of the order of millimetres or centimetres [3].

A remarkable feature of the lunar surface consists in the uniformity of this cover. Notwithstanding the fact that visual observations of the Moon have been made for over 300 years, and photometric measurements for more than 50 years, no single, even a small, horizontal area or object has so far been discovered on the Moon for which the contrast of brightness, in comparison with the surrounding background, changes perceptibly with the phase. This shows that the character of the microrelief is uniform over the whole visible surface of the lunar sphere, independently of the morphological structure and albedo of the different objects.

A study of the first photographs of the reverse side of the Moon in 1959, taken from the automatic interplanetary station launched in the U.S.S.R., showed that on the images of the lunar disk, darkening towards the limb for the greater part of the lunar circumference is absent; and where it is noted it should apparently be attributed to purely instrumental effects. This allows one to conclude—of course, for the time being only tentatively—that on the reverse side of the Moon the visible surface has a microrelief completely analogous to that which is so characteristic of the side turned toward the Earth.

Another feature which indicates the uniformity of the outer cover on the Moon is the very small differences in colour. According to the data of the new colorimetric catalogue of lunar objects, based on visual colorimetric observations conducted by me at the Tashkent Astronomical Observatory [6], the extreme differences in the colour index, including errors in measurement, do not exceed 0.11. The average value for the colour, expressed by the difference  $D$  of the colour indices of the Moon and Sun,

amount to 0.35. The continents and in general the bright parts are on the average a little redder than the maria, which can be seen from the figures given in Table 1. The dispersion of the colour for the maria and other dark objects was found to be somewhat larger than for the bright parts. However, a careful and repeated study of the disk of the full Moon, conducted under great magnification with the aid of refractors and reflectors, did not reveal a single, even small, object whose colour appreciably differed from that of the background.

TABLE 1

<i>Type of object or material</i>	<i>r</i>			<i>D</i>		
	Aver.	Extreme		Aver.	Extreme	
Moon, maria and floors of dark cirques	0.065	0.05	0.08	+0.339	+0.29	+0.40
Moon, pali	0.091	0.09	0.10	+0.349	+0.31	+0.37
Moon, continents and floors of craters with normal colouring	0.105	0.08	0.12	+0.347	+0.31	+0.38
Bright rays and craters with bright floors	0.140	0.10	0.18	+0.352	+0.31	+0.39
All parts of Moon together	0.090	0.05	0.18	+0.344	+0.29	+0.40
Volcanic slag, scoriae	0.060	0.02	0.14	+0.11	-0.13	+1.28
Volcanic tuff	0.193	0.06	0.43	+0.29	-0.15	+1.10
Pumice	0.354	0.13	0.55	+0.43	+0.05	+0.81
Dunite, peridotite	0.104	0.06	0.16	-0.01	-0.17	+0.25
Gabbro, norite	0.155	0.08	0.21	-0.04	-0.17	+0.12
Basalt	0.133	0.06	0.28	-0.05	-0.31	+0.15
Diabase	0.151	0.11	0.19	-0.02	-0.19	+0.13
Andesite	0.139	0.08	0.31	-0.02	-0.12	+0.10
Granite	0.244	0.04	0.70	+0.39	-0.09	+1.23
Metamorphic rocks	0.281	0.08	0.78	+0.26	-0.25	+0.99
Clays and schist	0.251	0.12	0.50	+0.33	-0.24	+1.53
Sand	0.240	0.10	0.40	+0.49	+0.06	+1.22
Sandstone	0.222	0.06	0.54	+0.66	+0.03	+1.54
Limonite, ortstein	0.131	0.05	0.35	+0.69	0.00	+1.24
Limestone, marl	0.325	0.06	0.80	+0.38	-0.13	+1.52
Stone meteorites	0.183	0.04	0.48	+0.10	-0.16	+0.36
Fusion crust of meteorites	0.052	0.02	0.17	+0.11	-0.10	+0.38

The differences in albedo on the Moon, although they are considerable (up to 3:1), amount to less than one-tenth of the differences in the albedo of terrestrial rocks (up to 50:1). Data available at the present time on the heat conductivity of the outer layer of the lunar surface obtained from thermoelectric and radio astronomical observations also furnish evidence in favour of the uniformity of this cover.

In order to identify the nature of the visible surface of the Moon wide

use is made of the empirical comparison of values for different optical parameters—such as, for example, albedo, colour, and polarization for lunar objects and for terrestrial rocks. However, this method is based on the assumption that the same colouring is characteristic for materials on the Earth and the Moon which are alike in mineralogical and petrographic composition. This is likely, but still far from certain. Besides, we can identify rocks on the Moon by comparison of their colour with terrestrial samples only in the case when we see on the Moon an exposed and completely fresh surface of those rocks of which the upper layers of the lunar crust consists. A very insignificant amount of contamination of extraneous origin or an insignificant change in the texture of the surface rocks themselves is sufficient to change the colour and make the substance unrecognizable for us.

Furthermore, in order that the results of such a comparison should be meaningful it is necessary to observe certain conditions. For example, the comparison of data for the Moon, which always represents averages for large areas of the surface, with individual samples of rocks of such a size as can be found in museums and collections, cannot give a satisfactory result. The fact is that there is a great variety in the colour of the minerals and the rocks; therefore, from rocks of any origin it may always be possible to select an individual sample which matches in colour the area of the Moon's surface being studied. In order to compare the terrestrial data with the observations of the Moon, it is necessary to use the statistical method and measure the necessary parameters for a great number of specimens of each kind of rock from which average values can be formed. In doing so it is very important to select specimens in such a way that the average values obtained will really be characteristic of the average colour which a broad area covered with a given kind of rock and observed from a great distance would have.

I wish also to mention that, in order to obtain reliable results, it is not sufficient to make a comparison of only one optical characteristic. To illustrate this I will cite an example. If we confine our attention only to the albedo, then a hypothesis could be maintained that the surface of the continents consists of ultrabasic magmatic rocks, and the surface of the maria is covered with volcanic slag. But if we invoke also the colorimetric data, the similarity disappears, inasmuch as the two types of rocks just mentioned do not have the reddish, or rather gray-brown, shade which characterizes the colour index of the Moon. There is also no agreement in the characteristics of heat conductivity, especially with regard to magmatic rocks.

A great deal of work on the comparison of the Moon with photometric and colorimetric observations of rocks has been accomplished in the course of a number of years at the Astronomical Observatory of the Leningrad University. There we studied more than 100 areas of the lunar surface and some thousands of the specimens of rock. The technique for the use of such material can vary. The simplest way is to compare the average and the extreme values, as was done in Table 1, where the albedo is expressed in the form of the brightness factor  $r$ , i.e. the ratio of the brightness of a given object to the brightness of an absolutely white surface under analogous conditions of illumination; and the colour, as before, is presented in the form of a colour excess  $D = C_0 - C_C$ . Here  $C_0$  is the colour index of a given



object under illumination by natural or artificial solar light (system of E. S. King), and  $C_{\odot}$  is the colour index of the Sun. It is evident that for a gray, i.e. a neutral-reflecting surface,  $D = 0$ ; for substances which have a blue or bluish colour,  $D$  will be negative; but for yellow, brownish, and reddish materials it will be positive. In our investigation of the colour of minerals and rocks we met with extreme values for  $D$  ranging from  $-1.0$  (colourful samples of lazurite) to  $+2.0$  (saturated-red limestone).

Another method consists in obtaining the distribution curves of specimens of each kind of rock according to the values of  $r$  and  $D$  [4]. An example of such curves for the Moon, granite and magmatic rock of basic and ultrabasic composition is presented in Fig. 1. Still another method consists in the

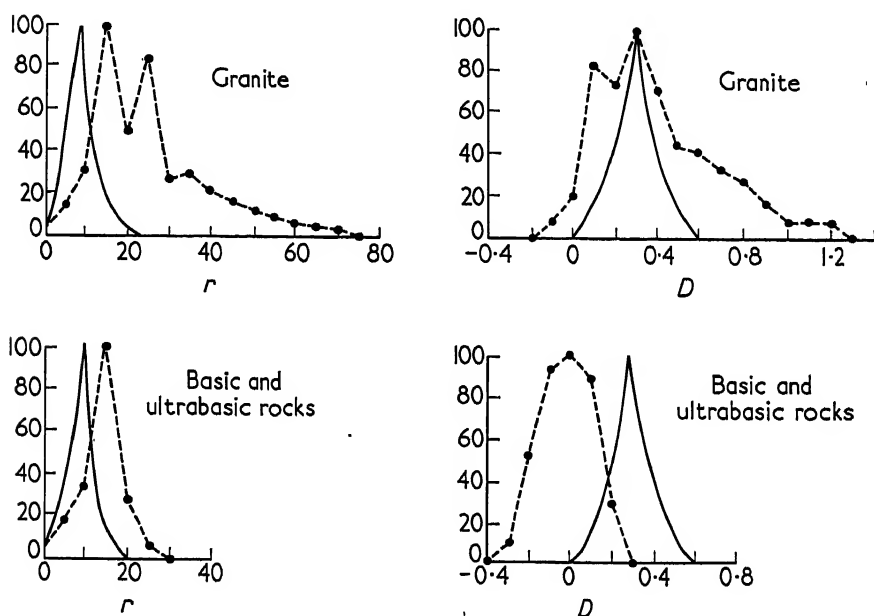


FIG. 1. Curves of the distribution of specimens according to albedo and colour excess  $D$ . At the top for granite; at the bottom for basic and ultrabasic rocks. Data for rocks—dotted line; for lunar objects—solid line.

construction of albedo-colour diagrams on which along one axis we plot the values of  $r$  and along the other those of  $D$ , defining a point for each specimen [5]. On Fig. 2 we plotted the points for granite and rocks of basic and ultrabasic composition. The points for lunar objects are not plotted, but the area occupied by them is marked off by a closed line.

The results of all these comparisons lead to the conclusion that no kinds of terrestrial rock (including meteorites) correspond to the lunar surface in reflectivity and colour. The basic difference consists in the fact that all the rocks investigated are on the average brighter than the Moon. An exception to this is special material, rarely met on the Earth, such as volcanic slag and the fusion crust of meteorites. Therefore, no combinations or mixtures of rocks will give an average albedo identical with that obtained for the Moon. Besides, nearly all terrestrial rocks exhibit very considerable dispersion

in albedo, and, especially, in colour—which is not the case on the lunar disk.

Thus, from the point of view of the optical properties, the lunar surface exhibits three characteristic peculiarities that distinguish it from all terrestrial rocks: namely, extremely low albedo, an almost identical colour, and a reflection diagram very elongated in the direction of the source of light. These peculiarities of the colour and structure of the substance which

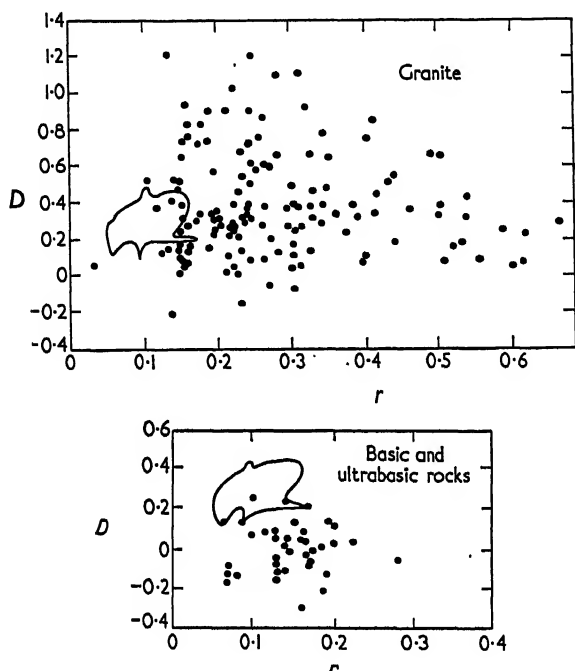


FIG. 2. Albedo-colour diagrams (by Sytinskaya). Above, for granite. Below, for basic and ultrabasic igneous rock. Area occupied by the points for lunar objects surrounded by solid line. (The points themselves are not shown in order to avoid overcrowding of the drawing.)

forms the outer layer of the surface of the Moon observed by us can be explained in various ways. The best explanation appears to be that those rocks which make up the outer layers of the lunar globe are always hidden from our view by a crust or film of subsequent origin—just as, on the Earth, the original rocks are usually covered by the products of weathering and soil. This crust originated under conditions on the Moon which are quite different from those which we have on the Earth. It should then be only natural that among terrestrial rocks we are unable to find anything similar to the surface layer on the Moon—particularly as far as the albedo, colour, and structure of the surface are concerned.

If our assumption is correct, then the usefulness of further investigation of the nature of the Moon's surface by such simple methods as photometry and colorimetry naturally becomes very limited. Nevertheless, we can draw certain conclusions about the formation of the dark porous crust overlying

the lunar surface. First of all we should distinguish between the endogenous and exogenous factors. On the Moon, due to the absence of atmospheric pressure and smaller force of gravity many processes—and, in particular, the hardening of the lava flows and the formation of vesicular structure on their surface—will proceed otherwise than on the Earth. Therefore, the surface of the rocks of volcanic origin can acquire a special structure at their formation. However, it appears more plausible that the outer covering of the Moon, characterized by its uniformity, was produced by external and not by internal forces; for it is just the external (and particularly, cosmic) influences which should have a uniform effect on all parts of the surface of the lunar globe. Often the impacts of meteoric bodies are indicated as being the basic factor in the formation of the surface crust on the Moon, as is assumed by the meteor-slag theory expounded in the report by Sytinskaya. A considerable effect may also be produced by different forms of radiation.

Further progress in the solution of the problem of the nature and origin of the lunar surface and of its characteristic microrelief by means of ground-based observations can come only from the use of new methods of research, and from a close collaboration between astronomers and geologists.

#### REFERENCES

1. Galileo Galilei, "Dialogue about Two of the Great Systems of the World—Ptolemaic and Copernican", Florence, 1632; English translation by S. Drake, Univ. of California Press (1953); or by G. de Santillana, Univ. of Chicago Press (1953).
2. Orlova, N. S. Comparison of the law of reflection of light for the Moon and certain kinds of rocks, *Vestnik Leningr. Univ.* **12**, 152–157 (1957).
3. Sytinskaya, N. N. Probable dimensions of the elements of the microrelief of the lunar surface, *Izv. com fizik. planet*, no. 1, 81–84 (1959).
4. Sharonov, V. V. Experimental petrographic investigation of lunar surface by combined application of photometric and colorimetric observations, *Astr. Zhurn.*, **31**, 442–552 (1954).
5. Sytinskaya, N. N. Origin and nature of the outer covering of the lunar surface according to data of comparative study of the albedo-colour diagrams, *Ucheni. Zap. Leningr. Univ.* **190**, 74–87 (1957).
6. Sharonov, V. V. A visual-colorimetric study of the lunar surface, *Astr. Zhurn.* **39**, 87–92 (1962).

# METEOR-SLAG THEORY OF THE LUNAR SURFACE

N. N. SYTINSKAYA

*Leningrad State University, Leningrad, U.S.S.R.*

In my communication I am confronted with the task of applying the results of photometric, colorimetric and thermal investigations of the Moon for certain conclusions regarding the nature and origin of the outer layer of the lunar surface. The considerations which I am to share with you in the present chapters have already been published by me under the title "Meteoric-Slag Theory of the Lunar Surface". This theory had to be developed and supplemented as results of new observations, measurements and theoretical calculations were obtained [2].

During the past 25-30 years in the U.S.S.R. many investigations were carried out for studying the albedo, colour, changes in brightness with directions of incident and reflected rays and other optical characteristics of the lunar surface. The results are briefly as follows. The lunar surface has everywhere a relatively uniform, very dark grayish-brown shade of colour. The differences in albedo are noticeable, but they are small and vary within the limits of 1:3,4. Still smaller are the differences in colour, which do not exceed the differences in colour index of 0.1-0.2. No kind of terrestrial rock in its mean colour has a sufficient resemblance to the lunar surface [3], [4]. The reflection of solar rays from regions of the lunar surface (which when seen in a telescope appear to be perfectly smooth) gives a reflection diagram for all angles of incidence sharply elongated toward the Sun. This proves that the Moon has a microrelief which is characterized by a high degree of fragmentation and steep, almost perpendicular, slopes [5].

The problem of the scale of this relief is interesting. Results of radar investigations of the Moon, carried out in various parts of the world, show that the lunar surface reflects radio waves in an entirely different manner than the light rays—namely, in an almost specular manner. It follows that the structure of the microrelief is considerably smaller than the wavelength of the radiation, which was used for radar observations. Thus the dimensions of the microrelief elements are definitely smaller than a meter, and it is most probable that they range within limits of one millimetre to several centimetres [6].

Of great importance for solving the problem concerning the nature of the lunar surface are the results of thermoelectric observations of the thermal radiation of the Moon itself during lunar eclipses and during a month. The extremely low values of heat conductivity obtained from such observations indicate that the outer layer of the lunar surface has a highly porous, vesicular structure [7].

From what has been said concerning the properties of the lunar surface layer we conclude that:

- (a) it cannot be a massive rock formation, nor magmatic, or sedimentary, because its heat conductivity properties would have to be different;
- (b) it cannot be mixed in composition, i.e. represent an alternation of

rocks with porous material; for in this case, in order to obtain the average values, corresponding to observational data, it would be necessary to assume unacceptably low values of heat conductivity for the porous fraction;

(c) it cannot consist of loose substances such as sand, gravel, or dust because such a substance, due to its limited slope angle, cannot have a surface with such steep irregularities which would give an indicatrix of reflection in agreement with that observed;

(d) it cannot be a surface consisting entirely of material brought from outside (of meteorites, cosmic dust) because continuous cover of this type would smooth out all differences of albedo.

Consequently, the positive properties of the lunar surface layer must be such that:

(a) it should consist of an extremely porous, vesicular material, because only such a material will possess properties compatible with observations of its heat conductivity;

(b) it should consist of loose, sufficiently coherent material, which could give sharp-rough structure and adhere to the steepest slopes;

(c) it should have originated in such a manner that its reflectivity is determined by the mineralogical or petrographic composition of rocks situated in the given region.

Terrestrial black volcanic slags show the best agreement with the above-enumerated properties. They are formed preferably on the surface of lava streams and represent congealed lava foam. From here we have borrowed the expression "slag" to be applied to the porous cover assumed to exist on the Moon.

At the present time, a majority of lunar investigators tend toward the view that the visible outer layer of the lunar surface represents the result of the treatment of basic parent rocks of the lunar crust by external factors. Several such factors have been mentioned, but the effective and most active undoubtedly are the impacts of meteorites and micrometeorites, accompanied by explosion phenomena. The latest results on the frequency of micrometeorites, obtained with the aid of artificial Earth satellites and cosmic rockets, show that the bombardment by micrometeorites is so intense (up to one impact per square centimetre per minute), that it can within a very short time change the structure of the outer layer of any region of the lunar surface.

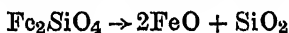
A comparison of the kinetic energy of motion of a meteoritic body with the heat absorbed in evaporation shows that the amount of this energy exceeds by far the quantity necessary for complete evaporation of the meteorite itself. It is highly probable that a considerable fraction of the surplus energy, liberated during the impact of a meteoric particle, is used for the conversion of the material of the lunar surface in the zone of impact into vapour. As is indicated by the calculations of Stanyukovich and Fedynsky [8] the mass of the matter of the lunar surface transformed into vapour may by hundreds and even thousands of times exceed the mass of the meteorite. The investigations by Gilvarry and Hill [9] lead to a conclusion that the temperature in the zone of explosion can be very high. Depending upon the velocity acquired during explosion, a fraction of the vapour molecules may escape from the Moon entirely, another is scattered over the whole surface of the Moon and the third precipitates in the zone of the explosion. To study the velocity distribution of molecules is a very difficult task. A complete solution of this problem is not yet available.

The meteoric-slag theory of the origin of the surface layer is based on the assumption that a sufficiently large part of the evaporating material condenses and precipitates near the place of explosion, forming a crust which consists of vesicular mass, with cavities separated by very thin walls. From the outside such a layer will show a spongy cellular structure. Light slags, lapilli and other products of volcanic eruptions may serve as a certain—possibly quite remote—analogy of such a structure. According to its low value of heat conductivity in vacuum and reflection diagram for the solar rays falling on it, such a matter may well be consistent with the observations of the lunar surface.

In addition, the high temperature of the explosion should lead to various chemical changes, so that the layer formed as a result may differ considerably in its mineralogical and chemical composition from the rock from which it originated.

A characteristic feature of details of the lunar surface is their low albedo, the values of which vary between 0.05–0.18 and on the average, amount to 0.07. A comparison of lunar data with the results of investigations of the terrestrial samples shows that the average albedos of all kinds of terrestrial rocks are higher than those of the surface of the Moon. The exceptions here are such formations as volcanic slag (mean albedo of 0.06) and the fusion crust of meteorites (mean albedo of 0.05). Consequently, any theory describing the structure and origin of the outer layer of the lunar surface should account for its dark colour.

The meteor-slag theory permits us to explain the low reflectivity in the following manner. Experiments show that many kinds of terrestrial magmatic rocks and a majority of meteorites acquire dark or even black colour under the influence of high temperature. After fusion in the flame of an electric arc, samples of meteorites and rocks ordinarily acquire black colour. The black colour is characteristic also for the fusion crust of meteorites. According to investigations by Yudin [10] it originates because of the presence of magno-magnetite, a mineral of the composition  $(\text{Fe}, \text{Mg})\text{O} \cdot \text{Fe}_2\text{O}_3$ , and forms during the decomposition of silicates of the olivine type. It is true that the fusion crust of the meteorites originates under conditions of the oxygen-rich terrestrial atmosphere. On the Moon, the dark colour may originate by the formation of ferric oxides due to the oxygen contained in the silicates, as for example takes place during the decomposition of the mineral fayalite:



The mineral ilcrite, which is natural ferrous oxide (i.e. corresponding to the composition  $\text{FeO}$ ), according to investigations by Yudin also takes part in the creation of the black colour of the fusion crust of meteorites. Under conditions prevailing on the lunar surface, at complex temperature and pressure distribution in the zone of the explosion, the origin of other ferric oxides, such as  $\text{Fe}_3\text{O}_4$  and  $\text{Fe}_2\text{O}_3$ , is quite probable. The reddish colour characteristic for the latter would correspond to the actual colour of the Moon. Furthermore, one cannot completely rule out the origin, on the Moon, of reddish ferric hydroxides of the type  $\text{Fe}(\text{OH})_3$  by the action of water included in the composition of silicates of the lunar surface, due to the formation of  $\text{H}_2\text{O}$  molecules by combining hydrogen ions of solar origin with oxygen atoms liberated during meteoric explosions, or as result of "icy" meteoric bodies falling on the Moon.

An opinion was expressed many times that lunar continents are formed by less heavy acidic magmatic rocks, while the maria consist of heavier basic rocks. Our hypothesis is in general agreement with this view. We recognize the fact that the albedo of the slaggy material should be the lower, the greater the content of ferric or ferrous oxide compounds in the initial (parent) basic rock. But, as is known, with the transition to basic and ultrabasic rocks the FeO content increases. This is why there is little likelihood that the lunar continents are formed by acidic rocks of the granite type, because rocks of this group (in view of the insignificant amount of FeO) acquire a light colour when fused in an arc flame. It can be assumed that the slaggy surface of the maria is made up predominantly of ultrabasic rocks, and of the continents by basic rocks, which determines the differences in albedo of the vesicular layer which originate as a result of meteoric bombardment.

In an analogous manner we can explain the dark surface colour also of other bodies of the solar system, which are devoid of atmosphere—as, for example, Mercury or the satellite IV of Jupiter. As can be judged by the available data, the meteor-slag theory of the structure and origin of the outer layer of the lunar surface is in agreement with all the facts known at the present time.

#### REFERENCES

1. Sytinskaya, N. N. Explosions of meteorites as a factor changing the surface of the Moon. *Vopr. Kosmogonii* 5, 13–18 (1957).
2. Sytinskaya, N. N. New data on meteor-slag theory of formation of the outer layer of the lunar surface. *Astr. Zhurn.* 36, 315–320 (1959).
3. Sharonov, V. V. Experimental petrographic investigation of lunar surface by combined application of photometric and colorimetric observations. *Astr. Zhurn.* 31, 442–552 (1954).
4. Sytinskaya, N. N. Origins and nature of the outer covering of the lunar surface according to data of comparative study of the albedo-colour diagram. *Uchen. Zap. Leningrad Univ.* 190, 74–87 (1957).
5. Orlova, N. S. Photometric relief of the lunar surface, *Astr. Zhurn.* 33, 93–100 (1956).
6. Sytinskaya, N. N. Probable dimensions of the elements of the microrrelief of the lunar surface. *Izv. Com. Fiz. Planet* no. 1, 81–84 (1959).
7. Jaeger, J. The surface temperature of the Moon. *Aust. J. Physics* 6, 10 (1953).
8. Stanyukovich, K. P. and Fedynsky, V. V. The destructive effect of meteoric impacts. *C.R. Acad. Sci. U.R.S.S.* 57, 129–132 (1947).
9. Gilvarry, J. J. and Hill, J. E. The impact of large meteorites. *Astrophys. J.* 124, 610 (1956).
10. Yudin, I. A. Non-transparent minerals of stony meteorites. *Meteoritika* 16, 78 (1958).

# ON THE PHOTOMETRIC HOMOGENEITY OF THE LUNAR SURFACE

N. P. BARABASHEV, V. I. EZERSKY

*Kharkov Astronomical Observatory, Kharkov, U.S.S.R.*

1. THE first photometric investigations of the lunar surface [1, 2] revealed the basic peculiarities of the reflecting properties, which proved to be characteristic of formations, with different morphological peculiarities and location position. These peculiarities were interpreted by Barabashev as being due to the very porous, rough relief of the lunar surface.

Minnaert, by applying the Helmholtz principle of reciprocity to photometry, provided the method for the investigation of the photometric homogeneity of the surfaces and atmospheres of the planets [3]. Investigations of the photometric homogeneity of the lunar surface should be based on the most complete photometric data, and include all the main morphological types of the lunar relief in different regions of the lunar disk.

2. Various comparisons were made for investigating the photometric homogeneity. On the basis of the photometric catalogue of V. A. Fedoretz [6] paired comparisons of brightness were made in areas which could be considered as interchangeable [4]. Altogether eighty-four such pairs were subjected to examination. A summary of the results is given in Table 1.

TABLE 1

<i>Groups</i>	<i>n</i>	$\delta_m \pm \sigma$	
I—I	18	0.11	0.09
II—II	17	0.13	0.11
I—II	39	0.19	0.13
I—III	6	0.07	0.07
II—III	4	0.05	0.03

Here  $n$  signifies the number of comparisons; group I the maria, sinus and palus, group II the continents and craters, group III the bright rays.  $\delta_m$  is the average arithmetical value of

$$\delta = \frac{r(i) - r(\beta)}{r(i)},$$

which determines the deviation from homogeneity, and  $\sigma$  is the mean square deviation.

One should bear in mind the fact that, in the comparison of objects belonging to one group, the average deviation is noticeably less than in the



comparison of details belonging to different groups. It is also noteworthy that the bright rays behave in the same way as the regions through which they pass.

3. Photometric measurements were made along the equator of the intensity of the Moon and parallel directions at different phase angles, and subsequently compared with the corresponding branches of the intensity distribution curves. The areas measured along the selected sections belonged to different types of formations. In this case, the photometric homogeneity of the Moon is revealed to a still greater degree [4].

The difference in the albedo, as in the case of the paired comparisons, was taken into account, assuming that the ratio of the albedos is equal to the ratio of the brightness at full Moon, and that the law of reflection has the form,  $\beta(i, \epsilon) = \beta_0 f(i, \epsilon)$ , where  $\beta_0$  is the brightness of a given detail at minimum phase angle equal to  $\alpha = 1.5^\circ$ .

4. On the basis of the data of the catalogue of Fedorets, indicatrices of reflection of different details of the lunar surface were constructed, and comparisons made in those cases when the necessary conditions were fulfilled. The following ratio was used

$$\frac{\beta(i, \epsilon)}{\beta(\epsilon, i)\beta_0} = \frac{\cos i}{\cos \epsilon}$$

From the catalogue data on the dependence of the brightness of the detail on the angle of incidence  $i$ , the angle reflection  $\epsilon$  and the phase angle  $\alpha$  only those values were selected which would include as far as possible a sufficiently large range of values of  $i$  with  $\epsilon$  deviating not more than  $\pm 1^\circ$ . In this way the brightness of a detail was determined depending on the angle of reflection (in a limited interval of values with  $\epsilon_{\min} \approx \varphi$ ) for a constant value of the angle of incidence.

As is seen from the data presented in Figs. 1, 2, and 3, the indicatrices

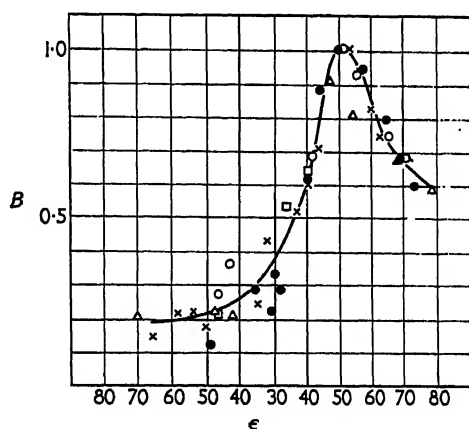


FIG. 1. ● N150  $i = 49^\circ 5$  Continent  
 x N165  $i = 50^\circ 4$  Oceanus Procellarum  
 ○ N144  $i = 42^\circ 7$  Continent  
 Δ N118  $i = 57^\circ 7$  Area alongside of light ray  
 □ N167  $i = 50^\circ 4$  Continent

$\varphi = -27^\circ 0$   $\lambda = +42^\circ 9$   
 $\varphi = +32^\circ 5$   $\lambda = -41^\circ 4$   
 $\varphi = -34^\circ 0$   $\lambda = +46^\circ 0$   
 $\varphi = +26^\circ 0$   $\lambda = -46^\circ 0$   
 $\varphi = -17^\circ 0$   $\lambda = -46^\circ 6$

are similar. It is also interesting that the indicatrices of reflection of the bright rays and those of neighbouring regions coincide. The latter circumstance is evidence in favour of the bright rays adopting the photometric structure of those regions through which they pass.

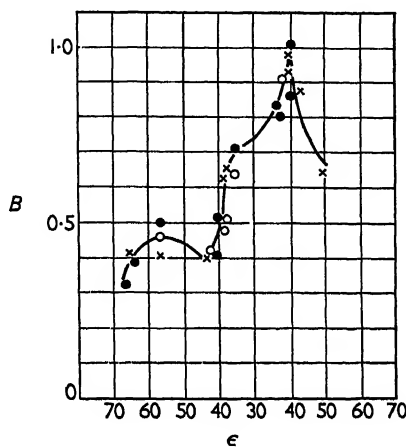


FIG. 2. ● N79a  $i = 47^{\circ}0$  Area alongside of Tycho ray  $\varphi = -35^{\circ}$   $\lambda = +7^{\circ}0$   
 × N79b  $i = 43^{\circ}0$  Tycho crater  $\varphi = -37^{\circ}$   $\lambda = +10^{\circ}0$   
 ○ N79c  $i = 41^{\circ}6$  area alongside of Tycho ray  $\varphi = -35^{\circ}$   $\lambda = +10^{\circ}0$

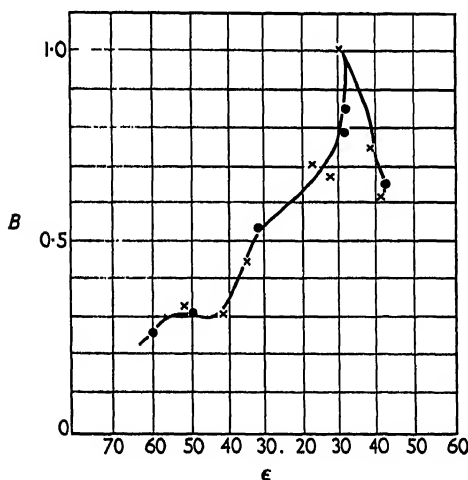


FIG. 3. ● N76  $i = 31^{\circ}4$  area beside light strip  $\varphi = +23^{\circ}0$   $\lambda = -22^{\circ}8$   
 × N45  $i = 30^{\circ}9$  light strip in Maro Imbrium  $\varphi = +23^{\circ}0$   $\lambda = -21^{\circ}8$

The photometric homogeneity of the lunar surface evidences the important role of external, cosmic factors exerting isotropic action, on the formation of the microrelief of the lunar surface.

## REFERENCES

1. Barabashev, N. P. *A. N.* 217 (1917).
2. Markov, A. V. *A. N.* 221, 285 (1924).
3. Minnaert, M. *Astrophys. J.* 93, 403 (1941).
4. Barabashev, N. P. and Ezersky, V. I. *Izv. plan. Kom.* no. 1 (1960).
5. Barabashev, N. P. and Ezersky, V. I. *Izv. plan. Kom.* no. 2 (1960).
6. Fedorets, V. A. *Trudy Khark. astron. Obs.* no. 2 (10) (1952).

# COLOUR AND SPECTRAL CHARACTERISTICS OF THE LUNAR SURFACE

V. G. TEYFEL

*Astrophysical Institute, Kazakhstan  
Academy of Sciences, Alma-Ata, Kazakh S.S.R.*

IN the broad complex of optical studies of the Moon, the most complete information which does not lead to differences of opinion is available only for the photometric characteristics of its surface. The colour and polarization characteristics of the Moon's surface have been studied in less detail; and as far as the question of the colour contrasts on the Moon's surface is concerned, no unanimity of opinion has existed until recently, since colorimetric observations conducted by various investigators have often produced contradictory results. At the same time, the question of the existence and magnitude of colour differences on the surface of the Moon is not an academic one. The colour of the lunar surface reveals just such characteristics of its physical state as do other optical characteristics—such as photometric and polarizing peculiarities which inform us about the microstructure of the surface layer of the Moon. The observed colour of the lunar formations characterizes also the external layer, which represents the result of protracted and continuous influences on the lunar surface of various external factors—such as meteorites, micrometeorites, cosmic rays, and ultraviolet, corpuscular and X-ray radiation of the Sun, etc. Differences in colour of lunar features, just as differences in the albedo, depend on the characteristics of the basic lunar rocks and not on the changes which these rocks have undergone in the course of time. Therefore, although the alteration of characteristics of the external layer of these rocks does not permit comparison of the external optical characteristics of the Moon's topography with terrestrial rocks with certainty, one can, by means of various photometric and colour data, draw a number of conclusions about the characteristics of emerging basic rocks found on its surface.

A sufficient number of colorimetric observations of lunar details has disclosed the presence of appreciable colour differences on the surface of the Moon. However, according to various investigations, the magnitude of colour contrasts varied from several hundredths to one magnitude and more of the normal colour index. Furthermore, Barabashev raised the question concerning the legitimacy of regarding the colour index as a unique characteristic of colour differences of lunar formations [1], as separate spectrophotometric observations of the Moon revealed a nonuniform variation of the brightness of lunar details along the spectrum.

In order to clarify these problems, it was necessary to have systematic spectral observations of the Moon. Such observations have commenced only in the last 3 or 4 years at several observatories in the Soviet Union. In particular, spectrophotometric observations of the Moon have been conducted systematically since 1956 in Alma Ata, with the 200 mm Maksutov meniscus reflector and the spectrograph ASP-9.

The primary aim of these observations was to obtain spectrograms

of extended regions of the Moon, on which it was possible to measure the intensity distribution in the spectrum of separate areas. Since the main task was to reveal the spectral differences of lunar formations, an area of the Moon's surface in Mare Vaporum was chosen, as a reference standard. The intensity distribution in the spectrum of this area was measured relative to the intensity of stellar spectra. Altogether ninety areas were observed in fifteen regions of the lunar surface, six to eight spectrograms being measured for each. In this way, relative spectral curves were constructed for these areas, permitting one to assess the differences of spectral reflectivity of different details on the lunar surface.

The spectral distribution curves of most lunar objects show a smooth, almost monotonous, intensity variation along the spectrum. For several features, the differences in spectral intensities exceed the mean square error of the result  $\sigma_A = \pm 0.02-0.03$ . No unusual anomalies have been noted in the intensity distribution in the visible spectral region, with the exception of a conspicuous decrease in the reflectivity for  $\lambda < 420m\mu$  for several objects in Mare Imbrium and other regions. The general differences of spectral curves of lunar formations are noticeably smaller than, for example, those of stony meteorites, according to the investigations of Krinov [2] (Fig. 1).

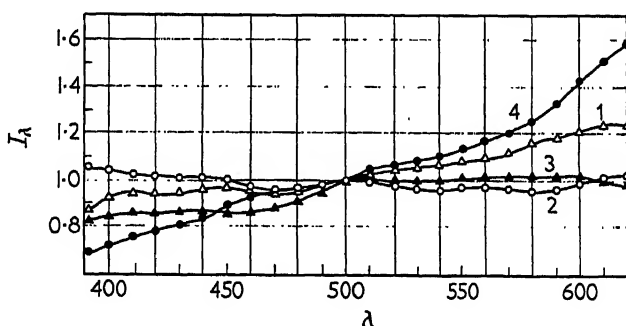


Fig. 1. Comparison of the relative spectral curves of the lunar surface and stony meteorites which differ most in colour (according to Krinov).

- (1) The Moon—north-west part of continent. (2) The Moon—the continent between Mare Fecunditatis and Mare Nectaris. (3) Meteorite "Mogoi". (4) Meteorite "Andronitsky".

A comparison of the spectrum of the standard region with that of  $\alpha$  Lyrae also shows that the lunar surface is characterized by a monotonous distribution of energy in the spectrum of reflected light, even in comparison with the spectra of hot stars (Fig. 2). The smooth variation of the spectral curves permits one to characterize them by the relative photometric gradient, either in the whole spectral interval  $\lambda\lambda 390-620m\mu$  or, at least, in the half intervals of wave lengths. The limits of spectrophotometric gradients of the investigated lunar details are not large:  $G(390-620m\mu)$  from  $-0.06$  to  $+0.41$ ,  $G_1(390-500m\mu)$  from  $-0.08$  to  $+0.49$ ,  $G_2(510-620m\mu)$  from  $-0.20$  to  $+0.52$ . These limits correspond in the spectral scale to 0.6 of the spectral class  $dG$ . The regions of the maria are characterized by the lowest mean value of  $\bar{G}$ , the lunar craters by the highest. For the maria and craters we have  $\bar{G}_1 > \bar{G}_2$ , while for the continental areas and craters rays  $\bar{G}_1 < \bar{G}_2$ .

For 50% of all the objects investigated, the spectrophotometric gradients in half spectral intervals computed in the whole spectral interval, the function  $\log I(\lambda^{-1})$  is almost linear in the visible spectral region. Moreover, the deviations of individual gradients from the mean obey the normal law or errors.

As Lipsky [3] indicated, the results of spectrophotometry of the lunar surface may be influenced by polarization in the spectrograph and by the polarization of the lunar surface varying with wave length. With the instrument used by us, as shown by investigations, the degree of polarization did not vary with wave length and in the above-mentioned interval of wave lengths equals 0.07.

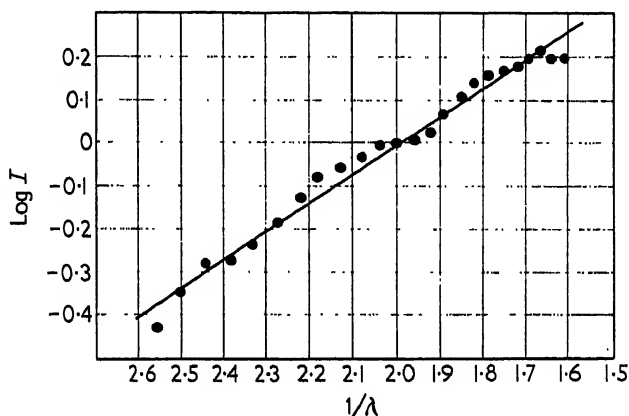


FIG. 2. Intensity distribution in the spectrum of Maro Vaporum, in relation to  $\alpha$  Lyrae.

Spectropolarimetric investigations of nineteen lunar objects in three regions of the Moon were carried out. For this purpose, spectra of lunar regions were photographed near the quadratures in three positions of a polyvinyl polaroid placed in front of the slit of the spectrograph. No less than two spectrograms were measured for each position angle of the polaroid. These showed that the variation of polarization with wave length is insignificant (not more than 0.05 to 0.07) and decreases toward the red. This agrees well with the Umov effect, according to which the lunar surface has a reddish colour in comparison to that of the illuminating sunlight. The variation of polarization with wavelength follows, in general, the same empirical relationship of polarization and the albedo of lunar features obtained by Sytinskaya [4] from the observations of Lio in integrated light. Monochromatic values of polarization may be influenced by the luminescence of lunar rocks which decreases, decreasing the values of  $P_\lambda$  obtained from observations in spectral regions in which bands of intense luminescence are present.

As we have mentioned above, the spectral curves of lunar features show a monotonous variation of intensity with the wave length. Therefore, the spectral differences in the visible spectral region can be defined uniquely by the colour index (or the colour excess  $CE$ ). A comparison of the relative photometric gradients and the colour excess of lunar details shows a distinct relationship (within the limits of accidental deviations) between the two.

The relation between  $G$  and  $CE$  is linear and expressed by the formula  $G = 2.27CE$ , which is close to the ratio  $G = 2.00 CE$ , computed according to the formula for the spectrophotometric gradient.

Thus, colorimetric observations based on measurements of the brightness of lunar features in two to four regions of the spectrum should yield the same results as the spectrophotometric observations. The comparison of our spectroscopic results with the colorimetric data of Barabashev and Chekirda reveals a close agreement in the limiting colour differences on the lunar surface.

Instead of time-consuming measurements of spectrograms in mass determinations of the colour properties of areas of the Moon's surface, it is possible to restrict oneself to computations of the colour indices of lunar objects from the photometric profiles of the spectrograms of extended regions across the dispersion in the corresponding wave lengths. Such spectrocolorimetric observations permit the investigation of the colour characteristics of a much larger number of lunar details of comparatively small size than does conventional spectrophotometry. In order to reduce the errors of measurement of the photographic method, it is necessary to photograph each area several times. In this way a catalogue was compiled in 1958 which gives the normal colour indices of 262 areas of the Moon, based on the measurements of ten to fourteen spectrograms of each of the eleven regions. In 1959 some spectrograms, obtained near the true full Moon at a phase angle of  $3^{\circ}$ – $4^{\circ}$ , were used to determine the colour indices and the relative intensity of 1442 areas of the Moon in sixty-two regions, uniformly distributed over the visible lunar disk.

The result of these investigations was, first of all, the establishment of the limits of colour differences on the lunar surface, which equal  $0^{\text{m}}.21$ – $0^{\text{m}}.25$  in units of the normal colour index. The colour index of lunar features varies between  $0^{\text{m}}.72$  and  $0^{\text{m}}.97$  while the amplitude of colour differences in the maria and continental regions is almost identical. The maxima of the numerical distribution of colour indices for the maria and continents are also almost identical and included within the limits  $CI = 0^{\text{m}}.79$ – $0^{\text{m}}.84$ .

The most interesting result of spectrocolorimetric investigations is the relationship between the colour and relative brightness of lunar features. The fact that the brighter features of the lunar surface also prove to be redder, was noted by many investigators—in particular, by Radlova [6] from colorimetric measurements. This relationship shows up more distinctly in spectrophotometric investigations, although the range of colour differences is about twice smaller than in the photographic investigations of Radlova, i.e. the lunar details on the brightness-colour diagram (Fig. 3) occupy a more limited region.

The relationship between colour and brightness is numerically characterized for each investigated region of the lunar surfaces by two values: the gradient of relationship

$$G = \frac{\Delta CE}{\Delta \log I_{550}},$$

and the correlation coefficient  $r$ . Investigations of the relationship of colour-brightness for sixty-two regions of the Moon gave values of  $G$  from 0.45

to 3.00, with a maximum of statistical distribution  $G = 0.60$  to 0.80 and correlation coefficients from 0.34 to 0.90. The comparison of  $G$  and  $r$  (Fig. 4) shows that, with the general increase of  $G$  together with the decrease of  $r$ ,

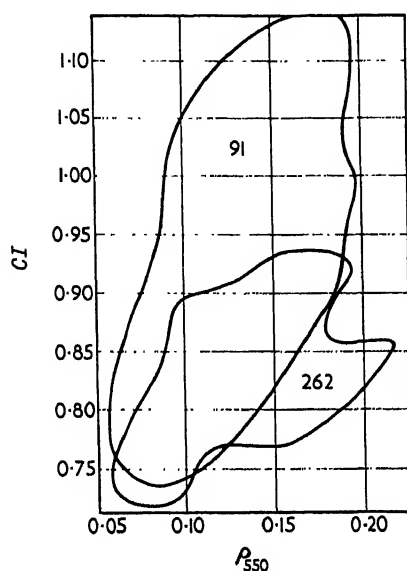


FIG. 3. Comparison of diagrams of brightness-colour (the brightness coefficient—colour index) according to the observations of L. N. Radlova (91 objects) and the author (262 objects).

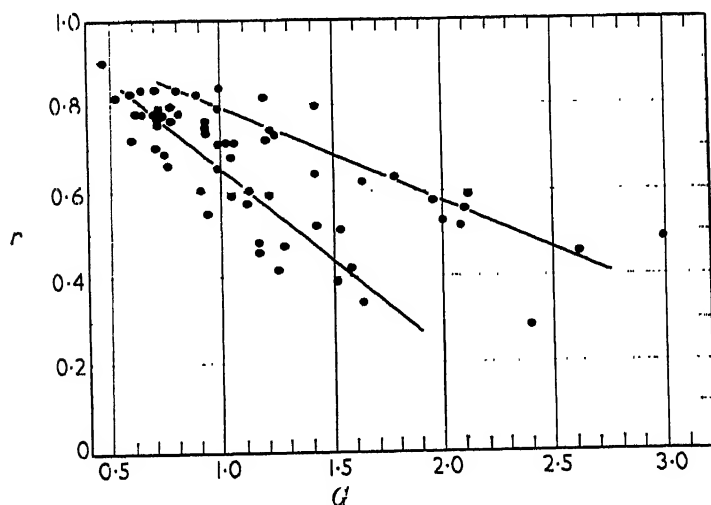


FIG. 4. Diagram of relationships between  $G$  and  $r$  for sixty-two regions of the lunar surface.

two branches are visible on the graph: with small and large values of  $G$ , at the same values of  $r$ . This distribution is noticeably linked with the morphological characteristics of the region. Thus the majority of regions investigated



in Mare Serenitatis, in Mare Imbrium, and in the region of Mare Crisium are in the right-hand branch of the diagram (i.e.  $G$  is characterized by the greatest values both for large and small  $r$ ). Oceanus Procellarum, Mare Fecunditatis and continental regions, even at small  $r$  have comparatively small values of  $G$ , not exceeding 1.7. This shows that although the increase of dispersion of points on the colour-brightness diagram leads to an increase in  $G$ , it is not the only cause of differences of  $G$  in different regions of the lunar surface. Apparently here we have to do with real physical differences.

A study of the colour-brightness diagrams shows that even in regions where the correlation coefficient is high, there are objects which deviate from this relationship. The crater Aristarchus especially stands out in this respect. While having a high relative brightness, its colour excess is smaller than that which follows from the colour-brightness relation. The measurements of twenty spectrograms taken in the region of Oceanus Procellarum, including Aristarchus, showed that the colour of Aristarchus deviates from the linear colour-brightness relation in the mean by  $\Delta CE_G = -0^m.48 \pm 0^m.04$  (Fig. 5). Of the twenty-three remaining objects measured in this

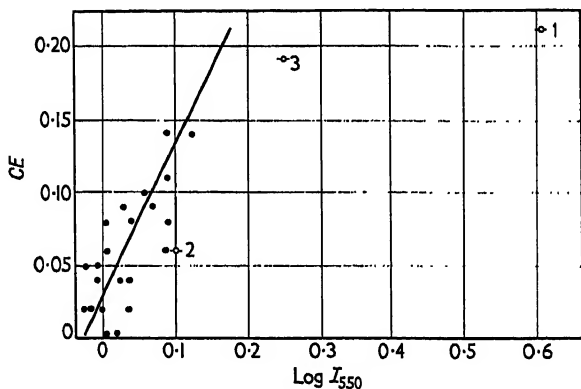


Fig. 5. The deviation of colour of Aristarchus (1) and neighbouring areas of the Moon (2 and 3) from the colour-brightness relation in Oceanus Procellarum.

region, two other objects show essential deviations: the ray system of Aristarchus ( $-0^m.16$ ) and the dark intervening space between the crater and the rays ( $-0^m.11$ ). Matter spread over the interior of the crater and its ray system differs from the matter of the surrounding surface. This is also indicated by the intense luminescence of Aristarchus, which was detected by Kozyrev [7], and by the somewhat increased polarization of this crater noted by Markov [8]. It is hardly possible that the colour peculiarities of the crater can be explained by its luminescence, as that would require excess luminescent radiation up to 56%. Besides,  $\Delta CE_G$  does not show a dependence on the phase angle.

The relation between colour and brightness of lunar objects is apparently the result of tectonic evolution, in the process of which a crumbling of the primary lunar crust took place, accompanied by lava outflow and the sinking of fragments of the crust into the lava. The bright substances of the lunar crust fused with the darker greenish materials of the lava in different proportions, which led to the formation of a multiplicity of bright

spots on the dark area of the maria. These spots are also distinguished from the dark areas of the maria by colour, which is especially evident in Mare Serenitatis.

The computation of the theoretical colour and brightness relation, assuming blending of materials with different colour and brightness, gives curves of variation of the colour index with brightness, which satisfactorily represent the observed colour-brightness relationship for various regions of the Moon. Different slopes of the curves correspond to different materials. The correlation coefficient for these materials shows (for sufficiently exact determinations of the colour excesses and relative brightnesses of the respective details) whether in a given region of the Moon only two kinds of rock are present, blended in different proportions. The low coefficient of correlation in a given region of the Moon's surface reveals that, in this region, the colour-brightness relationship is weakly expressed or completely absent. This is due to the presence of blending of three or more kinds of lunar rock in such a region. A deposit of the material of bright rays and rings on the surface, which already consists of a mixture of two rocks may serve as the simplest example. Therefore, in future investigations of the colour-brightness relationship, it will be necessary to measure the brightness-colour characteristics in limited regions of the lunar surface, i.e. areas where rays are present, areas without rays, and the floors of large craters. From the respective values of  $G$  and  $r$ , it will be possible to reach conclusions on the similarity and difference of the composition of materials of a given region of the lunar surface, and of the rays diverging from various craters.

The viewpoint that, on the lunar surface, we do not observe basic lunar rocks which have not been subjected to the influence of external factors, can now be assumed to be widely accepted. On the other hand, the observed differences of optical characteristics of lunar features clearly point to a difference in the composition of rocks of different areas of the Moon. External factors were unable completely to obliterate these differences, including the colour-brightness relation.

The opinion has repeatedly been expressed that continental regions of the Moon are formed of lightly coloured rock, similar to the terrestrial acidic rocks of the type of granite, and the maria regions of basic and ultrabasic rocks of the basaltic type. The hypothesis, proposed recently by Miyamoto [9] on the origin of the maria and continental regions, is based on such a conjecture. But in such a case, the changes in the colour characteristics of the continental and maria regions would have followed a different course: the continental areas would have become darker and bluer, those of the maria darker and redder. Rough calculations show [10] that the observed brightness-colour characteristics of the lunar surface cannot be a result of processing of the rocks, similar to terrestrial granite and basalt, under the action of only external factors. The assumption seems more natural that even those parts of the surface of the Moon which were not subject to subsequent processing by external factors possessed colour differences which were not so sharply expressed as for terrestrial rocks. The smoothing of contrasts could have been due to endogenous processes: eruptions, outflow of lava, the fusion of rocks with different characteristics, etc.

In conclusion, we wish to mention a number of tasks to be performed by spectroscopic and other methods of investigation, which should be undertaken in the near future:

(a) In further spectral investigations it is necessary to eliminate the existing diversity in referring the spectral measurements to different standard objects. It is necessary to establish and investigate a standard reference area on the Moon as a spectrophotometric reference. Since observations of the Moon should be made at all phases, it is expedient to select three areas in the western, central and eastern zones of the Moon. These areas should be compared spectrophotometrically. Besides the standard reference areas can serve for the control of spectrophotometric measurements made at various observatories. Having taken the spectrum of the reference area and of the standard star ( $\alpha$  Lyrae) observers at any observatory may compare their results and eliminate personal errors inherent in the reduction of spectrograms.

The following reference areas of the Moon with a more or less uniform surface brightness are proposed.

TABLE 1.

<i>Region of the Moon</i>	$\varphi$	$\lambda$	<i>The Slit of Spectrograph Established on the Line of</i>
Mare Crisium	+15°0	+65°0	Agarum Promontory—toward the north from Cape Olivum.
Mare Vaporum	+13°0	+5°0	Manilius—Bode A
Oceanus Procellarum near Grimaldi	-3°0	-61°0	Flamsteed—North edge of Grimaldi.

(b) It is desirable to investigate, not isolated objects of the lunar surface located arbitrarily on the disk of the Moon, but all areas and objects in small, well-defined regions of the Moon. These regions (squares) should be selected in accordance with the relative age of the formations, located in the respective parts of the lunar surface. In this way, it should be possible to construct maps of the distribution of optical characteristics in specific regions of the Moon, gradually approaching the compilation of a complete physical map of the Moon.

(c) It is probable that areas of the Moon with extreme values of the brightness and colour coefficients are most similar to the parent lunar rocks. These are the darker areas of the maria and the brighter areas of the mountainous regions (not rays), and craters. It is possible that, while the bright areas of the mountain regions were formed from comparatively bright magmatic rocks, the bright walls of the craters were covered with a deposit of dust and gaseous products of eruption. It is desirable to investigate such objects in order to elucidate the differences in their photometric, spectral, and polarization characteristics.

(d) Spectropolarimetric investigations, which as yet have the character of preliminary experiments, should also be extended to a larger number of lunar formations for a statistical study of their age characteristics, and also anomalies in the dependence of polarization on wavelength, due to luminescence and other causes.

## REFERENCES

1. Barabashov, N. P. *Circ. Kharkov, astr. Obs.* no. 15 (1956).
2. Krinov, E. *Astr. Zhurn.* **17**, 40 (1940.)
3. Lipsky, Y. N. *Astr. Circ. Acad. Sci. U.S.S.R.* **155**, 9 (1954).
4. Sytinskaya, N. N. *Astr. Circ. Acad. Sci. U.S.S.R.* **168**, 18 (1956).
5. Teyfel, V. G. *Astr. Zhurn.* **37**, 703 (1960).
6. Radlova, L. N. *Astr. Zhurn.* **20**, 1 (1943).
7. Kozyrev, N. A. *Izv. Crim. astrophys. Obs.* **16**, 148 (1956).
8. Markov, A. V. *Izv. Pulkovo*, **20**, no. 158, 5, 138 (1958).
9. Miyamoto, S. *Contrib. Inst. Astrophys. Kwasan Obs.* no. 90 (1960).
10. Teyfel, V. G. *Trudy Sect. astrobot.* **8**, 165 (1960).



# THE COLOUR OF THE BRIGHT RAYS ON THE MOON

L. N. RADLOVA

*Institute of Scientific Information, Moscow, U.S.S.R.*

THE systems of rays on the surface of the Moon are of great importance for selenology because, on any hypothesis concerning the origin of the lunar craters, the formation of bright rays and aureolae should be the results of some kind of explosive phenomena. At the present time two views regarding the nature of bright rays are most widely held. According to one of these, the rays are cracks in the crust of the Moon, filled with lava; while according to the other, the rays are formed by matter ejected from the zone of a crater and spread over a previously existing relief. Photometric and colorimetric data allow the reliability of these two hypotheses to be evaluated.

I have carried out visual and photographic measurements of the colour of several such rays. Visual measurements were made in the autumn of 1956 at the Tashkent Astronomical Observatory with the aid of a Rosenberg astrophotometer, the blue wedge of which was used as a colorimeter. With the aid of this wedge and the polarization system of the photometer the brightness and colour of the comparison field of the photometer, illuminated with an incandescent light, were compared with those of various regions along the rays and the background of continents. I measured three of the brightest rays of the crater Tycho, three rays of the system belonging to the crater Copernicus and two rays originating from crater Kepler. The results of measurement are expressed in the form of special colour indices, the zero-point of which was identified with the mean light of the lunar surface, obtained by measuring the colour of several points on the lunar disk, selected so that their mean corresponded to the mean value for a large number of objects [1].

In the photographic method, photographs of the full Moon which I obtained in 1939 were used with the Tashkent normal astrograph in three following spectral regions: ultraviolet ( $\lambda = 380 \text{ m}\mu$ ), photographic ( $\lambda = 430 \text{ m}\mu$ ) and photovisual ( $\lambda = 560 \text{ m}\mu$ ). On these photographs the density along the rays of crater Tycho was measured with the aid of a Hartmann microphotometer. The visual as well as the photographic observations revealed that the colour of the rays differs but very little from the mean colour of the Moon. For some rays a small systematic change of colour along the ray was noted; but this lies within the limits of observational errors ( $\pm 0.010$  for the visual method and  $\pm 0.15$  for the photographic).

Thus, the measurements confirmed the subjective impression that the rays differ from the background only in brightness, but not in colour. Taking into account that rays and rings differ also only slightly from the background by their albedo and the law of light reflection, it can be considered probable that the surface of the rays consists basically of the very

same material as the surface of the continents, but somewhat more finely pulverized. This leads us to give preference to the hypothesis regarding such rays as filled cracks.

#### REFERENCE

1. Radlova, L. N. *Astr. Zhurn.* **20**, 1-13 (1943).

# A STUDY OF THE ANGLE OF REPOSE OF SOME LOOSE MATERIALS AND ITS BEARING ON THE HYPOTHESIS OF A DUST LAYER ON THE LUNAR SURFACE

N. S. ORLOVA

*Astronomical Observatory of the Leningrad State University, U.S.S.R.*

AMONG the numerous hypotheses to explain the observed peculiarities of the outer layer of the lunar surface, some consider this layer to consist of loose material of volcanic ashes or dust. The basic objection to this view is the fact that such a layer of loose material cannot give a microstructure of the surface that would correspond to the law of the reflection of light from the lunar surface which follows from the observations. The scattering diagram of illuminating rays for a given area of the lunar surface, at all angles of incidence, is known to be very elongated in the direction of the light source. This is illustrated in Fig. 1, where the average scattering diagrams

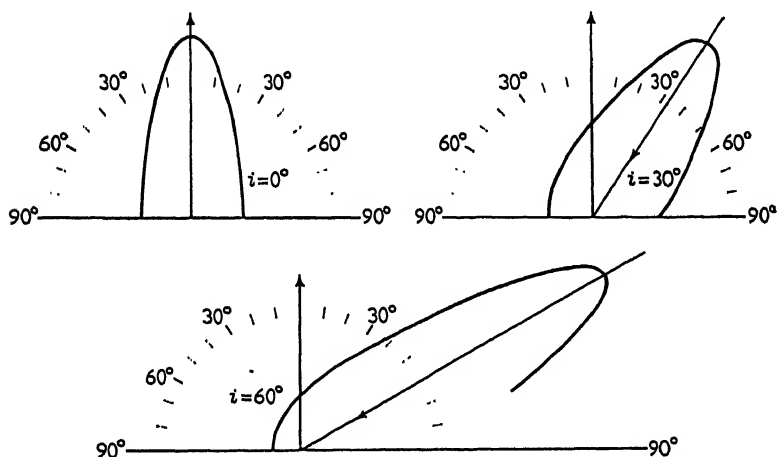


FIGURE 1.

for the lunar maria are plotted for the angles of incidence of light  $i = 0^\circ, 30^\circ, 60^\circ$ . Experiments show that such diagrams can be reproduced only by those formations the surfaces of which are thickly covered by deep depressions with steep walls and sharp edges. Loose material cannot be maintained on surfaces with great angles of repose and, consequently, is capable of producing unevenness only on the slopes.

In order to study this situation more precisely, the experiments were set up in the laboratory for determining the angle of repose for different specimens of loose material: sand, dust, volcanic ash, and other materials. If the cone of accumulated material of one kind or another is viewed from a sufficiently great distance, its projection on the picture plane can be regarded



as orthographic. If, in addition, the line of sight is perpendicular to the axis of the cone, then the apparent angle of the slope of the sides of a triangle by which the cone is represented will be equal to the actual angle formed by the generating lines of the cone with the plane of the horizon. Therefore, for the actual measurements we used a medium-sized telescope provided with an ocular micrometer. The wires of this micrometer were set parallel with the slopes of the cone. The readings of the corresponding position angles enabled us to obtain angles of slope for thirty-eight kinds of different materials.

Subsequently, we determined the size of the angles of repose of terrestrial volcanoes. It is known that the cones of volcanoes are formed from materials which are thrown out of the crater at the time of eruption—bombs, lapilli, ashes, and other loose materials. The angles of repose of volcanic cones of piled-up loose material were obtained by photographs published in special issues and photographic atlases of volcanoes of different countries. By making use of the sources indicated we determined the angles of repose of fifty-eight volcanic cones.

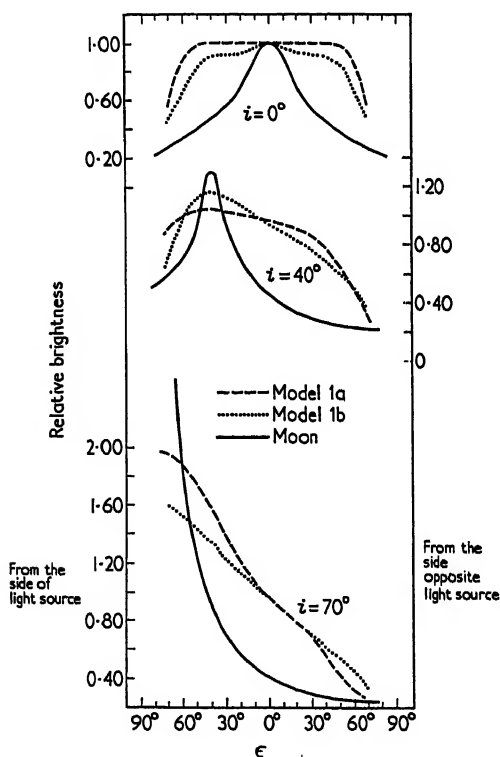


FIGURE 2.

A summary of the material obtained is given in Table 1. It contains the values for the average angles of repose and the limits of angles of repose for different groups of objects. We see that, in all cases, the angle of repose does not exceed  $45^\circ$ .

TABLE 1. Angles of Repose

Order No.	Materials	No. of Observations	Angle of Repose	
			Limits	Average
1	Crushed Stone	3	40°-43°	42°
2	Pebbles	9	32°-40°	36°
3	Gravel	10	32°-40°	37°
4	Coarse Sand	15	29°-36°	34°
5	Medium Sand	21	30°-41°	34°
6	Fine Sand	23	29°-42°	34°
7	Dust	24	32°-45°	41°
8	Volcanic Ashes	2	30°-35°	33°
9	Volcanic Slope Material	58	27°-42°	34°

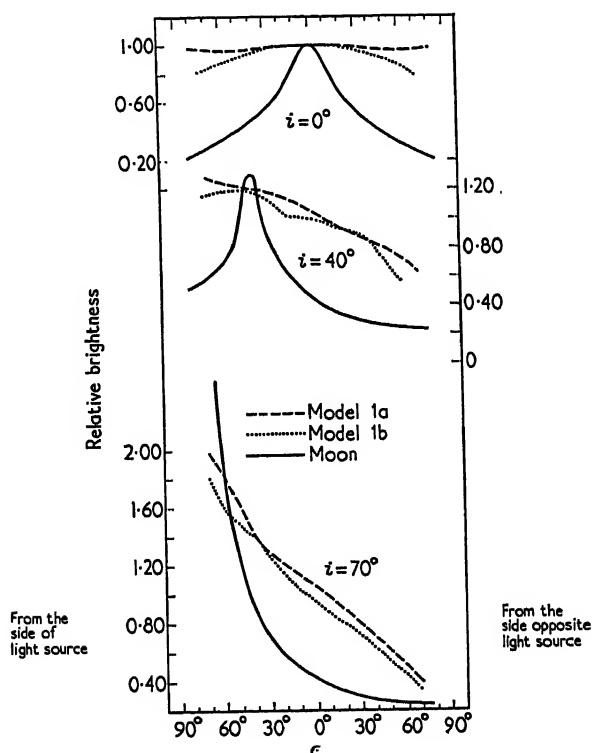


FIGURE 3.

In order to study the photometric relief of a rough surface with the maximum angles of repose of 45°, models specially prepared in the laboratory were investigated. Of these, the first consisted of a surface completely covered by four-sided pyramids, and the second by three-sided pyramids

with the sides inclined at  $45^\circ$ . The scattering diagrams of these models in the plane of incidence of the beam were determined by a device specially designed for this purpose at the Astronomical Observatory of the Leningrad University. The measurements of each model were done twice. The first model was measured at first in such a way that one of the horizontal edges of the pyramids at all angles of  $\epsilon$  was perpendicular to the line of sight. In the second measurement, the model was turned in azimuth through  $45^\circ$ . The second model with the three-sided pyramids was at first also set in a position in which the edges of the pyramid were perpendicular to the line of sight. For the second measurement the model was turned in azimuth through  $90^\circ$ .

The results obtained for the first and second models are shown in graphical form on Figs. 2 and 3 for angles of incidence of light  $i = 0^\circ$ ,  $40^\circ$ , and  $70^\circ$ . The angles of reflection  $\epsilon$  in the plane of the angle of incidence are through the abscissae, and the average values  $M$  for the brightness, referred to the value of brightness when  $i = \epsilon = 0^\circ$  (adopted as unity) are the ordinates. The dotted lines show the curves for the laboratory models, and the solid lines represent the corresponding curves for the lunar maria in accordance with the data published earlier by the author.

As was expected, the laboratory curves are not at all similar to what one observes on the lunar surface. Thus we come to the conclusion that if under the natural lunar conditions (smaller gravitational acceleration, absence of atmosphere, etc.) the angles of repose of loose materials have the same values as on the Earth, large areas of the surface of the Moon cannot be covered by loose material.

# FORMATION OF LUNAR CRATERS AND BRIGHT RAYS AS A RESULT OF METEORITE IMPACTS

K. P. STANYUKOVICH, V. A. BRONSHTEIN

*All-Union Astronomical and Geodetic Society, Moscow, U.S.S.R.*

The phenomena accompanying the impact of large meteorites on the surface of the Moon or of the Earth can be examined on the basis of the theory of explosive phenomena if we assume that, instead of an exploding meteorite moving inside the rock, we have an explosive charge (equivalent in energy), situated at a certain distance under the surface.

As an example, we shall consider a crater produced by an explosion of a charge buried at a depth of 30 m below the ground, which was carried out for the purpose of seismographic investigations. The crater has the diameter of 5 m and the depth of 2 m, i.e. parameters which are typical for meteoritic craters of this scale.

The theory of the formation of craters as a result of meteoritic impacts on the Moon's and Earth's surfaces was developed by K. P. Stanyukovich, first in 1937, and is being developed further at the present time [1-6]. The basic results can be expressed by the following formulas.

The radius of the explosion crater:

$$R_B = \sigma \left[ \eta \frac{Mu_0^2}{2Q} \right]^{1/3} \quad (1)$$

The total depth of the crater:

$$h_0 = \left[ \frac{3\bar{\eta}\eta Mu_0^2}{8\pi\rho Q} \right]^{1/3} \quad (2)$$

The mass of "exploded" material, ejected from the crater (in the case of the Moon):

$$M_B = \frac{\pi\rho}{15} \sigma^3 \eta \frac{Mu_0^2}{2Q}, \quad (3)$$

where  $M$  and  $u_0$  are mass and velocity of the meteorite;  $Q$  is the density of energy spent for the destruction (evaporation) of the medium;  $\delta$  is the coefficient depending on properties of the medium;  $\bar{\eta}$  is the efficiency of impact (portion of energy changing into energy of explosion);  $\eta$  is the coefficient determining the penetration depth of meteorite and the radius of destruction zone as a function of the velocity, shape and density of the meteorite, and the properties of the medium;  $\rho$  is the density of the medium. Thus, for conditions of the landing of "Lunik-2" on the Moon, we obtain  $M_B = 3 \times 10^3 M \approx 1000$  tons (for the container). The values of all the coefficients are given in [5].

Interesting experiments, simulating the kinetic impact (at velocities of 4.5—7.5 km/sec) have been described recently by Charters [7]. The filming

at a rate of about 1.2 million frames per second demonstrates the process of crater formation caused by the impact of a small particle. The impinging body and the medium appear to acquire for a certain time the properties of a liquid. The cumulative phenomenon is observed in experiments with actual liquids; this phenomenon consists of the fact that a stream, carrying the droplet on the top, ascends from the centre of the crater.

The experiments in simulation of lunar craters, conducted recently by Benevolensky [8], are of interest in this respect. In contrast with the experiments of Wegener [9] and Sabaneyev [10], who dropped lumps of cement into a powder-like layer of a substance, Benevolensky dropped compact particles into a layer of semi-liquid hardening mass, such as the cement or gypsum. As a result of the cumulation phenomenon, craters were obtained with a clearly expressed central peak (Figs. 1 and 2). However,

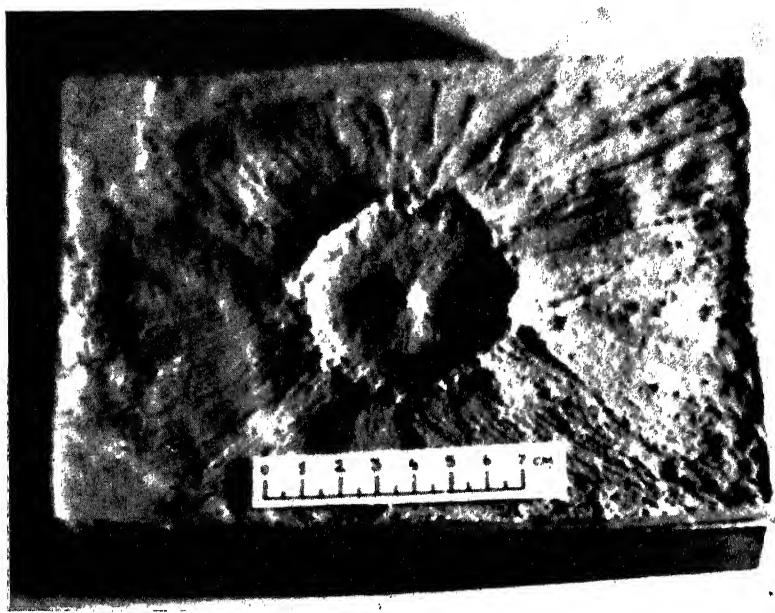


FIG. 1. A model of a lunar crater in a layer of hardened cement. Illumination at an angle of  $35^\circ$ . (According to A. M. Benevolensky.)

this peak was not obtained in all cases. We can assume that the formation of central peaks of lunar craters is associated with the impacts of meteorites against the Moon's surface in a molten state.

The opinions of each author differ somewhat on the question concerning the mechanism of formation of crater walls. Thus Stanyukovich assumes that the walls of lunar craters are of depository origin. If we assume the isotropic distribution of ejected masses according to the angles of ejection, and if we consider the range of scattering as a function of the angle of ejection, then the greatest amount of matter will fall in the centre and on the wall. This viewpoint is substantiated in various papers [3-5].

BronshTEN assumes that, since the structure of craters from explosions

on the Earth as well as of meteoritic and lunar craters is described by one law formulated by Baldwin [11], there are no reasons for attributing depository origin to the walls. The latter are formed as a result of radial shifts in a horizontal direction from the centre of crater, which is evident from experiments conducted by Charters [7]. This viewpoint is supported also by the circumstance that the walls of large craters (in contrast to bright rays which are unquestionably depository formations) are not superposed on the

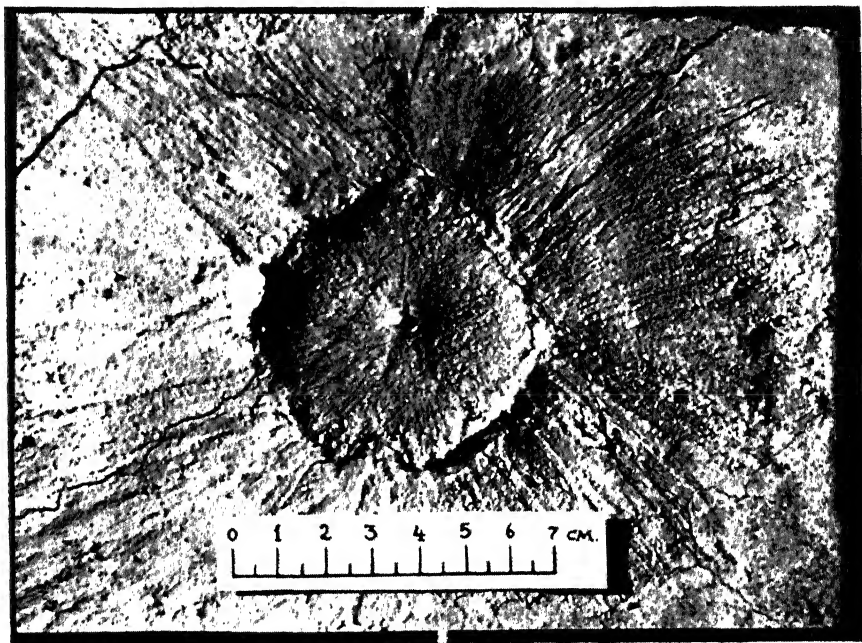


FIG. 2. A model of a lunar crater in a layer of hardened cement. Illumination at an angle of  $65^\circ$ . Soil cracks are clearly visible. (According to A. M. Benevolensky.)

surrounding relief, but appear to accommodate this relief to themselves. There is no doubt, however, that the deposition of rock takes place and exercises an appreciable flattening effect on the relief of the bottom of craters as well as of its walls.

The bright rays can be explained by ejections of matter from the crater; the longest rays being formed by the matter escaping at small angles with respect to the horizon, possibly through cracks in the wall of an already formed crater, as was assumed by Bronshten and Chistyakov [4, 12].

On the impact of very large meteorites against the lunar crust, the propagation of the shock wave downward to the layer of semi-liquid magma, situated beneath the crust, may cause an acceleration of the motion of crust matter in the region of the rarefaction wave, generated on transition of the shock wave from the solid crust into magma. As a result, the cleavage of an appreciable mass of the matter will take place under the crater already formed below, on the side of magma, which will facilitate the outflow of magma outwards and cause lava eruption. In approximately the same way we

can consider the mechanism of lava eruptions on impacts of gigantic meteorites, within the framework of hypothesis proposed by Urey [13] and supported by Levin [14].

### REFERENCES

1. Stanyukovich, K. P. On the impact of meteorites against the surface of planets. 1938 (manuscript). Account in *Astr. Zhurn.* 14, 240 (1937).
2. Stanyukovich, K. P. and Fedynsky, V. V. Concerning the destructive action of meteoritic impacts. *C.R. Acad. Sci. U.R.S.S.* 57, 129 (1947).
3. Stanyukovich, K. P. Elements of the physical theory of meteors and crater-forming meteorites. *Meteoritics*. 39 (1950).
4. Stanyukovich K. P. and Bronshten, V. A. The role of external cosmic factors in evolution of the Moon. "The Moon", ed. Markov, Chapter VIII (1960).
5. Stanyukovich, K. P. Elements of the theory of impact of solids with high (cosmic) velocities. "Artificial Earth Satellites", issue no. 4. Publishing House of the Academy of Sciences U.S.S.R. pp. 86-117 (1960).
6. Stanyukovich, K. P. Concerning one effect in the field of aerodynamics of meteors. *News of the Academy of Sciences U.S.S.R., Department of Technical Sciences, Mechanics and Machine Construction*, no. 5, 3-8 (1960).
7. Charters, A. C. *Sci. Amer.* 203, 128 (1960).
8. Benevolensky, A. M. The role of cumulative processes in formation of lunar ring-shaped mountains. *Bull. astr.-geodet. Soc. U.S.S.R.*, no. 30 (37) (1960).
9. Wegener, A. "The Origin of the Moon and Its Craters" (1923).
10. Sabaneyev, P. F. *Bull. astr.-geodet. Soc. U.S.S.R.* no. 13 (20) (1953), no. 16 (23) (1955), no. 17 (24), (1956), no. 21 (28) (1958).
11. Baldwin, R. B. "The Face of the Moon", Chicago University Press, (Chicago (1949).
12. Bronshten, V. A. and Chistyakov, V. F. On the origin of craters with rays on the Moon. *Bull. astr.-geodet. Soc. U.S.S.R.* no. 26 (33) (1960).
13. Urey, H. C. The origin of the Moon's surface features. *Sky and Telesc.* 15, 108, 161 (1956).
14. Levin, B. J. History of Moon's rotation and rheological properties of its matter. *Problems in Cosmogony*, 6, 56 (1958).

# SOME RESULTS DEDUCED FROM SIMULATION OF LUNAR CRATERS

P. F. SABANEYEV

*Rostov University, Rostov, U.S.S.R.*

It has been repeatedly noted that formations possessing all the attributes of lunar craters are produced in a layer of some loose materials, placed on a level and firm base, on dropping of a lump—made likewise of a loose substance—into such materials. The experiments demonstrate the possibility of obtaining in this way individual special features of separate craters, as well as their combinations, and of clarifying the origin of many enigmatic features of the Moon's relief.

Figure 1 shows the picture of a model of a crater produced in a cement

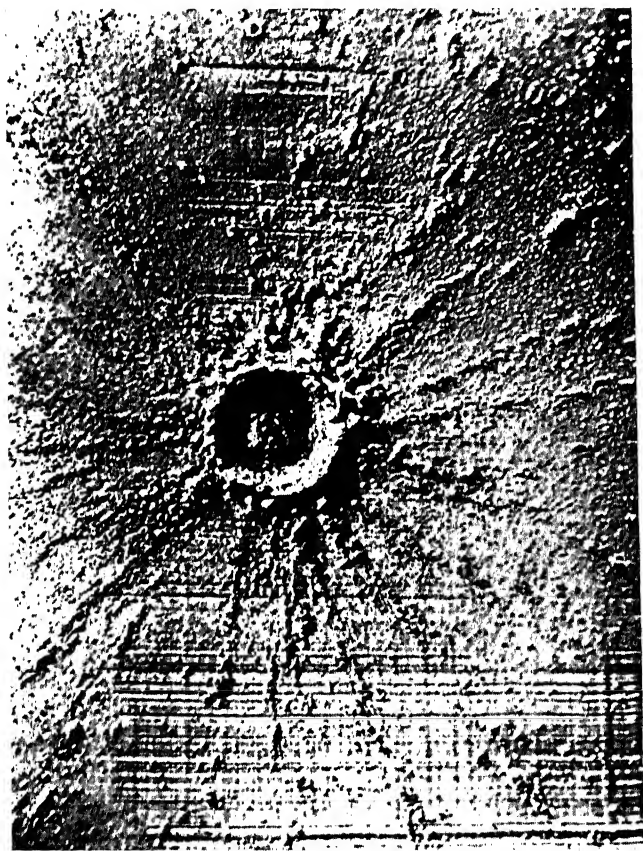


FIG. 1. Model of a crater produced in cement layer.



layer. On this picture we can readily distinguish the basic attributes: ring-shaped wall, having locally a fold structure with steep inner and slanting outer slopes; lowered inner region with central elevation, and ray ejection of matter. Sometimes, particularly when experiments are conducted under conditions of reduced gravity, the inner slopes of craters are stepped and terrace-like. Figure 2 shows the picture of two models obtained in a cement layer of greater thickness. These forms have the same basic attributes, but qualitatively differ. The diameters of ring-shaped walls are smaller here, central peaks expressed very weakly (to the point of being virtually absent), internal slopes of ring-shaped walls very steep, and the number of ejections is small. These models are obtained in the soil of a varying firmness; model I was formed in a layer the firmness of which increased with depth; model II originated in a naturally loose layer. The inner region of the first model is nearly horizontal, the radius of its junction with the ring-shaped wall small, and the number of ejections in this region negligible. The second model is distinguished by the rounded-off shape of the cross-section profile and by a slightly greater number of ejections.

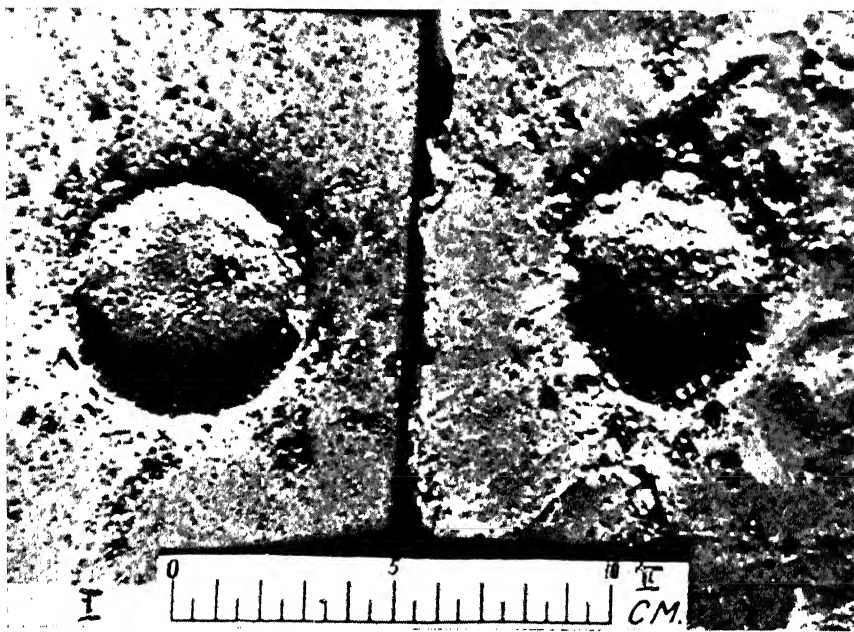


FIG. 2. Two models obtained in a cement layer of greater thickness.

The combinations of craters shown in Figs. 3 and 4, are obtained easily by a successive dropping of the lumps. The synchronous dropping of two adjacent masses produces formations as such presented in Fig. 5. Figure 6 shows the picture of the model of a crater, and Fig. 7 its diagram; the model was obtained in a layer of cement, 1 mm thick, placed on a spherical base ( $R = 300$  mm), by dropping the batch weighing 6 g from a height of 1.50 m. The central angle of the model is  $14^\circ$ . The tops of the ring-shaped wall are lower than the central part of the spherical base. This model is comparable to Mare Crisium, the central angle of which is equal to approximately  $12^\circ$ .



FIG. 4. Crater combination formed by successive dropping.

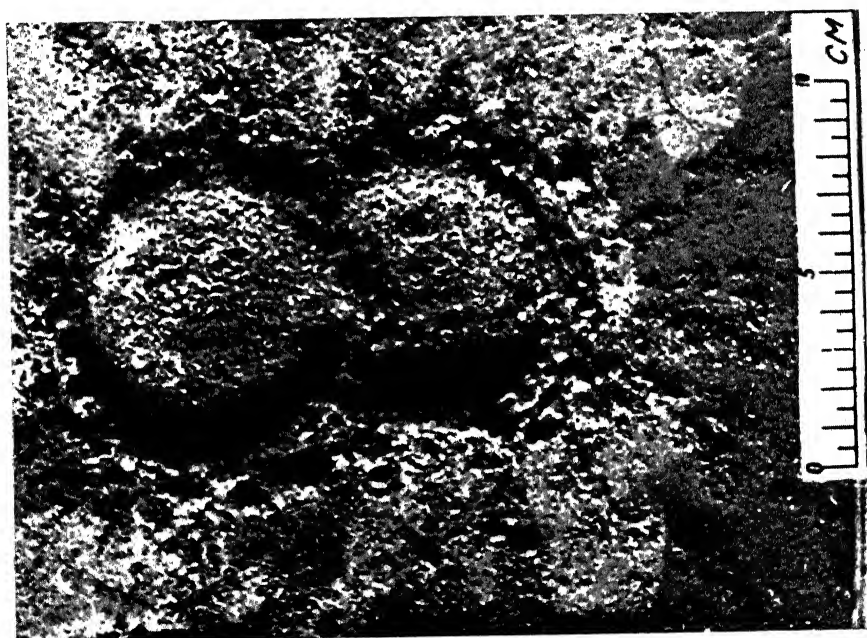


FIG. 3. Crater combination formed by successive dropping.

Under experimental conditions, the central angle of  $14^\circ$  constitutes the maximum at which the shape of a crater retains regular geometric dimensions.

The increase in the weight of dropped material caused the formation on the spherical surface of a crater of a greater size with a distorted regularity of ring-shaped wall. The emerging figures are nearly square or approximating the polyhedron (Fig. 8). Here the presence of rectilinear wall sections, connected into a broken line, and the accumulations of matter at the inner slopes (indicated by arrows) are characteristic. We can follow the consistent serration of inner slopes and the presence of ray structures on outer slopes.



Fig. 5. Formed by synchronous dropping of two adjacent masses.

The similarity between basic attributes of lunar craters and models obtained by the above-indicated method is hardly in doubt. Hence follows the advisability of studying in detail the conditions of formation of such models, in order to establish the most important circumstances under which the major mountainous formations of the Moon originated.

It was necessary to explain the dependence of the form and dimensions of models on such factors as the physical properties of impinging matter, its form, angle of incidence, velocity and size of dropping matter, atmospheric medium, magnitude of gravity, and also on mechanical properties of the soil and its stratigraphic structure.

The series of experiments, conducted according to the above-indicated programme, made it possible to explain the following basic features:

1. The greatest similarity between models and lunar objects is attained by dropping matter with a negligible cohesion of its constituent particles.



FIGURE 6.

Even an insignificant hardening of the impinging matter is sufficient to increase the acuity of the central mound and decrease the diameters of ring-shaped walls. A further hardening causes disturbances in the structure to such an extent that they lose their similarity with lunar objects. If, under experimental conditions, the impinging matter is absolutely rigid (steel ball), we note the emergence of formations which are comparable only with small craters on the Moon, terrestrial meteoritic craters and explosions craters.

2. The similarity indicated above is attained only if the impinging matter possesses the shape of figures of revolution—such as a sphere, hemisphere, cone, and ellipsoid of revolution, provided that their projections in the direction of incidence are circular.

3. The angle of incidence with respect to horizon exerts an appreciable effect on the structure of the models. Only an absolutely perpendicular drop yields a completely symmetric structure of the cross-section profile of the crater and a uniform orientation of ejections in all directions.

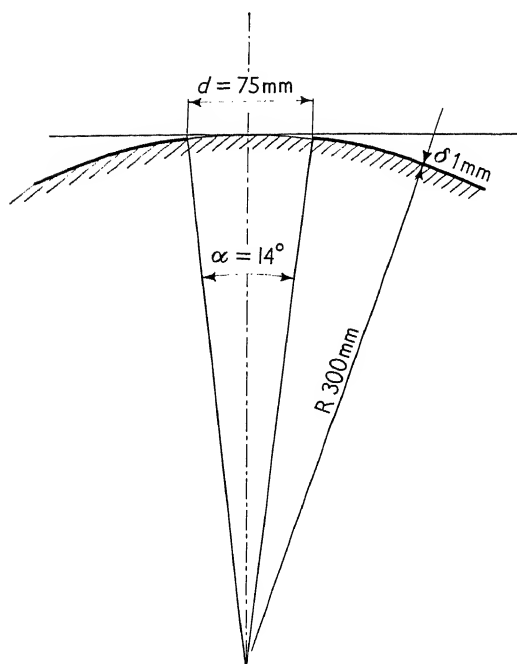


FIG. 7. Diagram of crater model shown in Fig. 6.

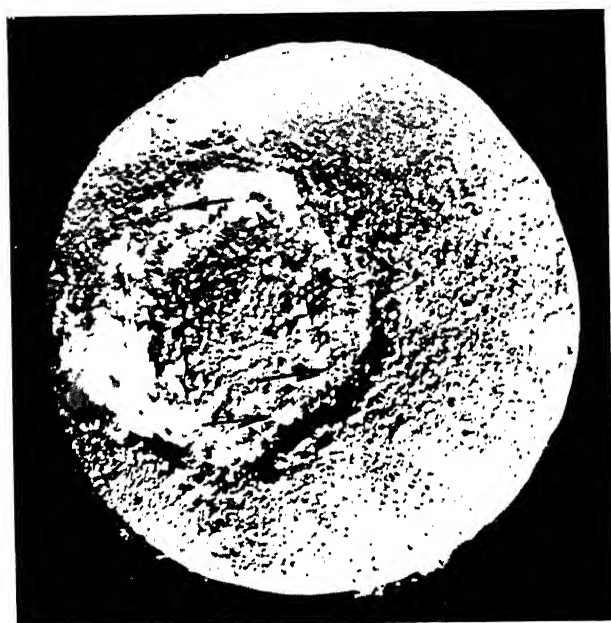


FIG. 8. Larger crater formed by increasing the weight of the dropped material.

Formations with an elliptic wall, which are unstable in form and dimensions, and the radial ejections in one direction, are produced on oblique incidence. At very small angles, the similarity of models to lunar objects is lost.

4. The increment in impact velocity of descending matter causes an increase in the diameter of a crater only up to a definite limit.

5. The dimensions of models increase with the increment in the amount of impinging matter.

6. The experiments in the simulation of craters under vacuum conditions demonstrated that the presence of atmospheric medium introduces no essential changes in the process of crater formation. Variations in the density of atmospheric medium cause only the development or abatement of individual facets of this process. The height and acuity of central peaks, and the height of ring-shaped walls, increase with the decrement in the density of atmospheric medium. The diameter of ring-shaped walls decreases somewhat. At the barometric pressure of 10 mm Hg and lower, the ejections from the dropped matter tend to form dense nimbi of short rays directly at the ring-shaped wall, and individual spots at a distance from this wall.

7. The decrement in gravity introduces also no essential variations into the process involved in crater formation, and affects only the development of its individual aspects. The heights of ring-shaped walls decrease when the ground is very weak. The speeds of solid ejections are lower. The curvature of ejection trajectories increases. The formation of ground ejections in the form of large fragments constitutes a distinctive peculiarity.

8. It was made clear that no powders constituting perfectly loose materials—such as, e.g. ground quartz or pure aluminium oxide—can be used as a ground material. The models having a satisfactory similarity with lunar objects are obtained only in a ground endowed with properties of the solid. Cement, alabaster, flour, lycopodium, and other such powders, constitute loose substances only if they occur in a large mass. These materials are most suitable for simulation, because they possess in a thin layer the properties of the solid with a lower firmness.

The firmness of the ground affects to a substantial extent the structure of models. Figure 9 (left side) shows a model produced by dropping alabaster into a layer of loose cement. A deep internal region, containing virtually all the impinging material, is characteristic here. The ejections in this model consist of the matter of the ground. The right-hand picture shows a model produced on retention of all the previous experimental conditions; however, this model is produced in a ground consisting of alabaster, solidified by pressure, on impact of a cement lump. In this case we obtained a crater of smaller diameter, and the depth was also smaller. The ray ejections involved only the impinging matter. Figure 10 demonstrates a change in the profile of the crater's cross-section as a function of the depth of the soil subject to deformation under experimental conditions.

When all experimental conditions remain unchanged, the diameter of models increases with the decrease in the depth of the ground layer, and their depth decreases. The central peak is formed in all cases; however, with increasing depths of the ground, this peak is insignificant and hardly distinguishable. The dimensions of the peak increase with decreasing depth of the ground, and the peak acquires the character of a major structural element of the model. The number of ejections is small with greater depths of the

ground, and the ejections consist only of ground matter. The opposite phenomenon is observed at a small thickness of the ground; the amount of ejected matter increases, and the content of impinging substance in this matter is greater.

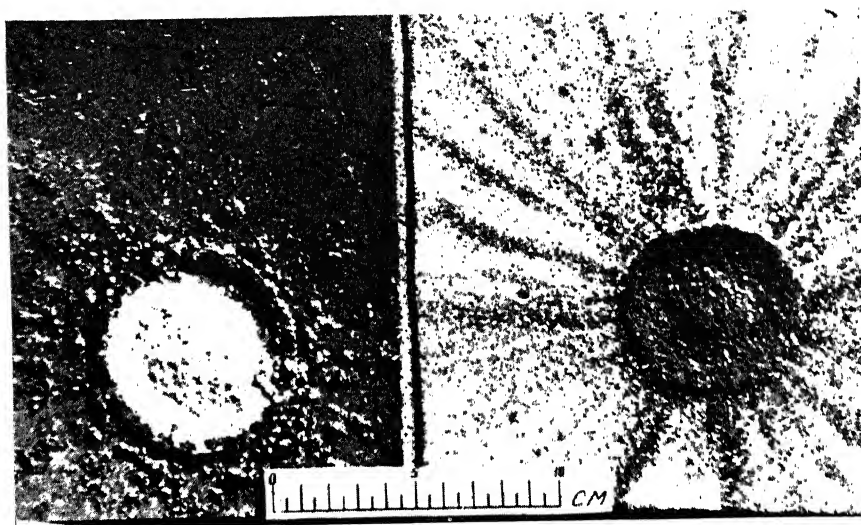


FIG. 9. Craters produced (*left*) by dropping alabaster into loose cement; (*right*) by dropping a cement lump into alabaster.

The presence of a very firm substrate under a thin layer of the soil yielding to deformation is not a necessary condition for producing the forms comparable with lunar objects. The models having a satisfactory similarity with large lunar craters can be obtained also in a thick layer of the ground, provided that the firmness of the latter increases gradually with the depth. At the same time, a level (or nearly level) floor of the crater is a characteristic special feature.

9. The ejection of soil fragments always accompanies the formation of crater models. The diagrams of the trajectories of these ejections are shown in Fig. 11. The ejections from the internal region of the crater originate during the process of its formation immediately near the central peak, where they have maximum velocity. The ejection velocity decreases gradually, and reaches the smallest value near the terminal edge of the ring-shaped wall.

The angle of elevation of the trajectories of fragments obtained under experimental conditions was approximately the same, and always much greater than that of trajectories of ejections of the dropped substance. We discovered that a portion of the fragmentary matter has a speed exceeding the velocity of impact of the crater-forming substance.

The ejection of the ground beyond the limits of the ring-shaped walls always produces strictly radial rays. However, these rays are distinctly visible only in the immediate vicinity of the crater itself. At a distance they yield individual groups of deposits and spots of a shallow matter. The large fragments, falling into a less firm ground, may produce small secondary craters. Under experimental conditions, when the ground and the impinging

matter consisted of cement, the dimensions of small secondary craters constituted most often 0.2–2% of the diameter of the major crater. Less frequent was the formation of secondary craters with a dimension of 5–6%, and a size of 10–12% was exceptional. The small secondary craters are

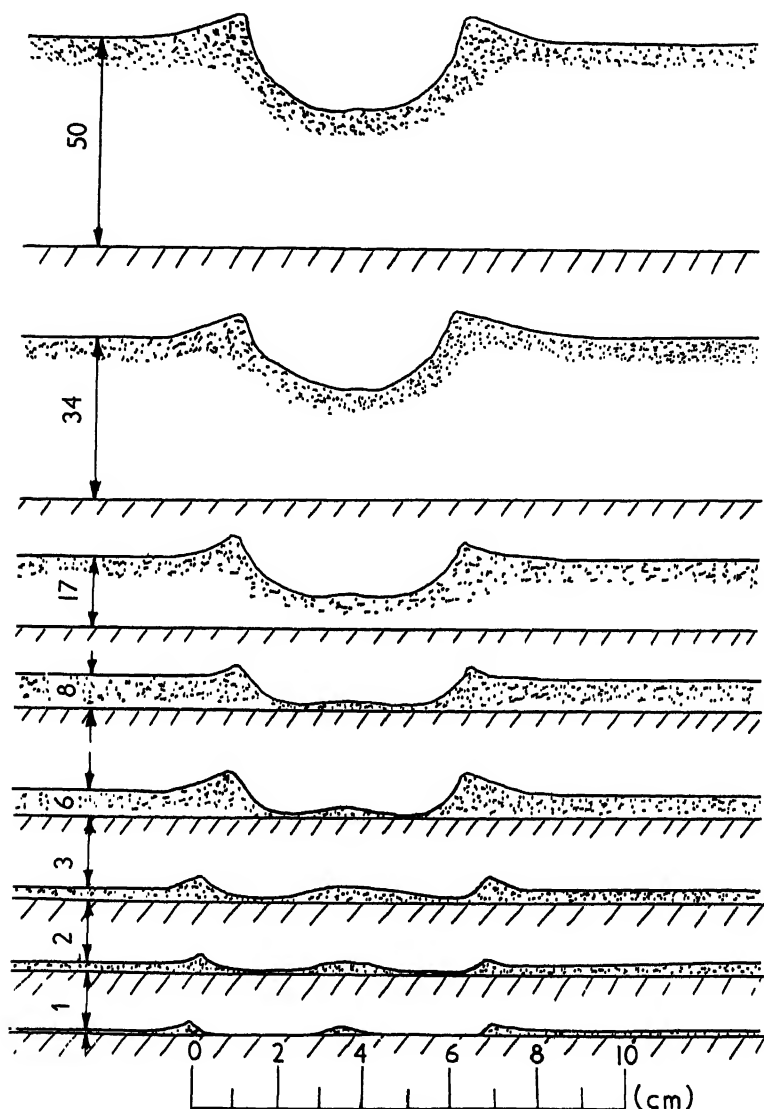


FIG. 10. Change in profile of crater cross-section as a function of depth of soil.

always formed at some distance from the major crater, and for their formation the fragments themselves must have sufficient supply of kinetic energy.

The most remote craters may have their own ray systems. A characteristic special feature of secondary craters consists in their tendency to unite into groups composed of small, almost exactly rectilinear chains. Figure 12



shows the picture of secondary craters. Clearly visible here is a crack, connecting three craters arranged in one line, produced on fixation of the model by wetting it with water. In order to fix small surface features of the model, the latter was wetted slightly by sprinkling. Upon formation of a thin

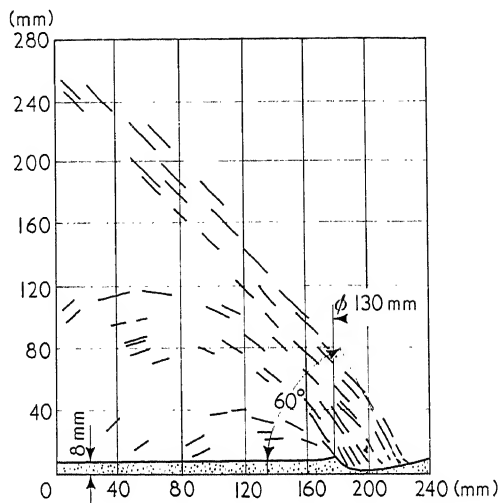


FIG. 11. Trajectory of ejection of soil fragments accompanying crater formation.



FIG. 12. Secondary craters.

surface crust the wetting was conducted more intensively until the liquefaction of cement beneath this crust was achieved; this liquefaction caused the cracking of the crust.

It should be noted that, regardless of the method of producing cracks in the layer of soil (mechanical, physico-chemical, etc.), these cracks always tend to unite the chain of small craters. The impinging matter forms, on its ejection beyond the limits of the crater, straight bands of a finely dispersed matter. Under experimental conditions the range of this kind of ejections is usually somewhat smaller than the flight range of fragmentary matter, which is explained by a smaller elevation angle of trajectories and by an increased aerodynamic resistance of finely pulverized particles. This kind

of ray begins frequently at a certain distance from the ring-shaped wall. The eccentricity in orientation of a portion of rays is revealed almost consistently.

Breaks of the wall's edge cause the formation of unilaterally oriented bands of dropped matter. The above experimental material, as well as the results of experiments with the hydraulic model which made it possible to observe rapidly occurring phenomena in a form fixed for a long time, permitted setting up the scheme of the crater formation process shown in Fig. 13.

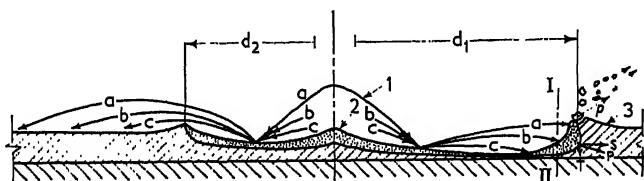


FIG. 13. Cross section

- (1) The cone of dropped matter. (2) Dropped matter which was deposited inside the crater. (3) Superficial, deformed ground.

The mass of impinging matter, consolidating and expanding the ground layer, produces an initial depression in this ground. A portion of its matter, having lost the initial resource of kinetic energy, forms the central peak. The remaining portion of the matter produces a stream radially diverging from this peak. Due to the re-distribution of kinetic energy induced by impact, the speed of this stream turns out to be higher than the speed of impact.

The radially diverging streams, reflected from the bottom of the formation and from each other, produce in a weak ground (see the right-hand part of the diagram) a ring-shaped chamber in which pressure  $P$  is created. A break of the upper edge of the ring-shaped wall occurs in quadrant I under the action of this pressure. The fragments, emerging at the same time, produce ejections and accumulations near the ring-shaped wall. In quadrant II the pressure force  $P$  is divided into two components: I—the force consolidating the soil, and  $T$ —the force expanding it, i.e. producing breaking stresses in this soil. Upon an impact against the wall of the ring-shaped chamber the impinging matter is deposited at the floor of the crater, and its penetration beyond the limits of the ring-shaped wall is negligible.

The pressure in the ring-shaped chamber decreases in proportion to the amount of used-up impinging matter and to the increase in diameter of the crater. The increase in diameter of the ring-shaped wall is discontinued at the moment when equilibrium is established between the dynamic thrust of the radially diverging stream flow and the resistance of the ground.

If equilibrium sets in before the crater-forming matter is used up the latter begins to accumulate near the ring-shaped wall and the level of the floor of the crater increases. In this case the conditions obtain for ejection of the crater-forming matter beyond the limits of the ring-shaped wall (right-hand part of the diagram). The ejections of the crater-forming matter may occur also with greater force of its fall and with a negligible thickness of the soil, through breaks in the ring-shaped wall. At the same time, conditions are created for ejection of fragments of the ground with a speed exceeding the speed of the initial impact.

## CONCLUSIONS

Experience shows that, under laboratory conditions, we can obtain models of craters with all the attributes characteristic for lunar objects and with the correlation of basic dimensions. By varying the conditions of formation we can obtain models which are similar to specific formations on the Moon. This indicates the analogy of the general scheme of processes involved in their creation.

In the crater formation scheme described above we do not detect anything that might change substantially on increase of the scale of the phenomenon and transposition to the lunar conditions. This is valid for relatively moderate speeds of infall, i.e. for a case wherein the impact does not cause any substantial changes in the state of the matter.

Specifically, the conclusions reduce to the following statements:

1(a) Craters and maria with a clearly expressed perimeter emerged as a result of the infall of dense, homogeneous and definitely circular masses of loose matter.

(b) Considerable dimensions of craters and a great range of ejections indicate, first of all, the impact of great masses of matter, but cannot be considered as an incontrovertible proof of very high speeds of impact.

(c) The circular form of the craters indicates that the fall of the matter was essentially vertical. A slight ovality of the ring-shaped wall, the irregularity of internal structure and the orientation of ejections in any one predominant direction indicate possible occurrence of falls inclined to the horizon most frequently rather steeply. All this points out that the impact had occurred mainly under the action of lunar gravity, with a relatively moderate speed on the order of 2400–3000 m/sec. The formation of craters was accompanied by an appreciable heat liberation; however, explosive phenomena could not have taken place at the same time. Only small craters with bright rings can be related to explosive formations on the Moon's surface. Precisely these formations turn out to be morphologically comparable with terrestrial meteoritic craters and pits caused by explosions.

(d) The virtual absence of twin forms with a straight partition indicates a considerable dissociation of falling masses in space before they have been attracted by the Moon. These premises make it possible to assume the past existence, near the Earth, of a large number of small-mass satellites besides the Moon. The orbits of these satellites were close to the Moon's orbit, which brought about their infall on the Moon's surface and which caused the formation of craters.

The cohesion of these satellites was insignificant. They constituted the planetary embryo.

2. An appreciable number of small craters may have emerged as secondary formations. They were produced as a result of fragments being ejected during the formation of large craters.

3. The Moon's surface is covered with matter consisting of hard rock with a lower firmness than the deeper layers. It is possible that the cohesion of the surface material increases with depth.

The surface layers in the regions of large craters consist largely of accumulated and fragmentary matter made coherent by subsequent processes of mineralization.

A considerable amount of heat must have been released during the crater

formation, and a portion of the impinging substance and ground matter should have melted completely. Hence, we can assume that outer layers of the Moon's surface contain an appreciable amount of hardened splash chondrules. These chondrules may have, upon fracture, a microporphyrlic structure, the result of incomplete melting of the initial ground matter.

4. The formation of craters was accompanied by the ejection of fragments of surface rocks into interplanetary space. We can assume that a considerable portion of chondrite-type meteorites may have originated in this way.

5. Individual special features of the structure of each lunar crater are explained first of all by stratigraphic conditions existing, in place of its formation, mechanical properties of rocks and, possibly, by the influence of atmospheric medium. The individual features of the crater's structure are finally determined by the state of tectonic conditions in the locality where the crater was formed.

#### REFERENCES

1. Stanyukovich, K. P. and Fedynsky V. V. Concerning the destructive action of meteoritic impacts. *U.R. Acad. Sci. U.S.S.R.* 57, no. 2 (1947).
2. Sabaneyev, P. F. Concerning the origin of lunar craters. *Bull. astr.-geodet. Soc. U.S.S.R.*, no. 13/20 (1953).
3. Sabaneyev, P. F. On the origin of small craters on Moon's surface. *Bull. astr.-geodet. Soc. U.S.S.R.*, no. 16/25 (1955).
4. Sabaneyev, P. F. Causes of differences in the structure of bright ray aureoles of craters. *Bull. astr.-geodet. Soc. U.S.S.R.*, no. 17/24 (1956).
5. Sabaneyev, P. F. Results on the models of lunar craters under vacuum conditions. *Bull. astr.-geodet. Soc. U.S.S.R.*, no. 17/24 (1956).
6. Sabaneyev, P. F. Results of modeling of lunar craters at reduced gravity. *Bull. astr.-geodet. Soc. U.S.S.R.*, no. 21/28 (1958).
7. Sabaneyev, P. F. Results of modeling of lunar craters in a ground of non-uniform firmness. *Bull. astr.-geodet. Soc. U.S.S.R.*, no. 23/30 (1958).
8. Sabaneyev, P. F. Results of modeling of lunar craters on a spherical surface. *Bull. astr.-geodet. Soc. U.S.S.R.*, no. 24/31 (1959).
9. Sabaneyev, P. F. Note on the problem of the origin of meteorites. *Bull. astr.-geodet. Soc. U.S.S.R.*, no. 25/32 (1959).



# PROCESSES ON THE LUNAR SURFACE

T. GOLD

*Cornell University, Ithaca, N.Y., U.S.A.*

THE coloration of the Moon in light and dark areas requires a remarkably specific interpretation and is therefore a good starting point for the discussion of processes on the lunar surface. It is generally true that the high ground is light and the low flat ground is dark. Generally the ray material ejected from craters both in the high and the low ground is light (there are a few exceptions). The light ray material is present only in association with craters judged youngest on all other evidence, and it must therefore be supposed that such ray material does not show on the surface for long, compared with the age of most features.

Most simple interpretations of these effects run into difficulties. If, for example, it was supposed that the darker material was lava which had filled the low ground, then it would be necessary to suppose that infalling meteoritic dust had not obliterated that distinction of color. The only way it could have failed to do that would be by removing through evaporation more than it supplied to the Moon. This is a possibility stressed by F. L. Whipple; I do not believe it to be the case. One would then have to suppose that the ray material is also removed in the course of time, to account for the disappearance of the older rays. Why then is ray material in the dark ground—supposed lava in this explanation—just as light as the ray material in the highlands?

Both highland and maria ground would in this case have on their surface pulverized material due to the destruction from the small-scale impacts, and such material would nevertheless have to appear darker where it is "lava" than where it is highland ground. Why then does the other finely powdered material making up the rays not maintain a similar distinction?

If, on the other hand, the infalling material adds more than it evaporates (as I think more likely in accord with a theory of origin by solid accretion) then the conclusion has to be avoided that it all will be covered with a layer of uniform material. Even the present rate of infall, which presumably is lower than the rate has been in the remote past, would already suffice to do this in a few million years. Such a conclusion is clearly ruled out unless there are other processes which all the time make for a differentiation between low and high ground.

It seems that a satisfactory explanation can be found only if one allows the possibility of transportation of material over the lunar surface. In that case the following sequence of events may take place: material may constantly be removed from the high ground, presumably in finely powdered form, and migrate to the low ground. All the ionizing radiation from the Sun and the particle bombardment which the Moon receives is absorbed in a very thin layer of material on the surface, and this material therefore will show very substantial radiation damage. It is known that most silicates change to a darker color as a consequence of such crystallographic damage.

If the dark color is now attributed entirely to radiation damage, then those areas whose material has longest been exposed on the surface will appear the darkest. On the slopes of the highlands fresh material would constantly be exposed as the erosion proceeds. On the low ground the top layer will be composed of material which had been on the surface for the period of at least its entire migration. Areas of sediment would therefore be dark, eroding areas would be light. The rate of infalling meteoritic powder would have to be low enough by comparison with the surface migration so as not to dominate the coloration.

The appearance of the rays can then also be explained. They would now be composed of the same basic material, only in a different physical form on the low ground and the high ground. It is therefore not surprising that an explosion throwing out ray material will generate rays of similar coloration. As in the process of the explosion the finely divided material certainly gets heated, probably to the vicinity of its melting point, any crystallographic radiation damage which it may still have possessed would disappear, and the light color would result in each case. The same process of radiation darkening will then suffice to assure the disappearance of the rays at a faster rate than any other physical process that can be discerned to have occurred on the lunar surface, and this is clearly what is required.

Since no other way has been suggested of accounting adequately for the coloration effects, it seems that one has to take account of surface transportation and investigate both its consequences as well as the processes that could give rise to it.

The lunar formations strongly suggest that a process of erosion has taken place that has greatly reduced the height of older formations. This reduction in height may in some cases be as much as 4 km, but for the great majority of crater formations the amount missing, compared with new craters of the same diameter, is much less than that. I have elsewhere stressed [1, 2, 3] the importance that electrostatic forces may have for transporting finely powdered material downhill and I have considered the possibility that all low flat ground may be the consequence of the deposition of material transported from the high ground. The type of erosion process that would then be required would have to be one that characteristically causes very flat deposition, for the Moon shows quite generally a remarkably abrupt division between the low flat and the high rugged ground. The erosion process must therefore have the property of transporting particles with almost zero limiting friction, so as to make flat deposits. On the other hand, it must be an extremely slow process working at a rate of denudation of the high ground of considerably less than one micron per year, if an age of 4 or 5 billion years for the older features of the Moon is assumed.

In general in an erosion process one can discuss two phases, namely the liberation of a particle into the transportable phase, and the actual transportation mechanism. What we would require for the erosion on the Moon is that the bottleneck should be in the first process. Particles should not easily be made available in a transportable form, but once they are so available the transportation mechanism should take them to fill in any local minimum of height, even if the approaches to that minimum possess only extremely slight gradients. A "fluidization" process is required in which the material that is fluidized is very fluid indeed so as to fill in low regions almost as flat as a liquid would have done, but where on the other hand only

a very small amount of material is at any time put into this extremely fluid form. As we shall see electrostatic processes are of the kind that can do just that.

We have investigated many actions that may be responsible for the transportation of material over the lunar surface, and electrostatics seems by far the most important. Thermal variations, radiation pressure, forces arising from traces of gas, cycles of evaporation and condensation, all these would seem in the present circumstances to be unimportant agencies compared with a variety of electrostatic effects that must be expected.

In no case could substantial amounts of material be moved as large pieces, and the transportation must certainly be preceded by a destruction into fine powder. Meteoritic impacts will certainly do this, as will also the radiation effects if the dust produced is constantly swept away and therefore does not give protection. It may even be that dust is an original major constituent of the Moon, which of course will have been tightly compacted at some depth but may not have been subjected to any great compaction or heating close to the surface. In any event dust is likely to be common on the Moon's surface and the thermal measurements certainly require a material of low thermal conductivity and low volumetric specific heat, which would fit well with dust.

Light as well as the harder radiations and the particle bombardment from the Sun all cause the emission of secondary electrons on the surface. Electrostatic effects can then be expected. They will be limited to phenomena on a scale small compared with the Debye length in the resulting electron gas, or the general solar system plasma, while on a scale larger than this all electrostatic effects will be shorted out. The Debye length in the densest electron gas that may be produced above the lunar surface would still be as large as some centimeters, and it is certain that small dust particles will therefore acquire quite erratic charges which are not immediately discharged by the surrounding plasma. Two processes can then be distinguished that would cause surface creep. Firstly it will occur that neighboring particles will acquire a large charge of similar sign in the course of these erratic charge distributions, mainly caused by the sunlight and the photoelectric effect. Two such particles may then jump apart if they are not too firmly welded to each other. Such a process of "electrostatic hopping" may tend to move particles frequently and make them jump a little way. The statistical consequence of such hopping as of any other surface agitation would of course be a transportation downhill.

An estimate of the effectiveness of such a process can be made as follows: If the photoelectrons had a mean energy of say 1 eV, then the departure of the potential of one particle from the mean will occur in a random way until it has reached a substantial fraction of 1 V. Within one-tenth of a volt the addition and subtraction of electrons at random but statistically equal rates will make it a simple random walk problem. For a particle of a size of  $10\ \mu$ , the removal of 1000 electrons will imply a potential of about one-tenth volt. At a rate of emission of  $10^{11}$  electrons/cm<sup>2</sup> sec the removal of say 200 electrons by this statistical process would occur on an average once every 4 seconds, and since any particle will spend a substantial fraction of its life, namely nearly half, at a positive potential exceeding one-tenth volt, any pair of particles may jump every 10 seconds. For this case the force separating them initially would be  $2.5 \times 10^{-9}$  dynes, which is considerably



in excess of the weight of such a particle, and is a force that would have to be compared with any possible slight adhesion between neighboring particles.

An electrostatic process that may be of considerably greater importance for the surface transportation is one of electrostatic "gliding". This occurs in the following way: the constant emission of electrons from the Moon's surface will produce a distribution of potential whereby the body of the Moon itself is at a potential of several volts positive, surrounded by a space-charge of electrons, mostly in transit between emission and return to the lunar surface. The outer fringes of this space-charge cloud approach zero potential—the potential at infinity.

One can follow the usual discussion of the potential distribution in a thermionic space-charge. For an emission of  $10^{11}$  electrons/cm<sup>2</sup> sec the space-charge cloud would be confined almost entirely to a height of less than 2 cm and most of the potential gradient would occur within the first few millimeters above the surface (for a smaller rate of emission these dimensions would be larger). The total potential to which the Moon will in fact be raised is hard to estimate, since it depends critically on the density and temperature of the solar system plasma in its vicinity, but it can safely be predicted to be between 3 and 30 V. For the present discussion it is only the potential gradient close to the surface that matters and this is only very insensitively dependent upon the value of this potential. The distribution of charge and potential near the surface is given by the great number of low energy photoelectrons while it is only the manner in which the space-charge and potential tails off far away that is dependent on the few high energy photoelectrons (Fig. 1).

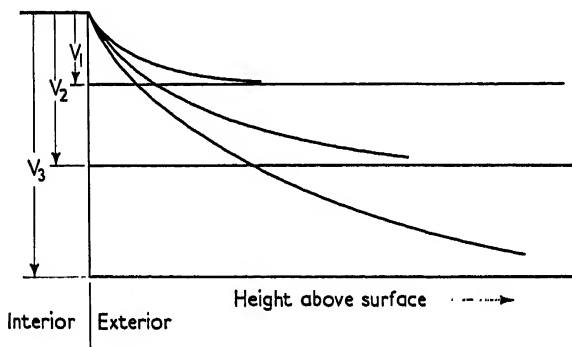


FIG. 1. A schematic diagram to illustrate the distribution of potential above the lunar surface. Whether the potential of the Moon is raised to  $V_1$  or  $V_2$  or  $V_3$  does not affect significantly the field near the surface. The near field is determined by the large number of low energy electrons released from the surface by photo-effect or bombardment. The far field and the total excursion of potential are determined by a small number of high energy electrons and a current bringing in electrons from the general ambient plasma.

An estimate of the potential gradient just above the surface that the space-charge may produce would be in the neighbourhood of 3 V/mm or a field of one-tenth esu. Any dust grain which is lifted some millimeters

above the surface for any reason whatever may then experience a force large enough to cause it to float. With 100 electrons missing from the dust grain, which will be a very common situation, it would experience a force of  $5 \times 10^{-9}$  dyn, sufficient to float particles of  $1 \times 1 \times 10 \mu$  in size. Substantially larger charges than this can be occurring frequently, and the process may then work with lower rates of electron emission.

If any disturbances occur on the surface that release and lift up dust grains such as the impacts of micrometeorites, or the electrostatic hopping discussed earlier, then the grains that are so lifted up will find the potential gradient insufficient to support them anywhere except in a very thin layer above the surface. If a particle was lifted up to a great height then it will no doubt fall back to the surface with the electric effect unable to arrest its momentum. But if it had been lifted up to a height not greatly in excess of that at which it could float, then it may remain suspended.

Any slope on the Moon's surface will now cause such a floating particle to glissade downhill. It will be supported above the surface everywhere, but there will be no force whatever resisting the component of gravity parallel to the inclined surface, and the particle will thus make a frictionless descent. The distance to which it can go in this way must be limited in practice by the roughness of the ground, for in this frictionless glissade it will soon acquire a speed where even a slight undulation of the ground will be sufficient to imply inertial forces which will exceed the electrostatic support. Particles will thus be precipitated in such places and it is probable that this will in general result in the smoothing out of slopes and the filling in of all small depressions. This glissading process would make it possible for the low regions to be filled in very nearly accurately flat, for the particles that are lifted will there continue their frictionless flow even over the slightest gradients. As we have seen earlier the interpretation of erosion and deposition would require just such a flow of material where at any time only a very small quantity was being transported but where the fluidity of the material in transit is extremely high.

The thermal data which are now available from radio thermal measurements appear to fit the dust hypothesis of the lunar surface very well. The uppermost layer may be composed of material that has a density of between one-third and one-sixth of the compact solid, with a grain size in the general range between 1 and  $10 \mu$ . The slight welding that occurs commonly (though not always) at the contact point between two grains when their surfaces are free from adsorbed gases, will in fact allow a very loose structure to be built up. In the absence of such welding the dust grains would tend to slide closer together and pack more tightly, while in the vacuum case many particles will remain supported when they first make contact and a fluffy, very compressible structure is likely to result. On the mare type of ground all would be dust only according to the present interpretation. On the highlands most of the surface would also be dust, but a certain fraction of denuded more solid material must be showing through at all local high spots. On a scale of centimeters the ground must be expected to have been rough enough to assure the existence of very many local minima of height. Since all those must get filled up before a further transportation of dust downhill can take place, it is likely that a large proportion of the ground there would be filled to a height of at least a few centimeters and possibly more. Even though most of the highland surface would also be dust in this explanation, it would

generally be dust that had only suffered a short surface exposure and new material would constantly be exhibited. All this is therefore still lighter than dust that has come to be deposited in the lowlands and is no longer stirred up and turned over.

The radio thermal data quoted by Salomonovich support the conclusion—quite contrary to any lava hypothesis—that the mare type of ground is the one of the smaller heat conductivity. This is what would be expected if the high ground had a mixture of dust and solid material on the surface or if the solid material was generally present at a shallow depth, while on the low ground the dust was generally deep.

The interpretation of the lunar features in terms of dust is by no means in conflict with cracks and steep slopes that are seen in a few places in the maria. On the scale on which such things can be seen at present—about 1 km—the dust would certainly be compacted and it would have enough internal friction to allow vertical slopes to be exposed. The common formation of rills that are circumferential near the edges of the maria could be accounted for by the compression of the dust deposit as more and more dust is sedimented. The dust layer would sink most where the dust is deepest, which is likely to be in the middle of a mare, and this distortion is in the sense of stretching the surface most in the vicinity of the periphery where rills would therefore be expected to appear in a peripheral pattern.

Radio thermal measurements have now shown that the crust of the Moon below the diurnally varying layer is at a temperature of 25 to 30°C below the freezing point of water. This leads to an interesting consequence. If the Moon was initially composed of hydrated silicates like the Earth, then the release of internal heat will have caused water or water vapor to percolate towards the surface. In the case of the Earth such water could come freely through all the pores of the ground and accumulate there to make the oceans. In the case of the Moon the situation is quite different. Not only would any water reaching the surface quickly evaporate into space and be lost, but there is also now a different process of percolation through the ground. That layer in which the temperature is below the freezing point of water, which is likely to be more than 1 and less than 10 km thick, would block the escape of water by freezing up all interstices. Water could escape to the surface in large cracks in which it flows sufficiently fast not to be cooled to the temperature of the surrounding material, but all the fine cracks and gaps in the material will be filled with ice. At a depth that may be estimated of the order of 30 m, the evaporation to the outside will keep the ground free from ice, but below that depth the evaporation would be extremely slow so that even a very slight rate of supply from beneath would compensate. It is hard to escape the conclusion that there is a general ice-table in the lunar ground, for extremely slight rates of liberation of internal water would have been sufficient to form it. The existence of such an ice-table will of course become an important topic for lunar exploration in the future.

There are some lunar formations which are hard to account for by the processes of meteoritic impact and surface erosion, but which suggest that some internal motion has taken place. It may be that the water below the surface, the internal glaciation as it were, may be responsible for some of these features.

The author is grateful to the General Motors Corporation for support of this and associated experimental work.

REFERENCES

1. Gold, T. The lunar surface, *Mon. Not. R. astr. Soc.*, **115**, 585 (1955).
2. Gold, T., Dust on the Moon, "Vistas in Astronautics," Vol. II. Pergamon Press (1959).
3. Gold, T., The Moon, "Space Astrophysics", McGraw-Hill (1961).



# LABORATORY SIMULATION OF LUNAR LUMINESCENCE†

J. E. GEAKE, H. LIPSON, M. D. LUMB

*Physics Department, College of Science and Technology,  
Manchester, England*

WORK has recently begun in the Physics Department of the Manchester College of Science and Technology on an attempt to simulate lunar luminescence in the laboratory. This programme is running parallel with that of our colleagues in the Manchester University Astronomy Department, who are making observations of the luminescent spectrum of the Moon itself. Our instruments are as yet only partly completed, but we will describe briefly what they are to consist of, in the hope that we may benefit from the comments of others in the same field, and arrange to co-ordinate our work with theirs.

The instrument is to consist of three parts; a small evacuated chamber in which dust or rock samples may be placed, equipment for exciting luminescence, and a recording photoelectric spectrophotometer for investigating the luminescent spectrum.

## EXCITATION EQUIPMENT

Provision is being made to excite luminescence by means of either UV radiation or corpuscular beams (protons of 10–120 keV and possibly electrons); X-radiation may also be used.

The UV excitation equipment is practically complete, and consists of a choice of two lamps: (a) a hydrogen lamp, which gives a continuum between 2000 Å and 3500 Å and is followed either by filters giving crude wavelength selection over 500 Å bands, or by a small monochromator (Hilger D290) giving bands a few Å wide; (b) a mercury lamp followed by filters, giving radiation mainly at 2537 Å.

The proton source, construction of which has started, will consist of a hydrogen-ion source copied from one at Birmingham University, a high-voltage supply variable from 10–120 kV, and a single-stage accelerating tube consisting of a Pyrex glass cylinder supporting the accelerating electrodes. The ion source will be RF excited, and supplied with hydrogen gas through a nickel leak. A bend in the system between the poles of an electro-magnet, just before the sample chamber, will enable protons to be selected from the impure ion beam. The proton beam will be used at a density (about  $10^3/\text{cc}$ ) which simulates the solar proton stream received by the Moon.

The high-voltage supply will be the smoothed output of an RF oscillator; the output polarity will be reversible, so that electrons from a filament source may be accelerated as an alternative form of excitation.

†Supported by Contract AF61(052)-379 between the Department of Astronomy, University of Manchester, and the Geophysics Research Directorate, Air Research and Development Command, U.S. Air Force, through its European office in Brussels.

## OPTICAL EQUIPMENT

The luminescent spectrum will be investigated by means of an  $f/9$  Ebert grating monochromator, which is nearly complete, and is shown in Fig. 1. It is of four-poster construction, with a single 14-in. spherical mirror of 72 in. radius of curvature lying on its back on a nine-point support on the base plate. The grating is suspended from the top plate on a pair of kinematic pivots made from 1-in. steel bearing balls. The entrance and exit slits are symmetrically placed on either side of the grating, and mounted in focusing tubes. A series of pre-set fixed slits are used, which locate kinematically when interchanged. The spectrum is to be scanned by tilting the grating by means of a lever and micrometer drum. The drive for this, which will consist of a synchronous motor and change gears, has yet to be made.

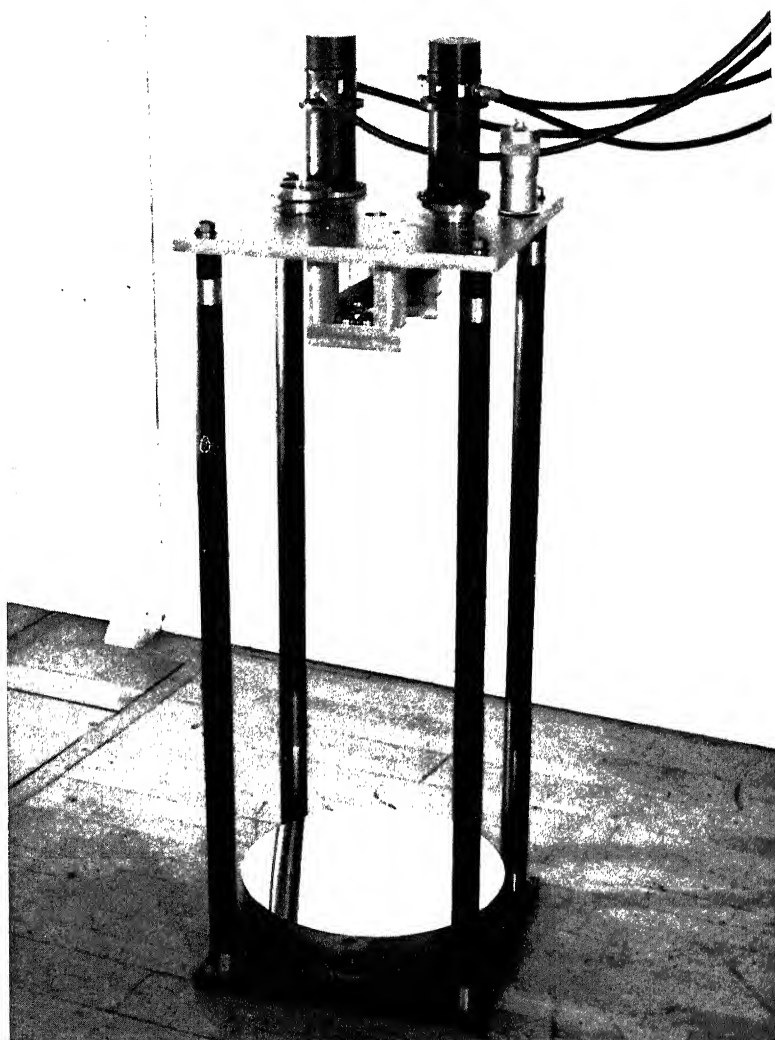


FIG. 1. An  $f/9$  Ebert grating monochromator.

A mirror will direct the light from the sample to the entrance slit of the monochromator. Two photomultipliers will be attached to the monochromator: one to the exit-slit mounting, to scan the spectrum as the wavelength passed is varied, and the other so as to receive a sample of the undispersed light just after the entrance slit.

The grating to be used is a 5 in.  $\times$  4 in. Bausch and Lomb replica with 1200 lines/mm and blazed at about  $26^\circ$ , or 7500 Å in the first order. This enables the range 3500 Å to 11 000 Å to be used at reasonable efficiency in the first order with a dispersion of about 12.0 mm/Å (8 Å/mm), and up to

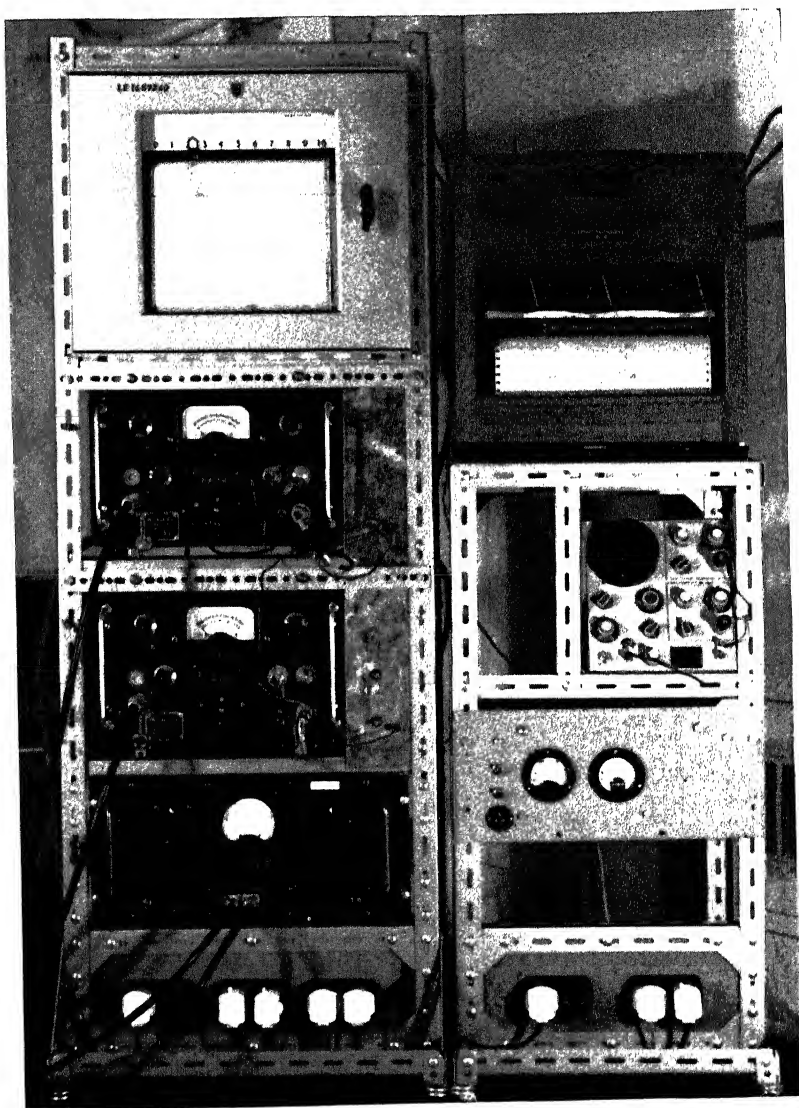


FIG. 2. Electronic equipment.



about 5500 Å in the second order with double the dispersion. This large grating is used to obtain a high luminosity (as defined by Jacquinot): the potentially high resolving power is not needed for the present luminescence investigations, but is a useful by-product which may be used for other purposes.

#### ELECTRONIC EQUIPMENT

The electronic equipment is virtually complete, as shown in Fig. 2, and consists of a two-channel photometer and a ratio-taking recorder. One channel will scan the spectrum while the other monitors the undispersed light to remove the effect of source fluctuations. The detectors to be used alternatively are pairs of EMI 6256 or 9558 photomultipliers, each followed by a DC amplifier. A potentiometric recorder has been modified to take ratios. A separate three-channel recorder monitors the two channel outputs and repeats the ratio alongside.

#### OTHER EQUIPMENT

The sample chamber and corpuscular beam source will be evacuated (to about  $10^{-6}$  mm of mercury) by a 2 in. oil diffusion pump. Provision is being made for either heating or cooling the sample, and for measuring its temperature. The incident corpuscular flux will be measured by means of an ionization chamber, with a grid to repel secondary emission.

The work described is being carried out under contract with the USAAF to whom we are grateful for funds. We are also grateful to Mr. J. McConnell for constructing the mechanical parts of this equipment, and to the Manchester College of Science and Technology for providing facilities.

# LUNAR LUMINESCENCE†‡

J. F. GRAINGER, J. RING

*Department of Astronomy, University of Manchester, England*

PHOTOMETRY of the penumbra of lunar eclipses over a considerable number of years has shown an excess of light over that which can be reasonably explained as an effect of the Earth's atmosphere. Link [1, 2] introduced the hypothesis of surface luminescence on the Moon and showed that it could account for the eclipse phenomenon. However, it is clear that eclipse observations cannot be used to investigate the detailed spectrum and distribution of the luminescent regions. A more powerful approach was suggested by Link [3] which has subsequently been called the "line depth" method.

Let us suppose that in the wavelength interval  $\lambda$  to  $\lambda + d\lambda$ , the flux of solar energy at the Earth's surface is  $I(\lambda)d\lambda$ . A Fraunhofer line at wavelength  $\lambda_0$  will show up in a graph of  $I(\lambda)$  against  $\lambda$  as indicated in Fig. 1(a). Let us define the depth of the line as

$$R = \frac{\text{Deepest level}}{\text{Continuum level}}.$$

In the case of the Sun we have

$$R_s = \frac{b}{a}. \quad (1)$$

In the absence of luminescence, the light received from the Moon is simply the sunlight incident upon it, attenuated by a constant factor  $r$ . Thus, in the lunar spectrum, the same lines will appear with the depth

$$R_m = \frac{rb}{ra} = R_s. \quad (2)$$

However, in the presence of luminescence, there will be an additional amount of light,  $k$ , which we may suppose constant over the width of the Fraunhofer line; for even if the luminescence spectrum has the usual band structure, these bands are likely to be at least fifty times as wide as the Fraunhofer line (see the dotted line of Fig. 1(b)). In this case the depth of the line in the lunar spectrum will be

$$R_m = \frac{rb + k}{ra + k} \neq R_s. \quad (3)$$

We can express the amount  $k$  of luminescence in terms of the continuum

†Astronomical Contributions from the University of Manchester, Series III, no. 88.

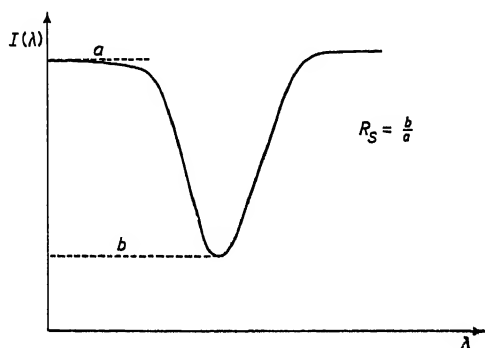
‡Supported under Contract AF61(052)-378 between the Department of Astronomy, University of Manchester and the Geophysics Research Directorate, Air Research and Development Command, U.S. Air Force, through its European Office and by a grant from the D.S.I.R.

level in the absence of luminescence (a simple relation exists between this and the observed continuum) by means of the dimensionless parameter  $\rho$ , defined by

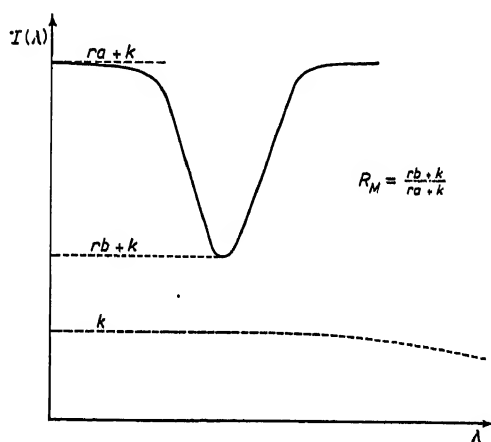
$$k = \rho a. \quad (4)$$

If so, equation (3) becomes,

$$R_m = \frac{b + \rho a}{a(1 + \rho)} = \frac{R_s + \rho}{1 + \rho}. \quad (5)$$



(a)



(b)

FIG. 1. Fraunhofer line in the spectrum of (a) the Sun (b) the Moon (with luminescence).

the solution of which gives

$$\rho = \frac{R_s - R_m}{R_m - 1}. \quad (6)$$

Thus measurement of  $R_s$  and  $R_m$  is sufficient to give the fractional luminescence.

Observations have been made using this method by Dubois [4] and Kozyrev [5]. The former used a variety of solar spectrographs of different

dispersions and has taken many plates of different lunar regions, but restricted his observations to five prominent Fraunhofer lines in the visible spectrum. Kozyrev, on the other hand, using a single low dispersion spectrograph (50 Å/mm at 3900 Å) has observed several points on the Moon, but only in the *H* and *K* lines. This makes it difficult to compare the results obtained by these two observers; however, they have both found evidence for the existence of luminescence and have also reported time-variations in its intensity.

Both these observers used photographic spectrographs and did not seem to have considered fully the effect of inherent errors in photometry on their derived luminescent intensities. Since these intensities amount frequently to only a few per cent of the continuum, it is necessary to perform a detailed analysis of the photometric accuracy required from an ideal instrument before more meaningful results can be obtained.

A consideration of equation (6) assuming errors of  $\delta R_m$  and  $\delta R_s$  in  $R_m$  and  $R_s$  leads to an error  $\delta\rho$  in the percentage luminescence given by:

$$\delta\rho^2 = \left( \frac{1+\rho}{1-R_s} \right)^2 [(1+\rho)^2 \delta R_m^2 + \delta R_s^2], \quad (7)$$

which reduces to

$$\left( \frac{\delta\rho}{\rho} \right)^2 = \left[ \frac{1+\rho}{\rho(1-R_s)} \right]^2 [(\rho + R_s)^2 + R_s^2] f^2, \quad (8)$$

where  $f$  is the fractional error in  $R_m$  and  $R_s$ —i.e.,

$$\delta R_m = f \cdot R_m \quad \text{and} \quad \delta R_s = f \cdot R_s.$$

With a photographic spectrograph there are several sources of error contributing to  $\delta R_m$  and  $\delta R_s$ . Kozyrev's work showed that the Eberhard effect may lead to a spurious change in line depth. In any event, the accuracy in a measured intensity from a single plate will seldom be better than 5%; and the lack of dynamic range in the photographic process may give larger errors at the bottom of a deep line. If we accept the accuracy of 5% in an intensity measurement, then a ratio can be measured at best to 7%.

It is clear that, for a significant difference of line-depth, the ratios  $R_m$  and  $R_s$  must differ by at least  $2\delta R$ . This leads to a minimum detectable luminescence

$$\rho_{min} = \frac{0.14 R_s}{1 - 1.14 R_s}. \quad (9)$$

Thus values of  $R_s$  of 0.1, 0.2 and 0.5 give  $\rho_{min}$  of 1.5%, 4% and 16% respectively. Even the detection of a typical luminescent intensity ( $\sim 10\%$ ) necessitates the use of solar lines with at least 60% absorption at the resolution employed.

However, equation (8) permits us to calculate the fractional error in  $\rho$  as a function of  $\rho$  and  $R_s$ . Typical values are given in Table 1.

It is clear from this that the above minimum detectable amounts will not, in fact, be of any value quantitatively owing to their large uncertainties. They should only be recorded as "luminescence detected, but not accurately measurable".

TABLE 1. Table of Fractional Errors in  $\rho$ 

$R_s$ $\rho$ in %	0.1	0.2	0.3	0.4	0.5	0.6
5	0.29	0.59	0.76	> 1	> 1	> 1
10	0.19	0.35	0.55	0.82	> 1	> 1
15	0.16	0.27	0.41	0.60	0.88	> 1
20	0.15	0.23	0.35	0.50	0.72	> 1

If, however, we can somehow make the error in  $R_s$  negligible in comparison with that in  $R_m$ —which should after all be possible, since the solar lines do not fluctuate and can therefore be measured many times—then the expression for  $\delta\rho$  becomes:

$$\delta\rho = \frac{(1+\rho)^2}{1-R_s} \delta R_m, \quad (10)$$

which on being expressed in terms of  $\delta R_m/R_m$  becomes

$$\delta\rho = \frac{(1+\rho)(\rho+R_s)}{1-R_s} \left( \frac{\delta R_m}{R_m} \right). \quad (11)$$

If we can also increase the accuracy of  $R_m$  to about  $1\frac{1}{2}\%$  then we can write the fractional error in  $\rho$  as:

$$\frac{\delta\rho}{\rho} = \frac{3(1+\rho)}{200\rho} \frac{\rho+R_s}{1-R_s}. \quad (12)$$

Substituting typical figures again of  $\rho = 10\%$  and  $R_s = 0.1$ , we obtain

$$\frac{\delta\rho}{\rho} = 0.04$$

i.e. a luminescence of  $10\%$  can be determined as

$$(10 \pm 0.4)\%$$

using a line of depth 0.1. With the previous method, the fractional error was about five times larger (see Table 1).

Even a luminescence of  $1\%$  can be found with a fractional error of about 0.2 using a line with  $R_s = 0.1$  whereas previously it was below the limit of detectability. The very act of observing the lines produces an apparent profile which is shallower than the true one, owing to the finite resolving power of the spectrometer. Whilst it is easily shown that the apparent profiles are still related to the luminescent intensity by the same equation, this effect necessarily increases the uncertainty in the result. Thus the ideal spectrometer should be more than adequate to resolve the narrowest line of interest. The only possible way of achieving these improvements, and also removing the severe limitations on dynamic range which the photographic plate presents, is to use a spectrometer of high dispersion with a photoelectric device as detector. An instrument incorporating these advantages will be described below.

The observations described above have been used to arrive at a specification for an ideal instrument to observe lunar luminescence. If the spectrum is to be explored thoroughly, many lines must be studied; and to allow reasonable photometric accuracy, the spectrometer should completely resolve them. This suggests an instrumental profile of about  $0.2 \text{ \AA}$ , which should correspond to the smallest details seen on the Moon—i.e. the slit should subtend about one second of arc on the sky. If the luminescent intensity is only a few per cent of the scattered sunlight, the photometry must not have errors greater than 1%.

Let us consider an idealized astronomical spectrometer as shown in Fig. 2. Light from the telescope mirror (diameter  $D_0$ ) forms an image in the

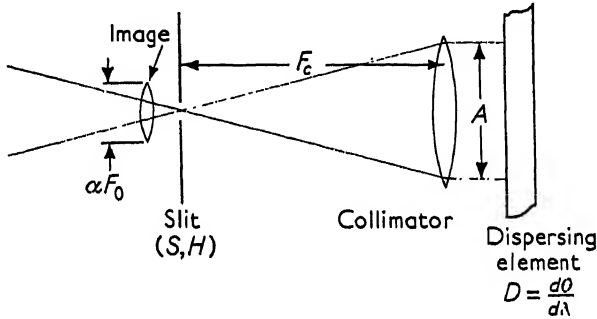


FIG. 2. Idealized astronomical spectrometer.

plane of the entrance slit. The size of this image will be the product of the focal length ( $F_0$ ) of the telescope and the angle subtended by the object (the detail on the Moon being investigated). Let  $S$  and  $H$  represent the width and length of the entrance slit,  $F_c$  the focal length of the collimator and  $D_c$  the aperture of the dispersing element. The angular dispersion  $d\theta/d\lambda$  of this element is represented by  $D$ . The wavelength range given by the slit width will be

$$\delta\lambda = \frac{d\theta}{D} = \frac{S}{F_c D}. \quad (13)$$

The region studied on the Moon will be rectangular, with sides of angular extent

$$\alpha_H = \frac{H}{F_0}, \quad \alpha_S = \frac{S}{F_0}. \quad (14)$$

If one wishes to study the lunar surface in the greatest detail,  $\alpha_S$  and  $\alpha_H$  will both be about one second of arc, but for certain features (rays, for example) the slit may be placed along the object studied with a consequent increase in permissible slit length, resulting in a greater signal. Equations (13) and (14) lead to the relation

$$\alpha_S = \frac{F_c D}{F_0} \delta\lambda \quad \text{or} \quad D = \frac{\alpha_S F_0}{\delta\lambda F_c} = \frac{\alpha_S}{\delta\lambda} \cdot \frac{D_0}{D_c} \quad (15)$$

assuming that the focal ratios of telescope and collimator are equal. The flux of light  $\phi$  from this object must be as high as possible to allow a short time of observation.

If  $B$  is the brightness of the lunar surface (in photons/Å/sq cm/sec/ster), then

$$\phi = \frac{1}{4}\pi D_0^2 B \alpha_S \alpha_H \delta \lambda.$$

If we fix  $\alpha_S = \alpha_H$  and  $\delta \lambda$  at one second of arc and 0.2 Å respectively, we see that (if  $D$  is expressed in seconds per Å)

$$D = 5 \frac{D_0}{D_c} \quad \text{or} \quad D \cdot D_c = 5 D_0, \quad (17)$$

$$\phi = \frac{B\pi}{20} D_0^2. \quad (18)$$

Thus the flux of light will increase with the area of the telescope mirror; but to match a given telescope we shall need to reach a certain product of diameter of dispersing element and dispersive power. If we consider a 50-in. mirror, we find that a grating of about 4 in. diameter with a blaze angle of approximately 30° is required.

It has been shown that the low photometric accuracy of the photographic plate makes it of doubtful value in these observations. However, the photo-multiplier cell can easily give an accuracy of 1%; and since the number of spectral elements to be investigated is only of the order of one or two hundred, its overall sensitivity will be comparable with that of the plate. The photo-cell will be about one hundred times more sensitive, but the spectral elements must be explored sequentially and not simultaneously as with the plate. The dark current of the cell will set the limit to the flux required; but the following calculation shows that, with the instrument considered, this flux is sufficient. The Moon can be regarded as having a brightness of  $+3^m.5$  per square second of arc. One may assume a flux of some  $1.2 \times 10^5$  photons/sec/Å from an object of this size and brightness into a 50-in. mirror, leading to a rate of  $2.5 \times 10^4$  photons/sec into 0.2 Å. If the cell has a quantum efficiency of 10% and again of about  $10^6$  we may expect a photo-current of  $4 \times 10^{-10}$  amp at the collector, as compared with a dark current of the order of  $10^{-12}$  amp from a selected cell cooled with solid carbon dioxide. An integration time of 10 sec will reduce photon shot noise to below the assumed uncertainty of 1%.

This calculation suggests that a d.c. amplifier and recorder can be used to display the line profiles as the spectrum is scanned across the exit slit of the spectrometer. Previous experiments have shown that the worst problem with such a photoelectric monochromator arises from scintillation; but with an extended object this is unlikely to cause trouble. In any case, the difficulty can be overcome by taking the ratio of the intensity measured at the exit slit to that entering the spectrometer.

On the basis of this analysis we have constructed a photo-electric spectrometer specifically to investigate lunar luminescence, using the f/5 Newtonian focus of the 120-cm telescope at Asiago. The dispersing element is a Bausch and Lomb grating (135 × 110 mm No. 33-53-18-36) used with spherical mirrors (Fig. 3). The Newtonian arrangement was introduced after earlier

experiments had shown that off-axis systems—even the Ebert–Fastie mounting—introduced severe loss of resolution due to aberrations consequent upon the use of this high relative aperture. The theoretical resolving power of the grating is 320 000 in second order, leading to an instrumental width of  $0.01 \text{ \AA}$  at  $4000 \text{ \AA}$ . Since it normally operates with equal entrance and exit slits equivalent to  $0.2 \text{ \AA}$  or more, the instrumental profile is triangular, with good suppression of the wings. The focal length is 560 mm, giving a dispersion of  $6.5 \text{ \AA/mm}$  at  $3900 \text{ \AA}$ . The optical components are mounted on a magnesium alloy baseplate. The spectral region of interest is first selected

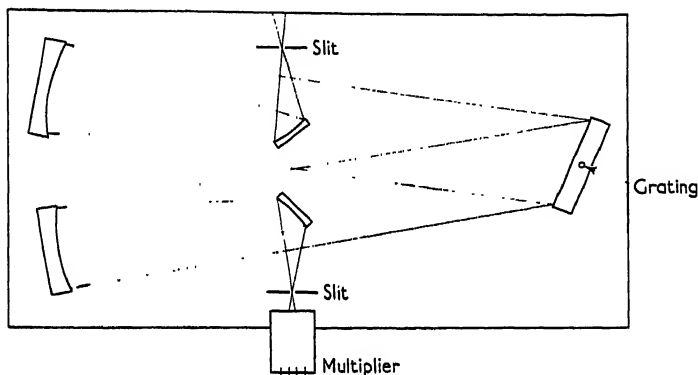


FIG. 3. Luminescence spectrometer.

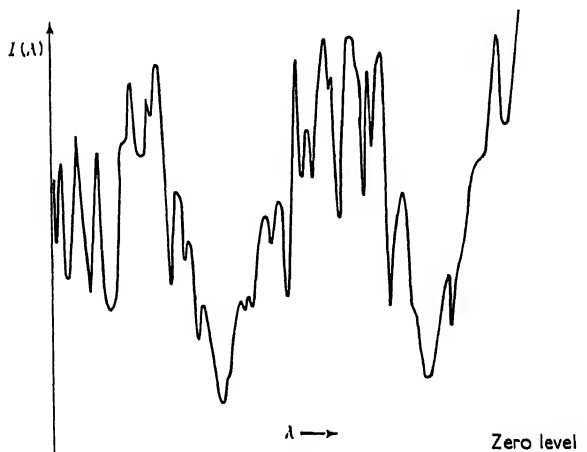


FIG. 4. *H* and *K* lines in the spectrum of moonlight.

by turning the grating, and then the spectrum is scanned across the exit slit by rotating its Newtonian flat. This rotation is effected by means of a motor-driven micrometer screw which bears on a 500-mm arm attached to the small mirror support. A photomultiplier cell is mounted behind the exit slit and can be cooled with solid  $\text{CO}_2$ . The electronic system comprises an Avo d.c. amplifier (type 1388B) and a potentiometric recorder. Full-scale deflection can be obtained from a current of  $3 \times 10^{-13} \text{ amp}$  (corresponding to



a light flux at the photo-multiplier cathode of a few tens of photons per second).

Preliminary experiments with this instrument have shown that, using an area on the Moon 30 secs. long and 1 sec. wide, with a spectral resolution of  $0.25 \text{ \AA}$ , we obtain a photo-current of  $10^{-9}$  amp, whilst the dark current is less than  $10^{-12}$  amp. Figure 4 shows a scan of the  $H$  and  $K$  lines of moonlight obtained in 30 min, from which it is clear that the instrument is eminently suitable for the investigation of lunar luminescence by the "line-depth" method; observations will begin at Asiago in March 1961.

#### REFERENCES

1. Link, F. *C.R.Acad. Sci., Paris* **223**, 978 (1946).
2. Link, F. *Bull. astr. Insts. Csl.* **2**, 131 (1951).
3. Link, F. *Trans. int. astr. Un.* **VII**, 135 (1950).
4. Dubois, J. *Rozpr. České Akad. Věd*, **69**, Part 6 (1959).
5. Kozyrev, N. A. *Izv. Crim. astrophys. Obs.* **16**, 148 (1956).

# INVESTIGATION OF THE POLARIZATION PROPERTIES OF THE SURFACE OF THE MOON

E. K. KOHAN

*Pulkovo Observatory, Leningrad, U.S.S.R.*

At this time of the rapid development of cosmonautics, one of the basic problems of investigation of the Moon appears to be the problem of the matter covering the surface of the Moon. A comparison of various characteristics obtained from studies of the individual regions of the Moon with analogous characteristics of terrestrial rocks led various authors [1-16] to a conclusion that the surface of the Moon is covered with a very porous substance. The mean dimensions of irregularities, as suggested by Barabashev [4] equal 2 to 5 mm, and according to Sytinskaya [2] from 0.1 mm to 10 cm. Fesenkov [17] assumes that the surface of the Moon represents a combination of relatively large grains with weak bonds between each other.

The school of planetary investigators at the Leningrad State University assumes [6-12] that the porous, vesicular substance resembles in structure a volcanic slag. It originated from basic rocks as a result of their transformation under the effect of explosions accompanying the impact of meteorites striking the surface of the Moon. The Kharkov school of planetary investigators [1-4] considers, on the other hand, that the surface of the Moon is not similar to a fused one, but that it is most probably covered with finely crushed tuff rocks with grains of the order of several mm, and in some places large-grain volcanic ashes.

According to the measurements by Markov [5] a comparison of polarization of details of the lunar surface with polarization of fused surfaces of meteorites does not confirm the hypothesis of the continuous fusion of the surface of the Moon. The French scientist Lyot [16] assumes that the Moon is possibly covered by a mixture of ashes with various albedo. The very same conclusion was reached by Dollfus [14-15]. However, Van Diggelen [13] doubts the presence of volcanic ashes on the Moon.

Our experiment is devoted to the study of polarization characteristics of lunar surface formations and numerous ground rocks in accordance with two Stokes parameters: namely, the degree of polarization and angle of orientation of the plane of polarization of the reflected light. We selected thirty-five regions on the surface of the Moon belonging to various types of formations (Fig. 1 and Table 2). These include conventional maria, crater-type maria, craters with central peaks, bays and regions on the continent. They were investigated at various phase angles.

Using the conclusions of the above-quoted authors about the probable dimension of the micro-relief of the Moon, we investigated terrestrial specimens in nonpulverized as well as in pulverized state (with grain dimensions of  $d < 0.25$  mm;  $0.25$  mm  $< d < 1$  mm;  $1$  mm  $< d < 3$  mm) at various angles of incidence and two angles of reflection ( $\epsilon = 0^\circ$  and  $\epsilon = 45^\circ$ ).

The terrestrial specimens which were given to us by Khabakov and Sharonov are listed in the following Table 1:

TABLE 1

<i>No.</i>	<i>Name</i>	<i>Source</i>
1.	Obsidian quaternary	Caucasus Minor
2.	Andesite bubbly lava, quaternary	ditto
3.	Basalt quaternary	ditto
4.	Basalt quaternary	Georgia
5.	Gneissic granite	Transbaikal
6.	Massive biotite granite	ditto
7.	Quartz	Ukraine
8.	Columnar quartz	Eastern Transbaikal
9.	Ocherous limonite	Ural
10.	Volcanic tuff	Trans-Carpathian regions
11.	Volcanic tuff	Georgia
12.	Highly vesicular volcanic slag	—



FIG. 1. Thirty-five areas selected.

Lunar observations were conducted with the aid of the Pulkovo electropolarimeter, attached to the camera shown on Fig. 2. Observations of terrestrial rocks were made with the same electropolarimeter attached to the indicatometer of the planetary laboratory of the Leningrad University.

The use of a rotating polaroid and compensating device, enabling to record large oscillograph deflections and, consequently, large amplitudes of the variable component, permitted to measure the low polarization with a large degree of accuracy at phases close to full Moon. The results so obtained are shown on Fig. 3.

The plane of polarization of moonlight was referred to the intensity equator by observing the polarization of the bright diurnal sky in the zenith, utilizing the fact that the plane of polarization of the sky coincides with the vertical plane of the Sun [18]. For terrestrial rocks this is realized by observing the light reflected by a marblite mirror, in which the plane of polarization coincides with the plane of incidence and reflection.

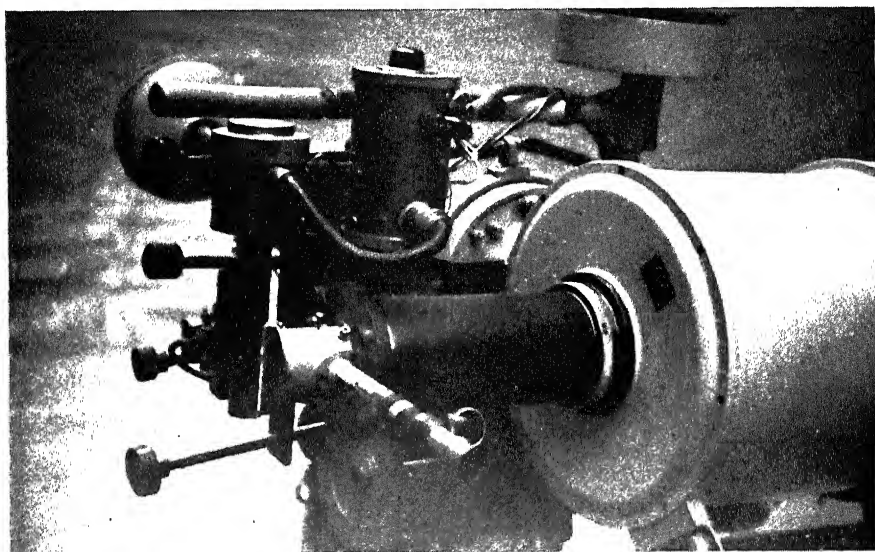


FIG. 2. Pulkovo electropolarimeter camera.

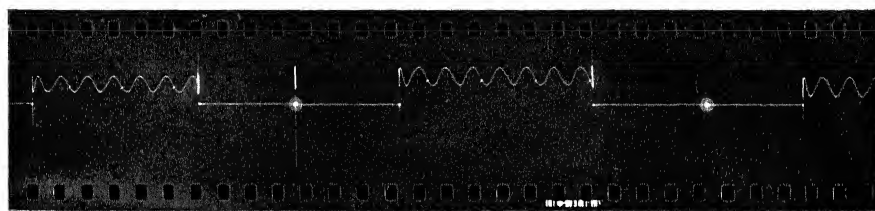


FIG. 3. Results obtained from a rotating polaroid and compensating device.

On the basis of results obtained by studying the angle of orientation of the plane of polarization  $\gamma$ , it is possible to conclude that:

1. The angle of orientation of the plane of polarization on the Moon for a given phase does not depend on the position of the detail on the lunar surface—i.e. it does not depend upon the angle of reflection  $\epsilon$  (Table 2).
2. This angle depends upon the phase angle  $\psi$  (Fig. 4). At large phase

TABLE 2

No.	Phase angle, date Name	−97°	−53°	−20°	8°	Lunar coordinates	
		4.III	8.III	11.III	13.III	$\varphi$	$\lambda$
1	Albategnius		67°	−21°	−26°	−11°7	+4°5
2	Alphonsus		66°		−25°	−12°8	−3°3
3	Archimedes		66°	−19°	−22°	+23°0	−47°1
4	Aristarchus			−17°		+29°8	−4°0
5	Vendelinus	83°	68°	−21°	−25°	−17°0	+61°6
6	Copernicus		65°	−19°	−25°	+6°0	−22°0
7	Hipparchus		66°	−22°	−24°	−5°0	+5°1
8	Grimaldi			−25°	−25°	−5°2	−67°1
9	Sinus Iridum (100)		66°	−17°	−27°	+45°0	−32°5
10	Sinus Iridum (101)		67°	−19°	−27°	+75°0	−47°0
11	Catharina	88°	66°	−20°		−17°7	+23°0
12	Kepler			−19°	−22°	+7°5	−37°8
13	Clavius		66°	−20°	−26°	−58°0	−15°0
14	Cleomedes	87°	65°	−20°	−25°	+27°3	+56°0
15	Copernicus		66°	−19°	−27°	+9°0	−20°0
16	Langrenus	88°	64°	−15°	−20°	−8°5	+60°7
17	Maginus		64°	−17°	−26°	−51°0	−8°0
18	Cleomedes mainland	87°	63°	−19°	−28°	+27°0	+71°0
19	Mare Humorum		67°	−18°	−27°	−22°6	−37°6
20	Mare Imbrium		66°	−16°	−27°	+40°0	−28°0
21	Mare Fecunditatis	84°	67°	−20°	−28°	−3°1	+56°0
22	Mare Crisium	85°	65°	−17°	−25°	+20°0	+61°1
23	Mare Nectaris	86°	66°	−18°	−27°	−15°0	+34°1
24	Mare Tranquilitatis	87°	67°	−19°	−26°	+8°0	+30°0
25	Mare Serenitatis	98°	66°	−19°	−25°	+25°9	+17°0
26	Oceanus Procellarum		70°	−17°	−24°	−4°9	−36°1
27	Plato		66°	−19°	−24°	+51°2	−10°0
28	Posidonius	86°	65°	−19°	−26°	+31°9	+29°5
29	Ptolemaeus		65°	−20°	−25°	−8°1	−2°8
30	Theophilus	88°	62°	−17°		−11°7	+26°8
31	Tycho		66°	−18°	−24°	−43°0	−11°1
32	Fokidides			−20°	−24°	−53°0	−57°0
33	Fracastorius	86°	67°	−20°	−27°	−21°2	+32°3
34	Schiller			−21°	−27°	−52°0	−39°0
35	Schickard			−19°	−30°	−43°0	−55°4

Average: 86° 66° −19° −25°  
 $\pm 1^{\circ}5 \pm 1^{\circ}0 \pm 1^{\circ}3 \pm 1^{\circ}7$

angles the plane of polarization of moonlight coincides with the plane of the intensity equator, a rapid rotation of the polarization plane begins at  $\psi = 40^{\circ}$ ; at  $\psi = 10^{\circ}$  it equals  $90^{\circ}$ ; during full Moon the plane of polarization coincides once more with the plane of the intensity equator.

In the case of terrestrial rocks the angle of orientation of the plane of polarization:

3. does not depend on the degree of pulverization;

4. does not depend on the angle of reflection at which observations are made;

5. depends upon the phase angle (Fig. 5) where I designates the curve for granite, II—for tuff, III—for ochrous limonite, IV—for slag. At large phase angles the plane of polarization coincides with the plane passing through the specimen, illuminator and electropolarimeter; a rapid rotation of the plane of polarization begins at  $\psi = 28^\circ$ .

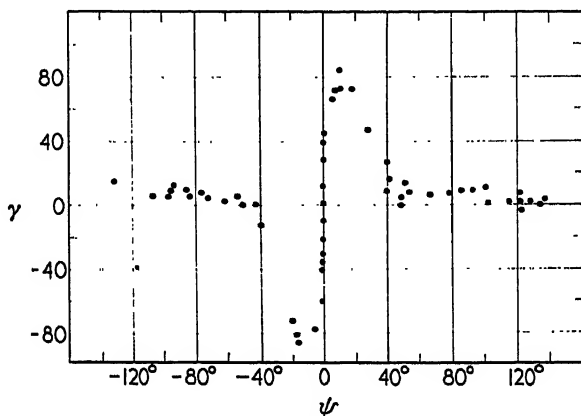


FIGURE 4.

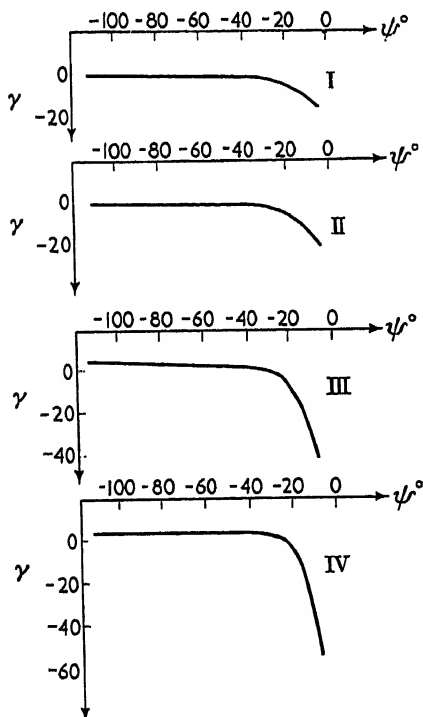


FIGURE 5.

6. In the case of limonite and volcanic slag, the most rapid rotation of the polarization plane is observed, which is similar to the rotation of the polarization plane of moonlight. In other terrestrial rocks, including volcanic tuff, the angle of rotation is considerably smaller.

In contrast to the similar nature of rotation of the plane of polarization of different regions of the lunar surface, the degree of polarization exhibits greater variety. The maximum degree of polarization of different lunar features decreases in the following order: maria, bays, crater maria, craters with central peaks, and the continents. Figure 6 shows the dependence of

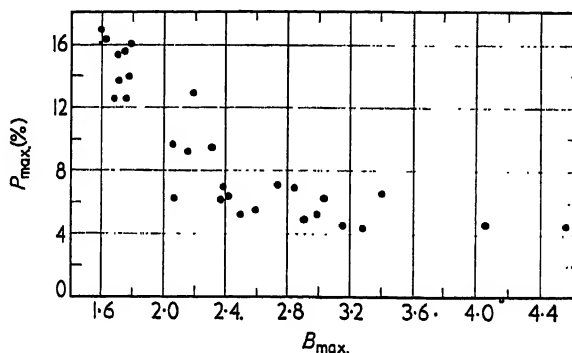


FIGURE 6.

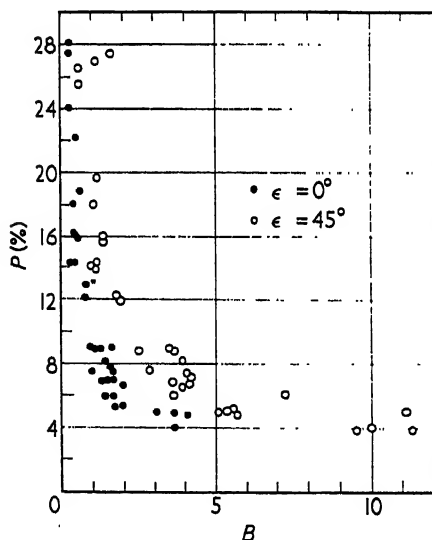


FIGURE 7.

maximum degree of polarization, found by our measurements, on the maximum brightness of the given detail according to Fedorets [19]. Exactly the same dependence is also obtained for the terrestrial rocks (Fig. 7), where we plotted the magnitudes of the degree of polarization at  $\psi = 80^\circ$

for various degrees of pulverization, taken from the graphs which show the dependence of the degree of polarization on the phase angle, and corresponding values of relative brightness obtained by the same instruments. From here it is evident that the darker the investigated sample, the greater its polarization. Maximum degree of polarization depends upon the pulverization of the rock (Fig. 8), i.e. the diameter of the grains  $\alpha$ ; the larger the grains, the greater the degree of its polarization.

Figure 9 shows the degree of polarization of the measured terrestrial rocks at  $\psi = 80^\circ$  for various degrees of pulverization. The numbers from the left to the right under each line denote the degree of polarization for rocks with

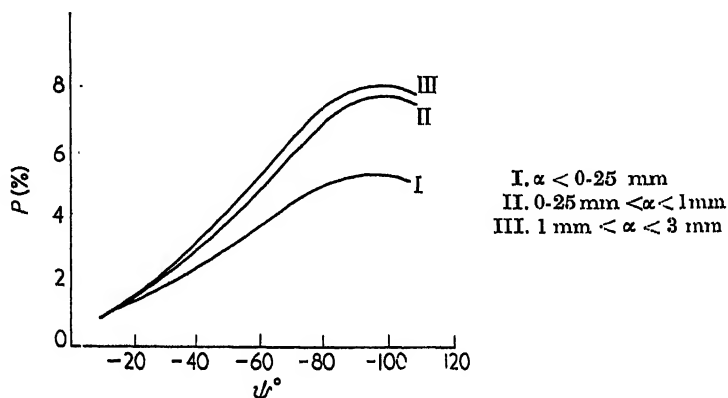


FIGURE 8.

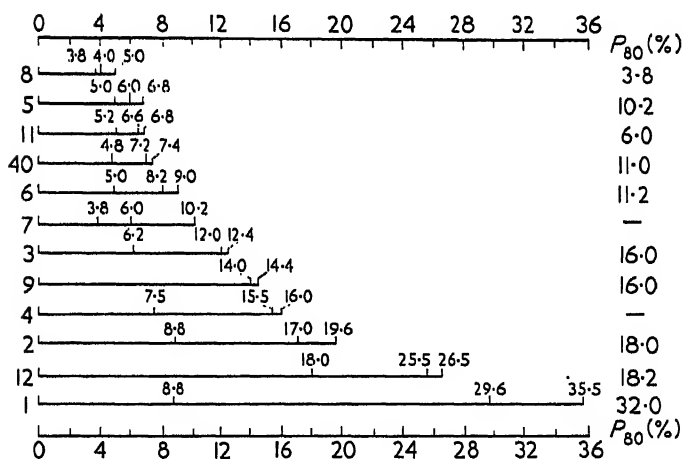


FIGURE 9.

$d < 0.25$  mm;  $0.25 \text{ mm} < d < 1 \text{ mm}$  and  $1 \text{ mm} < d < 3 \text{ mm}$ . The number at the end of each line shows the degree of polarization at the same phase angle for rocks in a non-pulverized state. The numbers on the left correspond to the ordinal number of the rock in Table I. It is evident from this diagram that the degrees of polarization  $p$  of rocks in a pulverized state  $d \leq 0.25$  mm do not differ greatly from each other. At  $0.25 \text{ mm} < d < 1 \text{ mm}$ ,  $p$  for various



rocks varies in different ways. On a further increase in grain size  $p$  changes only slightly. Thus the magnitude of the degree of polarization cannot be used as an indicator of the accurate scale of the microrelief of the lunar surface.

If we examine the inclination of the curves representing the degree of polarization of lunar regions and terrestrial rocks (Figs. 10, 11) as well as the

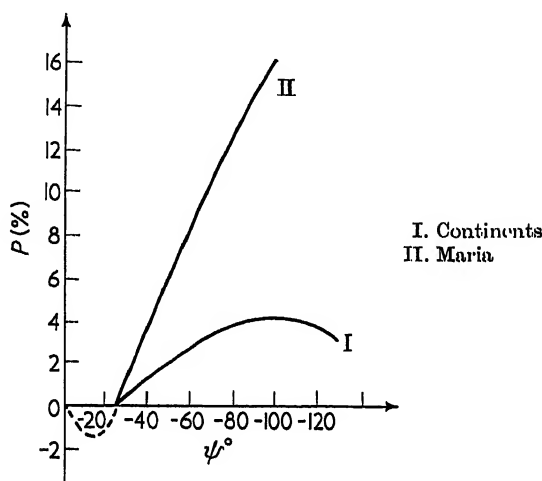


FIGURE 10.

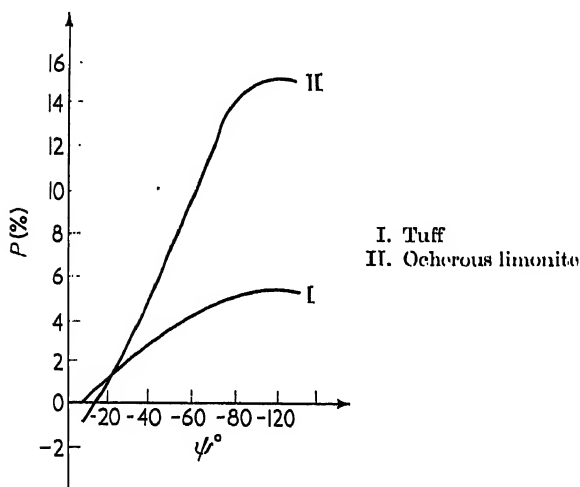


FIGURE 11.

magnitude of maximum degree of polarization, we can discern an analogy with several samples of terrestrial rocks. From these diagrams we see that at phases close to zero the degree of polarization may be zero or negative.

These results lead us to the following conclusions. As far as change in

the angle of orientation of the polarization plane are concerned, ochrous limonite and volcanic slag match closely the characteristics of moonlight. However, as the degree of polarization of volcanic slag is larger than that of the Moon, it becomes necessary to assume that the polarization characteristics of the lunar surface come closest to those of ochrous limonite. The degree of polarization of limonite is, on the average, equal to the degree of polarization of lunar maria.

The curve showing the change in the degree of polarization with the phase angle for volcanic tuff (Fig. 11-I) is analogous to the curve for lunar continents (Fig. 10-I), but the angle of rotation of the polarization plane has no such analogy.

## REFERENCES

1. Barabashev, N. P. Publication no. 19, Astronomical Observatory of Kharkov University, Publishing House of Kharkov State University (1958).
2. Barabashev, N. P. and Chokirda, A. T. *Astr. Zhurn.* **36**, 851 (1959).
3. Barabashev, N. P. and Chokirda, A. T. *Izv. Kom. Fiz. Planet.* no. 1 (1959).
4. Barabashev, N. P. and Garazha, V. I. Publication no. 21, Astronomical Observatory of Kharkov University, Publishing House of Kharkov State University (1960).
5. Markov, A. V. *Izv. glavn. astr. Obs. Pulkovo* no. 158 (1958).
6. Orlova, N. S. *Astr. Zhurn.* **33**, 93 (1956).
7. Orlova, N. S. *Festn. Leningr. Gos. Univ.* **12**, 152 (1957).
8. Sytinskaya, N. N. *Uchen. Zap. Leningrad Gos. Univ.* **190**, 74 (1957).
9. Sytinskaya, N. N. "Problems of Cosmogony". Publishing House of the Academy of Sciences of the U.S.S.R., Moscow (1957).
10. Sytinskaya, N. N. *Astr. Zhurn.* **36**, 2 (1959).
11. Sytinskaya, N. N. *Izv. Kom. Fiz. Planet.* no. 1 (1959).
12. Sharonov, *Astr. Zhurn.* **31**, 442 (1954).
13. Van Diggelen, J. *Rech. astr. Obs. Utrecht* **14**, no. 2 (1959).
14. Dollfus, A. *Ann. Astrophys.* **19**, 83 (1956).
15. Dollfus, A. *Ann. Astrophys. Suppl.* **4** (1957).
16. Lyot, B. *Ann. Obs. Paris (Meudon)* **8**, no. 1 (1929).
17. Fesenkov, V. G. *Astr. Zhurn.* **37**, 496 (1960).
18. Tverskoy, P. N. "Course on Meteorology". Gidrometizdat IL—Foreign Literature (1951).
19. Fedorova, V. A. *Trud. Kharkovsk. astr. Obs.* **2**, 50 (1952).



# FIRST RESULTS FROM OBSERVATIONS OF THE MOON BY MEANS OF A POLARIMETER

V. P. DZHAPIASHVILI, L. V. KSANFOMALITI

*Abastumani Astrophysical Observatory, Academy of Sciences,  
Georgian S.S.R.*

UNTIL recently, no instrument was available for a direct measurement of the degree of light polarization and of the angle determining the position of the polarization plane. The degree of polarization was calculated by formula

$$P = \frac{\Phi_{\max} - \Phi_{\min}}{\Phi_{\max} + \Phi_{\min}}$$

from the measurements of the maximum  $\Phi_{\max}$  and minimum  $\Phi_{\min}$  light fluxes through an analyzer. A laborious additional reduction of the observational data was necessary for obtaining the final characteristics of light polarization.

In order to improve the method of observation and the accuracy of results in studies of the polarization properties of the Moon and planets, an automatic electronic polarimeter [1, 2], was designed and constructed at the Abastumani Observatory. It provides for a direct reading of the above-indicated quantities. The instrument is analogous to an electronic computer solving the equation

$$P = \frac{x-y}{x+y}.$$

The solution is obtained in less than 0.01 sec (one cycle).

The instrument adjusts itself automatically (in no more than 0.10 sec) to any brightness within a wide range. When used as a photometer, the total sensitivity of the instrument is not less than the eleventh stellar magnitude, which corresponds to  $10^{-11}$  lumen. The polarimeter was designed for operation with the 40 cm refractor ( $f = 680$  cm) of the Abastumani Astrophysical Observatory in conjunction with extensive investigations of polarization properties of lunar and planetary surfaces conducted at this Observatory. Figure 1 shows the curve of flux  $F_{\text{in}}$  on the instrument input against stellar magnitude  $m$  of the observed object. The instrument is equipped with additional automatic elements facilitating its use. The scale readings and the number of measurements are recorded on the photographic film by pressing the button.

The first test observations were conducted in the spring of 1960. The instrument was examined as a photometer, as well as a polarimeter. An extensive programme of stellar, lunar and planetary observations was carried out.

For monitoring purposes we selected the stars from Hiltner's catalogue [3]. The observations of lunar formations were compared with earlier observations, conducted also at Abastumani with another instrument [4].

Table 1 shows an example of the testing of the instrument on the stars:

TABLE 1

<i>Star</i>	<i>Magnitude</i>	<i>Date and Universal Time of Observation</i>	<i>P<sub>1</sub>%</i>	<i>P<sub>2</sub>%</i>
BD +20°3649	5 <sup>m</sup> .09	29 Sept. 1960, 18 <sup>h</sup> :40 <sup>m</sup>	0.9	0.8
BD +18°4085	6.93	29 Sept. 1960, 19:40	6.2	6.2

In this table  $P_1$  denotes the degree of star polarization, averaged from our three measurements, and  $P_2$ —Hiltner's data [3]. The examination of this table shows that the difference between these two series of observations is small and does not exceed 0.1%.

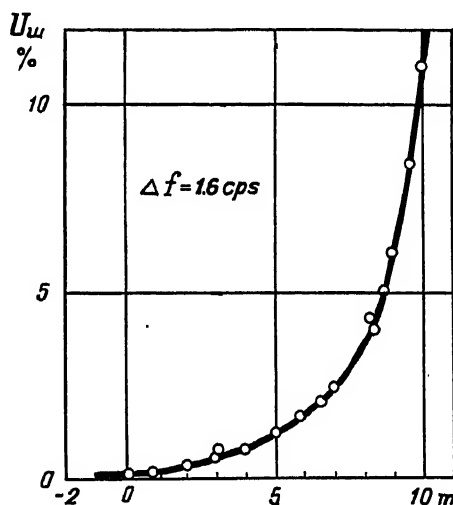


FIG. 1. Light flux on the input of instrument vs. stellar magnitude of the object under observation.

Table 2 presents some results of observations of lunar craters near quadrature when the polarization is maximum. Here  $P_1$  designates the degree of polarization obtained by authors with the polarimeter described above attached to the 40-cm refractor, and  $P_2$  denotes the degree of polarization obtained at Abastumani during 1950–1953 [4] with the 33-cm reflector ( $f = 500 \text{ cm}$ ), taking into account stray polarization introduced by mirrors of this instrument. The values  $P_2$  are taken from curves for the corresponding phase angles.

The examination of this table shows that the values of  $P_1$  and  $P_2$  are in good agreement for the overwhelming majority of craters. Aristarchus is the only exception; the maximum polarization as measured in 1950–1953 exceeds by two to three times that obtained in 1960. The observational data, obtained by Dzhapiashvili in 1956–1960 using the electropolarimeter

TABLE 2

<i>Lunar Crater</i>	<i>Date and Universal Time of Observation</i>		<i>Phase Angle</i>	<i>P<sub>1</sub>%</i>	<i>P<sub>2</sub>%</i>
Archimedes	11 Oct. 1960,	23 <sup>h</sup> 55 <sup>m</sup>	+82°0	10.2	11.3
Ptolemaeus	12 Oct. 1960,	0:05	+82°0	7.4	7.6
Kepler	13 Oct. 1960,	0:45	+93°1	6.5	9.3
Herodotus	13 Oct. 1960,	0:32	+93°1	9.7	9.7
Aristarchus	12 Oct. 1960,	1:30	+82°6	4.5	11.2
Aristarchus	13 Oct. 1960,	0:15	+93°0	4.4	12.0

of Myuhkyurya's design [5], installed at the Abastumani Observatory, as well as the measurements by Kohan carried out on this instrument during about the same period and already published [6], show that after 1956 the maximum degree of polarization of Aristarchus was always about 4%.

During observations with 33-cm refractor in 1950–1953 a diaphragm of 0.3 mm in diameter was used, which (the scale of the reflector being 41"/mm) corresponds to areas of 12"3 in diameter on the Moon. Beginning with 1956, the diaphragm of 0.05 mm in diameter has been used, which (the scale of the refractor being 30"3/mm) isolates areas with angular dimensions of 1'52 on the Moon. The comparison of these diaphragms (12"3 and 1'52) suggests that, since the angular diameter of Aristarchus is rather small ( $\approx 28''$ ), the errors in guiding might have caused in 1950–1953 a partial admixture of the light of adjacent regions, which are characterized by a greater polarization, and—as a result—a false increase in polarization of the crater itself.

However, on examination of Table 3 such a suggestion must be rejected.

TABLE 3

<i>Lunar Crater</i>	<i>Linear Diameter (in km)</i>	<i>Angular Diameter</i>
Aristarchus	52	28''
Herodotus	44	23'5
Kepler	40	21''

Indeed, as is evident from the table, Kepler and Herodotus have smaller diameters than Aristarchus, but the results of the measurements of their degree of polarization in 1950–1953 and in 1956–1960 (Table 2) are in good agreement. Particular attention must be paid to Herodotus which is situated alongside of Aristarchus and—in the presence of guiding errors during 1950–1953—should also exhibit an increased polarization, probably owing to the similar nature of the part of Oceanus Procellarum surrounding these craters. And so, there inadvertently arises a question: were there any changes inside the crater Aristarchus since 1953 which might have caused a decrease in the degree of polarization? In any case, a decrease in polarization is unquestionable; and in view of this it appears to us that a further detailed examination of the floor of Aristarchus is of great interest.

The results presented in Table 2 were obtained by observations through a rotating polaroid without light filters. As regards observations through the polaroid in combination with light filters, we must note that all objects on the Moon's surface show an increase in the degree of polarization with decreasing wavelength, in accordance with Umov's principle [7].

An essentially new possibility offered by our polarimeter consists in obtaining a complete polarization chart of the Moon by the method of inter-linear resolution (with appropriate attachment). The authors quite recently devoted considerable time to this highly interesting work, and obtained the first experimental raster samples and test images of the Moon at various phases. A section of one of them is shown on Fig. 2. We must emphasize

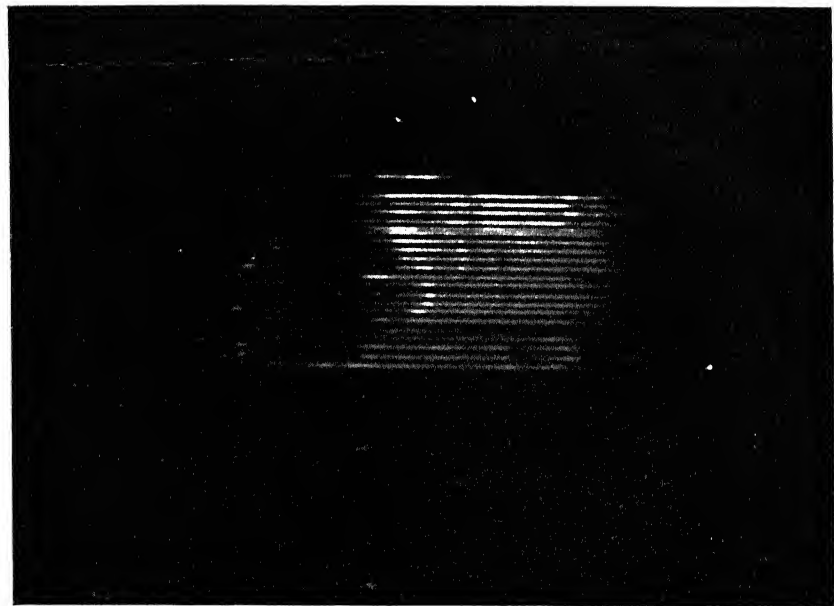


Fig. 2. Fragment of polarization chart of the Moon, 12 January 1961. Phase angle  $\psi = +114^\circ$ . Twenty lines (corresponding to the Moon's diameter) of resolution out of 100. Dark regions indicate the absence of polarization, and the brightest regions correspond to polarization of more than 20%. The great dark region near the terminator is the equatorial part of Oceanus Procellarum. (Test image.)

that the new method has nothing in common with photography through the analyzer, as this method transmits brightnesses exclusively in polarized light, being independent of the orientation of the analyzer.

Certain solutions are already available, which make it possible to improve this method.

#### REFERENCES

1. Ksanfomaliti, L. V. Electronic automatic polarization photometer of the Abastumani Astrophysical Observatory. "11th Scientific Conference of Research Students and Junior Scientific Workers." Publishing House of the Academy of Sciences, Tbilisi, Georgian SSR (1960).

2. Ksanfomaliti, L. V. Automatic Electropolarimeter, Model IEP23. *Trans. Astr. Obs. of the Kharkov State Univ.* 14 (1962).
3. Hiltner, W. A. Polarization of stellar radiation. III. The polarization of 841 stars. *Astrophys. J.* 114, 241 (1951).
4. Dzhapiashvili, V. P. A study of polarization properties of formations on the lunar surface, according to electrophotometric measurements. Monograph. *Bull. Abastumani Astrophys. Obs.* 21 (1957).
5. Myuhkyurya, V. I. Differential recording electrophotometer for measuring the brightness, colour and polarization of celestial objects (Author's Abstract of the Candidate's Thesis), Leningrad (1954).
6. Kohan, E. K. An investigation in three spectral regions of the degree and position angle of the plane of polarization of light, reflected by lunar formations. *News Bulletin of the Committee on Planet. Physics.* 1, 41-53 (1959).
7. Umov, H. A. *I'lys. Z.* 6, 674 (1905).





# ECLIPSE TEMPERATURES OF THE LUNAR CRATER TYCHO

WILLIAM M. SINTON

*Lowell Observatory, Flagstaff, Arizona, U.S.A.*

SHORTHILL, Borough, and Conley discovered during the total eclipse of the Moon on 13 March 1960 that the floor of the crater Tycho did not cool as much as the surrounding area, but remained some 40 to 60° warmer [1]. They found that other rayed craters, specifically Copernicus and Aristarchus, also remained warmer than their surroundings.

Using the pyrometer developed here [2], attached to the 42 in. Lowell reflector, I observed the temperature of Tycho during the total eclipse on 5 September 1960. The measurements were made with a  $1.5\mu$  bandwidth at  $8.8\mu$ , and calibration was made by direct comparison with blackbodies of known temperature. An aperture of  $27''.9$  defined the observed area of the Moon. For the most part, scans were made across the lunar disk by turning off the telescope drive. The telescope was set upon Tycho and allowance was made for the expected lunar motion in declination, and then the telescope was moved to the same declination at the leading edge of the Moon.

Clouds interfered with the first part of the initial penumbral phase and again after about one-half hour of totality. Observations could not be continued beyond that. Since the initial temperature was not recorded, Tycho was observed again on the following night and the temperature obtained is assumed to be the initial temperature as well.

Figure 1 shows two of the scans; one is before the traversed chord of

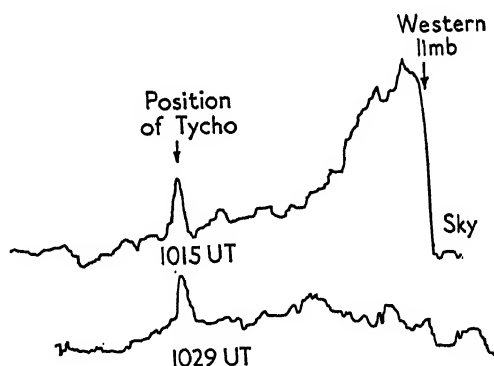


FIG. 1. Two scans across Tycho. They illustrate the rapid temperature decay of most of the Moon's surface and the relative constancy of Tycho's temperatures during the eclipse.

the Moon is completely in the umbra, while the other is after the chord is completely shadowed. The time interval between crossing the western limb and crossing Tycho was calculated and compared to the tracings obtained before totality. Such a comparison is shown in Fig. 1. The agreement is good, showing that the warmer region is indeed Tycho.

Figure 2 shows the temperatures observed for Tycho as dots; crosses designate the temperatures of the region around Tycho found by taking the mean of the deflections on either side of the bump. Several theoretical curves, which assume different combinations of dust and rock, are taken from papers of Jaeger [3] and Jaeger and Harper [4], and they are also shown in the figure. The curve for thick dust agrees well with measurements of the Tycho environs. The measurements of Tycho, itself, agree well in general shape with the curve for 0.5 mm of dust on top of rock; they show little change during totality. A similar curve, if computed for a slightly thinner dust layer, would fit the points better. The computation of this curve requires numerical integration.

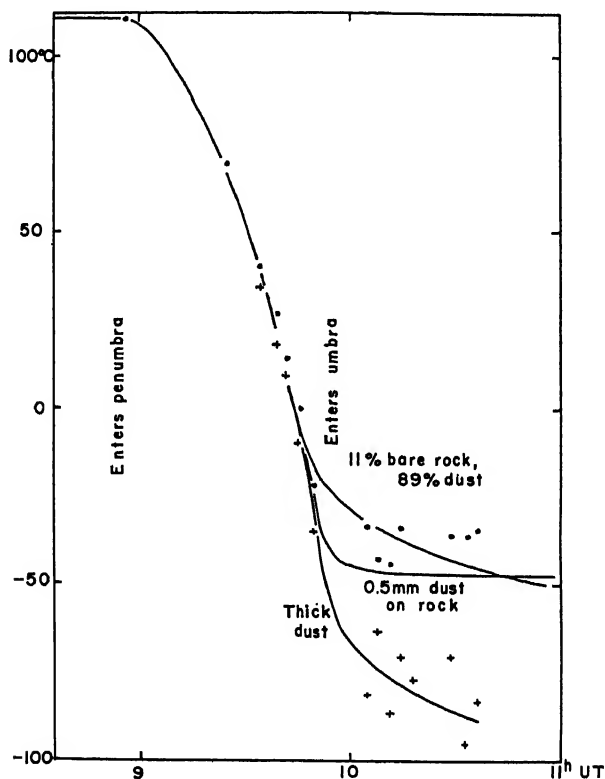


FIG. 2. The temperatures of Tycho (dots) and Tycho's environs (crosses) during the eclipse. Several theoretical curves for different models are shown.

However, the thickness of the dust layer that would fit the observations better can be determined by assuming that, after totality has commenced, the heat radiated from the surface is equal to the heat conducted through the layer. This is expressed by

$$\sigma T^4 = (T_0 - T)k/d,$$

where  $\sigma$  is the Stefan-Boltzmann constant,  $T$  is the surface temperature,  $T_0$

is the temperature of the upper surface of the rock,  $k$  is the thermal conductivity, and  $d$  is the thickness of the layer. Jaeger and Harper assumed  $k = 2.8 \times 10^{-6}$  in cgs units. The temperatures during totality, which they computed by numerical integration, are adequately derived from the above formula if  $T_0$  is 0.73 of the pre-eclipse temperature. From this formula and the observed eclipse temperature of Tycho, the thickness of the dust layer is 0.3 mm.

Another possible model was considered, that of bare boulders lying in a field of dust, and the curve for this model is also shown. The agreement with the dust-layer model is decidedly better. In the case of the two points that are lower temperature, the scans very likely crossed only the edge of Tycho.

From the 0.3 mm thickness of dust a maximum age of Tycho has been derived. The influx of solid matter on the Earth is assumed by Whipple [5] to be several thousand tons per day. In order to build up a 0.3 mm dust layer of density 2 at this rate,  $10^7$  years are required. Since high-velocity particles are apt to fracture and erode rock surfaces, this age will be an upper limit.

Tycho, because its rays overlie many other features, is certainly one of the most recent major craters, but it is now possible to set a more accurate appraisal of its age.

Tycho, however, is not the only feature that can be dated by this method because, as was mentioned, Shorthill, Borough, and Conley also found that Aristarchus and Copernicus are warmer than their neighborhoods. Possibly most rayed craters can be dated by this method. The relative thickness of dust (and the relative ages) of two craters is given by the formula

$$d_1/d_2 = (T_2/T_1)^4(T_{0,1}-T_1)/(T_{0,2}-T_2),$$

where  $T_1$  and  $T_2$  are the observed crater temperatures when they are shadowed, and  $T_{0,1}$  and  $T_{0,2}$  are 0.73 times the pre-eclipse temperatures of the two craters.

To date 17 ray craters have been observed during an eclipse, and all of these except Proclus were warmer than their environs.

#### REFERENCES

1. Shorthill, R. W., Borough, H. C. and Conley, J. M. *Publ. astr. Soc. Pacif.* **72**, 481 (1960).
2. Sinton, W. M. *Lowell Obs. Bull.* **4**, 260 (1959).
3. Jaeger, J. C. *Aust. J. Phys.* **6**, 10 (1953).
4. Jaeger, J. C. and Harper, A. F. A. *Nature, Lond.* **166**, 1026 (1950).
5. Whipple, F. L. In R. Jastrow, ed. "The Exploration of Space", Macmillan, New York, 7 (1960).



# V. RADIO OBSERVATIONS OF THE MOON



# RADIO EMISSION OF THE MOON, ITS PHYSICAL STATE, AND THE NATURE OF ITS SURFACE

V. S. TROITSKY

*Institute of Radio Physics, U.S.S.R.*

## 1. INTRODUCTION

RECENTLY experimental data have been obtained on lunar radio emission which enable one to solve the problem as to which model of structure for its upper layer corresponds to reality: single layer (homogeneous structure of the covering) or a widely distributed two-layer-dust cover [1]. They also enable one to draw more definite conclusions as to the physical properties, thermal conditions, and structure of lunar material.

Let us consider briefly the results of the theoretical and experimental research of the radio emission of the Moon obtained up to the present time†. The first measurements of the radio emission of the Moon on  $\lambda = 1.25$  cm showed that this emission depends essentially on the phase and has a constant and variable component, the latter which is well approximated by a sinusoid [2] (see, for example, [19]). The maximum of the variable component shows a lag in phase relative to maximum illumination of the Moon by the Sun. This fact is explained in [2] as a result of the heating of a sufficiently thick layer of the material of the surface, which therefore shows a certain retardation. The formula for the heating of the surface itself at the centre of the lunar disk can be written as

$$T_s = T_0 + T_1 \cos \Omega t + T_2 \cos 2\Omega t + \dots, \quad (1)$$

where  $\Omega$  is the angular velocity of rotation of the Moon, equal to  $2.46 \cdot 10^{-6}$  rad/sec ( $\Omega t = 0$  corresponds to the full Moon); and  $T_0$ ,  $T_1$ ,  $T_2$ , are the mean value and the first and second harmonics of the true temperature of the surface, respectively. For the two models, the brightness temperature of the centre of the disk is described by the expression (2), (3) (the higher harmonics are not taken into consideration),

$$T_e = (1-R)T_0 + (1-R) \frac{T_1}{m_g m_s} \cos(\Omega t - \xi_s - \xi_s), \quad (2)$$

where  $T_{e0} = (1-R)T_0$  is the constant component and  $T_{e1} = (1-R)T_1/m_g m_s$  is the amplitude of the first harmonic of the variable component of radio temperature, and

$$m_g = \sqrt{1 + 2\delta + 2\delta^2}, \quad \xi_s = \tan^{-1} \frac{\delta}{1 + \delta} \quad (3)$$

denotes the weakening of the variable component of radio emission and the

† See also [15].



lag in phase due to the basic layer of the material,  $m_s$  and  $\xi$  are the weakening and shift in the dust layer.  $R$  is the coefficient of reflection of electromagnetic waves depending on the dielectric constant  $\epsilon$  of the lunar material.  $\delta = l_E/l_T$ , where  $l_T$  is the depth of penetration of the heat wave into the lunar material, and  $l_E$  is the depth of penetration of the electromagnetic wave or the depth from which the radio emission emerges from the surface weakened by a factor of  $e = 2.71$ .  $l_E$  determines the thickness of the layer of the material responsible for the radio emission observed at a given wavelength.

In the general case, if the permeability  $\mu = 1$ ,

$$l_E = \frac{v}{4\pi f \sqrt{\epsilon}} \left[ -\frac{1}{2} + \frac{1}{2} \sqrt{1 + \left( \frac{2\sigma}{\epsilon f} \right)^2} \right]^{-1/2} \quad l_T = \sqrt{\left( \frac{2k}{\rho c \Omega} \right)}, \quad (4)$$

where  $\sigma = \sigma(f)$  is the electric conductivity of the material of the Moon at a given frequency  $f$ ;  $k$ ,  $\rho$ , and  $c$ , are their thermal conductivity (in cal/cm. deg.sec), density (in g/cm<sup>3</sup>), and specific heat capacity (in cal/deg) respectively;  $v$  = being the velocity of light in a vacuum.

The values of  $T_0$  and  $T_1$  are connected with the maximum  $T_m$  and minimum  $T_n$  temperatures attained on the surface, at the lunar midday and midnight. They depend on the law  $\eta(\beta)$  of variation of the temperature of the surface with the angle of incidence  $\beta$  of the solar rays. The theory gives

$$T_0 = T_n + a_0(T_m - T_n); \quad T_1 = a_1(T_m - T_n), \quad (5)$$

where, consistent with the experimental data,  $\eta(\beta) = \cos^{1/2} \beta$ ,  $a_0 = 0.382$  and  $a_1 = 0.558$ . The experimental data obtained at  $\lambda = 1.25$  cm did not satisfy the expressions (2), (3) for a single-layer model ( $m_s = 1, \xi_s = 0$ ), but agreed better with the two-layer model characterized by the parameters  $m_s = 1.8$ ,  $\xi_s = 22^\circ$ .

In [4] it was shown that the experimental curve given in (2) can be approximated by a curve with a phase shift  $\xi = 35^\circ$  which satisfies the single-layer model. Subsequent measurements of the radio emission on the wave lengths of 1.63 cm [6], 0.8 cm [7], and 0.86 cm [8] also did not give well-defined results. Within the limits of observational errors in the measurements of the intensity and the phase of the radio emission, all of them can be made to agree with both the two-layer and the single-layer models.

In view of this the analysis of the experimental results was made in accordance with the theory of the single-layer model. As a result the applicability of the law

$$\delta/\lambda = \text{const} \quad (6)$$

characterizing the physical properties of lunar material at the cm as well as mm wave lengths was detected [4] and confirmed [6] in a broader frequency range. From here followed the constancy of the loss tangent of lunar material in this range of wave lengths.

It was noted that the same property is shown by ceramic dielectrics containing silicon and aluminium oxides.

Further computation of the parameters characterizing the lunar material did not lead to sufficiently concordant results. Thus, starting from the universally accepted thermal parameters of the lunar material

$$(k\rho c)^{-1/2} = \gamma = 1000, \quad c = 0.2,$$

and  $\rho = 2(l_T \simeq 2 \text{ cm})$  it was found that  $l_E(3) \simeq 10 \text{ cm}$  at  $\lambda = 3.2 \text{ cm}$ . If one considers the lunar material as a dielectric, then  $\sigma(3) = 6 \times 10^8$  in c.g.s. units. This value proved to be more than half an order of magnitude greater than the data known from literature for some dry terrestrial material [9]. Thus in the case of a single-layer model, there arose the difficulty of explaining the high electric conductivity of the lunar material in comparison with some terrestrial ones. In [4] it was pointed out that this "contradiction" is eliminated if the two-layer model is considered. Thus the problem of the structure of the upper layer of the Moon's crust remained intricate and obscure.

In order to solve this problem, at the Gorky Radio Astronomical Station of the SRRPI measurements were made of the radio emission of the Moon in widely spaced wave lengths, ranging from  $\lambda = 0.4 \text{ cm}$  [10] to  $3.2 \text{ cm}$  [11], with greater precision of the absolute measurements than was obtained previously with comparative diagrams of the antennas. These data proved to be decisive for specifying the model, and definitely indicated a quasi-homogeneous structure of the surface layer of the Moon. For a comparison of the electric parameters of lunar and terrestrial material, measurements have been made at  $\lambda = 3.2 \text{ cm}$  of the loss angle and dielectric constant of some terrestrial volcanic rocks of Armenia and Kamchatka (tuff, tufo-lava volcanic slag, obsidian pumice, clay, etc.). We measured the specimens which, in accordance with the investigations of Barabashev and his collaborators at the Kharkov Observatory, proved to correspond closely with the lunar material in their optical characteristics (albedo, colour, polarization, indicatrix of reflection, etc.) [5]. In the present investigation the new data are analyzed, resulting conclusions made on the physical properties of the superficial layer and a homogeneous model constructed on their basis.

## 2. SOME BASIC CONCLUSIONS FROM THE EXPERIMENTAL DATA ON THE NATURE AND PHYSICAL STATE OF THE SURFACE LAYER OF THE MOON

In Table 1†, besides the basic data at  $\lambda = 0.4, 1.63$  and  $3.2 \text{ cm}$ , all experimental data on the intensity of radio emission that have been obtained up to the present time are included, for a comparison of the experimental data with theoretical experimental characteristics that depend least on the conditions of measurements. The quantities independent of the precision of absolute measurements are the phase shift  $\xi$  and the value inverse to the relative variation of the intensity of radio emission  $M = T_{e0}/T_{e1}$ .

The values  $\xi$  and  $M$  are interrelated and depend on the wave length. The character of their interdependence is determined by the structure of the surface of the Moon. In order to find out to which of the models the experimental data correspond, a  $\xi-M$  diagram was constructed. On it theoretical curves corresponding to both models as well as the experimental points were plotted. The theoretical value of  $M$  for both models is, according to (2), equal to  $M = m_g m_s T_0/T_1$ , and the corresponding phase shift

† The specimens for the measurements were kindly placed at our disposal by N. P. Barabashev and V. I. Ezersky. Measurements were made by V. D. Krotikov.

‡ The value  $T_e$  in the second and next to last lines of the table corresponds to the brightness temperature at the centre of the disk. In the remaining cases  $T_e$  is equal to  $\int |T \Omega F d\Omega| / \int F d\Omega$  - i.e. it is intermediate between the brightness and average temperature for the disk, differing from each other by a value of the order of 8% [2] [3].

TABLE 1

$\lambda(\text{cm})$	$T_{e0}$	$T_{e1}$	$\xi$	Intensity of radio emission	$M = \frac{T_{e0}}{T_{e1}}$	$\delta$	$\xi_{\delta}$	$\delta/\lambda$	$l_e(\text{cm})$	off. $10^2$	Authority
3.2	245°	15.5°	50°	230° + 14.5° cos( $\Omega t$ - 50°)	15.9	7.0	41°	2.2	70°	0.5	Troitsky, Strezhneva [11]
3.2	230°	17°	45°	230° + 17° cos( $\Omega t$ - 45°)	13.5	5.8	40°	1.8	58°	0.6	Salomonovich [12]
1.63	224°	36°	40°	230° + 37° cos( $\Omega t$ - 40°)	6.23	2.4	35°	1.5	24°	0.7	Zelinskaya, Troitsky, Fedoseyev [6]
1.25†	215°	36.3°	35°	230° + 39° cos( $\Omega t$ - 40°)	5.93	2.3	35°	1.8	23°	0.6	Piddington, Minnett [2]
0.86‡	180°	35°	35°	230° + 45° cos( $\Omega t$ - 35°)	5.15	1.9	33°	2.2	19°	0.5	Gibson [8]
0.8	197°	32°	40°	230° + 37° cos( $\Omega t$ - 40°)	6.15	2.4	35°	2.9	24°	0.4	Salomonovich [7]
0.8§	210°	40°	30°	230° + 44° cos( $\Omega t$ - 30°)	5.25	1.9	33°	2.4	19°	0.4	Salomonovich [12]
0.4	230°	73°	24°	230° + 73° cos( $\Omega t$ - 24°)	3.15	0.9	25°	2.2	9°	0.5	Kislyakov [10]

† Corrected value of the phase (see text and [4]).

‡ Approximation by the author.

§ Variable component — first harmonic from the intensity variation curve.

$\xi = \tan^{-1}(\delta/1+\delta) + \xi_s$ . By substituting for  $\delta$  its expression through  $M$  we obtain the following theoretical dependence between  $\xi$  and  $M$

$$\xi = \tan^{-1} \frac{-\frac{1}{2} + \sqrt{\frac{1}{4} + \frac{1}{2} \left[ \left( \frac{M}{m_s} \cdot \frac{T_1}{T_0} \right)^2 - 1 \right]}}{\frac{1}{2} + \sqrt{\frac{1}{4} + \frac{1}{2} \left[ \left( \frac{M}{m_s} \cdot \frac{T_1}{T_0} \right)^2 - 1 \right]}} + \xi_s. \quad (7)$$

In order to evaluate this function it is necessary to know the value of  $T_0/T_1$ . It transpires from (5) that this relationship depends basically on the coefficients  $a_0$  and  $a_1$ , and remains practically unaltered by a change in the ratio between  $T_n$  and  $T_m$  within their limits of uncertainty. For  $\eta(\beta) = \cos^2 \beta$ ,  $T_n = 125^\circ \text{ K}$  [13], and  $T_m = 407^\circ \text{ K}$  [14] this ratio is equal to

$$\frac{T_0}{T_1} = 1.48. \quad (8)$$

For actual computation let us take the round value 1.5, found also experimentally (see below). In order that a definite wave should correspond to each point of the plane  $M, \xi$ , it is also necessary to consider the relation between  $\delta$  and  $\lambda$  for the base and also (in the case of the two-layer model) the homogeneous layer. For the computation the linear relation was taken, which corresponds ordinarily to the dielectric. On Fig. 1 we present the theoretical curves  $\xi(M)$  plotted in accordance with (7). Curve 1 corresponds to the single-layer model  $m_s = 1, \xi_s = 0$ , for the material for which  $\delta = 2\lambda$ . The black dots on the curve correspond to the wave lengths  $\lambda = 0.4, 0.8$ ,

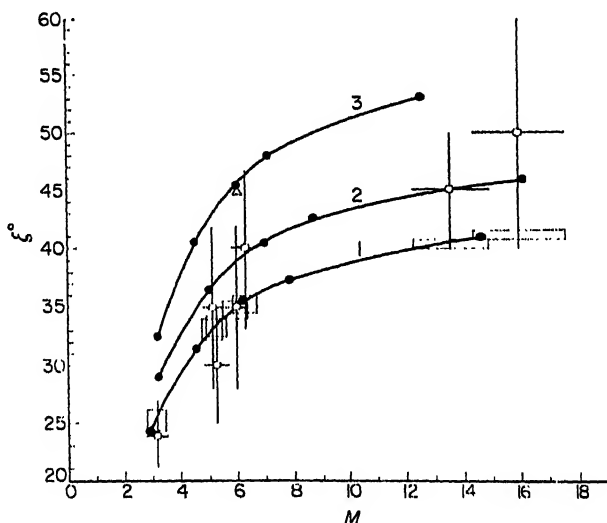


FIG. 1. Theoretical dependence of the phase lag of the first harmonic of the radio emission of the Moon on the ratio of the constant component to the amplitude of the first harmonic of the emission for a cycle: 1. Homogeneous structure of the surface, 2.—3. Two-layer-dust. Black dots — theoretical values for wave lengths  $\lambda = 0.4, 0.8, 1.25, 1.63$  and  $3.2$  cm.

1.25, 1.63 and 3.2 cm. If, however, this material is covered by a very thin layer of dust characterized by the parameters  $m_s = 1.1$ ,  $\xi = 5^\circ$ , then one obtains the curve 2. With increasing thickness of the layer the corresponding curves will shift upwards and to the right. Finally, if the base layer on the rock, for which  $\delta = 1.15$ , is covered with a thicker layer characterized by the parameters  $m_s = 1.4$ ,  $\xi_s = 15^\circ$  (a layer about half as thick as in [2]), then we get the curve 3. The experimental values of  $M$  and  $\xi$  for each wave length presented in the table are indicated by circles†, with indication of the limits of possible error in  $M$  and  $\xi$ . As is seen from the curve, the experimental points uniquely correspond to the one-layer model, and cannot be reconciled simultaneously with the two-layer dust model. For example, the phase lag obtained in [2] for  $\lambda = 1.25$  cm,  $\xi = 45^\circ$  (the point in Fig. 1 is marked by a triangle) agrees well with the two-layer model as represented by curve 3 in Fig. 1. However, the data for  $\lambda = 3.2$  cm and  $\lambda = 0.4$  cm do not fall on this curve. If for  $\lambda = 3.2$  cm the theoretical phase,  $\xi = 45^\circ$ , for the two-layer model with a very thin layer of dust comes within the limits of the experimental values, for  $\lambda = 0.4$  cm the theoretical phase  $32^\circ$  diverges again considerably from the experimental value. Many other combinations of the base and dust layer were considered, but all of them deviate much more from experimental data even at shorter wave lengths. It turns out that if we select the parameters of the two-layer-dust model in order to satisfy the data on some single wave length or for previously obtained data on near wave lengths (0.8 cm—1.6 cm), then for the wave lengths of the new wide interval it becomes impossible to do so. In trying to accomplish this it is necessary to thin out the dust layer to the point of disappearance. Thus one may consider the homogeneous structure of the surface layer of the Moon experimentally proved‡. If so, then for the phase lag it is of advantage to use its value computed by (3) from the experimentally determined value  $m_s$  instead of the inaccurate value  $\xi$  directly measured. In accordance with this, on Fig. 1 the values of  $M$  and the phase lag  $\xi_s$  are marked for each wave length by rectangles which determine the limit of errors. As can be seen, these values lie precisely on the curve for the one-layer model.

† The point corresponding to 0.8 mm [7] is not indicated as it clearly contradicts the whole series of measurements (see column 4 of the table).

‡ Apparently one still observes a tendency towards an increase in the phase shift with the increase in the wave length, as compared with the theoretical values for the one-layer model. However, this can be explained not only by an assumption on the inhomogeneity of this layer with depth. More probably this may be connected by different emission of the maria and the continents, observable already at  $\lambda = 0.4$  cm [31]. Actually with reception on an antenna with a wide diagram the observed phase-curve of radio emission can be represented by a sum of two sinusoidal phase-curves: one for the eastern half of the Moon, where large maria are present and which lags behind the full Moon, and the other for the western half covered predominantly by continents, and which precedes the full Moon by the same angle. If the maria gives a greater variable component than a continent, then for the total emission we shall observe a supplementary lag in phase, proportional to this difference in emission. Inasmuch as the amplitude decreases with the increase of the wave length, the effect of the difference in emission on the shift will increase—and this is actually observed. In connection with this point in the investigation of radio emission with sharp directional diagrams, the orientation of the antenna on the centre of the disk (as was done in [12]) can lead to considerable errors. In this case, in the course of the cycle due to libration the diagram passes through maria and continents distorting thereby the actual course of radio temperature.

Let us consider now the dependence of  $M$  and  $\xi$  on the wave length. On Fig. 2 the experimental values of  $M$  for each wave length are plotted. Through the points one can draw a straight line, which practically corresponds to the theoretical one, constructed according to (3), and shows that the amplitude of the oscillations decreases almost linearly with the wave length. On the drawing the line is extrapolated to  $\lambda = 0$ . Since for  $\lambda \simeq 0$ , the emission originates from the topmost layer of the surface itself, the intercept

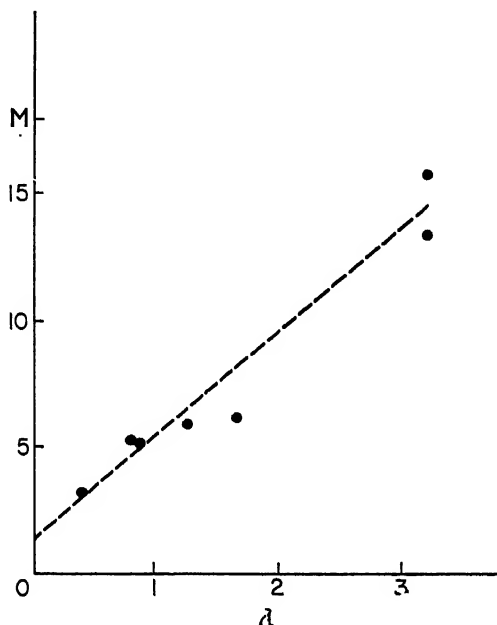


FIG. 2. Experimental values of ratio of the constant component to the amplitude of the first harmonic of radio emission in dependence on the wave length.

on the  $y$  axis gives the value of  $M$  for this layer—i.e. the value of the ratio  $T_0/T_1$ . Thus the data for the range of the wave lengths present an interesting possibility of direct determination of the ratio of the constant component of the temperature to the first harmonic of the variable component on the topmost layer of the Moon†. The value of this ratio, which is determined by permissible differences of inclinations of straight line, does not exceed the limits 1.3—1.7 and, on the average, is equal to

$$\frac{T_0}{T_1} = 1.5, \quad (9)$$

which corresponds to the theoretical value indicated above for this ratio.

The frequency dependence of the (theoretical) phase lag for  $\delta = 2\lambda$  is shown in Fig. 3. On Fig. 4 we plotted the dependence on  $\lambda$  of the value  $(1+2\lambda) \tan \xi$ , proportional to  $\xi$ . As can be seen, the experimental points follow a straight line, which extrapolated to  $\lambda = 0$ , as expected, passes through  $\xi = 0$ .

† Similarly one can find experimentally the ratio for the second harmonic.

Since the value  $T_0/T_1$  was determined experimentally, then, in accordance with the formulas (2) and (3), one can compute the value of  $\delta$  for each wave length. The corresponding values are given together with the ratio  $\delta/\lambda$  in Table 1. As can be seen, this ratio remains constant within the limits of

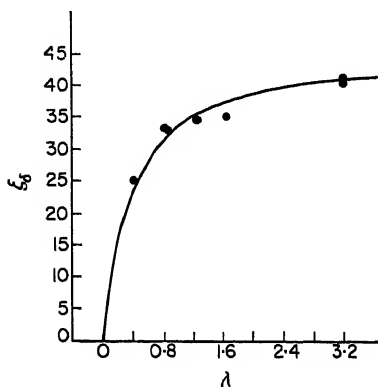


FIG. 3. Theoretical dependence of the phase-lag of the variable component of radio-emission on the wave length for  $\delta = 2\lambda$ .

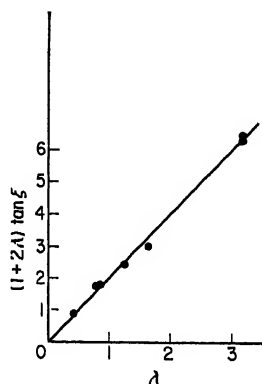


FIG. 4. Another representation of the curve 3.

the errors of measurement in the whole observed interval of frequencies, and is equal to

$$\frac{\delta}{\lambda} = 2\text{cm}^{-1}; l_e = 2\lambda l_T. \quad (10)$$

The establishment of this law is important; for it allows definite conclusions to be drawn on the chemical composition of the outermost surface of the Moon. Let us consider this question in more detail. The rather large absolute values of  $l_e$ , obtained from (10) practically for any assumed values of the thermal parameters (for which  $l_T \geq 1$  cm) lead, in accordance with (4), to the conclusion that  $2\sigma/\epsilon f \ll 1$ —i.e. the lunar material proves to be a rather good dielectric; for which

$$l_e = \frac{v\sqrt{\epsilon}}{4\pi\sigma}. \quad (11)$$

From this and from (10) it necessarily follows, that the effective electrical conductivity of lunar material is proportional to the frequency—i.e.  $\sigma = \sigma_0 f/f_0$ . This leads to the constancy of the loss tangent in the range of

$$\tan \Delta = 2\sigma/\epsilon f$$

the frequencies of the measurements.

Such a behaviour is characteristic of solid dielectrics and different rocks which contain as basic components quartz ( $\text{SiO}_2$ ) and corundum ( $\text{Al}_2\text{O}_3$ ). The conductivity (or loss angle), as is known [16], depends on the amount of mixtures of oxides of light metals ( $\text{CaO}$ ,  $\text{MgO}$ ,  $\text{Na}_2\text{O}$ ,  $\text{K}_2\text{O}$ , and others)

and oxides of iron ( $\text{Fe}_n\text{O}_m$ ). In Table I the values of  $\sigma/f$  (in absolute units) obtained for various wave lengths are given.

If the outer layer of the rocks were to contain even some small amounts of admixtures of powdered meteoritic iron, the dependence of the electrical conductivity on the frequency would be essentially different. As experimental investigations of artificial dielectrics show ([17] and [18]), the loss tangent of such a dielectric increases with the increase in the frequency  $f$  somewhat faster than  $f^{1/2}$ —i.e. the conductivity increases  $\sim f^{3/2}$ . The dielectric acquires such properties already with a 2 to 3% concentration of the metallic powder by volume. In this case, the loss angle of the lunar material would be considerably larger than that of terrestrial rocks of similar composition. It is not difficult to see that, in this case, the constant quantity instead of (10) would be the ratio  $\delta/\lambda^{3/2}$ . Also  $M$  would become proportional to  $\xi^{3/2}$  instead of  $\lambda$ , as is actually the case (see Fig. 2). Thus the character of the dependence of the electrical conductivity on the frequency, and to some extent also its magnitude enables us to affirm that the outer layer of the Moon behaves like a dielectric with a composition close to that of terrestrial rocks. However, it is at present impossible to conclude from the radio data which types of rocks should be given preference. For this purpose one needs a more precise and reliable determination of the electrical conductivity of the lunar material and for this, as we shall see below, it is necessary to know more precisely the values of  $[k\rho c]^{-1/2}$  and  $c$  as well as a laboratory investigation of electrical conductivity of different material at ultra-high frequencies. Apparently, such a characteristic as electrical conductivity may prove to be a very reliable index of the identity of terrestrial and lunar materials.

### 3. FURTHER DEVELOPMENT OF THE SINGLE-LAYER MODEL AND PHYSICAL PROPERTIES OF LUNAR MATERIALS

#### (A) GENERAL RELATIONSHIPS

From the facts obtained above and the new data on the electrical properties of terrestrial material, one can deduce some of the parameters characterizing lunar material. The dielectric nature of the upper layer, and the very probable identity of the average chemical composition with the average composition of terrestrial material, derived from the radio data, justify the comparison made below of the values of the electrical parameters of the lunar and terrestrial material and the conclusions drawn therefrom. However, due to the limitations of the experimental data, what follows in this section should be regarded more as a development of the method and the selection of comparison parameters than the deduction of new results.

Let us consider in more detail the obtained relation (10). By substituting from (11) and (4) it is not difficult to obtain a relationship connecting the electrical and thermal parameters of the lunar material in the form

$$\frac{\sqrt{\epsilon \tan \Delta}}{\rho} = 88 \times 10^{-6} \text{ cgs.} \quad (12)$$

Thus the measurement of the radio emission of the Moon, if the thermal parameters are known, gives a possibility of determining some combination of the electrical parameters of the lunar material and vice versa.



In (12)  $\gamma$  is known directly from the optical measurements. Its most precise value has been obtained, apparently, from eclipse observations and equals 900 (taking into account the corrections given below). The value of  $c$  for aluminium silicates with sufficient accuracy is equal to 0.2. Hence, for the material of the Moon we get

$$\zeta = \frac{\tan \Delta}{\rho} \sqrt{\epsilon} = (1.6 \pm 0.2) \times 10^{-2}. \quad (13)$$

It is clear that for a comparison with terrestrial rocks, we should measure for each of them exactly the same combination of parameters,

$$\zeta' = \frac{\tan \Delta'}{\rho'} \sqrt{\epsilon'}$$

as a function of density (porosity) of  $\rho'$  of the rock (here and in subsequent cases the prime indicates the terrestrial rocks). This value is basically determined by the nature of the material. Thus, by using (13), we can identify a group of terrestrial rocks similar to the lunar ones in density and nature.

Let us consider the character of the change of  $\zeta'$ . In the existing literature on dielectrics the connection of  $\epsilon$  of solids with the density (porosity) has been developed in some detail (see, for example, [20], [21], and [22]); and the conclusions confirmed experimentally (see, for example, [23] and [24]). The connection between the density and the loss angle has been studied much less. The existing theoretical works (see, for example, [25]) lead to complicated expressions not as yet confirmed experimentally. We make use of a simplified expression following from the logarithmic formula of Lichtenener [16] which, apparently, is applicable for porous substances with small  $\epsilon$  ( $\leq 5$ ), and partly confirmed experimentally at UHF [24]; namely,

$$\frac{\tan \Delta'_{cp}}{\rho_{cp}} = \frac{\tan \Delta'_k}{\rho'_k}, \quad (14)$$

where  $\rho'_k$  and  $\Delta'_k$  are the density and loss angle of the terrestrial material in a dense crystalline or amorphous state (porosity absent) and  $\rho_{cp}$  and  $\Delta_{cp}$  are the average density and loss angle of the same porous material.

The dielectric constant  $\epsilon$  of the porous material depends on the degree of porosity and the dielectric constant  $\epsilon_k$  of the substance in the naturally dense state (when pores are absent). For a porous solid dielectric the following formula of Odelevsky [20] and Levin [21] is generally accepted:

$$\epsilon = \epsilon_k \left( 1 - \frac{3x}{\frac{2\epsilon_k + 1}{\epsilon_k - 1} + x} \right), \quad (15)$$

where  $x = 1 - (\rho_{cp}/\rho_k)$  is the volumetric concentration of the pores. For the powdered state we have Boettcher's formula [22]

$$\frac{\epsilon - 1}{3\epsilon} = \frac{\epsilon_k - 1}{\epsilon_k + 2\epsilon} \frac{\rho_{cp}}{\rho_k}. \quad (16)$$

The two formulas lead to closely the same results.

The average density can in general change in the interval  $0 < \rho_{cp} \leq \rho_k$ , and  $\epsilon$  changes in the interval  $1 \leq \epsilon \leq \epsilon_k$ , while for the terrestrial rocks at UHF  $\epsilon_k \simeq 4.5$ . Thus, in dependence on  $\rho_{cp}$ ,  $\zeta_1$  for each material cannot vary more than  $\sqrt{\epsilon} \simeq 2$  to 2.5 times. For such variations of density as are possible on the Moon, the variations of  $\zeta'$  apparently do not exceed 1.5. This dependence on  $\rho_{cp}$  enables one to estimate with sufficient precision the density of the lunar material. Let us note that there exists another possibility of independent determination by radio emission of the value  $\epsilon$ , and from this the density  $\rho$  of lunar material, discussed in [26] and [27].

(B) COMPARISON WITH TERRESTRIAL ROCKS; DENSITY AND DIELECTRIC CONSTANT OF LUNAR MATERIAL

In specimens of terrestrial rocks measured at  $\lambda = 3.2$  cm the density did not vary. The specimens of different rocks had a density comprised in the interval  $0.5 \leq \rho' \leq 1.25$ , a dielectric constant  $1.65 \leq \epsilon' \leq 3.3$ , and loss tangent  $6 \cdot 10^{-3} \leq \tan \Delta \leq 23 \cdot 10^{-3}$ . The specimens were measured in dry state under ordinary conditions†.

A striking result was the fact that the ratio  $\tan \Delta / \rho'$  proved to be practically identical for all rocks under investigation, and equal to

$$\frac{\tan \Delta'}{\rho'} = (1.5 \pm 0.3) \times 10^{-2}. \quad (17)$$

If the group of rocks investigated is identified with those on the Moon, then—in whatever physical state of (porosity and pulverization) they may be—the magnitude of the ratio (17) should remain the same. Accordingly, by substituting (17) in (13) we find that the material on the Moon should have a dielectric constant close to unity. On the average, one may conclude that  $\epsilon = 1.6$ . By substituting this value in (15) or (16) instead of  $\epsilon_k$  and  $\rho_k$ , the average magnitude  $\epsilon' = 2.8$  at  $\rho' = 1.2$  measured for the rocks, it is not difficult to find that a density of the rock  $\rho_{cp} = 0.4$  to 0.5 corresponds to the derived dielectric constant. Let us, therefore, adopt for the lunar material the values of

$$\epsilon = 1.6 \quad \text{and} \quad \rho_{cp} = 0.5. \quad (18)$$

This conclusion seems to be quite natural since, if the rocks investigated under terrestrial conditions had a density of the order of unity, then under lunar conditions the density of such rocks can only be less due to the considerably more favourable conditions for the formation of highly porous material. The conclusion as to the lower density of the lunar rocks than that accepted previously is supported also by the observed high radio temperature of the Moon [11]. Actually, according to (15) or (16), a low  $\epsilon$  corresponds to a low value for the average density of a substance; and this leads to an increase in the emission capacity ( $I-R$ ) in the radio range. The new value  $\epsilon = 1.6$ , in comparison with the earlier accepted values of  $\epsilon = 3$  to 5, gives an increase in the intensity of the radio emission (radio temperature) of the Moon by 6 to 10%, which essentially reduces the earlier observed difference between the optical and the radio temperature.

† Air instead of a vacuum cannot introduce any appreciable changes in the results for  $\epsilon$  and  $\tan \Delta$ .

Thus our comparison shows that the investigated rocks can, in a first approximation, be identified according to their electrical parameters, with those on the Moon. It should be noted that the values  $\gamma$ , leading to  $\xi$  consistent with the data of the electrical conductivity of the investigated terrestrial rocks and the high intensity of radio emission, lie in a relatively narrow interval  $800 \leq \gamma \leq 1200$ . This is evidence of the sufficient precision and reliability of the adopted value of  $\gamma = 900$  and points to good agreement of these values with the conductivity. The former contradiction between these data thus completely disappears.

#### (C) HEAT CONDUCTIVITY AND DEPTH OF PENETRATION OF THE THERMAL AND ELECTROMAGNETIC WAVES

The derived values  $\gamma = 900$  and  $\rho = 0.5$ , give for the material of the Moon (for  $c = 0.2$   $k = 1.25 \times 10^{-5}$  instead of the earlier value of  $k = 3 \times 10^{-5}$   $\rho = 2$ ). The depth of the penetration of the heat wave will be equal to

$$l_T = \sqrt{\left(\frac{2k}{\rho c \Omega}\right)} \simeq 10 \text{ cm.} \quad (18a)$$

From here, and also from (10), the thickness of the radiating layer for waves of the centimetre and millimetre range is

$$l_E \simeq 20 \lambda. \quad (19)$$

In accordance with (13) and (18), the loss tangent of the lunar material corresponding to  $\rho = 0.5$  and  $\epsilon = 1.6$  is

$$\tan \Delta \simeq 0.6 \times 10^{-2}.$$

The effective electrical conductivity at  $\lambda = 3.2$  cm is, accordingly, equal to

$$\sigma(3) = 4.5 \times 10^7 \text{ in c.g.s. units.}$$

#### (D) TEMPERATURE OF THE SURFACE OF THE MOON

The experimental values of  $T_0/T_1$  and the measured value of the constant component  $T_{e0}$  of radio temperature allow for a unique determination of  $T_n$  and  $T_m$  at the given law  $\eta(\beta)$ . For this it is of advantage to use some mean value of  $T_{e0}$ , derived from measurements at different wave lengths. However, one must make certain that the temperature gradient (due to the flow of internal heat) at the upper layer of the material, responsible for radio emission, is sufficiently small. The values of the gradients given in various investigations are much higher than the minimum value necessary for detection by means of measurements on centimetre and millimetre wave lengths [28], [29]. If the most reliable value of the flux which is given in [30] and equal to  $0.25 \times 10^{-6}$  cal/cm<sup>2</sup>sec is adopted—then  $k(\partial T/\partial x) = 0.25 \times 10^{-6}$ . Hence, even for the lowest estimate of thermal conductivity ( $K = 3 \times 10^{-6}$ ) the gradient  $(\partial T/\partial x) < 0.1$  deg/cm—i.e. at the depth of the order of 1 m from which we still receive the emission at  $\lambda = 3$  cm, a difference in temperature of less than  $10^\circ$  K can be expected. This could give an increase in the average radio temperature on this wave length in comparison with the millimetre wave of less than  $5^\circ$ . It follows that in the observed range of

wave lengths the constant component of radio temperature should be practically identical for all the wave lengths, and the observed nonsystematic dispersion is due to observational errors.

The weighted average for the constant component of the radio temperature of the centre of the disk

$$T_{e0} = 230^\circ \text{K}$$

is adopted. The error in this value apparently does not exceed  $\pm 5\%$ . Hence, with  $\epsilon = 1.6$  we obtain  $T_0 = 234^\circ \text{K}$  and in accordance with (9)  $T_1 = 156^\circ \text{K}$ . By substituting this in (5) we derive the following values of the true temperatures of the surface of the Moon.

$$T_n = 127^\circ \text{K}, \quad T_m = 407^\circ \text{K}$$

at midnight and noon, respectively.

The radio temperature of the centre of the disk is, consequently, for  $\epsilon = 1.6$

$$T_e = 230^\circ + \frac{155^\circ}{\sqrt{(1+2\delta+2\delta^2)}} \cos(\Omega t - \xi). \quad (19a)$$

The values  $T_n = 125^\circ \pm 5^\circ$  and  $T_m = 407^\circ \text{K}$  obtained in the infrared region ( $\lambda = 8$  to  $12\mu$ ) do not contradict, within the limits of the precision of measurements, the higher temperatures found from the radio data. The computations of  $\gamma$  from optical observational results on the temperature curve of the eclipse and night temperature of the Moon [1] are based on the temperature of the subsolar point  $T_m = 374^\circ$  obtained theoretically, as is now known, from a too low value of the solar constant. It is not difficult to reduce the results of the optical eclipse to the night temperature. In accordance with [1] the experimental temperature curve at the time of the eclipse corresponds to a theoretical curve with the parameter

$$\sigma E T_m^3 t_0^{1/2} \gamma \sqrt{0.1}$$

equal to 1.5. In this case for  $T_m = 374^\circ \text{K}$  and the radiating capacity  $E = 1$  ( $\sigma$  and  $t_0$ , constants)  $\gamma = 1026$ . At  $T_m = 407^\circ \text{K}$  and an average albedo of  $8\%$  ( $E = 0.92$ ) the same parameter is obtained with  $\gamma = 800$ . The approximate corrections to Jaeger's curves [1] for the dependence of the surface temperature on the phase gives for  $T_n = 127^\circ \text{K}$  the value  $300 \leq \gamma \leq 600$ . Thus the values found for  $T_n$  and  $T_m$  bring the optical data for  $\gamma$ , obtained from the eclipse and lunations to better mutual agreement†. As is seen, the optical and radio data on temperature are in need of more precise and reliable measurements.

From the above facts the following conclusions can be drawn:

1. The surface layer of lunar material is quite homogeneous in its physical properties, at least to the depth of the order of 1 m, and is characterized by  $\gamma = 900$ . The hypothesis of a nonhomogeneous two-layer structure is not in accordance with the data on radio emission.

2. By its electrical parameters the upper layer of the Moon can be satisfactorily identified with terrestrial volcanic rocks, and cannot contain

† This discrepancy was especially noted in [1].

any significant admixture of dispersed meteoritic iron. This confirms the view of the endogenous origin of the upper layer.

3. A comparison of the electrical parameters of the lunar material with terrestrial rocks leads necessarily to the conclusion of a low density of lunar material of the order of 0.5 gr/cm<sup>3</sup>, due, for example, to their great porosity which may attain 80% by volume. This, together with the low thermal conductivity, calls for the assumption of very loose porous material, or, perhaps a dust structure. However, at such low density the latter is less likely. More definite conclusions on this may be obtained from radio measurements if more precise determinations are made of optical and radio data as well as detailed investigations of the electrical and thermal parameters of terrestrial materials. However, we already possess optical data (such as the scattering indicatrix, dependence of polarization on the phase of the Moon) refuting the pulverized state of the material on the topmost surface [19], [32], or [15]; and consequently, in accord with the proved homogeneity of the surface layer in depth.

4. The radio data for the temperature and the basic thermal parameters of the upper surface layer of the Moon agree satisfactorily with the optical data for the same parameters.

#### REFERENCES

1. Jaeger, J. C. *Aust. J. Phys.* 6, 10 (1953).
2. Piddington, J. H. and Minnett, N. C., *Aust. J. sci. Res.* 4A, 450 (1951).
3. Troitsky, V. S. *Astr. Zhurn.* 31, 511 (1954).
4. Troitsky, V. S. "Transactions of the 5th Conference on Problems of Cosmogony". Publishing Office of the Academy of Sciences of the U.S.S.R., Moscow, 99 (1956).
5. Barabashev, N. P. and Chekirda, A. T. *Izv. Kom. Fiz. Planet.* no. 1 (1959); *Astr. Zhurn.* 851 (1959).
6. Zelinskaya, M. R., Troitsky, V. S. and Fedoseyev, L. I. *Astr. Zhurn.* 31, 643 (1959).
7. Salomonovich, A. E. *Astr. Zhurn.* 35, 129 (1958).
8. Gibson, J. E. *Proc. Inst. Radio Engrs. N.Y.* 46, 1, 280 (1958).
9. Shillerov (translator) "Propagation of Ultrashort Waves". Soviet Radio (1954).
10. Kislyakov, A. G. *Radiofizika*, in press (Compendium of the Transactions of the Symposium on the Moon).
11. Strezhneva, K. M. and Troitsky, V. S. *Radiofizika*, in press.
12. Salomonovich, A. E. These Proceedings, pp. 491-496.
13. Sinton, W. M. These Proceedings, pp. 469-471.
14. Sharonov, V. V. "The Nature of Planets."
15. Markov, A. V. ed. "The Moon". Publishing Office of Literature on Physics and Mathematics, Moscow (1960).
16. Skanavi, G. I. "Physics of Dielectrics". State Publishing Office of Foreign Technical Literature, Moscow (1949).
17. Kelly, J. M., Stenoien, J. O. and Isbell, D. E. *J. appl. Phys.* 24, 258 (1953).
18. Swarup, S. *Electronic. Radio Eng.* 35, 5 (1958).
19. Pawsey, J. L. and Bracewell, R. N. "Radio Astronomy", translation edited by I. S. Shklovsky. Foreign Literature, Moscow (1958).
20. Odelevsky, V. I. *J. tech. Phys., Moscow* 21, 667 (1951).
21. Levin, L. "Theory of Modern Waveguides". Foreign Literature, Moscow (1954).
22. Boettcher, C. J. E. "Theory of Electric Polarization". New York (1952).
23. Myshkin, V. G. *Fizika izv. vuz.* no. 3 (1958).
24. Parnas, Y. M. and Lebedeva, K. I. Physics of Dielectrics "Transactions of the 2nd All-Union Conference on Dielectrics". Publishing House of the Academy of Sciences of the U.S.S.R., Moscow (1960).
25. Burak, I. N. and Zhilenkov, N. V. *Fizika Izv. vuz.* no. 6 (1958).
26. Troitsky, V. S. and Tseytlin, N. M. *Radiofizika izv. vuz.* no. 5 (1960).
27. Troitsky, V. S. *Astr. Zhurn.* in press.

## 45. RADIO EMISSION OF THE MOON

489

28. Fremlin, J. H. *Nature, Lond.* **183**, 239 (1959).
29. Jaeger, J. C. *Nature, Lond.* **183**, 1316 (1959).
30. Levin, B. J. and Mayeva, S. V. *C.R. Acad. Sci. U.R.S.S.* **133**, 44 (1960).
31. Coates, R. J. American Astronomical Society Meeting, Canada (1959).
32. Sytinskaya, N. N. *Astr. Zhurn.* **36**, 315 (1959).



# THERMAL RADIO EMISSION OF THE MOON AND CERTAIN CHARACTERISTICS OF ITS SURFACE LAYER

A. E. SALOMONOVICH

*Lebedev Physics Institute, Academy of Sciences, U.S.S.R.*

In order to use the data on the radio emission of the Moon as a basis for conclusions regarding the characteristics of the surface layer of the lunar crust, additional data or assumptions about the properties of this layer are necessary. The use of high-resolution radio telescopes reduces to a certain extent the unavoidable arbitrariness in the selection of parameters. Observations with the 22-m radio telescope of the Physics Institute, Academy of Sciences, made it possible to evaluate certain characteristics of the surface layer without relying entirely on optical data.

The observations were made in 1959-60 at the 0.8, [2, 3], 2.0 [4], 3.2 [5] and 9.6 cm [6] wave lengths. At the wave length of 9.6 cm the brightness temperature averaged over the disk of the Moon was measured at a co-incidence of antenna diagram axis with the centre of the disk. Since the width of the diagram at the level of 3 db was 19', practically the temperature of the central part of the disk was measured. The antenna parameters were determined from data of measurements of discrete sources of radio emission [7]. The brightness temperature, within the accuracy of relative errors of measurement ( $\pm 2\%$ ), was found to be independent of the phase of the Moon and equal to 230° K. The errors in determining the absolute brightness temperature amounted to  $\pm 15\%$ .

At 3.2, 2 and 0.8 cm wave lengths the antenna pattern of the radio telescope was  $6.3 \sim 4'$  and  $\sim 2'$  respectively, which after correcting for the antenna smoothing enabled to obtain a two-dimensional distribution of radio brightness over the lunar disk ("radio image" of the Moon).

On Figs. 1 and 2 examples of the distributions obtained at  $\lambda = 0.8$  and 3.2 cm are given. The region of maximum radio brightness shifts systematically along the lunar equator following the sub-solar point. Furthermore, there is a constant weakening of brightness in the direction from the equator to the poles, due to a decrease of surface temperature with latitude  $\psi$ . The deviations of the radio-isophotes from axial symmetry observed on many radio images are, possibly, connected with various properties of separate regions on the surface of the Moon; but this conclusion needs verification.

The phase dependence of radio brightness distribution leads to periodic brightness temperature variations in the centre of the disk  $T_c$ . These variations are maximum at the 0.8 cm wave length [8] where they are noticeably anharmonic; the mean values  $T_c = T_0$  were determined with an accuracy of  $\pm 15\%$  and on 0.8, 2.0 and 3.2 cm wave lengths they were found to equal 210° K, 190° K, 223° K, respectively. An analysis of the results of measurement at 0.8 and 2 cm wave lengths, carried out by a previously proposed



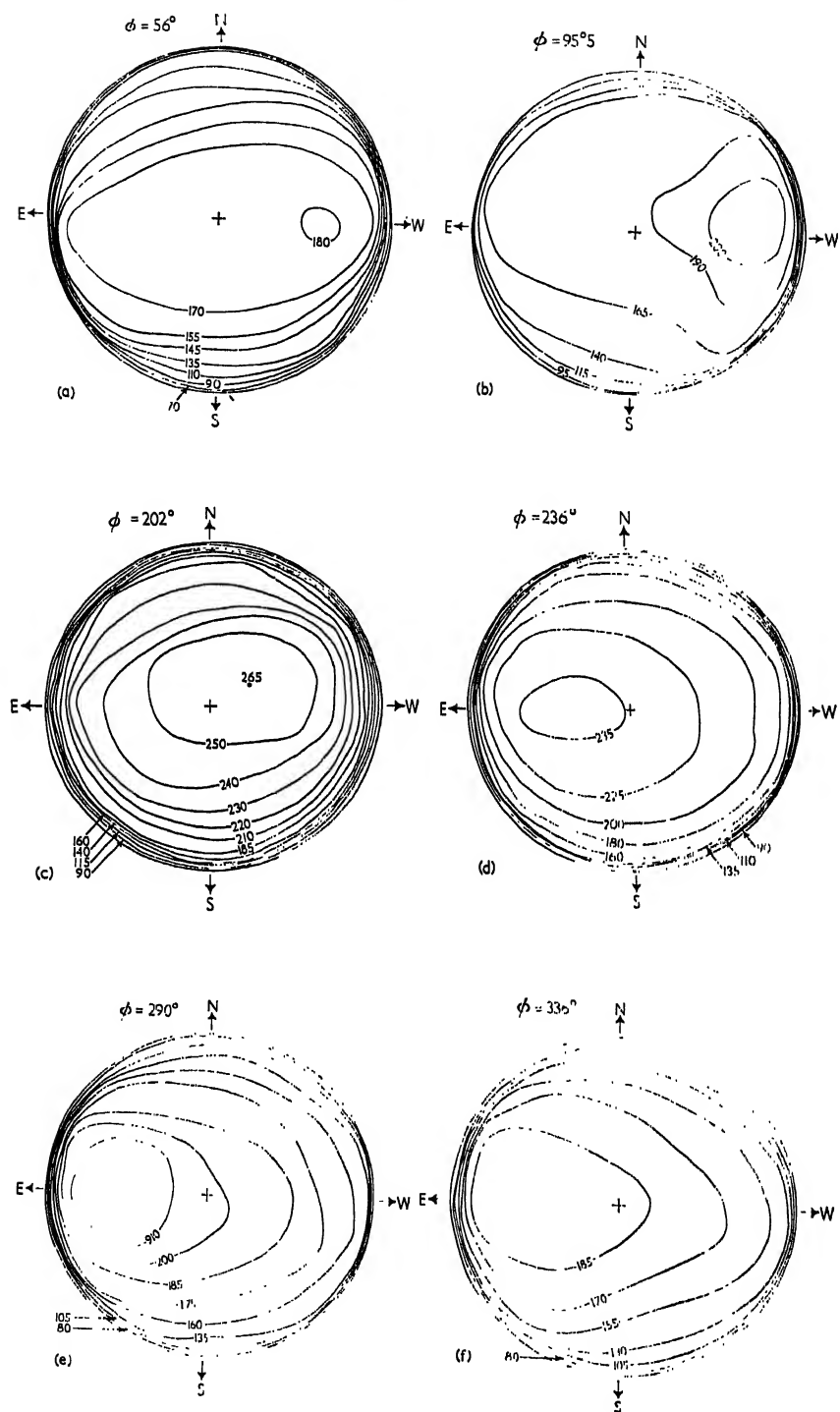


FIGURE 1.

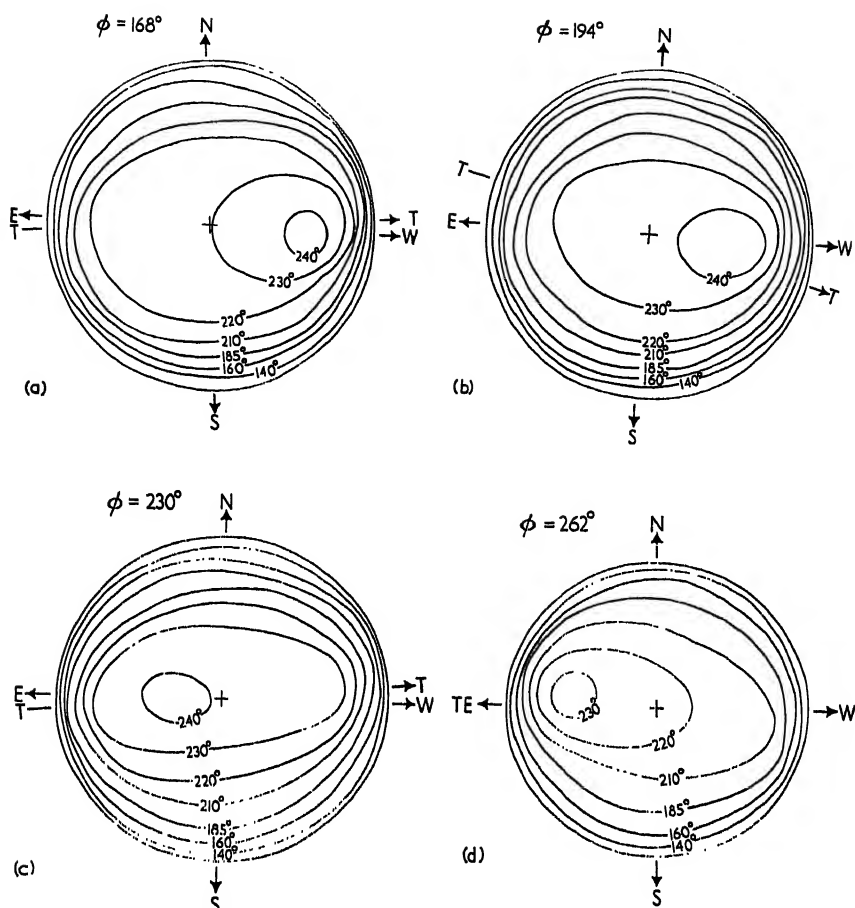


FIGURE 2.

method showed that the effective dielectric constant of the surface layer does not exceed 2, and the latitudinal distribution of surface temperature is given approximately by the function  $\cos^2 \psi$ . During further reductions we also took into account the more accurate values of surface temperatures in the centre of the disk at lunar noon ( $407^\circ \text{K}$ ) and midnight ( $125^\circ \text{K}$ ) measured in the infrared region of the spectrum.

In the following table are given the ratios of the first harmonic  $T_1$  to  $T_0$ , as well as the ratios of the depth of penetration of radio and the first harmonic of the thermal wave  $\delta_1$  [9]. Listed also are the phase lags of the first harmonic of the variable component of radio temperature relative to the optical phase  $\xi$ . We utilized the values obtained with the radio telescope of the Physics Institute, Academy of Sciences, on 0.8, 2.0, 3.2, 9.6 cm, as well as the published results by Piddington and Minnett (1.25 cm [10]), Troitsky, Selinskaya and Fedoseyev (1.63 cm [11]) and Mezger (20.5 cm [12]).

For  $\lambda > 1 \text{ cm}$ ,  $\delta_1/\lambda \approx 2$ . At 0.8 cm,  $\delta_1/\lambda = 2.5$ , which is somewhat higher than the indicated value, although it is close to it. The constancy of the

TABLE 1

$\lambda$ (cm)	$T_e/T_0$	$\delta$	$\delta_1\lambda$	$\xi$ (calculated)	$\xi$ (observed)	$C$
0.8	0.20	2.0	2.5	34	$30 \pm 5$	0.85
1.25	0.17	2.4	1.9	35	45(?)	
1.63	0.16	2.3	1.4	35	34	
2.0	0.10	4.4	2.2	39	$40 \pm 5$	0.40
3.2	0.075	6.1	1.9	41	$45 \pm 5$	0.29
9.6	$< 0.02$	$> 24$	$> 2.4$	—	—	
	—	—	—	—	—	
20.5	$< 0.02$	$> 25$	$> 1.2$	—	—	

ratio  $\delta_1/\lambda$  is evidence of the approximate constancy of layer properties responsible for radio emission in the 1 to 3 cm range.

For a comparison with Jaeger's calculations [13] the mean values  $T_0$  of brightness temperatures, obtained on 0.8, 2 and 3.2 cm ( $210^\circ \pm 15\%$ ,  $190^\circ \pm 15\%$  and  $223^\circ \pm 15\%$  respectively) were reduced to the more reliably measured value of  $230^\circ$  K measured on 9.6 cm. The parameter  $C = \sqrt{\pi}/\delta_1$  given in Jaeger's calculations is also listed in the table for 0.8; 2 and 3.2 cm. The phase variation curves of the lunar radio temperature, computed by Jaeger, were corrected by taking into account the more accurate values of surface temperatures listed above. The observational results by Pettit and Nicholson [14] could be explained assuming that

$$(kpc)^{-1/2} = 300 \pm 450.$$

On the other hand, the constant component of brightness temperature  $230^\circ \pm 10\%$ , derived by us, corresponds to  $(kpc)^{-1/2} = 300 \div 1000$ . Jaeger's curves were modified and plotted for  $(kpc)^{-1/2} = 380$  and  $(kpc)^{-1/2} = 1000$ , using values of  $C$  which correspond to  $\delta_1$  obtained at 0.8, 2.0 and 3.2 cm. The observed phase variation curves of brightness temperature at the centre of the disk agree with the above theoretical curves within the limits of observational errors (Fig. 3).

The above data give more definite evidence than those obtained previously in favour of the one-layer model. For this it is necessary that

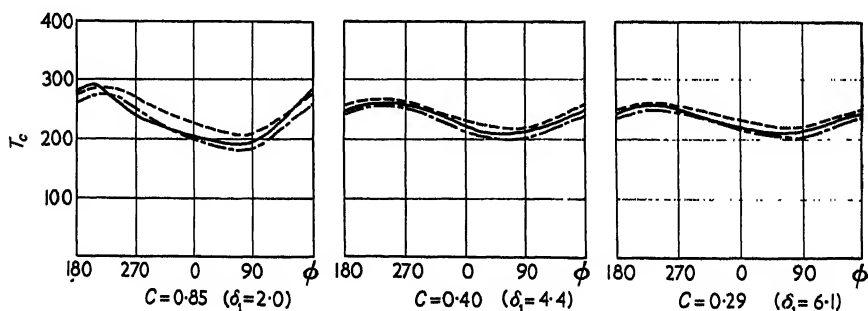


FIGURE 3.

---- corresponds to  $(kpc)^{-1} = 380$

..... corresponds to  $(kpc)^{-1} = 1000$

$(k\rho c)^{-1/2} < 10^3$ , which is in favour of a very porous and not dense material. This is also confirmed by the relatively low value of the effective dielectric constant ( $1 < \epsilon < 2$ ). An estimate of the depth of penetration of the thermal wave made for  $(k\rho c)^{-1/2} = 600$  and  $\epsilon = 1.5$ , leads to an effective density of the radiating layer equal to  $0.5 \text{ g/cm}^3$ . At these assumptions  $K = 3.5 \times 10^{-5}$  and the depth of thermal wave penetration is  $\sim 20 \text{ cm}$ . Adopting  $\delta_1 = 2\lambda$  we obtain a depth of penetration of electromagnetic waves  $40\lambda$ . The loss angle at  $\lambda = 2 \text{ cm}$  is in this case equal to  $\sim 10'$ .

A higher value of the parameter  $\delta_1$  for the  $0.8 \text{ cm}$  wave length indicates apparently a certain decrease in density and thermal conductivity toward the surface. Gradual changes of these properties with depth are only to be expected.

#### REFERENCES

1. Salomonovich, A. E. *Radiotekh. Elektron.* **4**, no. 12, 2092 (1959).
2. Amenitsky, N. A., Noskova, R. I. and Salomonovich, A. E. *Astr. Zhurn.* **37**, 185 (1960).
3. Losovsky, B. Y. and Salomonovich, A. E. Theses of a Report presented at the Plenum of the Commission on Radioastronomy, November, 1960.
4. Salomonovich, A. E. and Koshechenko, V. N. *Radiofiz. Izv. Vuzov* **4**, 4, 591 (1961).
5. Koshechenko, V. N., Losovsky, B. Y. and Salomonovich, A. E. *Radiofiz. Izv. Vuzov* **4**, 4, 596 (1961).
6. Koshechenko, V. N., Kuzmin, A. D. and Salomonovich, A. E. *Radiofiz. Izv. Vuzov* **4**, 3, 425 (1961).
7. Karachun, A. M., Kuznin, A. D. and Salomonovich, A. E. *Radiotekh. Elektron.* **6**, 3, 430 (1961).
8. Kaidanovsky, N. L. and Salomonovich, A. E. *Radiofizika Izv. Vuzov* **4**, 1, 40 (1961).
9. Troitsky, V. S. *Astr. Zhurn.* **31**, 512 (1954).
10. Piddington, J. H. and Minnett, H. C. *Aust. J. sci. Res.* **2A**, 63 (1949).
11. Troitsky, V. S., Zolinskaya, M. R. and Fedoseyev, I. N. *Radiofizika* **3** (1959).
12. Mozger, P. G. and Strassl, H. *Planetary Space Sci.* **1**, 213 (1959).
13. Jaeger, J. C. *Aust. J. Phys.* **6**, 10 (1953).
14. Pettit, E. and Nicholson, S. B. *Astrophys. J.* **71**, 102 (1930).



# THERMAL RADIO EMISSION OF THE MOON AT A WAVE LENGTH OF 10 cm

V. N. KOSHCHENKO, A. D. KUZMIN, A. E. SALOMONOVICH  
*Lebedev Physics Institute, Academy of Sciences, U.S.S.R.*

THE investigations of intensity and phase dependence of the thermal radiation of the Moon at various wave lengths of the radio-range are very important for clarifying the properties and structure of the Moon's surface layer.

In the 10-cm range the radio emission of the Moon was investigated by Kaydanovsky, Turusbekov and Khaikin [1], and also by Akabane [2]. According to the data in [1], the constant component of brightness temperature of the Moon, averaged over the disk is  $T_{br0} = 130^\circ \text{K}$ ; and the variable component due to the dependence of brightness temperature on the phase of the Moon, is absent within the limit of accuracy of 8%. However, according to data in [2],  $T_{br0} = 315^\circ \text{K}$ , and the amplitude of the variable component attains 25%. Besides the results just quoted, the paper by Piddington and Minnett [3] contains a reference to a single measurement at the 10-cm wave length, yielding  $T_{br} = 215^\circ \text{K}$ .

Since the results of these investigations differ still appreciably (probably due to an insufficient accuracy in estimates of the parameters of the utilized radio telescopes), we have at present no clear conception of the intensity of thermal radio emission of the Moon in the 10-cm range and of its dependence on the phase. In order to obtain more reliable data, we have conducted a cycle of observations of the radio emission of the Moon at 9-6-cm wave length.

The observations were carried out by means of the 22-cm radio telescope at the Physical Institute of the Academy of Sciences, U.S.S.R. [4]. For a receiver a modulation radiometer, briefly described in [5] was used. The calibration of antenna temperature was carried out with the aid of a gas-discharge noise generator placed in the channel of the equivalent. For the time constant of 4 sec, the fluctuation sensitivity was  $0.5^\circ \text{K}$ . The antenna temperature of the Moon varied from day to day as a function of the apparent angular diameter of the Moon within the range of  $132$ – $154^\circ \text{K}$ . The transits in azimuth through the centre of lunar disk were controlled by means of an optical sighting device during observations carried out on days when the Moon was optically visible. When the Moon was invisible (cloudiness, new Moon), the antenna of the radio telescope was aimed at the calculated position of the centre of its disk. The transits in azimuth were conducted with the differential speed of 2–3 minutes of arc per minute of time. In consecutive transits the position of axis was shifted in the elevation angle. From recordings thus obtained those corresponding to the maximum value of antenna temperature were selected, thereby excluding non-central passages.

The conversion of the antenna temperature into the brightness tempera-

ture  $T_r$ , averaged over the disk, was made by means of the relation

$$T_{br} = \frac{4\pi T_{br}}{(1-\beta)G \int_{\Omega} F(\varphi, \theta) d\Omega}. \quad (1)$$

The gain  $G = 2.6 \times 10^5 \pm 15\%$  and scattering coefficient  $\beta = 0.32$  of the antenna were determined earlier [6] from the discrete source of radio emission, Taurus A, whose flux density at  $\lambda = 9.6$  cm was assumed to be equal to  $p = 709 \times 10^{-26}$  W m $^{-2}$  c $^{-1}$ ). The integral

$$\int_{\Omega} F(\varphi, \theta) d\Omega,$$

was determined by numerical integration of the directivity pattern of the antenna,  $F(\varphi, \theta)$  within the limits of the visible disk of the Moon  $\Omega_{\zeta}$ .

The results of observations, carried out from 8 April to 28 May 1960, are shown in Fig. 1, where the values of the Moon's brightness temperature,

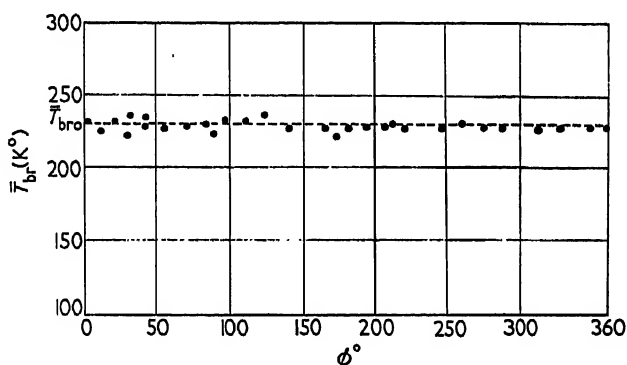


FIG. 1. Results of observations carried out between 8 April and 28 May 1960.

averaged over the visible disk, are plotted as a function of the Moon's phase. The average value of the Moon's brightness temperature at  $\lambda = 9.6$  cm is  $T_{br0} = 230 \pm 4.5^\circ$  K $^\dagger$ . It is clear from Fig. 1 that—within the limits of observational accuracy—there is no regular deviation of  $T_{br}$  from the average value. Consequently, at the wave length of 9.6 cm the amplitude of the variable component does not exceed 2%. Thus, the conclusions of [2] on the presence of a variable component of 25% must be regarded as erroneous.

The magnitude of the constant component of the Moon's brightness temperature as given in [2] is apparently also overestimated. On the other hand, the data on the constant component of temperature, as given in [1] are apparently greatly underestimated.

Our results for  $T_{br0}$  are in good agreement with the measurements in 20 cm range, carried out on 25 m radio telescopes by Mezger and Strassl [7] who obtained  $T_{br0} = 250^\circ$  K  $\pm 12\%$ , and with the single measurement by

$^\dagger$  Apart from that, there is a systematic error of 15%, caused mainly by the inaccuracy in determination of antenna parameters.

Westerhout [8] ( $T_{bro} = 232 \pm 50^\circ \text{K}$ )†. No phase variation of  $T_{br}$  was revealed in measurements reported in [7] within the accuracy of 2%. The slight increase in brightness temperature at transition from 10 cm to 20 cm (taking into account systematic errors due to an inaccurate knowledge of the parameters of radio telescope antennas) apparently cannot as yet be regarded as real, although it does not contradict the concept of temperature increase with penetration into the depth of lunar crust. To clarify this interesting problem, it would be advisable to conduct measurements of the Moon's thermal radiation at longer wave lengths.

The virtual absence of phase variation on decimetre waves is compatible with existing concepts of the mechanism of the Moon's thermal radio emission [10].

#### REFERENCES

1. Kaidanovsky, N. L., Turusbekov, M. T. and Khaikin, S. E. "Transactions of Fifth Conference on Problems of Cosmogony". Publishing House of the Academy of Sciences, U.S.S.R. page 347, 1956.
2. Akabane, K. *Proc. imp. Acad. Japan* **31**, 161 (1955).
3. Piddington, J. H. and Minnett, H. C. *Aust. J. sci. Res.* **4A**, 459 (1951).
4. Salomonovich, A. E. *Radio Eng. Electron.* **4**, 2092 (1959).
5. Kuznin, A. D., Levchenko, M. T., Noskova, R. I. and Salomonovich, A. E. *Astr. Zhurn.* **37**, 975 (1960).
6. Karachun, A. M., Kuzmin, A. D. and Salomonovich, A. E. *Radio tekhn. Electron.* **6**, 430 (1961).
7. Mezger, P. G. and Strassl, H. *Planetary Space Sci.* **1**, 213 (1959).
8. Westerhout, G. *Bull. astr. Insts Netherlands.* **14**, 215 (1958).
9. Mezger, P. G. *Z. Astrophys.* **46**, 234 (1958).
10. Troitsky, V. S. *Astr. Zhurn.* **31**, 511 (1954).

† Taking into account the correction of 0.86, made by Mezger [9]





# THE PHASE DEPENDENCE OF RADIO EMISSION OF THE MOON ON 3.2 cm

K. M. STREZHNEVA, V. S. TROITSKY

*Radio-Physics Research Institute, U.S.S.R. Academy of Sciences, U.S.S.R*

The absolute measurements of the intensity of radio emission of the Moon, carried out with the aid of more advanced equipment and method of calibration, made it possible to reveal its variation with the phase, and yielded the value of the effective temperature for the centre of the disk practically equal to  $T_1 = 245^\circ + 15.5^\circ \cos(\Omega t - 50^\circ)$ , the ratio of penetration depth of the electric wave to the thermal wave equal to 6.0, and  $\delta/\lambda = 2.0$ .

The dependence of the radio emission of the Moon at 3.2 cm on its phase has not been revealed until recently. The basic task of our work consisted in measuring the phase dependence of the radio temperature at 3.2 cm, with a more accurate method of measurements of absolute intensity than had been used previously [1]. For this purpose we employed a new method of antenna calibration [2], a more precise method of measurements and reduction of the data (taking into account the effect of background noise of the antenna), and new improved equipment [3]. Before the results are discussed it is, however, advisable to give an account of the method of measurement.

## 1. METHOD OF MEASUREMENT OF THE ANTENNA TEMPERATURE

The absolute measurements of the antenna temperature of the Moon were made by the method of calibration using natural noises of the antenna [4] with a modernization [5] allowing for an automatic reduction of the absorption in our atmosphere. The measurement procedure consisted, as usual, of two operations:

1. Measurement of the difference between signals of the antenna, the beam of which was directed skyward to the height of the Moon (to the right or left of the Moon), and the "cold" radiation standard (having the surrounding temperature) connected instead of the antenna.

2. Measurement of the signal increment when directing the antenna beam toward the Moon.

A more precise analysis of this procedure yields the following results. The temperature of the signal at the output of the antenna directed skyward to the height of the Moon  $h$  will be [2]

$$T_1(h) = T_n(h)(1 - \beta)\eta + T_\varphi(h) + T_0(1 - \eta), \quad (1)$$

where  $\eta$  is the antenna efficiency;  $\beta$ , the coefficient of power dissipation apart from the specified major lobe;  $T_n(h)$ , the effective radio-temperature of the sky at an altitude  $h$ ;  $T_\varphi(h)$ , the background temperature of antenna output which is equal to  $T_g(h)\eta\beta$ , wherein  $T_g(h)$  is the mean temperature of the background according to minor lobes, allowing for the atmosphere and ground radiation; and  $T_0$  is the temperature of antenna material. Let

the temperature of the cold standard be  $T_x = T_0 + \Delta t$ . The first operation yields

$$k\eta_n = T_x - T_1(h) = \Delta t - T_n(h)(1 - \beta)\eta - T_\varphi(h) + T_0\eta, \quad (1a)$$

where  $\eta$  is the deflection of the output meter on switching the latter from the antenna to the standard, measured in mm; and  $k$  is the sensitivity of equipment, measured in  $^\circ/\text{mm}$ .

In aiming the antenna beam at the Moon, as a result of a slight change of the antenna direction only in azimuth, the temperature of the antenna—induced by the radiation of background [1]—will not vary and therefore the second procedure yields

$$kn_l = T_{al}\eta, \quad (2)$$

where  $\eta_l$  is the deflection of the output meter on directing the antenna toward the Moon, and  $T_{al}$  is the antenna temperature of the lunar radio emission attenuated in the atmosphere.

Excluding  $k$ , from (1) and (2) we obtain the final expression for determining the antenna temperature from the radiation of the Moon, or of any other source

$$T_{al} = \frac{n_l}{n_n} \left[ T_0 - T_n(h)(1 - \beta) - \frac{1}{\eta} T_\varphi(h) + \frac{1}{\eta} \Delta t \right]. \quad (3)$$

It is obvious from the expression thus obtained that in precise measurements we must know, and take into account, the background temperature and the antenna efficiency, introduced as corrections. In some cases it is advisable to represent expression (3) in a somewhat different form. According to [7],

$$T_n(h) = T_\varphi \{1 - \exp(-\gamma_0/\sin h)\},$$

where  $T_\varphi = T_0 - \Delta T$ ;  $T_0$  being the temperature of atmosphere near the ground, and  $\gamma_0$  the absorption of the entire atmosphere in the zenith.  $\Delta T$  depends on  $h$  and  $\lambda$ ; for  $\lambda = 3.2$ , at  $h > 5^\circ$  (plane atmosphere),  $\Delta T \simeq 30^\circ \text{ K}$ . Inasmuch as the Moon is being observed at altitudes for which the atmosphere can be considered plane,  $T_{al} = T_{al}^0 \exp(-\gamma_0/\sin h)$ , where  $T_{al}^0$  is the antenna temperature in the absence of atmospheric absorption. By substituting expressions  $T_H(h)$  and  $T_{al}$  in (3) we obtain

$$T_{al}^0 = \frac{n_l}{n_n} T_0 \left[ 1 + \beta \frac{1 - \exp(-\gamma_0/\sin h)}{\exp(-\gamma_0/\sin h)} + \frac{\Delta T(1 - \beta)}{T_0} \cdot \frac{1 - \exp(-\gamma_0/\sin h)}{\exp(-\gamma_0/\sin h)} + \frac{\Delta t - T_\varphi(h)}{\eta T_0 \exp(-\gamma_0/\sin h)} \right], \quad (4)$$

where, as we know,

$$T_{al}^0 = \frac{\int_{\omega} T_l F d\Omega}{\int_{4\pi} F d\Omega}, \quad (5)$$

where  $\omega$  is the solid angle of the Moon;  $T_l$ , the distribution of radio brightness temperature over the Moon's disk; and  $F$ , the power diagram of the antenna.

Let us now evaluate the separate terms. For  $\lambda = 3.2$  cm,  $\gamma_0 = 0.02$  neper and for all altitudes  $h \geq 5^\circ$   $1 - \exp(-\gamma_0/\sin h) = \gamma_0/\sin h$ . Since in all measurements the Moon's altitude was not less than  $h = 20^\circ$ ,  $\gamma_0/\sin h \leq 0.06$ . At  $\beta = 0.2^\dagger$ , the second term in (4) constitutes about 1% and can be neglected while the third term amounts to no more than 0.5% at  $\Delta T = 30^\circ$ , and the fourth term can introduce a correction of up to 5 to 7%. Thus, with a sufficient degree of accuracy,

$$T_{at}^0 = \frac{n_l}{n_n} T_0 \left[ 1 + \frac{\Delta t - T_\varphi(h)}{\eta T_0} \right]. \quad (6)$$

This formula served for calculations of the antenna temperature. The quantity  $T_\varphi(h)$  was determined by the method described in [2] and constituted, at  $h > 20^\circ$  or  $30^\circ$ ,  $25^\circ$  K for the horizontal polarization and  $35^\circ$  K for the vertical. The quantities  $T_0$ ,  $\Delta t$  and  $\eta$  were determined for each measurement.

## 2. DETERMINATION OF MOON'S RADIO TEMPERATURE

As the width of the antenna pattern was comparable with angular dimensions of the Moon, we can determine from (5) only the Moon's average temperature over the disk with the weight of the diagram (8); cf., e.g. [9]. Indeed, multiplying and dividing (5) by

$$\int_{\omega} F d\Omega$$

we find that

$$T_{at}^0 = T_{lF} = \frac{\int_{\omega} F d\Omega}{\int_{4\pi} F d\Omega} = T_{lF}(1 - \beta_l), \quad (7)$$

where

$$T_{lF} = \frac{\int_{\omega} T_l F d\Omega}{\int_{\omega} F d\Omega} \quad (8)$$

<sup>†</sup> In measurements for angles  $h > 20^\circ$  it is advisable to determine  $\beta$  in expression (1) by assuming that the angular dimension of the major lobe is of the order of the background inhomogeneity—i.e.  $10$ – $15^\circ$ . This corresponds to the value of  $\beta$  given above.

is the weighted average radio-temperature of the Moon, and

$$\beta_l = \frac{\int_{4\pi-\omega} F d\Omega}{\int_{4\pi} F d\Omega} \quad (9)$$

is the coefficient of "scattering," indicating—on examination of transmission—the fraction of the power radiated by the antenna outside the Moon's solid angle. The quantity of  $T_{lF}$ —for any diagram—is obviously comprised within the range of values corresponding to the radio brightness temperature of the central part of Moon's disk  $T_l(0)$  (sharp diagram) and to the average temperature over the disk (a diagram width much greater than the angular dimensions of the Moon)

$$T_l = \omega^{-1} \int_{\Omega} T \Omega d\Omega.$$

Allowing for the fact that the decrease of brightness temperature  $T$  occurs only within the range of a narrow ring of  $2'-3'$  of arc. (cf. [8] and [12]) and that the beam width is  $36'$ , we must assume that our determined value of  $T_{lF}$  is closer to the value of  $T_l(0)$  than to the value  $T_l$ . However, the difference between these limits is small and constitutes about 10% cf. [8] and [12].

It is obvious from equation (7) that the determination of  $\beta_l$  is necessary for determining  $T_l$ . A method for measuring the scattering coefficient on a reflecting sheet was proposed and investigated in [2]. The quantity

$$\beta_{\Omega_0} = \int_{4\pi-\Omega_0} F d\Omega / \int_{4\pi} F d\Omega$$

is measured with the angular dimension of the sheet  $\Omega_0$ . We shall express  $T_{al}^0$  through this measured quantity. Multiplying and dividing (7) by

$$\int_{\Omega_0} F d\Omega,$$

we obtain

$$T_{al}^0 = T_{lF} \frac{\int_{\omega} F d\Omega}{\int_{\Omega_0} F d\Omega} (1 - \beta_{\Omega_0}). \quad (10)$$

Hence it is evidently advisable to select  $\Omega_0$  equal to the Moon's solid

angle (cf. [10], and also [6]). However, since the latter varies during a cycle, this does not eliminate the necessity for calculating the ratio of the integrals for each measurement and, consequently, also the necessity of knowing the antenna diagram. The error of measurements will be minimal when  $\Omega_0$  is selected to be of the order of the solid angle of the major antenna lobe. The coefficient  $\beta$  of antenna scattering was measured by the method of reflecting sheet, described in [2], for two dimensions of the circular sheet: one with the visible angular radius  $r_0 = 48'$  and solid angle  $\Delta\Omega_0 = \pi r_0^2/4$ , and another with the visible angular radius  $r_m = 16' \cdot 5$  (see Fig. 1), equal to the maximum



FIG. 1. Reflecting sheet with radius  $r_0 = 16' \cdot 5$ .

angular radius of the Moon. Let us designate by  $\alpha$  the ratio of integrals in (10). For every measurement this quantity changes in accordance with the variation in angular dimensions of the Moon. We note that  $T_{IF}$  should be virtually independent of the Moon's dimension (or a small quantity of second order in comparison with the dependence on  $\alpha$ ). For an axially-symmetric diagram.

$$\alpha = \frac{\int_0^r F(\theta) \sin \theta d\theta}{\int_0^{r_0} F(\theta) \sin \theta d\theta}, \quad (11)$$

where  $r_0$  and  $r$  are the sheet radius and the given radius of the Moon respectively. However,  $r = r_m - \Delta r$ , where  $r_m$  is the maximum radius of the

Moon during a cycle. Assuming that  $r_0 \neq r_m$ , we obtain

$$\alpha = \frac{\int_0^{r_m} F(\theta) \sin \theta d\theta - \int_r^{r_m} F(\theta) \sin \theta d\theta}{\int_0^{r_0} F(\theta) \sin \theta d\theta} = \alpha_0 - \Delta\alpha, \quad (12)$$

where

$$\alpha_0 = \frac{\int_0^{r_m} F(\theta) \sin \theta d\theta}{\int_0^{r_0} F(\theta) \sin \theta d\theta}; \quad \Delta\alpha = \frac{\int_r^{r_m} F(\theta) \theta d\theta}{\int_0^{r_0} F(\theta) \theta d\theta} = \frac{F(r_m)r_m(r_m-r)}{\int_0^{r_0} F(\theta) \theta d\theta} \quad (13)$$

Thus we obtain the following final expression for  $T_{al}$ :

$$T_{al}^0 = T_{lF}(\alpha_0 - \Delta\alpha)(1 - \beta_{r_0}), \quad (14)$$

which was used for the calculation of  $T_{lF}$ . In the case of  $r_0 = r_m$  we have

$$T_{al}^0 = T_{lF}(1 - \Delta\alpha)(1 - \beta_{r_m}). \quad (15)$$

Let us note that  $\beta_r$  or  $\beta_{r_m}$  are the antenna parameters which are determined only by the geometry of the antenna; and therefore it is sufficient to measure them once during each period of observation. In this case, the above-indicated method for measurement of the antenna temperature is advisable.

However, if the reflecting sheet and the "black body" radiating area [2] can be used for each given measurement of the Moon's radiation, it is more expedient to determine the antenna temperature by another procedure, eliminating the necessity of taking into account the background temperature of the antenna. Indeed, by determining the difference of the received radiation of the sheet and of the "black body" radiating area we obtain

$$kn_k = (T_0 - T_{\text{sheet}})(1 - \beta_{r_0})\eta, \quad (15a)$$

where  $T_0$  is the temperature of the "black" area;  $T_{\text{sheet}}$  is the effective temperature of the sheet, dependent mainly on the scattering and reflection of sky radiation in the corresponding angle [6].

According to the second procedure (equation 2), the increment of the signal from the Moon yields  $kn_l = T_{al}\eta$ . From both measurements

$$T_{al} = \frac{n_l}{n_k}(T_0 - T_{\text{sheet}})(1 - \beta_{r_0}) = \exp[-\gamma(h)]T_{al}^0 \quad (16)$$

Finally, according to (7),

$$T_{lF} = \frac{n_l}{n_k}(T_0 - T_{\text{sheet}})\frac{1 - \beta_{r_0}}{1 - \beta_l} \exp[\gamma(h)], \quad (17)$$

where

$$\frac{1 - \beta_{r_0}}{1 - \beta_l} = \frac{\int F d\Omega}{\int_{\omega} F d\Omega} = \alpha. \quad (17a)$$

It may appear advisable to employ this method also with a single use of the sheet, having measured once and for all (by means of the thermal calibration) the quantity  $(T_0 - T_{\text{sheet}})(1 - \beta_{r_0})$ , in formulas (16) and (17) which constitutes in essence a constant parameter of the system ( $T_{\text{sheet}}$  on centimetre wave changes very slightly with prevailing meteorological conditions). However, in order to determine this quantity, it is necessary to measure independently the efficiency  $\eta$  and this, as we know [2], requires taking into account the background noise of the antenna; and once we do so we revert again to the method discussed above.

If the value in the expression for temperature

$$T_1 = (T_0 - T_{\text{sheet}})(1 - \beta_{r_0})\eta_1$$

is found from one measurement, (where  $\eta_1$  is the efficiency at the moment of sheet measurement) and then  $T_x = T_{al}\eta_x$  measured (where  $\eta_x$  is the antenna efficiency on the days when the Moon is observed) we have  $T_{al} = T_x(T_0 - T_{\text{sheet}})(1 - \beta_{r_0})\eta_1/\eta_x$ , or

$$T_{lf} = \frac{T_x}{T_1}(T_0 - T_{\text{sheet}})\frac{1 - \beta_{r_0}}{1 - \beta_l}\exp[+\gamma(h)]\frac{\eta_1}{\eta_x}. \quad (18)$$

As can be easily verified, the background noise of the antenna, similarly entering into the expressions for  $\eta_1$  and  $\eta_x$  affects the result practically insignificantly. However, since the antenna efficiency varies appreciably with the meteorological conditions (air humidity, in our case, by  $\pm 12\%$ ), this method may produce larger errors or dispersion of the data than in the case of application of the above method of separate measurement of the antenna temperature and the antenna parameter  $\beta$ .

We note that, as is evident from above expressions, the systematic errors of the applied method of measurements consist mainly of the error of the determination of  $T_{\text{sheet}}$ . This quantity can be calculated (see (6)) and measured. According to the calculation for  $\lambda = 3.2$  cm and  $20 < T_{\text{sheet}} < 60$ , the measurements yielded  $T_{\text{sheet}} \simeq 40^\circ \text{K} \pm 10^\circ$ . Thus, an inaccurate knowledge of  $T_{\text{sheet}}$  can lead to a systematic error in  $T_{lf}$  (through error in  $\beta$ ) of not more than  $\pm 7-10\%$ .

### 3. THE MEASUREMENTS AND RESULTS

The measurements of lunar radio emission were conducted in both planes of polarization during the optical visibility of the Moon (visual aiming of antenna) from August to October 1959 and from May to September 1960. However, reliable data, which revealed without ambiguity the phase dependence of lunar radio emission, were obtained only in September 1960.



These data are presented in our paper. The earlier data are used for determining the average radio temperature. A 4-meter paraboloid with a round waveguide feed served as the antenna of the radio telescope. The antenna efficiency, measured according to natural noise [4], constituted on the average  $\eta = 0.85$  and varied with meteorological conditions by not more than  $\pm 12\%$ . The scattering coefficient of the antenna outside the solid angle of the sheet  $\Delta\Omega_0 = \pi r_0^2/4$ , where  $r_0 = 48'$ , is according to measurements  $\beta_{r_0} = 0.35$ , and outside the solid angle  $\Delta\Omega_m = \pi r_m^2/4$ , where  $r_m = 16.5'$ , is  $\beta_{r_m} = 0.75$ . The radiometer had the threshold sensitivity of  $0.5^\circ$  for the time-constant of 1 sec, with which all measurements were conducted. The output was registered by a recorder during 1 min; the antenna orientation toward the Moon's centre was maintained at the same time. The thermal calibration was carried out in order to monitor the performance of the radiometer and determine the antenna efficiency. The curve of  $T_{lf}$  plotted against the phase shown on Fig. 2, was obtained as a result of the reduction of the data by means of equations (3), (14) and (15)<sup>†</sup>. As the systematic difference in measurement in both planes of polarization (of the order of 1–1.5%) may have been due to instrumental effects (some change in the pattern, varying background temperature, etc.), this difference was

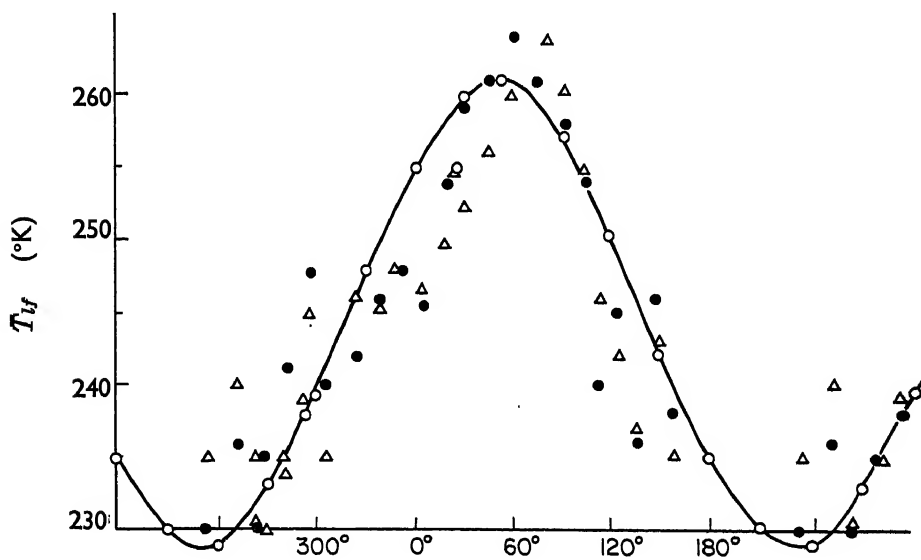


FIG. 2. Moon's radio-temperature vs. phase curve.

●—Moon's temperature in vertical polarization.

△—Moon's temperature in horizontal polarization.

eliminated on Fig. 2 by multiplying the data in vertical polarization by a constant multiplier. The reduction factor was found from the ratio of mean radio temperatures for both directions of polarization.

Besides calibration of the antenna using the reflecting sheet, calibration was also made by means of a standard horn [4]. Within the limits of errors

<sup>†</sup> Each point corresponds to 5–6 measurements.

both gave the same values of  $T_{IF}$ . In the reduction we used the antenna diagram, obtained by means of the Sun, and reduced to the diagram of a point-source by selection of an equivalent diagram reproducing the observed diagram found by graphical integration. The reality of the true diagram thus obtained, is demonstrated by the fact that the direction cosine  $D_0$ , calculated according to the diagram, equals precisely  $D(1 - \beta_{r_0})$ , where  $D$  is the direction cosine measured by means of the horn, and  $\beta_{r_0}$  is the diagram outside the adopted scattering, measured according to the sheet.

We note finally that the calculation of  $T_{IF}$ , carried out from the measurements of  $\beta_{r_0}$  with the sheet  $r_0 = 48'$  (equation 14), and from measurements with a sheet equal to maximum dimension of the Moon's disk  $r_m = 16.5'$  (equation 15), where the accurate value of the pattern is not required (the diagram enters only in the correction  $\Delta\alpha$  constituting no more than 2 or 3%), led to the same values within 1 to 2%. We reduced the data also by means of equation (18), assuming that  $\eta_1/\eta_x = 1$ . As was to be expected, this increased slightly the dispersion of values of  $T_{IF}$ ; however, it gave the same value of temperatures within 1 to 2%. Finally, we reduced the data obtained from measurements of three 1959 cycles, carried out with a double-mirror antenna calibrated according to the square sheet. The average temperature of the Moon was also found to be  $245^\circ \text{K}$ . Taking into account the systematic error of the method and of the calibration of parameters, we consider that the error of absolute values does not exceed  $\pm 15\%$ . The precision of relative measurements is not more than  $\pm 1\%$ ; this is seen directly from the dispersion of the experimental points. It is clear from Fig. 2 that the variation curve of  $T_{IF}$  is slightly asymmetric; however, it is approximated rather satisfactorily by the expression

$$T_{IF} = 245^\circ + 15.75 \cos(\Omega t - 50^\circ). \quad (a)$$

By comparing the ratio of the variable component to the average radio-temperature with the theoretical ratio from expressions for the brightness radio-temperature and the average radio-temperature over the disk [12], we obtain for the quantity  $\delta$  (equal to the penetration depth ratio of electric wave to thermal wave [8]) the value  $\delta \simeq 6.0$ . Accordingly,  $\delta/\lambda \simeq 2.0$ , which corresponds satisfactorily to the estimate made in [1] and to measurements at other wave lengths [11]. In case of a one-layer model the phase shift should be  $\xi = \tan^{-1} \delta/(1 + \delta) = 41^\circ$ . This is less than the quantity observed, although still within the error range of its determination.

The rather large constant component of the radio-temperature, which we have found, is—in our opinion—more reliable than that obtained in [1], where the radio emission of the Moon was determined with the same antenna by the method of comparison with the known radio emission of the Sun from the expression

$$T_{IF} = \frac{T_s}{T_{as}} \cdot \frac{\int_{\Omega} F d\Omega}{\int_{\Omega} F d\Omega} T_{at},$$

(cf. [6]), where  $T_s$  is the Sun's temperature and  $T_{as}$  is the antenna temperature of the Sun. If the data on the antenna temperatures obtained in [1] are re-reduced, using the derived parameters of the antenna, then for the constant component of radio-temperature we obtain the value  $T_{10} = 250^\circ\text{K}$ . If we use the later, more accurate value of the radio-temperature of the quiet Sun [13], equal to  $16\,000^\circ\text{K}$  (previously  $T = 13\,000^\circ\text{K}$  was adopted), then we obtain  $T_{10} = 224^\circ\text{K}$ , which is compatible with the value now obtained within the limits of observational errors. The higher value of the constant component necessitates the revision of the values of certain physical parameters of the Moon. As regards the excessive phase lag, we can hardly base any conclusions on this fact, because the accuracy of lag determination is not higher than  $+10^\circ$ †, and the curve of variation of the radio emission is rather asymmetric.

In conclusion, we wish to express our gratitude to N. M. Tseytlin for carrying out the calibration of the antenna and for his assistance in the data reduction.

#### REFERENCES

1. Troitsky, V. S. and Zelinskaya, M. R. "Transactions of the Fifth Conference on Cosmogony". Publishing House of the Academy of Sciences U.S.S.R., Moscow, 99 (1956).
2. Troitsky, V. S. and Tseytlin, N. M. *Radiophysics* 3, 667 (1960).
3. Rakhlin, V. L. "Instruments and Technique of Experiment". (In press.)
4. Troitsky, V. S. *Radio Engineering and Electronics* 1, 601 (1956); 2, 935 (1957).
5. Salomonovich, A. E. *Astr. Zhurn.* 35, 120 (1958).
6. Troitsky, V. S. and Tseytlin, N. M. *Radiophysics* 5, 3 (1961).
7. Zhevakin, S. A., Troitsky, V. S. and Tseytlin, N. M. *Radiophysics* 1, 2, 19 (1958).
8. Troitsky, V. S. "Transactions of the Fifth Conference on Cosmogony". Publishing House of the Academy of Sciences U.S.S.R., Moscow, 325 (1956).
9. Markov, A. V. ed. "The Moon". GIFML, Moscow (1960).
10. Molchanov, A. P. *Radiophysics* 3, 722 (1960).
11. Zelinskaya, M. R., Troitsky, V. S. and Fedoseyev, L. I. *Astr. Zhurn.* 31, 643 (1959). 643 (1959).
12. Troitsky, V. S. "Report to the Plenary Session of Radioastronomy Board". (November 1960.)
13. Krotikov, V. D., Porfiryev, V. A. and Troitsky, V. S. *Radiophysics* 4, 1004 (1961).
14. Bondar, L. N., Zelinskaya, M., Porfiryev, V. A. and Strezhneva, K. M. *Radiophysics* 5, 4 (1962).
15. Krotikov, V. D. *Radiophysics* 5, 3 (1962).
16. Kamenskaya, S. A., Semonoy, B. I., Troitsky, V. S., and Plechkov, V. M. *Radiophysics* 5, 5 (1962).

† The uncertainty in the determination of the phase shift is due to the dispersion of points  $0.01 \times 240 \approx 2.4$ , which comprises a considerable fraction of the variation amplitude of  $17^\circ$ . This dispersion may result in a shift of  $\pm \tan^{-1}(2.4/17) = \pm 8-10^\circ$ .

# THE RADIO EMISSION OF THE MOON ON 4 mm

A. G. KISLYAKOV

*Radio-Physics Research Institute U.S.S.R. Academy of  
Sciences, U.S.S.R.*

THE aim of this communication is to present the results of an experimental research on the intensity of the radio emission of the Moon at 4 mm and to describe the method followed in observations and reductions. It was established that the radio brightness of the Moon,  $T_r$ , varies during the lunation according to the law:  $T_r = 230^\circ + 73^\circ \cos(\Omega_0 t - 24^\circ)$  K. The accuracy in measuring the absolute value of Moon's radio temperature is about  $\pm 10\%$ . The comparison between the phase dependence of the radio emission of the Moon at 4 mm and the data from observations of the radio temperature of the lunar disk on other wave lengths demonstrated that the homogeneous model of Moon's surface is in good agreement with the experimental data.

## 1. INTRODUCTION

Numerous measurements of the Moon's radio brightness within the range of wave lengths from 75 cm to 0.8 cm turned out to be insufficient [1, 2] for solving the problem of the existence of a sharp gradient of thermal conductivity in the surface layer of lunar ground. This gradient can be simulated approximately, as was proposed by Jaeger [3], by the layer of a vesicular substance with a low thermal conductivity (say, dust), overlying a solid base characterized by greater thermal conductivity. The results of observations of the phase dependence of the Moon's radio brightness on waves from 1.6 cm to 0.8 cm [4-7] are satisfied equally by the single-layer (homogeneous) model of the surface of lunar ground and by the Jaeger model, in which the thickness of the layer with a low thermal conductivity (lower by one order of magnitude than that of the base) may attain several millimeters. The ambiguity of interpretation of these experimental data is caused by an insufficient width of the wave-range [8] in which it was possible to detect and measure the fluctuations in the radio brightness of the Moon during lunation, as well as by the low accuracy in measuring the phase shift of radio emission of the Moon relative to its optical phase. In order to solve the problem of the structure of the lunar surface we must examine the phase dependence of the Moon's radio emission at sufficiently separated wave lengths [8]. In this connection it is of interest to measure the Moon's radiation on wave lengths longer than 1.6 cm and on those shorter than 0.8 cm.

As we know [9], only single measurements of Moon's radio brightness were made on 4.3 mm. The accuracy of these measurements is low ( $\pm 25\%$ ); and, in addition, their small number does not permit to determine the constant and variable components of the radio temperature of the Moon.

We present below the results of a study of phase dependence of the Moon's radio emission at 4 mm. The measurements were conducted in the summer of 1960 in a mountainous region near Elbrus at the elevation of

3150 m above sea-level. This place was selected for observations in order to weaken the effect of atmospheric absorption on the accuracy of measurements.

## 2. EQUIPMENT AND METHOD OF MEASUREMENTS

The observations of Moon's radio emission were conducted by means of a radio telescope consisting of a parabolic reflector antenna (with the beam-width of 25' on one-half power level), and a modulation radiometer of 4-mm wave range. The mirror and radiometer were mounted on the azimuthal-vertical setup. The external view of the radio telescope is shown on Fig. 1.



FIG. 1. External view of the radio telescope.

It is known [10, 11] that we can eliminate the thermal calibration of the radiometer by measuring the radio brightness of an extraterrestrial source. Actually the calibration is accomplished according to noise level of the antenna and thermal radio emission of the atmosphere. The measurement of radio brightness of the extraterrestrial source can be reduced to the following procedure: (1) aiming of the antenna at the source; (2) subsequent aiming of the antenna at the region of the sky near the source; and (3) aiming of the antenna at the "black" region with temperature equal to that of surrounding air,  $T_0$ . For each one of three positions of the radio telescope

antenna the output signal of the radiometer is equal to  $\alpha_l$ ,  $\alpha_n$  and  $\alpha_0$ , respectively. It is evident that

$$\alpha_l \sim T_l e^{-\gamma\eta(1-\beta)} + T_n \eta(1-\beta) + T_\delta \eta \beta_n + T_{n\delta} \eta \beta_n + T_0(1-\eta), \quad (1)$$

$$\alpha_n \sim T_n \eta(1-\beta) + T_\delta \eta \beta_l + T_{n\delta} \eta \beta_n + T_0(1-\eta), \quad (2)$$

$$\alpha_0 \sim T_0 \eta(1-\beta) + T_\delta \eta \beta_l + T_{0\delta} \eta \beta_n + T_0(1-\eta), \quad (3)$$

where the quantity  $T_l$  is determined by the formula

$$T_l = \frac{\int_{\Omega_l} T_l(\Omega) F(\Omega) d\Omega}{\int_{\Omega_A} F(\Omega) d\Omega}, \quad (4)$$

$T_l(\Omega)$  being the distribution of radio temperature over the Moon's disk,  $\Omega_l$ , the Moon's solid angle;  $F(\Omega)$ , the directivity pattern of the radio telescope antenna;  $\Omega_A$ , the solid angle in which  $F(\Omega)$  is known. The major lobe of the directivity pattern is known usually in a certain solid angle. It is necessary that  $\Omega_A \geq \Omega_l$ . The quantity  $\beta$  is the antenna dissipation factor outside the solid angle  $\Omega_A$ , i.e.

$$\beta = \frac{\int_{4\pi - \Omega_A} F(\Omega) d\Omega}{\int_{4\pi} F(\Omega) d\Omega}. \quad (a)$$

The product  $T_l(1-\beta)$  is the temperature of the antenna directed at the Moon, for the case of no losses in the antenna or the atmosphere. The quantity  $T_l$  would then be the antenna temperature when the conditions enumerated above are satisfied, as well as in the absence of antenna dissipation outside the angle  $\Omega_A$ . For the sake of brevity  $T_l$  will henceforth denote simply the antenna temperature.

Furthermore, the following abbreviations are used in equations (1-3):  $\gamma = F_0 \sec \theta$  is the coefficient of absorption in atmosphere in the direction of the source ( $\theta$  is the zenith angle of the source, and  $F_0$  is the complete vertical absorption in atmosphere);  $T_n = T_m(1 - e^{-\gamma})$  is the effective temperature of the atmosphere in the direction of  $\theta$ , and  $T_m$  the mean kinetic temperature (weighted in absorption) of the atmosphere between the source and the receiving antenna;  $\eta$  the efficiency of antenna;  $\beta_l$  the isotropic part of dissipation of the radio telescope antenna, and  $\beta_n$  its anisotropic part, wherein  $\beta_l + \beta_n = \beta$ .  $T_\delta$  is the temperature of the background, surrounding the antenna, averaged over the isotropic lobes of antenna;  $T_{n\delta}$  is the background temperature averaged over the anisotropic lobes, with antenna directed skyward; and, finally,  $T_{0\delta}$  is the background temperature, averaged over the anisotropic lobes, with the antenna directed toward the "black" region. The same mountain slope was used always as the "black" region under conditions prevailing at Elbrus.

From equations (1-3) we can obtain

$$T_l = qe\gamma [T_0 - T_n + (T_{0\delta} - T_{n\delta})\beta_n(1-\beta)^{-1}], \quad (5)$$

where  $q = (\alpha_l - \alpha_n)/(\alpha_0 - \alpha_n)$ . In the treatise (13) the quantity  $T_m$  is calculated as equal to†

$$T_m = T_0 - bHs(\gamma)(e\gamma - 1)^{-1}, \quad (6)$$

† The calculations were conducted on the assumption of a plane atmosphere and, therefore, formula (6) is valid for not too large values of  $\theta$ .

where  $b$  is a constant determining the rate of temperature decrease in the atmosphere with the elevation  $h$  above sea-level;  $T(h) = T_0 - bh$ ;  $H$  is the effective height of atmosphere, and the function  $s(\gamma)$  is a rather rapidly converging series

$$s(\gamma) = \sum_{k=1}^{\infty} \frac{\gamma^k}{k \cdot k!}. \quad (b)$$

On substitution of equation (6) in (5) the latter assumes the form

$$T_t = q \left\{ T_0 \left[ 1 + \frac{bH}{T_0} s(\gamma) \right] + \Delta T \right\}, \quad (7)$$

where

$$\Delta T = e\gamma(T_{0s} - T_{ns})\beta_n(1-\beta)^{-1}. \quad (c)$$

The second member (in brackets) of formula (7) represents the correction for the temperature variation in the atmosphere. If this temperature were constant, then  $b = 0$  and the correction would vanish.

We should note that, in some well-known experimental works [14-16] the authors failed to take into account the anisothermal structure of the atmosphere in the reduction of their experimental data. This may cause appreciable errors if the absorption in atmosphere is sufficiently great and the elevation of the object under investigation sufficiently low above the horizon. Thus it is known [14, 15], that the quantity  $F_0 \sim 0.5n_\gamma$  and  $bH/T_0 \sim 0.1$  or  $4.3$  mm (for the standard atmosphere [17]); therefore, the correction for anisothermal structure for a source at the zenith amounts to approximately 5%. The function  $s(\gamma)$  increases rapidly with the increase in zenith angle (cf. Fig. 2) and, at  $\theta = 70^\circ$ , the correction attains already

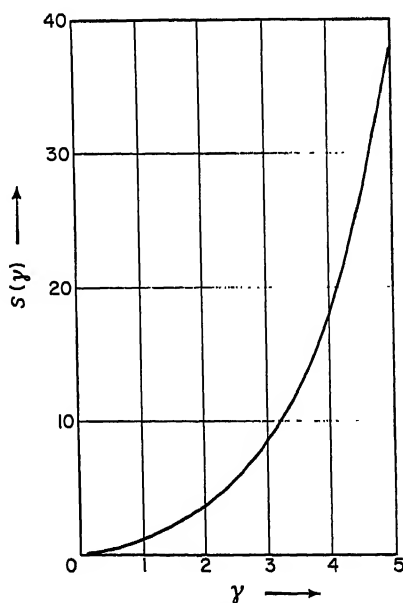


Figure 2.

20%. Under conditions prevailing at Elbrus the correction for variation in temperature of the atmosphere did not exceed a few per cent.

The last bracketed member in (7) is due to the anisotropic distribution of the dissipated radiation of the radio-telescope antenna. The author in [13] describes an experiment, by means of which he has succeeded in estimating the quantity  $\Delta T$ . It turned out that, for the employed antenna system,  $\Delta T \sim 0.07T_0$  and does not depend (within  $\pm 3\%$ ) on the elevation of the source above the horizon (in the range of  $\theta$  angles from  $20^\circ$  to  $80^\circ$ ).

The procedure described above—namely, aiming of the antenna at the source, sky and black region—was repeated ten to fifteen times in each measurement of the Moon. The records of deviations of the output of the radiometer were processed according to formula (7) and averaged. The temperature of the antenna  $T_l$ , thus obtained, was used in further reductions, during which the transition was effected from the quantity  $T_l$  to the Moon's temperature  $T_i$  (weighted mean over the disk). The equation (4) can be presented in the form

$$T_l = T_i \int_{\Omega_l} F(\Omega) d\Omega \bigg/ \int_{\Omega_A} F(\Omega) d\Omega = \alpha T_i, \quad (8)$$

where

$$T_l = \int_{\Omega_l} T_l(\Omega) F(\Omega) d\Omega \bigg/ \int_{\Omega_l} F(\Omega) d\Omega. \quad (d)$$

The quantity  $T_l$  is intermediate between the Moon's radio temperature (averaged over the disk) and the temperature of the Moon's central part. Taking into consideration the fact that the radio brightness of the lunar disk changes only at the limb [18], we can assume with a sufficient degree of accuracy [4] that the quantity  $T_l$  is equal to the radio temperature of the central part of the Moon.

In determining the coefficient  $\alpha$ , the integral in the denominator of (8) was calculated graphically, and the integral in the numerator of (8) could be found analytically, since—within the angular dimensions of Moon's disk—the shape of major lobe of directivity pattern was very close to a Gaussian curve. The main lobe of the directivity pattern of the radio telescope antenna was found within the necessary limits (approximately in the range of  $\pm 50'$  from the direction of maximum radiation of the antenna) by selecting the initial pattern of such a shape that the curve of Sun's transit across the major lobe, calculated in accordance with this pattern, would coincide with the experimental curve. This selection yielded the value of  $25'$  for the width of major lobe on one-half power level (the same figure was obtained from the calculation based on the curve given in [19]). In one case the directivity pattern of antenna was measured on a flat peak of the mountain ridge. The last experiment also yielded the value of beamwidth close to  $25'$  on one-half power level.

The coefficient  $\alpha$  was calculated with an allowance for variations in visible dimensions of the Moon during the lunation.



## 3. RESULTS OF OBSERVATIONS

The observations, conducted during three lunar cycles (June–August), made it possible to obtain the dependence of radio temperature of the Moon,  $T_l$ , on its phase. Figure 3 shows the graph of this dependence. The moment of full Moon was taken as the zero time reference in phase reading. The experimental points of the graph coincide well with the sine curve:

$$T_l = 230^\circ + 73^\circ \cos(\Omega_0 t - 24), \quad (9)$$

where  $\Omega_0$  is the frequency of lunation. The dispersion of most experimental points relative to curve (9) does not exceed 3%. This dispersion determines the accuracy in measurements of relative values of the constant and variable components of the Moon's radio temperature. The absolute values of the temperature are subject to an error of about 10%. The basic sources of errors consist in the inaccuracy of allowance for the anisotropy of dissipation of the antenna system (the error of which may attain roughly 8%), as well as in the approximate determination of the major lobe of directivity pattern of the antenna (which may result in an error of about 5% in  $T_l$ ). Thus, the total RMS error, together with the fluctuation error, may attain

$$(64 + 25 + 9)^{\frac{1}{2}} \simeq 10\%.$$

The accuracy of the phase shift measurement in (9) is about  $\pm 3^\circ$ .

## 4. DISCUSSION OF RESULTS

It has already been noted in the introduction that three values of the radio temperature of the central part of the Moon on 4.3 mm are quoted in Coates's paper [9]. If his data are plotted on the graph in Fig. 3 we find that they coincide well with the curve (9); (the points are marked with crosses). As can be seen from the graph in Fig. 3, the curve of phase behaviour of the

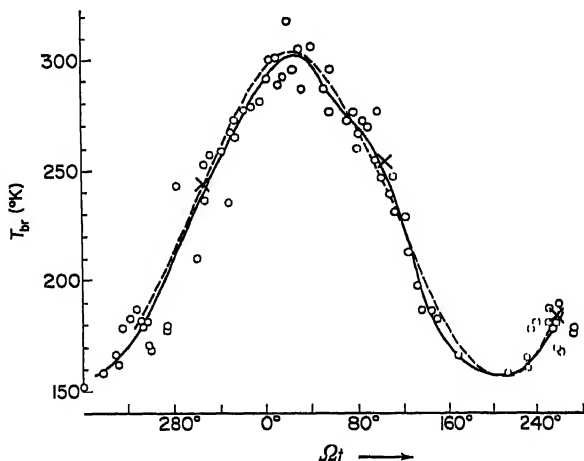


FIG. 3. Intensity of radio emission vs. optical phase of the Moon.

Moon's radio temperature in 4-mm wave range does not seem to contain any significant higher-harmonic components.

The analysis of the phase-dependence curve, plotted in accordance with

the averaged experimental points, demonstrated that the amplitudes of the second and third harmonic of the lunation frequency do not exceed in any case 10% of the amplitude of the first harmonic. It follows from the theory for the homogeneous model of the Moon's surface [18] that the amplitude of second-harmonic oscillation of the radio temperature for the central part of lunar disk constitutes roughly 18% of the amplitude of the first harmonic. Inasmuch as the harmonics have a tendency to smooth out upon averaging over the disk [18] this experimental result is in agreement with theoretical expectations. It also does not contradict the results obtained in observations of Moon's radio emission on 8.2 mm [6] and 1.25 mm [5]. However, it apparently differs from the data obtained for the radio temperature of the Moon's central part at 8.6 mm [7]. The phase effect of the intensity of radio emission of the Moon at 8.6 mm presented in [7], revealed fairly intensive higher harmonic components. However, since the author of [7] published only the averaged experimental curve of the phase effect, the question of the significance of his basic data remains uncertain—a fact which renders their interpretation difficult†.

We shall now use the present experimental data for determination of the parameters of lunar ground. It is known from the theory for the homogeneous model of the lunar surface [refs. 8 and 18] that

$$T_l = 245^\circ + 162^\circ \frac{\cos(\Omega_0 t - \xi)}{\sqrt{(1 + 2\delta + 2\delta^2)}} \text{ K}, \quad (10)$$

where

$$\xi = \tan^{-1}[\delta/(\delta + 1)] \quad (11)$$

and  $\delta$  is the ratio of attenuation factors of the thermal and electric waves in the lunar ground.

By comparing formulas (9) and (10) we can ascertain easily that the value of constant component of Moon's radio temperature, obtained experimentally, coincides (within the limits of the accuracy of measurement) with that calculated theoretically. It is evident from equations (9)—(11) that the parameter  $\delta$  of lunar ground can be found from the phase-shift of radio emission  $\xi$ , as well as from the ratio of constant and variable components of the Moon's radio temperature. The first method yields  $\delta' = 0.8 \pm 0.2$ , and the second leads to the value  $\delta'' = 0.88 \pm 0.15$ . This coincidence (within the limits of observational errors) of the values of parameter  $\delta$ , found by different methods, attests to the adequacy of the homogeneous model of the lunar surface and of the experimental data obtained in this work.

Thus the parameter  $\delta/\lambda$  ( $\lambda$  being the wavelength) equals  $2.2 \pm 0.3$  according to measurements made in 4-mm wavelength range, revealing that, for lunar rocks, the quantity  $\delta/\lambda$  is constant [4]. The observations of the phase dependence of the Moon's radio emission at 1.63 cm [4] yield  $\delta/\lambda = 1.5 \pm 0.2$  and, as a result of recent measurements [20] conducted on 3.2 cm, the authors of [20] found  $\delta/\lambda = 2.2 \pm 0.4$ . The constancy of the parameter  $\delta/\lambda$  in the entire wavelength range from 3.2 cm to 0.4 cm bears witness to the homogeneity of composition of the Moon's crust to a depth of the order of

† One should note that the investigations in [7] were conducted using an antenna with the beamwidth of  $12^\circ$  on one-half power level, i.e. with a higher directivity than that used by the author of this investigation.

100 cm (since the penetration depth of thermal wave for the lunar soil constitutes about 15 cm [8]).

In conclusion, we wish to note that, in order to obtain more accurate data concerning the properties of the lunar ground at a depth of a few millimetres, it is necessary to examine the Moon's radio emission on wavelengths shorter than 0.4 cm.

The author takes advantage of this opportunity to express his gratitude to V. S. Troitsky for directing the work, and to N. M. Tseytlin for the fruitful discussion. Highly valuable also was the assistance in processing of experimental data, rendered by M. R. Zelinskaya and V. A. Porfiryov, for which the author is sincerely grateful.

#### REFERENCES

1. Troitsky, V. S. "Transactions of the 5th Conference on Problems of Cosmogony" Publishing House of the Academy of Sciences U.S.S.R., Moscow, 325 (1956).
2. Barabashev, N. P. *et al.* "Moon". GIFML, Moscow. Chapter VI (1960).
3. Jaeger, J. C. *Aust. J. Phys.* **6**, 10-21 (1953).
4. Zelinskaya, M. R., Troitsky, V. S. and Fedoseyev, L. I. *Astr. Zhurn.* **36**, no. 4, 643-647 (1959).
5. Piddington, J. H. and Minnet, H. C. *Aust. J. sci. Res.*, **2A**, 63-74 (1949).
6. Salomonovich, A. E. *Astr. Zhurn.* **35**, 129-136 (1958).
7. Gibson, J. E. *Proc. Inst. Radio Engrs.*, N.Y. **46**, 280-286 (1958).
8. Troitsky, V. S. *Astr. Zhurn.* **39**, 73 (1962).
9. Coates, R. J. Paper for presentation at the A.A.S. meeting at Toronto, Canada, 1 Sept. 1959.
10. Troitsky, V. S. *Radio Engineering and Electronics*, **2**, 935-937 (1957).
11. Whitehurst, R., Copeland, J. and Mitchell, F. *Proc. Inst. Radio Engrs.*, N.Y., **45**, 1410 (1957).
12. Zhevakin, S. A., Troitsky, V. S., Tseytlin, N. M. *News of Institutions of Higher Learning. Radiophysics Series*, **1**, 19-26 (1958).
13. Kislyakov, A. G. *News of Institutions of Higher Learning. Radiophysics Series*, **4**, 433 (1961).
14. Coates, R. J. *Proc. Inst. Radio Engrs.*, N.Y., **46**, 122-126 (1958).
15. Straiton, A. H., Folbert, C. H. and Britt, C. O., *J. Appl. Phys.*, **29**, 776-782 (1958).
16. Whitehurst, R. *et al. Astr. J.*, **62**, 38 (1957).
17. Zhevakin, S. A. and Troitsky, V. S. *Radio Engineering and Electronics* **4**, 21-27 (1959).
18. Troitsky, V. S. *Astr. Zhurn.* **31**, 511-528 (1954).
19. Kaidanovsky, N. L. *Radio Engineering and Electronics* **1**, 683 (1956).
20. Troitsky, V. S. and Strezhneva, K. M. *News of Institutions of Higher Learning. Radiophysics Series* **4**, 600 (1961).

# RADAR MEASUREMENTS OF THE LUNAR SURFACE

G. H. PETTENGILL, J. C. HENRY

*Lincoln Laboratory, Massachusetts Institute of Technology,  
Massachusetts, U.S.A.*

In this paper some recent measurements of the radio echo power scattered by the lunar surface are reported. These measurements were made at a radio frequency of 440 Mcps using a parabolic reflector of 84 ft diameter and a peak transmitted power of approximately 2.5 MW. The received echo power was processed by a high-speed digital computer which is an integral part of the measuring system.

Figure 1 shows the mean received echo power plotted as a function of delay, when a transmitted pulswidth of 65  $\mu$ sec was employed. The results shown represent an integration over approximately 20 min of time. Since we know the Moon to be very nearly a sphere, we may define an angle  $\varphi$ , measured at its center between the radius to the center of the lunar disc (point of first radar contact) and the radius to the point at which we are considering reflection or scattering to take place (see Fig. 2). Let  $a$  be the lunar radius, and  $y$  the depth from the point of first contact with the surface to the region in question. Then  $\varphi$  may be expressed as

$$\varphi = \cos^{-1}(1 - y/a). \quad (1)$$

Now, since  $\varphi$  is also the angle at which the incident radiation strikes and then leaves the surface, we may express the measured power distribution in range,  $y$ , alternatively as a function of angle  $\varphi$ . The measured power level at any range will be the result of an integration over a small annular region of the surface defined by the length of the transmitted pulse. This area, for a pulse of duration  $\tau$ , will be

$$\Delta A = \pi a^2 \tau c \quad (2)$$

independent of  $y$ . Thus we may transform easily to the angular coordinate as shown in Fig. 3. For convenience, since many scattering laws are expressed in powers of  $\cos \varphi$ , returned power density has been plotted against  $\cos \varphi$  on logarithmic scales.

Perhaps the most obvious qualitative feature of the returns is the presence of two distinctly different regimes. First is seen the rapidly decaying specular-type echo associated with near-normal reflection from the center of the disc. Then at a value for  $\varphi$  of about  $35^\circ$  (corresponding to a delay of several milliseconds) a weaker but more slowly varying diffuse component becomes visible which persists until the region of the limb is reached.

The sharp echo at the leading edge was first noticed by Trexler [1] and is in marked contrast to the scattering behaviour of the lunar surface at visible [2] and infrared [3] wavelengths where no such highlight is noticed. A response so peaked at normal angles of incidence implies, of course, a considerable surface smoothness at radar wave lengths. Careful measurements by Hey and Hughes [4] and others show that the mean gradient of the smooth

portions of the surface is approximately one in twenty. It should be remembered, however, that only a comparatively small region of the lunar surface (about  $5^\circ$  in radius) is sampled by this technique, and that the results may not necessarily apply to the entire surface.

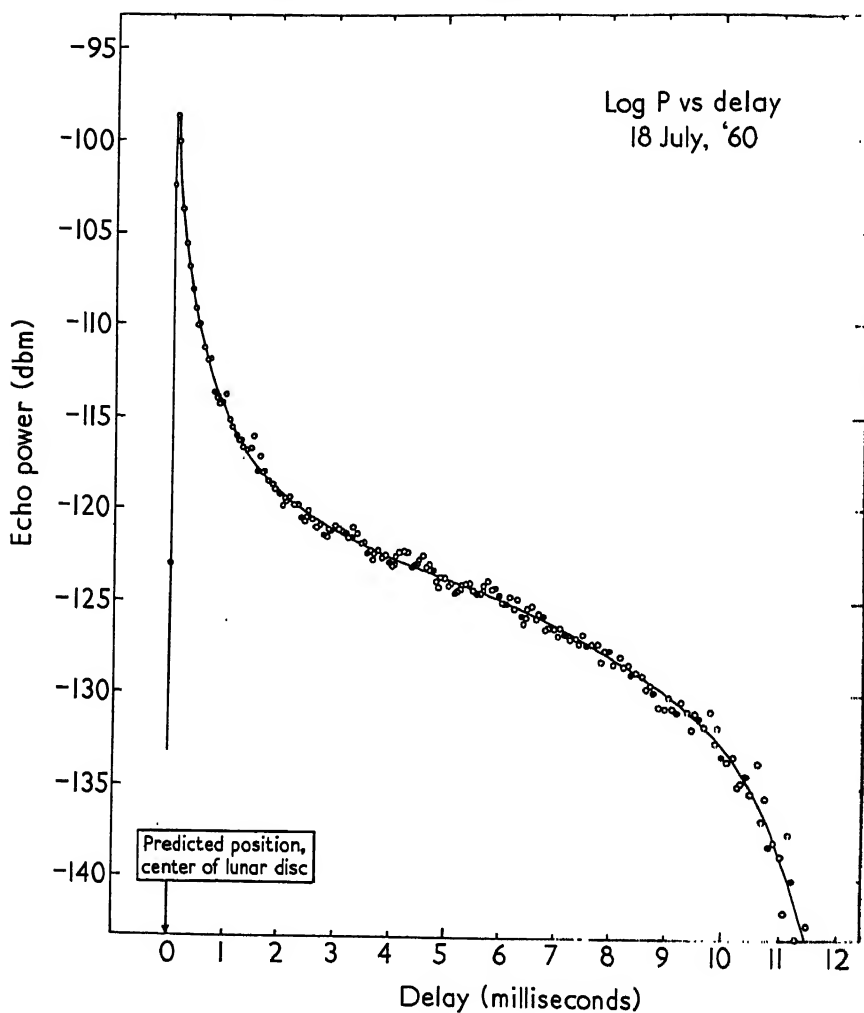


FIG. 1. Plot of received power vs. delay for signals received from the Moon. These measurements were taken by the Millstone Radar at MIT Lincoln Laboratory using 100- $\mu$  sec transmitted pulses and a receiver bandwidth of 35 Kcps. Data taken at 0730 EST 18 July 1960.

The diffuse component evident in Figs. 1 and 3 was not discovered until the advent of radars with a very high product of power and aperture because it is so much weaker than the specular echo. In spite of its low power density, however, integration of this component over the entire lunar disc shows that it contributes approximately 20% of the power contained in the total returned signal. The angular behavior of the diffuse component seems to lie between the Lommel-Seeliger and Lambert scattering laws with an

angular dependence of scattered power approximately as  $\cos^{3/2} \phi$ . It is interesting to note that this is close to the behavior found by Pettit and Nicholson [3] for scattering in the infrared. By integrating the observed

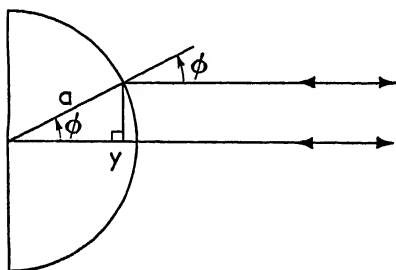


FIG. 2 Geometry for converting range measurements to angle of incidence.

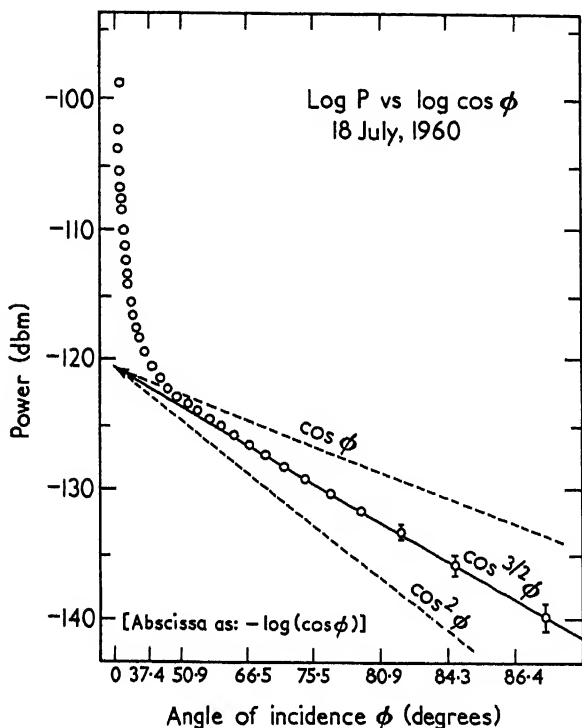


FIG. 3. Plot of received power vs. angle of incidence with respect to the lunar surface.

dependence (assuming that it may be extrapolated to  $\phi = 0$  without serious error), the total contribution of the component may be found from

$$\begin{aligned}
 I_D &= P'_0 a / \tau \int_0^{\pi/2} \cos^{3/2} \phi \sin \phi \, d\phi \\
 &= 2aP'_0 / 5\tau
 \end{aligned}
 \quad \left. \vphantom{\int_0^{\pi/2}} \right\}$$

where  $P'_0$  is the extrapolated value for power from the diffuse component at  $\varphi = 0$ . A similar integration may be carried out numerically for the specular component and it is found to contribute about four times the amount due to the diffuse scattering. The angular dependence of the specular component (when the diffuse contribution has been removed) appears to be well represented empirically over the entire range of measured values by the expression

$$P_S = P_0 \exp(-10.5 \sin \varphi). \quad (4)$$

At present the theoretical interpretation of this dependence is not completely clear, but it should be noted that the angular radius of the apparent lunar disc is proportional to  $\sin \varphi$ . No correspondence with the theories advanced by Daniels [5], Brown [6], or Senior and Siegel [7] has yet been established.

In order to relate the measured power ratio back to the actual fraction of the lunar surface which may be responsible for each type of scattering, the directivity of each scattering law must be determined. The directivity factor  $g$  is a measure of the amount of energy scattered back towards the radar as compared to the average of that scattered into all directions. The generalized bistatic electromagnetic scattering cross-section cannot be determined directly by radar measurements of the Moon, since bistatic measurements are not feasible at present (note that this limitation does not apply to optical measurements made using the Sun as illuminator). However, in some cases the behavior can be inferred. For example, Lambert's law is defined as

$$\sigma_L(\varphi, \varphi') \sim \cos \varphi \cos \varphi', \quad (5)$$

with  $\varphi$  as the angle of incidence and  $\varphi'$  the angle of emergence measured with respect to the normal-to-the-surface. For this law,  $g = 8/3$ . Similarly, by making measurements over the course of a month, Pettit and Nicholson [3] find (using our definitions) that

$$\sigma_{IR}(\varphi, \varphi') \sim \frac{\cos \varphi'}{(1 + \cos \varphi)(0.46 \cos \varphi' + \sin \varphi')}, \quad (6)$$

yielding  $g \cong 5/2$ .

For a smooth, specularly reflecting sphere, the resulting directivity is unity; in fact, the sphere will scatter equal power in all directions. It seems likely that the directivity for sharply peaked distributions will, therefore, also be close to unity. Under these assumptions, the rough areas of the lunar surface, which appear to scatter approximately as Pettit and Nicholson's infrared law, will be approximately 2.5 times as effective in back-scattering as the smooth portions.

Measurements of the absolute power returned have enabled Trexler [1], Evans [8], and Fricker [9] to calculate the radar cross-section of the Moon. These measurements are all in fair agreement, spanning the frequency region 100 to 400 Mcps. Fricker's results are probably the most accurate, yielding a CW radar cross-section of  $0.074 \pm 0.01$  times the geometrical cross-section of the Moon. Since we have already determined that most of the specular energy is returned from near normal incidence to the surface, we may assume a power reflection coefficient  $\rho_N$  to be associated with the materials near

he center of the lunar disc

$$\rho_N \approx \left( \frac{k^{1/2} - 1}{k^{1/2} + 1} \right)^2, \quad (7)$$

where  $k$  is the dielectric constant. The permeability is assumed to be unity and the conductivity zero. The integrated radar cross-section for each component may thus be set equal to

$$\sigma = fg\rho_N\pi a^2, \quad (8)$$

where  $f$  is the corresponding fraction of power. If we assume the above values for  $g$  and insert the total measured cross-sections for the two components, only 9% of the surface need be responsible for the diffuse scattered component. For the reflectivity, we find  $\rho_N = 0.064$  and, consequently,  $k = 2.81$ . Dielectric constants for dry rocks and silicate material of the Earth's surface are in the neighborhood of five. The apparent discrepancy may, perhaps, be caused by a low density of the surface material, at least for those flat areas responsible for the nearly specular reflection. Gold [10]

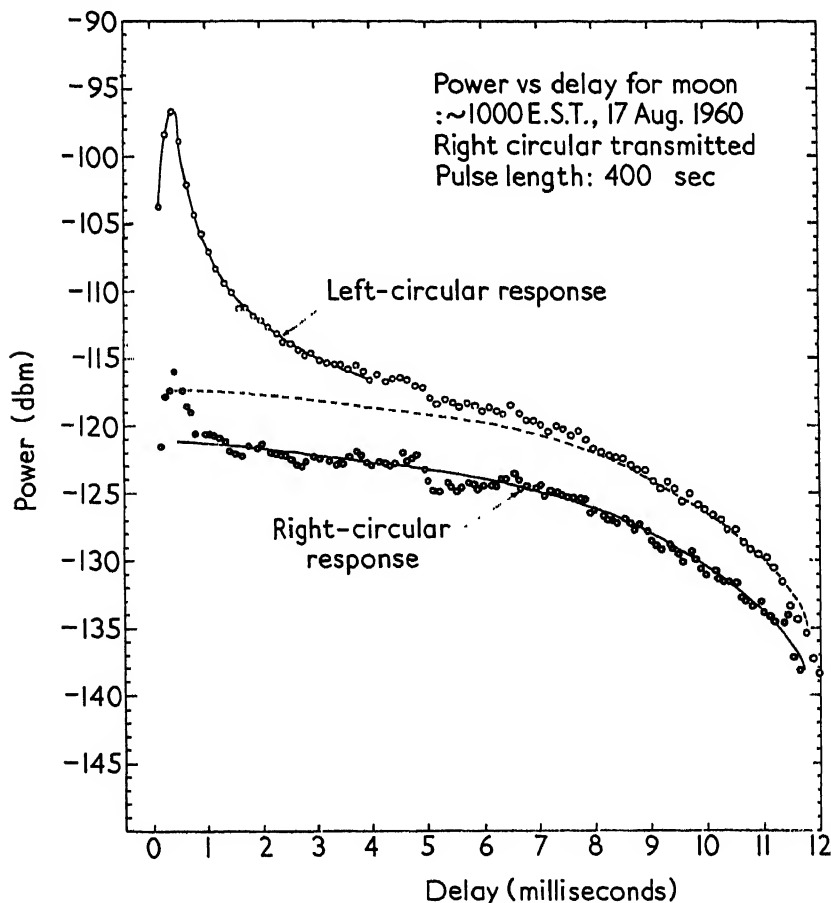


FIG. 4. Lunar echo power vs. delay for two orthogonal received polarizations.



and Van Diggelen [11] have suggested, on both theoretical and observational grounds, that the crater floors may have a spongy texture of reduced density. Thus, a radio wave incident on these regions would encounter a region of low density with associated low reflectivity. Reflections from denser layers below the surface (if they exist) would suffer absorption in the upper layer and likely would not be seen. Assuming this explanation, we find a surface porosity of approximately two for the flat areas. Note that if the material responsible for the diffuse scattering has a lower porosity (i.e. a more compact structure), as seems possible, the estimate of the fraction of the surface responsible for this type of scattering must be revised downward (changing this fraction will have only a second-order effect on our calculations involving the smooth portions of the surface). In fact, if we assume a mean density characteristic of terrestrial rocks, a mere 5% of the surface need contribute to the diffuse scattering in order to explain the observed results.

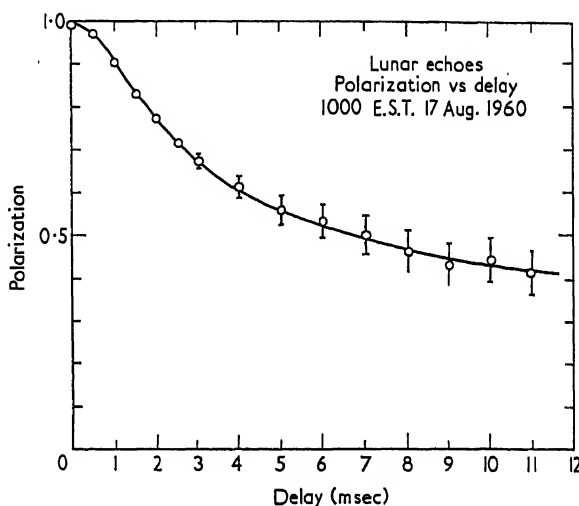


FIG. 5. Polarization vs. delay for lunar echoes.

If the association of the echo "tail" with a diffusely scattering surface is correct, one would expect to find the returned signal significantly depolarized at greater delays as compared to the nearly specular component observed near the beginning. In order to determine this effect, a right-circularly polarized transmission was directed at the Moon and both right- and left-circularly polarized received radiation were recorded. Circular polarization was used, since such a mode is not subject to magneto-ionic perturbation in the Earth's ionosphere.

In the absence of depolarization, all energy would be returned in the circular sense opposite to that which was transmitted. It may be seen from Fig. 4, however, that while the initial return is highly polarized as expected, there is a substantial amount of energy received in the channel corresponding to depolarization. The polarization of the returned wave may be defined by

$$P = \frac{I_L - I_R}{I_L + I_R}, \quad (9)$$

where  $I_L$  and  $I_R$  are the scattered intensities for left- and right-circular received polarizations, respectively. Figure 5 plots this quantity for the data shown in Fig. 4. It is clear that a substantial amount of depolarization is associated with the echoes occurring near the lunar limb.

## REFERENCES

1. Trexler, J. H. *Proc. Inst. Radio Engrs.*, N.Y. **46**, 286 (1958).
2. Markov, A. V. *Astr. Zhurn.* **25**, 172 (1948).
3. Pettit, E. and Nicholson, S. B. *Astrophys. J.* **71**, 102 (1930).
4. Hey, J. S. and Hughes, V. A. "International Astronomical Union: Paris Symposium on Radio Astronomy". Stanford University Press, Stanford, 13 (1959).
5. Daniels, F. B. *Nature, Lond.* **187**, 399 (1960).
6. Brown, W. *Jet Propulsion Lab. Tech. Release* no. 34-54 (April 1960).
7. Senior, T. B. A. and Siegel, K. M. *J. Res. Nat. Bur. Stand.* **64**, D, 217 (1960).
8. Evans, J. V. *Proc. Phys. Soc. B.*, **70**, 1105 (1957).
9. Fricker, S. J. *et al. J. Res. Nat. Bur. Stand.* **64D**, 455 (1960).
10. Gold, T. *Mon. Not. R. Astr. Soc.* **115**, 585 (1955).
11. Van Diggelen, J. *Rech. Astr. Obs. Utrecht* **14**, part II (1960).
12. Pottengill, G. H. *Proc. Inst. Radio Engrs*, N.Y. **48**, 933 (1960).
13. Leudabrand, R. L. *et al. Proc. Inst. Radio Engrs*, N.Y. **48**, 932 (1960).



# OBSERVATIONS OF RADIO EMISSION OF THE MOON AT 2.3 cm WITH THE PULKOVO LARGE RADIO TELESCOPE

N. L. KAYDANOVSKY, V. N. IHSANOVA, G. P. APUSHKINSKY,  
O. N. SHIVRIS

*Pulkovo Observatory, Leningrad, U.S.S.R.*

THE measurement of the amplitude of variation of the brightness temperature  $T_a$  at the centre of the lunar disk enables, as is shown in [1], to evaluate the magnitude of the equivalent conductivity  $\sigma$  of the material of the lunar crust. The amplitude of variation of brightness temperature  $T_a$  can be determined with the aid of radio telescopes with high resolving power by direct measurements of the brightness temperature  $T_e$  in the course of a lunation. Such measurements require that the area efficiency  $\sigma$  of the antenna and conditions of calibration of the receiving apparatus over the period of observations to be constant, and this is hard to ensure.  $T_a$  can also be determined by measuring the shift of the centre of gravity of radiation  $x_u$  [2]†, resulting from the fact that the variable component of brightness temperature, in superimposing itself on the constant component, distorts the symmetry of the curves of equal light intensity (isophotes) relative to the central meridian, and shifts the point of maximum brightness away from the centre of the disk in the direction of the subsolar point, as  $T_a$  is a function  $x_u$ .

The measurement of the displacement  $x_u$  requires only that the coefficient of amplification of the receiver in the course of one observation remains constant. The magnitude of the displacement of the centre of gravity along the diameter perpendicular to the line of the horns is given by

$$x_u = \frac{\int_0^{2\pi} \int_0^{R_\zeta} T_e r^2 \sin \lambda \, dr \, d\lambda}{\int_0^{2\pi} \int_0^{R_\zeta} T_e r \, dr \, d\lambda}, \quad (1)$$

where  $r$  and  $\lambda$  are the polar coordinates of the points on the disk of the Moon and  $R_\zeta$  is the radius of the disk (Fig. 1). For the purposes of our computations, we assume that the brightness temperature, in accordance with [1], is given by

$$T_e = (1-R) \left[ T_n + \frac{a_0}{2} D \eta(\psi) + \sum_{n=1}^{\infty} \frac{a_n D \cos(n\omega t - n\varphi - \xi_n)}{\sqrt{1 + 2\delta_n \cos \alpha' + 2\delta_n^2 \cos^2 \alpha'}} \right] \quad (2)$$

where  $R$  is the coefficient of reflection;  $T_n$ , the night temperature of the surface;  $D$ , the difference between the temperature at the point under the

† The values for  $x_u$  computed in [2] are too high as, in the computations, the decrease in the radiating capacity towards the limb was not taken into account.

Sun and the night temperature;  $\varphi$  and  $\psi$  the selenographic longitude and latitude, respectively;  $\eta$  is the function which determines the latitudinal and longitudinal course of the variable component of the temperature on the surface;

$$a_n = -\frac{1}{\pi} \int_{-\pi}^{+\pi} \eta(Z) \cos nZ dZ$$

i.e. the Fourier coefficients;  $\omega$  is the angular velocity of rotation of the Moon; and  $\xi_n = \tan^{-1} \delta_n / (1 + \delta_n)$  is the shift of the phase of the variable component of the brightness temperature as compared to the temperature on the surface;  $\delta = \beta/\chi$  is the ratio of the depth of penetration of the electromagnetic wave  $1/\chi$  to the depth of penetration of the thermal wave  $1/\beta$ ; and  $\alpha'$  is the angle of incidence of the beam from the depth of the crust to the surface. The maximum shift of the centre of gravity of the radiation occurs at moments

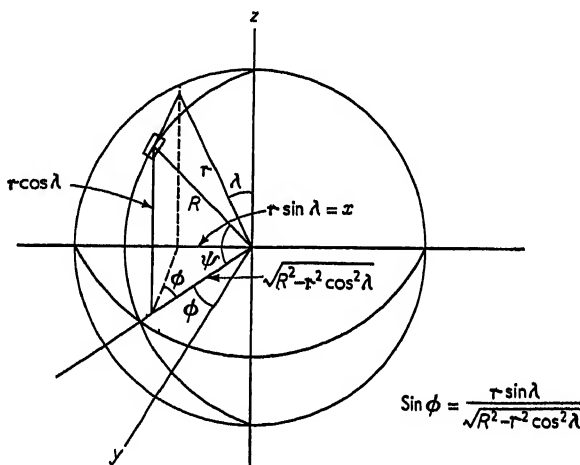


FIGURE 1.

when

$$\omega t - \xi = \pi/2 = 3\pi/2; \quad (2a)$$

and if we discard the higher harmonics in (2) and set  $\cos \alpha' \approx 1$  as well as  $\cos^2 \alpha' \approx 1$  the brightness temperature of the disk assumes the form

$$T_{e\pi/2;\pi 3/2} = (1-R) \left[ T_n + \frac{a_0}{2} D\eta(\psi) \right] \pm \frac{(1-R)a_1 D\eta(\psi)}{\sqrt{(1+2\delta+2\delta^2)}} \sin \varphi \quad (3)$$

Hence,

$$x_u = \pm \frac{\frac{a_1 D}{\sqrt{(1+2\delta+2\delta^2)}} \int_0^{2\pi} \int_0^{R\zeta} \frac{(1-R)\eta'(r\lambda) r^3 \sin^2 \lambda}{\sqrt{(R\zeta - r^2 \cos^2 \lambda)}} dr d\lambda}{2\pi T_n \int_0^{R\zeta} (1-R)r dr + \frac{a_0}{2} D \int_0^{2\pi} \int_0^{R\zeta} (1-R)\eta'(r\lambda) r dr d\lambda} \quad (4)$$

A knowledge of the form of the functions  $(1-R)$  and  $r(\psi)$  makes it possible to calculate the integrals in (4) and determine the numerical relation between the value of the maximum displacement of the centre of gravity of radiation  $x_u$  and the amplitude of the variable component of brightness temperature at the centre of the disk

$$T_{e\text{ var}} = \frac{a_1 D(1-R_v)}{\sqrt{(1+2\delta+2\delta^2)}}. \quad (5)$$

In the theory of radio emission of the Moon [1], it was assumed for the sake of simplicity that the plane of the orbit of the Moon lies in the ecliptic and that the librations are absent. Therefore, the conclusion that the centre of gravity of radiation is always to be found on the line joining the horns of the lunar crescent cannot be taken to be strictly true. With the rapid tilt of the line of the horns as well as the axis of rotation of the Moon from day to day it is possible that the centre of gravity of the radiation may lag as a result of the delay in the change of the temperature of the radiating layer with a change in the illumination of the Moon by the Sun.

Since, however, the angles of the tilt of the axis of the Moon do not exceed  $\pm 24^\circ$ , and the rapid tilt of the line of the horns only occurs close to

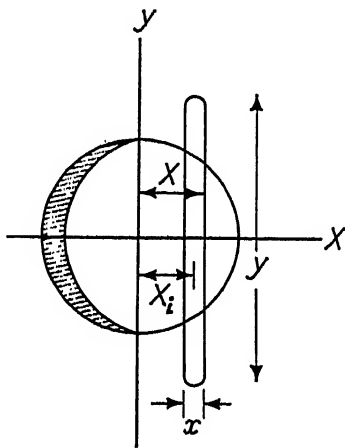


FIGURE 2.

the new and full Moon (when the shift of the centre of gravity of the radiation is generally small), the departure of the centre of gravity of the radiation from the diameter perpendicular to the line of the horns can be disregarded in the first approximation, at least near the quadrature. One can determine the coordinate of the centre of gravity of radiation  $x_u$  with the aid of a radio telescope of narrow beam cross-section, for which the direction of the major axis is parallel to the line of the horns. The antenna temperature for a narrow beam cross-section, during the transit of the Moon (Fig. 2), is

$$T_{at} = \frac{T_{ei} y_i}{y}, \quad \text{where} \quad T_{ei} = \frac{1}{y_i} \int T_e(x_i y_i) dy_i \quad (6)$$

denotes the average brightness temperature of a strip of the Moon the radiation of which is received by the antenna;  $y_i$  is the major size of the strip; and  $y$ , the effective size of the beam along its major dimension. The curve of the transit of the Moon through this fan-beam reproduces the curve of the products of the average brightness temperatures of the strips by their height.

The  $y$ -coordinate of the the centre of gravity of the plane figure which is limited by the curve of passage relative to the vertical, passing through the centre of the curve relative to the zeros is given by

$$x_y = \frac{\int T_{at} x dx}{\int T_{at} dx}. \quad (7)$$

With a sufficiently narrow beam we have, in accordance with (6),

$$x_y = \frac{\iint T_e(xy) x dx dy}{\iint T_e(xy) dx dy}, \quad (8)$$

which coincides with the coordinate  $x_u$  (eqs. 1-4) provided that the line of the horns is parallel to the major axis of the diagram and is perpendicular to the line of transit. As the directivity diagram of the radio telescope widens in comparison with the angular diameter of the Moon, the coordinate of the centre of gravity of radiation begins to deviate from the coordinate  $x_y$  of the plane figure limited by the curve of transit. With a broad diagram of directivity the transit curve will reproduce the form of the beam cross-section, and the displacement of the centre of gravity of radiation will produce only a general displacement of the curve. It is possible to detect the displacement of the centre of gravity by such a method only when it is not too small in comparison with the beamwidth.

Between October and December of 1959 observations of the Moon were made with the Pulkovo large radio telescope [3, 4] on  $\lambda = 2.3$  cm. A part of the working surface of the radio telescope was used with a variable profile, whose beam diagram had an angular size of  $2'$  in the horizontal direction and from  $20'$  to  $1^\circ$  in the vertical, depending on the elevation of the Moon. The axis of the beam diagram of the radio telescope was oriented along the meridian, while the curves of transit of the Moon through the fixed antenna diagram were recorded at culmination, when the axis of the Moon and the line of the horns were nearly perpendicular. The moment of the upper culmination of the Moon was recorded. As a result of small errors in setting the feed of the radio telescope (of the order of  $\pm 10''$ ) the moment of the passage of the central meridian of the Moon through the axis of the beam diagram and the moment of upper culmination did not always coincide. Therefore, the position of the central meridian was established when reducing the records of the curves of transit. The position of the zero points of the transit curve (corresponding to the limb) cannot be reliably determined from the records. Therefore, a line equidistant from the sides of the curve (Fig. 3) was constructed on the diagram tape on which the curve of the passage was recorded. It is clear that, on the average, such a line should intersect the zero line at the point equidistant from the zero points of the curve. The perpendicular to the zero line at the point of its intersection with the mean line determines then the position of the central meridian of the Moon. From this perpendicular,

the coordinate of the centre of gravity of the plane figure, limited by the curve, was measured; and the displacement of the centre of gravity of the radio emission of the Moon relative to the geometrical centre was found in this way.

Figure 4 shows the results of the measurement of the displacement of the centre of gravity of lunar radio emission in dependence on the phase. The course of the curve of displacement can be approximated (at new Moon  $\omega t = 0$ ) by the equation

$$x_u = 0.17 \sin(\omega t - 35^\circ). \quad (9)$$

The maximum displacement of the centre of gravity of the radio emission from the Moon on  $\lambda = 2.3$  cm occurs  $35-40^\circ$  after the quadrature and attains  $0.17'$  with a precision of  $\pm 30\%$ . The considerable scatter of the points on the curve of Fig. 4 is, apparently, to be explained by the slow

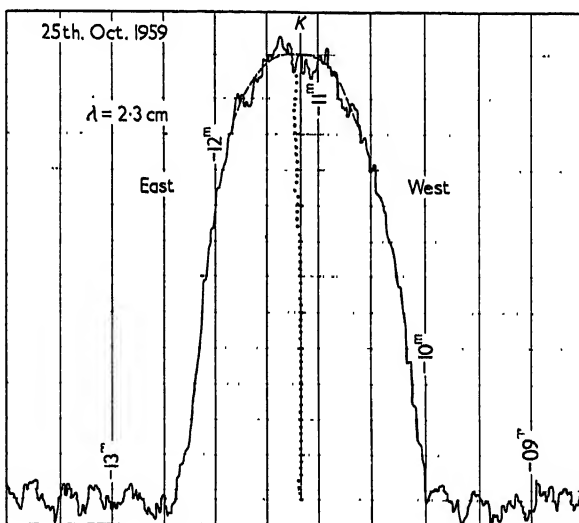


FIGURE 3.

variations in the coefficient of the amplification of the receiver. Rather high requirements should be set for the stability of the receiver used for such measurements, since the linear change in the coefficient of amplification during the time of the recording (about 2m) by 10% can cause in the recording an apparent displacement of the centre of gravity of radiation by 1% of the diameter. By the magnitude of the maximum displacement of the centre of gravity of radiation, which occurs at the time of effective quadrature, when

$$\omega t - \xi = \frac{\pi}{2} = \frac{3}{2}\pi$$

one can, by using the expression (4), determine the amplitude of brightness



temperature

$$T_{e \text{ var}} = \frac{a_1 D(1-R_\eta)}{\sqrt{(1+2\delta+2\delta^2)}}$$

if the radiation capacity  $(1-R)$  and the function  $\eta(\psi)$  are known.

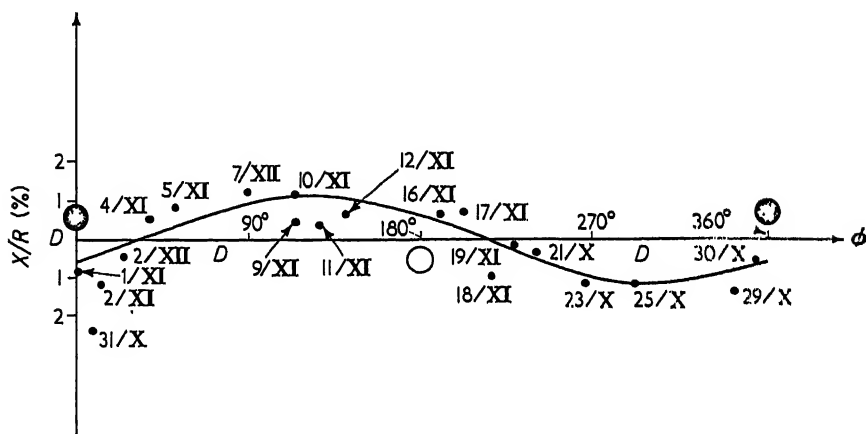


FIGURE 4.

For determining the numerical relation between  $x_\mu$  and  $T_{e \text{ var}}$  it was assumed that  $\eta(\psi) = \cos \frac{1}{2}\psi$  and  $\epsilon = 2$ . As a result of numerical integration it was found that

$$T_{e \text{ var}} = 11^\circ \cdot 3 \frac{x_\mu}{R_\odot} \% \quad (10)$$

Hence, and also from (9) it follows that the amplitude of the variable component of brightness temperature at the centre of the disk of the Moon is

$$T_{e \text{ var}} = 13.5^\circ \pm 4''.$$

The authors wish to express their thanks to Prof. S. E. Khaikin for his valuable consultation, and to engineer A. A. Novush for taking part in the observations.

#### REFERENCES

1. Troitsky, V. S. *Astr. Zhurn.* **31**, 511 (1954).
2. Kaydanovsky, N. L., Turusbekov, N. T. and Khaykin, S. E. "Transactions of the 5th Conference on Problems in Cosmogony". Publishing Office of the Academy of Sciences, Moscow 347 (1956).
3. Khaikin, S. E. and Kaydanovsky, N. L., *N.T.E. (Scientific and Technical Era)* **2**, 19 (1959).
4. Khaikin, S. E., Kaydanovsky, N. L., Yosepkins, N. A. and Shvris, O. N. *Publ. Obs. cent. Nicolas XXI*, **5**, 164, 3.

# SOME PHYSICAL CONSTANTS OF THE LUNAR SURFACE AS INDICATED BY ITS RADAR SCATTERING AND THERMAL EMISSION PROPERTIES

T. B. A. SENIOR, K. M. SIEGEL<sup>†</sup>, A. GIRAUD

*The University of Michigan Radiation Laboratory, Ann Arbor,  
Michigan, U.S.A.*

## 1. INTRODUCTION

THE purpose of this paper is to summarize some of the results of lunar studies carried out in the Radiation Laboratory of The University of Michigan during the past 3 years. Apart from an associated program which is the subject of a later paper [1] by Fensler *et al.*, these studies have been confined mainly to an analysis of radar scattering and thermal emission data, but in the course of this work, values have been obtained for some of the physical constants of the lunar surface.

The first part of the paper is concerned with the scattering of radar signals by the Moon, and with a theory which has been proposed to account for the observed features of the returns. As a consequence of the theory it is possible to determine the electromagnetic parameters of certain portions of the lunar surface and, in particular, it is found that the relative permittivity (or dielectric constant) is about 1.1. Following this the thermal radio emission from the Moon is considered, and by use of the electromagnetic parameters obtained above, the thermal parameters of the lunar surface are deduced from an analysis of the thermal emission observed experimentally. The values for these new parameters turn out to be compatible with the character of the lunar surface suggested by the radar data.

## 2. RADAR SCATTERING

In order to use the radar data to study the electromagnetic parameters of the lunar surface, it is necessary first to consider the manner in which the radar waves are scattered. During the 15 years which have elapsed since radar contact with the Moon was first reported, a large number of such experiments have been carried out; and though the initial ones suggested that the Moon was behaving as a rough scatterer at these frequencies (just as it does at optical wavelengths) later experiments indicated that this was not so. And, indeed, as the sensitivity of the equipment improved, the differences between the observed returns and the returns predicted on the basis of a uniformly rough scatterer became more and more apparent. In other words, it became necessary to assume a more directive scattering process at the lunar surface with an increased concentration of the returned power in the direction of specular reflection.

It was at this stage that the present authors became interested in the problem from a theoretical aspect, and from an examination of the polarization and shapes of returned pulses they felt that a scattering process closely

<sup>†</sup> Now at the Conduction Corporation, Ann Arbor, Michigan.

akin to that for a smooth body would explain the dominant features of the returns. Such a theory was proposed by Senior and Siegel in a paper [2] presented at the IAU Symposium on Radio Astronomy in Paris (1958) and further developed in a subsequent paper [3].

In this theory the starting point is a model for the Moon which is essentially smooth as regards the bulk of its radar scattering properties, but which possesses many individual scattering areas each of which is capable of returning a specular type of signal to the Earth. Because of the existence of more than one scattering area, the term "quasi-smooth" was used to describe the lunar surface.

The various scattering areas on the Moon appear to be concentrated around the point which is nearest to the Earth and their number decreases with increasing distance from the central point. This can be attributed to the distribution of surface slopes on the Moon, and to the fact that relatively little of the surface is inclined at more than a few degrees to the "mean" lunar sphere. As a result, the portions of the surface which are suitably orientated to reflect energy back to the Earth are located near to the front of the Moon, and this in turn is responsible for the oft-quoted fact that the major portion of the returned power comes from a region which is no more than a third of the Moon's radius in extent. It is hardly necessary to add that if the Moon were observed from a point in space *other* than the Earth, one would expect to find a similar set of scattering areas distributed around the point on the Moon nearest to the transmitter and the receiver. In other words, it does not follow that the visible side of the Moon must be unique in its radar scattering properties.

If the Moon is illuminated by a pulse of long duration, or by a cw signal, the return will build up as the incident pulse moves over the Moon and a peak will be reached when all the scattering areas are illuminated. This peak will correspond to the addition, with appropriate phases, of the signals from the various areas. On the other hand, pulses of sufficiently short duration are a tool by means of which we can separate out the returns from individual areas and thus, with a short pulse of perhaps 2 to 5  $\mu\text{sec}$  in length, at least the first few peaks in the return can *each* be attributed to the return from a single scattering area. Even with short pulses, however, the later peaks may still be due to interference as the result of two or more scattering areas lying within the same annular region on the Moon.

It will be appreciated that this break-up of the initial peak as the pulse length is decreased is the crux of the difference between the present theory and the one proposed by Pettengill and Henry [4], and since this difference in the interpretation of the data has a marked effect upon the values of the electromagnetic constants obtained using the two theories, it may be desirable to say a few words about it at this stage.

According to Dr. Pettengill, the large initial peak found when using a pulse length of 70  $\mu\text{sec}$  can be directly related to the reflection coefficient of the surface; and from a measurement of this peak a dielectric constant of (about) 2.8 is then deduced. On the other hand, if the pulse length is reduced, the magnitude of the initial peak is also reduced; and for a pulse length of only a few microseconds the decrease which is observed is of order 20 db. With pulses of this length, the return is found to consist of a large number of "spikes", and at least the first few of these would seem to have a degree of consistency suggesting that they are the returns from individual scatter-

ing areas. On this basis, the peak obtained with longer pulses is in fact the result of adding together the returns from many areas; and since the addition must be carried out with due regard to phase, the magnitude of the initial peak is not a direct measure of the reflection coefficient of any one area. With this interpretation the exponential law which is found to describe the shape of the initial peak is related to the distribution of the scattering areas, and to calculate the electromagnetic constant it is necessary to examine the return from one of these alone. As we have seen, the most straightforward method of doing this is to use pulses of only a few microseconds duration.

Let us, therefore, consider the return obtained when using pulses of order  $5 \mu\text{sec}$ . The first peak then corresponds to the power returned by the scattering area which is nearest to the Earth, and from a measurement of this peak we can determine both the form of the associated area and also its reflection coefficient.

For this purpose we require experimentally-determined values of the initial peak in a short pulse return at a variety of different wavelengths. But, unfortunately, relatively few experiments have been carried out using pulses of a few microseconds; and most of the data on the power return have been obtained with long pulses or even with cw. All of the available data have been summarized in Table I, where the power is given as a multiple

TABLE I  
Power Return from the Moon—Experimental Data

<i>Wavelength</i>	$\sigma/\pi a^2$	<i>Probable Error</i> (where known)	<i>Source</i>
0.10 m	$4 \times 10^{-4}$	—	Hey and Hughes
0.14 m	$3 \times 10^{-4}$	$\pm 4$ or $5\text{db}$	Yaplee
0.33 m	$9 \times 10^{-2}$	$\pm 3\text{db}$	Aarons
0.61 m	$5 \times 10^{-2}$	$\pm 3\text{db}$	Bleviss and Chapman
0.73 m	$7 \times 10^{-2}$	$\pm 3\text{db}$	Frieker
0.75 m	$1 \times 10^{-1}$	$\pm 3\text{db}$	Leadabrand
1.00 m	$7 \times 10^{-2}$	$\pm 3\text{db}$	Trexler
1.49 m	$7 \times 10^{-2}$	$\pm 3\text{db}$	Aarons
1.50 m	$8 \times 10^{-2}$	$\pm 3\text{db}$	Trexler
1.99 m	$5 \times 10^{-2}$	—	Webb
2.5 m	$1 \times 10^{-1}$	$\pm 3\text{db}$	Evans
3.0 m	$1 \times 10^{-1}$	$\pm 3\text{db}$	Leadabrand

of  $\pi a^2$ , with  $a = 1.74 \times 10^6 \text{ m}$ ;  $\pi a^2$  will therefore be recognized as the radar cross-section of a smooth perfectly conducting sphere whose radius is equal to that of the Moon. The source of the data is indicated, and in interpreting these results an essential factor is the pulse length employed. Thus, the first measurement of  $\sigma$  was made using  $5 \mu\text{sec}$  pulses, whilst the second was with pulses of  $2 \mu\text{sec}$ . All the other measurements were, however, made using very long pulses, and this is the explanation for the marked difference in magnitude between the first two results and the remainder.

In order to make use of the last ten values of  $\sigma$  in our analysis, it is necessary to deduce from these the initial peak values which would have been

observed had the experiments been carried out with short pulses, and since the initial peak in such a return is also (in general) the maximum return which occurs, it is possible to do this using the measured modulation losses found by Trexler. The modulation loss is, in essence, a measure of the decrease in the peak return consequent upon using pulses of a given length rather than cw, and if such "corrections" are applied to the data, we arrive at the following results:

$\lambda = 0.10$ m,	$\sigma = 4 \times 10^{-4}\pi a^2$
$\lambda = 0.14$ m,	$\sigma = 3 \times 10^{-4}\pi a^2$
$\lambda = 0.33$ m,	$\sigma = 5.4 \times 10^{-4}\pi a^2$
$\lambda = 0.61$ m,	$\sigma = 3.2 \times 10^{-4}\pi a^2$
$\lambda = 0.73$ m,	$\sigma = 4.3 \times 10^{-4}\pi a^2$
$\lambda = 0.75$ m,	$\sigma = 6.3 \times 10^{-4}\pi a^2$
$\lambda = 1.00$ m,	$\sigma = 4.7 \times 10^{-4}\pi a^2$
$\lambda = 1.49$ m,	$\sigma = 4.2 \times 10^{-4}\pi a^2$
$\lambda = 1.50$ m,	$\sigma = 5.3 \times 10^{-4}\pi a^2$
$\lambda = 1.99$ m,	$\sigma = 3.0 \times 10^{-4}\pi a^2$
$\lambda = 2.5$ m,	$\sigma = 6.3 \times 10^{-4}\pi a^2$
$\lambda = 3.0$ m,	$\sigma = 6.3 \times 10^{-4}\pi a^2$

Each of these is now interpreted as the scattering cross section of the first scattering area at the corresponding wavelength; and it can be seen that there is relatively little change in  $\sigma$  over this frequency range—just a slight tendency for the cross section to increase with decreasing frequency.

This lack of wavelength-dependence indicates the type of surface area which is responsible for the initial peak return. Thus, it cannot be a flat area, or a corner reflector, since the cross section of this is proportional to  $\lambda^{-2}$ ; similarly it cannot be a projection (such as a cone) since the cross section here is proportional to  $\lambda^2$ . And proceeding in this way we are finally led to the conclusion that the scattering area is merely part of a curved surface. The cross section of this is wavelength-independent, and given by  $\pi$  times the product of the principal radii of curvature at the point in question, with an additional factor which is the power reflection coefficient for the material which constitutes the scattering area.

Let us now *assume* that the radii of curvature are the same as the radius of the mean lunar sphere. The numbers in the above display then represent values for the power reflection coefficient, and the expression for this in terms of the electromagnetic parameters is known. The very slight wavelength dependence now arises from the conduction current term; and by fitting the formula for the reflection coefficient to the experimental data using the method of least squares we can determine the electromagnetic constants. The fitted curve, along with the experimental results, are shown in Fig. 1, and the corresponding electromagnetic constants are

$$\epsilon/\mu = 7.6 \times 10^{-6} \text{ mhos}^2,$$

$$s/\mu = 2.7 \times 10^2 \text{ mhos/henry},$$

where  $\epsilon$  is the permittivity,  $\mu$  the permeability and  $s$  the conductivity of the material.

It is now apparent that from a power measurement alone we cannot

determine  $\epsilon$ ,  $\mu$  and  $s$  individually; but if the permeability is equal to that of free space, then

$$\epsilon = 9.6 \times 10^{-12} \text{farads/m}$$

corresponding to a relative permittivity of approximately 1.08, and

$$s = 3.4 \times 10^{-4} \text{mhos/m.}$$

Both of these values are smaller than might have been expected, and few if any naturally occurring substances on Earth, apart from liquids or gases, have a relative permittivity as low as 1.1. Although this is no reason for ruling out the possibility of an appropriate *lunar* substance, it may be of interest to note that if  $\mu$  is not equal to  $\mu_0$ , but is greater by some factor  $x$ , then  $\epsilon$  and  $s$  are both increased by this same factor.

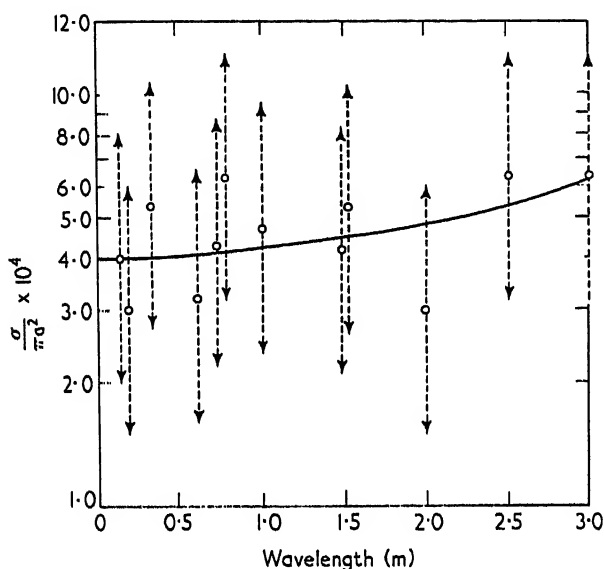


FIG. 1. Comparison between theory and experiment.

It should also be pointed out that a substance whose conductivity is zero would fit the experimental results within the quoted experimental errors. The reflection coefficient would then be wavelength-independent and represented by a horizontal line in Fig. 1. The corresponding value of  $\epsilon/\mu$  is

$$\epsilon/\mu = 7.7 \times 10^{-6} \text{mhos/m;}$$

and with a permeability equal to that of free space the relative permittivity is 1.09.

Even if we ignore the conductivity, or assume the permeability to be greater than that of free space, the reflection coefficient remains very small and equal to (about)  $5 \times 10^{-4}$ . It is, therefore, tempting to look around to see if there is any modification to the theory which would significantly increase this value. One obvious way is to assume that the reflection occurs at a place where the radii of curvature are not equal to the radius of the Moon,

but are appreciably less. If, for example, the radii were smaller by a factor of 10, the power reflection coefficient deduced from the experimental data would be increased by a factor of  $10^2$ , and the resulting relative permittivity would go up to about 1.5—which is not inconsistent with certain dry sands on Earth.

Unfortunately, this modification has at least one unpleasant consequence. In a short pulse return from the Moon the second major peak is similar to the first in all important respects, and is certainly not greater in size in the majority of instances; and to a somewhat lesser extent this is also true of the third and fourth peaks. It then becomes necessary to assume that each of the corresponding scattering areas has radii of curvature which are appreciably less than that of the Moon itself, and this must be true for all aspects of the Moon regardless of which scattering areas happen to be nearest to the Earth. To the authors, at least, such regions of reduced radius of curvature seem intuitively unlikely; and although we have examined several other possibilities for increasing the reflection coefficient, none of them has appeared acceptable.

Moreover, it is clear that the analysis by means of which the reflection coefficient has been obtained could be applied to scattering areas other than the one nearest to the Earth by considering the later peaks in a short pulse return; and we are, therefore, led to similar result for these scattering areas also. Bearing in mind that, because of the libration of the Moon, a given set of areas will not always preserve the same position relative to the Earth, we now have a collection of isolated areas all close to the center of the Moon's disk and all having a reflection coefficient of about  $5 \times 10^{-4}$ .

It would, therefore, appear that significant portions of the lunar surface must have a relative permittivity as low as 1.1; and it is natural to ask how a permittivity as low as this can be associated with a non-liquid, non-gaseous substance, and how such a value affects the interpretation of the observed data on the thermal emission from the Moon. As the second question is answered more easily, we shall now go on to consider the thermal radio emission in the millimeter and centimeter wavelength ranges.

### 3. THERMAL EMISSION

It is well known that from a measurement of the variable component of the Moon's effective temperature a relationship can be found which involves both the electromagnetic and thermal constants of the surface material; and a knowledge of one set then serves to determine the other. In the past it has been customary to postulate values for the electromagnetic constants and to deduce the thermal constants from these, and the thermal constants have varied depending upon the particular choice of the electromagnetic constants. On the other hand, a more straightforward derivation is now possible, since values for the electromagnetic constants are available as a consequence of our theory; and if the interpretation of the radar results is correct, the values for the thermal constants will be that much more accurate than hitherto obtained.

To analyse the measurements of the thermal emission, it is necessary to know the absorption coefficient of the lunar surface for electromagnetic waves; and this takes us back to a discussion of the radar reflection coefficient. It will be recalled that the values for the power reflection coefficient deduced

from the radar observations showed a slight increase with increasing wavelength, but at the smaller wavelengths the curve is almost horizontal (see Fig. 1). The thermal measurements extend, however, over the wavelength range from 20 cm to 4 mm, whereas the smallest wavelength at which radar observations have been carried out is 10 cm. It seems, therefore, reasonable to assume that over the thermal emission band the reflection coefficient is independent of wavelength.

The formula for the power reflection coefficient is

$$|R|^2 = \left| \frac{1 - \sqrt{(\epsilon' + i\epsilon'')}}{1 + \sqrt{(\epsilon' + i\epsilon'')}} \right|^2, \quad (1)$$

where  $\epsilon'$  and  $\epsilon''$  are the real and imaginary parts of the relative permittivity and the permeability has been given the value for free space. Now  $\epsilon''$  is proportional to the product of the conductivity  $s$  and the wavelength  $\lambda$ ; and if  $|R|^2$  is to be independent of wavelength it is necessary that either  $\epsilon''$  is zero (implying zero conductivity) or the conductivity is inversely proportional to the wavelength. In any case, however,  $\epsilon''$  is small compared with  $\epsilon'$ , so that the electromagnetic absorption coefficient is

$$\alpha = \frac{2\epsilon''\pi}{\lambda \sqrt{\epsilon'}}; \quad (2)$$

and since  $\alpha$  must be non-zero in order to explain the experimental results on thermal emission, it must be assumed that the conductivity is proportional to  $1/\lambda$ . A more convenient form of equation (2) is then

$$\epsilon' = (2\pi d\epsilon'')^2 \quad (3)$$

where  $d$  is a dimensionless constant given by

$$d = \frac{1}{\alpha\lambda}; \quad (4)$$

$d$  can be interpreted as the skin depth measured in wavelengths.

Once it is assumed that  $\epsilon''$  is independent of wavelength, a knowledge of  $|R|^2$  no longer determines  $\epsilon'$  and  $\epsilon''$  separately, but merely leads to a set of associated values. From the radar data, the mean reflection coefficient is found to be approximately  $5 \times 10^{-4}$ , and if equation (1) is then solved for  $\epsilon'$  and  $\epsilon''$ , the results shown in Table 2 are obtained. The solutions

TABLE 2  
Electromagnetic Penetration as a Function of  $\epsilon'$

$\epsilon'$	$100\epsilon''$	$d$
1.099 (7)	0.71	23.5
1.096	2.56	6.50
1.090	4.76	3.90
1.080	5.85	2.83
1.060	7.78	2.10
1.040	8.87	1.83
1.020	9.43	1.71



given here are only a selection of those which are possible, and have been limited to ones for which  $\epsilon''$  is positive (with zero excluded) and  $\epsilon' > 1$ .

From the measured values of the thermal emission it is found that the effective temperature of the lunar surface contains two components: a constant one, and one which is a function of the lunar day. Based on a homogeneous model for the Moon, the former can be expressed mathematically as an integral involving the reflection coefficient of the surface; and since the reflection coefficient is known, the integral can be evaluated. If the variable component is Fourier-analysed and only the first harmonic retained, an integral form for this expression can also be obtained but then the integrand is a function of the ratio  $\gamma$  of the thermal to the electromagnetic absorption in addition to being a function of the reflection coefficient. Nevertheless, the integral can be evaluated numerically to give an expression for a quantity  $A\gamma$  as a function of the absorption ratio  $\gamma$ , where  $A\gamma$  is a normalized form of the amplitude of the variable temperature component; and by inverting the expression it is then possible to infer the value of  $\gamma$  from a measured value of  $A\gamma$ . It should be pointed out, however, that the range over which the integrals have to be evaluated depends upon the beam-width of the antenna used in the measurement of the temperature; and, accordingly, the theoretical values of both the constant and variable temperature components may change from experiment to experiment.

Turning now to the measured data on the lunar temperature components, we have summarized in Table 3 the results of experiments in which the

TABLE 3  
Effective Temperature of the Lunar Surface

Wavelength (cm)	$T_c(^{\circ}\text{K})$	$T\gamma(^{\circ}\text{K})$	Source
0.43	220	60	Coates
0.80	197	$> 39.5$	Salomonovich
0.86	225	45	Gibson
1.25	216	36.4	Piddington and Minnett
1.36	224	36	Troitsky <i>et al.</i>
2.2	220	20	Grebenkemper
3.2	183	$< 13$	Troitsky and Zelinskaya
20.5	250	$< 5$	Mezger and Strassl

variable component was measured or bounds upon it obtained.  $T_c$  and  $T\gamma$  are here the constant and variable components respectively of the Moon's effective temperature measured in degrees Kelvin. On the basis of the assumed model for the lunar surface the constant component should be independent of wavelength; but though quite a variation is evident, this can be attributed either to calibration errors or to the fact that this component was inferred from measurements carried out only over restricted portions of the lunar day. On the other hand, the variation must be removed before comparison with the theory; and since the average value of  $T_c$  is approximately  $215^{\circ}\text{K}$ , the values for  $T\gamma$  have been normalized to this† in Table 4. The appropriate values of  $A\gamma$  are also shown, as are the corresponding  $\gamma$ 's.

† It is probable that the true value of  $T_c$  is somewhat larger than  $215^{\circ}\text{K}$ .

TABLE 4  
Normalized Data

$T\gamma(^{\circ}\text{K})$	$A\gamma$	$\gamma$
58.8	0.42	0.9
> 43.2	> 0.31	< 1.5
43.1	0.31	1.5
36.4	0.26	2.0
34.7	0.25	2.1
19.6	0.14	4.0
< 15.3	< 0.11	> 5.2
< 4.3	< 0.03	> 20

These values of  $\gamma$  are plotted as a function of  $\lambda$  in Fig. 2, and if the points are fitted to the theoretical expression

$$\gamma = \beta d\lambda \quad (5)$$

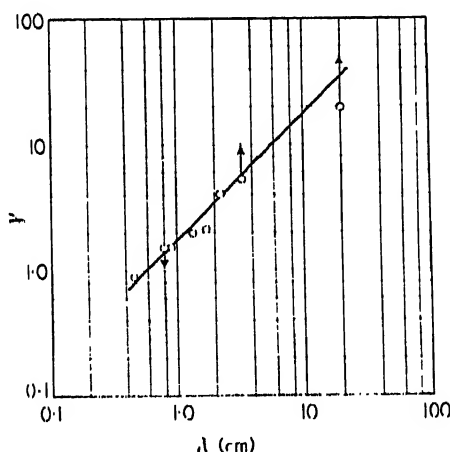


FIG. 2. Comparison between theory and experiment.

using the method of least squares, it is found that

$$\beta d = 1.7. \quad (6)$$

The resulting curve is shown, and is seen to be in reasonable agreement with the data.

Having obtained  $\beta d$ , the analysis is almost complete. It will be recalled that  $d$  is known for each value of the relative permittivity  $\epsilon'$  consistent with the radar observations. Thus,  $\beta$  is similarly known, and since  $\beta$  is given in terms of the thermal conductivity  $k$  and the volumetric specific heat  $c$  by the definition

$$\beta = \left( \frac{\omega c}{2k} \right)^{1/2},$$

where  $\omega$  is the angular frequency of the apparent revolution of the Sun about the Moon, a knowledge of  $\beta$  provides us with a relationship between  $k$  and  $c$  in the form

$$\left(\frac{k}{c}\right)^{1/2} = \frac{1.1 \times 10^{-3}}{\beta}. \quad (7)$$

In addition, however,  $k$  and  $c$  can also be obtained in the combination  $(kc)^{-1/2}$  from an analysis of optical eclipse observations. Observations of this type have been made by many experimenters and, in general, the values found for  $(kc)^{-1/2}$  have been of order 1000. In order to have a definite value to feed into the calculations, we have selected the one obtained by Wessellink [5] on the basis of a homogeneous model of the Moon, and this gives

$$(kc)^{-1/2} = 920. \quad (8)$$

From equations (7) and (8) we can now calculate the values of  $k$  and  $c$  corresponding to the various permittivities, and these are shown in Table 5.

TABLE 5  
Physical Constants of the Lunar Surface

$\epsilon'$	$\beta$	$k(\text{cal sec}^{-1}\text{cm}^{-1}\text{deg}^{-1})$	$c(\text{cal deg}^{-1}\text{cm}^{-3})$
1.099	0.072	$1.7 \times 10^{-5}$	$7.1 \times 10^{-2}$
1.096	0.262	$4.6 \times 10^{-6}$	$2.6 \times 10^{-1}$
1.090	0.436	$2.7 \times 10^{-6}$	$4.3 \times 10^{-1}$
1.080	0.601	$2.0 \times 10^{-6}$	$5.9 \times 10^{-1}$
1.060	0.810	$1.5 \times 10^{-6}$	$8.0 \times 10^{-1}$
1.040	0.929	$1.3 \times 10^{-6}$	$9.2 \times 10^{-1}$
1.020	0.994	$1.2 \times 10^{-6}$	$9.8 \times 10^{-1}$

The first column gives a selection of the possible  $\epsilon'$ 's, and though all of them are compatible with the radar observations, it is likely that the higher values are more probable. The second column is related to the depth of penetration of the heat wave:  $2\pi/\beta$  is the so-called heat wavelength, and accordingly would appear to be anything from 5 cm up to 1.0 m. The upper limit corresponds to the largest possible  $\epsilon'$ , and is certainly higher than the values estimated by Wessellink [5] for the homogeneous model and by Jaeger [6] for the two-layer model.

The last two columns in Table 5 show the thermal conductivity and the volumetric specific heat and as a result of the small values of  $\epsilon'$  now employed the values of  $k$  are larger by about an order of magnitude than previous estimates, whilst the values of  $c$  are smaller by about the same amount. Nevertheless, the values of  $k$  still seem to be consistent with a loose material, such as dust, *in vacuo*, and the low value of the volumetric specific heat almost certainly implies an equally low value for the density, which also supports the hypothesis of a loosely packed material.

#### 4. CONCLUSIONS

It is now apparent that the lunar scattering theory used in the interpretation of the radar data is reasonably consistent in its predictions about

the physical constants of the lunar surface. Nevertheless, much still remains to be done. In the first place, there is the need for additional experimental evidence either for or against the theory, and in this connection more radar experimental results obtained with very short pulses would be particularly valuable. In addition, there is the problem posed by the very low permittivity deduced from this theory and on which the calculation of the thermal constants is based. It is natural to ask the question whether it is possible that certain Earth substances could have a permittivity as small as this when placed in the environment of the Moon. The substance would probably occur as a very fine powder and, on the Moon, it is to be expected that the packing factor would be low. In recent months we have been giving some attention to the way in which the permittivities of selected substances *do* vary as the particle size and packing factor are decreased. This represents part of the laboratory program previously referred to, and will be discussed in the paper by Fensler *et al.* [1].

### 5. ACKNOWLEDGMENTS

The study of the radar characteristics of the Moon was supported by the National Aeronautics and Space Administration (NSG-4-59), and the analysis of the thermal emission properties was financed by the Army Map Service through the Autometric Corporation. Their assistance is gratefully acknowledged.

### REFERENCES

1. Fensler, W. E., *et al.* These Proceedings, pp. 545-565.
2. Senior, T. B. A. and Siegel, K. M. "Paris Symposium on Radio Astronomy" ed. Bracewell, R. N. Stanford University Press (1959).
3. Senior, T. B. A. and Siegel, K. M. *J. Res. nat. Bur. Stand.* **64D**, 217 (1960).
4. Pottengill, G. H. and Henry, J. C. These Proceedings, pp. 519-525.
5. Wessink, A. J. *Bull. astr. Insts. Netherlands* **10**, 351 (1948).
6. Jaeger, J. C. *Proc. Camb. phil. Soc.* **49**, 355 (1953).



# THE ELECTROMAGNETIC PARAMETERS OF SELECTED TERRESTRIAL AND EXTRATERRESTRIAL ROCKS AND GLASSES

W. E. FENSLE<sup>†</sup>, E. F. KNOTT, A. OLTE, K. M. SIEGEL<sup>†</sup>

*Radiation Laboratory, The University of Michigan, U.S.A.*

## INTRODUCTION

DETERMINATION of the physical properties of the surface layers of celestial bodies is one of the areas of research in radar astronomy. Radar pulses reflected from such a body contain information about the reflecting surface. Information concerning the composition and density of the outer layer of the lunar surface derived from radar echoes is of practical importance in view of proposed lunar landing.

Senior and Siegel [1] have deduced the ratios of the electromagnetic constants of these areas of the Moon responsible for initial scattering of radar echoes back to Earth. These ratios are:

$$\frac{\epsilon/\epsilon_0}{\mu/\mu_0} = 1.09,$$

$$\frac{\sigma}{\mu/\mu_0} = 3.4 \times 10^{-5} \text{ mhos},$$

where  $\epsilon$ ,  $\mu$  and  $\sigma$  are permittivity, permeability and conductivity, respectively, and the subscript "0" denotes free space.

Both of these ratios are quite small. In the case of the first-mentioned ratio, the relative permittivity is 1.09 times the relative permeability and, when  $\mu = \mu_0$ , equals 1.09 exactly. No solid terrestrial material having such electro-magnetic constants is known to the authors. Only foam-like materials, or gases, are likely to approach relative permittivities of order 1.09.

Optical and infrared measurements indicate that the lower bound in the prevalent key particle sizes on the surface of the Moon is  $10 \mu$ . Measurements of microwave radiation from the surface of the Moon predict an upper bound between 300 to 1000  $\mu$ . Thus the expected sizes of the most predominant particles probably lie between 30 and 100  $\mu$ .

Taking a different approach, theories dealing with likely lunar surface materials have been presented by O'Keefe [2], Urey [3], and many others. These theories suggest solid materials found or simulated on the Earth.

In view of this we started a program, starting with measurements of the electromagnetic constants of solid materials of reasonable volumes, and then proceeded to break up some of these solids into smaller and smaller pieces and measured the average permittivities of each mixture. The idea was to see how closely the electromagnetic constants of these materials and their form would approach those predicted from the electromagnetic measurements of the Moon.

<sup>†</sup> Now at the Conductron Corporation, Ann Arbor, Michigan.

The scientific exploration prior to human lunar landing should not only reveal the depth of the outer layer of the lunar surface, but the electromagnetic constants of the base layer as well [4]. Then the correlation between the electromagnetic and the geological parameters would yield the hardness and the load bearing capability of the lunar surface. Therefore, measurements of the electromagnetic constants of representative rocks are presented and analyzed. Some preliminary results on the geological parameters are included as well.

#### SOLID CHONDRITIC METEORITES

Two samples of chondritic meteorites were purchased from the American Meteorite Museum, Sedona, Arizona. One sample came from a fall which occurred at 7-00 p.m. on 25 November 1943, at Leedy, Oklahoma, the total known weight of which was 50 kg. The second sample came from Plainview, Texas: although this meteorite was found in 1917, the date of the fall is unknown. The total known weight of this fall was about 680 kg. In the discussion to follow, the two meteorite samples will be identified by their places of fall.

In these chondritic meteorites small specks of iron-nickel alloy are distributed in a rock-like base. Thus, strictly speaking, the chondritic meteorites are electromagnetically not homogeneous; and since the metallic particles are not spherical, a slight degree of anisotropy may also be present.

Toroidal configuration was used to measure the static permeability of the meteorites. Rectangular slabs were cut from the meteorite samples and the d.c. conductivity measured in a parallel plate device. The permittivity compared to conductivity was insignificant at d.c. Measurements to determine the permittivity and the permeability in the frequency range from 420 to 1800 Mc were carried out in a coaxial line.

#### D.C. MEASUREMENTS OF PERMEABILITY

The ballistic method was used to measure the static permeability of the meteorites. The experimental procedure outlined by Stout [5] was followed and is a common one.

The toroidal test samples were of rectangular cross section; one toroid of each meteorite sample was available. Matching toroids of polystyrene also were fabricated for use as references.

The measurements were carried out for magnetizing currents up to 3 amp for the meteorites and 0.75 amp for polystyrene. Unless special cooling arrangements are made, the ohmic heating of the primary becomes too great for polystyrene, resulting in softening of the core, which is, of course, accompanied by undesirable changes in physical dimensions. Thus, magnetizing currents for the polystyrene cores were held to 0.75 amp or less.

The relative permeability of the meteorite cores has been calculated from the measurements and values are shown in Table 1.

TABLE 1. D.C. Permeability of Chondrites

<i>Meteorite</i>	$\mu_r$
Leedy, Oklahoma	$1.20 \pm 0.06$
Plainview, Texas	$2.04 \pm 0.1$

The results indicate that chondritic meteorites are feebly magnetic. A simple test with a small permanent magnet convinces one that the metal particles imbedded in the chondrite are rather strongly magnetic. However, the metal particles are suspended in a non-magnetic medium; and thus one is not surprised to find that, in the average sense, the stone meteorites are only feebly magnetic.

#### MEASUREMENTS OF CONDUCTIVITY

Originally, low frequency measurements were contemplated to determine the complex permittivity of the chondrites. Rectangular sample slabs with the dimensions given in Table 2 were fabricated, two from the Plainview, Texas chondrite and one from the Leedy, Oklahoma. The slabs were to be inserted between parallel plates and the measurements of the parallel resistance and capacitance would then have enabled us to find a permittivity descriptive of the material. However, the measurements showed that the parallel resistance was less than the capacitive reactance, approximately by a factor of  $10^5$ , for both chondrites. This meant that the conductivity alone adequately described them at very low frequencies.

TABLE 2. Dimensions of the Chondrite Slabs

<i>Sample</i>	<i>Sample dimensions</i>		
	(a)	(b)	(c)
	<i>cm</i>	<i>cm</i>	<i>cm</i>
Plainview, Texas I . .	0.712	3.40	7.21
Plainview, Texas II . .	0.253	3.40	7.21
Leedy, Oklahoma. . .	0.712	3.40	7.21

The vertical deflection on an oscilloscope was calibrated for current and the horizontal deflection for voltage. The faces of the slab carrying the currents were painted with a thin layer of silver paint.

The voltage was applied between the silverized faces only for a few seconds—long enough to take a reading. This was necessary in order not to change the temperature of the chondrite. The measurements were carried out in the long direction (*c*) and the medium direction (*b*) for all three slabs. The measured results, current density as a function of applied field intensity, are shown in Fig. 1.

For the Plainview, Texas chondrites the current density is a non-linear function of the applied field intensity even at low levels of field. It also depends on the direction in the slab, and varies from sample to sample. The Leedy, Oklahoma chondrite behaved as a somewhat more linear medium. It also gave the same current density in the long and medium direction for the same field strength. The Leedy, Oklahoma chondrite had lower current densities by a factor of  $10^3$  than the Plainview sample.

Conductivity measurements of stoney meteorites (Kelley, Arriba, Richardson, Rose City, Estacado) have been done previously by Evernden and Verhoogen [6] at 60 cps. The conductivity varied from  $2 \times 10^{-5}$  mhos/m for the very stony meteorites (Kelley) to 14 mhos/m for the ones with more metallic phase (Rose City). It is clear that our measurements of the Plainview and Leedy chondrites fall within this range.



It was also discovered that the conductivity of the Plainview chondrites exhibits a rather strong temperature coefficient. In Fig. 2 the temperature dependence of one of the samples is plotted. From this graph, assuming a straight line, we obtain a conductivity temperature coefficient of  $1.3 \times 10^{-3}$  mhos/m/C°.

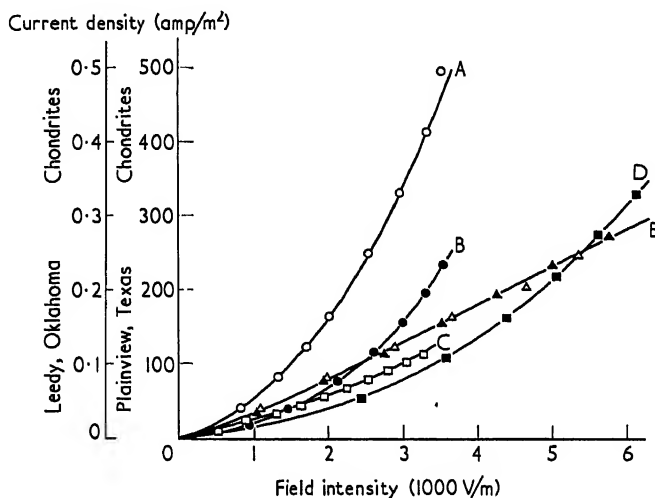


FIG. 1. D.C. Electrical characteristics of chondrites at 25° C.

Curve	Chondrite	Conduction axis
A—○	Plainview, Texas I	c
B—●	Plainview, Texas I	b
C—□	Plainview, Texas II	c
D—■	Plainview, Texas II	b
E—△	Leedy, Oklahoma	c
▲	Leedy, Oklahoma	b

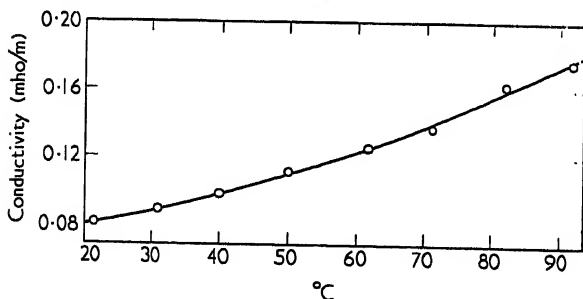


FIG. 2. Temperature dependence of conductivity. Plainview-I chondrite, c orientation. Field intensity = 1390 volts/meter.

#### UHF MEASUREMENTS OF PERMEABILITY AND PERMITTIVITY

Since the meteorites are not strictly homogeneous, one must be sure that the frequency is sufficiently low so that only a single mode may freely propagate in the sample. The multi-mode difficulty prevented us from using the rectangular waveguide configuration to determine the electromagnetic parameters. In the coaxial waveguide there is no cut-off property for the principal mode. The cut-off frequency of the next higher order mode is

controlled by the radii of the cylinders. The coaxial configuration was used to measure the electromagnetic parameters in the frequency range from 420 to 1800 Mc.

There are two waveguide techniques available by which to determine the complex permeability and permittivity of samples inserted in the waveguide. One, called the "general" method, allows samples of any length. The analysis of this method follows from measurements of impedance [7] at the front face of the sample for short circuit and open circuit terminations at the rear face. Any two reactive terminations may be used, but the advantage of using open and short circuits is considerable in that the subsequent calculations are simplified. The other, called the "thin sample" method [8], is merely a simplification of the general method. The simplification arises from the approximation that, if the electrical length of the sample is small compared to a radian, the hyperbolic tangent of the electrical length is equal to the electrical length itself. The thin sample method was used for all the UHF measurements.

Four chondrite samples were measured. Two were Leedy, and two were Plainview chondrites. Each toroidal sample had an outer diameter of 2.540 cm and an inner diameter of 1.105 cm. Table 3 serves to identify the chondrites. The Plainview toroid broke upon completion of the static measurements and the Plainview, Texas I and II listed in the table are new samples. The Leedy I is a toroid that was used for static magnetic measurements.

TABLE 3. Identification of the Chondrites

<i>Chondrite</i>	<i>Sample number</i>	<i>Thickness, cm.</i>
Plainview, Texas	I	0.1595
Plainview, Texas	II	0.1593
Leedy, Oklahoma	I	0.7142
Leedy, Oklahoma	II	0.2558

Both sides of each sample were measured—that is, a measurement was made with one face turned toward the generator and another measurement was made with that face turned away from the generator. Thus the description I-A means that face A of sample I was presented toward the generator, and I-B indicates that the opposite face was turned toward the generator.

The dielectric constants (the real part of relative permittivity) and the loss tangents of the meteorite samples measured are listed in Table 4. These constants were computed using the corrected reflection coefficient and assuming that  $\mu_r = 1$ . Three independent runs were taken on each sample, i.e. three reflection coefficients were measured whose average value was then corrected for the junction effect of the transition. Repeatability of the runs was good.

The shift of a voltage minimum from empty line condition to the condition of line with sample was more or less random for the permeability measurements. In some cases the shift was away from the generator, which was expected, and in other cases, towards the generator, which, in truth, is highly improbable. This is evidence of the limit in the precision of the measurement

TABLE 4. UHF Permittivity of Chondrites

Frequency, Mc.	420	600	800	1000	1200	1400	1600	1800
Sample I-A Plainview, Texas	$\epsilon'_r$ tan $\delta$ 45.9 0.193	39.0 0.184	36.9 0.175	35.9 0.181	35.4 0.195	33.1 0.174	33.0 0.177	32.3 0.178
Sample I-B Plainview, Texas	$\epsilon'_r$ tan $\delta$ 43.6 0.199	37.4 0.190	36.6 0.160	34.2 0.165	34.6 0.179	33.7 0.205	32.4 0.169	32.1 0.172
Sample II-A Plainview, Texas	$\epsilon'_r$ tan $\delta$ 30.9 0.138	26.8 0.129	27.5 0.134	26.9 0.134	27.2 0.140	26.2 0.134	26.2 0.128	25.4 0.125
Sample II-B Plainview, Texas	$\epsilon'_r$ tan $\delta$ 30.4 0.134	27.0 0.131	27.0 0.128	26.6 0.135	27.2 0.139	26.6 0.141	26.5 0.128	25.7 0.134
Sample I-A Leedy, Oklahoma	$\epsilon'_r$ tan $\delta$ 11.1 0.0367	10.7 0.0340	10.7 0.0367	10.4 0.0390	10.6 0.0254	10.9 0.0471	11.0 0.0383	11.0 0.0556
Sample I-B Leedy, Oklahoma	$\epsilon'_r$ tan $\delta$ 11.1 0.0366	11.2 0.0346	10.8 0.0351	10.5 0.0395	10.7 0.0240	11.1 0.0463	11.0 0.0415	10.9 0.0549
Sample II-A Leedy, Oklahoma	$\epsilon'_r$ tan $\delta$ 13.8 0.0285	11.2 0.0281	12.1 0.0346	12.6 0.0339	12.6 0.0378	12.4 0.0421	12.0 0.0349	11.9 0.0413
Sample II-B Leedy, Oklahoma	$\epsilon'_r$ tan $\delta$ 13.9 0.0261	11.4 0.0336	12.0 0.0367	12.5 0.0358	12.0 0.0352	12.4 0.0318	11.8 0.0354	11.9 0.0386

Note:  $\epsilon'_r$  = real part of relative permittivity

$$\tan \delta = \frac{\epsilon'' + \sigma/\omega}{\epsilon'}$$

and amounts to an error in the determination of the nodal shift by about 0.005 cm. The 0.005 cm error was roughly constant for all frequencies. The maximum  $\mu_r$  of the chondrites measured is then, at most, 1.02 in the UHF region, and probably is closer to 1, perhaps 1.01.

The error associated with the real part of the permittivity depends primarily on the accuracy with which we may measure the shift in the voltage minimum, while error in the loss tangent arises from errors in determining the standing wave ratio. The shift in voltage minimum could be measured to within  $\pm 0.005$  cm. This error includes the error of positioning the sample in the line. This gives a probable error in the real part of permittivity of no more than 2 per cent. The error in the loss tangent of the Plainview meteorite is of the order of 2 per cent, while in the Leedy chondrite it is 20 per cent. This considerable difference in error is because the former meteorite is considerably more lossy than the latter. Higher losses mean lower standing wave ratios which lend themselves to accurate measurement.

#### DISCUSSION

The relative permeability of the Leedy chondrite starting from 1.20 at D.C. decreased practically to unity at ultrahigh frequencies. The same end point was also approached by the Plainview sample, starting with a relative permittivity of 2.04 at D.C. The iron-nickel alloy grains in the chondrites are susceptible to strong magnetization. However, the intervening rock-like substance effectively breaks the magnetic circuit from grain to grain, and thus the over-all effect is small. At ultrahigh frequencies the very high conductivity of metal grains shields the interior of the grain from the fields, and thus the relative permeability tends to approach unity.

The D.C. conductivity of the Leedy chondrite is of the order of  $4 \times 10^{-5}$  mhos/m. Two samples were measured from Plainview, Texas. One of the samples was relatively thin. The D.C. conductivity varied from 0.016 to 0.115 mhos/m, depending on direction, sample, field strength, and temperature. It is clear that the conductivities of the chondrite meteorites are very low compared to good conductors, but they are high compared to good insulators.

The real part of the relative permittivity of the two Leedy samples is approximately between 11 and 13 from 420 to 1800 Mc, with the loss tangent (or loss factor) of the order of 0.03. The Plainview samples varied from 25 to 46 approximately in the real part of the relative permittivity, with the loss tangent of the order of 0.15. In this meteorite the loss appears to be an order of magnitude higher than in the previous one. The measurements are rather well repeatable when the samples are reversed, indicating that they appear fairly homogeneous at these wavelengths. A possible exception is the first sample from Plainview which had a rather large iron grain in it.

It was not possible to measure the permittivity at 1000 cps, because the conductivity is sufficiently large to make the displacement current negligible at such a low frequency. It follows, of course, that at D.C. the permittivity is even less significant.

#### SOLID TEKTITES

At this point it is pertinent to summarize briefly the electromagnetic measurements carried out by some of the authors [10] on solid tektites.

Dr. E. P. Henderson of the Smithsonian Institution in Washington kindly loaned us, for non-destructive tests, six Australites, three Indochinites, four Philippinites, one Moldavite, and a sample of Libyan Desert glass.

The requirement to preserve the tektites ruled out the standard methods for measuring electromagnetic parameters since such methods require either cutting the materials or obtaining the exact solution for the diffraction field, which is patently impracticable because of the irregular shapes involved. Thus, in practice, no exact method for obtaining the desired parameters can be devised.

However, approximate measuring methods are available; and if one restricts oneself to the Rayleigh region (that is, where one uses an incident electromagnetic field of wavelength considerably larger than the major dimension of the body to be measured) two methods of measurement are feasible. One method is that of obtaining the bistatic radar cross-sections for various polarizations and from these deduce the electromagnetic parameters. The second method is based upon perturbation of resonant frequency and "Q" of a resonant cavity, when a body is placed inside the cavity. The electromagnetic parameters of the material can be calculated from the changes in value of the cavity parameters. The second method appeared to be both more accurate and simpler than the first, and was chosen for these measurements.

The tektites were between 2-7 cm long and a wavelength of 60 cm (500 Mc) was used, thus assuring that we were well within the Rayleigh region. In these tests each tektite was approximated by an equivalent ellipsoid, and in the results each axis, i.e.  $a$ ,  $b$ ,  $c$ , had a uniquely polarized internal field, and a somewhat different permittivity. The real part of the dielectric constant† for these glasses is shown in Table 5. The difference between Sample 20 which is the Libyan Desert glass, and the tektites should be noted. As had been suspected, the permeability of the tektites was so low that no significant shift in the resonant frequency of the cavity could be detected when permeability tests were made.

#### PERMITTIVITY AS A FUNCTION OF PARTICLE SIZE

An investigation was made to determine the manner in which permittivity varies as a solid sample is reduced into finer and finer fragments. For the materials to be reduced sea sand (which is readily available in various grain sizes), plate glass, tektites from Bohemia, a Plainview chondrite, basalt (New Jersey), scoria (Oregon) and pumice (Utah) were selected.

The ordering of the grain sizes was done by the use of standard sieves. The range of particle sizes in each batch thus obtained is given in Table 6. It is clear that such an ideal grading of particles as shown in the table could occur only if they were spherical. The grain shapes varied, some were cubical, some spherical, some spheroidal, and some splinterlike. Thus the boundaries are to be taken in a rough sense only. The batch containing the smallest particles is labeled as dust. No sieves were available to establish the particle size accurately because the particles were exceedingly small. To get a distribution curve a microscope was used to measure particle sizes and to count the particles. Most of the particles were about  $1\mu$  in size for the dust grade.

† Dielectric constant is equal to the relative permittivity.

TABLE 5. Real part of the Dielectric Constant of Tektites

<i>Tektite No.</i>	<i>Polar a</i>	<i>Polar b</i>	<i>Polar c</i>	<i>Average</i>
17A	7.62	6.29	5.67	6.53
17B	5.37	5.55	8.31	6.41
17C	6.77	6.21	6.97	6.65
17D	5.81	5.32	8.03	6.39
17E	5.62	6.14	7.98	6.58
17F	5.48	6.86	9.27	7.20
18A	7.02	5.96	5.88	6.29
18B	5.92	6.97	7.66	6.85
18C	5.54	5.74	6.73	6.00
19	5.37	6.14	6.77	6.09
20	3.88	4.54	4.05	4.16
21A	6.10	6.10	6.08	6.09
21B	5.92	7.66	8.64	7.41
21C	7.43	6.79	6.07	6.76
21D	6.42	7.10	7.81	7.11

The particle-size distribution for the four dust grade powders shown in Table 7 were obtained by the microscope method of measurements in which an attempt was made to classify the individual particles as to nominal size in 5 or 10  $\mu$  increments. A small amount of powder was placed in a container of acetone and mixed vigorously. Upon placing a drop of solution on a glass specimen slide, the acetone evaporated leaving the dry particles dispersed over a circular area. Neither the density nor the mixture of the particles was constant as one moved from the outer rim to the center of the circular patch. The finer particles were grouped at the outside strip, and as one moved towards the center, the proportion of the bigger particles increased. Starting approximately from one-third of the radius, the particle density was practically zero. The particle distribution was approximately symmetrical along the direction of circumference. The particles were counted in two narrow tracks normal to each other, using a microscope.

TABLE 6. Grading of Particles

Grain Size	Range of Particle Size, microns	
	Maximum	Minimum
7	6000	2000
6	2000	840
5	840	420
4	420	177
3	177	90
2	90	44
1	44	2 (approx.)
Dust Grade	50	0.1

TABLE 7. Particle Size Distribution for the Dust Grades

Material	Frequency of occurrence in per cent						
	0-5 $\mu$	5-10 $\mu$	10-20 $\mu$	20-30 $\mu$	30-40 $\mu$	40-50 $\mu$	50-60 $\mu$
Sea Sand . . .	98.52	1.0	0.4	0.70	—	0.01	—
Plate Glass . . .	76.86	12.7	7.1	1.80	0.77	0.63	0.14
Tektite . . .	87.03	9.8	2.7	0.30	0.05	0.05	0.07
Plainview, Tex. Chondrite . . .	96.23	3	0.6	0.09	0.02	0.03	0.03

The method used for grinding each specimen should be pointed out, since the contamination of the sample is an ever present problem in the grinding process. As obtained, the sea sand was in grade 5 particle size. It was ground in a porcelain ball mill partially filled with pebbles and then graded into batches using the sieves. The dust grade was ground from grade 1 sand; hardened steel balls were used in the ball mill. No iron contamination could be observed using a strong permanent magnet.

The plate glass was crushed by hand using a pair of pliers. The first four grades were obtained in this manner. They were subsequently ground to finer powders in a ball mill. Flint pebbles were used for the first three sizes and hardened steel balls for the dust grade. A small amount of iron contamination of the glass dust could be observed by employing a strong permanent magnet. The glass particles had a tendency to be splinterlike.

Six small tektites from Bohemia were purchased from Ward's Natural Science Establishment; one was saved, and the rest were first crushed and then ground into dust with a mortar and pestle. Thus the contamination is very small for the tektite dust.

The Plainview chondrite was ground in a hand mill with cast-iron grinding plates. The meteorite was relatively soft so that it is believed that the contamination problem is not a severe one. However, the magnetic test could

not be applied since the meteorite is originally magnetic. The dust grade chondrite was obtained by grinding the total available in all other grades in the porcelain jar mill, using hardened steel balls for grinding action.

The New Jersey basalt also was ground in the hand mill. Unfortunately, the hardness of basalt was such that some of the cast iron was worn away from the plates of the mill and became part of the fragmentized sample. The main iron impurities were easily removed magnetically from grades 4, 5 and 6 because iron particles were much more magnetic than the basalt particles. However, practically all particles in grades 3, 2 and 1 seemed magnetic and the effectiveness of the magnetic clean-up is not known. With respect to the problem of contamination, an unsuccessful attempt was made to establish the relative amount of magnetic material in the basalt. A small piece of it was ground to fine powder with a mortar and pestle, guaranteeing zero iron contamination. The relative amount of magnetic material was then to be established in the uncontaminated sample. However, all the powder seemed to respond to a permanent magnet, but not quite as energetically as the fine sample from the mill.

The scoria was found to be slightly magnetic and use of the grinding mill was avoided. The sample was fragmentized mainly by crushing in a steel vice, and iron contamination is small. Pumice is quite soft and was reduced to powder by merely rubbing two blocks of the material together.

The sea sand and plate glass could be considered as homogeneous, and thus the different grades are of the same material. On the other hand, the chondrite, the basalt, the scoria and the pumice consist of different minerals of various hardness and toughness so that upon crushing one may expect them to fragmentize preferentially. Upon grading the crushed sample by the sieves there was no guarantee that each grade would contain the grains of each mineral in the same proportions as in the solid sample. It is extremely difficult to get rid of this variable. This problem exists in all the grades, except the chondrite dust, which represents the whole meteorite.

Two coaxial sample holders, different by a factor of 4 in volume, were fabricated of aluminum. Guard rings were provided to insure that fringe capacitance was not entering into the capacitance measurements. A sample of carbon tetrachloride was measured in both sample holders as a check and its permittivity found to be within 3 per cent of the accepted value. Thus it is felt that the measurements reported are accurate to the same order.

Prior to measurement each sample was heated in an oven for at least 30 minutes at 105°-110° C. In many instances the samples were heated for greater lengths of time. It was discovered that measurements on a given sample were repeatable whether it has been stored in the oven for a half-hour or for 2 days. It is felt that the half-hour period was adequate to guard against moisture condensing on the particle surfaces.

The sample holder was placed in a vertical position and was loaded with the graded particles through a funnel. Care was taken to let them fall naturally into the cylinder in order to get as low a packing factor as possible. Grade 1 of both sand and glass particles exhibited a tendency for the particles to cling together. It was thought at first that not all the moisture had been driven off the samples. However, after 15 hours of vacuum heating at 180° C, the clinging nature had been reduced but slightly. The only explanation that we can offer is that the particles acquire charges which give rise to interparticle attraction.



Packing factor is defined here as the ratio of the density of the reduced sample to the density of the material making up the particles. The density of the reduced sample is evaluated from the knowledge of the weight of the sample which filled the known volume of the sample holder. Table 8 lists the densities of the materials upon which the values of packing factor are based. Since pumice and scoria are porous, the packing factor is less than unity for the unfragmentized state.

TABLE 8. Densities of the Solid Materials

<i>Material</i>	<i>Specific gravity</i>
Cheap Plate Glass . . .	2.49
Sea Sand . . . . .	2.64
Moldavite . . . . .	2.37
Plainview, Texas Chondrite	3.61
Basalt (New Jersey) . . .	2.96
Scoria (Oregon) . . . . .	2.58
Pumice (Utah) . . . . .	2.13

## DISCUSSION

Table 9 summarizes the relative permittivities and the packing factors obtained from the measurements for the various grain sizes. The result was obtained from three measurements which were averaged. The repeatability was good. In general we observe that the relative permittivity decreased with the particle size. Also the packing factor decreased with the particle size. It was observed that for particles larger than  $100\mu$  the permittivity did not depend on moderate tapping of the sample holder. However, for particles less than  $100\mu$  in size a significant increase in the relative permittivity of all materials could be brought about by tapping the sample holder. For example, by a gentle but prolonged tapping the relative permittivity of Grade 1 sand was increased from 1.94 to 2.58 and the corresponding packing factor from 0.355 to 0.580. Similar results were measured for plate glass. The relative permittivities listed are the minimum values obtainable. The smallest relative permittivities obtained were practically the same for sand, plate glass, moldavite, and pumice, with the Plainview chondrite not very far behind.

The relative permittivities presented in Table 9 may be plotted either as a function of particle size or as a function of packing factor. Relative permittivities as a function of particle size are shown in Figs. 3 and 4. The particle size plotted is one which was judged to be the most predominant in each grade of particles. The range of permittivities obtainable for the same powders is shown as solid segments for sand and glass particles. This property of the particles is not indicated on the graphs for the other materials, but it is to be understood. For sand, plate glass, and chondrite the measured points are joined by a dashed curve to indicate the expected behavior of the relative permittivity as a function of particle size. For basalt, scoria, and pumice the relative permittivity does not decrease uniformly with the particle size. This may indicate preferential fragmentation upon reducing the sample so that the particles in each grade do not represent correctly the proper proportions of the minerals in the solid specimen. In addition, for these

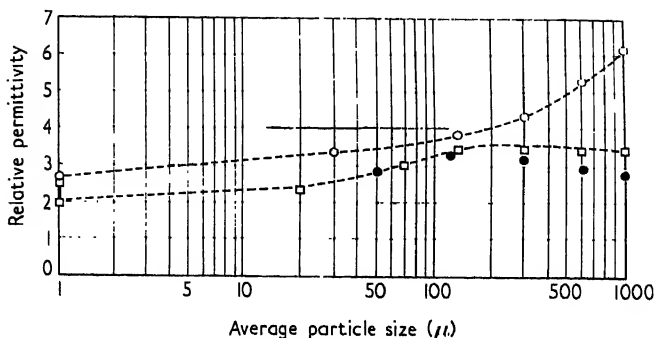


FIG. 3. Relative permittivity vs. particle size.

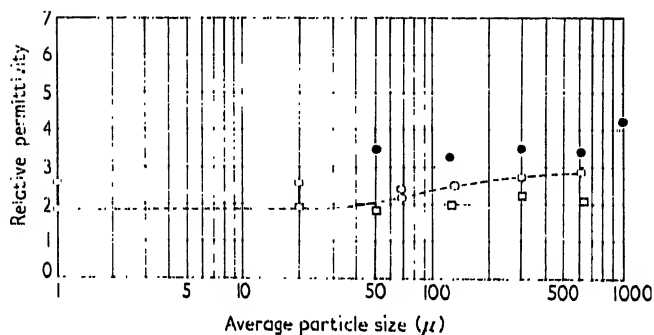


FIG. 4. Relative permittivity vs. particle size.

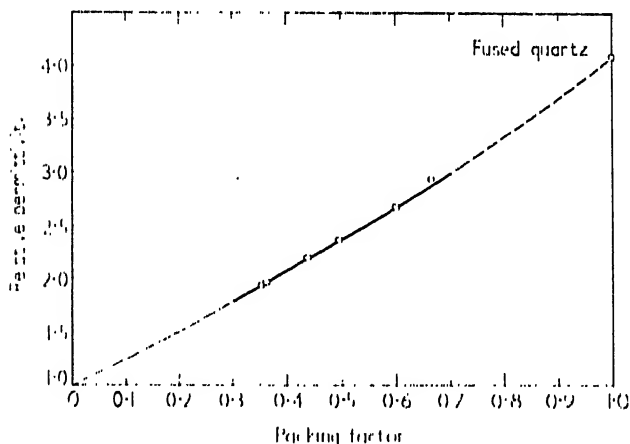


FIG. 5. Relative permittivity vs. packing factor for sand (at 1000 cps).

materials it was very difficult to estimate the preponderant particle size for the finer powders shown. To emphasize these observations the measured points have not been connected by a dotted curve.

If the relative permittivity is plotted as a function of the packing factor, it is observed that for the reduced materials the relative permittivity is to first order a linear function of the packing factor. As an illustration, the sand results are shown in Fig. 5. The end-points of the curve are known

TABLE 9. Relative Permittivity of Fragmentized Materials at 1000 cps.

Material	Grain size	Solid	6	5	4	3	2	1	Dust
Sea Sand	$F$	1.00	—	0.657	0.600	0.497	0.440	0.355	0.363
	$\epsilon'_r$	3.78†	—	2.92	2.68	2.36	2.19	1.94	1.90
Plate Glass	$F$	1.00	0.588	0.522	0.501	0.495	0.441	0.320	0.271
	$\epsilon'_r$	7.30	3.38	3.40	3.35	3.36	3.01	2.27	1.96
Moldavite	$F$	1.00	—	—	—	—	—	—	0.305
	$\epsilon'_r$	5.38	—	—	—	—	—	—	1.91
Plainview, Texas Chondrite	$F$	1.00	0.537	0.519	0.452	0.409	0.383	—	0.346
	$\epsilon'_r$	$\ll \sigma'_r/\omega$	6.12	5.21	4.33	3.83	3.32	—	2.66
Basalt (New Jersey)	$F$	1.00	0.495	0.431	0.432	0.415	0.374	—	—
	$\epsilon'_r$	26.7	4.14	3.34	3.43	3.24	3.43	—	—
Scoria (Oregon)	$F$	0.864	0.414	0.419	0.470	0.485	0.436	—	—
	$\epsilon'_r$	6.08†	2.80	2.90	3.14	3.19	2.83	—	—
Pumice (Utah)	$F$	0.392	—	0.310	0.373	0.336	0.296	—	—
	$\epsilon'_r$	2.29†	—	2.02	2.23	2.03	1.88	—	—

Explanations:  $F$ —Packing Factor,  $\epsilon'_r$  = real part of relative permittivity.

$\sigma'_r/\omega$ —ratio of conductivity to angular frequency.

†Taken for fused quartz (9)

‡Solid sample permittivity.

and the expected curve joining the end-points with the measured points is shown dashed. The curve for the sand is somewhat more linear than for the other materials. From this curve it is concluded that if by one means or another one can reduce the packing factor then the relative permittivity will also be reduced.

Packing factors for congregations of particles which are not spherical and which are not of the same size have been measured here. It is interesting to note that for solid spherical particles of identical size, one may easily compute the packing factor. Two limiting cases are distinguished. If the spheres are stacked in a cubical lattice, then a spherical particle is found in each cube whose edge is the diameter of the sphere. The volume of the sphere to that of the enclosing cube gives the packing factor which comes to  $\pi/6$ , or 0.524. This is the lowest packing factor obtainable with all spheres in contact with each other at four points. It is independent of the diameter of the sphere. The highest packing factor is obtained for the tetrahedral lattice which follows from the cubical lattice if alternate layers of spheres are shifted in the diagonal direction a distance  $\sqrt{2}a$ , where  $a$  is the radius of the sphere. Each layer then would rest in the holes of the lower layer, and the packing factor for this configuration is  $\sqrt{2}\pi/6$ , or 0.740, again independent of sphere size. It seems intuitively obvious that if identical spheres are dumped in a container that they will approach a packing factor of 0.740. Our measurements show that when the particles are not spherical, considerably lower packing factors are obtainable than for the spheres, and that the packing factor depends rather significantly also on the particle size.

The lowest packing factors are reached for the dust grade powders, for which the particle size is of the order of the wavelength of light. For the reduced materials, as already observed, the dielectric constant is to first order a linear function of the packing factor. As the packing factor becomes zero the dielectric constant would become unity, and one would be tempted to deduce that by making the particles size sufficiently small one could produce the packing factor vanishingly small. However, this does not seem to be the case. Upon closer examination of Table 9 it is seen that for sea sand the packing factor has changed but little from Grade 1 to dust grade, but the predominant particle sizes differ between the two grades at least by a factor of 10. The packing factors also become very sensitive to tapping the sample holder, as already mentioned, as the grain size becomes less than  $100\mu$ . It was also observed that the low packing factor of No. 1 and dust grade appeared to be partially caused by the air trapped between the grains. For Grade 1 sand this was confirmed in a separate experiment which showed that the minimum packing factor at an air pressure equal to 1 mm of Hg was higher by 35 per cent than the minimum packing factor at normal air pressure. However, it is to be expected that by making the grain size considerably less than  $1\mu$  one would have a dust which could be kept in agitation by the air molecules and thus become a gas of a sort. In this case the packing factor would be very close to zero.

The loss tangents of the reduced materials also were measured. These were independent of particles size for all except basalt. Table 10 lists the loss tangents of those materials for which loss tangents were constant. In the case of basalt, Table 11, the loss tangents decreased with grain size. This may show that there was some preferential fragmentation of the basalt upon reducing.

TABLE 10. Loss Tangent of Fragmentized Materials

<i>Material</i>	<i>Loss tangent</i>
Sea Sand . . . .	0.04
Plate Glass . . . .	0.05
Moldavite . . . .	0.02
Plainview Chondrite .	0.05
Scoria (Oregon) . . .	0.04
Pumice (Utah) . . .	0.04

TABLE 11. Loss Tangent of Fragmentized New Jersey Basalt

<i>Grain size</i>	<i>Loss tangent</i>
Solid	0.444
6	0.114
5	0.101
4	0.105
3	0.094
2	0.068

## ROCKS AND MINERALS

Permittivity and conductivity were determined for forty-four rocks and minerals which were obtained from Ward's Natural Science Establishment, Rochester, New York. The classifications of the minerals are Ward's.

In addition, petrographic analysis as well as analyses to determine speed of sound in the rocks and the density of the rocks were made under sub-contract to the Rensselaer Polytechnic Institute. The contributors to the program were, T. S. Ahrens, J. R. Dunn, F. B. Gerhard, Jr., S. Katz, and J. L. Rosenholtz.

Shear wave analysis is now being undertaken by them. Their work should be considered preliminary; but, on the other hand, the authors feel the results reported are worthy of being correlated with the electromagnetic results that are obtained for the same rocks and for this reason their work is included in Table 12.

For electromagnetic measurements twenty-one of the samples were cut into 3 in.  $\times$  1½ in.  $\times$  ½ in. slabs while the remaining twenty-five were cut into 1½ in.  $\times$  ½ in.  $\times$  ⅜ in. slabs: variation of thickness in all slabs was less than 10<sup>-3</sup> in.

The two faces of each slab were coated with a silver paint, such as it used for printed circuits, in order to produce equipotential faces during the tests. Porous samples and those which were highly conductive, were not so coated. See Fig. 6 for a flow diagram of the experiment.

Before testing, the samples were heated (in an oven) at 110° C for 20

hours. After this heating, samples were stored in capped jars containing a desiccant until tested. Thus, it is believed that any effects of moisture on results of these tests have been minimized. In some earlier measurements, the dielectric properties and conductivity of several unbaked samples were measured. It was found that the results were highly dependent upon moisture content. In general, the permittivity and conductivity of the unbaked samples were about double that reported here.

It was found that the dissipation factor of heated-stored samples is approximately half that of samples stored openly in the ambient atmosphere.

Loss tangents were computed from dissipation factors read from the impedance bridge.

Since, as has been noted before although the reasons are obscure (see for example, Reference 11), conductivities of materials of these types change with time, resistance was measured at 10 sec. and 1, 2, and 3 min after application of the electric field. Ten-second and 3-min readings are recorded in the tables as Initial and Final Conductivity respectively.

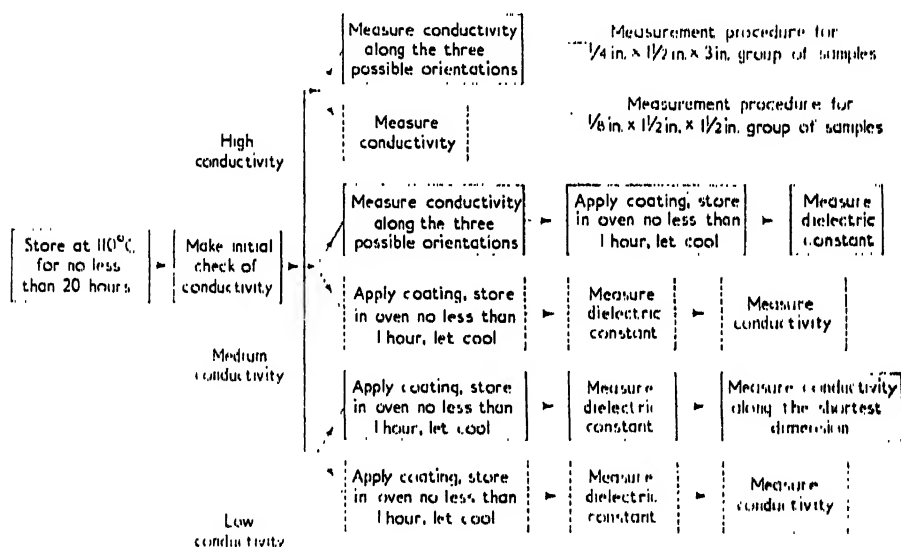


FIG. 6. Flow diagram of electromagnetic measurements.

Ten seconds is the minimum practicable, since this time is required to manipulate the controls of the bridge.

Samples having conductivities on the order of  $10^{-12}$  mhos/meter may be in error by as much as 30 per cent, while those samples having conductivities on the order of  $10^{-9}$  are believed to be accurate to within 5 per cent; loss tangents near  $10^{-2}$  are accurate to about 10 per cent while those near  $10^{-1}$  are accurate to within 5 per cent.

In certain of the samples (30, 36, 37, 28, 42, 44 and 45 in the tables) conductivity was measured along the long (3-in.) axis. It was impossible to measure the dielectric constant of samples 35, 37, 28, 42 and 44 due to the high conductivity of these samples.

TABLE 12. Ultrasonic and Electromagnetic Parameters of Rocks and Minerals

Sample No.	Name†	Source	Rel. perm. ( $\epsilon'/\epsilon_0$ )	Electromagnetic measurements			Mean vel. (km/s)	Density (gm/cc)	Velocity of compressional waves
				Loss tangent	D.C. conductivity Initial (mho/m)	D.C. conductivity Final (mho/m)			
1	Andesite	San Juan Co., Colo.	19.3	0.213	$1.3 \times 10^{-8}$	$1.7 \times 10^{-8}$	5.50	2.700	
2	Hornblende And.	Mt. Shasta, Calif.	4.87	0.024	—	$9.6 \times 10^{-12}$	2.58	2.32	
3	Andesite Porphyry	Boulder Co., Colo.	7.65	0.032	—	$4.9 \times 10^{-11}$	5.25	2.68	
4	Basalt	Lintz, Rhenish-Prussia	17.4	0.42	$3.1 \times 10^{-8}$	$2.8 \times 10^{-8}$	5.79	3.00	
5	Hornblende Basalt	Chaffee Co., Colo.	9.94	0.103	$1.6 \times 10^{-11}$	$1.1 \times 10^{-11}$	5.23	2.59	
6	Olivine Basalt	Jefferson Co., Colo.	8.89	0.057	$1.1 \times 10^{-10}$	$2.2 \times 10^{-10}$	5.40	2.73	
7	Olivine Bas. Cellular	Washington	5.50	0.033	—	$1.1 \times 10^{-11}$	2.78	2.44	
8	Vesicular Basalt	Chaffee Co., Colo.	6.51	0.038	$1.2 \times 10^{-11}$	$5.0 \times 10^{-12}$	5.27	2.57	
9	Ol. Bas. Porphyry	Boulder Co., Colo.	22.9	0.412	$6.2 \times 10^{-8}$	$5.3 \times 10^{-8}$	5.59	2.83	
10	Andesite Breccia	Ouray, Colo.	7.56	0.026	$6.6 \times 10^{-11}$	$5.2 \times 10^{-11}$	4.52	2.73	
11	Mica Dacite Por.	Boulder Co., Colo.	8.84	0.080	$3.5 \times 10^{-11}$	$2.4 \times 10^{-11}$	6.12	2.67	
12	Diabase	Mount Tom, Mass.	10.8	0.113	$8.6 \times 10^{-10}$	$8.0 \times 10^{-10}$	5.41	2.97	
13	Mica-Aug. Peridotite	Murfreesboro, Ark.	10.0	0.114	$3.1 \times 10^{-10}$	$5.4 \times 10^{-10}$	3.98	2.67	
14	Pumice	Millard Co., Utah	2.29	0.103	—	$5.3 \times 10^{-12}$	Not measured		
15	Rhyolite	Chaffee Co., Colo.	4.85	0.018	$9.4 \times 10^{-11}$	$1.9 \times 10^{-10}$	4.03	2.39	
16	Rhyolite	Castle Rock, Colo.	4.00	0.054	$1.8 \times 10^{-10}$	$7.9 \times 10^{-10}$	3.22	2.05	
17	Diorite Porphyry	Jackson, Wyo.	12.3	0.25	$4.5 \times 10^{-9}$	$4.1 \times 10^{-9}$	5.21	2.91	

† Ward's Designation

TABLE 12—(continued)

Sample No.	Name†	Source	Rel. perm. ( $\epsilon' / \epsilon_0$ )	Electromagnetic measurements			Mean rel. vel. (km/s)	Density (gm/cc)
				Loss tangent	D.C. conductivity Initial (mho/m)	Final (mho/m)		
18	Rhyolite Porphyry	Chaffee Co., Colo.	5.40	0.027	$1.4 \times 10^{-11}$	$4.5 \times 10^{-11}$	2.85	2.91
19	Scoria	Nr. Klamath Falls, Okla.	6.08	0.041	—	$1.6 \times 10^{-11}$	4.25	2.23
20	Trachyte Porphyry	Bannockbury Twp, Ontario	8.19	0.040	$1.8 \times 10^{-11}$	$1.4 \times 10^{-11}$	5.82	2.62
21	Sanidine Trachyte	Chaffee Co., Colo.	7.39	0.057	$1.9 \times 10^{-11}$	$8.2 \times 10^{-11}$	3.19	2.45
22	Tuff	Nr. Cripple Creek, Colo.	5.32	0.028	$8.1 \times 10^{-12}$	$5.3 \times 10^{-12}$	4.32	2.42
23	Volcanic Breccia	Park Co., Colo.	4.88	0.017	$3.2 \times 10^{-11}$	$9.3 \times 10^{-11}$	4.14	2.19
24	Dunite	Jackson Co., North Carolina		Not measured			6.15	3.25
25	Bytownite Gabbroic	Duluth, Minn.		Not measured			6.51	2.75
26	Volcanic Ash	San Luis Obispo Co., Calif.		Not measured			1.24	1.38
27	Diorite	Salem, Mass.	21.3	0.186	$5.8 \times 10^{-9}$	$5.3 \times 10^{-9}$	6.29	2.99
28	Alkali Granite	Woodbury, Vt.	6.82	0.067	$7.3 \times 10^{-12}$	$2.2 \times 10^{-12}$	4.90	2.66
29	Obsidian	Lake Co., Oregon	7.76	0.027	$7.2 \times 10^{-9}$	$1.1 \times 10^{-8}$	5.67	2.35
30	Basalt	Somerset Co., N.J.	26.7	0.444	$7.0 \times 10^{-9}$	$6.7 \times 10^{-9}$	6.31	2.97
31	Quartz Monzonite	Westerly, R.I.	6.23	0.028	—	$2.2 \times 10^{-12}$	5.67	2.65
32	Sandstone	Columbia Co., Pa.	4.84	0.008	—	$2.2 \times 10^{-12}$	1.96	2.61
33	Kaolin	Drybranch, Ga.	7.29	0.179	$3.8 \times 10^{-11}$	Not measured	1.21	1.58

† Ward's designation



TABLE 12—(continued)

Sample No.	Name†	Source	Electromagnetic measurements				Velocity of compressional waves	
			Rel. perm. ( $\epsilon'/\epsilon_0$ )	Loss tangent	D.C. conductivity Initial (mho/m)	D.C. conductivity Final (mho/m)	Mean vel. (km/s)	Density (gm/cc)
34	White Marble	Tate, Ga.	9.84	0.012	—	$2.2 \times 10^{-12}$	5.22	2.71
35	Graphite	Ceylon		Not measurable		$4.0 \times 10^3$	2.93	2.16
36	Limonite	Alabama	18.9	0.145	—	$3.7 \times 10^{-9}$	5.24	3.55
37	Pyrrhotite	Ontario		Not measurable		$4.3 \times 10^3$	4.60	4.55
38	Pyrite	Colorado		Not measurable		2.14	7.46	4.81
39	Microcline	Ontario	6.52	0.027	$5.5 \times 10^{-12}$	$2.2 \times 10^{-12}$	6.52	2.57
40	Albite	Ontario	11.7	0.195	$3.5 \times 10^{-11}$	$5.1 \times 10^{-12}$	6.28	2.63
41	Pyroxene (Diopside)	Quebec	8.30	0.013	—	$2.2 \times 10^{-12}$	6.72	3.08
42	Hematite	Michigan		Not measurable		$8.1 \times 10^{-3}$	6.65	4.93
43	Bytownite	Minnesota	-7.61	0.048	—	$3.3 \times 10^{-10}$	6.78	2.71
44	Magnetite	New York		Not measurable		$2.9 \times 10^{-1}$	5.02	4.81
45	Hornblende	Ontario	14.0	0.64	—	$3.5 \times 10^{-8}$	6.14	3.32
46	Augite	New York	9.22	0.042	$7.0 \times 10^{-11}$	$1.8 \times 10^{-11}$	3.67	3.26
47	Tremolite	New York	6.30	0.013	—	$2.2 \times 10^{-12}$	4.77	2.86

† Ward's designation

## CONCLUSIONS

We conclude that the meteorites, tektites, glasses and rocks as found on Earth do not have correct electromagnetic properties to be akin to the materials as found on the outer layer of the surface of the Moon. We find that by crushing materials so that we obtain particle sizes which are in the regions indicated by optical, infrared, and passive microwave data, the electromagnetic constants approach those values obtained by electromagnetic diagnostics of the lunar surface. We feel that tests under vacuum conditions similar to the vacuum conditions found at the lunar surface might easily reduce the electromagnetic constants of some of the materials, under loosely packed conditions, to values in the expected region. This work is continuing.

The electromagnetic constants of the meteorites, rocks, and tektites have been measured and we find that, especially for meteorites, the results are sufficiently different to be worthy of note on their own merits. For example, the non-linear property of the electromagnetic conductivity for certain stony meteorites was quite unexpected.

## ACKNOWLEDGMENT

We would like to acknowledge the support of the Autometric Corporation under its contract with the Army Map Service of the Corps of Engineers for supporting our efforts on crushed meteorites, rocks, and passive electromagnetic analysis. We would like to acknowledge the assistance obtained under NASA Grant NsC4-4-59 under which we obtained results on tektites and meteorites. R. Wolford and M. Brunschwig helped with some of the measurements. The advice of R. Hiatt and Professor M. Stout on the measurements technique is gratefully acknowledged.

## REFERENCES

1. Senior, T. B. A. and Siegel, K. M. *J. Res. nat. Bur. Stand.* **64D**, 217-229 (1960).
2. O'Keefe, J. *Nature, Lond.* **181**, 172-173 (1958).
3. Urey, H. C. Personal communications (1959, 1960).
4. Fensler, W. R., Senior, T. B. A. and Siegel, K. M. *Aero/Space Eng.* **18**, 38-41 (1959).
5. Stout, M. B. "Basic Electrical Measurements", Prentice-Hall, New York (1950).
6. Evernden, J. F. and Verhoogen, J. *Nature, Lond.* **178**, 106-107 (1956).
7. Birks, J. B. *Proc. phys. Soc., Lond.* **60**, 282-292 (1948).
8. Conrad, E. E. *et al. J. appl. Phys.* **27**, 346-350 (1956).
9. Von Hippel, A. "Dielectric Materials and Applications". Technology Press of MIT and John Wiley & Sons, New York, 311 (1958).
10. Otto, A. and Siegel, K. M. *Astrophys. J.* **133**, 706-717 (1961).
11. Keller, G. V. and Lieustro, P. H. *Geol. Surv. Bull.* 1052-H (Washington, GPO) (1959).



## AUTHOR INDEX

*Italic numbers indicate pages on which complete references are to be found*

### A

Aarons, J., 535  
 Ahrens, T. S., 201, 560  
 Akabane, K., 497, 499  
 Alcaraz, A., 255  
 Alfón, H., 136  
 Alter, D., 220, 263, 264, 270  
 Amenitsky, N. A., 495  
 Amstutz, C., 254  
 Ananyan, A. A., 235, 256  
 Anders, E., 135, 144, 147, 148, 256  
 Arthur, D. W. G., 96, 100, 114, 119, 125

### B

Baker, P. E., 243, 244, 257  
 Baldwin, R. B., 134, 196, 255, 294, 300, 417, 418  
 Banfield, A. F., 256  
 Barabashov, N. P., 23, 201, 255, 378, 384, 395, 398, 399, 402, 407, 453, 461, 477, 488, 518  
 Baranov, V. I., 256  
 Barcroft, D. P., 221  
 Barker, R., 220  
 Barkhatov, D. P., 256  
 Barth, T. F. W., 255  
 Baum, R. M., 221  
 Beer, W., 221  
 Behre, C. H., Jr. 256  
 Benevolensky, A. M., 416, 417, 418  
 Beringer, R., 199, 255  
 Bessel, F. W., 104, 105  
 Billings, M. P., 255  
 Birch, F., 257  
 Birks, J. B., 565  
 Bleifuss, R., 241, 257  
 Blovis, B. G., 535  
 Bobrovnikoff, N., 277, 287  
 Boehk, I. A., 161  
 Bootcher, C. J. E., 484, 488  
 Bogatov, G. B., 23  
 Bond, W. H., 220  
 Bondarenko, L. A., 23  
 Bonoff, N., 190, 255, 257, 262  
 Borel, E., 262  
 Borough, H. G., 256, 469, 471  
 Bracowell, R. N., 488, 543

Broido, I. I., 44  
 Brousse, J. J., 256  
 Browin, F. D., 220  
 Britt, C. O., 518  
 Broding, R. A., 241, 242, 257  
 Bronshten, V. A., 416, 417  
 Brown, D. C., 99, 100  
 Brown, H., 256  
 Brown, O. D. R., 257  
 Brown, W., 522, 525  
 Brunswick, M., 201, 255, 565  
 Buckingham, J., 221  
 Bulanov, S. I., 287  
 Bullard, F. M., 256  
 Bülow, K. von, 169, 201, 222, 254, 255  
 Burak, I. N., 488  
 Buscombe, W., 285  
 Bystrov, S., 64

### C

Caldwell, R. L., 243, 256  
 Camichel, J., 325  
 Casey, R. D., 232, 233, 256  
 Castel, J. H., 238, 256  
 Chandrasekhar, S., 139, 148  
 Chamberlin, R. T., 255  
 Chao, E. C. T., 255  
 Chapman, S., 535  
 Charters, A. G., 415, 417, 418  
 Chokirala, A. T., 201, 255, 384, 402, 461, 488  
 Chistyakov, Y. N., 372, 373, 374, 378, 417  
 Chudakov, A. Y., 52  
 Clastre, M., 325  
 Clinenhagen, J. L., 287  
 Coates, R. J., 489, 516, 518, 540  
 Collins, B. W., 256  
 Conley, J. M., 256, 469, 471  
 Conrad, E. E., 565  
 Copeland, J., 518  
 Craig, H., 219, 256

### D

Dana, J. D., 169  
 Daniels, F. B., 522, 525  
 Darwin, G. H., 259  
 Degtyareva, K. I., 23

Deshpande, B. G., 256  
 Dicke, R. H., 199, 255  
 Dietz, R. S., 294, 300  
 Doležal, E., 256  
 Dolginov, S. S., 52  
 Dollfus, A., 117, 194, 257, 325, 373, 376,  
 453, 461  
 Dubois, J., 446, 452  
 Dunn, R. J., 560  
 Dzhapiashvile, V. P., 464, 467

## E

Eaton, J. P., 255  
 Eberhardt, G., 144  
 Eggleton, R. E., 300  
 Eroshenko, E. G., 52  
 Escher, B. G., 196, 255  
 Evans, J. V., 522, 525, 535  
 Evernden, J. F., 547, 565  
 Ezerskaya, V. A., 384  
 Ezersky, V. I., 273, 277, 285, 286, 384,  
 398, 477

## F

Faust, G. T., 219, 256  
 Fauth, P., 320  
 Fedorets, V. A., 41, 42, 44, 378, 380,  
 384, 395, 396, 398, 458  
 Fedoseyev, L. I., 478, 488, 493, 495,  
 510, 518  
 Fedynsky, V. V., 392, 394, 418, 431  
 Fensler, W. E., 533, 543, 565  
 Fesenkoy, V. G., 372, 453, 461  
 Field, G. B., 46, 52  
 Fielder, G., 320  
 Finn, J. C., Jr., 175, 257  
 Firsoff, V. A., 257, 372, 378  
 Fish, R. A., 144, 145, 148  
 Fisher, Y. W. I., 221  
 Folbert, C. H., 518  
 Fowler, W. A., 136, 144, 145, 147, 148  
 Franz, J., 5, 38, 102, 114, 115, 125, 129  
 Fremlin, J. H., 224, 256, 371, 378, 489  
 Fricker, S. J., 522, 525, 535

## G

Galilei, G., 385, 390  
 Garazha, V. I., 384, 461  
 Gentili, M., 325  
 Gerard, V. B., 252, 257  
 Gerhard, F. B., Jr. 560  
 Gibson, J. E., 257, 478, 488, 518, 540  
 Gilbert, G. K., 178, 255, 294, 300  
 Gilvarry, J. J., 199, 255, 295, 300, 372,  
 378, 392, 394

Gold, T., 199, 255, 295, 300, 371, 378,  
 439, 523, 525  
 Goles, G. G., 144, 148  
 Goodacre, W., 117, 321  
 Goyna, A. I., 23  
 Grebenkemper, F., 540  
 Green, J., 173, 175, 179, 255, 257  
 Greenstein, J., 144, 145, 147  
 Gurevich, L. E., 155  
 Gutenberg, B., 160, 167

## H

Haar, D. ter, 139, 148  
 Haas, W. H., 221  
 Hackman, R. J., 300  
 Haid, R., 45, 52  
 Harper, A. F. A., 257, 470, 471  
 Haser, L., 287  
 Hatherton, T., 242, 257  
 Hayakawa, M., 256  
 Hayn, F., 63, 64, 65  
 Healy, J., 256  
 Henderson, E. P., 148, 257, 552  
 Henry, J. C., 534, 543  
 Herbig, G. H., 143  
 Herring, J. R., 257  
 Herzberg, G., 287  
 Hey, J. S., 519, 525, 535  
 Heyden, F. J., 358  
 Hiat, R., 565  
 Hill, J. E., 392, 394  
 Hiltner, W. A., 463, 464, 467  
 Hippel, A. von, 565  
 Hole, G. A., 220  
 Houtgast, L., 46, 52, 287  
 Hoyle, F., 136, 144, 145, 147  
 Hughes, V. A., 519, 525, 535

## I

Isboll, D. E., 488

## J

Jacquinet, P., 443  
 Jaeger, J. C., 256, 257, 394, 470, 471,  
 487, 488, 489, 494, 495, 511, 518, 542,  
 543  
 Jeans, J. H., 137, 148  
 Johnson, R. C., 285

## K

Kaiser, J. R., 209  
 Kalinyak, A. A., 265, 267  
 Karachun, A. M., 495, 499  
 Karus, Y. V., 241, 256  
 Katz, S., 560

Kaydanovsky, N. L., 495, 497, 499, 518, 532  
 Koller, G. V., 256, 565  
 Kelly, J. M., 488  
 Kendall, M. G., 88, 100  
 Kennedy, G. C., 209, 256, 257  
 Key, H. C., 221  
 Khabakov, A. V., 371, 454  
 Khaikin, S. E., 497, 499, 532  
 King, E. S., 388  
 King, R. B., 285  
 Kislyakov, A. G., 478, 488, 518  
 Knott, G., 221  
 Koban, E. K., 372, 373, 465, 467  
 Komárek, G., 209  
 König, A., 109  
 Kopál, Z., 46, 52, 117, 126, 133, 147, 194, 300, 360  
 Koshechenko, V. N., 495  
 Koziel, K., 106, 109  
 Kozyrev, N. A., 46, 52, 145, 217, 220, 222, 224, 256, 257, 259, 273, 277, 285, 286, 287, 342, 404, 407, 446, 447, 452  
 Krieger, J., 113, 317, 321  
 Krinov, E. L., 256, 400, 407  
 Krotikov, V. D., 477  
 Ksanfomaliti, V. N., 466, 467  
 Kuiper, G. P., 117, 119, 125, 126, 129, 137, 157, 167, 183, 224, 256, 294, 295, 300, 322, 324  
 Kuno, H., 169, 255  
 Kuprevich, N. F., 368  
 Kuzmin, A. D., 495, 499

## L

Lambert, W. D., 216, 256  
 La Paz, L., 257  
 Laronov, L. V., 256  
 Lawrie, J. A., 252, 257  
 Leandabrand, R. L., 525, 535  
 Lebedeva, K. I., 488  
 Lebedinsky, A. I., 155  
 Ledoux, P., 136, 137, 148  
 Leroy, J., 325  
 Levchenko, M. T., 499  
 Levin, B. J., 167, 418, 489  
 Levin, L., 484, 488  
 Licastro, P. H., 565  
 Licht, A. L., 257  
 Lichtener, J., 484  
 Link, F., 445, 452  
 Lipschütz, M., 135, 147, 256  
 Lipsky, Y. N., 23, 401, 407  
 Loewy, M., 344  
 Loguchov, Y. I., 52  
 Lohrmann, W., 117, 221

Losovsky, B. Y., 495  
 Lowman, P. D., 254  
 Lukyanov, V. S., 164  
 Lyot, B., 257, 325, 344, 453, 461  
 Lyustikh, Y. N., 256

## M

MacDonald, G. A., 255  
 MacDonald, G. J. F., 144, 147, 163, 167  
 Machado, P., 255  
 Mädlér, J. H., 117, 221  
 Madsen, B. M., 255  
 Makarenko, F. A., 256  
 Makovetskiy, P. V., 44  
 Markov, A. V., 44, 378, 398, 404, 407, 453, 461, 488, 510, 525  
 Markowitz, W., 80  
 Marshall, C. H., 295, 300  
 Martin, P. W., 257  
 Martina, E. F., 240, 243, 250, 257  
 Mayeva, S. V., 161, 167, 489  
 Mazzoni, A., 256  
 McBirney, A. F., 192, 255  
 McConnell, J., 444  
 McKeller, A., 285, 287  
 McKeller, I. G., 256  
 Manyaylov, A. A., 255  
 Meyer, V. A., 256  
 Mezger, P. G., 493, 495, 497, 499, 540  
 Mikhailov, A. A., 260  
 Mikhailov, V. Y., 23  
 Minakami, T., 179, 255  
 Minnaert, M. J. G., 287, 305, 398  
 Minnett, H. G., 257, 478, 488, 493, 495  
 Mitchell, F., 518  
 Miyamoto, S., 177, 254, 405, 407  
 Molechanov, A. P., 510  
 Mooney, H. M., 241, 257  
 Moore, E., 105  
 Moore, P., 37, 38, 220  
 Morey, G. W., 177, 254  
 Mulders, G. F. W., 287  
 Murota, T., 255  
 Murthy, V. R., 144, 148  
 Myshkin, V. G., 488  
 Myukhyura, V. I., 465, 467

## N

Nagata, T., 241, 257  
 Nagy, B., 219, 256  
 Nambu, M., 255  
 Nefedyev, A. A., 63, 64, 65  
 Nemoto, T., 253, 256  
 Neugebauer, M., 52  
 Nichols, R. L., 186, 255  
 Nicholson, S. B., 223, 256, 494, 495, 521, 522, 525

Nikolayev, A. G., 52  
 Nockolds, S. R., 219, 256  
 Noskova, R. I., 495, 499  
 Novush, A. A., 532

## O

Oana, S., 256  
 Odelevsky, V. I., 484, 488  
 Öhman, Y., 376, 378  
 O'Keefe, J. A., 545, 565  
 Olte, A., 565  
 Öpik, E. J., 141, 147, 148  
 Orlova, N. S., 385, 390, 394, 461  
 Oswald, P., 175

## P

Parnas, Y. M., 488  
 Patel, S. M., 285  
 Pawsey, J. L., 488  
 Pease, F. G., 291  
 Pekeris, C. L., 216  
 Perret, F. A., 255  
 Perry, S. H., 148, 257  
 Pettengill, G. H., 525, 534, 543  
 Pettit, E., 223, 256, 372, 373, 374, 494, 495, 521, 522, 525  
 Pickering, W. H., 220  
 Piddington, J. H., 257, 478, 488, 493, 495, 497, 499, 518, 540  
 Pillow, M. E., 285  
 Plechkov, V. M., 510  
 Poldervaart, A., 209, 254, 256, 257  
 Polozhentseva, M., 264  
 Poppendiek, H. F., 220  
 Porfiryev, V. A., 518  
 Proctor, R. A., 184, 255  
 Puisseux, P., 344  
 Pushkov, N. V., 52

## R

Rackham, T. W., 129  
 Radlova, L. N., 402, 403, 407, 410  
 Radzievsky, V. V., 150  
 Rakhlin, V. L., 510  
 Ramsey, W. H., 157  
 Rankama, K., 257  
 Razbitnaya, E. P., 150  
 Rein, N. F., 150  
 Reynolds, J. A., 144, 148, 226, 256  
 Richards, A. F., 255  
 Ringwood, A. E., 135, 147  
 Roedder, E., 254  
 Rösch, J., 117, 344, 359, 360  
 Rosenholtz, J. L., 560  
 Roux, J., 255

Rubey, W. W., 209, 256  
 Ruskol, E. L., 155, 157, 167

## S

Sabanyev, P. F., 416, 418, 431  
 Safronov, V. S., 155, 167  
 Sahama, T. G., 257  
 Salomonovich, A. E., 438, 478, 488, 499, 510, 518, 540  
 Saundor, S. A., 102, 103, 106, 114, 125  
 Schairer, J. F., 257  
 Schmidt, J., 117, 126, 221  
 Schmidt, O. J., 150  
 Schrader, C. D., 240, 243, 250, 257  
 Schrutka-Rechtenstamm, G. von, 102, 129  
 Schwartz, E. H. L., 230  
 Scott, J. H., 232, 256  
 Secchi, A., 221  
 See, T. J. J., 199, 255  
 Sen Gupta, S. N., 256  
 Senior, T. B. A., 522, 525, 543, 545, 565  
 Serdyukova, A. S., 256  
 Shaler, N. S., 169  
 Sharonov, V. V., 390, 394, 454, 461, 488  
 Shchegolev, D. E., 40, 42, 44  
 Shviris, O. N., 532  
 Shklovsky, I. S., 488  
 Shoemaker, E. M., 134, 198, 254, 255, 296, 300  
 Shorthill, R. W., 222, 223, 224, 256, 469, 471  
 Sicardi, L., 255  
 Siegel, K. M., 522, 525, 543, 545, 565  
 Sinton, W. M., 371, 372, 374, 378, 471, 488  
 Sippel, R. F., 243, 256  
 Skanavi, G. I., 488  
 Smolukhovsky, M., 372, 376  
 Somers, E. V., 257  
 Spicer, H. C., 257  
 Spurr, J. E., 169, 197, 201, 255  
 Stanyukovich, K. P., 392, 394, 415, 418, 431  
 Starkova, A. G., 167  
 Starodubtsev, A. M., 510  
 St. Clair, D., 256  
 Stein, R. J., 220  
 Steiner, A., 219, 256  
 Stenoien, J. O., 488  
 Stout, M., 546, 565  
 Straiton, A. H., 518  
 Strassl, H., 495, 497, 499, 540  
 Strezhnova, K. M., 478, 488, 510, 518  
 Stripling, A. A., 257  
 Sucksdorf, E., 46, 52

Suess, H. E., 147, 169

Swarup, S., 488

Swings, P., 278, 279, 283, 287

Sytinskaya, N. N., 209, 256, 284, 287,  
382, 389, 390, 394, 401, 407, 453, 461,  
489

## T

Tajima, H., 257

Takahashi, K., 256

Tawde, N. R., 285

Teyfel, V. G., 384, 407

Thorarinsson, S., 191

Thornton, F. H., 221

Tilloy, C. E. E., 219, 256

Trexler, J. H., 519, 522, 525, 535, 536

Troitsky, V. S., 478, 488, 493, 495, 499,  
510, 518, 532, 540

Trouvelot, E., 221

Tsuytlin, N. M., 483, 510, 518

Turusbekov, M. T., 497, 499, 532

Turner, F. J., 177, 254

Tverskoy, P. N., 461

Tyurmina, L. O., 52

## U

Uffen, R. J., 179, 255

Ulinich, F. R., 46, 52

Uinov, H. A., 466, 467

Urey, H. C., 133, 144, 147, 148, 149,  
152, 155, 158, 163, 167, 209, 219, 254,  
256, 294, 300, 418, 545, 565

## V

Vakulov, I. V., 52

Van Bemmelen, R. W., 176, 195, 219,  
254, 257

Van Diggelen, J., 376, 378, 453, 461,  
524, 525

Verhoog, J., 177, 178, 197, 254, 255,  
547, 565

Vernov, S. N., 52

Voshev, A. V., 241, 256

Vinogradov, A. P., 167, 257

Vlček, O. S., 205, 208, 255

Vlodavets, V. I., 255

Voldan, J., 205, 255

## W

Wall, J., 220

Washington, H. S., 255

Watts, C. B., 109, 111

Webb, J., 535

Wegenor, A., 416, 418

Weimer, T., 63, 102

Wessolink, A. M., 199, 255, 376, 377,  
542, 543

Westcott, E. M., 232, 256

Westerhout, G., 499

Whipple, F. L., 199, 255, 433, 471

Whitaker, E. A., 119, 125, 322

Whitehurst, R., 518

Wiik, H. B., 219, 256

Wilhelm, R. S., 257

Wilkins, H. P., 37, 38, 117, 126, 220

Wilkins, W. H., 221

Wilks, S. S., 88, 100

Williams, H., 176, 179, 254, 255

Wolff, F. L. von, 169, 201

Wolford, R., 565

Wright, F. E., 199, 255

## Y

Yakovkin, A. A., 55, 57, 58, 63, 64, 65

Yapleo, B. S., 535

Yosepkina, N. A., 532

Yodor, H. S., 179, 255

Yokoyama, I., 257

Yoshimura, J., 256

Yudin, I. A., 393, 394

## Z

Zablocki, C. J., 256

Zelinskaya, M. R., 478, 488, 493, 495,  
510, 518, 540

Zharkov, V. N., 46, 52, 164, 167

Zhevakin, S. A., 510, 518

Zhilonkov, N. V., 488

Zhuzgov, L. I., 52

Zimmerman, G. W., 257

Zoellner, F., 372

Zotov, P. P., 228, 256

Zuckernik, V. B., 241, 256